



# Electric and Hybrid Vehicles

Power Sources, Models, Sustainability, Infrastructure and the Market



Edited by  
Gianfranco Pistoia



# ELECTRIC AND HYBRID VEHICLES

## POWER SOURCES, MODELS, SUSTAINABILITY, INFRASTRUCTURE AND THE MARKET

**Gianfranco Pistoia**

*Consultant, Rome, Italy*

*Gianfranco.pistoia0@alice.it*



**ELSEVIER**

Amsterdam • Boston • Heidelberg • London • New York • Oxford

Paris • San Diego • San Francisco • Singapore • Sydney • Tokyo

Elsevier  
Radarweg 29, PO Box 211, 1000 AE Amsterdam, The Netherlands  
Linacre House, Jordan Hill, Oxford OX2 8DP, UK

First edition 2010

Copyright © 2010 Elsevier B.V. All rights reserved

No part of this publication may be reproduced, stored in a retrieval system or transmitted in any form or by any means electronic, mechanical, photocopying, recording or otherwise without the prior written permission of the publisher

Permissions may be sought directly from Elsevier's Science & Technology Rights Department in Oxford, UK: phone (+44) (0) 1865 843830; fax (+44) (0) 1865 853333; email: [permissions@elsevier.com](mailto:permissions@elsevier.com). Alternatively you can submit your request online by visiting the Elsevier web site at <http://elsevier.com/locate/permissions>, and selecting Obtaining permission to use Elsevier material

#### Notice

No responsibility is assumed by the publisher for any injury and/or damage to persons or property as a matter of products liability, negligence or otherwise, or from any use or operation of any methods, products, instructions or ideas contained in the material herein.

#### **British Library Cataloguing in Publication Data**

A catalogue record for this book is available from the British Library

#### **Library of Congress Cataloging-in-Publication Data**

A catalog record for this book is available from the Library of Congress

ISBN: 978-0-444-53565-8

For information on all Elsevier publications  
visit our website at [books.elsevier.com](http://books.elsevier.com)

Printed and bound in the Great Britain

10 11 10 9 8 7 6 5 4 3 2 1

Working together to grow  
libraries in developing countries

[www.elsevier.com](http://www.elsevier.com) | [www.bookaid.org](http://www.bookaid.org) | [www.sabre.org](http://www.sabre.org)

ELSEVIER

BOOK AID  
International

Sabre Foundation

# CONTRIBUTORS

**Paul Albertus**

Department of Chemical Engineering, University of California, Berkeley, CA 94720, USA

**James E. Anderson**

Systems Analytics and Environmental Sciences Department, Ford Motor Company, Dearborn, Michigan, USA

**Ashish Arora**

Exponent Failure Analysis Associates, 23445 North 19<sup>th</sup> Avenue, Phoenix, AZ 85027, USA

**Jonn Axsen**

Institute of Transportation Studies, University of California at Davis, 2028 Academic Surge, One Shields Avenue, Davis, CA 95616, USA

**Thomas H. Bradley**

Department of Mechanical Engineering, Colorado State University, Fort Collins, CO 80523-1374, USA

**Michel Broussely**

Formerly Scientific Director of Specialty Battery Division at Saft, France, 53 Avenue de Poitiers, 86240 Ligugé, France

**Andrew F. Burke**

Institute of Transportation Studies, University of California at Davis, 2028 Academic Surge, One Shields Avenue, Davis, CA 95616, USA

**Mark A. Delucchi**

Institute of Transportation Studies, University of California at Davis, Davis, CA, 95616, USA

**Ibrahim Dincer**

Faculty of Engineering and Applied Science, University of Ontario, Institute of Technology (UOIT), Oshawa, Ontario, Canada

**Matthieu Dubarry**

Hawai'i Natural Energy Institute, SOEST, University of Hawai'i at Manoa Honolulu, HI 96822, USA

**Ulrich Eberle**

Hydrogen, Fuel Cell & Electric Propulsion Research Strategy, GM Alternative Propulsion Center Europe, Adam Opel GmbH, IPC MK-01, 65423 Rüsselsheim, Germany

**Tiago Farias**

Department of Mechanical Engineering, IDMEC/IST, Instituto Superior Técnico, Technical University of Lisbon, Av. Rovisco Pais, 1 Pav. Mecânica I, 1049-001 Lisboa, Portugal

**Horst E. Friedrich**

Institute of Vehicle Concepts, German Aerospace Center (DLR), Stuttgart, Germany



**Daniel D. Friel**

Battery Management Solutions, Texas Instruments, Inc., 607 Herndon Parkway, Suite 100, Herndon, VA 20170, USA

**John Garbak**

U.S. Department of Energy, Washington, DC 20585, USA

**Benjamin Geller**

Department of Mechanical Engineering, Colorado State University, Fort Collins, CO 80523-1374, USA

**Maria Grahn**

Department of Energy and Environment, Physical Resource Theory, Chalmers University of Technology, Göteborg, Sweden

**Rittmar von Helholt**

Hydrogen, Fuel Cell & Electric Propulsion Research Strategy, GM Alternative Propulsion Center Europe, Adam Opel GmbH, IPC MK-01, 65423 Rüsselsheim, Germany

**Mohammed M.Hussain**

National Research Council – Institute of Fuel Cell Innovation, Vancouver, British Columbia, Canada

**Kenneth S. Kurani**

Institute of Transportation Studies, University of California at Davis, 2028 Academic Surge, One Shields Avenue, Davis, CA 95616, USA

**Jennifer Kurtz**

National Renewable Energy Laboratory, Golden, CO 80401, USA

**Bor Yann Liaw**

Hawai'i Natural Energy Institute, SOEST, University of Hawai'i at Manoa Honolulu, HI 96822, USA

**Timothy E. Lipman**

Transportation Sustainability Research Center, University of California–Berkeley, 2614 Dwight Way, MC 1782, Berkeley, CA, 94720-1782, USA

**Thomas Livernois**

Exponent Failure Analysis Associates, 39100 Country Club Drive, Farmington Hills, MI 48331, USA

**Chris Manzie**

Department of Mechanical Engineering, University of Melbourne, Victoria, Australia

**Tony Markel**

National Renewable Energy Laboratory, 1617 Cole Blvd., Golden, CO 80401, USA

**Julien Matheys**

Department of Electrical Engineering and Energy Technology (ETEC), Vrije Universiteit Brussel, Pleinlaan 2, Brussels, Belgium

**Noshirwan K. Medora**

Exponent Failure Analysis Associates, 23445 North 19<sup>th</sup> Avenue, Phoenix, AZ 85027, USA

**Peter Mock**

Institute of Vehicle Concepts, German Aerospace Center (DLR), Stuttgart, Germany

**John Newman**

Department of Chemical Engineering, University of California, Berkeley, CA 94720, USA

**Fabio Orecchini**

GRA (Automotive Research Group) and CIRPS (Interuniversity Research Centre for Sustainable Development), “La Sapienza” University of Rome, Piazza S. Pietro in Vincoli 10, 00184 Rome, Italy

**Ahmad A. Pesaran**

National Renewable Energy Laboratory, 1617 Cole Blvd., Golden, CO 80401, USA

**Casey Quinn**

Department of Mechanical Engineering, Colorado State University, Fort Collins, CO 80523-1374, USA

**Todd Ramsden**

National Renewable Energy Laboratory, Golden, CO 80401, USA

**Marc A. Rosen**

Faculty of Engineering and Applied Science, University of Ontario, Institute of Technology (UOIT), Oshawa, Ontario, Canada

**Adriano Santiangeli**

GRA (Automotive Research Group) and CIRPS (Interuniversity Research Centre for Sustainable Development), “La Sapienza” University of Rome, Piazza S. Pietro in Vincoli 10, 00184 Rome, Italy

**Stephan A. Schmid**

Institute of Vehicle Concepts, German Aerospace Center (DLR), Stuttgart, Germany

**Carla Silva**

Department of Mechanical Engineering, IDMEC/IST, Instituto Superior Técnico, Technical University of Lisbon, Av. Rovisco Pais, 1 Pav. Mecânica I, 1049-001 Lisboa, Portugal

**Kandler Smith**

National Renewable Energy Laboratory, 1617 Cole Blvd., Golden, CO 80401, USA

**Bent Sørensen**

Department of Environmental, Social and Spatial Change, Bld. 11.1, Universitetsvej 1, Roskilde University, PO Box 260, DK-4000 Roskilde, Denmark

**Sam Sprik**

National Renewable Energy Laboratory, Golden, CO 80401, USA

**Jan Swart**

Exponent Failure Analysis Associates, 23445 North 19<sup>th</sup> Avenue, Phoenix, AZ 85027, USA

**Peter Van den Bossche**

Erasmus Hogeschool Brussel, Nijverheidskaai 170, Anderlecht, Belgium

**Joeri Van Mierlo**

Department of Electrical Engineering and Energy Technology (ETEC), Vrije Universiteit Brussel, Pleinlaan 2, Brussels, Belgium

**Timothy J. Wallington**

Systems Analytics and Environmental Sciences Department, Ford Motor Company, Dearborn, Michigan, USA

**Keith Wipke**

National Renewable Energy Laboratory, Golden, CO 80401, USA

**Calin Zamfirescu**

Faculty of Engineering and Applied Science, University of Ontario, Institute of Technology (UOIT), Oshawa, Ontario, Canada

# PREFACE

In the last 10–15 years, people have become acquainted with vehicles powered not only by an internal combustion engine (using gasoline, diesel or gas), but also by an electric motor. These hybrid electric vehicles (HEVs) afford a reduction of fuel consumption in city driving and reduce emissions, but this is only the first stretch of a long road that will hopefully end with zero-emission electric vehicles (EVs) allowing long-range driving.

The first vehicles produced at the beginning of the last century were electric, powered by lead-acid batteries, but they were soon abandoned because of the limited battery performance and the availability of fossil fuels at reasonable costs. However, the situation has radically changed in recent years; high fuel price and dramatic environmental deterioration have led to reconsider the use of batteries, whose performance, on the other hand, has been steadily increasing since the early 1990s.

Nickel-metal hydride (almost exclusively used to the end of 2009, e.g. in Toyota Prius and Honda Insight) and the forthcoming Li-ion batteries (now used in recently produced electric vehicles, e.g. Nissan Leaf and Mitsubishi i-MiEV) have satisfactory energy and power features. In this book, the performance, cost, safety and sustainability of these and other battery systems for HEVs and EVs are thoroughly reviewed (particularly in Chapters 8 and 13–19).

Attention is also given to fuel cell systems, as research in this area is more active than ever, and prototypes of hydrogen fuel cell vehicles are already circulating (e.g. Honda FCX Clarity and GM Hydrogen4), although their cost places commercialization a long-way ahead (Chapters 9–12).

Throughout this book, especially in the first chapters, alternative vehicles with different powertrains are compared in terms of lifetime cost, fuel consumption and environmental impact. The emissions of greenhouse gases have been particularly dealt with.

In general, how far is, and how much substantial will be, the penetration of alternative vehicles into the market? The answer to this question has to be based on the assumption of models taking into account such factors as the fraction of electricity produced by renewable sources and the level of CO<sub>2</sub> considered acceptable (as is done especially in Chapters 4 and 21). However, according to some surveys, many drivers seem less attracted by environmental issues and more by vehicle performance and cost. In this respect, improvement of the battery, or fuel cell, performance and governmental incentives will play a fundamental role.

An adequate recharging infrastructure is also of paramount importance for the diffusion of vehicles powered by batteries and fuel cells, as it may contribute to overcome

the so-called “range anxiety”. The battery charging techniques proposed are summarized in Chapter 20, while hydrogen refueling stations are described in Chapter 12.

Finally, in Chapter 22, the state of the art of the current models of hybrid and electric vehicles (as of the beginning of 2010) is reviewed along with the powertrain solutions adopted by the major automakers.

Gianfranco Pistoia



# Economic and Environmental Comparison of Conventional and Alternative Vehicle Options

Ibrahim Dincer<sup>1</sup>, Marc A. Rosen and Calin Zamfirescu

Faculty of Engineering and Applied Science, University of Ontario, Institute of Technology (UOIT), Oshawa, Ontario, Canada

## Contents

1. Introduction	1
2. Analysis	2
2.1 Technical and economical criteria	3
2.2 Environmental impact criteria	5
2.3 Normalization and the general indicator	10
3. Results and Discussion	11
4. Conclusions	15
Acknowledgement	15
Nomenclature	16
Greek symbols	16
Subscripts	16
References	16



## 1. INTRODUCTION

Of the major industries that have to adapt and reconfigure to meet present requirements for sustainable development, vehicle manufacturing is one of the more significant. One component of sustainability requires the design of environmentally benign vehicles characterized by no or little atmospheric pollution during operation. The design of such vehicles requires, among other developments, improvements in powertrain systems, fuel processing, and power conversion technologies. Opportunities for utilizing various fuels for vehicle propulsion, with an emphasis on synthetic fuels (e.g., hydrogen, biodiesel, bioethanol, dimethylether, ammonia, etc.) as well as electricity via electrical batteries, have been analyzed over the last decade and summarized in Refs [1–3].

In analyzing a vehicle propulsion and fueling system, it is necessary to consider all stages of the life cycle starting from the extraction of natural resources to produce

<sup>1</sup> Corresponding author: Ibrahim.Dincer@uoit.ca

materials and ending with conversion of the energy stored onboard the vehicle into mechanical energy for vehicle displacement and other purposes (heating, cooling, lighting, etc.). All life cycle stages preceding fuel utilization on the vehicle influence the overall efficiency and environmental impact. In addition, vehicle production stages and end-of-life disposal contribute substantially when quantifying the life cycle environmental impact of fuel-propulsion alternatives. Cost-effectiveness is also a decisive factor contributing to the development of an environmentally benign transportation sector.

This chapter extends and updates the approach by Granovskii et al. [1] which evaluates, based on actual cost data, the life cycle indicators for vehicle production and utilization stages and performs a comparison of four kinds of fuel-propulsion vehicle alternatives. We consider in the present analysis two additional kinds of vehicles, both of which are zero polluting at fuel utilization stage (during vehicle operation). One uses hydrogen as a fuel in an internal combustion engine (ICE), while the second uses ammonia as a hydrogen fuel source to drive an ICE. Consequently, the vehicles analyzed here are as follows:

- conventional gasoline vehicle (gasoline fuel and ICE),
- hybrid vehicle (gasoline fuel, electrical drive, and large rechargeable battery),
- electric vehicle (high-capacity electrical battery and electrical drive/generator),
- hydrogen fuel cell vehicle (high-pressure hydrogen fuel tank, fuel cell, electrical drive),
- hydrogen internal combustion vehicle (high-pressure hydrogen fuel tank and ICE),
- ammonia-fueled vehicle (liquid ammonia fuel tank, ammonia thermo-catalytic decomposition and separation unit to generate pure hydrogen, hydrogen-fueled ICE).

The theoretical developments introduced in this chapter, consisting of novel economic and environmental criteria for quantifying vehicle sustainability, are expected to prove useful in the design of modern light-duty automobiles, with superior economic and environmental attributes.



## 2. ANALYSIS

We develop in this section a series of general quantitative indicators that help quantify the economic attractiveness and environmental impact of any fuel-propulsion system. These criteria are applied to the six cases studied in this chapter. The analysis is conducted for six vehicles that entered the market between 2002 and 2004, each representative of one of the above discussed categories. The specific vehicles follow:

- Toyota Corolla (conventional vehicle),
- Toyota Prius (hybrid vehicle),
- Toyota RAV4EV (electric vehicle),

- Honda FCX (hydrogen fuel cell vehicle),
- Ford Focus H<sub>2</sub>-ICE (hydrogen ICE vehicle),
- Ford Focus H<sub>2</sub>-ICE adapted to use ammonia as source of hydrogen (ammonia-fueled ICE vehicle).

Note that the analysis for the first five options is based on published data from manufacturers, since these vehicles were produced and tested. The results for the sixth case, namely, the ammonia-fueled vehicle, are calculated, starting from data published by Ford on the performance of its hydrogen-fueled Ford Focus vehicle. It is assumed that the vehicle engine operates with hydrogen delivered at the same parameters as for the original Ford design specifications. However, the hydrogen is produced from ammonia stored onboard in liquid phase. Details regarding the operation of the ammonia-fueled vehicle are given subsequently.

The present section comprises three subsections, treating the following aspects: economic criteria, environmental criteria, and a combined impact criterion. The latter is a normalized indicator that takes into account the effects on both environmental and economic performance of the options considered.

## 2.1 Technical and economical criteria

A number of key economic parameters characterize vehicles, like vehicle price, fuel cost, and driving range. In the present analysis, we neglect maintenance costs; however, for the hybrid and electric vehicles, the cost of battery replacement during the lifetime is accounted for. Note also that the driving range determines the frequency (number and separation distance) of fueling stations for each vehicle type. The total fuel cost and the total number of kilometers driven are related to the vehicle life.

The technical and economical parameters that serve as criteria for the present comparative analysis of the selected vehicles are compiled in [Table 1.1](#). For the Honda FCX the listed initial price for a prototype leased in 2002 was US\$2,000, which is estimated to drop below US\$100 in regular production. Currently, a Honda FCX can be leased for 3 years with a total price of US\$21.6. In order to render the comparative study reasonable, the initial price of the hydrogen fuel cell vehicle is assumed here to be US\$100.

The considered H<sub>2</sub>-ICE was produced by Ford during the years 2003–2005 in various models, starting with model U in 2003 which is based on a SUV body style vehicle with a hybrid powertrain (ICE + electric drive) and ending with the Ford Focus Wagon which is completely based on a hydrogen-fueled ICE (this last model is included in the analysis in [Table 1.1](#)). The H<sub>2</sub>-ICE uses a shaft driven turbocharger and a 217l pressurized hydrogen tank together with a specially designed fuel injection system. The evaluated parameters for a H<sub>2</sub>-ICE Ford Focus Wagon converted to ammonia fuel are listed in the last row of [Table 1.1](#). The initial cost is lower than that of the original ICE Ford Focus due to the fact that the expensive hydrogen fuel tank and safety system are



**Table 1.1** Technical and economical characteristics for selected vehicle technologies

Vehicle type	Fuel	Initial price (USk\$)	Specific fuel consumption <sup>a</sup> (MJ/100 km)	Specific fuel price (US\$/100 km)	Driving range (km)	Price of battery changes during vehicle life cycle <sup>b</sup> (USk\$)
Conventional	Gasoline	15.3	236.8 <sup>c</sup>	2.94	540	1 × 0.1
Hybrid	Gasoline	20.0	137.6	1.71	930	1 × 1.02
Electric	Electricity	42.0	67.2	0.901	164	2 × 15.4
Fuel cell	Hydrogen	100.0	129.5	1.69	355	1 × 0.1
H <sub>2</sub> -ICE	Hydrogen	60.0 <sup>d</sup>	200	8.4	300	1 × 0.1
NH <sub>3</sub> -H <sub>2</sub> -ICE	Ammonia	40.0 <sup>e</sup>	175	6.4 <sup>f</sup>	430	1 × 0.1

<sup>a</sup> Fuel consumption based on driving times divided as 45% on highway and 55% in city.

<sup>b</sup> Life cycle of vehicle is taken as 10 years.

<sup>c</sup> Heat content of conventional gasoline is assumed to be its lower heating value (LHV = 32 MJ/l).

<sup>d</sup> Estimated based on gasoline ICE to H<sub>2</sub>-ICE conversion data from Atlantic Hydrogen [4].

<sup>e</sup> Estimated based on assumption that the costs of the fuel tank + fuel distribution + fuel safety systems are negligible with respect to the H<sub>2</sub>-ICE vehicle.

<sup>f</sup> Estimated for US\$6.4/kg of ammonia.

replaced with ones with negligible price, because ammonia can be stored in ordinary carbon steel cylinders. Moreover, NH<sub>3</sub> is a refrigerant that satisfies onboard cooling needs, reducing the costs of the balance of plant.

For the ammonia-fueled vehicle, previous results of Zamfirescu and Dincer [3] are considered. Based on a previous study [1], it is estimated for the electric vehicle that the specific cost is US\$569/kWh of nickel metal hydride (NiMeH) batteries which are typically used in hybrid and electric cars. The specific cost of an electric car vehicle decreased in recent years to below US\$500/kWh (and in some special cases to below US\$250/kWh). Here, we assume the same figure as Granovskii et al. [1], that is, US\$570/kWh, which is considered more conservative. For gasoline and hybrid vehicles, a 40 l fuel tank is assumed, based on which determines the driving range.

Annual average prices of typical fuels over the last decade are presented in Fig. 1.1, based on Energy Information Administration (EIA) [5]. Few and approximate data are available for historical trends of hydrogen fuel prices, so the results by Granovskii et al. [1, 6] are considered to obtain hydrogen price trends.

Here, hydrogen price trends are derived based on the assumption that the price of low-pressure hydrogen, per unit energy content, is about the same as the price of gasoline [3]. The hydrogen fuel price accounts for the cost of energy required to compress the hydrogen from 20 bar, the typical pressure after natural gas reforming [7], to the pressure of the vehicle tank, which is on the order of 350 bar. The compression energy is estimated to be approximately 50 kJ of electricity per MJ of hydrogen in the vehicle. The cost of ammonia is taken from the analysis by Zamfirescu and Dincer [3].

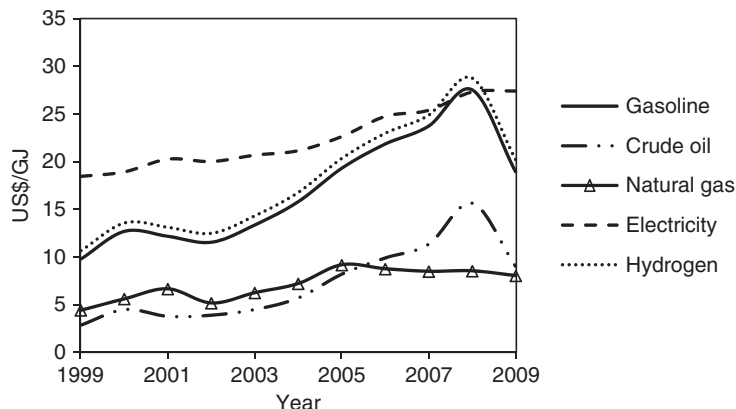


**Figure 1.1** Historical price trends of selected energy carriers.

## 2.2 Environmental impact criteria

Two environmental impact elements are accounted for in this study of fuel–powertrain options for transportation: air pollution (AP) and greenhouse gas (GHG) emissions. The main GHGs are CO<sub>2</sub>, CH<sub>4</sub>, N<sub>2</sub>O, and SF<sub>6</sub> (sulfur hexafluoride), which have GHG impact weighting coefficients relative to CO<sub>2</sub> of 1, 21, 310, and 24,900, respectively [8]. SF<sub>6</sub> is used as a cover gas in the casting process for magnesium, which is a material employed in vehicle manufacturing. Impact weighting coefficients (relative to NO<sub>x</sub>) for the airborne pollutants CO, NO<sub>x</sub>, and VOCs (volatile organic compounds) are based on those obtained by the Australian Greenhouse Office [9] using cost–benefit analyses of health effects. The weighting coefficient of SO<sub>x</sub> relative to NO<sub>x</sub> is estimated using the Ontario Air Quality Index data developed by Basrur et al. [10]. Thus, for considerations of AP, the airborne pollutants CO, NO<sub>x</sub>, SO<sub>x</sub>, and VOCs are assigned the following weighting coefficients: 0.017, 1, 1.3, and 0.64, respectively.

The vehicle production stage contributes to the total life cycle environmental impact through the pollution associated with the extraction and processing of material resources and manufacturing. As indicated in Table 1.2, it is also necessary to consider the pollution produced at the vehicle disposal stage (i.e., at the end of life). The data in

**Table 1.2** Gaseous emissions per kilogram of curb mass of a typical vehicle

Life cycle stage	CO (kg)	NO <sub>x</sub> (kg)	GHGs (kg)
Materials extraction	0.0120	0.00506	1.930
Manufacturing	0.000188	0.00240	1.228
End-of-life disposal	$1.77 \times 10^{-6}$	$3.58 \times 10^{-5}$	0.014
Total	0.0122	0.00750	3.172

Table 1.2 are on the basis of the curb mass of the vehicle (i.e., the vehicle mass without any load or occupants).

The AP emissions per unit vehicle curb mass, denoted  $AP_m$ , are obtained for a conventional car case by applying weighting coefficients to the masses of air pollutants in accordance with the following formula:

$$AP_m = \sum_1^4 m_i w_i \quad (1.1)$$

Here,  $i$  is the index denoting an air pollutant (which can be CO, NO<sub>x</sub>, SO<sub>x</sub>, or VOCs),  $m_i$  is the mass of air pollutant  $i$ , and  $w_i$  is the weighting coefficient of air pollutant  $i$ .

The results of the environmental impact evaluation for the vehicle production stage are presented in Table 1.3 for each vehicle case. The curb mass of each vehicle is also reported. We assume that the ammonia-fueled vehicle has the same curb mass as the H<sub>2</sub>-ICE vehicle from which it originates. The justification for this assumption comes from the fact that the ammonia and hydrogen vehicles have system components of similar weight, because the car frame is the same, the engine is the same, and the supercharger of the hydrogen vehicle likely has a similar weight as the ammonia decomposition and separation unit of the ammonia-fueled vehicle, etc. Since the engines of the hydrogen and ammonia-fueled vehicles are similar to that of a conventional gasoline vehicle, the environmental impact associated with vehicle manufacture is of the same order as that for the conventional vehicle.

We assume that GHG and AP emissions are proportional to the vehicle mass, but the environmental impact related to the production of special devices in hybrid, electric and fuel cell cars, for example, NiMeH batteries and fuel cell stacks, are evaluated separately. Accordingly, the AP and GHG emissions are calculated for conventional vehicles as

$$AP = m_{\text{car}} AP_m \quad (1.2a)$$

**Table 1.3** Environmental impact associated with vehicle production stages

Vehicle type	Curb mass (kg)	GHG emissions (kg)	AP emissions (kg)	GHG emissions per 100 km of travel <sup>a</sup> (kg/100 km)	AP emissions per 100 km of travel (kg/100 km)
Conventional	1,134	3,595.8	8.74	1.490	0.00362
Hybrid	1,311	4,156.7	10.10	1.722	0.00419
Electric	1,588	4,758.3	15.09	1.972	0.00625
Fuel cell	1,678	9,832.4	42.86	4.074	0.0178
H <sub>2</sub> -ICE	1,500	3,600	9.00	1.500	0.00400
NH <sub>3</sub> -H <sub>2</sub> -ICE	1500	3,500	8.00	1.400	0.00300

<sup>a</sup> During vehicle lifetime (10 years), an average car drives 241,350 km (DoE Fuel Economy [11]).

$$\text{GHG} = m_{\text{car}}\text{GHG}_{\text{m}} \quad (1.2\text{b})$$

For hybrid and electric vehicles the AP and GHG emissions are evaluated as

$$\text{AP} = (m_{\text{car}} - m_{\text{bat}})\text{AP}_{\text{m}} + m_{\text{bat}}\text{AP}_{\text{bat}} \quad (1.3\text{a})$$

$$\text{GHG} = (m_{\text{car}} - m_{\text{bat}})\text{GHG}_{\text{m}} + m_{\text{bat}}\text{GHG}_{\text{bat}} \quad (1.3\text{b})$$

Finally, the environmental impact for fuel cell vehicles is found as

$$\text{AP} = (m_{\text{car}} - m_{\text{fc}})\text{AP}_{\text{m}} + m_{\text{fc}}\text{AP}_{\text{fc}} \quad (1.4\text{a})$$

$$\text{GHG} = (m_{\text{car}} - m_{\text{fc}})\text{GHG}_{\text{m}} + m_{\text{fc}}\text{GHG}_{\text{bat}} \quad (1.4\text{b})$$

Here,  $m_{\text{car}}$ ,  $m_{\text{bat}}$ , and  $m_{\text{fc}}$  are, respectively, the masses of cars, NiMeH batteries, and the fuel cell stack;  $\text{AP}_{\text{m}}$ ,  $\text{AP}_{\text{bat}}$ , and  $\text{AP}_{\text{fc}}$  are AP emissions per kilogram of conventional vehicle, NiMeH batteries, and the fuel cell stack; and  $\text{GHG}_{\text{m}}$ ,  $\text{GHG}_{\text{bat}}$ , and  $\text{GHG}_{\text{fc}}$  are GHG emissions per kilogram of conventional vehicle, NiMeH batteries, and fuel cell stack. The masses of NiMeH batteries for hybrid and electric cars are 53 kg (1.8 kWh capacity) and 430 kg (27 kWh capacity), respectively.

The mass of the fuel cell stack is about 78 kg (78 kW power capacity). According to Rantik [12], the production of 1 kg of NiMeH battery requires 1.96 MJ of electricity and 8.35 MJ of liquid petroleum gas. The environmental impact of battery production is presented in Table 1.4, assuming that electricity is produced from natural gas with a mean efficiency of 40% (which is reasonable since the efficiency of electricity production from natural gas varies from 33% for gas turbine units to 55% for combined-cycle power plants, with about 7% of the electricity dissipated during transmission).

The material inventory for a proton exchange membrane fuel cell (PEMFC) is presented in Table 1.5, based on data of Handley et al. [13] and Granovskii et al. [6].

**Table 1.4** Environmental impact related to the production of NiMeH batteries and PEMFC stacks

Equipment	Mass (kg)	Number per vehicle life	AP emissions per vehicle life (kg)	GHG emissions per vehicle life (kg)
NiMeH battery for hybrid vehicle	53	2	0.507	89.37
NiMeH battery for electric vehicle	430	3	6.167	1,087.6
PEMFC stack for fuel cell vehicle	78	1	30.52	4,758.0

**Table 1.5** Material inventory of a PEMFC stack

Component	Material	Mass (kg)
Electrode	Platinum	0.06
	Ruthenium	0.01
	Carbon paper	4.37
Membrane	Nafion membrane	5.64
Bipolar plate	Polypropylene	16.14
	Carbon fibers	16.14
	Carbon powder	21.52
End plate	Aluminum alloy	2.80
Current collectors	Aluminum alloy	1.14
Tie rod	Steel	2.05
Total		69.87

Source: Refs [6, 13].

The environmental impact of the fuel cell stack production stage is expressed in terms of AP (air pollution) and GHG emissions (Table 1.4, last row). Compared to NiMeH batteries, the data indicate that the PEMFC production stage accounts for relatively large GHG and AP emissions. The manufacturing of electrodes (including material extraction and processing) and bipolar plates constitutes a major part of the emissions.

Additional sources of GHG and AP emissions are associated with the fuel production and utilization stages. The environmental impacts of these stages have been evaluated in numerous life cycle assessments of fuel cycles, (e.g., [6, 14–16]). We also use the results of Granovskii et al. [6, 15] for quantifying the pollution associated with fuel production and utilization stages.

Regarding electricity production for the electric car case, three scenarios are considered here:

1. electricity is produced from renewable energy sources and nuclear energy;
2. 50% of the electricity is produced from renewable energy sources and 50% from natural gas at an efficiency of 40%;
3. electricity is produced from natural gas at an efficiency of 40%.

Nuclear/renewable weighted average GHG emissions are reported by Granovskii et al. [15] as 18.4 tons CO<sub>2</sub>-equivalent per GWh of electricity. These emissions are embedded in material extraction, manufacturing and decommissioning for nuclear, hydro, biomass, wind, solar, and geothermal power generation stations.

AP emissions are calculated assuming that GHG emissions for plant manufacturing correspond entirely to natural gas combustion. According to a study by Meier [17], GHG and AP emissions embedded in manufacturing a natural gas power generation plant are negligible compared to the direct emissions during its utilization. Taking these

**Table 1.6** GHG and air pollution emissions per MJ of electricity produced

Electricity-generation scenario	GHG emission (g)	AP emission (g)
1	5.11	0.0195
2	77.5	0.296
3	149.9	0.573

**Table 1.7** GHG and air pollution emissions per MJ fuel (LHV) for fuel utilization stage

Fuel	GHG emissions, g	AP emissions, g
Hydrogen from natural gas		
Scenario 1	78.5	0.0994
Scenario 2	82.1	0.113
Scenario 3	85.7	0.127
Gasoline from crude oil	84.0	0.238

factors into account, GHG and AP emissions for the three scenarios for electricity generation are calculated and presented in [Table 1.6](#).

As noted previously, onboard hydrogen charging of fuel tanks on vehicles requires compression. In this study we consider the energy for hydrogen compression to be provided by electricity. In [Table 1.7](#), GHG and AP emissions are reported for hydrogen vehicles for the three electricity-generation scenarios considered, accounting for the environmental effects of hydrogen compression. GHG and AP emissions for gasoline utilization in vehicles are also reported in [Table 1.7](#).

The environmental impact of the fuel utilization stage, as well as the overall environmental impact (including the fuel utilization, vehicle production, and disposal stages), are summarized in [Table 1.8](#). The H<sub>2</sub>-ICE vehicle results in [Table 1.8](#) are based on the assumption that the only GHG emissions during the utilization stage are associated with the compression work needed to fill the fuel tank of the vehicle. When combusting hydrogen, the tailpipe exhausts only water vapor. The GHG effect of water vapor emissions is neglected in this analysis, as it is deemed minor with respect to the effect of the other emitted gases (listed above). For the ammonia fuel vehicle, a very small amount of pump work is needed to fuel the tank, but compression work is not required. Therefore, ammonia fuel is considered here to emit no GHGs during fuel utilization. However, some AP caused by imperfect combustion is assumed for the ammonia fuel vehicle, which is on the order of magnitude of that for the H<sub>2</sub>-ICE vehicle.

**Table 1.8** Fuel utilization stage and overall GHG and air pollution emissions (per 100 km of vehicle travel) for different vehicle types

Vehicle type	Fuel utilization stage		Overall life cycle <sup>a</sup>	
	GHG emissions (kg/100 km)	AP emissions (kg/100 km)	GHG emissions (kg/100 km)	AP emissions (kg/100 km)
Conventional	19.9	0.0564	21.4	0.0600
Hybrid	11.6	0.0328	13.3	0.0370
Electric <sup>b</sup>				
Scenario 1	0.343	0.00131	2.31	0.00756
Scenario 2	5.21	0.0199	7.18	0.0262
Scenario 3	10.1	0.0385	12.0	0.0448
Fuel cell <sup>b</sup>				
Scenario 1	10.2	0.0129	14.2	0.0306
Scenario 2	10.6	0.0147	14.7	0.0324
Scenario 3	11.1	0.0165	15.2	0.0342
H <sub>2</sub> -ICE	10.0	0.014	11.5	0.0180
NH <sub>3</sub> -H <sub>2</sub> -ICE	0.0	0.014	1.4	0.0170

<sup>a</sup> During vehicle lifetime (10 years), an average car drives 241,350 km (DoE Fuel Economy [11]).

<sup>b</sup> Scenarios refer to electricity-generation scenarios.

## 2.3 Normalization and the general indicator

To allow different cars to be compared when various kinds of indicators are available (e.g., technical, economical, and environmental), a normalization procedure is proposed. A normalized indicator value of one is chosen to correspond to the best economic and environmental performance among the six vehicle types considered. Normalized indicators for vehicle and fuel costs and GHG and AP emissions are now introduced.

The general expression for the normalized indicator of impact is

$$(\text{NInd})_i = \frac{\left(\frac{1}{\text{Ind}}\right)_i}{\left(\frac{1}{\text{Ind}}\right)_{\max}} \quad (1.5)$$

where  $(1/\text{Ind})_i$  are reciprocal values of indicators like vehicle and fuel costs, GHG, and AP emissions,  $(1/\text{Ind})_{\max}$  is the maximum of the reciprocal values of those indicators,  $(\text{NInd})_i$  is the normalized indicator, and the index  $i$  denotes the vehicle type.

A driving range indicator quantifying the vehicle displacement with one full tank or one fully charged battery is also introduced, as follows:

$$(\text{NInd})_i = \frac{(\text{Ind})_i}{(\text{Ind})_{\max}} \quad (1.6)$$

where  $(\text{Ind})_i$  denotes the driving range indicator for the six types of vehicles (denoted by index  $i$ ) considered here and  $(\text{Ind})_{\max}$  denotes the maximum value of the driving range indicators.

Normalized technical–economical and environmental indicators for the six vehicles types and the three electricity–generation scenarios are reported in Table 1.9. A generalized indicator is introduced, representing the product of the normalized indicators (which is a simple geometrical aggregation of criteria without weighting coefficients). The general indicator is also normalized according to Eq. [1.6]. The general indicators provide a measure of how far a given car is from the “ideal” one (which has a corresponding general indicator of one), for the factors considered.



### 3. RESULTS AND DISCUSSION

The normalized indicators are used to compare the fuel–powertrain cases. In Fig. 1.2, the dependence is illustrated of the normalized general indicator on the electricity–generation scenario for each of the considered vehicles (using data from column 8 of Table 1.9). These results indicate that hybrid and electric cars are competitive if nuclear and renewable energies account for about 50% of the energy to generate electricity. If fossil fuels (in this case natural gas) are used for more than 50% of the energy to generate electricity, the hybrid car has significant advantages over the other five. For electricity–generation scenarios 2 and 3, however, the ammonia–fueled vehicle becomes the most advantageous option, based on the normalized general indicator values.

The results from Table 1.9 (scenario 3) indicate that the electric vehicle is inferior to the hybrid one in terms of vehicle price, range and AP emissions. The simplest technical solution to increase its range is to produce electricity onboard the vehicle. Since the efficiency of electricity generation by means of an ICE is lower than that of a gas turbine unit (typically the efficiency of a thermodynamic cycle with fuel combustion at constant pressure is higher than that one at constant volume), it could make sense on thermodynamic grounds to incorporate a gas turbine engine into the electric vehicle. The application of fuel cell systems (especially solid oxide fuel cell stacks) within gas turbine cycles allows their efficiency to be increased to 60% [18].

The pressure of the natural gas required to attain a vehicle range equal to that of a hybrid vehicle is more than two times less than the pressure of hydrogen in the tank of the fuel cell vehicle. So, corresponding to the efficiency of electricity generation from natural gas ( $\eta = 0.4–0.6$ ), the required pressure in the tank of a hypothetical electric vehicle could decrease from 170 to 115 atm.

Assuming the cost and GHG and AP emissions corresponding to the hypothetical electric car production stage are equal to those for the electric prototype, the normalized indicators for the different onboard electricity–generation efficiencies can be determined



**Table 1.9** Normalized economic and environmental indicators for six vehicle types

Vehicle type	Scenario <sup>a</sup>	Normalized indicators					General indicator	Normalized general indicator
		Car cost	Range	Fuel cost	GHG emissions	AP emissions		
Conventional	1	1	0.581	0.307	0.098	0.126	0.00220	0.2090
Hybrid	1	0.733	1	0.528	0.105	0.204	0.00830	0.0550
Electric	1	0.212	0.177	1	0.610	1	0.02290	0.0200
Fuel cell	1	0.154	0.382	0.532	0.098	0.247	0.00076	0.6050
H <sub>2</sub> -ICE	1	0.255	0.322	0.110	0.122	0.42	0.00046	1
NH <sub>3</sub> -H <sub>2</sub> -ICE	1	0.382	0.462	0.140	1	0.44	0.01087	0.042
Conventional	2	1	0.581	0.307	0.098	0.283	0.00494	0.2085
Hybrid	2	0.733	1	0.528	0.105	0.459	0.01865	0.0552
Electric	2	0.216	0.177	1	0.194	0.649	0.00481	0.2141
Fuel cell	2	0.154	0.382	0.532	0.095	0.525	0.00156	0.6600
H <sub>2</sub> -ICE	2	0.255	0.322	0.110	0.122	0.94	0.00103	1
NH <sub>3</sub> -H <sub>2</sub> -ICE	2	0.382	0.462	0.140	1	1	0.02470	0.0420
Conventional	3	1	0.581	0.307	0.098	0.283	0.00494	0.0210
Hybrid	3	0.733	1	0.528	0.105	0.459	0.01865	0.0557
Electric	3	0.212	0.177	1	0.117	0.379	0.00166	0.6265
Fuel cell	3	0.154	0.382	0.532	0.092	0.497	0.00143	0.7273
H <sub>2</sub> -ICE	3	0.255	0.322	0.110	0.122	0.94	0.00104	1
NH <sub>3</sub> -H <sub>2</sub> -ICE	3	0.382	0.462	0.140	1	1	0.02471	0.0421

<sup>a</sup> Refers to scenario for electricity generation.

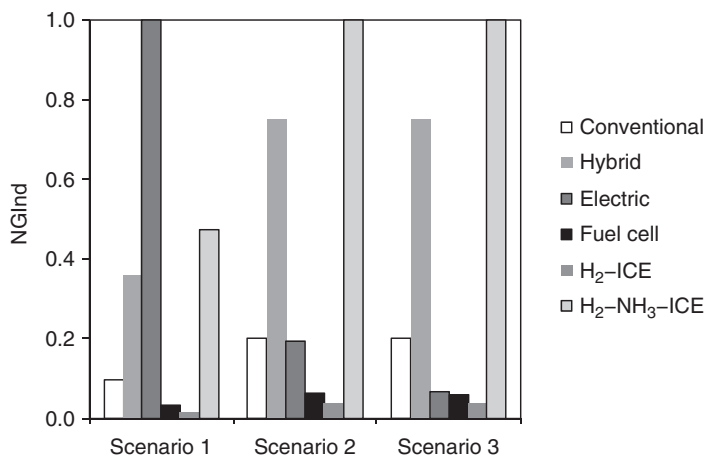


**Figure 1.2** Dependence of the normalized general indicator, NGInd, on electricity-generation scenario for four types of vehicles.

**Table 1.10** Normalized economic and environmental indicators for hybrid and hypothetical electric vehicles with different efficiencies for onboard electricity generation

Vehicle type	Onboard electricity generation efficiency ( $\eta$ )	Normalized indicators					General indicator
		Vehicle cost	Range	Fuel cost	GHG emissions	Air pollution emissions	
Hybrid	–	1	1	0.316	0.720	0.954	0.217
Electric	0.4	0.289	1	0.663	0.725	0.718	0.0997
Electric	0.5	0.289	1	0.831	0.867	0.863	0.180
Electric	0.6	0.289	1	1	1	1	0.289

(see Table 1.10). An optimization is needed to obtain the optimal relationship between capacities of batteries and the characteristics of a gas turbine engine.

The gas turbine engine has many advantages over the conventional ICE: the opportunity to use various kinds of liquid and gaseous fuels, quick starts at low air temperatures, high traction qualities, and simplicity of design. The main reason the implementation of gas turbine engines into light-duty vehicles in the 1960s failed was their poor ability to change fuel consumption with varying traffic conditions. Then, the gas turbine engine was considered for use in directly converting fuel energy into mechanical work to drive an automobile. The application of a gas turbine unit only to generate electricity permits this weakness to be overcome, when the gas turbine is integrated with a high-capacity battery and electric motor. The introduction

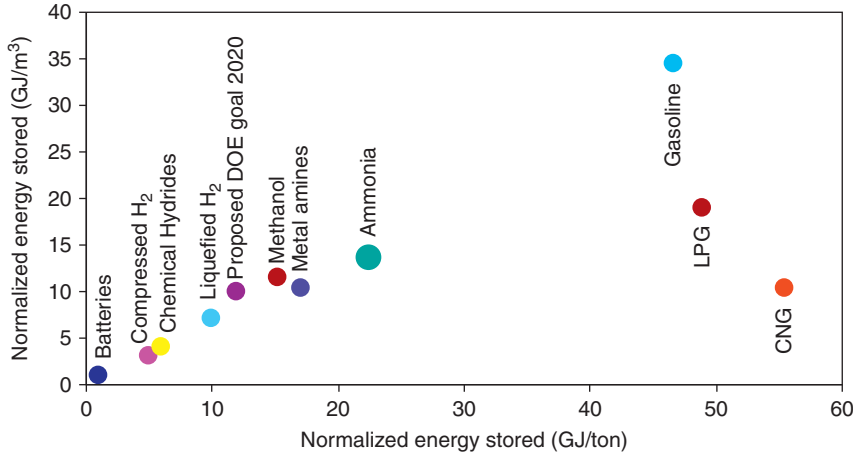


**Figure 1.3** Energy stored in the fuel tank per unit mass and per unit volume for various fuels.

of ion-conductive membranes and fuel cells into a gas turbine cycle can further increase the efficiency and decrease AP emissions [19].

It is informative to compare the energy stored in a fuel tank per unit fuel mass or fuel volume, for the fuels (energy carriers) considered here (gasoline, electricity, and hydrogen and ammonia). These results are shown in Fig. 1.3 and include, for comparative purposes, other fuels like methanol, liquefied petroleum gas, and compressed natural gas. Assuming reasonable efficiencies for the heat engine, a modified version of Fig. 1.3 is developed and shown in Fig. 1.4. This diagram illustrates the energy delivered at the shaft, which is the product of the energy stored in the fuel tank and the engine efficiency. For the hydrogen-from-ammonia case, as well as for the hydrogen-fueled

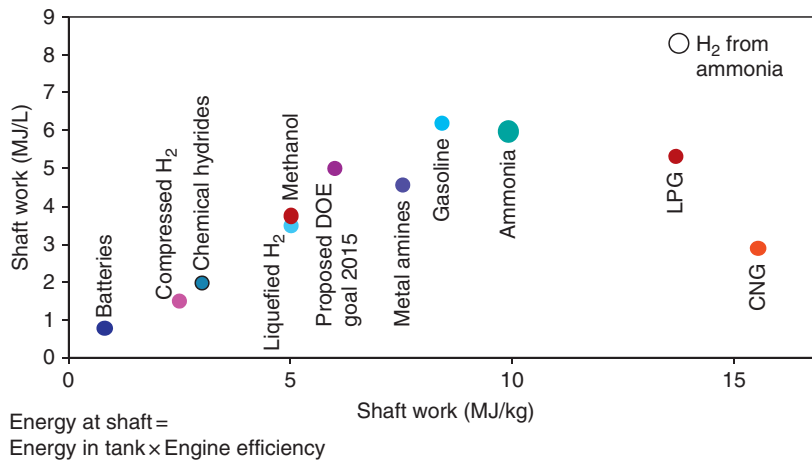


**Figure 1.4** Energy available at engine shaft per unit fuel volume and fuel mass for various fuels.

vehicles, we assume here a 50% efficiency. In fact, the hydrogen-from-ammonia vehicle considered operates with a hydrogen-fueled engine, so the efficiency of this engine and of the H<sub>2</sub>-ICE are equal. It can be observed from Fig. 1.4 that, if one generates hydrogen from ammonia onboard a vehicle, the energy retrieved at the engine shaft is superior to that of a conventional gasoline-fueled engine and to that of hydrogen-fueled systems. Thus, using ammonia as a hydrogen source appears to be an attractive option.



## 4. CONCLUSIONS

Using actual data, an economic and environmental comparison is performed of six types of vehicles: conventional, hybrid, electric, hydrogen fuel cell, H<sub>2</sub>-ICE, and ammonia-to-hydrogen. The analysis shows that the hybrid and electric cars have advantages over the others. The economics and environmental impact associated with use of an electric car depends significantly on the source of the electricity:

- If electricity is generated from renewable energy sources, the electric car is advantageous to the hybrid vehicle.
- If the electricity is generated from fossil fuels, the electric car remains competitive only if the electricity is generated onboard.
- If the electricity is generated with an efficiency of 50–60% by a gas turbine engine connected to a high-capacity battery and electric motor, the electric car is superior in many respects.
- For electricity-generation scenarios 2 and 3, using ammonia as a means to store hydrogen onboard a vehicle is the best option among those analyzed.

The implementation of fuel cells stacks and ion-conductive membranes into gas turbine cycles could permit the efficiency of electricity generation to be further increased and AP emissions to be further decreased. It is concluded, therefore, that the electric car with capability for onboard electricity generation represents a beneficial option and is worthy of further investigation, as part of efforts to develop energy efficient and ecologically benign vehicles.

The main limitations of this study are as follows: (i) the use of data which may be of limited accuracy in some instances; (ii) the subjectiveness of the indicators chosen; and (iii) the simplicity of the procedure used for developing the general indicator without using unique weighting coefficients. Despite these limitations, the study reflects relatively accurately and realistically the present situation and provides a general approach for assessing the combined technical–economical–environmental benefits of transportation options.

## ACKNOWLEDGEMENT

The authors acknowledge the support provided by the Natural Sciences and Engineering Research Council of Canada.

## NOMENCLATURE

AP	air pollution
GHG	greenhouse gas
Ind	indicator
LHV	lower heating value, MJ/kg
$m$	mass, kg
NGInd	normalized general indicator
NiMeH	nickel metal hydride
NInd	normalized indicator
PEMFC	proton exchange membrane fuel cell
VOC	volatile organic compound
$w$	weighting coefficient

## GREEK SYMBOLS

$\eta$	energy efficiency
--------	-------------------

## SUBSCRIPTS

bat	battery
car	car
m	mass
max	maximum
fc	fuel cell
$i, j$	indexes

## REFERENCES

1. M. Granovskii, I. Dincer, M.A. Rosen, J. Power Sources 159 (2006) 1186.
2. C. Zamfirescu, I. Dincer, J. Power Sources 185 (2008) 459.
3. C. Zamfirescu, I. Dincer, Fuel Process. Technol. 90 (2009) 729.
4. Atlantic Hydrogen. Hydrogen Fueled Vehicles can be Ordered Today. <http://www.atlantichydrogen.net/vehicles.html>, 2009 (accessed 10.10.09).
5. EIA. Annual Energy Outlook 2009, With Projections to 2030. Department of Energy/Energy Information Administration, Report 0383.
6. M. Granovskii, I. Dincer, M.A. Rosen, Int. J. Hydrogen Energy 31 (2006) 127.
7. P.L. Spath, M.K. Mann, Life Cycle Assessment of Hydrogen Production via Natural Gas Steam Reforming, Report NREL/TP-570-27637, 2001.
8. J.T. Houghton, L.G. Meira Filho, B.A. Callander, N. Harris, A. Kattenberg, K. Maskell (Eds.), Climate Change 1995: The Science of Climate Change, Cambridge University Press, New York, 1996.
9. Australian Greenhouse Office. Emissions Analysis of Alternative Fuels for Heavy Vehicles, Report EV45A/2/F3C, 2009.
10. S. Basrur, D. Pengelly, M. Campbell, R. Macfarlane, A. Li-Muller, Toronto Air Quality Index: Health Links Analysis, Report, Toronto Public Health, 2001.
11. DoE Fuel Economy. United States Department of Energy, Energy Efficiency, and Renewable Energy. <http://www.fueleconomy.gov>, 2009 (accessed 01.09.09).
12. M. Rantik, Life Cycle Assessment of Five Batteries for Electric Vehicles Under Different Charging Regimes, Report, KFB-Stockholm, 1999. <http://www.kfb.se/pdfer/M-99-28.pdf>, 2009 (accessed 10.10.09).
13. C. Handley, N. Brandon, R. Vorst, J. Power Sources 106 (2002) 344.

14. J.C. Sparrow, *Alternative Transportation Fuels: Issues and Developments*, Nova Science Publishers, New York, 2003.
15. M. Granovskii, I. Dincer, M.A. Rosen, *J. Power Sources* 157 (2006) 411.
16. M.F. Horddeski, *Alternative Fuels: The Future of Hydrogen*, CRC Press, Boca Raton, USA, 2007.
17. P. Meier, *Life Cycle Assessment of Electricity Generation Systems and Applications for Climate Change Policy Analysis*, Report No. UWFDM-1181, Fusion Technology Institute, 2002.
18. S. Chan, H. Ho, Y. Tian, *J. Power Sources* 109 (2002) 111.
19. M. Granovskii, I. Dincer, M.A. Rosen, *Chem. Eng. J.* 120 (2006) 193.



# Lifetime Cost of Battery, Fuel-Cell, and Plug-in Hybrid Electric Vehicles

Mark A. Delucchi<sup>\*1</sup> and Timothy E. Lipman<sup>\*\*</sup>

<sup>\*</sup>Institute of Transportation Studies, University of California at Davis, Davis, CA 95616, USA

<sup>\*\*</sup>Transportation Sustainability Research Center, University of California–Berkeley, 2614 Dwight Way, MC 1782, Berkeley, CA, 94720-1782, USA

## Contents

1. Introduction	20
2. Lifetime Cost of Battery-Electric Vehicles	22
2.1 Introduction	22
2.2 BEV concepts	23
2.3 BEV drivetrain costs	24
2.3.1 Batteries for BEVs	24
2.3.2 Electric motors and motor controllers for BEVs	26
2.3.3 Accessory systems for BEVs	26
2.4 Nonenergy operating and maintenance costs	27
2.5 Energy-use costs for BEVs	27
2.5.1 Energy use of BEVs	27
2.5.2 Cost of electric fuel	28
2.6 External costs of BEVs	28
2.7 Discussion of BEV cost estimates	29
3. Lifetime Cost of Plug-In Hybrid Electric Vehicles	31
3.1 Introduction	31
3.2 PHEV concepts	32
3.3 Component costs	32
3.3.1 Overview	32
3.3.2 Batteries	32
3.3.3 Electric motor and motor controller	35
3.3.4 Engine, exhaust system, and transmission	35
3.3.5 Accessory power	37
3.4 Nonenergy operating and maintenance costs	37
3.4.1 Overview	37
3.4.2 Maintenance and repair costs	37
3.4.3 Other nonenergy operating costs	39
3.5 Energy-use costs	39
3.5.1 Overview	39
3.5.2 Energy use of PHEVs	39
3.5.3 The price of electricity and the total annual electricity cost	42

<sup>1</sup> Corresponding author: [madelucchi@ucdavis.edu](mailto:madelucchi@ucdavis.edu)

3.6	External costs of PHEVs	42
3.7	Discussion of PHEV cost estimates	44
4.	Lifetime Cost of Fuel-Cell Electric Vehicles	45
4.1	Introduction	45
4.2	Component costs	45
4.2.1	Overview	45
4.2.2	Fuel-cell system	46
4.2.3	Hydrogen storage system	49
4.3	Nonenergy operating and maintenance costs	50
4.3.1	Maintenance and repair costs	50
4.3.2	Other nonenergy operating costs	53
4.4	Energy-use costs	53
4.4.1	Energy use of FCEVs	53
4.4.2	Cost of fuel	54
4.5	External costs of FCEVs	55
4.6	Discussion of FCEV cost estimates	56
5.	Discussion	57
	Acknowledgments	58
	References	58



## 1. INTRODUCTION

Concerns about climate change, urban air pollution, and dependence on unstable and expensive supplies of foreign oil have lead policy makers and researchers to investigate alternatives to conventional petroleum-fueled internal combustion engine vehicles (ICEVs) in transportation. Because vehicles that get some or all of their power from an electric drivetrain can have low or even zero emissions of greenhouse gases (GHGs) and urban air pollutants (see Lipman and Delucchi, this volume, for a review of the climate-change impacts of advanced electric vehicles (EVs)) and can consume little or no petroleum, there is considerable interest in developing and evaluating advanced EVs, including battery electric vehicles (BEVs), plug-in hybrid electric vehicles (PHEVs), and fuel-cell electric vehicles (FCEVs). However, although there are no technical barriers to developing EVs that perform as well as do petroleum ICEVs, it is not yet clear whether advanced EVs can be developed economically. No manufacturer is producing advanced EVs in large quantities, and the prices quoted for demonstration vehicles produced in small quantities tell us nothing about long-run manufacturing costs at high production volumes. Moreover, the manufacturing cost is not the only relevant cost metric: vehicles that have higher initial costs might have lower operating and maintenance costs and as a result might have lower total costs over their lifetime. And even if advanced EVs have higher lifetime *consumer* costs than do comparable ICEVs, they still might have lower lifetime *social* costs, on account of having lower “external” costs (which we will explain below).



To address these issues, in this chapter we review estimates of the full social lifetime cost of BEVs, PHEVs, and FCEVs. The full social lifetime cost of a vehicle comprises all of the initial and periodic costs of owning and operating a vehicle, including some nonmarket costs that are incurred by society as a whole (external costs). Because initial costs, such as the cost of the whole vehicle, and future periodic costs, such as the cost of fuel, are incurred at different times, and in cost–benefit analysis the *timing* of costs and benefits matters (because of the opportunity, cost of money, and for other reasons), initial costs and periodic costs must be put on the same temporal basis before they can be added together. This can be accomplished either by taking the *present value* (PV) of future costs and adding this PV to actual initial costs, or else by *amortizing* initial costs over the life of the vehicle or component and adding the amortized cost stream to actual periodic costs. These two approaches give the same results, because they are just different expressions of the same mathematical relationship between present and future costs.

Researchers typically distinguish between initial costs, such as the cost of the whole vehicle, and periodic costs, such as fuel and operating costs, because initial costs are an important part of the total lifetime cost but also because the initial cost of the vehicle is of interest in itself. The initial cost of an advanced EV typically is estimated by starting with the cost of a comparable gasoline ICEV and then subtracting the costs of components not used in the EV (e.g., an exhaust and emission control system) and adding the cost of extra or modified components in the EV. The extra or modified components in the EV can include a traction battery, an electric motor, a motor controller, a fuel cell, a hydrogen storage system, and a modified engine and transmission.

Operating and maintenance costs include energy, insurance, maintenance, repair, registration, tires, oil, safety- and emission-inspection fees, parking, and tolls. Because all of these costs except parking and tolls are related to vehicle cost, total vehicle weight, or vehicle power train characteristics, and EVs have a different cost, weight, and power train than do ICEVs, all types of EVs can have different operating and maintenance costs than do ICEVs. A comprehensive comparative lifetime cost analysis therefore should estimate all operating and maintenance costs except parking and tolls (and in fact, even the private cost of parking and tolls can be different for EVs, if public policy provides incentives for clean vehicles by subsidizing parking and toll costs). However, as we shall see, most EV lifetime cost studies conducted to date have considered only energy costs.

Initial costs and the operating and maintenance costs described above are explicit dollar costs that consumers pay in market transactions as part of the cost of owning and using a vehicle. They constitute what we will call the *private* or *consumer* lifetime cost. However, the production and use of motor vehicles also generates other impacts, such as those related to air pollution, that are not borne entirely by consumers in their market transactions related to vehicle ownership and use, but rather are borne diffusely by society as a whole. Economists call these impacts *externalities* because they are “external” to private decision making in market transactions. The estimated dollar value of an

externality is an *external cost*. Private costs plus external costs, with adjustments for noncosts transfers (see Section 4.6), constitute the *social* lifetime cost of the vehicle.

The production and use of motor vehicles and motor-vehicle infrastructure generates a wide range of externalities: air pollution, climate change, the macroeconomic impacts of dependence on unstable and expensive foreign oil, water pollution, noise, death and injury and destruction from crashes, delay from congestion, habitat destruction, and more. For a review of the external costs of transportation in the United States, see Ref [1]. The substitution of an electric drivetrain for an internal combustion engine (ICE) drivetrain can affect the external costs of motor-vehicle air pollution, climate change, oil dependence, noise, and water pollution (which, as noted above, is why EVs are being considered as alternatives to petroleum ICEVs.) Several studies, reviewed below, have included at least some of these external costs as part of an analysis of the social lifetime cost of advanced EVs.

In the following sections, we discuss component costs, nonenergy operating and maintenance costs, energy costs, and external costs, for BEVs, PHEVs, and FCEVs. We conclude each section and then the whole chapter with a general discussion of the estimates.



---

## 2. LIFETIME COST OF BATTERY-ELECTRIC VEHICLES

### 2.1 Introduction

Of the advanced EV types examined here, BEVs have the longest history. In fact, BEVs date back to the late 1800s. However, a modern series of vehicles was introduced by various automakers in the 1980s and 1990s. Along with the introduction of vehicles such as the General Motors EV-1, the Toyota RAV4-EV, and the Ford Ranger EV, a series of battery EV cost studies were conducted to examine the commercial prospects of these vehicles should they become further developed and reach higher volumes of production. These include several studies conducted by us (Lipman and Delucchi) that form the early basis for this assessment [2–5].

The introduction of BEVs in the 1990s was occurring as the California Air Resources Board (CARB) was looking to battery technology as the leading near term path to “zero-emission” vehicles (ZEVs). The term ZEV was used to describe vehicles that produced no *tailpipe* emissions of regulated pollutants, ignoring pollution from the power plants used to recharge EVs.

An important point with regard to the analysis of the potential manufacturing, retail, and lifetime costs of BEVs is that the critical issue of battery cost and performance has evolved greatly over the past 15 years and will continue to evolve for the foreseeable future. In the early 1990s, the dominant battery technology was lead-acid, with investigations into other chemistries such as sodium–sulfur and zinc–bromine. By the mid-1990s the nickel–metal hydride (NiMH) battery chemistry emerged as a more attractive

option for many EV applications owing to better energy density than lead-acid, but still with good power characteristics. At this point, lithium-ion (Li-ion) was only an emerging technology, with highly uncertain cost and performance characteristics and concerns about safety from battery flammability.

Moving forward to 2010, NiMH is still the main battery technology used in hybrid vehicles, but the next generation of PHEVs and BEVs is demanding the use of Li-ion technologies because of their superior performance and energy storage characteristics. What is clearer now than in the late 1990s with regard to Li-ion is that the technology can offer excellent performance but at what appears to be a relatively high cost (in \$/kWh) in the near term. How far and how quickly Li-ion battery prices can fall in higher volume production, while still assuring good battery durability, remains a critical question.

Thus, early studies of BEVs based on Li-ion batteries appear to be somewhat optimistic regarding those battery costs, based on what is now known, although we note that the “learned out” high-volume production cost of key Li-ion technologies is still unknown. Perhaps what was most unappreciated several years ago is that it is not only the costs of the Li-ion battery modules that are of issue, but also the costs of the rest of the battery management system (BMS), which is necessarily more intricate than for NiMH owing to the specific characteristics of Li-ion batteries that require special care (e.g., owing to their thermal characteristics and needs for voltage monitoring of groups of cells to ensure good performance). The life of Li-ion batteries also is quite important, because as mentioned in the introduction the cost per mile of the battery is a function of the cycle life (which translates into mileage life) as well as of the initial cost.

## 2.2 BEV concepts

BEVs are the simplest type of EV from a conceptual perspective, using electrical power from a single source—the electrochemical battery—to power one or more electric motors. Typically, a single electric motor is connected to the front axle through a simple one- or two-speed gearbox, but there are several other possible variations in the driveline architectures. One significant variation is to use a series of four “hub motors” attached to each wheel rather than a single drive motor.

Of course, the battery itself is composed of many cells that are composed into modules, which in turn are grouped into packs. This can be done various ways using series and parallel connections between groups of cells and/or modules. BEV electric motors typically operate at a few hundred volts, meaning that a minimum of about 100 cells is required (e.g., 100 Li-ion batteries with cell voltage of 3.6 V could produce 360 V if arranged in series). However some vehicles have many more but smaller cells, up to tens of thousands, configured in complex arrays with parallel and series connections. Also, in addition to the basic battery pack, a “balance of plant” of thermal management and voltage-monitoring systems is required to prevent overcharging and to detect earlier-than-expected cell degradation or failure.

The battery pack is typically the largest and most expensive component of the BEV, often by several-fold for longer-range vehicles. Especially since it is the sole power source, BEV applications require combined performance from the battery in producing both power (for acceleration) and energy (for sustained driving range). In practice, this means that battery engineers must strive to provide the best combination possible for the vehicle application they are targeting, within the limits of the battery chemistry they are using.

Finally, it is worth noting that one concept for BEVs is to have the battery pack itself be readily removable and “swappable.” This allows for extended driving range through the use of battery swap stations and an arrangement for consumers to lease rather than own their batteries. Systems have been demonstrated that can accomplish the battery swap very rapidly, in around 1 min for the battery pack swap itself and a few minutes for the complete operation [6]. While somewhat complex to administer, this type of service could help to reduce the key issue of limited range coupled with long recharge time for BEVs.

## 2.3 BEV drivetrain costs

The costs of manufacturing BEVs versus conventional vehicles can be estimated through a series of “parts replacement” exercises, where the components not needed in the BEV are “stripped out” and the replacement components needed for the EV are added in. This method has been widely used, and is generally appropriate for BEVs that are built along those lines—for example, on a conventional vehicle chassis “platform” that is adapted for use for the EV. Alternately, one may consider the concept of a much lighter weight design, to reduce the costs of the EV drivetrain components. This is a strategy widely advocated by some industry analysts; for example, see reference [7]. Clearly, this basic vehicle design choice has major implications for BEV driveline costs, as smaller and cheaper drivetrain components can be traded off with the costs of producing lighter (but typically more expensive) vehicle chassis based on high-strength steel, aluminum, and/or carbon fiber composite materials.

In a series of studies in the late 1990s we reviewed and analyzed the costs of complete EVs as well as their drivetrains and key components [2–5]. Subsequent to these studies, noteworthy efforts in the 2000s included those by university and other research groups [8–10]. The results of these more recent EV driveline cost analysis efforts are summarized in Table 2.1.

### 2.3.1 Batteries for BEVs

The costs of batteries for BEVs were the subject of many cost studies in the 1990s, including two by us [1, 3]. We add to those previous reviews here and in Section 3.3.2.

Kromer and Heywood [8] consider two sets of battery assumptions for a 200-mile range BEV: (1) 150 Wh/kg and \$250/kWh and (2) a much more optimistic case of

**Table 2.1** Summary of published estimates of BEV costs

Cost study	Total or incremental retail price of BEV or driveline <sup>a</sup>					
Kromer and Heywood (2007) [8] BEV with 200-mile range	<i>Base case</i> \$10,200 incremental BEV price			<i>Optimistic case</i> \$6,900 incremental BEV price		
Thomas (2009b) [17] BEV with 320/480-km (200/300-mile) range (200-mile cost based on MIT estimates shown above)	<i>320-km (200-mile) range</i> \$10,200 incremental BEV price			<i>480-km (300-mile) range</i> \$12,119 incremental BEV price		
Delucchi and Lipman (2001) <sup>b</sup> [2]	<i>Total BEV retail price estimates by assumed driving range (year 2000 US\$)</i>					
Mid-sized BEV (lead-acid battery)	<i>50 miles</i> \$23,363	<i>65 miles</i> \$24,553	<i>80 miles</i> \$25,918	<i>95 miles</i> \$27,510	<i>110 miles</i> \$29,422	<i>125 miles</i> \$31,814
Mid-sized BEV (NiMH battery)	<i>65 miles</i> \$25,984	<i>90 miles</i> \$28,034	<i>115 miles</i> \$30,261	<i>140 miles</i> \$32,834	<i>165 miles</i> \$35,759	<i>190 miles</i> \$39,223
Mid-sized BEV (Li-ion battery)	<i>100 miles</i> \$26,135	<i>140 miles</i> \$27,678	<i>180 miles</i> \$29,174	<i>220 miles</i> \$30,791	<i>260 miles</i> \$32,448	<i>300 miles</i> \$34,268
Argonne National Lab (Vyas et al., 1998) [18]	<i>Total BEV retail price estimates by year and BEV production volume</i>					
Subcompact BEV Minivan BEV	<i>2000 (&lt;10K/year)</i> \$18,500–41,400 \$27,300–63,500	<i>2005 (10–40K/year)</i> \$18,300–35,900 \$27,100–53,900	<i>2010 (&gt;40K/year)</i> \$17,800–32,900 \$26,300–49,400	<i>2020 (&gt;40K/year)</i> \$17,700–30,300 \$26,000–44,100		
Eaves and Eaves (2004) [9] EV driveline cost	\$19,951 (complete EV driveline)					
Offer et al. (2010) [10] BEV driveline cost (25 kWh battery) ICE comparison driveline cost Difference (extra price for BEV driveline)	<i>2010</i> \$26,700 \$2,200 \$24,500			<i>2030, low/high/average</i> \$6,200/\$9,530/\$7,865 \$2,400/\$2,530/\$2,465 \$3,800/\$7,000/\$5,400		

<sup>a</sup>Note that in some cases the figures refer to full retail prices of BEVs, while in other cases the figures refer to total incremental costs, relative to comparable conventional vehicles. The Eaves and Eaves (2004) [9] figure is for the total cost of the EV driveline – no comparison to a conventional vehicle is offered.

<sup>b</sup>High-volume production in all cases. Conventional vehicle comparison price is \$20,085.

300 Wh/kg and \$200/kWh. In the first case (their base case) the battery cost for the 200-mile range BEV is \$12,000 and in the optimistic case it is \$8,400 (for batteries of 48 and 42 kWh, respectively, owing to the smaller and lighter vehicle and battery possible with the better battery energy density).

Eaves and Eaves [9] arrive at a Li-ion battery cost of \$16,125 for a BEV that has a 64.5 kWh battery pack that makes it capable of a 300-mile (500 km) range (thus assuming a battery specific energy of 143 Wh/kg). This is derived from a \$250/kWh estimate for high-volume production of Li-ion batteries in a previous national lab study.

Offer et al. [10] consider a much smaller BEV battery pack of 25 kWh as “the lower limit considered acceptable for an electric vehicle.” They estimate a current cost of \$25,000 (or \$1,000/kWh), with year 2030 “optimistic,” “pessimistic,” and “average” estimates of \$5,000, \$7,500, and \$6,250, respectively (translating to \$200/kWh, \$300/kWh, and \$250/kWh).

One difficulty with some of these studies of battery costs for vehicles is the need to consider the BMS or more generally the “balance of plant” needed to support the use of the battery in the vehicle. This is especially important in the case of Li-ion batteries, which have significant needs for cooling and are sensitive to overcharging. The BMS is a significant cost item for advanced batteries, acting as the integration component for the battery and vehicle systems, but some studies are not explicit about the extent to which they include the costs of the BMS as well as the battery pack itself.

### **2.3.2 Electric motors and motor controllers for BEVs**

The electric motor and motor controller propulsion systems comprise the other key set of components for BEVs, along with the battery power system. The motor controller in particular has evolved in recent years with the use of insulated gate bipolar transistors (IGBTs) as high-power switching devices in place of the previously used MOSFETs (metal-oxide-semiconductor field-effect transistors). Along with better integration of other components and reduced parts counts, motor controllers have improved in performance and decreased in cost and complexity over the past few decades. Meanwhile, electric motors have also improved in terms of their torque and power density and energy efficiency characteristics. See Subsection 3.3.3 and Lipman [5] for more discussion of these electric motor and controller costs.

### **2.3.3 Accessory systems for BEVs**

BEVs require battery chargers that can be included onboard the vehicle or even integrated into the motor controller unit. There has been previous experience with both conductive and inductive charging systems, but a new standard has emerged based on the SAE J1772 standard and a plug design pioneered by the Yazaki Group. This standard allows up to what has come to be defined as “Level 2” charging at power levels of up to 16.8 kW (120–240 V AC power at up to 70 A). Along with these charging

standards, an active area of research and industry interest is the interface between the charging system, and when and how it is operated, and the local utility grid. For details on these BEV charging and utility grid issues, see this recent review [11].

Also the presence of a fuel-fired heater can have a significant impact on vehicle energy use, and to some extent cost as well. For example, for use in colder climates the 1997/1998 General Motors S-10 Electric pickup truck had the option of a fuel-fired heater, using diesel fuel stored in a 1.7-gallon tank [12]. The off-board charger (if any) and potential addition of a fuel-fired heater are the main accessory issues for BEVs compared to regular vehicles.

## 2.4 Nonenergy operating and maintenance costs

In addition to costs of electric fuel, discussed below, BEVs typically offer the advantage of lower maintenance costs compared with conventional vehicles. There are many fewer moving parts in BEVs, the electric motors are essentially maintenance free, and there is no need for periodic oil changes. There are needs for periodic battery pack inspections, but overall maintenance costs for BEVs are expected to be relatively low. For example, we have previously estimated that the annual maintenance costs for BEVs could be about 28% lower than for conventional gasoline vehicles on an annualized basis [2]. By contrast, MIT's *On the Road in 2020* study [13] assumes that maintenance costs for BEVs are the same as for gasoline ICEVs.

## 2.5 Energy-use costs for BEVs

The following sections describe the energy use of BEVs, and the costs associated with the electric fuel that they consume. Unlike PHEVs, which use a somewhat complex combination of electricity and another fuel, or FCEVs, which use hydrogen with uncertain costs in a consumer setting, the costs of refueling BEVs are relatively more straightforward and well-understood.

### 2.5.1 Energy use of BEVs

The energy use of BEVs is relatively straightforward to estimate, particularly in the absence of auxiliary fuel-fired heaters that have been proposed for colder climates as alternatives to electric heaters. Since the amount of waste heat produced from the resistance of the BEV battery system and electric motor controller is much lower than from conventional vehicles, auxiliary cabin heating can be an issue.

Energy use of BEVs is typically expressed in watt-hours per mile or kilometer (Wh/mile or Wh/km), and can be defined and measured at the battery pack terminals or the "wall plug." This value typically ranges from about 200 Wh/mile (124 Wh/km) for small EVs to up to 400 Wh/mile (249 Wh/km) for larger vehicles. For example, the extensively tested Toyota RAV4 "small SUV" type of EV has an energy-use value (measured at the battery terminals) of 301 Wh/mile or 187 Wh/km. This energy use rate



is based on reported energy use of 270 Wh/mi (168 Wh/km) city and 340 Wh/mi (211 Wh/km) highway [14] and assuming the “55/45” city/highway mileage split established for U.S. government certification purposes.

As BEV technology slowly improves in the future, vehicle energy use should also be somewhat reduced (assuming vehicle performance remains relatively constant). This could be the result of improved motors and motor controllers, improved batteries with lower internal resistance characteristics, better integration of components, and lower auxiliary system losses. In an overall sense, however, vehicle size and weight and level of performance are the key determinants of overall energy use, as is the case for conventional vehicles.

### **2.5.2 Cost of electric fuel**

Electricity for BEVs is generally less costly than other fuels including gasoline. Many utilities now offer special “time of use” (TOU) rates for EV owners that can be used in conjunction with separate utility meters to charge for the electricity used for EV charging. Since BEVs can typically be recharged at night when power is typically cheaper, they benefit from these TOU rates. Furthermore, separate metering allows BEV owners to prevent their electricity usage from accruing to their regular household electrical bill, which in many regions has a tiered structure that penalizes high rates of usage.

For a recent review of the electricity costs associated with BEV charging in various regions of the United States, including utility regions where TOU rates are available, see Lidicker et al. [15]. The study examines three different gasoline price periods in comparing the costs of fueling BEVs and conventional vehicles, and finds that depending on region and price period (during 2008–2009 when prices were highly variable), BEVs can cost consumers from a few hundred to a few thousand dollars per year less than conventional vehicles to fuel. The savings associated with charging off-peak versus on-peak is found to be relatively modest, however, on the order of \$1.00–\$2.00/day. This suggests that to avoid on-peak charging, consumers may need stronger “price signals” than are typically available—an issue that could become important with significant levels of BEV market penetration.

## **2.6 External costs of BEVs**

The external costs of BEVs differ from those of conventional vehicles in that air pollutants are produced in different places and in different types and amounts, and there are reduced externalities associated with oil use, GHG emissions, and vehicle noise. In previous work [2], we have estimated the difference in external costs between BEVs and conventional vehicles to be in the range of 0.4–3.7 cents per mile, with a best estimate of 1.1 cents per mile (in year 2000 US\$). These external cost differences between BEVs and conventional vehicles are primarily in the form of air pollution



and oil-use related externalities, with climate change and noise being smaller factors [2]. See also the discussion in Section 4.5 of Thomas [16], who estimates air pollution, climate change, and oil-dependence external costs of ICEVs, BEVs, PHEVs, and FCEVs.

## 2.7 Discussion of BEV cost estimates

Along with the earlier “generation 1” cost studies conducted in the 1990s, a few additional BEV cost studies have been performed more recently in the 2000s, and these are also reviewed here. For an earlier review and presentation of modeling results focusing on the details of the cost studies conducted in the early 1990s, see our previous work [2, 3].

The BEV cost studies conducted thus far, by academic groups, government research laboratories, and consulting firms, have generally concluded that the incremental retail purchase prices of BEVs were at least a few and up to tens of thousands of dollars more than those of conventional vehicles. However, it is important to note that studies that have considered vehicle costs on a lifetime basis have often shown that the additional purchase costs of BEVs can potentially be recouped through reduced fuel and other operational costs over time. Key factors in that regard are not only the relative vehicle costs, but also the relative costs of electricity and gasoline for consumers in particular settings.

Tables 2.1 and 2.2 present the initial cost and lifetime cost estimates from studies performed by government agencies, coalitions, and research organizations from the mid-1990s through the present. As shown in Table 2.1, all studies conclude that BEV manufacturing costs and retail prices will be higher than conventional vehicle costs in the near-term, but a few studies suggest that BEV costs could relatively quickly drop to levels comparable to those of conventional vehicles, particularly on a lifetime basis.

The differences in the results of the studies summarized in Table 2.1 can be explained partly by variations in assumptions regarding the types of vehicles analyzed, the assumed volume of vehicle production, the range and energy efficiency of the analyzed vehicle, the life and cost of the battery, and the costs of accessories and additional equipment needed for the BEV. This additional equipment includes battery chargers, vehicle heating and cooling systems, and electrical power steering units. Key characteristics in this regard are called out in the table, but we refer readers to the original studies for additional details, with regard to key assumptions and the relative level of the full range of BEV drivetrain components that are included.

Overall, BEV costs are estimated to be from ten thousand dollars or more (US\$10,000+) in the near-term than the comparable ICE vehicles to which they are compared, falling to a projected several thousand dollars (US\$3,500–US\$12,000) in the future in high-volume production in some studies (and depending on the size and type of battery pack assumed). See the results in Table 2.1 for details. Note that there is

**Table 2.2** Summary of published estimates of BEV lifetime cost

Cost study	Lifetime cost (levelized cost per mile or total lifetime incremental cost)					
Delucchi and Lipman (2001) <sup>a</sup> [2]	<i>Levelized cost per mile estimates by assumed driving range (year 2000 \$ per mile)</i>					
Mid-sized BEV (lead-acid battery)	<i>50 miles</i> \$0.45	<i>65 miles</i> \$0.46	<i>80 miles</i> \$0.46	<i>95 miles</i> \$0.49	<i>110 miles</i> \$0.53	<i>125 miles</i> \$0.58
Mid-sized BEV (NiMH battery)	<i>65 miles</i> \$0.52	<i>90 miles</i> \$0.53	<i>115 miles</i> \$0.55	<i>140 miles</i> \$0.60	<i>165 miles</i> \$0.66	<i>190 miles</i> \$0.73
Mid-sized BEV (Li-ion battery)	<i>100 miles</i> \$0.44	<i>140 miles</i> \$0.46	<i>180 miles</i> \$0.48	<i>220 miles</i> \$0.51	<i>260 miles</i> \$0.54	<i>300 miles</i> \$0.57
Argonne National Lab (Vyas et al., 1998) [18]	<i>Levelized cost per mile estimates by year and BEV production volume (\$ per mile)</i>					
Subcompact BEV Minivan BEV	<i>2000 (&lt;10K/year)</i> \$0.30-0.72 \$0.44-1.08	<i>2005 (10-40K/year)</i> \$0.27-0.60 \$0.39-0.89	<i>2010 (&gt;40K/year)</i> \$0.25-0.48 \$0.37-0.72	<i>2020 (&gt;40K/year)</i> \$0.24-0.42 \$0.33-0.60		
NYSERDA (Booz-Allen and Hamilton, 1995) [19]	<i>Levelized cost per mile estimates by year and BEV production volume (\$ per mile)</i>					
Compact BEV	<i>1998 (40K/year)</i> \$0.36	<i>2000 (41K/year)</i> \$0.33	<i>2002 (107K/year)</i> \$0.27	<i>2004 (243K/year)</i> \$0.24		
IEA/OECD [20]	<i>Total lifetime incremental cost or (savings) vs. gasoline by near-term/long-term and price of oil<sup>b</sup></i>					
	<i>Near term</i>			<i>Long term</i>		
BEV (150 km range) BEV (200 km range)	<i>(US \$60/barrel oil)</i> \$16,000 \$22,000	<i>(US \$120/barrel oil)</i> \$10,000 \$17,000	<i>(US \$60/barrel oil)</i> \$4,500 \$8,000	<i>(US \$120/barrel oil)</i> (\$1,000) \$2,000		

considerable variation in the results of the studies, showing the wide range of possible variation depending on the type and size of battery included, the manufacturing production volume of the vehicles, and the timeframe considered (where potential “learning curve” improvements can be considered for the future).

Some studies estimate the vehicle lifetime cost, which includes the costs of operating and maintaining the vehicles as well as purchasing them (Table 2.2). As shown in Table 2.2, BEV lifetime costs are typically somewhat higher than for conventional vehicles but the results depend significantly on the gasoline price and (to a lesser extent) the electricity prices assumed. As discussed above, the addition of social costs adds more to the overall costs of conventional vehicles than for BEVs, owing to the lower emissions, oil-use, and noise from BEVs, by perhaps 1 cent per mile (as a central estimate within a range of about 0.5–4 cents per mile) on a vehicle lifetime cost basis [2].



### 3. LIFETIME COST OF PLUG-IN HYBRID ELECTRIC VEHICLES

#### 3.1 Introduction

PHEVs have attracted the interest of researchers and policy makers because they can reduce consumption of petroleum [21], emissions of GHGs, and emissions of urban air pollutants [22]. PHEVs are likely to cost more than conventional ICE gasoline vehicles, primarily because of the relatively high cost of batteries, but also may have lower energy-use costs. In this section we analyze the lifetime cost of PHEVs, focusing on detailed original research published over the last 10 years.<sup>1</sup>

The lifetime cost of a PHEV includes amortized initial costs and operating costs. The initial cost of a PHEV typically is estimated with respect to the initial cost of a gasoline ICEV, by adding the cost of the additional components in a PHEV (e.g., battery, motor, controller, transmission, and small engine) and subtracting the cost of gasoline ICEV components not used in a PHEV (e.g., a large engine and exhaust system). Operating costs include energy, maintenance and repair, and insurance costs. Most studies estimate only the cost of major PHEV components and the cost of energy.

We begin with an overview of basic PHEV concepts. We then examine estimates of component costs, non-energy operation and maintenance costs, and energy costs. In the discussion of energy costs, we review simulations of the power train energy use of PHEVs. We conclude with a discussion of the strengths and weaknesses of current PHEV cost estimates and highlight some directions for future research. In this PHEV section, we express all costs in year 2009 dollars unless noted otherwise.

<sup>1</sup> We do not consider simple calculations, such as those of Scott et al. [23] and Silva et al. [24] in which an assumed price premium for PHEVs (\$1,000–\$10,000 per car in Ref. [23] and \$4,000–\$10,000 in Ref. [24]) is compared with the reduced energy costs (based on gasoline at \$2.50–\$3.50/gallon and electricity at \$0.12/kWh in Ref.[23], and gasoline at 0.54–1.35 /l and electricity at 0.057–\$0.104 euros/kWh in [24]), at an assumed discount rate (8% in [24]).

## 3.2 PHEV concepts

Two important differences separate a PHEV from a non-plug-in hybrid electric vehicle (HEV). PHEVs have (1) a larger battery and (2) the ability to recharge the battery from the electricity grid. A PHEV can operate in two different modes depending on the state of charge (SOC) of the battery. The first is *charge-depleting* (CD) mode, during which the battery discharges from its beginning state (e.g., 100% charged). We describe PHEVs by their CD range, which we express as PHEV-X, where X is the number of km a PHEV can be driven in CD mode. For example, PHEV-32 specifies that the plug-in hybrid has a range of 32 km (20 miles). After reaching the end of its CD range, a PHEV will switch to *charge-sustaining* (CS) mode, during which the PHEV operates much like an HEV, using regenerative braking and power from the engine to keep the average SOC constant. The switch to CS operation is triggered by the battery reaching a specified SOC (e.g., 30%).

The control strategy and vehicle design determine whether the PHEV's CD mode of operation is all-electric or blended. *All-electric* means that the vehicle operates on only the electric motor for the specified CD range. In this case, the CD range is often referred to as the all-electric range (AER). If the CD mode is *blended*, the electric motor and ICE are both used to power the vehicle. In general, an all-electric PHEV will require a larger electric motor and battery than a blended PHEV. We discuss this more in Section 3.5.2.

## 3.3 Component costs

### 3.3.1 Overview

PHEVs have several components that conventional ICEVs do not have: a large traction battery, an electric motor, and a motor controller. The engine, transmission, and emission control and exhaust system in a PHEV are different from those in an ICEV, and the climate control system also might be different. In the following sections, we review estimates of the costs of the components that are different in PHEVs. In some cases we express component costs relative to the total “incremental” cost of a PHEV, which is the difference between the total initial cost of a complete PHEV and the total initial cost of a complete gasoline ICEV.

### 3.3.2 Batteries

All cost studies reviewed here estimate that the battery pack is the most expensive component of a PHEV. A battery pack comprises individual modules, an enclosure for the modules, management systems, terminals and connectors, and any other pertinent auxiliaries. The studies shown in Table 2.3 find that the battery pack cost is 50–87% of the estimated incremental cost of the PHEV at high-volume production.

The earliest study in our review, published by the Electric Power Research Institute (EPRI) [25], is one of the most comprehensive. Graham et al. [25] used CARB's Battery Technical Advisory Panel (BTAP) report [27] to estimate the cost of NiMH batteries produced at 100,000 or more units per year. The BTAP report estimated that the lowest probable specific cost for batteries in BEVs is \$250/kWh. To calculate the specific cost of

**Table 2.3** Battery pack cost versus total incremental cost for mid-sized PHEVs

Study	Cost year	Battery type	CD range (km)	Total incremental PHEV cost (\$)	Battery power/energy ratio (1/h)	Battery module specific cost (\$/kWh)	Battery pack cost (\$) (% of total incremental cost)
Kromer and Heywood (2007) [8]	2007	Li-ion	16	3,000	13.5	420	1,500 (50)
			48	4,300	5.5	320	2,800 (65)
			96	6,100	2.9	270	4,800 (79)
EPRI 2001 (Graham et al., 2001) [25]	2000	NiMH	32	3,278	9.1	320	2,638 (80)
			96	6,866	5.5	270	5,757 (84)
Simpson (2006) [26]	2006	Li-ion	32	4,836	4.9	265	3,966 (82)
			96	7,605	2.6	241	6,650 (87)

the PHEV battery, Graham et al. [25] multiplied the BTAP battery cost estimate by the ratio of the specific energy of the PHEV battery to the specific energy of the EV battery. This method assumes that materials costs are the largest influence on the cost of the battery module and that the material cost of the battery is inversely proportional to the specific energy of the battery for a given storage capacity.

EPRi also published a report in 2004 that deals primarily with advanced batteries for various EVs, including PHEVs [28]. Duvall et al. [28]. used an updated version of the year 2000 CARB's life cycle cost model, with new assumptions about other major component costs, but used the assumptions of Graham et al. [25] for NiMH battery cost.

Simpson [26] used the vehicle-energy-use simulator ADVISOR to model several PHEV designs with various CD ranges, and then estimated the cost of both Li-ion and NiMH batteries at the module and pack level for each PHEV design. He used battery-cost curves developed in the 2001 EPRi [25] report to estimate module and pack costs, as follows:

$$\text{Battery module cost (long-term)} : \$/\text{kWh} = 11.1 \times P/E + 211.1$$

where  $P/E$  = power/energy ratio.

$$\text{Battery pack cost} : \$ = (\$/\text{kWh} + 13) \times \text{kWh} + 680$$

Simpson assumed that NiMH batteries would be used in near-term PHEVs (2005–2010) and that Li-ion batteries would be available for use in the longer term (2015–2020). On the basis of interviews with battery suppliers and other experts, he estimated that NiMH batteries for near-term PHEVs would be twice as expensive as Li-ion batteries for long-term PHEVs.

Kromer and Heywood [8] based their estimates of future Li-ion battery costs on previous studies, such as Refs. [27] and [29]. Consistent with the BTAP report [27], they assumed that material costs for batteries are 50% of the total cost, that materials costs decrease by 2.5%/year, that manufacturing costs and profit margin remain constant over time, and that the present cost of high-energy batteries is \$300/kWh. They estimate costs for production volumes above 100,000 units/year.

Table 2.3 presents the specific cost estimates in the studies reviewed above. All of the studies cited estimate the specific cost of the battery module as a function of the power-to-energy ratio. The power-to-energy ratio and the specific cost decrease as the CD range increases because the battery will require the same peak power to meet the requirements of the drive cycle used to design the PHEV, regardless of the CD range.

The lifetime cost per mile of the battery is a function of the initial cost of the battery, the cycle life of the battery, and the salvage value of the battery at the end of its life. Both EPRi studies in Table 2.3 suggest that the battery in a PHEV may have a nonzero salvage value at the end of its useful life in the vehicle. The 2001 EPRi report [25] uses a salvage value of \$100/kWh, assuming that the battery is replaced when its capacity has

been reduced to 80% of its original capacity. The 2004 EPRI report [28] takes a more conservative approach and estimates the salvage value of the battery by multiplying the projected new module cost at the time of replacement by the percentage of battery life remaining. This assumes that the battery has another useful application after being used in a PHEV and that the value is proportional to the remaining battery life. For a PHEV-32, the 2004 EPRI report [28] estimates a salvage value of about \$15/kWh.

### **3.3.3 Electric motor and motor controller**

The electric motor provides motive power to the axle, and the motor controller varies the torque and speed of the electric motor as needed. The cost of these components can be a significant proportion of the total incremental cost of a PHEV.

The 2001 EPRI report [25] modeled PHEVs with a DC brushless permanent magnet motor, because this type of motor is smaller, less complex, and typically more efficient than an induction motor and is easier to control than an AC motor. The authors estimated the cost of the motor on the basis of several studies of traction motor costs [5, 30, 31] and came up with the cost formula of  $\$13.70/\text{kW} + \$190$ , which equates to about  $\$16/\text{kW}$  for the motor sizes considered in their study. Based on a review of previous cost estimates, Graham et al. [25] projected the cost of a PHEV motor controller to be equal to  $\$7/\text{kW} + \$165$ .

The 2004 EPRI report [28] estimated the cost of a brushless permanent magnet motor to be about  $\$16/\text{kW}$ , but suggested that with high production volumes of these motors and other devices that use permanent magnets the cost could drop to  $\$10.50/\text{kW}$ . The study estimated that motor controllers for PHEVs will cost around  $\$10/\text{kW}$ , assuming that the IGBTs used in the controllers will also be used in fuel cell and distributed power systems and therefore will be produced in relatively high volumes.

On the basis of a 2005 National Research Council (NRC) report on FreedomCAR [32] and a 2002 report by Energy and Environmental Analysis, Inc. [33] on the cost and performance of conventional vehicles and hybrids, Kromer and Heywood [8] estimated the cost of the PHEV motor and controller in 2030 to be  $\$15/\text{kW} + \$200$  (2007 \$). Table 2.4 summarizes estimates of the cost of electric motors and controllers in PHEV cost studies. See Lipman and Delucchi [34, 35] for a detailed analysis of the cost of electric motors and controllers for HEVs.

### **3.3.4 Engine, exhaust system, and transmission**

The engine and exhaust system are likely to be smaller for a PHEV than for an ICEV because the electric power train shares the burden of propulsion. The 2001 EPRI report [25] estimated engine costs using a set of curves developed at General Motors that show base-engine cost versus engine power in kilowatt. For a 4-cylinder engine, the base-engine cost function was approximately  $\$11/\text{kW} + \$400$ . EPRI estimated that the total engine cost, including a thermal management system at  $\$0.236/\text{kW}$  of peak engine

**Table 2.4** OEM cost estimates for mid-sized car PHEV components (2008 \$, converted from original dollar basis by the PPI)

Author	CD range (km) and control strategy <sup>a</sup>	Motor and controller (\$)	Engine (\$)	Transmission (\$)	Exhaust system (\$)
Simpson (2006) [26]	16 B	1,170	1,855	NR	NR
Kromer and Heywood (2007) [8]	16, 48, 96 B	803	3,715 <sup>b</sup>	w/engine	301
EPRI 2001 (Graham et al., 2001) [25]	32 AE	1,933	1,469	785	251
Simpson (2006) <sup>c</sup> [26]	32 B	1,503	1,887	NR	NR
Burke (2007) [36]	32 B	1,099	1,500	NR	NR
Simpson (2006) <sup>c</sup> [26]	96 B	1,575	1,937	NR	NR
EPRI 2001 (Graham et al., 2001) [25]	96 AE	3,154	1,116	785	188

NR = not reported, OEM = original equipment manufacturer.

<sup>a</sup> AE = all-electric, B = blended.

<sup>b</sup> Kromer and Heywood [8] reported engine and transmission cost as one value.

<sup>c</sup> Engine, battery, and motor cost calculated from equations given in Simpson's study [26].

power, was \$2,107 for the ICEV, \$1,170 for a PHEV-32, and \$889 for the PHEV-96 (in 2000 \$) [25].

The 2001 EPRI report [25] also calculated the cost of the exhaust system (including the catalytic converter) based on the engine size. For the ICEV, the exhaust system costs \$250; for the PHEV-32, the exhaust system costs \$200; and for the PHEV-96, the exhaust system costs \$150 (in 2000 \$) [25].

Simpson [26] used the aforementioned engine-cost equations in EPRI 2001 to calculate an engine cost of \$2,300 for the ICEV, \$1,706 for a PHEV-32, and \$1,749 for a PHEV-96 (in 2006 \$).

In their 2001 report, EPRI assumed that PHEVs would have a continuously variable transmission (CVT) rather than an automatic transmission with discrete gearing ratios because of the lower cost and performance advantage of the CVT [25]. EPRI estimated that the CVT in a PHEV-32 and a PHEV-96 would cost \$625 (in 2000 \$), which is about 60% of the cost of an automatic transmission from a model year 2000 Chevrolet Lumina. Table 2.4 summarizes the estimates of the cost of the electric motor and controller, engine, transmission, and exhaust system.

EPRI's estimates of the cost of the electric motor are significantly higher than the estimates from the other studies, but its estimate of the engine cost is lower. This



difference stems from EPRI's choice of a PHEV with an AER, which demands a larger electric motor to meet the peak power demand without engaging the correspondingly smaller engine.

### **3.3.5 Accessory power**

EPRI's 2001 report estimated that, in a PHEV, a power steering pump, an air-conditioning compressor and condenser, and an accessory power module to run lighting and other electrical loads would cost a total of \$300 (in 2000 \$) [25]. The 2004 EPRI report [28] assumed the same cost. For comparison, in an ICEV, a power steering pump, an air-conditioning compressor and condenser, and a generator/alternator were estimated to cost a total of \$210.

## **3.4 Nonenergy operating and maintenance costs**

### **3.4.1 Overview**

As discussed in the introduction to this chapter, operating and maintenance costs include energy (which we consider in a separate subsection), insurance, maintenance, repair, registration, tires, oil, safety- and emission-inspection fees, parking, and tolls. Most of these are likely to be different for PHEVs than for gasoline ICEVs. However, PHEV lifetime cost studies conducted to date generally have considered only energy costs and, in some instances, maintenance and repair costs.

### **3.4.2 Maintenance and repair costs**

Table 2.5 summarizes estimates of PHEV maintenance costs from the EPRI 2001 and 2004 studies [25, 28] and estimates of HEV (not PHEV) maintenance costs from Lipman and Delucchi [35] and a cost calculator of the U.S. Department of Energy (DOE) [37].

Both of the EPRI studies report that PHEV maintenance costs, including parts and labor, are likely to be lower than those for ICEV [25, 28], in part because in a PHEV the engine shares the propulsion load with the electric drivetrain and hence is likely to have less wear than the engine in an ICEV. Both EPRI studies also assume that the front brake pads and rotors in a PHEV would last about twice as long as they would in an ICEV, because regenerative braking spares the front brake pads and rotors in a PHEV from wearing as quickly as those in an ICEV.

The DOE cost calculator also indicates that an HEV is slightly cheaper to maintain than a comparable ICEV, but the DOE estimates in general are much lower than EPRI's. Because the methods and assumptions used in DOE cost calculator are not completely explicit, it is impossible to fully explain the differences between the DOE and EPRI estimates. The calculator documentation notes that it bases annual maintenance costs on mileage and estimates developed by Vincentric, LLC, an automotive data services company, but does not report the detailed estimates. It appears from the documentation that the estimate of lower HEV maintenance costs is based on longer

**Table 2.5** Maintenance cost estimates (2008 \$)<sup>a</sup> for mid-sized vehicles

Study	Vehicle lifetime (km)	Vehicle type	Lifetime maintenance cost	Lifetime maintenance cost (\$/km)
EPRI 2001 (Graham et al., 2001) <sup>b</sup> [25]	161,000	ICEV	5,853	0.0364
		HEV	5,371	0.0334
		PHEV-32	4,861	0.0302
		PHEV-96	4,464	0.0277
EPRI 2004 (Duvall et al., 2004) <sup>b</sup> [28]	188,000	ICEV	6,450	0.0342
		PHEV-32	4,122	0.0219
	241,000	ICEV	8,475	0.0352
		PHEV-32	5,118	0.0212
Lipman and Delucchi (2003) <sup>c</sup> [35]	273,530	ICEV	12,094	0.0442
		HEV “full” hybrid	13,407	0.0490
U.S. DOE (2008) <sup>d</sup> [37]	161,000	ICEV	3,301	0.0205
		HEV	3,107	0.0193

<sup>a</sup> Adjusted from the original dollars to year 2008 dollars using the CPI for vehicle maintenance and repair [38].

<sup>b</sup> To put the two EPRI studies on the same basis, we used the nondiscounted maintenance costs from Appendix A in EPRI 2004 [28] and subtracted tire costs from the total maintenance costs, because EPRI 2001 [25] did not include tire costs.

<sup>c</sup> Lipman and Delucchi [35] report maintenance costs for a mid-sized ICEV (based on Ford Taurus) and a comparable mid-sized “advanced full” HEV with an electric drivetrain that provides 40% of the total vehicle power requirement. They estimate maintenance costs of \$617/year for the ICEV and \$684/year (year 2000 \$) for the HEV, and a vehicle lifetime of 15 years.

<sup>d</sup> We used the DOE cost calculator to obtain estimates of average annual maintenance costs for several mid-sized ICEVs (the Toyota Camry, Honda Civic, Nissan Altima, and Hyundai Elantra) and HEVs (the Toyota Prius and Camry, Honda Civic, and Nissan Altima). We ran the calculator for 10,000 miles/year (16,100 km/year) and multiplied the average annual cost by 10 years to obtain a lifetime maintenance cost without discounting—comparable to what is reported in the EPRI studies.

service intervals for components like the brakes and spark plugs. It follows that for PHEVs, which would have smaller engines and larger electric drivetrains compared to HEVs, the maintenance costs would likely be even lower.

By contrast, the maintenance cost estimates by Lipman and Delucchi [35], which are the most detailed, result in HEVs having slightly *higher* maintenance costs than ICEVs. Their estimation method has several steps: (1) estimate fleet-average lifetime maintenance and repair costs for ICEVs, in dollars per vehicle per year, using data from the Bureau of the Census data; (2) distinguish maintenance and repair costs that are the same for HEVs and ICEVs, costs that are unique to ICEVs or HEVs, and costs that are “common to but not exactly the same” for ICEVs and HEVs; (3) estimate the HEV costs relative to the ICEV costs for those costs that are unique to HEVs and common to but not the same for HEVs and ICEVs; (4) convert the fleet-average lifetime estimates into year-by-year maintenance cost schedules, for different vehicle types; (5) update costs to a target year using the consumer price index (CPI); and (6) estimate HEV maintenance and repair “common” costs relative to ICEV costs based on components sizes and then

aggregate all maintenance and repair cost estimates for each vehicle type. This method results likely in relatively high maintenance cost estimates because it assumes that there are maintenance requirements for the novel HEV components (which are assumed zero in some studies) and in effect accounts for the more complex nature of the HEV driveline. We also note that the studies in Table 2.5 assume that EV batteries require no maintenance. This assumption probably is reasonable, because maintenance costs for advanced EV batteries are likely to be relatively minor, but there are small costs associated with periodic inspecting and tightening battery connectors that could be included in a more complete study.

### **3.4.3 Other nonenergy operating costs**

Compared with ICEVs, PHEVs will have different insurance costs, because these are partly a function of vehicle value (which is different for PHEVs); different tire costs, because these are partly a function of vehicle weight; different registration costs, because these are a function of vehicle value or vehicle weight; and different emission-inspection fees, because these are related to the characteristics of the engine and emission control system, which will be different for PHEVs. However, as indicated above, we have not found an analysis that quantifies these differences for PHEVs specifically. Lipman and Delucchi [34, 35] evaluate these other nonenergy operating costs for a range of non-plug-in HEVs, and estimate that an “advanced” mid-sized HEV with a relatively large electric power train (providing 40% of the total required power) has a 15% higher insurance cost per kilometer than does the comparable ICEV, due to the higher initial cost of the HEV, but lower lubricating oil, tire, and registration costs, the latter two on account of the lower estimated vehicle weight of the HEV. We expect that results would be qualitatively similar for PHEVs.

## **3.5 Energy-use costs**

### **3.5.1 Overview**

The energy cost per mile of a PHEV is the product of two independent factors: the price of energy, in \$/British thermal unit (BTU) and the energy-use rate, in BTUs/mile, for each source of energy. In this section we focus on the electricity cost per mile. The price of electricity depends in part on whether the utility’s pricing structure distinguishes peak demand periods from off-peak periods. The energy-use rate depends in part on the size and control strategy of the electric power train. We discuss both of these factors next.

### **3.5.2 Energy use of PHEVs**

The power train energy use of PHEVs depends on a number of factors that have been treated differently in the literature. A particularly important and uncertain factor is the control strategy that dictates if the PHEV will operate on battery power alone or if both the gasoline engine and electric motor will propel the vehicle. One control option is to

design the PHEV to have an AER over a specified drive cycle; in this case, the engine will turn on only once the battery has reached a predetermined SOC and from then until the next recharging will operate as a CS hybrid (e.g., the Toyota Prius). We refer to this as the all-electric or AE design strategy.

An alternate strategy, termed *blended* mode, allows the engine to turn on in response to power demands that exceed the capacity of the electric drivetrain. Gonder and Markel [39] described two variations on the blended control scheme. The first, an *engine-dominant* blended strategy, uses battery power to supplement engine operation and keep the engine running at its best possible efficiency. This provides the best petroleum fuel economy over the longest distance. The other control option is the *electric-dominant* blended strategy. Under this scheme, the objective is to power the vehicle using the electric power train as much as possible and to turn on the engine only if the vehicle encounters a transient load beyond the capabilities of the electric motor and battery. As shown in Table 2.6, most PHEV studies have selected the electric-dominant blended control strategy, which we will designate ED.

A PHEV with an AE control strategy will have higher power train costs but lower energy costs than will a PHEV with a blended ED control strategy. It will have higher power train costs because it will need a larger battery and power train in order to provide maximum driving range on electricity. However, this can be offset somewhat by the lower cost of a smaller engine. It will have lower energy costs because the cost per mile of electricity is less than the cost per mile of gasoline and an AE PHEV is designed to run almost exclusively on electricity. The design that minimizes the total lifetime cost (amortized initial costs plus operating costs) depends on the desired AER, the actual driving patterns, the power demands of the drive cycle, and other factors. To our knowledge nobody has analyzed in detail the lifetime costs of different PHEV designs.

Table 2.6 summarizes the results of several studies of PHEV design and energy use. Simpson [26] used an iterative Microsoft Excel spreadsheet model to estimate the appropriate component sizes based on performance requirements such as 0–60 mph acceleration time and maximum speed, and then calculated the mass of the sized components and the resultant total mass of the vehicle. This designed vehicle then was simulated in ADVISOR, a dynamic vehicle energy-use model that determines gasoline and electricity consumption over various drive cycles [26]. The resultant energy-use estimates are shown in Table 2.6.

Gonder et al. [40] also used ADVISOR to simulate the performance of PHEVs. They simulated PHEV performance over standard driving cycles, such as the US06 cycle, but also simulated a real-world driving cycle based on GPS data from 227 vehicles in the St. Louis metropolitan area. As shown in Table 2.6, the modeled gasoline consumption was lower for the real-world, GPS-based drive cycle than for the combined UDDS/HWFET and US06 drive cycles (4.06 l/100 km vs. 4.34 l/100 km and 5.06 l/100 km, respectively). Conversely, electricity consumption was higher for the

**Table 2.6** Modeled component specifications and fuel consumption for mid-sized PHEVs

Author	Model	Control strategy <sup>a</sup>	CD Range (km) <sup>b</sup>	Engine power (kW)	Motor power (kW)	ESS power (kW)	ESS energy (kWh)	Curb mass (kg)	Drive cycle <sup>c</sup>	Fuel consumption (l/100 km)	Electricity consumption (Wh/km)	SOC window <sup>d</sup>	
Gonder et. al (2007) [39]	ADVISOR	ED	32	79.4	43.6	47	9.4	1,488	Comb.	4.36	59	NR	
									RW	4.06	87		
										US06	5.94	NR	
			64	81.9	48	51.8	18.5	1,567	Comb.	3.49	97.6	NR	
								RW	3.10	131.1			
								US06	4.57	NR			
Simpson (2006) (near-term) [26]	Excel Model and ADVISOR	ED	32	85	47	62.23	12.7	1,678	Comb.	6.0	60	47%	
			64	91	51	68.64	20.8	1,824	Comb.	4.8	104	59%	
Simpson (2006) (long-term) [26]	Excel Model and ADVISOR	ED	32	81	43	57.82	11.8	1,531	Comb.	5.7	58	47%	
			64	83	45	60.8	19	1,598	Comb.	4.5	96	59%	
Kromer & Heywood (2008) [8]	ADVISOR	ED	16	48	38	43	3.2	1,296	Comb/Adj	2.3	119.9	60%	
			48	50	40	45	8.2	1,338	Comb/Adj	1.54	115.6	70%	
			96	53	42	48	16.5	1,434	Comb/Adj	1.09	113.7	75%	
Burke (2007) [36]	ADVISOR	AE	32	75	65	80–100	10	1,372	NR <sup>e</sup>	6.2	154.7	50%	

<sup>a</sup> ED = electric-dominant, AE = all-electric.

<sup>b</sup> CD range is the design goal, not actual range on each cycle.

<sup>c</sup> Drive cycles: RW = real-world as modeled by GPS in Gonder et al. [40]. Comb. = weighted combination of HWFET and UDDS cycles. Comb/Adj: combined, adjusted HWFET/FTP drive cycle, calculated as follows: Comb/Adj = (0.45) (FCHW/0.78) + (0.55) (FCFTP/0.9), where FCHW and FCFTP are the fuel consumption in the HWFET and FTP drive cycles, respectively. FTP = Federal Test Procedure; HWFET = Highway Fuel Economy Test; UDDS = Urban Dynamometer Driving Schedule.

<sup>d</sup> SOC window = ratio of required energy to ESS total energy. Describes the amount by which the battery may be discharged.

<sup>e</sup> Drive cycle not specified. Assumed to be driven such that 70% of miles are in CD mode and 30% in CS mode [41].

real-world cycle than in the combined UDDS/HWFET drive cycle (87Wh/km vs. 59 Wh/km). These findings suggest that the standard EPA test driving cycles do not capture the range of speeds and accelerations in real-world driving, and that these differences can significantly affect energy use of PHEVs. Specifically, it is possible that PHEV analyses based on the EPA drive cycles (e.g., [8, 36]) underestimate the electricity consumption and overestimate the gasoline consumption of PHEVs.

### 3.5.3 The price of electricity and the total annual electricity cost

Table 2.7 shows how five studies treat several factors in the calculation of the total annual electricity bill for a PHEV: annual driving distance, CD range, charging time of day, and electricity prices. Of particular interest here are the assumptions related to the electricity price.

The EPRI 2001 and 2004 reports [25, 28] and Kromer and Heywood [8] assumed that PHEV charging would occur at off-peak times and would face relatively low off-peak electricity prices of 5.0–7.5 cents/kWh. By contrast, Parks et al. [42] assumed that the PHEV would be charged once per day at an *average* electricity price of 8.6 cents/kWh, and Simpson [26] assumed that PHEV charging would face the 2005 U.S. average electricity price of almost 10 cents/kWh. Which assumption is more reasonable—an average electricity price or an off-peak price—depends on how people respond to price differentials. On this issue there have been conflicting findings: although several studies show that in general (as opposed to in the specific case of EV charging), time-of-use rates do cause consumers to shift their electricity usage to low-price off-peak periods [43–45]; other studies (e.g., [46]) have shown little to no effect on consumer behavior due to price differentials. Furthermore, to our knowledge there are no studies of the effects of time-of-use rates specifically on consumers who own EVs.

The annual electricity cost of a PHEV depends on the number of miles traveled on electricity and the price of electricity. Parks et al. [42] and the EPRI 2001 report [25] estimate higher annual electricity use, and subsequently higher annual electricity cost, than the other studies. EPRI 2004 [28] and Kromer and Heywood [8] estimate similar annual costs; the differences are due to the choice of annual mileage and CD range.

## 3.6 External costs of PHEVs

Thomas [16] has estimated the external costs of gasoline ICEVs, BEVs, PHEVs, and hydrogen FCEVs. We discuss these in Section 4.5. In general, we can say that to the extent that PHEVs have lower emissions of GHGs (see Lipman and Delucchi, Chapter 5 of this volume) and urban air pollutants and use less petroleum than do petroleum ICEVs, PHEVs will tend to have lower external costs. Because PHEVs still use some petroleum, whereas BEVs and FCEVs do not, the reduction in external costs

**Table 2.7** PHEV electricity cost (2009 \$)<sup>a</sup>

Report	Annual driving distance	CD range	Charging frequency	Electricity price (\$/kWh)	Annual electricity cost (\$)
EPRI 2001 (Graham et al., 2001) [25]	16,100 km (10,000 miles)	32 km (20 miles) 96 km (60 miles)	Nightly	0.075	136 267
EPRI 2004 (Duvall et al., 2004) <sup>b</sup> [28]	18,800 km (11,700 miles) 24,100 km (15,000 miles)	32 km (20 miles) 32 km (20 miles)	Nightly	0.056	61 69
Simpson (2006) [26]	24,100 km (15,000 miles)	32 km (20 miles)	Nightly	0.099	139
Kromer and Heywood (2007) [8]	24,100 km (15,000 miles)	48 km (30 miles)	Nightly	0.050	75
Parks et al. (2007) [25]	22,370 km (13,900 miles)	32 km (20 miles)	Once/day	0.086	168

<sup>a</sup> Inflated prices using CPI from [http://www.bls.gov/data/inflation\\_calculator.htm](http://www.bls.gov/data/inflation_calculator.htm).<sup>b</sup> EPRI 2004 [28] annual electricity cost based on small battery scenarios.

with PHEVs will be less than the reduction with BEVs and FCEVs (this is consistent with Thomas's [16] results).

Furthermore, as discussed more fully in Section 4.6 (the social lifetime costs of FCEVs), in a social-cost analysis the relevant cost metric for petroleum fuel is not the *price* of the fuel but rather the *cost* of the fuel, and in the case of petroleum the cost can be much less than the price. This by itself *reduces* the social cost of petroleum ICEV relative to the private cost of petroleum ICEVs, because the private cost is based on the price that consumers actually pay. These two factors—the relatively modest reduction in external costs with PHEVs, and the price-cost effect that tends to reduce the social lifetime cost of petroleum ICEVs—are likely to result in the social cost of PHEVs relative to the social cost of ICEVs being similar to the private cost of PHEVs relative to the private cost of ICEVs.

We believe that the conclusion of Lipman and Delucchi [34] who analyze the external costs of HEVs, applies generally to the external costs of PHEVs:

*The general conclusion is that the most likely value of external costs (e.g., about \$0.20/gallon for our best estimates) are not large relative to either absolute gasoline prices...or to the range of the breakeven price due to uncertainty in the private lifetime costs. We do not think this means that external costs should be ignored, but rather that one should not expect the results of a social-cost analysis of HEVs to be dramatically different from the results of a private-cost analysis. In other words, consideration of external costs is not likely to appreciably relieve us of the need to find the most cost-effective vehicle designs and to reduce battery costs as much as possible (p. 131).*

### 3.7 Discussion of PHEV cost estimates

In this chapter, we reviewed the recent literature on lifetime cost of PHEVs. In all studies, battery cost is the main driver of the incremental cost of a PHEV over an ICE vehicle, but none of the studies we reviewed conducted detail original research in this area. Although PHEV batteries currently are very expensive, with some advances in battery technology and manufacturing processes, batteries have the potential to be much cheaper when mass produced. However, we are interested here in the *lifetime* cost per mile of the battery, and this is a function of the battery lifetime, which is uncertain and has not yet been modeled in detail. Further research on the cost and lifetime of batteries and other EV components is warranted.

Nonenergy operating and maintenance and repair costs are likely to be different for PHEVs than for ICEVs, but no study has examined all of these differences systematically and in detail for PHEVs specifically. A few studies have considered maintenance costs, generally not in great detail. More work in this area is needed.

As mentioned above, estimates of the energy-use cost of PHEVs depend critically on assumptions regarding the price of electricity and the energy use of the vehicle. The control strategy is particularly important in determining energy use and is one of the



most uncertain aspects of PHEV design. In addition, the drive cycle (i.e., the range of speeds and accelerations over a given distance) the vehicle is subjected to can have a significant effect on the vehicle's energy consumption. Both the control strategy and test drive cycle warrant further examination so PHEV energy use can be modeled more accurately.

Our qualitative assessment of the external costs of PHEVs compared with ICEVs suggests that the social cost of PHEVs relative to the social cost of ICEVs will be similar to the private cost of PHEVs relative to the private cost of ICEVs. Overall, we feel that the current analyses are not comprehensive or detailed enough to allow for a full delineation of the differences in social lifetime cost between PHEVs and ICEVs.



## **4. LIFETIME COST OF FUEL-CELL ELECTRIC VEHICLES**

### **4.1 Introduction**

FCEVs use a fuel cell to convert the chemical energy in hydrogen and oxygen directly into electrical energy. A fuel cell differs from both a rechargeable (or secondary) storage battery, such as is used in BEVs, and a heat engine, although it is much more similar to the secondary battery than to the heat engine. Fuel cells and batteries are electrochemical devices; the main difference between them is that in a battery, the electricity-producing reactants are regenerated in the battery by the recharging process, whereas in a fuel cell, the electricity-producing reactants are continually supplied from sources external to the fuel cell itself: oxygen from the air and hydrogen from a separate onboard storage tank. The hydrogen can be stored as such on the vehicle, or can be stored on the vehicle in the form of methanol and then reformed into hydrogen and CO<sub>2</sub> onboard the vehicle. However, because methanol reforming reduces the energy efficiency of the vehicle, adds complexity, and produces CO<sub>2</sub> and other pollutants, most analysts assume that hydrogen is stored on the vehicle as such, typically at high pressures. All of the recent cost analyses reviewed here assume that FCEVs have high-pressure hydrogen storage tanks.

Hydrogen FCEVs combine the best features of battery EVs—zero emissions, high efficiency, quiet operation, and long life—with the long range and fast refueling time of ICE vehicles. If FCEVs can be developed economically, they will be general-purpose ZEVs, and will be an important component of a strategy for reducing dependence on oil, mitigating global warming, and improving urban air quality, at an acceptable cost.

### **4.2 Component costs**

#### **4.2.1 Overview**

A hydrogen FCEV has an electric motor and transmission, an electric motor controller, a fuel cell, and a high-pressure hydrogen storage system. It also may have a battery or other electricity storage device, such as an ultracapacitor, to be able to store the electrical

energy from regenerative braking and to supplement the power supply from the fuel cell. In previous subsections (Sections 2.3.1, 3.3.2, and 3.3.3), we have reviewed estimates of costs of electric motors, motor controllers, and batteries for EVs. Here we discuss estimates of the cost of fuel cells and the cost of onboard hydrogen storage systems.

#### 4.2.2 Fuel-cell system

The cost of a fuel-cell system can be analyzed in several parts: (1) the fuel-cell stack, consisting mainly of the electrodes, electrolyte, flow field, and housing; (2) the fuel-cell auxiliaries for heating, cooling, and water management; (3) the air-compression system; (4) the fuel processing system, if the vehicle stores methanol rather than hydrogen; and (5) electronic controls and electrical integration. In a cost analysis, key parts of the fuel-cell stack itself are the platinum catalyst and the proton-conducting polymer membrane.

Here we review a series of detailed estimates of fuel-cell system costs by Directed Technologies, Inc. (DTI) [47–49] and by Arthur D. Little (ADL) (later TIAX) [50–52]. DTI and ADL estimated costs in detail, at high volumes of production, for current technology and future technology systems. We then review a recent detailed analysis by Sun et al. [53] that relies in part on the work of DTI and ADL.

*Directed Technologies Inc. (DTI).* DTI has done detailed cost analyses of FCVs for over 10 years, with sponsorship from DOE and auto companies. In 1998 they published a detailed report on hydrogen fuel cell costs in high-volume production (500,000 power plants per year), based on prototypes or “reasonable extrapolations,” but no technological “breakthroughs” [47]. The results of this are shown in Table 2.8. In 2001, DTI carried out another analysis of FC costs as a function of production volume (500, 10,000, 30,000, and 500,000 units/year), this time assuming methanol rather than hydrogen and explicitly based on then-currently available technology [48]. As shown in Table 2.8, the DTI 2001 estimates of the cost of current fuel-cell technology are nearly an order of magnitude higher than their 1998 estimates of “future” technology costs.

DTI updated its analysis again in 2007, estimating the cost of a direct hydrogen fuel-cell system at three technology levels (year 2006, 2010, and 2015), and five different annual vehicle production volumes (1,000, 30,000, 80,000, 130,000, and 500,000 vehicles per year) [49] (Table 2.8). The 2007 analysis uses an extremely detailed costing method that consider machine costs, machine utilization rates, detailed materials costs, corporate taxes, equipment life, and so on. The 2007 analysis indicates that fuel cells with year 2015 technology produced in high volume will cost \$59/kWe-net (Table 2.8), or about \$4,700 for the 80-kWe-net system.

*Arthur D. Little (ADL)/TIAX LLC.* Like DTI, ADL/TIAX has performed a series of fuel-cell cost analyses over the past decade. (When ADL declared bankruptcy in 2002, TIAX LLC hired the ADL personnel involved in analyses of fuel-cell systems and continued that line of work.) First, ADL [50] did a detailed “factory” cost analysis of

**Table 2.8** DTI estimates of fuel-cell system cost (\$/kWe-net, except as noted)

Fuel	Reformate	Hydrogen	Hydrogen			
Study author (year)	James et al. (2001) <sup>a</sup> [48]	Lomax et al. (1998) <sup>b</sup> [47]	James and Kalinoski (2007) <sup>c</sup> [49]			
FC net power (kWe)	50	50	80			
Year of technology	~2001	~2000–2010	2006		2015	
Units/year	500,000	500,000	30,000	500,000	30,000	500,000
<i>Fuel cell subsystem</i>						
Membrane	26	0.4–0.6	15.00	4.31	12.04	3.30
Catalyst	86	8–13	49.01	43.77	10.07	8.98
Balance of stack	58	11–16	41.18	18.65	27.56	12.70
<i>Fuel-cell stack subtotal</i>	<i>170</i>	<i>20–30</i>	<i>105</i>	<i>67</i>	<i>50</i>	<i>25</i>
Air, water, coolant, misc.	30	n.e.	60	43	50	34
<i>Subtotal fuel-cell subsystem</i>	<i>200</i>	<i>n.e.</i>	<i>~165</i>	<i>110</i>	<i>~100</i>	<i>59</i>
Controls, BOP, misc.	12	n.e.	See air, water, coolants, misc			
Fuel processor <sup>d</sup>	49	n.e.	n.a.			
<i>Total</i>	<i>262</i>	<i>n.e.</i>	<i>n.a.</i>			

n.e. = not estimated, n.a. = not applicable.

<sup>a</sup> The estimates of membrane and catalyst cost include fabrication as well as material costs. The “controls, BOP, misc.” category includes stack assembly.

<sup>b</sup> Estimates are for the stack only, and do not include: turbo-compressor, humidifiers, or cooling system. Lomax et al. [47]. report costs per kWe-gross; we assume costs per kWe-electric net are 10% higher. (The gross output of the fuel-cell stack is before any system auxiliaries; the net output is net of the power consumption of system auxiliaries.)

<sup>c</sup> Estimates converted from \$/kW-gross by multiplying by ratio of gross power to net power ( $87.1/80 = 1.089$ ). Year of dollars not specified. “Balance of stack” includes stack assembly and stack conditioning and testing, and is calculated by difference between reported stack total and reported membrane and catalyst costs. “Air, water, coolant, misc.” is calculated as the difference between “subtotal fuel-cell subsystem” and “fuel-cell stack subtotal.”

<sup>d</sup> The “fuel processor” cost category includes the reactor, the reformate loop, and the fuel loop.

**Table 2.9** ADL estimates of fuel-cell-system cost (\$/kWe-net)

Fuel	Reformate	Reformate	Hydrogen	Hydrogen
Study author (year)	ADL (2000) [50]	Carlson and Thijssen (2002) <sup>a</sup> [51]	Carlson and Thijssen (2002) <sup>a</sup> [51]	Lasher et al. (2007) [52]
FC net power (kWe)	50	50	50	80
Year of technology	~2000	“Future”	“Future”	~2007
Units/year	500,000	500,000	500,000	500,000
<i>Fuel-cell subsystem</i>				
Precious metals in stack	52	14	10	
Membrane, plates, air supply, cooling, other	125	58	44	
<i>Subtotal fuel-cell subsystem</i>	177	72	54	67 (31 stack only)
Balance of plant	10	5	3	
Fuel processor/H <sub>2</sub> storage	86	28	30	n.e
Assembly/labor/depreciation	21	14	15	
<i>Total</i>	294	118	102	

n.e. = not estimated.

<sup>a</sup>Note: values read from graph in Carlson and Thijssen [51].

fuel cells for transportation. They assumed year–2000 performance data, but high volumes of production. They defined their “factory” cost basis explicitly and in detail. Their estimates for a mass-produced (500,000 units/year) 50 kWe-net system (with a methanol reformer) are shown in Table 2.9.

In 2002, ADL complemented its analysis of costs given current technology with an analysis of future costs assuming projected technology [51]. The future-technology scenario assumed much higher current density, much lower platinum loading, and lower membrane and balance-of-plant costs than in the current-technology scenario. The resulting estimates for a mass-produced (500,000 units/year), 50 kWe-net future-technology system, with either hydrogen or methanol storage, are shown in Table 2.9. In the ADL analyses, the catalysts, reformers, membrane, and other fuel-cell subsystem components cost much less in the future-technology scenario than in the current-technology scenario.

Finally, Lasher et al. [52] report the most recent results from this line of research (Table 2.9). They estimate costs of high-volume production of a direct-hydrogen fuel-cell system, for year 2010 and 2015 technology levels. They use the same manufacturing cost software used by James and Kalinoski [49], but they estimate that the complete fuel-cell subsystem costs \$67/kWe-net (Table 2.9)—much less than James and Kalinoski’s estimate for year 2006 technology (Table 2.8).

*Comparison of DTI and ADL/TIAX estimates.* The ADL definition of “factory” cost appears to be very similar to the DTI definition of cost, and the definition of high-volume production is identical (500,000/year) in both sets of studies, so the DTI estimates are reasonably comparable with the ADL estimates. Specifically, we can compare estimates of complete systems using reformat with current technology [48, 50], and estimates of the fuel-cell stack only using hydrogen, with future technology [47, 51]. The most recent ADL and DTI estimates cannot be directly compared because of lack of detail in the most recent ADL estimates.

These comparisons reveal the following:

- The DTI and ADL estimates of *total* system costs for current-technology fuel-cell systems are similar, but there are differences in the details;
- DTI estimates lower costs for future-technology hydrogen fuel-cell stacks;
- DTI estimates lower costs for current-technology reformers;
- DTI and ADL estimate similar membrane costs in the current-technology scenarios, but DTI’s estimate of future-technology membrane costs appears to be much lower than ADL’s; and
- DTI and ADL estimate similar platinum costs in the future-technology scenarios, but DTI estimates a higher cost in the current-technology scenario, mainly because of a higher assumed platinum price. This highlights the importance of carefully estimating platinum-catalyst cost.

*Sun et al. (2010).* Sun et al. [53] combine cost estimates from DTI and ADL with independent estimates of catalyst costs, and estimate that a fuel-cell system, including the stack, air management, water management, and thermal management, will cost \$57/kW of stack power output, at high volumes of production. This is close to DTI’s estimate of the cost of a future-technology fuel-cell system (Table 2.8).

### **4.2.3 Hydrogen storage system**

Hydrogen must be compressed, liquefied, or reacted with or contained in other materials in order to be stored conveniently onboard a vehicle. It is simplest and perhaps most economical to compress hydrogen and store it in specially designed high-pressure vessels consisting of a metal or metal-polymer container wrapped with carbon fiber. In this section we analyze the cost of these sorts of high-pressure vessels for hydrogen.

The cost and weight of high-pressure vessels is a function of the cost and weight of the materials, the manufacturing process, the storage pressure, and the amount of hydrogen stored. For high-pressure fiber-wrapped cylinders, one of the key cost factors is the cost of the carbon fiber used to wrap the metal or metal-polymer container. Table 2.10 summarizes several detailed estimates of the manufacturing cost of high-pressure hydrogen storage containers.

For storage at 10,000 psi, the estimates of the cost of storing 4.6 kg of hydrogen—enough for a 300-mile range in a mid-sized FCEV that gets an gasoline-equivalent fuel economy of 61 mpg—range from about \$1,800 to \$3,000, with our best estimate being

**Table 2.10** The manufacturing cost of high-pressure hydrogen storage containers in mass production (2005 US\$)<sup>a</sup>

Author	Organization	Storage pressure (psi)	OEM cost (\$-OEM/kWh-H <sub>2</sub> ) (HHV)	OEM cost for 4.6 kg H <sub>2</sub> (\$)
Mitlitsky et al. (2000) <sup>b</sup> [54]	Lawrence Livermore National Laboratory	5,000	5.6	1,020
TIAX LLC (2004) <sup>c</sup> [55]	TIAX LLC	5,000 10,000	9.1 11.3	1,650 2,050
Abele (2006) [56]	Quantum Hydrogen Storage Systems	10,000	10–17	1,810–3,080
Lasher et al. (2007) <sup>d</sup> [57]	TIAX LLC with others	5,000 10,000	10.2 15.7	1,840 2,840
Sun et al. (2010) <sup>e</sup> [53]	University of California, Davis	10,000	12.1	2,200

HHV = higher heating value, LHV = lower heating value, OEM = original equipment manufacturer, HHV-H<sub>2</sub> = 141.9 MJ/kg or 39.4 kWh/kg, LHV-H<sub>2</sub> = 120.1 MJ/kg or 33.4 kWh/kg.

<sup>a</sup> Where necessary we updated to year 2005 using the Bureau of Labor Statistics' Producer Price Indices ([www.bls.gov/ppi/](http://www.bls.gov/ppi/)) for gas cylinders and metal pressure vessels (we estimate a 2.4%/year price change).

<sup>b</sup> Mitlitsky et al. [54] estimate that a 5,000 psi carbon-fiber-wrapped tank with a solenoid and pressure-relief device and holding 3.58 kg of hydrogen would cost \$640 in mass production given then "current" materials costs. We have increased their estimate by 10% to account for regulators, sensors, pipes, and fill port, which are included in most of the other estimates but apparently not in Mitlitsky et al.

<sup>c</sup> TIAX [55] reports \$10.5/kWh for 5,000 psi, and \$13.0/kWh for 10,000 psi, including tank materials, assembly, regulators, fill port, valves, etc. The estimates appear to be in year 2004 US\$ and to be based on the LHV of hydrogen.

<sup>d</sup> Lasher et al [57]. report \$12/kWh for 5,000 psi, and \$18.50/kWh for 10,000 psi, for 5.6 kg hydrogen, including tank materials, tank production (which they call "processing"), and the "balance of plant," which includes regulators, fill port, valves, sensors, and pipes and fittings. The estimates appear to be in year 2005 US\$, and to be based on the LHV of hydrogen.

<sup>e</sup> Sun et al. [53] estimate that H<sub>2</sub> tank cost (2005 constant US\$) = 467.76 × full tank H<sub>2</sub> fuel (kg) + 50.

between \$2,000 and \$2,600 (year 2005 US\$). We estimate that the amortized *retail* level cost of the hydrogen storage system (where the retail-level cost is equal to the OEM [original equipment manufacturer] cost estimated in Table 2.10 plus the overhead and mark-ups of the automobile manufacturer and the dealer) is about 5% of the total private lifetime cost per mile of a FCEV.

## 4.3 Nonenergy operating and maintenance costs

### 4.3.1 Maintenance and repair costs

Hydrogen FCEVs, like BEVs, should have lower maintenance and repair costs than gasoline ICEVs (see Section 2.4). However, there appear to be no recent published analyses of maintenance and repair costs for FCEVs. In MIT's *On the Road in 2020* study, Weiss et al. [13] Assume that maintenance and repair costs are the same for all vehicle types, at \$0.036/km. The Advanced Vehicle Cost and Energy-Use Model (AVCEM) [58], used in the analyses of Sun et al. ([53], see Table 2.11), estimates that maintenance

**Table 2.11** Overview of recent hydrogen FCEV cost studies

Study group	MIT [8,13,60]	Oak Ridge National Laboratory (ORNL) [61]	National Research Council [62]	EUCAR [63]	Imperial College London [10]
Region	U.S. and several European countries	U.S.	U.S.	Europe	UK
Timeframe	2020, 2030, 2035	2012–2025	2010–2050	2010+	2010, 2030
Vehicle type	Mid-sized car, light truck	Light-duty vehicle	Light-duty vehicle	Compact five-seater European sedan	Saloon car
Vehicle energy-use model	ADVISOR simulation	No formal model	No formal model	ADVISOR simulation	No formal model
Vehicle cost	Retail price and OEM cost estimates from literature review and industry experts: \$3,000–\$5,300 incremental retail price of future FCEV relative to future ICEV	Drive train cost estimate from HyTrans model [64] assuming a constant glider cost and that DOE technical targets are met for fuel cell system	ORNL learning curve model for estimates of FCEV cost and investment costs	Vehicle retail price increment expected beyond 2010 at 50K vehicles per year; maintenance costs not considered	Power train cost estimates form reports by the International Energy Agency
Fuel cost	Estimated cost of raw materials plus cost of fuel production plus cost of fuel distribution, in the year 2020, with accounting for uncertainty	Estimates of full cost of dispensed H <sub>2</sub> from DTI’s HyPro model [65] (\$2.5–\$3.25/kg-H <sub>2</sub> )	Estimates of dispensed H <sub>2</sub> costs from UC Davis hydrogen-supply cost model SSCHISM [66]	Estimated cost of raw materials plus cost of fuel production plus cost of fuel distribution and refueling	Optimistic and pessimistic assumptions regarding fuel price, based on literature review
External costs	Not included	Not included	Not included	Not included	Not included

(Continued)

**Table 2.11** (continued)

<b>Study group</b>	<b>Princeton [67]</b>	<b>Lee et al. [68]</b>	<b>H2Gen [16,17]</b>	<b>UC Davis [53]</b>
Region	U.S. (Southern California)	Korea	U.S.	U.S.
Timeframe	Not specified	2007, 2015	2005–2100	2010–2025
Vehicle type	Mid-sized automobile (four to five passengers)	Sport utility vehicle	Light-duty vehicle	Mid-sized automobile
Vehicle energy-use model	No formal model	No formal model	No formal model	Advanced Vehicle Cost and Energy-Use Model (AVCEM) [58]
Vehicle cost	Vehicle first cost estimates (retail costs of drivetrain and body) based on engineering and cost models from several sources)	Vehicle price estimated from the data given by Hyundai Motor Company.	Based on FCEV cost estimates by Kromer and Heywood [8]	Based on AVCEM [58] with extensive supplemental analysis of fuel-cell costs, using learning-curve model
Fuel cost	Lifetime fuel cost calculated from fuel economy and levelized fuel price (8% discount rate, 12,000 miles/year, 10-year lifetime)	Fuel utilization costs calculated based on fuel efficiency and driving distance, using data from Hyundai motors	Assume NRC estimate, based on DOE H2A project ( <a href="http://www.hydrogen.energy.gov/h2a_analysis.html">www.hydrogen.energy.gov/h2a_analysis.html</a> ), of H <sub>2</sub> cost at time of hydrogen fueling system “break even” (\$3.30/kg-H <sub>2</sub> )	Estimates of dispensed H <sub>2</sub> costs from UC Davis hydrogen-supply cost model SSCHISM [66,69]; ~3.50/kg-H <sub>2</sub>
External costs	Estimates of damage costs from air pollution GHG emissions, and oil supply insecurity, based on literature review and additional analysis	Damage costs or prevention costs for regulated air pollutants and GHG emissions	Estimates of external costs of urban air pollution, GHG emissions and oil dependence, based on review and analysis of literature	Detailed estimates of damage costs from air pollution (including upstream pollution), climate change, energy security, and noise



and repair and oil-filling costs are 20% lower for hydrogen FCEVs, but this specific result is not reported in Sun et al. [53].

### 4.3.2 Other nonenergy operating costs

In MIT's *On the Road in 2020* study, Weiss et al. [13] Assume that the insurance cost per kilometer for an ICEV is \$0.05 and that the cost for an FCEV is equal to  $\$0.025 + \$0.025 (RP_{\text{FCEV}}/RP_{\text{ICEV}})$ , where  $RP_{\text{FCEV}}$  is the estimated retail price of the FCEV and  $RP_{\text{ICEV}}$  is the estimated retail price of the ICEV. This method, which assumes that half of the insurance cost is proportional to vehicle value, is a simplified version of the more disaggregated calculation in AVCEM [58], used in Sun et al. [53]. Weiss et al. [13] Estimate that the insurance cost per kilometer of a hydrogen FCEV is 14% higher than the insurance cost per kilometer of a gasoline ICEV, whereas AVCEM estimates that the FCEV insurance cost is only 5% higher. The method of Weiss et al. [13] Probably overestimates the insurance cost of FCEVs, because the portion of insurance that is related to vehicle value probably does not scale linearly with vehicle value, and because insurance related to vehicle value typically is not carried for the life of the vehicle.

Weiss et al. [13] Assume that license, registration, and "excise tax" costs per kilometer scale with vehicle value and are 25% higher for FCEVs than for gasoline ICEVs. By contrast, AVCEM assumes that registration fees are based on weight and hence are not higher for FCEVs, and that vehicle emission-inspection fees are lower.

## 4.4 Energy-use costs

### 4.4.1 Energy use of FCEVs

FCEVs generally will have two to three times the fuel economy (in miles per kilojoule of travel) of comparable gasoline ICEVs, because electric drivetrains are extremely efficient (over 80% on a work-out/energy-in basis), and fuel cells themselves are up to 50% efficient. Sun et al. [53] Use the detailed energy-use model built into AVCEM [58] to estimate that a mid-sized hydrogen FCEV gets 57 miles per gasoline-energy-equivalent gallon versus 20.1 mpg for the comparable gasoline ICEV. AVCEM performs a second-by-second simulation of all of the forces acting on a vehicle over a specified drive cycle. This energy-use simulation is used to accurately determine the amount of energy required to move a vehicle of particular characteristics over a specified drive cycle, with the ultimate objective of calculating the energy cost per mile *and* the size of the engine, battery, fuel-cell system, fuel-storage system, and electric drivetrain necessary to satisfy user-specified range and performance requirements.

The cost of these components is directly related to their size; hence, the importance of an accurate energy-use and performance analysis within a lifetime cost analysis. The energy-use simulation in AVCEM is the standard textbook application of the physics of work, with a variety of empirical approximations, to the movement of motor vehicles. For more details on this type of modeling, see also Haraldsson [59].

As indicated in [Table 2.11](#), most analyses of the lifetime cost of hydrogen FCEVs have not used a formal model of vehicle energy use. In studies that do not simulate energy consumption in detail, energy use either is assumed or else is estimated on the basis of assumptions regarding absolute or relative drivetrain efficiency. However, two of the studies in [Table 2.11](#)—the MIT studies and the EUCAR study—have used the ADVISOR model to simulate FCEV energy use. Like AVCEM, ADVISOR simulates vehicle energy use second-by-second over specified drive cycles. ADVISOR is a “backward facing” model, which means that every second, the required torque and rotational speed are calculated at the wheel and then traced backward to the engine. The algorithms in ADVISOR are similar to but in some cases more detailed than those in AVCEM.

Using ADVISOR, Kromer and Heywood [8] estimate that an FCEV has 2.3 times greater gasoline-energy-equivalent fuel economy than a year 2030 gasoline ICEV. By comparison, in the Sun et al. [53] Work using AVCEM, described above, the FCEV is estimated to have 2.8 times greater gasoline-energy-equivalent fuel economy.

#### **4.4.2 Cost of fuel**

A number of studies have made or used detailed estimates of the cost of hydrogen fuel ([Table 2.11](#)). Much of this work uses cost information from the U.S. DOE’s Hydrogen Analysis (H2A) project. The H2A project brought together a range of hydrogen experts to thoroughly review and analyze data pertaining to the cost of producing, delivering, and dispensing hydrogen. Estimates from H2A are used directly or indirectly in the NRC, ORNL (Oak Ridge National Laboratory), H2Gen, and UC Davis studies ([Table 2.11](#)).

Sun et al. [53] Estimate hydrogen fuel cost with the UC Davis Steady State City Hydrogen Infrastructure System Model (SSCHISM) [66, 69]. SSCHISM combines census, geographic, and energy price data for different cities with hydrogen infrastructure models to estimate hydrogen costs, efficiency and emissions as a function of the hydrogen pathway, and the market penetration of hydrogen vehicles. The cost estimates in SSCHISM are based on DOE’s H2A program and other sources. The SSCHISM model estimates that the full cost of compressed hydrogen (from natural gas or coal) delivered to motorists is in the range of \$3/kg to \$4/kg, or about \$21/GJ to \$28/GJ, excluding taxes. As shown in [Table 2.11](#), in Sun et al., [53] the delivered cost, in the year 2025, is about \$3.50/kg.

The ORNL [61] analysis of FCV market penetration used the HyPro model developed by Directed Technologies, Inc. [65]. HyPro estimates the \$/kg cost of hydrogen at the pump as the sum of production, terminal, delivery, dispensing, and other costs [65]. Like SSCHISM, HyPro uses estimates and data developed in the DOE’s H2A project. HyPro estimates that the full cost of compressed hydrogen delivered to the motorist is in the range of \$2.50/kg to \$3.50/kg, depending on the feedstock cost and other factors [65].

The most comprehensive analyses thus indicate that the full cost of hydrogen dispensed to the motorist is in the range of \$2.50/kg to \$4.00/kg, with the cost of a high-pressure dispensing station being around \$0.50/kg to \$1.00/kg of this. The range \$2.50/kg to \$4.00/kg corresponds to a pretax gasoline cost of about \$2.30 to \$3.70, on a gasoline-energy-equivalent basis. This is slightly above current gasoline pretax costs in the United States (on the order of \$2.50/gallon), but when the fuel price (in \$/gallon-gasoline-energy-equivalent) is divided by the fuel economy, which as discussed in Section 4.4.1 is 2–3 times higher for FCEVs, the resultant fuel cost per mile of an FCEV is roughly half that of a gasoline ICEV.

#### 4.5 External costs of FCEVs

Ogden et al. [67], Thomas [16], and Sun et al. [53] Estimate the external costs of FCVs as part of an analysis of the social lifetime cost of FCEVs (Table 2.11). Ogden et al. [67] Estimated air pollution, climate change, and energy-security costs. Air pollution and climate-change costs, in \$/km, were estimated by multiplying emissions in g/km by damages in \$/g. GHG emissions were taken from the GREET model [70], and unit damage costs in \$/g were calculated by adjusting estimates of damages in Europe [71] to U.S. population density. An oil-supply insecurity cost was estimated based on U.S. military expenditures for the Persian Gulf and the fraction of Persian Gulf exports to the United States.

Thomas [16] estimated the external costs of urban air pollution, GHG emissions, and oil dependence for HEVs, PHEVs, BEVs, and hydrogen FCEVs. The GREET model [70] was used to calculate emissions of air pollutants and GHGs and consumption of oil. Unit health damage costs from air pollution were derived from the average of several estimates of costs in the United States and Europe. The GHG damage cost was assumed to be \$25 per metric ton of CO<sub>2</sub> in 2010, increasing linearly to \$50/ton by 2100. A societal cost of \$60/barrel was assumed for “oil dependence,” including the “military costs of securing petroleum” and the “economic costs of oil dependence.” With these assumptions, Thomas [16] estimated the total external cost (air pollution, plus GHGs, plus oil dependence) for a light-duty vehicle fleet using different fuels and power trains in the United States In the year 2100. The study found costs of about \$515 billion/year for a fleet of gasoline ICEVs; about \$225 billion/year for gasoline PHEVs; and about \$30 billion/year for BEVs and hydrogen FCEVs. Thus, Thomas [16] estimates that BEVs and hydrogen FCEVs reduce external costs by over 90%.

Sun et al. [53] Provide the most comprehensive estimates of the external costs of hydrogen FCEVs. They use the AVCEM model [58] and additional analysis (included references [72–75]) to estimate the external costs associated with oil use, air pollution, climate change, and noise. Oil-use costs comprise the cost of the Strategic Petroleum Reserve, macroeconomic costs from oil price shocks, wealth transfers from U.S. consumers to foreign oil producers (a cost only in the U.S. national accounting), the military

costs of oil use, and the cost of water pollution due to oil use. Air pollution costs comprise health effects (such as premature mortality), reduced visibility, crop losses, and damages to forests and materials. The external costs of air pollution include the impacts of emissions from the “upstream” life cycle of fuels as well as emissions from vehicle themselves, and the external costs of climate change include the impacts of emissions from the vehicle life cycle as well as from the full life cycle of fuels. The upstream life cycle of fuels includes energy feedstock production, transportation, and storage, and fuel production, transportation, storage, and distribution. The vehicle cycle includes vehicle assembly and the life cycle of materials used in vehicles.

Sun et al. [53] Estimate that the present value of the total lifetime external cost ranges from about \$200 to almost \$5,000 for hydrogen FCEVs and from about \$800 to \$11,500 for gasoline ICEVs. By comparison, the present value of the total lifetime consumer cost is about \$62,000 for hydrogen FCEVs, and \$58,000 for gasoline ICEVs.

#### 4.6 Discussion of FCEV cost estimates

Generally, in the studies of Table 2.11, the higher initial cost of hydrogen FCEVs compared with gasoline ICEVs, due mainly to the high cost of the fuel cell and the hydrogen storage system (Sections 4.4.2 and 4.4.3), is not offset by lower fuel costs (Subsection 4.4.2), and as a result the private lifetime cost per kilometer of hydrogen FCEVs is estimated to be higher than that of gasoline ICEVs. However, because hydrogen FCEVs have lower external costs of air pollution, climate change, and oil dependency (Section 4.5), and because the social lifetime cost often is estimated as the private lifetime cost plus external costs, it is possible that the social lifetime cost of hydrogen FCEVs is comparable to or even less than the social lifetime cost of gasoline ICEVs. This is the general finding of Ogden et al. [67] (Table 2.11).

There is, however, one last issue to consider, mentioned in passing in Section 1. As discussed in Sun et al. [53], the social lifetime cost is equal to the private lifetime cost, plus external costs (discussed immediately above), *less any noncost transfers*. Examples of noncost transfers include fuel taxes, which are a transfer from consumers to the government, and producer surplus, which is producer revenue in excess of cost and is a noncost transfer from consumers to producers. Producer surplus in the oil industry can be very large, because many producers—especially those in the Middle East—have total long-run production costs well below the market price of oil. The result is that the social cost of gasoline—equal to the market price less the producer surplus per unit—can be much less than the private cost of gasoline, which is based on the market price. This means that, by this factor alone, the social cost of gasoline is *less* than the private cost of gasoline. In the case of gasoline ICEVs, this reduction of cost (over \$1,000, in present value terms) due to accounting for producer surplus, can be almost as large as the increase in cost due to accounting for external costs, especially when external costs are at the low end of an

estimated range. This means that in some cases—when external costs are relatively low— a social-cost comparison of gasoline with, say hydrogen FCEVs does not give appreciably different results than does a private-cost comparison [53].



## 5. DISCUSSION

Compared with conventional gasoline ICEVs, advanced EVs—BEVs, PHEVs, and FCEVs—have higher initial costs, lower fuel costs, lower external costs, possibly higher insurance costs, and possibly lower maintenance and repair costs. It thus is not immediately obvious how the full social lifetime cost of advanced EVs compares with the full social lifetime cost of gasoline ICEVs.

The formal estimation of the full social lifetime cost depends on a number of uncertain analytical details, including the following:

- the size of key components for EVs (batteries, fuel cells, hydrogen pressure vessels, electric motors), which depends on the desired performance and driving range and the energy efficiency of the vehicle;
- the cost of key materials for EV components, including, for example, lithium for batteries, platinum and membranes for fuel cells, and carbon fiber for pressure vessels;
- the lifetime of key components (e.g., cycles for batteries and pressure vessels, hours of operation for fuel cells);
- how manufacturing costs change with increasing production due to technological learning and economies of scale;
- the energy use of the EV, which depends on the technology and design of the power train, the drive cycle, the weight of the EV, the desired performance, and other factors;
- the cost of energy for the EV, which depends on feedstock costs, fuel production costs, fuel distribution costs, and fuel dispensing/delivery costs; fuel dispensing or delivery costs, in turn, depend on the type of fuel and the desired fuel delivery method (e.g., compressed vs. liquefied hydrogen; slow overnight battery charging vs. fast commercial battery charging);
- the relationship between insurance costs and vehicle value;
- the maintenance and repair requirements of advanced EV components and drivetrains;
- the magnitude of the changes in oil use and emissions of air pollutants and GHGs, and the dollar value of these changes, which in turn depend on assumptions and methods used to address a range of difficult-to-model problems, such as the costs of catastrophic climate change or the macroeconomic costs of oil-supply disruptions; and
- the treatment of noncost transfers, such as producer surplus and taxes and fees.

The analyses reviewed here suggest that with reasonably anticipatable technological progress, the social lifetime cost of advanced EVs can be close to the social lifetime cost of gasoline EVs. More work is needed in the areas listed above for more definitive conclusions, particularly as new advanced EV designs and concepts continue to emerge.

## ACKNOWLEDGMENTS

We thank Andrew Lentz for extensive research assistance and preparation of the material on the cost of PHEVs. We also thank the UC Davis STEPS program, the UC Davis PHEV Research Center, and the National Science Foundation's Material Use: Science Engineering, and Society (MUSES) program for support for research upon which this chapter is partly based.

## REFERENCES

1. M.A. Delucchi, D.M. McCubbin, External Cost of Transport in the U.S.A., A. de Palma, E. Quinet and R. Vickerman (Eds.), Handbook in Transport Economics, Edward Elgar Publishing, 2010, in press (Chapter 9), [www.its.ucdavis.edu/publications/2010/UCD-ITS-RP-10-10.pdf](http://www.its.ucdavis.edu/publications/2010/UCD-ITS-RP-10-10.pdf).
2. M.A. Delucchi, T.E. Lipman, *Transport. Res. D* 6 (2001) 371.
3. T.E. Lipman, A Review of Electric Vehicle Cost Studies: Assumptions, Methodologies, and Results, Report No. UCD-ITS-99-8, Institute of Transportation Studies, University of California, Davis, 1999.
4. T.E. Lipman, The Cost of Manufacturing Electric Vehicle Batteries, Report No. UCD-ITS-99-5, Institute of Transportation Studies, University of California, Davis, 1999.
5. T.E. Lipman, The Cost of Manufacturing Electric Vehicle Drivetrains, Report No. UCD-ITS-99-7, Institute of Transportation Studies, University of California, Davis, 1999.
6. J. Murphy, A high-tech twist on the filling station; in Japan, a California start-up unveils system for quickly swapping batteries in electric cars, *The Wall Street Journal*, May 9, 2009.
7. A. Lovins, D.R. Cramer, *Int. J. Vehicle Des.* 35 (2004) 50.
8. M. Kromer, J. Heywood Electric Power Trains: Opportunities and Challenges in the US Light-Duty Vehicle Fleet, Sloan Automotive Laboratory, Massachusetts Institute of Technology, Publication No. LFEE 2007-03 RP, May 2007.
9. S. Eaves, J. Eaves, *J. Power Sources* 130 (2004) 208.
10. G.J. Offer, D. Howey, M. Contestabile, R. Clague, N.P. Brandon, *Energy Policy* 38 (2010) 24.
11. T.E. Lipman, *Traffic Technol. Int.*, February/March (2009) 44–50.
12. General Motors Corp., General Motors' Electric Vehicles: Emergency Response Information, 1998.
13. M.A. Weiss, J.B. Heywood, E.M. Drake, A. Schafer, F.F. AuYeun, On the Road in 2020 — A Life-Cycle Analysis of New Automobile Technologies, Energy Laboratory Report MIT EL00-003, Massachusetts Institute of Technology, October 2000.
14. Alternative Fuels Data Center, Model Year 2002: Alternative Fuel Vehicles, National Renewable Energy Laboratory, 2001.
15. J. Lidicker, T.E. Lipman, S.A. Shaheen, Economic Assessment of Electric-Drive Vehicle Operation in California and the United States, Transportation Research Board Meeting, Paper #10-3667, 2010.
16. C.E. Thomas, *Int. J. Hydrogen Energy* 34 (2009) 9279.
17. C.E. Thomas, *Int. J. Hydrogen Energy* 34 (2009) 6005.
18. A.D. Vyas, R. Cuenca, L. Gaines, An Assessment of Electric Vehicle Life Cycle Costs to Consumers, SAE Technical Paper Series #982182, Society of Automotive Engineers, Warrendale, PA, 1998.
19. New York State Energy Research and Development Authority, Zero-Emission Vehicle Technology Assessment (Report No. 95-11), McLean, Virginia, Prepared by Booz-Allen and Hamilton, 1995.
20. International Energy Agency/Organization for Economic Cooperation and Development (IEA/OECD), Transport Energy and CO<sub>2</sub>: Moving Toward Sustainability, 2009.
21. L. Sanna, *EPRI J.* (2005) 8–17.
22. J. Douglas, *EPRI J.* (2008) 6–15.

23. M.J. Scott, M. Kintner-Meyer, D.B. Elliott, W.M. Warwick, J. EUEC, 1 (2007), [http://energytech.pnl.gov/publications/pdf/PHEV\\_Economic\\_Analysis\\_Part2\\_Final.pdf](http://energytech.pnl.gov/publications/pdf/PHEV_Economic_Analysis_Part2_Final.pdf).
24. C. Silva, M. Ross, T. Farias, *Energy Convers. Manag.* 50 (2009) 1735.
25. R. Graham, S. Unnasch, E. Kassoy, R. Counts, C. Powars, L. Browning, D. Taylor, J. Smith, et al., *Comparing the Benefits and Impacts of Hybrid Electric Vehicle Options*, Electric Power Research Institute (EPRI), 2001.
26. A. Simpson, 22nd International Battery, Hybrid and Fuel Cell Electric Vehicle Symposium and Exhibition, Yokohama, Japan, 2006.
27. M. Anderman, F.R. Kalhammer, D. MacArthur, *Advanced Batteries for Electric Vehicles: An Assessment of Performance, Cost, and Availability*, California Air Resources Board, Sacramento, CA, 2000.
28. M. Duvall, L. Browning, F. Kalhammer, W. Warf, D. Taylor, M. Wehrey, N. Pinsky, *Advanced Batteries for Electric-Drive Vehicles: A Technology and Cost-Effectiveness Assessment for Battery Electric Vehicles, Power Assist Hybrid Electric Vehicles, and Plug-in Hybrid Electric Vehicles*, Electric Power Research Institute (EPRI), 2004.
29. L. Gaines, R. Cuenca, *Costs of Lithium-Ion Batteries for Vehicles*, Center for Transportation Research, Energy Systems Division, Argonne National Laboratory, Argonne, IL, 2000.
30. A. Vyas, D. Santini, *HEV Cost Analysis for the EPRI Working Group*, Argonne National Laboratory, Argonne, IL, 2000.
31. R.M. Cuenca, L.L. Gaines, A. Vyas, *Evaluation of Electric Vehicle Production and Operating Costs*, Argonne National Laboratory, Argonne, IL, 1999.
32. National Research Council (NRC), *Review of the Research Program of the FreedomCar and Fuel Partnership*, Washington, D.C., 0-309-09730-4, 2005.
33. Energy and Environmental Analysis Inc. (EEA), *Analysis and Forecast of the Performance and Cost of Conventional and Electric-Hybrid Vehicles*, Contract No. 500-00-002 (WA 8), 2005.
34. T.E. Lipman, M.A. Delucchi, *Transport. Res. D* 11 (2006) 115.
35. T.E. Lipman, M.A. Delucchi, *Retail and Lifecycle Cost Analysis of Hybrid Electric Vehicle Designs*, UCD-ITS-RR-03-01, Institute of Transportation Studies, University of California, Davis, April 2003.
36. A.F. Burke, *Proc. IEEE* 95 (2007) 806.
37. U.S. Department of Energy, *Hybrid Cost Calculator*, Alternative Fuels & Advanced Vehicle Data Center, National Renewable Energy Laboratory, 2008.
38. US Bureau of Labor Statistics, *Consumer Price Index*, Government online database, 2008.
39. J. Gonder, T. Markel, *SAE World Congress & Exhibition*, Detroit, MI, 2007.
40. J. Gonder, T. Markel, A. Simpson, M. Thornton, *Transport. Res. Record* 2017 (2007) 26.
41. A. Burke, *Electric and Hybrid Vehicle Design and Performance*, in: M. Kutz (Ed.), *Environmentally Conscious Transportation*, John Wiley & Sons, Inc., Hoboken, NJ, 2008, pp. 129–190.
42. K. Parks, P. Denholm, T. Markel, *Costs and Emissions Associated with Plug-in Hybrid Electric Vehicle Charging in the Xcel Energy Colorado Service Territory*, National Renewable Energy Laboratory, NREL/TP-640-41410, 2007.
43. R.J. Sexton, N.B. Johnson, A. Konakayama, *J. Consum. Res.* 14 (1987) 55.
44. F.A. Wolak, *Residential Customer Response to Real-Time Pricing: The Anaheim Critical Peak Pricing Experiment*, Center for the Study of Energy Markets, UC Berkeley, 2007.
45. K. Herter, S. Wayland, *Energy* 25 (2009) 1561.
46. S. Lutzenhiser, J. Peters, M. Moezzi, J. Woods, *Beyond the Price Effect in Time-of-Use Programs: Results from a Municipal Utility Pilot, 2007–2008*, International Energy Program Evaluation Conference, Portland, OR, 2009.
47. F.D. Lomax, B.D. James, G.N. Baum, C.E. Thomas, *Detailed Manufacturing Cost Estimates for Polymer Electrolyte Membrane (PEM) Fuel Cells for Light Duty Vehicles*, Contract DE-AC02-94CE50389, Directed Technologies, Inc., Arlington, VA, August 1998.
48. B.D. James, C.E. Thomas, J. Ho, F.D. Lomax, Jr., *DFMA Cost Estimates of Fuel-Cell/Reformer Systems at Low/Medium/High Production Rates*, part II.F. of Fuel Cells for Transportation, FY 2001 Progress Report, U.S. Department of Energy Office of Transportation Technologies, December 2001, pp 44–49.
49. B.D. James, J.A. Kalinoski, *Mass Production Cost Estimation for Direct H<sub>2</sub> PEM Fuel Cell System for Automotive Applications*, DOE Hydrogen Program 2007 Annual Merit Review Proceedings, Project ID:FC28, Arlington, VA, May 15–18, 2007.



50. D. Arthur. Little (ADL), Cost Analysis of Fuel Cell System for Transportation, Baseline System Cost Estimate, Task 1 and 2 Final Report to the U.S. Department of Energy, Report 49739, Cambridge, MA, March 2000.
51. E.J. Carlson, J.H.J. Thijssen, Cost Analyses of Fuel Cell Stacks/Systems, part IV.A.4. of Hydrogen, Fuel Cells and Infrastructure Technologies, FY 2002 Progress Report, U. S. Department of Energy, Office of Hydrogen, Fuel Cells, and Infrastructure Technologies, Washington, D.C., November 2002, pp. 279–282.
52. S. Lasher, J. Sinha, Y. Yang, S. Sriramulu, Direct Hydrogen PEMFC Manufacturing Cost Estimation for Automotive Applications, DOE Hydrogen Program 2007 Annual Merit Review Proceedings, Reference D0362, Arlington, VA, May 15–18, 2007.
53. Y. Sun, J.M. Ogden, M.A. Delucchi, Societal Lifecycle Buy-Down Cost of Hydrogen Fuel-Cell Vehicles, *Transport. Res. Record* (2010, in press).
54. F. Mitlitsky, A.H. Weisberg, B. Myers, Vehicular Hydrogen Storage Using Lightweight Tanks, Proceedings of 2000 U.S. DOE Hydrogen Program Review, NREL/CP-570-28890, National Renewable Energy Laboratory, Golden, CO, 2000.
55. TIAX LLC, Cost Analysis of Fuel Cell Systems for Transportation — Compressed Hydrogen and PEM Fuel Cell System, Discussion Fuel Cell Tech Team FreedomCar, Detroit, MI, October 20, 2004.
56. A.R. Abele, Quantum Hydrogen Storage Systems, California ARB ZEV Technology Symposium, September 25–27, 2006.
57. S. Lasher, K. McKenney, Y. Yang, B. Rancatore, S. Unnasch, M. Hooks (TIAX LLC) Analyses of Hydrogen Storage Materials and on-Board Systems, DOE Merit Review, May 17, 2007.
58. M.A. Delucchi, Advanced-Vehicle Cost and Energy Use Model: Overview of AVCEM, UCD-ITS-RR-05-17(1), Institute of Transportation Studies, University of California, Davis, October 2005.
59. K. Haraldsson, On Direct Hydrogen Fuel Cell Vehicles — Modeling and Demonstration, Doctoral Thesis, KTH — Royal Institute of Technology, Department of Chemical Engineering and Technology Energy Processes, Stockholm, Sweden, 2005.
60. M.A. Weiss, J.B. Heywood, A. Schafer, V.K. Natarajan, Comparative Assessment of Fuel Cell Cars, Massachusetts Institute of Technology, Laboratory for Energy and the Environment, MIT LFEE 2003-001 RP, February 2003.
61. D.L. Greene, P.N. Leiby, B. James, J. Perez, M. Melendez, A. Milbrandt, et al., Analysis of the Transition to Hydrogen Fuel Cell Vehicles & the Potential Hydrogen Energy Infrastructure Requirements, ORNL/TM-2008/30, Oak Ridge National Laboratory, Oak Ridge, TN, March 2008.
62. National Research Council, Transitions to Alternative Transportation Technologies — A Focus on Hydrogen, The National Academies Press, Washington, D.C., 2008.
63. C. European, Well-to-Wheels Analysis of Future Automotive Fuels and Powertrains in the European Context, EUCAR/JRC/CONCAWE, Well-to-Wheels Report Version 2c, March 2007.
64. D.L. Greene, P.N. Leiby, Integrated Analysis of Market Transformation Scenarios with HyTrans, Oak Ridge National Laboratory, Oak Ridge, TN, ORNL/TM-2007/094, June 2007.
65. B. James, HyPro: Modeling the H<sub>2</sub> Transition, Prepared for the DOE Hydrogen Program, Directed Technologies Inc., May 9, 2007.
66. C. Yang, J. Ogden, *Int. J. Hydrogen Energy* 32 (2007) 268.
67. J.M. Ogden, R.H. William, E.D. Larson, *Energy Policy* 32 (2004) 7.
68. J.-Y. Lee, M. Yoo, K. Cha, T.W. Lim, T. Hur, *Int. J. Hydrogen Energy* 34 (2009) 4243.
69. C. Yang, J.M. Ogden, Steady State Model of Hydrogen Infrastructure for US Urban Areas, Institute of Transportation Studies, University of California, Davis, 2008.
70. M.Q. Wang, GREET 1.5 — Transportation Fuel-Cycle Model: Volume 1: Methodology, Development, Use, and Results, Report ANL/ESD-39, Argonne National Laboratory, Argonne, IL, August 1999.
71. A. Rabl, J.V. Spadaro, *Annu. Rev. Energy Environ.* 25 (2000) 601.
72. M.A. Delucchi, *J. Transp. Econ. Policy* 34 (2000) 135.
73. M.A. Delucchi, J. Murphy, *Energy Policy* 36 (2008) 2253.
74. P.N. Leiby, Estimating the Energy Security Benefits of Reduced U.S. Oil Imports, ORNL/TM-2007/028, Oak Ridge National Laboratory, Oak Ridge, TN, February 28, 2007.
75. M.A. Delucchi, D.R. McCubbin, The Contribution of Motor Vehicles and Other Sources to Ambient Air Pollution, UCD-ITS-RR-96-3 (16) rev. 2, Institute of Transportation Studies, University of California, Davis, 2004.





# Relative Fuel Economy Potential of Intelligent, Hybrid and Intelligent–Hybrid Passenger Vehicles

Chris Manzie<sup>1</sup>

Department of Mechanical Engineering, University of Melbourne, Victoria, Australia

## Contents

1. Introduction	61
2. Vehicle Models for Simulation Studies	65
2.1 Conventional powertrain vehicle model	65
2.2 Mild hybrid powertrain vehicle model	66
2.3 Full hybrid powertrain vehicle model	67
2.4 Initial performance comparisons	69
3. Velocity Scheduling Using Traffic Preview	70
3.1 Optimal velocity profiles using simplified models	70
3.2 Online velocity scheduling algorithms	73
3.3 Relative fuel saving potential through velocity shaping	77
4. Hybrid Vehicles with Telematics	80
5. Optimal Management of Hybrid Vehicles with Telematics	82
5.1 Formulation of the optimisation problem	82
6. Conclusions and Future Opportunities	88
Acknowledgements	89
Nomenclature	89
References	89



## 1. INTRODUCTION

Passenger safety has been a critical feature for automobile manufacturers as both consumers and legislators seek reduced risk in personal transportation. While the initial focus on passenger safety were passive approaches such as seat belts and vehicle crumple zones that mitigate the damage of a collision, more recently active devices (such as Adaptive Cruise Control) have been used to avoid collisions altogether. These active systems must typically gather information about the surrounding traffic environment through the use of sensors such as on-board radar.

<sup>1</sup> Corresponding author: manziec@unimelb.edu.au

The cost revolution in telematics experienced over the last decade has meant that these sensors are no longer the sole domain of high-end vehicles, and with the expected development of complementary metal-oxide-semiconductor (CMOS)-based radar-on-a-chip systems (see, e.g., [1]), these systems are set to become orders of magnitude cheaper and more prevalent among production vehicles.

Furthermore, with mobile communication systems now commonplace, the prospect of inter-vehicle and even vehicle-to-infrastructure communication pathways is well established and has been demonstrated in full-scale trials (e.g. [2, 3]). While automated highways and platooning scenarios are unlikely to eventuate in the near term, the smart infrastructure technology developed is being used for online traffic management systems in numerous countries already. Presently, systems such as Signal Coordination in Regional Areas of Melbourne (SCRAM) obtain information about traffic flows in urban environments automatically for use in scheduling traffic signals, so it is conceivable that this information could be made available to a suitably equipped vehicle. The information transfer from the network to the vehicle will also have clear advantages in route selection, as discussed in [4]. Meanwhile, potential sensor reduction in vehicles is also being facilitated through research efforts that look at enabling vehicle-to-vehicle communication using radar [5]. Consequently, a significant amount of information about the traffic flow a vehicle will shortly encounter may soon be available and there is the potential for this to enable other opportunistic use.

While passenger safety and large-scale traffic management have largely been responsible for the introduction of telematics to passenger vehicles, in parallel there has been a growing push for better fuel saving at the individual vehicle level on the part of consumers driven by both the rising cost of fuel and the concern over climate change. Hybrid powertrains represent a viable interim solution that overcomes the range and battery life issues that currently plague electric-only vehicles. The downside of a hybrid drivetrain is that the vehicle cost increases significantly, as two propulsion systems must be incorporated into the one vehicle.

An alternative, or even complementary, solution to powertrain hybridisation is to use the telematic technology already filtering into vehicles to improve fuel economy. In the road freight industry, the potential to include future information about road grade has been investigated [6, 7] by scheduling vehicle velocity and gear changes during highway driving. Improvements in fuel economy of up to 3.5% and a 40% reduction in gear changes were observed following the use of road grade prediction algorithms and global positioning system (GPS) data.

The majority of passenger driving is completed in urban scenarios and average journeys are around 10 minutes. This is a primary motivator for hybridising powertrains, as features such as engine shutoff when the vehicle is stationary and regenerative braking both provide fuel saving potential relative to a conventional powertrain. During highway driving, the hybrid vehicle will not offer fuel saving relative to an equivalent

conventional powertrain vehicle, as there is additional mass that must be carried, and the ability to recharge the batteries during regenerative braking events is minimal. Consequently, any comparison between a hybrid and a conventional vehicle should be conducted primarily on cycles featuring urban driving.

This is the focus of the work in [8, 9], where the relative fuel economy benefit of velocity scheduling using traffic flow information is assessed. While there are numerous urban drive cycles available, the work presented here will focus on three specific types. The first is the New European Drive Cycle (NEDC), which is used as it forms the regulatory cycle in both Australia and Europe.

As seen in Fig. 3.1, the NEDC is characterised by cyclical events and as a result has long been criticised for being unrepresentative of real-world driving dynamics [10]. Consequently, two further drive cycles are also considered – the United States Federal Test Procedure (US-FTP) drive cycle (Fig. 3.2) and the Australian urban drive cycle (Fig. 3.3).

In the absence of test vehicles, these three drive cycles will be assumed representative of the driving pattern of a typical vehicle in the later analysis, including how the typical vehicle reacts to existing traffic management signals. The critical assumption that will be made is the vehicle following this typical vehicle has some preview information about its future velocity profile available through the use of telematics. A conventional vehicle able to make use of the previewed traffic flow information to schedule its velocity profile will be designated hereon as an ‘intelligent vehicle’. In the case of a hybrid powertrain, the preview information may also be used to schedule the torque split between the

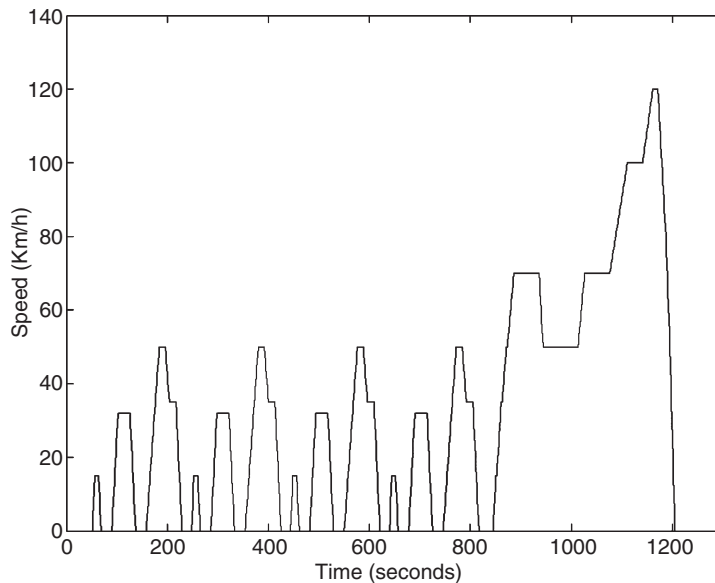


**Figure 3.1** The New European Drive Cycle (NEDC).

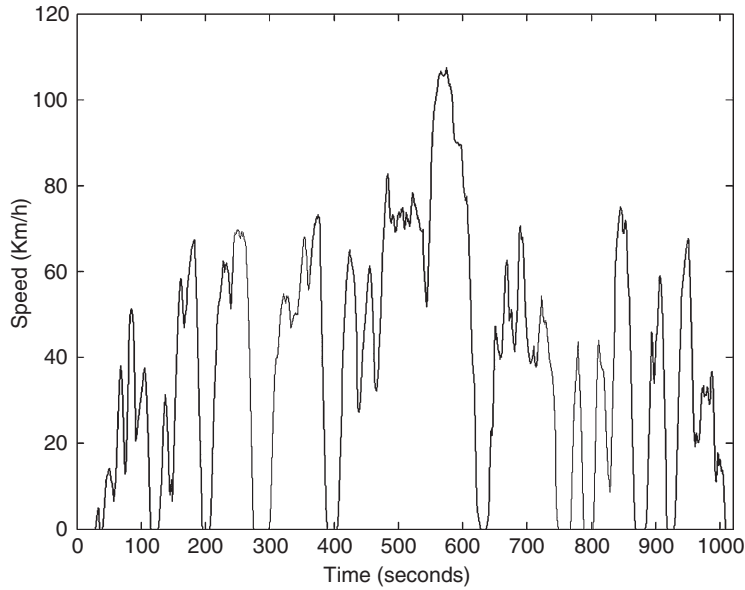


**Figure 3.2** The United States Federal Test Procedure (US-FTP) drive cycle.

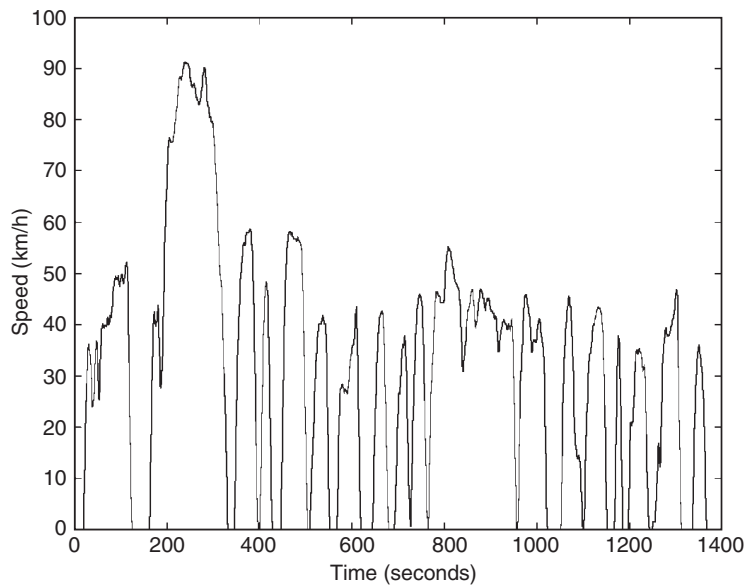


**Figure 3.3** The Australian urban drive cycle.

internal combustion engine and the electric motor, and such a vehicle will be designated an ‘intelligent-hybrid’. While this preview information is simply assumed available in this study, the algorithms required to fuse data from the different sources (e.g., on-board

devices, inter-vehicle communication systems, GPS and infrastructure–vehicle communication pathways) are discussed by several authors, for example [11].

To simulate fuel use of vehicles over the drive cycles, software packages such as ADVISOR [12] or PSAT [13] may be used. The ADVISOR software package provides a deterministic simulation environment based on quasi-static maps to represent functions such as fuel use in terms of engine speed and manifold pressure. While all dynamics are ignored using this approach, it does allow for hybrid and conventional powertrain vehicles to be simulated in one software package and has been found to give reasonably accurate fuel economy results over a specified drive cycle. Consequently, it has been used as the software tool in the work described here. The vehicle models used are specified in the following section.



## 2. VEHICLE MODELS FOR SIMULATION STUDIES

The choice of vehicle to be used as a benchmark is reasonably arbitrary, as the initial comparison here is not the absolute fuel consumption levels, but the fuel economy percentage gains possible following incorporation of telematics.

The vehicle treated as the benchmark is a 4.0l, six-cylinder sedan, representative of the most common vehicle size sold in the Australian market over the decade from 1995 to 2005. This vehicle was chosen as access to much of the data (including static maps of fuel use as a function of operating condition) required to develop the quasi-static simulation model which is described in [14] or was available through the ACART collaborative research centre.

### 2.1 Conventional powertrain vehicle model

The key parameters of the benchmark vehicle model corresponding to the 2002 production version of the Ford Falcon are listed in Table 3.1 and are very close to the current production model, with the exception that a six-speed gearbox is now used. The static maps corresponding to fuel use and power as functions of engine operating point also differ slightly from the 2009 production version resulting in approximately 5% improvement in fuel economy over an urban drive cycle and 4% higher peak power following nearly a decade of refinement. Thus, despite these slight differences between the models, given the detail available the model serves as a reliable benchmark for a conventional powertrain vehicle to be used in comparison with an equivalent hybrid powertrain.

A hybrid configuration of this vehicle does not currently exist, and to create a simulation model from scratch requires some informed guesses about what such a powertrain may look like. In the first instance, a mild hybrid is the most likely to appear in the marketplace but will not offer the comprehensive fuel economy benefits of full powertrain hybridisation. Both levels of hybrid vehicle model are described in the following two sections.

**Table 3.1** Baseline vehicle configuration

Total weight	1,642 kg
Chassis weight	1,000 kg
Frontal area	2.45 m <sup>2</sup>
Co-efficient of drag	0.366
Vehicle weight distribution	Front 55%, rear 45%
Centre of mass height	0.5 m
Vehicle length	5.00 m
Transmission	Manual, 5 speed
Transmission efficiency	95% (assumed constant through all gears)
Gear ratios	3.5:2.14:1.39:1:0.78
Final drive ratio	2.92
Gear changes	1 → 2 and 2 → 1 @ 24 km/hr 2 → 3 and 3 → 2 @ 40 km/hr 3 → 4 and 4 → 3 @ 64 km/hr 4 → 5 and 5 → 4 @ 75 km/hr
Tyre rolling radius	0.314 m
Tyre inertia	8,923 kg m <sup>2</sup>
Tyre pressure, $T_p$	240 kPa

## 2.2 Mild hybrid powertrain vehicle model

Many vehicle manufacturers are currently adopting mild hybrids as a precursor to facilitate the transition towards full hybrid vehicles. Mild hybrids are characterised by a conventional-sized internal combustion engine coupled with an electric motor of up to 15 kW. The mild hybrid is relatively cost-effective as the additional cost of the electric motor is offset by the removal of the starter motor and the alternator from the vehicle, while retaining the larger internal combustion engine does not require significant changes to existing manufacturing lines. Furthermore, consumer demand for large sedans and sports utility vehicles in non-European markets remains high, thereby favouring configurations with larger internal combustion engines.

Since the electric motor size in the mild hybrid is smaller than in the full hybrid configuration, it cannot be used as widely through the drive cycle and hence the torque split control design is simplified. Typically, in a mild hybrid configuration, the electric motor is used only for starting, to enable engine shutoff when the vehicle is stationary, and for some small power assist. There is clearly a relative reduction in motor utility compared to a full hybrid; however, fuel savings of the order of 10–15% may be observed relative to a non-hybrid vehicle. As an example, GM claims that by implementing a simple mild hybrid system on the 2007 model Silverado can achieve an overall fuel saving of 12%.

To simulate the mild hybrid vehicle, a 15 kW electric motor was chosen and the conventional vehicle described in Section 2.1 had its internal combustion engine downsized by an equivalent amount, thereby maintaining the performance characteristics of the original vehicle. The resulting fuel economy improvements through mild

hybridisation, primarily due to engine shutoff being enabled when the vehicle is stationary, are investigated in Section 2.4.

While the mild hybrid can be specified in a reasonably straightforward manner (i.e., downsizing the engine power by the equivalent electric motor power), the full hybrid has greater degrees of freedom in the configuration and requires careful construction, particularly if the performance of the vehicle is to be maintained. The solution to this challenging optimisation problem is the key to establish the best possible hypothetical hybrid performance and is the subject of the following section.

### 2.3 Full hybrid powertrain vehicle model

The constraint on the hypothetical full hybrid vehicle was that the drivability and performance of the original vehicle should not be significantly altered by hybridisation. A parallel hybrid configuration was deemed an appropriate choice given the power requirements of the baseline vehicle of Section 2.1. The parallel configuration allows the torque produced by both (or either) of the power sources to propel the wheels and is therefore considered the most realistic alternative. While some fuel economy benefits may be possible through serial connections of the electric motor and internal combustion engine, to achieve the power requirements of the benchmark vehicle (arising from the performance specifications) in a series, hybrid configuration would mean that the size and expense of the electric motor would be impractical.

Having decided on a parallel hybrid powertrain, the next step is to decide on the relative size of the electric motor and the internal combustion engine. This process begins with the selection of base engine and motor characteristics that are in the rough ballpark of the final elements on the hypothetical configuration. Provided the change is not too severe, linear scaling to each component can be applied during the optimisation process to produce the ideal combination. Engine downsizing is a well-known way of improving fuel efficiency in an internal combustion engine through reducing the frictional losses and weight, while turbocharging is used to maintain peak power from the engine [15]. Consequently a 1.3l, 71 kW turbocharged engine was chosen as a suitable starting point for the hybrid's internal combustion engine and scaled appropriately. A 49 kW permanent magnet brushless DC motor was chosen as the base motor to be scaled and the electric power was provided through nickel-metal hydride (NiMH) battery modules.

The optimal scaling of the internal combustion engine and the electric motor, along with the number of battery modules, must be performed such that the vehicle's performance characteristics are not unduly impacted. Constraints on the novel hybrid vehicle's acceleration through different speed ranges and the towing ability of the vehicle up a slope were necessary to match the vehicle performance, while other constraints such as the change in state of charge of the battery using a default torque split strategy are also

necessary. The optimal parameters were then obtained by minimising the fuel use over different drive cycles subject to these constraints using a particle swarm approach [16].

Two key features arose out of the optimisations performed. Firstly, if the vehicle experiences constant stop–start speed profiles (as in real-world urban driving), the optimal fuel economy is achieved with an electric motor of only slightly larger power capability than the internal combustion engine. Secondly, if there is minimal stop–start behaviour in the drive cycle (as in highway driving), the optimal configuration includes only a small electric motor, as the benefit of hybridisation is counteracted by the additional fuel required to transport the mass of the battery pack and electric motor. For drive cycles combining highway and urban components, the optimal configuration has an electric motor that monotonically decreases in size with the proportion of highway driving.

As the objective here is to establish the optimal hybrid configuration for urban driving (an environment best suited to hybrid vehicles), the vehicle was chosen to have an almost equal power ratio between the electric motor and the internal combustion engine, as listed in Table 3.2. However, it is worth noting that a production vehicle would probably have a larger internal combustion engine to electric motor ratio in order to achieve a balance between urban and highway cycles. As a consequence, the full hybrid fuel economies obtained using this model would represent the upper limit for a vehicle matching the performance characteristics of the benchmark described in Section 3.1.

The optimisation of configuration performed above requires a fixed torque split control architecture, and a rule-based algorithm was arbitrarily used during this process. Heuristic torque split control strategies include other rule-based [17] or fuzzy logic [18] designs that typically utilised the high low-speed torque characteristic of the electric motor. These approaches helped enable early hybrid implementations; however they potentially do not maximise fuel economy. In the initial results to be presented, a simple default strategy was used which (subject to constraints on the battery state of charge) uses the electric motor for slow city driving condition and assists the engine for peak acceleration, hill climbing and extremely fast highway driving conditions. Furthermore, the electric motor can act in reverse mode to become a generator to provide regenerative braking that recharges the on-board batteries.

As a possible alternative strategy considered later in this chapter, model-based methods for torque split control have been suggested as they may enable optimal fuel

**Table 3.2** Results of optimisation for hybrid vehicle configuration

IC engine power (scaled from a TC 1.31, 71 kW engine)	66 kW
Electric motor power (scaled from 49 kW PM brushless motor)	68 kW
Number of battery modules ( <i>D</i> size 1.2 V NiMH – 6 cells/module)	194



consumption. Dynamic programming approaches for series [19] and parallel hybrid configurations [20] may produce for the global optimal power split strategy over an entire drive cycle. While useful in identifying the global optimum, these approaches are not suited to real-time implementation, as they require *a priori* knowledge of the full drive behaviour, which is clearly infeasible.

More recent approaches have focussed on the problem of real-time applicability of the algorithm by approximating the complete optimal problem. One approach that improves practicality is centred on calculating the equivalent fuel consumption of the battery at all points in time and consequently allows the fuel and electrical energy to be combined in a single cost. This cost is then minimised instantaneously at each operating point using what is termed in [21] as an Equivalent Consumption Minimisation Strategy (ECMS) – however, the scaling factor between fuel and electrical energy use requires calibration using known drive cycle information.

The ability of ECMS to cope with unforeseen future driving behaviour was improved in [22]. In this work, the authors introduced probability factors to the equivalence factor to account for the future charging/discharging behaviour of the electrical energy. This instantaneous optimisation strategy can be applied online but is weak in reflecting the fuel–electric dependency at each operating point of the engine and motor because it assumes the linear equivalency of the fuel and electric energy obtained by averaging over the whole known drive cycle.

Alternative torque split strategies will be investigated in conjunction with velocity scheduling in the later part of this chapter.

## 2.4 Initial performance comparisons

Before considering the effect of any telematics, the baseline performance of each powertrain configuration described in Sections 2.1–2.3 was compared in terms of fuel economy over the three urban drive cycles. To prevent distortions in the fuel economy of the hybrid vehicles caused by unsustainable electric motor usage, the battery state of charge at the end of each cycle was constrained to be within 0.5% of its initial condition. The resulting economies are presented in Table 3.3.

**Table 3.3** Fuel economies for benchmark and hybrid vehicles

Drive cycle	Equivalent fuel economy (l/100 km)		
	Benchmark vehicle	Mild hybrid	Full hybrid
Australian urban	11.8	10.4 (11.9%)	10.1 (14.4%)
US-FTP	10.8	9.2 (14.8%)	8.2 (24.0%)
NEDC	10.6	9.3 (12.3%)	8.5 (19.8%)

Percentage improvement relative to the benchmark vehicle is given in parentheses.

In the case of the mild hybrid configuration, the vehicle's fuel economy improved from 11.81/100 km over the Australian urban cycle to 10.41/100 km as a result of this exercise. Over the other two drive cycles, similar improvement was noticed following hybridisation. These efficiency increases in the range of 10–15% are typical of the reported gains through mild hybridisation of a large vehicle and are primarily due to engine shutoff being enabled when the vehicle is stationary.

For the optimised hybrid configuration, the fuel economy is further improved for all three drive cycles, with 15–25% reduction observed relative to the benchmark conventional vehicle. Naturally, the fuel economy over urban drive cycles could be even better for a production version of all vehicles if the performance constraints imposed during the optimisation process were relaxed partially, or if further development in reducing the vehicle coefficient of drag or weight was achieved.

Having established the two levels of hybrid configuration and characterised their performance over different urban drive cycles, the performance of the conventional vehicle with its velocity trajectory shaped using surrounding information can be considered. The next section discusses velocity scheduling algorithms intended to minimise fuel consumption.



### 3. VELOCITY SCHEDULING USING TRAFFIC PREVIEW

There are several approaches that can be taken to specify the velocity profile to be used by the intelligent vehicle. In the first instance, the vehicle model can be simplified appropriately to allow the application of generic optimisation approaches such as Pontryagin's minimum principle [23]. This avenue is explored in Section 3.1. The alternative is to develop ad hoc approaches, but test these on more realistic vehicle models. This latter approach is discussed in Section 3.2 and allows more complexity to be investigated in the models and the results.

#### 3.1 Optimal velocity profiles using simplified models

If complete trip information is known *a priori*, optimal control theory may be used to develop a vehicle velocity profile that maximises fuel economy [24, 25]. In order to make the problem tenable for parametric solutions using Pontryagin's Minimum Principle, the following simplifying assumptions are necessary.

*Assumption 1:* The trip duration,  $T$ , and the final position of the vehicle,

$$x(T) = \int_0^T v(\tau) d\tau, \text{ are known at the commencement of the journey.}$$

*Assumption 2:* The gear ratio of the vehicle is fixed.

*Assumption 3:* The propulsive force generated by the engine is a linear function of the fuel use,  $m_{\text{fuel}}(t)$ , and vehicle speed,  $v(t)$ , according to:

$$F(t) = c_1 \frac{m_{\text{fuel}}(t)}{v(t)} - F_0 \quad [3.1]$$

The constant term,  $c_1$ , includes the internal efficiency of the engine and lower heating value of the fuel. The term  $F_0$  represents the engine braking force.

*Assumption 4:* The available propulsive force is constrained to the range:

$$F(t) \in [F_{\min}, F_{\max}] \quad [3.2]$$

*Assumption 5:* The vehicle speed and velocity are represented by simplified one-dimensional dynamic equations:

$$m_{\text{veh}} \frac{d}{dt} v(t) = F(t) - k_1 - k_2 v(t)^2 \quad [3.3]$$

$$\frac{d}{dt} x(t) = v(t) \quad [3.4]$$

The coefficient  $k_1$  represents constant load terms corresponding to road grade and rotating masses within the engine and  $k_2$  represents the coefficient of aerodynamic drag.

The average fuel economy is given by the total fuel used divided by the distance travelled and thus the following cost function may be proposed for minimisation:

$$J = \frac{\int_0^T m_{\text{fuel}}(\tau) d\tau}{\int_0^T v(\tau) d\tau} \quad [3.5]$$

From assumptions 1–5, the only schedulable input for the minimisation of [3.5] is the propulsive force applied by the vehicle,  $F(t)$ . To determine the optimal propulsive force,  $F^*(t)$ , it follows from assumption 1 and Eq. 3.5 that the problem can be restated as:

$$F^*(t) = \arg \min \int_0^T F(\tau) v(\tau) d\tau \quad [3.6]$$

subject to static and dynamic constraints [3.2]–[3.4].

The Hamiltonian for this problem can be stated in terms of the system parameters and adjoint state variables,  $p_1$  and  $p_2$ , as

$$H(t) = F(t) \left( v(t) + \frac{p_1(t)}{m_{\text{veh}}} \right) + p_1(t) \left( \frac{-k_1 - k_2 v(t)^2}{m_{\text{veh}}} \right) + p_2(t) v(t) \quad [3.7]$$

The adjoint state variable dynamic equations are given by

$$\frac{dp_1(t)}{dt} = 2k_2 v(t) \frac{p_1(t)}{m_{\text{veh}}} - F(t) - p_2(t) \quad [3.8]$$

$$\frac{dp_2(t)}{dt} = 0 \quad [3.9]$$

Pontryagin's minimum principle [23] states that for the system trajectory to be optimal, the following inequality must hold

$$H(F^*(t), v^*(t), x^*(t)) \leq H(F(t), v^*(t), x^*(t)) \quad \forall F(t) \quad [3.10]$$

The only place the schedulable control,  $F(t)$ , enters the Hamiltonian equation is through multiplication by  $\left( v(t) + p_1(t)/m_{\text{veh}} \right)$ . Defining  $\sigma \equiv \left( v(t) + (p_1(t)/m_{\text{veh}}) \right)$ , it follows from [3.2] that the inequality [3.10] can only be satisfied if the optimal propulsive force is described by

$$F^*(t) = \begin{cases} F_{\max} & \sigma(t) < 0 \\ F(t) & \sigma(t) = 0 \\ F_{\min} & \sigma(t) > 0 \end{cases} \quad [3.11]$$

This solution indicates that only three different propulsive forces make up the optimal fuel trajectory – a maximal force (acceleration) phase, a minimal force (acceleration) phase representing coasting and a singular phase when  $\sigma = 0$ . During the singular phase of the optimal trajectory, it is clear from the definition of  $\sigma$  that

$$v^*(t) = -\frac{p_1(t)}{m_{\text{veh}}} \quad [3.12]$$

To remain in the singular phase, it is also required that  $\sigma = 0$ . This second condition means that the following equality must hold:

$$0 = \frac{d}{dt} v^*(t) + \frac{1}{m_{\text{veh}}} \frac{d}{dt} p_1(t) \quad [3.13]$$

Substituting Eqs. [3.3] and [3.8] into [3.13] results in the algebraic equation:

$$\frac{1}{m_{\text{veh}}} \left( F(t) - k_1 - k_2 v^*(t)^2 \right) + \frac{1}{m_{\text{veh}}} \left( 2k_2 v^*(t) \frac{p_1(t)}{m_{\text{veh}}} - F(t) - p_2(t) \right) = 0 \quad [3.14]$$

Substitution of [3.12] to remove  $p_1(t)$  from [3.14] then leads to the solution for the velocity during the singular phase being given by

$$v^*(t)^2 = \frac{-p_2 - k_1}{3k_2} \quad [3.15]$$

Since  $p_2$  is constant from [3.9], Eq. [3.15] indicates that the velocity along the singular phase is also constant. Accordingly, the overall velocity trajectory for a vehicle moving a known distance in fixed time is optimal when it only encompasses three phases – a maximal acceleration phase, a constant velocity phase and a maximal deceleration phase. Furthermore, it can be shown that there will be at most one sign change in  $\sigma(t)$ , and thus each of these velocity phases can only occur at most once during the optimal trajectory.

### 3.2 Online velocity scheduling algorithms

The optimal velocity principle developed in Section 3.1 was adapted for continual online use in [9], where the velocity profile of an intelligent vehicle was modified using information about the surrounding traffic flow according to the intelligent vehicle velocity modification (IVVM) algorithm presented below.

#### **Algorithm 1: Intelligent Vehicle Velocity Modification (IVVM) Algorithm (Unconstrained Case).**

Estimate lead vehicle position at time  $T_p$  in the future according to

$$\hat{x}_{\text{lead}}(t + T_p) = x_{\text{lead}}(t) + \alpha \sum_{i=1}^{T_p/\Delta} \hat{v}_{\text{lead}}(t + i\Delta)\Delta \quad [3.16]$$

where  $\Delta$  is the sampling period (considered uniform) and  $\alpha$  is a conversion constant. In order to reach this predicted position with minimum stop–start behaviour, the intelligent vehicle should attempt to use a constant speed,  $v(t)$ , calculated as follows:

$$v(t) = \frac{\hat{x}_{\text{lead}}(t + T_p) - x_{\text{lead}}(t)}{\alpha T_p} \quad [3.17]$$

This process, using Eqs. 3.16 and 3.17, is repeated every time new information becomes available.

A comparison of the IVVM algorithm with the optimal result in [3.12] and [3.15] calculated from the simplified vehicle and powertrain model highlights several important considerations.

Firstly, both approaches advocate the use of a constant velocity phase although by necessity the velocity using the IVVM algorithm is continually updated each time new traffic information becomes available. The constant velocity calculated using the IVVM is essentially based on the vehicle reaching the vehicle in front at the end of the horizon and is thus a relative position-based algorithm. On the other hand, the optimal result from [3.15] is not an explicit solution for the velocity and requires a numerical solution to determine the value of velocity during the singular phase. This clearly requires more complexity in implementation than the approach described in Algorithm 1, but does offer the optimal constant velocity.

The second difference between the two approaches is that the IVVM approach does not include hard acceleration and deceleration phases, and consequently the IVVM velocity profile will be smoother overall but may need to contain higher instantaneous velocities to cover the same distance in the same time. This smoother profile, as illustrated in Fig. 3.4, is a positive effect in terms of likely passenger acceptance; however, it will have some fuel penalty if assumptions 1–5 are justified. There is some doubt on the veracity of some of these simplifying assumptions used in the optimal velocity controller development (e.g., assumption 3 does not penalise hard accelerations with wide open throttle) and consequently the degree of sub-optimality of Algorithm 1 is difficult to ascertain in general.

To investigate this difference quantitatively, the resulting fuel efficiencies of the vehicle undergoing all three possible velocity trajectories (i.e., original cycle, optimal cycle and IVVM modified cycle as shown in Fig. 3.4) were measured on the Australian urban cycle. The optimal cycle by necessity requires all future trip information at the start of the trip, while 60 second traffic preview was arbitrarily chosen for the IVVM

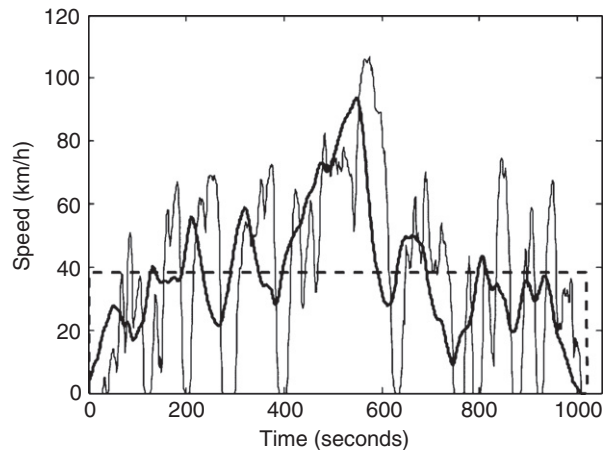


**Figure 3.4** Original Australian urban drive cycle (thin), intelligent vehicle velocity modification (IVVM) with 60 second preview (bold) and optimal trajectory (dashed) calculated from Pontryagin's minimum principle using simplified model.

algorithm. The resulting fuel economies were 11.81/100 km for the original cycle, 7.51/100 km for the IVVM cycle with 60 second preview and 7.31/100 km for the optimal cycle. This highlights that the fuel economy gain using the ‘optimal’ cycle is only slightly better than the IVVM, yet is much more intensive (to the point of infeasibility) in terms of its data requirements at the start of the trip.

As a further consideration, it is worth noting that the intelligent vehicles will not operate in complete isolation. The surrounding traffic and infrastructure will place constraints on the velocity profile that can actually be achieved. It becomes a difficult problem to include positional constraints into the optimal trajectory developed in Section 3.1; however, as the IVVM is a relative position-based algorithm, it is more easily modified in this regard. The algorithm presented as [Algorithm 2](#) below modifies the velocity trajectory to prevent overtaking, thereby ensuring that the vehicle meets all infrastructure and traffic enforced positional requirements.

### **Algorithm 2: Intelligent Vehicle Velocity Modification (IVVM) Algorithm (Overtaking Disallowed).**

**Step 1:** Find position trajectory of the vehicle in front of (leading) the intelligent vehicle over the preview duration, i.e.,

$$\hat{x}_{\text{lead}}(t + i\Delta) = x_{\text{lead}}(t) + \alpha \sum_{i=1}^j \hat{v}_{\text{lead}}(t + i\Delta)\Delta \quad \text{for } i = 1 \dots \frac{T_p}{\Delta} \quad [3.18]$$

Note that the sampling period  $\Delta$  is assumed constant, but Eq. 3.18 is readily adapted to non-uniform sampling.

**Step 2:** Set iteration number,  $j$ , to zero.

**Step 3:** For each  $j$ , find a candidate constant velocity over the next  $T_p - j$  seconds, such that the positions of the intelligent and leading vehicle are equal, i.e.  $\hat{x}(t + T_p - j\Delta) = \hat{x}_{\text{lead}}(t + T_p - j\Delta)$ . This candidate velocity is calculated according to

$$v^j(t) = \frac{\hat{x}_{\text{lead}}(t + T_p - j\Delta) - x(t)}{\alpha(T_p - j\Delta)} \quad [3.19]$$

**Step 4:** Develop a trajectory for the intelligent vehicle based on  $v^j(t)$  over the interval from the current time to  $T_p - j\Delta$ , i.e.,

$$\hat{x}(t + i\Delta) = x(t) + i\Delta\alpha v^j(t) \quad \text{for } i = 1 \dots \frac{T_p}{\Delta} \quad [3.20]$$

**Step 5:** Test whether the predicted intelligent vehicle trajectory overtakes the predicted ‘lead’ vehicle trajectory, and if necessary update the candidate constant velocity to avoid overtaking, i.e., if  $\hat{x}_{\text{lead}}(t + i\Delta) > \hat{x}(t + i\Delta)$  for  $i = 1 \dots (T_p/\Delta)$  then use  $v^j(t)$  as the intelligent vehicle’s velocity at time  $t$ . Otherwise, if  $\hat{x}_{\text{lead}}(t + i\Delta) \leq \hat{x}(t + i\Delta)$  for at least one value of  $i\Delta$ , then increment  $j$  and return to Step 3.

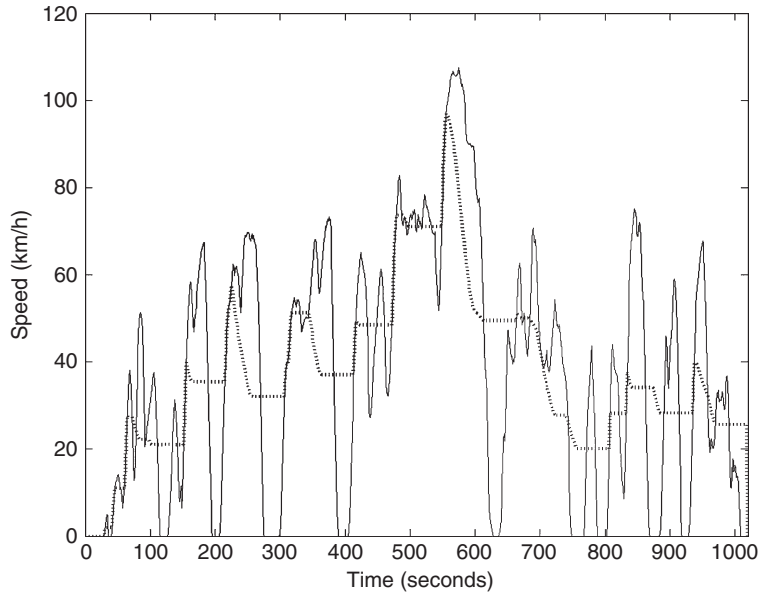


**Figure 3.5** Australian urban velocity profile (solid) and velocity profile (dotted) modified by Algorithm 2 with a traffic preview of 50 seconds.

In comparison with Algorithm 1, there are increased computational requirements associated with this modified IVVM algorithm; however, the additional complexity is very low. The effect of using Algorithm 2 is clear when the drive cycle of Fig. 3.5 is compared to the drive cycle found using Algorithm 1 (in Fig. 3.4). The inclusion of positional constraints enforces small constant velocity segments into the drive cycle, not unlike what would be expected if the optimal algorithm of Section 3.1 was employed over a subset of the drive cycle.

The satisfaction of the relative positional constraints imposed by the surrounding traffic is investigated for both IVVM algorithms, by examining the separation between the intelligent vehicle and its nominal position (if it followed the drive cycle exactly) in Fig. 3.6. It is clear that the original approach with 50-second preview information can result in the intelligent vehicle leading the traffic by as much as 200 m. This is clearly an infeasible result in many instances and is subsequently prevented using the modified algorithm. While large lags between the intelligent vehicle and the one in front are present in the high-speed region of the cycle (i.e., around 600 seconds), any overtaking is prevented. Naturally, further constraints may be imposed to avoid large gaps appearing between the intelligent vehicle and the leading traffic, although this is not pursued here.

In the following section, the fuel saving potential of velocity shaping through preview information provided by telematics is investigated, with the results placed in the context of the fuel saving achievable using an optimised hybrid configuration.



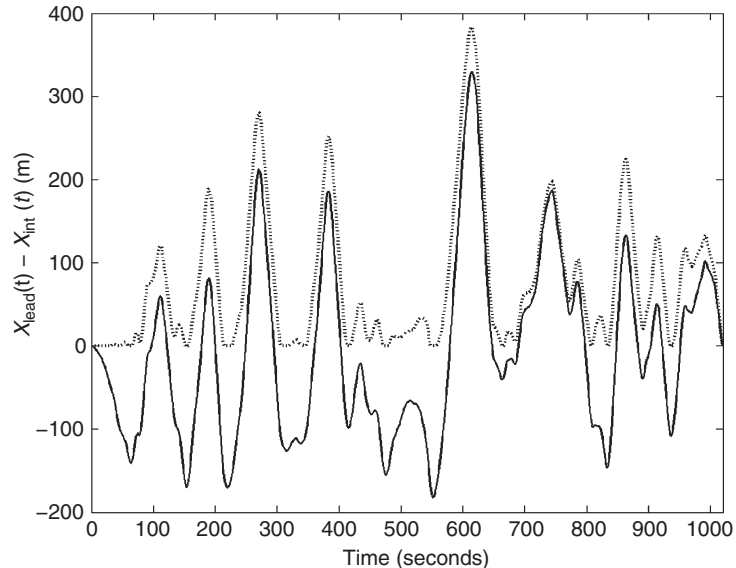


**Figure 3.6** Relative position comparisons between the lead and intelligent vehicles using Algorithm 1 (solid) and Algorithm 2 (dotted).

### 3.3 Relative fuel saving potential through velocity shaping

The fuel efficiency improvements possible through the application of the different velocity modification algorithms are now investigated. To place these numbers in context, the fuel savings are compared to those obtained through hybridising the powertrain in an optimal fashion, as discussed in Section 2.2.

The two IVVM algorithms both rely on traffic feedforward information. For the purposes of initial discussion, this is assumed available in terms of a preview *time*, that is, the intelligent vehicles velocity may be modified using information about the future traffic flow up to the preview length. Naturally, the longer the preview, the greater the possibility of adjusting the vehicle velocity favourably in terms of fuel efficiency. The downside to longer previews is the potential increase in telematic capability and associated cost.

In Figs. 3.7–3.9, the fuel economy over the three urban drive cycles is investigated for both IVVM algorithms as a function of traffic preview. The fuel economy for the optimised hybrid as identified in Table 3.3 is also shown for comparison.

There are three main points to arise out of these figures. Firstly, the fuel economy of the intelligent vehicle can match and generally better the fuel savings achievable through hybridisation. The feedforward information required to achieve this depends on the characteristics of the drive cycle, but for the real-world drive cycles that exhibit significant stop–start behaviour (the Australian urban and US-FTP), the trade-off occurs

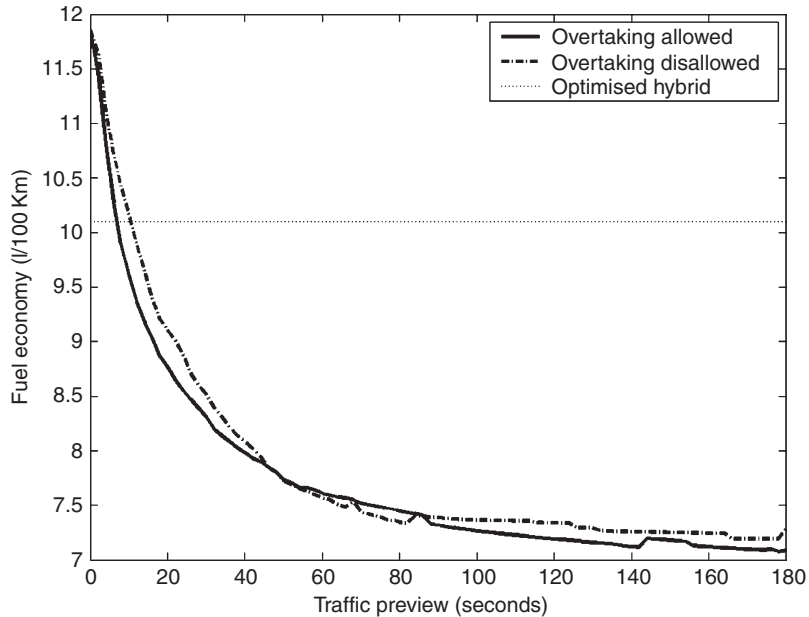


**Figure 3.7** Fuel economy as a function of preview information with overtaking allowed and disallowed using the Australian urban cycle. For reference, optimised hybrid fuel economy is also included.

at preview lengths of 7 and 60 seconds respectively. Furthermore, in all three drive cycles, the majority of the fuel saving possible through the velocity shaping occurs at relatively short previews (i.e., less than about 20 seconds). Thus, a real-world implementation would be entirely plausible and would certainly be more cost-effective than the hybrid alternative. While the results displayed for the NEDC are not as favourable in comparison with the optimal hybrid (a preview length of 182 seconds is required for the IVVM to match the hybrid’s fuel economy), the relationship between this legislative drive cycle and real-world driving is somewhat circumspect. Consequently, given the uncertainty surrounding the ability of this cycle to represent realistic driving, coupled with the unlikelihood of such a favourable hybrid configuration being built, there is still enough improvement via the velocity modification to warrant significant interest.

The second major point of interest regards the fuel economy ‘penalty’ incurred by preventing overtaking (i.e., using Algorithm 2). As seen in Figs. 3.7–3.9, for the most part there is very little difference between the two IVVM algorithms as the preview length changes. This indicates that the integration of the algorithm as an economy mode feature of a collision-preventing safety system such as an Adaptive Cruise Control system would be relatively straightforward but has significant impact on fuel economy.

The quantitative set of results presented in Table 3.4 show the fuel economy benefits of the various approaches at two preview lengths and reinforce the qualitative arguments

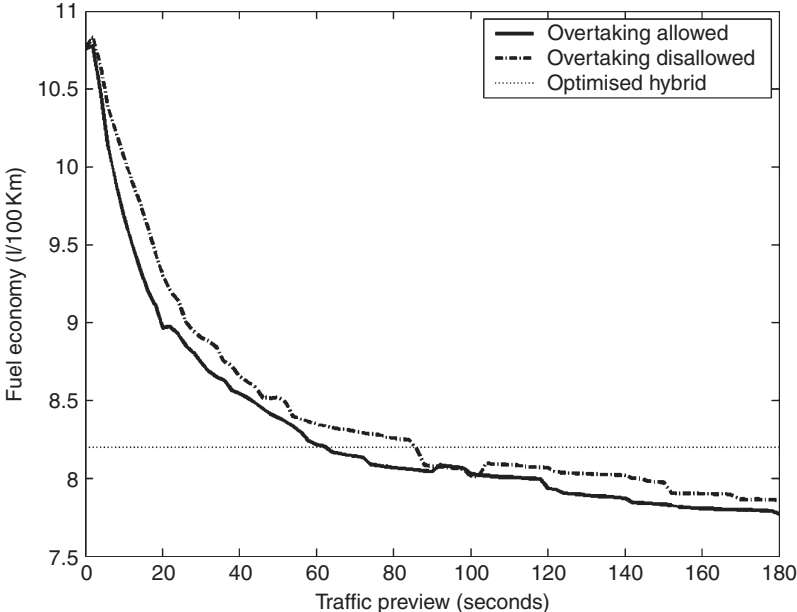


**Figure 3.8** Fuel economy as a function of preview information with overtaking allowed and disallowed using the United States Federal Test Procedure (US-FTP) cycle. For reference, optimised hybrid fuel economy is also indicated.

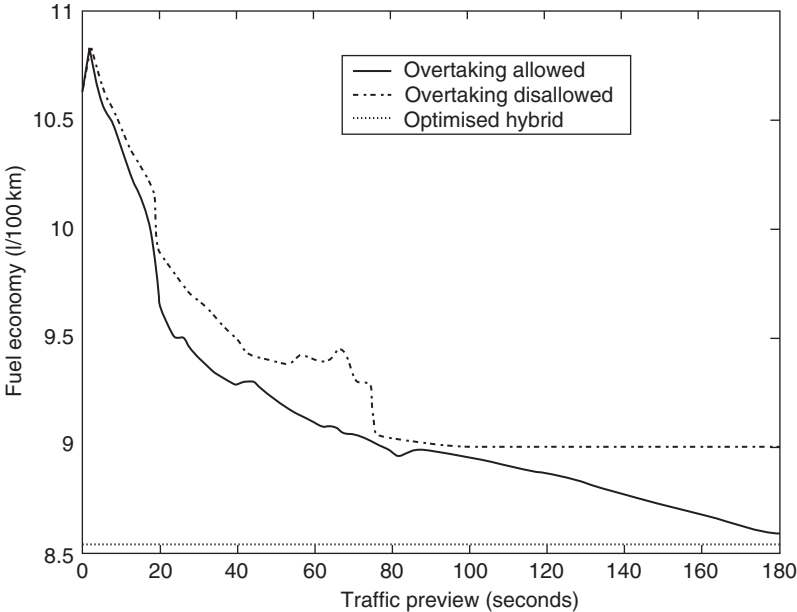


**Figure 3.9** Fuel economy as a function of preview information with overtaking allowed and disallowed using the New European Drive Cycle (NEDC). For reference, optimised hybrid fuel economy is also included.

**Table 3.4** Quantitative comparison of fuel economy (l/100 km) for different strategies

	Australian urban	US-FTP	NEDC
Benchmark vehicle	11.8	10.8	10.6
Optimised hybrid	10.1 (14%)	8.2 (24%)	8.5 (20%)
IVVM with 50 second preview	7.7 (34%)	8.4 (22%)	9.2 (13%)
IVVM with 50 second preview (no overtaking allowed)	7.7 (34%)	8.5 (21%)	9.4 (11%)
IVVM with 180 second preview	7.1 (40%)	7.8 (28%)	8.6 (19%)
IVVM with 180 second preview (no overtaking allowed)	7.2 (39%)	7.9 (27%)	9.0 (15%)
Theoretical optimal velocity <sup>a</sup>	7.3 (38%)	7.5 (30%)	7.5 (29%)

The percentage improvement relative to the benchmark vehicle is given in parentheses.

<sup>a</sup> Calculated from Section 1.

above. For completeness, the fuel efficiencies simulated using the optimal trajectories developed in Section 3.1 are also included and highlight that there are some limitations in the optimal approach since the IVVM outperforms it in a couple of cases despite only having a subset of the information. This is likely an artefact of the simplifying assumptions made in the derivation of the optimal trajectory. Importantly though, Table 3.4 also highlights the scale of the improvement possible through the velocity modification schemes, with double digit percentage gains seen in all drive cycles.



## 4. HYBRID VEHICLES WITH TELEMATICS

In the previous section, hybridisation and velocity modification were viewed as competing strategies at improving fuel consumption. In this section, they are considered as complementary and the fuel savings assessed if both technologies are integrated into one vehicle. To begin, the mild hybrid of Section 2.2 is considered followed by the full hybrid of Section 2.3.

The incorporation of telematics and the subsequent velocity shaping is achieved initially through a slightly modified version of the IVVM algorithm of Section 3. The modification is that a constant *distance* preview is used, rather than a constant preview *time*. This is mainly for comparison to establish the effect on fuel economy of, for example, a radar-based system with a certain range. The difference between the two approaches is that at high speed, the time-based preview decreases with constant distance preview and vice versa.

Fig. 3.10 illustrates how the fuel economy improves with look-ahead distance for both the conventional vehicle and the mild hybrid operating over the Australian urban drive cycle. The results are summarised quantitatively in Table 3.5, where it shows that the incorporation of mild hybrid electric vehicle (HEV) technology does offer some fuel

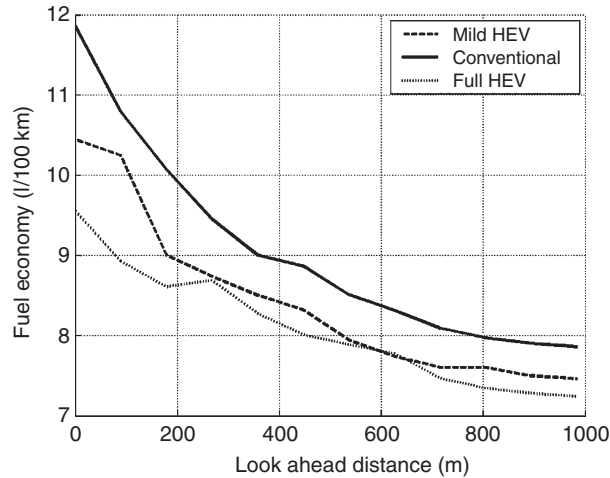


**Figure 3.10** Fuel economy as a function of distance over the Australian urban cycle for a conventional vehicle (solid), mild hybrid (dashed) and full hybrid (dotted) using the modified intelligent vehicle velocity modification (IVVM) algorithm.

**Table 3.5** Comparison of fuel economy (percentage improvement) using the IVVM algorithm with benchmark and mild hybrid vehicles

	No preview	150 m Preview	800 m Preview
Conventional	11.8	10.2	8.0
Mild HEV	10.4 (12%)	9.5 (7%)	7.6 (5%)

economy benefits when combined with the velocity shaping algorithm, although interestingly the percentage benefit decreases with increasing preview. This is a consequence of the IVVM algorithms tendency to remove all stationary behaviour from the drive cycle. While this works very well for a conventional powertrain vehicle, where the fuel use while idling is effectively ‘lost’, in a mild HEV this does not provide any advantage as the engine is shut off when the vehicle stops.

Furthermore, as the IVVM algorithm acts to smooth the surrounding traffic profiles, it consequently reduces the deceleration events the vehicle will undergo. This impacts on the ability of the mild HEV to benefit from regenerative braking events. It is therefore to be expected that the benefit provided by the mild hybridisation relative to the conventional powertrain decreases with increasing ability to avoid stop–start behaviour. As observed in Fig. 3.10, the difference does not asymptote to zero for large preview distances, which is most likely due to the difference in internal combustion engine sizes – that is, the slight downsizing obtained by hybridising offsets fuel use to a small degree even at constant velocity operation.

This apparent shortcoming of coupling the IVVM algorithm with a rule-based torque split strategy in mild HEV configurations was investigated further in [26]. In this work, an alternative to the IVVM that incorporated piecewise continuous (rather than constant) velocities through the horizon was considered, as well as addressing the torque split control problem using a variant on the ECMS of [21]. It was found that the potential improvement offered through these enhancements was minor (typically less than 1%) but indicated that further slight improvements might be possible. The optimal combination of torque split and velocity will be further investigated in Section 5.

To see the effect of full hybridisation compared to the mild hybrid configuration, the optimal hybrid determined in Section 2 was also tested on the modified IVVM algorithm (although the rule-based torque split strategy is still used at this stage). As can be seen from the dotted line in Fig. 3.10, there is an initial substantial fuel economy benefit to further degrees of hybridisation. However, as the preview distance increases, the IVVM algorithm decreases the advantage of any hybridisation relative to the conventional powertrain. This would infer that an appropriate configuration from a cost benefit analysis would be to reduce the amount of hybridisation as the preview information increases. Thus, given that the majority of the cost of hybridisation will be borne by the consumer while traffic preview information is principally at the cost of the regulatory body, this information can be extremely useful when considering fuel use from a macroscopic viewpoint.



## 5. OPTIMAL MANAGEMENT OF HYBRID VEHICLES WITH TELEMATICS

While useful from an indicative perspective, the results of Section 4 are still reliant to some degree on the torque management strategy of the hybrid vehicle. To fully exploit both the hybrid powertrain and the traffic information, an optimisation problem that minimises fuel use (and equivalent fuel use caused by discharging the batteries when the electric motor is used) must be solved. This optimisation problem is complicated due to constraints including limits on the torque available from each of the motor and engine, the allowable state of charge range of the battery, the relative position of the vehicle in traffic and the need for the vehicle to reach its destination. Furthermore, the components possess non-linear transfer functions – thus resulting in a non-trivial problem. In this section, optimal use of both technologies is considered and approaches to implement these strategies are discussed.

### 5.1 Formulation of the optimisation problem

In [20], the optimal torque split ratio,  $u(t)$ , over the entire drive cycle was found using a dynamic programming approach. In theory, if full drive cycle information is available *a priori*, this approach could potentially be extended to identify the optimal trajectories of

both torque split and vehicle velocity  $v(t)$ , to establish the absolute minimum fuel use achievable via the use of continuous torque split and velocity trajectories,  $\mathbf{u}$  and  $\mathbf{v}$ .

The optimisation problem is extremely challenging due to the presence of dynamic constraints (representing the vehicle motion and electrical and fuel energy usage), input constraints (the engine and motor capabilities) and state constraints (the relative position of the vehicle in traffic,  $x_{\text{lead}}(t) - x(t)$ , battery state of charge,  $q(t)$ , etc.). Furthermore, these constraints may be time-varying in the most general statement of the problem, shown in [3.21]:

$$[\mathbf{u}, \mathbf{v}] = \arg \min_{u, v} \int_0^T m_{\text{fuel}}(\tau) d\tau \quad [3.21]$$

subject to constraints from the following:

Equations of motion:  $\frac{dv}{dt} = f_1(F, v)$

Battery use:  $\frac{dq}{dt} = f_2(F, u)$

Fuel use:  $m_{\text{fuel}} = f_3(F, u)$

Velocity constraint:  $v(t) \in V(t)$

Torque split constraint:  $u(t) \in U$

Position constraint:  $x(t) \in X(t)$

State of charge constraint:  $q(t) \in S, q(0) = q(T_p)$

The dimensionality of the problem [3.21] when the trajectories of both inputs (velocity and torque split) are considered over the entire drive cycle represents an extremely challenging numerical problem. While the solution of this problem will provide the best possible fuel economy that can be obtained, it is infeasible for real-world implementation for two reasons: (i) the assumption of full knowledge of the traffic flow over the entire duration of the journey is required and (ii) the amount of computation required to arrive at the solution is massive. As a consequence, the optimisation problem must be restated to take into account these considerations.

Realistically, since only a small subset of the entire journey is available through the use of telematics, a suboptimal problem can be formulated that involves only the available information. A model predictive control (MPC) framework (see, e.g., [27]), whereby a model-based optimisation problem is solved over a receding horizon of  $N$  time steps rather than over the entire journey, is well suited to this application. The first step in the MPC approach is to specify the critical parts of [3.21] that will deliver a close-to-optimal solution, while simultaneously reducing the complexity of the problem.

It is apparent that the formulation of the cost function should include the effects of vehicle velocity, the battery state of charge and the consumption of both fuel and electricity. Previous approaches to torque split control such as the ECMS of [21] involve the sum of the weighted cost of fuel and electric power. The relative weighting (or equivalence factor,  $s$ ) is a fixed constant determined *a priori* for a given drive cycle. As

feedforward traffic information is assumed available in this work, the equivalence factor will be assumed calculable in time, leading to the optimisation problem to be solved over the prediction horizon stated in [28], as follows:

$$\mathbf{u}^*, \mathbf{v}^* = \arg \min \sum_{j=k}^{k+N} \hat{P}_f(u(j), v(j)) + s(j) \hat{P}_e(u(j), v(j)) \quad [3.22]$$

subject to constraints  $u \in [0, u_{\max}]$ ,  $x(k) < x_{\text{lead}}(k)$ ,  $v \in [0, v_{\max}]$  and  $dv/dt \in [(dv/dt)_{\min}, (dv/dt)_{\max}]$ .

To reduce the complexity of the optimisation, the state of charge constraint in [3.21] can be approximated using a soft constraint included in the equivalence factor,  $s(j)$ , of [3.22]. Thus the new equivalence factor,  $s^*$ , to be used in [3.22] is given by

$$s^*(j) = s(j) + K(q - q_{\text{init}}) \quad [3.23]$$

The value of  $K$  in [3.23] must typically be tuned to give desirable performance.

Note that the solution to [3.22]–[3.23] returns complete trajectories of both torque split and velocity (i.e.,  $\mathbf{u}^*$  and  $\mathbf{v}^*$  are vectors of length  $N$ ) but, as with all MPC approaches, only the first elements of the vector are implemented before the optimal results are recalculated. Furthermore, note that while various solution methods can be used, Sequential Quadratic Programming (SQP) is the approach used in the results presented here.

In order to maximise efficiency, the motor should run at peak efficiency as frequently as possible, with any surplus torque used to recharge batteries. This can result in torque split ratios higher than permitted by the rule-based controller in the development of the optimal hybrid configuration in Section 2. A true optimal configuration therefore needs to take into account the full system (i.e., hardware and controller specifications as well as operating constraints) and is a substantial system-wide optimisation exercise. The full hybrid vehicle used in this section was modified slightly from the one described in Section 2 to allow larger torque split ratios to be used.

Figs. 3.11 and 3.12 show the simulation of the vehicle with the non-linear, multi-input MPC algorithm controlling both torque split and vehicle velocity over the entire NEDC and US-FTP drive cycle. Initially, a 5 second prediction horizon was used in solving [3.22]–[3.23], which gives rise to several interesting observations.

Firstly, since the MPC approach uses a non-linear model, it is more accurate than the simplified models used in Sections 3.1 and 3.2, yet returns similar velocity trajectories. As the velocity profile returned by the algorithm maintains the smoothing characteristics obtained using the ad hoc IVVM approaches of Section 3.2, the IVVM algorithm may present a computationally beneficial alternative to a full MPC approach.

If the torque split in Figs. 3.11 and 3.12 is now considered, it is apparent that there are much higher frequency fluctuations during non-zero velocity segments of the cycle.



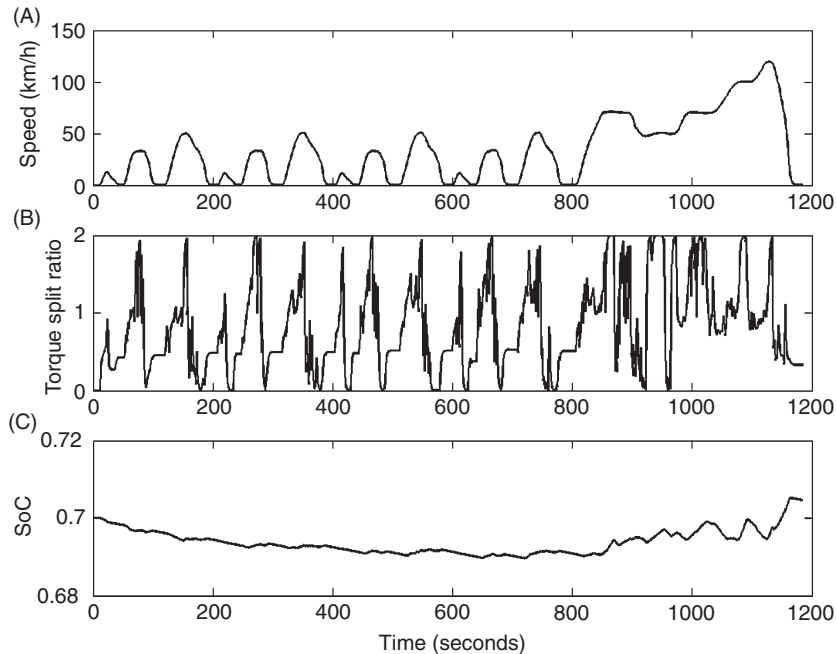


**Figure 3.11** Control inputs (A, B) and resulting state of charge (C) over the New European Drive Cycle (NEDC) using a 5 second preview and a model predictive control (MPC) controller.

When the vehicle is stationary, the torque required is zero and hence the value of  $u$  is irrelevant; however, it is interesting to note during the other segments of the cycles there are certain prevailing characteristics. During accelerations, the torque split ratio tends to increase, indicating that there is initial assistance provided by the electric motor, and this assistance tends to decrease as the state of charge decreases. When the vehicle is travelling at constant velocity, the torque split ratio is typically greater than one which indicates that the engine is being used to recharge the batteries following the acceleration, and in doing so moves the engine from a low-efficiency operating point to a higher operating point. Fig. 3.13 shows the operating points in torque–speed space over a portion of the drive cycle, and it is clear that the points are clustered about the maximum efficiency (with a small subset at the torque limits of the engine). There is some spread in the points, which may be partially due to the tolerance of the optimisation algorithm. However, these insights into optimal operating policies may be useful in developing more computationally tractable algorithms for online implementations.

Finally, it may also be observed that the battery state of charge remains within a relatively narrow corridor throughout the drive cycle. The reason for this may lie in the very short preview times relative to the length of the cycle and the soft constraint [3.23] that penalises variations (potentially too severely) from the initial state of charge. By

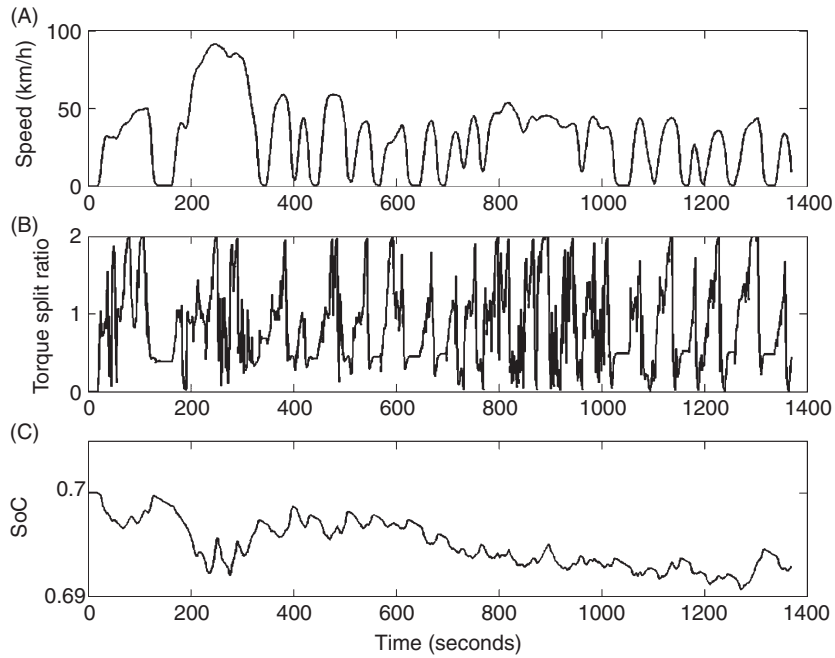


**Figure 3.12** Control inputs (A, B) and resulting state of charge (C) over the United States Federal Test Procedure (US-FTP) cycle using a 5 second preview and a model predictive control (MPC) controller.

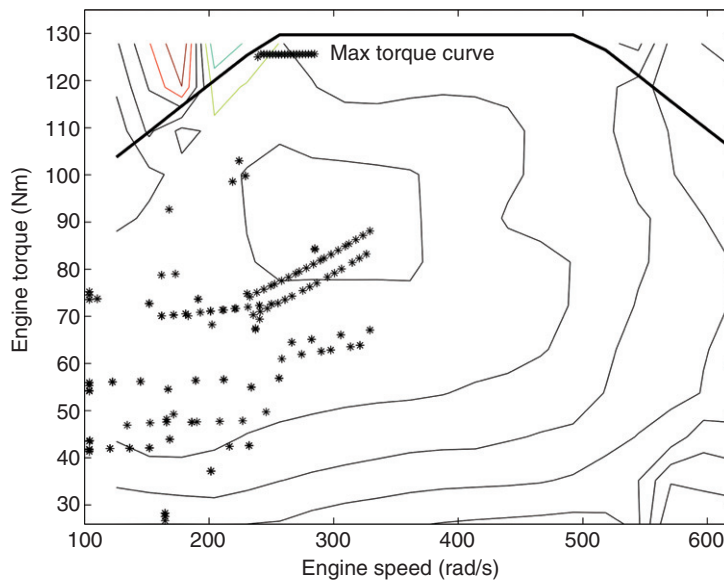


**Figure 3.13** Engine operating points over the New European Drive Cycle (NEDC), with efficiency contours and maximum torque curve superimposed.

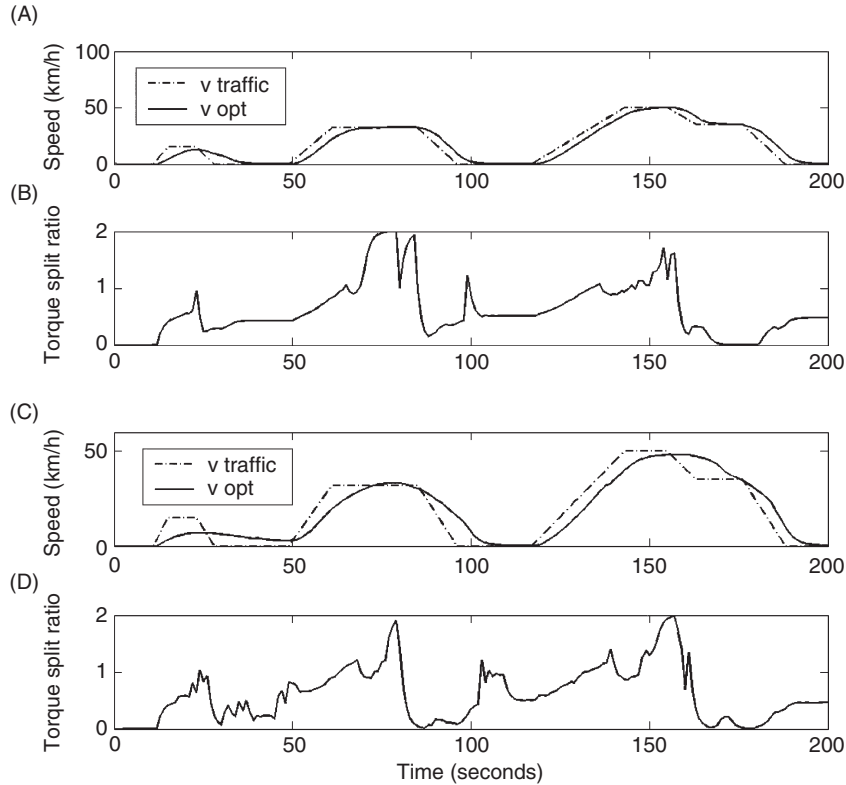


**Figure 3.14** Control trajectories using a model predictive control (MPC) approach with (A)–(B) 5 second and (C)–(D) 15 second preview over a 200 second subset of the New European Drive Cycle (NEDC).

increasing the preview time, there is the potential to introduce more scope for more use of the allowable battery range. Fig. 3.14 compares the control trajectories arising over subset of the NEDC with both 5 and 15 second previews. While the velocity is smoothed (in a similar way to the algorithms of Section 3) in both cases, there is no major change in the torque split ratio profile, and the same general trends are observed in both cases, thereby indicating that either a much larger prediction horizon is required, or the condition [3.23] dominates the torque split response.

In Table 3.6, a quantitative analysis of the improvement generated through both one-input MPC (whereby only the optimal torque split is calculated using the feedforward information) and two-input MPC (where both torque split and vehicle velocity are calculated) is presented. The results demonstrate that only minimal improvement is seen for the one-input case with increased preview, while more substantial improvements are observed if velocity is adjusted. Of course, the relatively short preview time may not offer the optimisation routine the opportunity to take into account both accelerations

**Table 3.6** Fuel economy improvements using non-linear model predictive controllers relative to rule-based approach with no look-ahead

Preview length (seconds)	Controlling torque split only (one-input MPC)		Controlling torque split and velocity (two-input MPC)	
	NEDC	US-FTP	NEDC	US-FTP
5	1.9%	2.0%	3.7%	2.1%
10	2.1%	2.4%	4.7%	3.6%
15	2.2%	2.5%	6.6%	4.7%

and decelerations within the sliding window, and consequently this may have an impact on the control trajectories generated. However, the computational burden associated with optimisations over long horizons using non-linear models is non-trivial and is the subject of ongoing work. The use of non-linear model reduction techniques [29] may prove extremely useful in this exercise.



## 6. CONCLUSIONS AND FUTURE OPPORTUNITIES

The prevalence of telematics, principally entering the automotive mainstream on the basis of safety, ensures that there is the potential to gather information about traffic flow conditions a vehicle may encounter in the near future. This information can then be utilised to great effect in scheduling vehicle velocity and consequently improve the overall fuel economy to a level better than achievable using hybrid technology alone. This highlights the impact that velocity shaping can have on real-world fuel economy, subject to driver acceptance that to date has been tacitly assumed in the absence of any relevant human factors research.

However, given that hybridisation and velocity shaping are essentially complementary approaches to minimise fuel use, there is also significant potential to consider using telematics to enable an intelligent hybrid vehicle – that is, a vehicle that uses future information on traffic flow to optimally schedule the velocity and torque management systems. Despite some significant advances, the best way to formulate this optimisation problem taking into account computational resources, model accuracy and problem constraints remains a matter of ongoing research.

Furthermore, it is apparent that the control approach used in torque split management and velocity scheduling cannot be decoupled from the hardware specification and optimisation – that is, true optimal performance can only be ascertained by taking a complete systems approach that encompasses all of the hardware and software configurations.

The next generation of hybrid vehicles available in the marketplace will likely include plug-in variants. This raises further opportunities for telematics to play a significant role in

the fuel optimisation. An on-board GPS system could be used to inform a controller about the vehicles proximity to a likely recharge station (home, office, etc.) and it is entirely conceivable that this could be fed into the vehicle's power management system. The optimisation complexity could be further increased by considering the relative cost (in dollar terms or even in emissions for 'green consumers') of using mains power against fuel to recharge the on-board batteries following electric motor use.

## ACKNOWLEDGEMENTS

Partial support of the research described in this chapter was provided by the Advanced Centre for Automotive Research and Testing (ACART), <http://www.acart.com.au>. The author would also like to thank Tae Soo Kim, Rahul Sharma, Harry Watson and Antonio Sciarretta for their useful discussions and input.

## NOMENCLATURE

$c_1$	Constant depicting engine efficiency and lower heating value of fuel
$f_i(\cdot)$	General non-linear equation representing the dynamics of the internal states in the hybrid vehicle
$F(t)$	Force supplied by engine at time $t$
$F^*(t)$	Optimal engine force at time $t$
$F_{\min}, F_{\max}$	Limits on available engine force
$F_0$	Engine braking force
$H(t)$	Hamiltonian
$k_1, k_2$	Constants corresponding to constant engine loads and aerodynamic drag coefficient
$m_{\text{fuel}}(t)$	Fuel mass used by engine at time $t$
$m_{\text{veh}}$	Vehicle mass
$p_1, p_2$	Adjoint state variables
$q(t)$	Battery state of charge in hybrid vehicle
$s(t)$	Equivalence factor at time $t$
$T_p$	Preview time in seconds
$u(t)$	Torque split of hybrid vehicle at time $t$
$v(t)$	Intelligent vehicle velocity at time $t$
$v^*(t)$	Optimal intelligent vehicle velocity at time $t$
$v_{\text{lead}}(t)$	Lead vehicle velocity at time $t$
$\hat{v}_{\text{lead}}(t)$	Predicted velocity of lead vehicle at time $t$
$x(t)$	Intelligent vehicle position at time $t$
$\hat{x}(t)$	Predicted position of intelligent vehicle at time $t$
$x_{\text{lead}}(t)$	Lead vehicle position at time $t$
$\hat{x}_{\text{lead}}(t)$	Predicted position of lead vehicle at time $t$
$X(t), V(t), U, S$	Constraints on position, velocity, torque split and state of charge in hybrid vehicle

## REFERENCES

1. B. Yang, E. Skafidas, R.J. Evans, Electron. Lett. 44 (2008) 738.
2. J.K. Hedrick, M. Tomizuka, P. Varaiya, IEEE Contr. Syst. Mag. 14 (1994) 21.
3. R. Rajamani, H.S. Tan, B.K. Law, W.B. Zhang, IEEE Trans. Contr. Syst. Technol. 8 (2000) 695.

4. D. Levinson, *Transport. Res. C – Emer. Technol.* 11 (2003) 75.
5. M. Heddebaut, J. Rioult, J.P. Ghys, C. Gransart, S. Ambellouis, *Meas. Sci. Technol.* 16 (2005) 1363.
6. A. Froberg, E. Hellstrom, L. Nielsen, SAE World Congress, Detroit, USA, 2006, 2006-01-1071.
7. E. Hellstrom, M. Ivarsson, J. Aslund, L. Nielsen, *Control Eng. Pract.* 17 (2009) 245.
8. C. Manzie, H.C. Watson, S. Halgamuge, K. Lim, *Proc. Inst. Mech. Eng. Part D–J. Automob. Eng.* 220 (2006) 67.
9. C. Manzie, H. Watson, S. Halgamuge, *Transport. Res. C – Emer. Technol.* 15 (2007) 1.
10. H.C. Watson, E.E. Milkins, 21st FISITA Congress, Paper 865042, Belgrade, 1986.
11. H.F. Durrant-Whyte, B.Y.S. Rao, H. Hu, *IEEE Int. Conf. Robot. 2* (1990) 1331.
12. K.B. Wipke, M.R. Cuddy, S.D. Burch, *IEEE Trans. Veh. Technol.* 48 (1999) 1751.
13. D.W.Z. Gao, C. Mi, A. Emadi, *Proc. IEEE*, 95 (2007) 729.
14. Y. Liu, PhD Dissertation in the Department of Mechanical and Manufacturing Engineering, The University of Melbourne, 1992.
15. H.G. Rosenkranz, H.C. Watson, W. Bryce, A. Lewis, *Proceeding of the Institution of Mechanical Engineering*, pp. 139–150, 1986.
16. K. Lim, Masters Dissertation in the Department of Mechanical and Manufacturing Engineering, The University of Melbourne, 2004.
17. N. Jalil, N.A. Kheir, M. Salman, American Control Conference, Albuquerque, USA, 4–6 June 1997, pp. 689–693.
18. N.J. Schouten, M.A. Salman, N.A. Kheir, *IEEE Trans. Contr. Syst. Technol.* 10 (2002) 460.
19. A. Brahma, Y. Guezennec, G. Rizzoni, American Control Conference, Chicago, USA, 1–3 September 2000, pp. 60–64.
20. F. Kirschbaum, M. Back, M. Hart, 15th IFAC World Congress, Barcelona, Spain, 21–26 July 2002.
21. G. Paganelli, S. Delprat, T.M. Guerra, J. Rimaux, J.J. Santin, 55th IEEE Vehicular Technology Conference, Birmingham, AL, USA, vol. 4, pp. 2076–2081, 6–9 May 2002.
22. A. Sciarretta, M. Back, L. Guzzella, *IEEE Trans. Contr. Syst. Technol.* 12 (2004) 352.
23. D.E. Kirk, *Optimal Control Theory. An Introduction*, Prentice-Hall, Englewood Cliffs, NJ, 1970.
24. A.P. Stoicescu, *Int. J. Vehicle Des.* 16 (1995) 229.
25. L. Guzzella, A. Sciarretta, *Vehicle Propulsion Systems. Introduction to Modeling and Optimization*, Springer, Berlin, New York, 2005.
26. T.S. Kim, C. Manzie, H. Watson, IFAC World Congress, vol. 17, Seoul, Korea, 6–11 July 2008.
27. J.M. Maciejowski, *Predictive Control with Constraints*, Prentice Hall, Harlow, 2002.
28. T.S. Kim, C. Manzie, R. Sharma, IEEE Conference on Systems, Man and Cybernetics, San Antonio, USA, 11–14 October 2009.
29. R. Sharma, D. Nestic, C. Manzie, *SAE Paper 2009-01-0684*, 2009.



# Cost-Effective Vehicle and Fuel Technology Choices in a Carbon-Constrained World: Insights from Global Energy Systems Modeling

Maria Grahn<sup>\*,1</sup>, James E. Anderson<sup>\*\*</sup>, and Timothy J. Wallington<sup>\*\*</sup>

<sup>\*</sup>Department of Energy and Environment, Physical Resource Theory, Chalmers University of Technology, Göteborg, Sweden

<sup>\*\*</sup>Systems Analytics and Environmental Sciences Department, Ford Motor Company, Dearborn, Michigan, USA

## Contents

1. Introduction	91
2. Method	92
2.1 Model structure	93
2.2 Energy demand	94
2.3 Primary energy sources and emission factors	94
2.4 Cost data	95
2.5 Constraints	95
2.6 Personal transportation	95
3. Results	104
3.1 Cost-effective fuel and vehicles	104
3.2 Impact of CCS and CSP	104
3.3 Impact of vehicle technology cost	107
4. Discussion and Conclusions	108
Acknowledgments	110
References	110



## 1. INTRODUCTION

Global climate change, caused by increasing levels of greenhouse gases in the Earth's atmosphere resulting from human activities, is a major issue that society is facing [1]. CO<sub>2</sub> released during fossil fuel combustion and deforestation is the single largest contributor to radiative forcing of climate change [1]. The United Nations Framework Convention on Climate Change has been ratified by 192 countries and calls for stabilization of greenhouse gas concentrations in the atmosphere at a level that would “prevent dangerous anthropogenic interference with the climate system” [2]. While there is no consensus on a precise level of CO<sub>2</sub> in the atmosphere that would prevent such

<sup>1</sup> Corresponding author: maria.grahn@chalmers.se

interference, levels in the range 350–550 ppm are often discussed. In the present work, we consider scenarios where CO<sub>2</sub> levels are stabilized at 450 ppm. The current global average atmospheric CO<sub>2</sub> concentration is 387 ppm and is increasing by approximately 2 ppm per year [3]. Substantial reductions in global CO<sub>2</sub> emissions over the rest of this century will be required to stabilize atmospheric CO<sub>2</sub> at 450 ppm. Light-duty passenger vehicles are responsible for approximately 11% of global fossil fuel CO<sub>2</sub> emissions [4].

Efforts to stabilize atmospheric CO<sub>2</sub> levels are complicated by many considerations, not least of which being the fact that CO<sub>2</sub> emissions are spread across different economic sectors (e.g., industrial, residential, commercial, transportation) and geographic regions. Given the magnitude of the CO<sub>2</sub> reduction task to achieve stabilization at 450 ppm, a multisector approach is needed where efforts will be taken to reduce, or limit, CO<sub>2</sub> emissions from all regions and economic sectors in a cost-effective manner.

To facilitate discussions of strategies to address climate change, the Global Energy Transition (GET) model [5–7], previously regionalized [8], was modified to include a more detailed description of passenger vehicle technology options (GET-RC 6.1) and was used to investigate the factors influencing cost-effective vehicle and technology choices in a carbon-constrained world.

It is important to understand the fuel and vehicle technology choices available for passenger vehicles and how actions in other energy sectors might impact these choices. There have been few published global long-term energy systems studies that analyze the competition of electricity, hydrogen (H<sub>2</sub>), and biofuels in the transportation sector [9–12]. Studies including plug-in hybrid electric vehicles (PHEVs) and battery electric vehicles (BEVs) (see, e.g., Gül et al. [11]) are neither global nor meet atmospheric CO<sub>2</sub> concentrations below 550 ppm.

The new GET-RC 6.1 model was used to quantify the potential impact of carbon capture and storage (CCS) technology and low CO<sub>2</sub> intensity electricity from renewable sources such as concentrating solar power (CSP) on cost-effective passenger vehicle fuel and technology options necessary to achieve stabilization of atmospheric CO<sub>2</sub> at 450 ppm. In the present work, CSP is both an energy technology and a proxy for other inexpensive low-CO<sub>2</sub> electricity-generating technologies that may be developed in the future.

The model was used to address three questions: (i) what cost-effective fuel and vehicle technologies might dominate in a carbon-constrained world? (ii) to what degree is the answer to the first question affected by the introduction of CCS and/or CSP? and (iii) how sensitive are the results to future vehicle cost assumptions?



## 2. METHOD

The linear programming GET model constructed by Azar et al. [5–8] covers the global energy system and is designed to meet exogenously given energy demand levels, subject to a CO<sub>2</sub> constraint, at the lowest system cost. A graphic depicting the main features in the model is shown in Fig. 4.1.



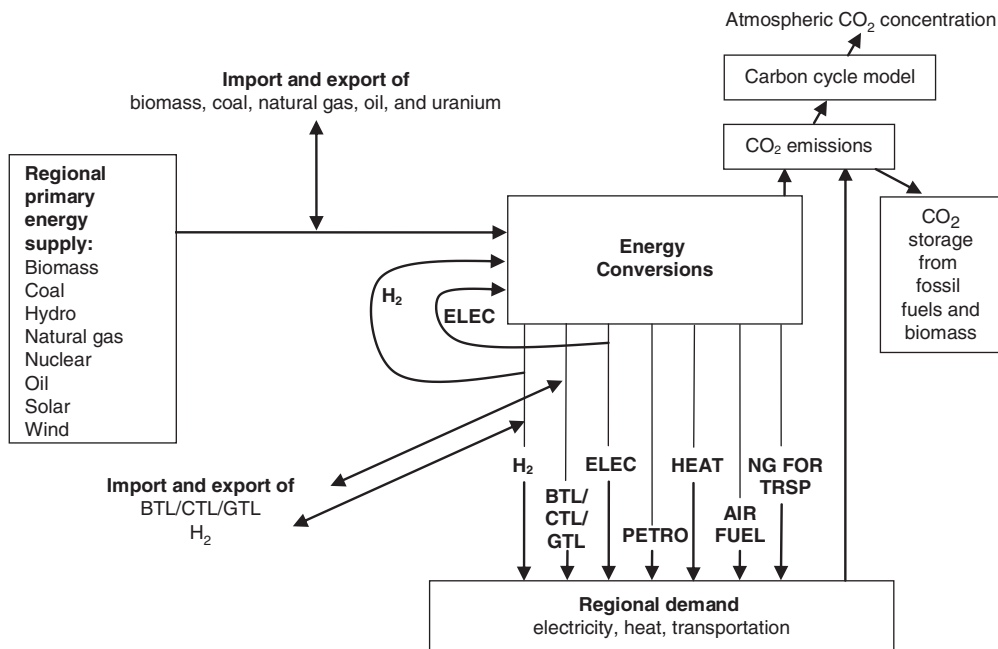


**Figure 4.1** The basic flow chart of supply and fuel choices in GET-R 6.1. Note that electricity and hydrogen can loop back to the energy conversions module allowing electricity to generate heat and allowing hydrogen to generate electricity and/or heat. H<sub>2</sub>, hydrogen; ELEC, electricity; HEAT, low and high temperature heat for the residential, service, agricultural, and industrial sectors; NG FOR TRSP, natural gas as transportation fuel; PETRO, diesel and gasoline; AIR FUEL, synthetic fuels for aviation.

### 2.1 Model structure

The world is treated as 10 distinct regions with unimpeded movement of energy resources between regions (with the exception of electricity) with costs ascribed to such movement. Regional solutions were aggregated to give global results. The pattern of allowed global CO<sub>2</sub> emissions was constrained according to the emission profile leading to an atmospheric CO<sub>2</sub> concentration of 450 ppm, developed by Wigley and co-workers [13]. The model does not consider greenhouse gases other than CO<sub>2</sub> and is run for the period 2000–2130 with 10-year time steps. We present and discuss the results from the time period 2010–2100.

The description of the energy system in the model is a simplification of reality in at least four important respects: (i) consideration of limited number of technologies, (ii) assumption of price inelastic demand, (iii) selections made only on the basis of cost, and (iv) “perfect foresight” with no uncertainty of future costs, climate targets, or energy demand. The model does not predict the future and is not designed to forecast the future development of the energy system. The model does however

provide a useful tool to understand the system behavior and the interactions and connections between energy technology options in different sectors in a future carbon-constrained world.

## 2.2 Energy demand

Energy demand is divided into three sectors: (i) electricity, (ii) transportation, and (iii) “heat” which comprises all stationary uses of energy except for those associated with generating electricity or transportation fuels. Emphasis was given to personal transportation in the present study.

Regional energy demand in the GET model is derived by combining World Energy Council projections of global population (increasing to 10 billion in 2050 and 11.7 billion in 2100) and estimates of the development of per capita income (IIASA/WEC scenario C1) [14], as well as assumptions regarding the activity demand (e.g., person-km, pkm, for personal transportation) associated with a given per capita income. For more details regarding the derivation of regional energy demand, see Azar et al. [5].

## 2.3 Primary energy sources and emission factors

In all areas except North America, Australia, Japan, Europe, and the Former Soviet Union, we assumed a biomass raw material cost of \$2/GJ. Higher costs were assumed in North America, Australia, and Japan (\$3/GJ), and in Europe and the Former Soviet Union (\$4/GJ). We have chosen to follow the regional biomass supply potentials described in Johansson et al. [15] adding up to a global potential of 205 EJ. This potential is similar to a recent Organization of Economic Cooperation and Development (OECD) estimation of 244.6 EJ [16]. Hoogwijk [17] also presents a similar biomass supply potential. For four different scenarios and two biomass production cost levels (lower than 2 USD/GJ and lower than 4 USD/GJ), she estimates the global supply potential to lie in the range of 130–439 EJ/year (with a mean value of 253 EJ/year) by the year 2050.

For global supply potential of oil and natural gas (NG), we have chosen approximately twice the present proved recoverable reserves, that is, 12,000 and 10,000 EJ, respectively [18, 19], and assumed a regional distribution following Johansson et al. [15]. For coal we have chosen a global supply potential of approximately 260,000 EJ following the total resource estimates in Rogner [20]. In the model, CO<sub>2</sub> emission constraints limit the use of fossil fuels (generally less than 10% of the coal supply potential is used within this century when meeting 450 ppm).

The CO<sub>2</sub> emission factors we have used are NG (15.4 kgC/GJ), oil (20.5 kgC/GJ), coal (24.7 kgC/GJ), and biomass (32 kgC/GJ) of delivered fuel [21]. Future use of nuclear, hydro, wind, biomass, and solar energy is assumed to contribute negligible CO<sub>2</sub> emissions.

## 2.4 Cost data

Data for vehicle technology as well as conversion plants and infrastructure (e.g., investment costs, conversion efficiencies, lifetimes, and capacity factors) are held constant at their “mature levels” (see Tables 4.1 and 4.2). Technological change is exogenous in the GET model, that is, the cost and performance of the technologies are independent of how much they are used. We assume mature technology costs throughout the time period considered. The model was tested to ensure that this assumption did not lead to an unduly rapid adoption of technologies. We further assume that all technologies are available in all regions. Global dissemination of technology is not seen as a limiting factor and thus is not included. All prices and costs are in real terms as future inflation is not considered. A global discount rate of 5% per year was used for the net present value calculations.

## 2.5 Constraints

Constraints on how rapidly changes can be made in the energy system have been added to the model to avoid solutions that are obviously unrealistic. This includes constraints on the maximum expansion rates of new technologies (in general, set so that it takes 50 years to change the entire energy system) as well as annual or total extraction limits on the different available energy sources.

The contribution of intermittent electricity sources (wind and solar photovoltaic (PV) is limited to a maximum of 30% of the electricity use. To simulate the actual situation in developing countries, a minimum of 30 EJ/ year of the heat demand needs to be produced from biomass during the first decades. For CCS, we assumed a storage capacity of 600 GtC [22], a maximum rate of increase of CCS of 100 MtC/year and negligible leakage of stored CO<sub>2</sub>.

The future role of nuclear energy is primarily a political decision and will depend on several issues such as nuclear safety, waste disposal, questions of nuclear weapons proliferation and public acceptance. We assume that the contribution of nuclear power does not exceed current levels.

## 2.6 Personal transportation

Electricity and H<sub>2</sub> are energy carriers; for simplicity, we include these as “fuels.” The model does not distinguish between gasoline and diesel fuels, which are lumped together as petroleum (petro). Five fuel options such as petro, NG, synthetic fuels (coal to liquid, CTL; gas to liquid, GTL; biomass to liquid, BTL), electricity, and H<sub>2</sub> and five vehicle technologies such as internal combustion engine vehicles (ICEVs), hybrid electric vehicles (HEVs), plug-in hybrid electric vehicles (PHEVs), battery electric vehicles (BEVs), and fuel cell vehicles (FCVs) were considered.

The relative efficiency values used in the model are derived from published studies (EUCAR [23], TIAX [24], GM [25], CONCAWE [26], and GREET version 1.7 [27]).

**Table 4.1** Cost data for transportation fuels

Primary energy	Secondary energy	Investment cost (\$/kW <sub>fuel</sub> )	Conversion efficiency	Life time (years)	Capacity factor	Annualized investment cost <sup>a</sup> (\$/GJ <sub>fuel</sub> )	O&M cost (\$/GJ <sub>fuel</sub> )	Distribution cost (\$/GJ <sub>fuel</sub> )	Primary energy price <sup>b</sup> (\$/GJ)	CO <sub>2</sub> storage cost <sup>c</sup> (\$/GJ <sub>fuel</sub> )	Total fuel cost <sup>d</sup> (\$/GJ <sub>fuel</sub> )
Oil	Petro	900	0.9	25	0.8	2.74	1.66	2.00	3.00	–	9.73
NG	NG	–	1	–	–	–	–	6.40	2.50	–	8.90
Biomass	BTL	1,000	0.6	25	0.8	3.05	1.84	3.47	2.00 <sup>e</sup>	–	11.69
NG	GTL	600	0.7	25	0.8	1.83	1.11	3.47	2.50	–	9.97
Coal	CTL	1,000	0.6	25	0.8	3.05	1.84	3.47	1.00	–	10.02
Biomass	H <sub>2</sub>	800	0.6	25	0.6	3.25	1.47	7.86	2.00 <sup>e</sup>	–	15.92
NG	H <sub>2</sub>	300	0.8	25	0.6	1.22	0.55	7.86	2.50	–	12.76
Coal	H <sub>2</sub>	700	0.65	25	0.6	2.84	1.29	7.86	1.00	–	13.53
Oil	H <sub>2</sub>	400	0.75	25	0.6	1.62	0.74	7.86	3.00	–	14.22
Solar	H <sub>2</sub>	2,000	1	25	0.25	19.49	3.69	7.86	0.00	–	31.04
Bio-CCS	H <sub>2</sub>	1,000	0.55	25	0.6	4.06	1.84	8.36 <sup>f</sup>	2.00 <sup>e</sup>	3.82	21.73
NG-CCS	H <sub>2</sub>	500	0.75	25	0.6	2.03	0.92	7.86	2.50	0.68	14.83
Coal-CCS	H <sub>2</sub>	900	0.6	25	0.6	3.66	1.66	7.86	1.00	1.37	16.21
Oil-CCS	H <sub>2</sub>	600	0.7	25	0.6	2.44	1.11	7.86	3.00	0.98	16.71
Infrastructure <sup>g</sup>	BTL/CTL/GTL	500	1	50	0.7	–	–	–	–	–	–
Infrastructure <sup>g</sup>	NG	1,500	1	50	0.7	–	–	–	–	–	–
Infrastructure <sup>g</sup>	H <sub>2</sub>	2,000	1	50	0.7	–	–	–	–	–	–

<sup>a</sup> Annualized investment cost  $C_I$  of energy conversion plant, calculated as  $C_I = \left( (1+r)^5 I / 10 \alpha C_f \right) \left( 1 - (1-1/T)^{10} / (1+r)^{10} \right)$ , where  $I$  is the investment cost,  $r$  is the discount rate (0.05/year),  $T$  is the life time, and  $C_f$  is the capacity factor. The constant  $\alpha = 31$  Ms/year is included to account for the conversion into GJ (remember 10 years per time step). The factor  $(1+r)^5$  reflects that investments are made between two time steps.

<sup>b</sup> Note that the stated primary energy costs do include neither scarcity rents (which are generated endogenously in the model) nor carbon taxes. To see the effect of an increasing carbon fee/tax, see Azar et al. [7].

<sup>c</sup> The CO<sub>2</sub> storage cost is \$10/tCO<sub>2</sub> (for CO<sub>2</sub> from fossil fuels) and \$20/tCO<sub>2</sub> (for CO<sub>2</sub> from biomass). The reason for the higher cost for biomass CO<sub>2</sub> is that we assume that facilities capturing CO<sub>2</sub> from biomass will typically be smaller (see Azar et al. [7] for more details). We have assumed that 90% of the carbon is captured.

<sup>d</sup> The total fuel cost is derived as primary energy cost/conversion efficiency +  $C_I$  + O&M cost + distribution cost + CO<sub>2</sub> storage cost.

<sup>e</sup> A biomass feedstock cost of \$2/GJ was assumed in all regions with the following exceptions: in North America, Australia, and Japan, the cost was set to \$3/GJ and in Europe and the Former Soviet Union, the cost was set to \$4/GJ.

<sup>f</sup> Longer transportation distances of biomass to bio-energy CCS plants add \$0.5/GJ to the distribution cost, since bio-energy plants are generally smaller than plants using fossil fuels.

<sup>g</sup> The incremental costs for investing in new infrastructure are based on the data presented in the last three rows and are included for each fuel option in column 9. The cost for distribution of conventional petro is set to \$2/GJ.

**Table 4.2** Cost data for heat and electricity options

Primary energy	Investment cost (\$/kW <sub>e</sub> )	Conversion efficiency	Life time (years)	Capacity factor	O&M cost (\$/GJe)	Primary energy price <sup>a</sup> (\$/GJ)	CO <sub>2</sub> storage cost <sup>b</sup> (\$/GJe)	Total prod. cost <sup>c</sup> (\$/GJe)
<b>Electricity</b>								
Biomass	1,200	0.5	25	0.7	2.21	2.00 <sup>d</sup>	–	10.39
Natural gas	500	0.55	25	0.7	0.92	2.50	–	7.21
Coal	1,100	0.5	25	0.7	2.03	1.00	–	7.86
Oil	600	0.5	25	0.7	1.11	3.00	–	9.19
Solar PV	1,200	1	25	0.25	2.21	0.00	–	13.91
Solar CSP	3,200	1	30	0.6	2.06	0.00	–	14.42
Hydro	1,000	1	40	0.7	1.84	0.00	–	4.92
Wind	600	1	25	0.25	1.11	0.00	–	6.95
Nuclear	2,000	0.33	25	0.7	3.69	1.00	–	13.68
Bio-CCS	1,700	0.3	25	0.7	3.13	2.00 <sup>d</sup>	7.01	23.23 <sup>e</sup>
NG-CCS	900	0.45	25	0.7	1.66	2.50	1.14	11.49
Coal-CCS	1,500	0.35	25	0.7	2.76	1.00	2.35	13.19
Oil-CCS	1,000	0.4	25	0.7	1.84	3.00	1.71	14.53
<b>Heat</b>								
Biomass	300	0.9	25	0.7	0.55	2.00 <sup>d</sup>	–	3.82
Natural gas	100	0.9	25	0.7	0.18	2.50	–	3.31
Coal	300	0.9	25	0.7	0.55	1.00	–	2.71

*(Continued)*

**Table 4.2** (Continued)

Primary energy	Investment cost (\$/kW <sub>e</sub> )	Conversion efficiency	Life time (years)	Capacity factor	O&M cost (\$/GJe)	Primary energy price <sup>a</sup> (\$/GJ)	CO <sub>2</sub> storage cost <sup>b</sup> (\$/GJe)	Total prod. cost <sup>c</sup> (\$/GJe)
Oil	100	0.9	25	0.7	0.18	3.00	–	3.87
Solar	400	0.9	25	0.25	0.74	0.00	–	4.64
Bio-CCS	500	0.8	25	0.7	0.92	2.00 <sup>e</sup>	2.63	8.29 <sup>f</sup>
NG-CCS	300	0.8	25	0.7	0.55	2.50	0.64	5.36
Coal-CCS	500	0.8	25	0.7	0.92	1.00	1.03	4.94
Oil-CCS	300	0.8	25	0.7	0.553	3.00	0.85	6.20

<sup>a</sup> Note that the stated primary energy costs do include neither scarcity rents (which are generated endogenously in the model) nor carbon taxes. To see the effect of an increasing carbon fee/tax, see Azar et al. [7].

<sup>b</sup> The CO<sub>2</sub> storage cost is \$10/tCO<sub>2</sub> (for CO<sub>2</sub> from fossil fuels) and \$20/tCO<sub>2</sub> (for CO<sub>2</sub> from biomass). The reason for the higher cost for biomass CO<sub>2</sub> is that we assume that facilities capturing CO<sub>2</sub> from biomass will typically be smaller (see Azar et al. [7], for more details). We have assumed that 90% of the carbon is captured.

<sup>c</sup> The total fuel cost is derived as primary energy cost/conversion efficiency + C<sub>f</sub> + O&M cost + distribution cost + CO<sub>2</sub> storage cost.

<sup>d</sup> A biomass feedstock cost of \$2/GJ was assumed in all regions with the following exceptions: in North America, Australia, and Japan, the cost was set to \$3/GJ and in Europe and the Former Soviet Union, the cost was set to \$4/GJ.

<sup>e</sup> Longer transportation distances of biomass to bio-energy CCS plants add \$0.5/GJ to the distribution cost, since bio-energy plants are generally smaller than plants using fossil fuels.

These studies provide relative efficiencies using a lower heating value (LHV) energy basis as is standard practice in the automotive industry. The model, however, uses higher heating values (HHVs) which is standard practice in the energy industry. Consensus relative efficiency values are first determined on an LHV basis and then each is converted to HHV basis by multiplying by  $(\text{LHV}_{\text{altfuel}}/\text{HHV}_{\text{altfuel}})/(\text{LHV}_{\text{petro}}/\text{HHV}_{\text{petro}})$ . While this conversion has no effect for petroleum-fueled vehicles (e.g., for Petro HEVs), it reduces the relative efficiency value for H<sub>2</sub>-fueled vehicles and increases the value for vehicles “fueled” by electricity. There is a lesser effect for certain synthetic fuels (alcohols) and NG, but this may be partly offset by higher efficiencies possible in IC engines for these higher octane fuels and thus the difference is considered negligible.

As seen in Table 4.3, these studies conclude that the efficiency of ICEVs fueled by synthetic fuels (Synth ICEV including BTL, GTL, and CTL) or NG (NG ICEV) is not greatly different from that by petroleum (Petro ICEV). Accordingly, we set the efficiency of Synth ICEVs and NG ICEVs equal to that of Petro ICEVs in the model. For H<sub>2</sub>-fueled ICEVs (H<sub>2</sub> ICEVs), the five reports provide efficiencies of 1.13–1.30 times that of Petro ICEVs. We adopt a value of 1.25 for the relative efficiency of H<sub>2</sub> ICEV on an LHV basis which is equivalent to 1.15 on an HHV basis. For HEVs, the five studies provide a range of relative efficiencies of 1.24–1.35, which will of course depend on the type and degree of hybridization. We adopt an average value of 1.3 for the relative efficiency of HEVs.

The estimates of the relative efficiency of BEVs in GREET 1.7 and in the TIAX study range from 3.5 to 3.6; we adopt a value of 3.5 for the year 2000 on an LHV basis which is 3.75 on an HHV basis. We gradually reduce this relative efficiency through the year 2100 to ensure that the powertrain efficiency does not exceed a reasonable level. The relative efficiency value (2.64 LHV basis; 2.85 HHV basis) in the year 2100 corresponds to an overall powertrain efficiency for BEVs of 85%. Over the period 2000–2100, the overall fuel efficiency of BEVs (and the electric component of PHEVs) increases by a factor of 1.5, as compared to a factor of 2.0 increase assumed for Petro ICEVs and all other vehicles.

For consistency and simplicity, we assume the relative efficiency of PHEVs when powered by electricity is the same as BEVs. We adopt the value of 1.5 for the relative efficiency of PHEVs when powered by petroleum as used in GREET 1.7 (IC engines in PHEVs could be downsized and operated at more efficient speed-load conditions than in HEVs). In the model, each PHEV energy fraction is handled separately. The overall relative efficiency of PHEVs depends on the fraction of distance traveled using electricity from the grid,  $x$ , and is given in the year 2000 by  $1/[(x/3.5) + (1-x)/1.5]$ , on an LHV basis. For example, if  $x = 0.65$ , then the overall relative efficiency of PHEVs is approximately 2.4, again on an LHV basis.

The values of 1.2 and 1.3 for the relative efficiencies of Petro FCVs and Synth FCVs are based on the values reported by CONCAWE. As seen in Table 4.3, there is

**Table 4.3** Efficiencies of different passenger vehicle technology fuel options relative to conventional petroleum internal combustion engine technology

Technology	EUCAR [23]	GREET 1.7 [24, 27] <sup>a</sup>	GM [25]	CONCAWE [26]	TIAX	This work 2000/2100	This work 2000/2100
Basis	LHV	LHV	LHV	LHV	LHV	LHV	HHV
Petro ICEV	1 <sup>b</sup>	1 <sup>b</sup>	1 <sup>b</sup>	1 <sup>b</sup>	1 <sup>b</sup>	1 <sup>b</sup>	1 <sup>b</sup>
Synth ICEV <sup>c</sup>	1.03	1.05–1.07	1	1	1.03/1.07	~1	1 <sup>c</sup>
NG ICEV	1	1.03–1.05	0.986	1.01	1	~1	1 <sup>c</sup>
H <sub>2</sub> ICEV	1.3	1.2–1.3	1.20	1.13	1.3	1.25	1.15
HEV	1.3	1.35	1.24	1.18	1.35	1.3	1.3
BEV	–	3.5	–	–	3.6	3.5/2.64	3.75/2.85
PHEV <sup>d</sup>	–	–	–	–	–	2.39/2.08 <sup>d</sup>	2.46/2.17 <sup>d</sup>
Petro mode		1.52–1.82	–	–	1.4	1.5	1.5
Elec mode	–	3.0	2.46	–	3.6	3.5/2.64	3.75/2.85
Petro FCV	–	–	–	1.17	–	1.2	1.2
Synth FCV <sup>c</sup>	–	–	–	1.28	–	1.3	1.3
H <sub>2</sub> FCV	2.4	2.32–2.64	2.36	2.02	2.0	2.0	1.8

Petro ICEV, Synth ICEV, NG ICEV, H<sub>2</sub> ICEV = internal combustion engine vehicle fueled by petroleum, synthetic fuel, natural gas, or gaseous hydrogen, respectively; HEV = hybrid electric vehicle; BEV = battery electric vehicle; PHEV = plug-in hybrid electric vehicle; Petro FCV, Synth FCV, H<sub>2</sub> FCV = fuel cell vehicle fueled by petroleum, synthetic fuel, or gaseous hydrogen, respectively; HHV = higher heating value; LHV = lower heating value.

<sup>a</sup>Values taken from Tables 3–7 in TIAX report [24].

<sup>b</sup>By definition.

<sup>c</sup>HHV-based relative efficiencies for vehicles fueled by synthetic fuels and natural gas were assumed to equal 1 given the small differences in HHV and LHV for synthetic fuels and natural gas relative to gasoline, and the consideration that lower LHV/HHV ratios for such fuels could be offset by higher efficiency due to their higher octane value.

<sup>d</sup>Derived values assuming 65% operation as Elec PHEV and 35% operation as Petro PHEV.

<sup>e</sup>Synthetic fuel here includes biofuel (BTL), coal-to-liquid (CTL), or gas-to-liquid (GTL).



reasonable agreement in the relative efficiency values for H<sub>2</sub> FCVs documented in the four literature sources. We adopt a value of 2.0 (LHV) in the year 2000 consistent with the recent assessments by CONCAWE [26] and TIAX [24].

Powertrain types and efficiencies for freight trucks were updated to be consistent with those assumed in the car sector.

An all-electric battery range of 65 km was adopted for PHEVs which enables approximately two-thirds of their daily driving distance to be powered by electricity from the grid on a single overnight charge [28]. HEVs have a relatively short all-electric range (~2 km). The all-electric range was set to 200 km for BEVs. As a sensitivity analysis, results from assuming 100 km are presented in Fig. 4.4.

Table 4.4 provides the incremental cost data relative to internal combustion engines powered by petroleum (Petro ICEVs) used in the model. These incremental costs are estimated for the technologies in their “mature” state. Fuel storage is a significant

**Table 4.4** Passenger (light-duty) vehicle energy use and cost data in the model

Fuel engine technology	Vehicle energy efficiency ratio (HHV) <sup>a</sup>		Vehicle cost (USD)	
	Year 2000 <sup>b</sup>	Year 2100	Base	Increment
Petro ICEV	1.0 <sup>c</sup>	1.0 <sup>c</sup>	20,000	–
Synth ICEV	1.0	1.0		100
NG ICEV	1.0	1.0		1,200–1,600
H <sub>2</sub> ICEV	1.15	1.15		1,500–3,600
HEV	1.3	1.3		1,300–1,900 <sup>d</sup>
BEV	3.75	2.85		8,000–23,000 <sup>d,e</sup>
PHEV <sup>f</sup>	2.46	2.17		3,000–8,000 <sup>d</sup>
Petro FCV	1.2	1.2		4,500–7,500 <sup>d</sup>
Synth FCV	1.3	1.3		4,500–7,500 <sup>d</sup>
H <sub>2</sub> FCV	1.8	1.8		4,900–7,900 <sup>d</sup>

Petro ICEV, Synth ICEV, NG ICEV, H<sub>2</sub> ICEV = internal combustion engine vehicle fueled by petroleum, synthetic fuel (CTL, GTL, or BTL), natural gas, or gaseous hydrogen, respectively; HEV = hybrid electric vehicle; BEV = battery electric vehicle, PHEV = plug-in hybrid electric vehicle; Petro FCV, Synth FCV, H<sub>2</sub> FCV = fuel-cell vehicle fueled by petroleum, synthetic fuel, or gaseous hydrogen, respectively.

<sup>a</sup> Tank-to-wheels energy (HHV basis) used by Petro ICEV divided by that for alternative technology.

<sup>b</sup> While it is clearly not appropriate to use mature costs for advanced technology during the beginning of the time period, this assumption did not compromise the study since advanced technologies did not enter the scenarios until later in the time period studied.

<sup>c</sup> By definition. The overall energy consumption (MJ/km) by Petro ICEVs in 2100 is a factor of 2 less than that in 2000.

<sup>d</sup> Battery cost of \$150–450/kWh, fuel cell stack cost of \$65–125/kW, hydrogen storage cost of \$1,500–3,500/GJ, and natural gas storage cost of \$1,000–1,300/GJ assumed.

<sup>e</sup> BEV cost based on 200-km driving range compared to 500-km range for the other technologies.

<sup>f</sup> Efficiency shown assumes that two-thirds of total distance traveled are powered via grid electricity. Synth HEV and Synth PHEV are also included in the model with efficiencies equal to Petro HEV and Petro PHEV with \$100 additional incremental cost.

component of vehicle cost for vehicles running on NG, H<sub>2</sub>, and batteries. As vehicle fuel consumption is assumed to steadily decline over the study period for all vehicle types, energy storage requirements for the assumed 500-km range also decline proportionally. For developing vehicle costs in GET-RC 6.1, we assume energy storage costs consistent with fuel consumption for each vehicle type in the year 2050, assuming a globally averaged vehicle size (consistent with 2.45 MJ/km for Petro ICEVs).

It should be stressed that the data in [Table 4.4](#) are based on literature estimates of potential mature technology costs [[24–27](#)] which we equate to costs in the period 2030–2050. It is unclear whether these costs will be realized in the future. The technology costs were assumed constant during the entire time period modeled. While it is clearly not appropriate to use mature costs for advanced technology during the beginning of the time period, this assumption did not compromise the study because advanced technologies are not required to meet the CO<sub>2</sub> constraints, and so were not selected by the model in the beginning of the time period. The base passenger vehicle with a conventional, internal combustion engine powered by petroleum is set to \$20,000. The incremental cost for a comparable vehicle powered instead by synthetic fuel (e.g., biofuel) is set to \$100 to cover for component modifications required to make the vehicle biofuel compatible [[29](#)]. For consistency, the incremental costs for other synthetic fuel vehicles were increased by \$100 relative to the comparable petroleum-powered vehicle.

Costs for alternative powertrain and alternative fuel technology in freight trucks were updated to be consistent with those assumed in the car sector.

Model runs assessed the sensitivity to variation of the following: battery costs from \$150/kWh (goal for long-term commercialization set by the US Advanced Battery Consortium [[30](#)]) to \$450/kWh (above which the model results were insensitive to battery cost); NG storage costs from \$1,000/GJ to \$1,300/GJ (consistent with estimation by CONCAWE [[26](#)]); H<sub>2</sub> storage costs from \$1,500/GJ (US Department of Energy target [[31](#)]) to \$3,500/GJ; and fuel cell (FC) stack costs from \$65/kW (Ballard [[32](#)]) to \$125/kW (CONCAWE [[26](#)]). Uytterlinde et al. [[33](#)] have recently provided incremental cost estimates of €2,000 for NG ICEVs and €1,800 for Petro HEVs in 2040 comparable to our estimates.

[Table 4.4](#) provides the vehicle energy efficiency and cost data for the different combinations of fuel and vehicle technologies included in the model.

To investigate the sensitivity of the results to costs assumptions, six cases were considered and the cost values are given in [Table 4.5](#). These cases add to earlier cases we have presented elsewhere [[34–36](#)]. Case 1 is based upon a battery cost of \$300/kWh, a H<sub>2</sub> storage cost of \$1,500/GJ, an NG ICE storage cost of \$1,300/GJ, and an FC stack cost of \$65/kW. Case 2 explores the impact of assuming a higher H<sub>2</sub> ICE storage costs and case 3 explores the impact of a higher FC stack cost. Cases 4 and 5 test the sensitivity to battery costs. Finally, case 6 tests the sensitivity to assuming a shorter driving range for

**Table 4.5** Cases for incremental costs of different interesting passenger vehicle technology and fuel options relative to conventional petroleum internal combustion engine technology explored in current work

Vehicle technology	Case 1 <sup>a</sup>	Case 2 (H <sub>2</sub> storage = \$3,500/GJ)	Case 3 (FC stack = \$95/kW)	Case 4 (battery = \$450/kWh)	Case 5 (battery = \$150/kWh)	Case 6 (BEV range = 100 km)
Petro ICEV	0	0	0	0	0	0
Synth ICEV	100	100	100	100	100	100
NG ICEV	1,600	1,600	1,600	1,600	1,600	1,600
H <sub>2</sub> ICEV	1,500	<b>3,600<sup>b</sup></b>	1,500	1,500	1,500	1,500
Petro HEV	1,600	1,600	1,600	<b>1,900<sup>b</sup></b>	<b>1,300<sup>b</sup></b>	1,600
Synth HEV	1,700	1,700	1,700	<b>2,000<sup>b</sup></b>	<b>1,400<sup>b</sup></b>	1,700
BEV	15,600	15,600	15,600	<b>23,300<sup>b</sup></b>	<b>7,900<sup>b</sup></b>	<b>7,900<sup>b</sup></b>
Petro PHEV	5,500	5,500	5,500	<b>8,000<sup>b</sup></b>	<b>3,000<sup>b</sup></b>	5,500
Synth PHEV	5,600	5,600	5,600	<b>8,100<sup>b</sup></b>	<b>3,100<sup>b</sup></b>	5,600
Petro FCV	4,500	4,500	<b>6,000<sup>b</sup></b>	<b>4,800<sup>b</sup></b>	<b>4,200<sup>b</sup></b>	4,500
Synth FCV	4,500	4,500	<b>6,000<sup>b</sup></b>	<b>4,800<sup>b</sup></b>	<b>4,200<sup>b</sup></b>	4,500
H <sub>2</sub> FCV	4,200	<b>5,500<sup>b</sup></b>	<b>5,700<sup>b</sup></b>	<b>4,500<sup>b</sup></b>	<b>3,900<sup>b</sup></b>	4,200

<sup>a</sup> Using natural gas storage = \$1,300/GJ, hydrogen storage = \$1,500/GJ, battery = \$300/kWh, FC stack = \$65/kW, and BEV driving range of 200 km.

<sup>b</sup> Values in bold-face type indicate those changed from case 1.

BEVs. It may be noticed that in most of the cases in Table 4.5, a lower base incremental cost is assumed for H<sub>2</sub> ICEVs than for NG ICEVs. These costs are consistent with the assumed on-board fuel storage costs of \$1,300/GJ for NG and \$1,500/GJ for H<sub>2</sub>, a subset of those presented elsewhere [34–36]. The greater incremental vehicle cost for NG ICEV here is the outcome of a higher fuel storage requirement (GJ) for NG due to the lower assumed efficiency of NG ICEVs compared to H<sub>2</sub> ICEVs (Table 4.3).



### 3. RESULTS

Four scenarios are considered: (A) where neither CCS nor CSP is available, (B) where CCS is available but CSP is unavailable, (C) where CSP is available but CCS is unavailable, and (D) where both CSS and CSP are available. The fuel and vehicle technology results for the global light-duty passenger vehicle fleet using case 1 for the four different scenarios (A–D) are presented in Fig. 4.2. The results from cases 2–5, assuming scenario A, that is, that neither CCS nor CSP is available, are presented in Fig. 4.3. In the figures, CTL and GTL (both from fossil sources) are combined for clarity.

#### 3.1 Cost-effective fuel and vehicles

In all scenarios, there is no single vehicle technology and fuel that dominates throughout the century. The diversity of solutions reflects (i) different regional resource availability and mobility demand, (ii) that relative cost-effectiveness between fuels and technology options changes over time due to increased carbon constraints, and (iii) oil and NG supply potentials become scarcer with time and this alone drives the introduction of alternative fuels.

#### 3.2 Impact of CCS and CSP

The availability of CCS and CSP has a profound influence on the lowest cost passenger vehicle fuel and technology choice in a carbon-constrained world. Without CCS or CSP (Fig. 4.2A), personal transportation changes from petroleum-fueled ICEVs to a combination of mostly HEVs and PHEVs fueled by petroleum and some ICEVs fueled by NG. Approaching 2100, these vehicles are replaced by FCVs and ICEVs fueled by H<sub>2</sub> (produced via solar energy).

The availability of CCS (compare Fig. 4.2B with 4.2A) extends the use of conventional petroleum-fueled ICEVs by a few decades, results in the use of more ICEVs and HEVs fueled by biofuels and CTL/GTL, and delays the introduction of H<sub>2</sub> (produced from coal with CCS). The system dynamic at work is that CCS provides relatively inexpensive low-CO<sub>2</sub> electricity and heat from coal which prolongs the use of traditional ICEVs. The availability of CCS leads to coal displacing biomass in the heat sector which allows increased production of transportation fuel from biomass (when CCS is not available, biomass is used mostly to provide heat). While CCS enables the

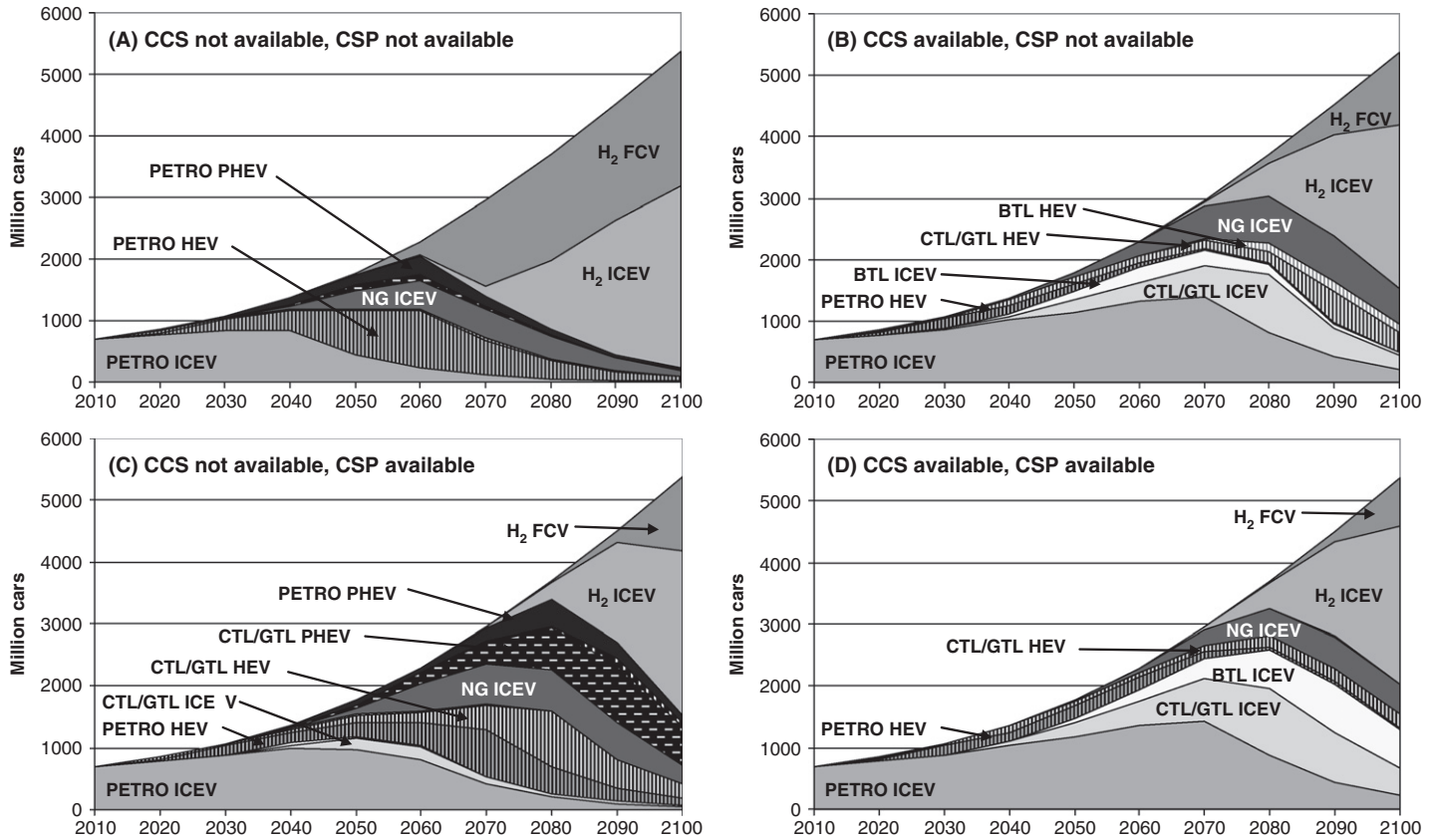


**Figure 4.2** Global passenger vehicle fleet (millions) consistent with data assumed in case 1, that is, a battery cost of \$300/kWh, a hydrogen storage cost of \$1,500/GJ, a natural gas storage cost of \$1,300/GJ, and an FC stack cost of \$65/kW, and (A) Neither CCS nor CSP available, (B) only CCS available, (C) only CSP available, or (D) CCS and CSP both available.

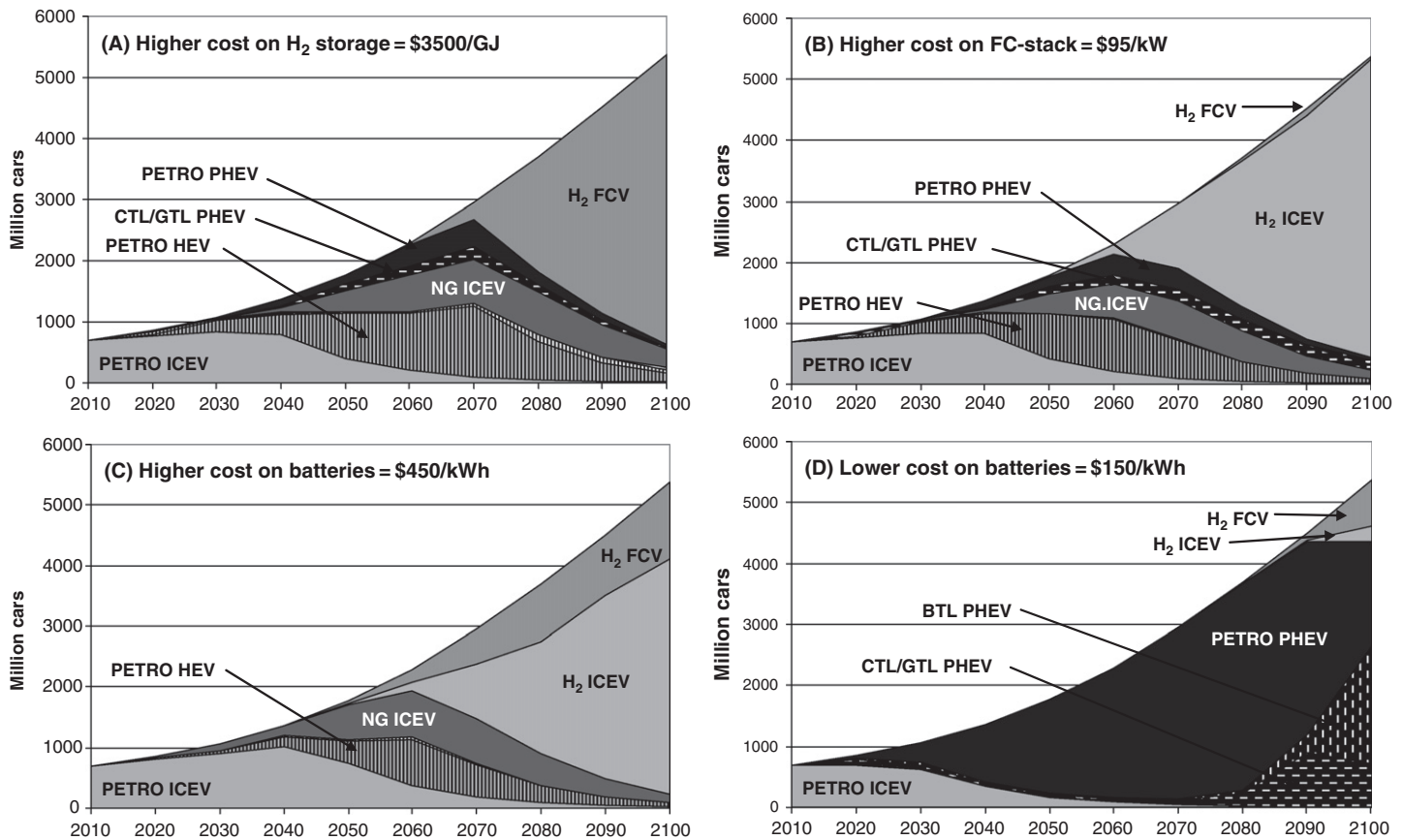


**Figure 4.3** Global passenger vehicle fleet (millions) from the scenario assuming neither CCS nor CSP available consistent with data assumed in (A) case 2 (higher H<sub>2</sub> storage cost, \$3,500/GJ), (B) case 3 (higher FC stack cost, \$95/kW), (C) case 4 (higher battery cost, \$450/kWh), and (D) case 5 (lower battery cost, \$150/kWh).

production of much cheaper  $H_2$  (from coal instead of solar), the overall importance of  $H_2$  decreases reflecting the fact that CCS enables nontransport sectors to realize more emission reductions at a lower cost than in the transport sector.

The availability of low- $CO_2$  electricity from CSP has somewhat different impacts. As seen by comparing Fig. 4.2C with 4.2A, when CSP is available, substantial volumes of PHEVs and HEVs fueled by petroleum and fossil synthetic fuels (GTL and BTL) are used at the expense of FCVs and ICEVs fueled by solar-based  $H_2$ . For the model assumptions leading to the results shown in Fig. 4.2C, biofuels are not a cost-effective strategy for the global passenger vehicle fleet to reduce  $CO_2$  emissions and BTL does not appear in the solution set. The system dynamic at work is similar to that described above for CCS, but with two effects: (i) CSP displaces fossil fuel-derived electricity and prolongs the use of petroleum-fueled ICEVs and (ii) CSP provides low- $CO_2$  electricity and promotes the electrification of passenger vehicles.

When both CSP and CCS are available (see Fig. 4.2D), cost-effective opportunities for  $CO_2$  reduction in other sectors allow substantial use of ICEVs powered by petroleum, GTL, and BTL (biofuel). As seen from Fig. 4.2D, when CSP and CCS are available, the adoption of advanced vehicle technology choices in the model is delayed until fairly late in the century.

### 3.3 Impact of vehicle technology cost

The impact of assumptions regarding future vehicle technology costs are illustrated in Fig. 4.3. The sensitivity to  $H_2$  storage costs are shown in Fig. 4.3A. Comparison of Figs. 4.3A with 4.2A shows that a higher cost for on-board storage of  $H_2$  increases the use of HEVs and PHEVs at the expense of the  $H_2$ -fueled vehicles. This observation illustrates the possible competition between vehicles powered by gaseous fuels and electricity in a carbon-constrained world. Increased cost of  $H_2$  fuel storage favors the electricity-powered options in all four scenarios. Interestingly, because FCVs are more efficient than ICEVs and need to carry less fuel, higher  $H_2$  storage costs disfavor FCVs less than ICEVs and so within the choices for  $H_2$ -powered vehicles (ICEV or FCV), the FCV vehicles become more dominant (in fact, as seen from Fig. 4.3A,  $H_2$  ICEVs are not chosen by the model in the \$3,500/GJ hydrogen storage case).

The sensitivity of the model results to FC stack cost is shown in Fig. 4.3B. Comparison of Fig. 4.3B with 4.2A shows that increasing the FC stack cost from \$65 to \$95/kWh results in essentially complete replacement of hydrogen FC with  $H_2$  ICE vehicle technology.

The sensitivity to variation of battery costs are shown in Figs. 4.3C and 4.3D. With increased battery price, and hence vehicle cost, PHEVs become less attractive (compare Fig. 4.3C with 4.2A). With a battery cost of \$450/kWh, PHEVs are not part of the lowest cost result. Comparison of Fig. 4.3D with 4.1A shows that PHEVs are a very attractive solution for battery costs at the low end of the range investigated (\$150/kWh).

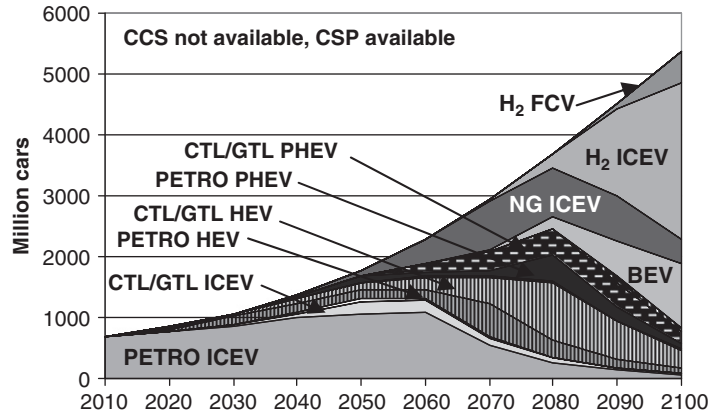


**Figure 4.4** Global passenger vehicle fleet (millions) consistent with data assumed in case 6, that is, halved driving range for BEVs (100 km) compared to case 1, in the scenario where CSP is available but CCS is assumed not to make it into commercial scale.

The impact of battery and FC stack cost when CCS and CSP are available shows the same trends discussed above when CSP and CCS are not available.

Even at the lowest battery cost, BEVs were not found to be a cost-competitive, large-scale technology under any scenario investigated, even though BEVs were allowed to compete with reduced functionality (200 km driving range instead of 500 km for all other vehicles). In an additional sensitivity analysis, we ran the model assuming 100 km driving range for BEVs (see Fig. 4.4 and case 6 in Table 4.5).

BEVs with a driving range of only 100 km are not directly comparable with the other car options in the model which have a range of 500 km. Nevertheless, a 100-km driving range might be a practical option for many city drivers. As shown in Fig. 4.4, BEVs are part of the lowest cost result in scenario C (where CSP is available and CCS is not available) with case 6 vehicle cost data. With an assumption of shorter driving range in scenario C, BEVs partially displace PHEVs (compare Fig. 4.4 with Fig. 4.2C).

Gaseous fuels (NG and H<sub>2</sub>) for HEVs and PHEVs were not explicitly considered here. As NG ICEVs and H<sub>2</sub> ICEVs were competitive, it is possible that the higher efficiencies associated with hybridization could make NG- and H<sub>2</sub>-fueled HEVs (and possibly PHEVs) competitive. Further work is needed to investigate this possibility.



## 4. DISCUSSION AND CONCLUSIONS

The goal of this work was to investigate the factors influencing the cost-effective vehicle and fuel technology choices in a carbon-constrained world. We approached this goal by further developing an existing global energy systems model with the most important addition being a more detailed description of light-duty vehicle technologies



(GET RC 6.1). The model is not intended to provide a forecast of the future, but it does provide insight into the system behavior. We have shown how CCS and CSP, technological options that have the potential to significantly reduce CO<sub>2</sub> emissions associated with electricity and heat generation, may affect cost-effective fuel and vehicle technologies for transport. We find that the availability of CCS and CSP have substantial impacts on the fuel and technology options for passenger vehicles in meeting global CO<sub>2</sub> emission target of 450 ppm at lowest system cost. Four key findings emerge as follows:

1. The introduction of CCS increases, in general, the use of coal (in the energy system) and ICEV (for transport). By providing relatively low-cost approaches to reducing CO<sub>2</sub> emissions associated with electricity and heat generation, CCS reduces the “CO<sub>2</sub> task” for the transportation sector, extends the time span of conventional petroleum-fueled ICEVs, and enables the use of liquid biofuels as well as GTL/CTL for transportation.
2. The introduction of CSP reduces the relative cost of electricity in relation to H<sub>2</sub> and tends to increase the use of electricity for transport (at the expense of H<sub>2</sub>).
3. The combined introduction of both CCS and CSP reduces the cost-effectiveness of shifting away from petroleum and ICEVs for a prolonged period of time (e.g., compare the results in Fig. 4.2D with those in Fig. 4.2A). Advanced energy technologies (CCS and CSP) reduce the cost of carbon mitigation (in the model) and therefore the incentives to shift to more advanced vehicle technologies.
4. The cost estimates for future vehicle technologies are very uncertain (for the time span considered) and therefore it is too early to express firm opinions about the future cost-effectiveness or optimality of different fuel and powertrain combinations. Sensitivity analyses in which these parameters were varied over reasonable ranges result in large differences in the cost-effective fuel and vehicle technology solutions. For instance, for low battery costs (\$150/kWh) electrified powertrains dominate and for higher battery costs (\$450/kWh) H<sub>2</sub>-fueled vehicles dominate, regardless of CCS and CSP availability. Thus, our results summarized above should not be interpreted to mean that the electricity production options alone will have a decisive impact on the cost-effective fuel and vehicle options chosen.

General results on cost-effective primary energy choices include observations that the use of coal increases substantially when CCS is available and that the use of solar energy (mainly solar-based H<sub>2</sub>) increases when neither CCS nor CSP is available.

Our findings have several policy and research implications. From a policy perspective, the findings highlight the need to recognize, and account for, the interaction between sectors (e.g., that illustrated by the impact of CCS availability in the present work) in policy development. From a research perspective, the findings illustrate the importance of pursuing the research and development of multiple fuel and vehicle technology pathways to achieve the desired result of affordable and sustainable personal mobility.

## ACKNOWLEDGMENTS

We thank Mats Willander (Department of Technology Management and Economics, Chalmers, Sweden); Christian Azar, Kristian Lindgren, Fredrik Hedenus, and Julia Hansson (Physical Resource Theory, Chalmers, Sweden); Sherry Mueller (Ford Motor Company, Dearborn, USA); Ichiro Sugioka (Volvo Monitoring and Concept Center, California); Roland Clift (University of Surrey, UK); and Patrik Klintbom (Volvo Technology Corporation, Sweden) for helpful discussions. Financial support from Swedish Energy Agency is gratefully acknowledged.

## REFERENCES

1. IPCC, *Climate Change 2007: The Physical Science Basis*, Cambridge University Press, Cambridge, United Kingdom and New York, USA. 2007. [www.ipcc.ch](http://www.ipcc.ch).
2. UNFCCC (2008), United Nations Framework Convention on Climate Change. The UNFCCC's objective was retrieved 01.12.2008 from [http://unfccc.int/essential\\_background/convention/background/items/1353.php](http://unfccc.int/essential_background/convention/background/items/1353.php) (accessed 06.09).
3. P. Tans, NOAA/ESRL. [www.esrl.noaa.gov/gmd/ccgg/trends](http://www.esrl.noaa.gov/gmd/ccgg/trends), 2009.
4. T.J. Wallington, J.L. Sullivan, M.D. Hurley, *Meteorol. Z.* 17 (2008) 109.
5. C. Azar, K. Lindgren, B.A. Andersson, Hydrogen or Methanol in the Transportation Sector? KFB-Report 2000:35, ISBN: 91-88371-90-5. [www.kfb.se/pdf/R-00-35.pdf](http://www.kfb.se/pdf/R-00-35.pdf)
6. C. Azar, K. Lindgren, B.A. Andersson, *Energy Policy* 31 (2003) 961.
7. C. Azar, K. Lindgren, E. Larson, K. Mollersten, *Climatic Change* 74 (2006) 47.
8. M. Grahn, C. Azar, K. Lindgren, *Biomass Bioenergy* 33 (2009) 360.
9. E. Endo, *Int. J. Hydrogen Energy* 32 (2007) 1347.
10. H. Turton, L. Barreto, *Int. J. Alternative Propulsion* 1 (2007) 397.
11. T. Gül, S. Kypreos, L. Barreto, Hydrogen and Biofuels – A Modeling Analysis of Competing Energy Carriers for Western Europe. Proceedings of the World Energy Congress, Rome, Italy, November 2007. Available at <http://www.worldenergy.org/documents/p000860.pdf>.
12. T. Takeshita, K. Yamaji, *Energy Policy* 36 (2008) 2791.
13. T.M.L. Wigley, Model for the Assessment of Greenhouse-Gas Induced Climate Change. <http://www.cgd.ucar.edu/cas/wigley/magicc/installation.html> (accessed 06.09)
14. IIASA/WEC, *Global Energy Perspectives to 2050 and Beyond*, World Energy Council, London, 1995. [www.iiasa.ac.at/cgi-bin/ecs/book\\_dyn/bookcnt.py](http://www.iiasa.ac.at/cgi-bin/ecs/book_dyn/bookcnt.py) (accessed 06.09).
15. T.B. Johansson, H. Kelly, A.K.N. Reddy, R.H. Williams, *Renewable Energy – Sources for Fuels and Electricity*, L. Burnham (Ed.), Island Press, California, USA, 1993.
16. OECD, *Biofuels: Is the Cure Worse Than the Disease?* Report SG/SD/RT(2007)3, Paris, 2007. [http://www.foeurope.org/publications/2007/OECD\\_Biofuels\\_Cure\\_Worse\\_Than\\_Disease\\_Sept07.pdf](http://www.foeurope.org/publications/2007/OECD_Biofuels_Cure_Worse_Than_Disease_Sept07.pdf) (accessed 06.09).
17. M. Hoogwijk, *On the Global and Regional Potential of Renewable Energy Sources*, Ph.D. Thesis, Utrecht University, Utrecht, the Netherlands, 2004.
18. P. British, *Statistical Guide of World Energy (Values for 2000)*. [www.bp.com](http://www.bp.com) (accessed 06.09).
19. World Energy Assessment, *Energy and the Challenge of Sustainability*. J. Goldemberg (Ed.), United Nations Development Programme (UNDP), United Nations Department of Economic and Social Affairs (UNESA) and World Energy Council (WEC). ISBN: 92-1-126126-0, USA, 2000.
20. H.H. Rogner, *Annu. Rev. Energ. Env.* 22 (1997) 248
21. E.P.A. Swedish. [www.naturvardsverket.se/upload/05\\_klimat\\_i\\_forandring/pdf/emissionsdata\\_koldioxid.pdf](http://www.naturvardsverket.se/upload/05_klimat_i_forandring/pdf/emissionsdata_koldioxid.pdf), 2008 (accessed 06.09).
22. IPCC, *Special Report on Carbon Dioxide Capture and Storage*, B.M. Ogunlade Davidson, H. de Coninck, M. Loos, L. Meyer (Eds.), 2005. [http://www.ipcc.ch/pdf/special-reports/srccs/srccs\\_wholereport.pdf](http://www.ipcc.ch/pdf/special-reports/srccs/srccs_wholereport.pdf) (accessed 06.09).
23. EC Alternative Fuels (EUCAR), *Market Development of Alternative Fuels*, Report of the European Commission, Alternative Fuels Contact Group, December 2003.

24. TIAX, Full Fuel Cycle Assessment Tank to Wheels Emissions and Energy Consumption, Report CEC-600-2007-003-D, February 2007 Available at <http://www.energy.ca.gov/2007publications/CEC-600-2007-003/CEC-600-2007-003-D.PDF>.
25. R. Choudhury, GM Well-to-Wheel Analysis of Energy Use and Greenhouse Gas Emissions of Advanced Fuel/Vehicle Systems – A European Study, 2002. [www.lbst.de/gm-wtw](http://www.lbst.de/gm-wtw) (accessed 06.09).
26. CONCAWE EUCAR JCR Report, Well-to-Wheels Analysis of Future Automotive Fuels and Powertrains in the European Context, European Commission, Luxembourg, 2006. <http://ies.jrc.ec.europa.eu/WTW> (accessed 06.09).
27. M. Wang, Greenhouse Gases, Regulated Emissions, and Energy Use in Transportation (GREET), Version 1.7, 2005. [www.transportation.anl.gov/pdfs/TA/353.pdf](http://www.transportation.anl.gov/pdfs/TA/353.pdf) (accessed 06.09).
28. D. Santini, M. Wang, PHEV Technology Analysis at Argonne. [www.transportation.anl.gov/pdfs/HV/548.pdf](http://www.transportation.anl.gov/pdfs/HV/548.pdf), 2008 (accessed 06.09).
29. TIAX, Ethanol Biofuels Implementation Plan, CEC-ARB Workshop on Developing a State Plan to Increase the Use of Alternative Transportation Fuels. [http://www.energy.ca.gov/ab1007/documents/2007-05-31\\_joint\\_workshop/presentations/JACKSON\\_ETHANOL\\_BIOFUELS\\_2007-05-31.PDF](http://www.energy.ca.gov/ab1007/documents/2007-05-31_joint_workshop/presentations/JACKSON_ETHANOL_BIOFUELS_2007-05-31.PDF), (accessed 31.05.07).
30. U.S. Advanced Battery Consortium. <http://www.uscar.org>, 2008 (accessed 06.09).
31. U.S. Department of Energy, Targets for On-Board Hydrogen Storage Systems. [www1.eere.energy.gov/hydrogenandfuelcells/storage/pdfs/targets\\_onboard\\_hydro\\_storage.pdf](http://www1.eere.energy.gov/hydrogenandfuelcells/storage/pdfs/targets_onboard_hydro_storage.pdf), 2008 (accessed 03.08)
32. Ballard Inc. <http://phx.corporate-ir.net/phoenix.zhtml?c=76046&p=irol-newsArticle&ID=985592&highlight>, 2008 (accessed 06.09).
33. M.A. Uytterlinde, C.B. Hanschke, P. Kroon. Effecten En Kosten Van Duurzame Innovatie in Het Wegverkeer; Een Verkenning Voor Het Programma 'De Auto Van De Toekomst Gaat Rijden', ECN, Petten 2007. <http://www.ecn.nl/publicaties/default.aspx?nr=ECN-E-07-106> (accessed 06.09)
34. M. Grahm, C. Azar, M.I. Willander, J.E. Anderson, S.A. Mueller, T.J. Wallington, *Envir. Sci. Technol.* 43 (2009) 3365.
35. M. Grahm, M.I. Willander, Conference Proceedings, EVS-24, Stavanger, Norway, May 13–16, 2009.
36. T.J. Wallington, M. Grahm, J.E. Anderson, S.A. Mueller, M.I. Willander, K. Lindgren, *Envir. Sci. Technol.* 44 (2010) 2702.



# Expected Greenhouse Gas Emission Reductions by Battery, Fuel Cell, and Plug-In Hybrid Electric Vehicles

Timothy E. Lipman<sup>\*1</sup> and Mark A. Delucchi<sup>\*\*</sup>

<sup>\*</sup>Transportation Sustainability Research Center, University of California–Berkeley, 2614 Dwight Way, MC 1782, Berkeley, CA, 94720-1782, USA

<sup>\*\*</sup>Institute of Transportation Studies, University of California at Davis, Davis, CA 95616, USA

## Contents

1. Introduction	114
1.1 Chapter scope and organization	115
2. Background and Previous Research	115
2.1 Overview of previous research	117
3. Formation of GHG Emissions from EV Fuel Cycles	118
3.1 Upstream emissions	119
3.1.1 Overview of estimates of upstream emissions	119
3.2 Combustion or “in-use” emissions	119
3.2.1 Combustion emissions of carbon dioxide—overview	120
3.2.2 Emissions of carbon dioxide from combustion engines	120
3.2.3 Combustion emissions of carbon dioxide from electricity generation	120
3.2.4 Emissions of methane from combustion engines	121
3.2.5 Emissions of methane from power plants	121
3.2.6 Formation and emissions of nitrous oxide from combustion engines	122
3.2.7 Emissions of nitrous oxide from power plants	122
3.2.8 Emissions of other greenhouse gases from EV fuel cycles	123
3.3 Emissions of CO <sub>2</sub> and other GHGs from the vehicle life cycle	123
4. Estimates of GHG Emissions from EV Fuel Cycles	124
4.1 LEM—overview	124
4.1.1 LEM—emission results for BEVs and FCVs	126
4.2 GREET model—overview	133
4.2.1 GREET—GHG emission results for BEVs and FCVs	134
4.3 Other EV GHG emission modeling efforts	134
4.4 Comparison of major modeling efforts	135
4.4.1 Comparison of GHG emissions estimates for BEVs and FCVs	135
4.4.2 Overview of GHG emissions estimates for PHEVs	137
4.4.3 Review of estimates of GHG emissions from PHEVs	140
4.4.4 Comparison of GHG emissions reductions from PHEVs	144
4.5 Comparison of GHG emissions reductions from EV types	145

<sup>1</sup> Corresponding author: [telipman@berkeley.edu](mailto:telipman@berkeley.edu)

5. Magnitude of Possible GHG Reductions—Scaling up the EV Industry	147
5.1 Scaling up the EV industry—how fast can it be done?	147
5.2 GHG reductions from a scaled up fleet of EVs	148
6. Key Uncertainties and Areas for Further Research	148
6.1 Key uncertainties in LCA analysis of GHGs from EV fuel cycles	149
7. Conclusions	150
Acknowledgments	151
References	151
Appendix	153



## 1. INTRODUCTION

Electric-drive vehicles (EVs) are widely promoted for their environmental and energy efficiency benefits. However, unlike conventional gasoline vehicles, whose emissions of greenhouse gases (GHGs) are a combination of “upstream” emissions from fuel production and distribution and “downstream” emissions from vehicle operation, emissions from EVs are more heavily or even entirely upstream in the fuel production and distribution process. In some ways this makes emissions from these vehicles easier to estimate, but there still are many complexities involved. This is particularly true for “plug-in hybrid” vehicles (or “PHEVs”) that use a combination of grid electrical power and another fuel that is combusted onboard the vehicle.

In the case of battery electric vehicles (BEVs) and fuel cell vehicles (FCVs), the emissions from the vehicles are entirely dependent on the manner in which the electricity and/or hydrogen (H<sub>2</sub>) are produced, along with the energy-use efficiency of the vehicle (typically expressed in “watt hours per mile/kilometer” for BEVs and “miles/kilometers per kilogram” for H<sub>2</sub>-powered vehicles). In the case of PHEVs, an upstream emission component results from the use of electricity from the wall plug or charger (along with upstream emissions from the production of the vehicle’s other fuel), but there can be also significant tailpipe emissions depending on travel patterns and the type of plug-in hybrid.

PHEVs with true “all-electric range” (AER) could allow drivers to some trips without the engine turning on at all (or at least very little), where the trip can be made almost entirely on the energy stored in the battery. However, some PHEVs are not designed for this and instead employ “blended mode” operation, where the design would be for the engine to turn of and on periodically. And in other cases, even for “series type” PHEVs with extensive AER, some engine operation is to be expected both on longer trips and in other cases where the PHEV battery becomes discharged before it can be charged again.

GNG emissions from conventional and alternative vehicles have been extensively studied over the past 20 or more years, but are still not fully understood and accounted for. This is particularly so with regard to some of the subtler aspects of vehicle three-way catalyst operation and emissions of trace gases, as well as some potentially important nuances

of upstream emissions from virtually all fuels due to the complexity of estimating various aspects of upstream emissions. These include, for example, difficulty in accurately assessing the true marginal emissions impacts from the increased use of power plants to charge BEVs and PHEVs, and some secondary aspects of upstream emissions that can be important such as the “indirect land use” change effects of the production of biomass for biofuel vehicles. GHG emission reductions from vehicles and fuels represent an important set of strategies for reducing emissions from the transportation sector, among various other options [1].

Additionally, some aspects of climate dynamics are still not completely understood, for example, with regard to the exact “radiative forcing” aspects of certain gases emitted by vehicles, especially fine particulates and conventional pollutants that appear to have relatively weak impacts but of uncertain magnitude and potentially even uncertain direction [2]. This renders some uncertainty in the overall impacts of the GHGs that are compounded by uncertainties in the exact levels of emissions themselves. With those caveats, this chapter presents much of what is known about the relative emissions of GHGs of these emerging EV types.

## 1.1 Chapter scope and organization

This chapter presents background on GHG formation from motor vehicles and then estimates of GHG emissions from various types of EVs from studies by research groups at universities, national labs, government agencies, and other groups. The GHG emissions estimates are compared and assessed, and key differences and suggestions for further research are presented.

Researchers generally distinguish emissions related to the life cycle of fuels and energy used to power the vehicle (the “fuel cycle”) from emissions related to the life cycle of the vehicle and the materials it is made from (the vehicle life cycle). In this chapter we focus mainly but not exclusively on fuel cycle emissions, because there has been relatively little work on vehicle life cycle emissions.

The chapter is organized as follows. First, background on the issue of GHG emissions from EVs is presented and previous research is reviewed. Second, the processes for the formation of GHG emissions from EV fuel cycles are discussed. Third, recent estimates of GHGs from EV fuel cycles are reviewed and compared. Fourth, the potential for EVs to rapidly scale-up to meet the climate challenge is examined. Finally, key uncertainties, areas for further research, and conclusions are discussed.



---

## 2. BACKGROUND AND PREVIOUS RESEARCH

Emissions from various types of alternative-fuel vehicles (AFVs) including EVs using electricity and H<sub>2</sub> as fuels have been reviewed and analyzed over the past few decades. This has occurred along with growing scientific and public recognition of the climate change problem and the role of transportation in contributing to it. This work

has revealed some interesting dynamics of GHG formation and emission from vehicle fuel cycles, particularly with regard to various nuances of upstream emissions from fuels and electricity production, secondary effects of fuels production on other aspects of the economy, and emissions of nitrous oxide ( $\text{N}_2\text{O}$ ) and other GHGs from combustion engine vehicles [3–6].

By way of further background it is worth noting that GHGs are a number of different gases and aerosols that have climatic impacts, including three that are commonly analyzed as parts of vehicle fuel and electricity fuel cycles—carbon dioxide ( $\text{CO}_2$ ), methane ( $\text{CH}_4$ ), and  $\text{N}_2\text{O}$ —as well as many refrigerant gases and various other gases and particulates that have climatic impacts (e.g., ozone, carbon monoxide ( $\text{CO}$ ), black soot, volatile organic compounds, etc.). Fig. 5.1 presents the “radiative-forcing” in terms of watts per square meter from the emissions of various classes of gases from 1750 through 2005. As shown,  $\text{CO}_2$  has the single largest effect, but various other gases and atmospheric species are significant as well. For example, ozone and aerosols—which are omitted from most analyses of GHG emissions from EVs—have had a greater absolute radiative forcing effect than has  $\text{N}_2\text{O}$  (Fig. 5.1).

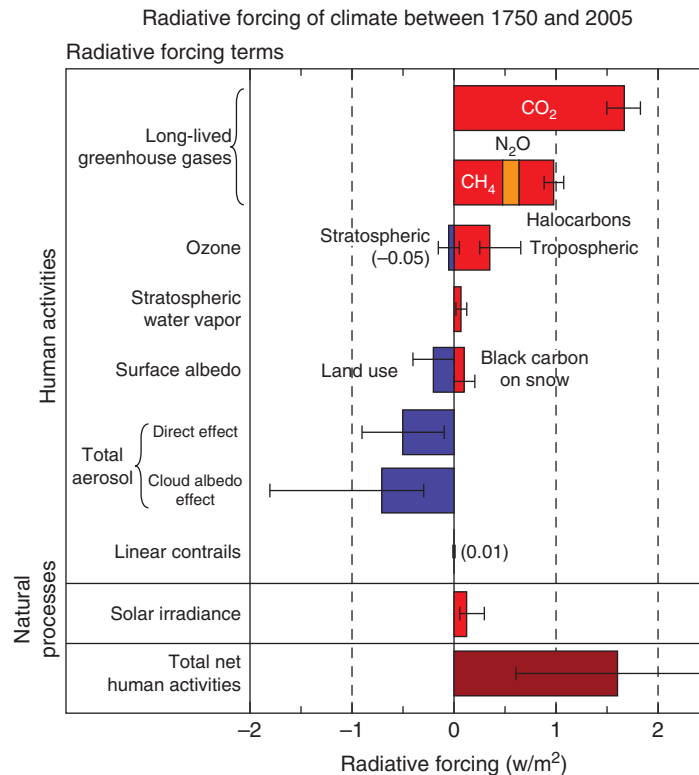


**Figure 5.1** Radiative forcing from GHGs from human activities and natural activities [2].

**Table 5.1** Atmospheric concentration and radiative forcing increases from key GHGs (1750–2007)

Gas	Preindustrial level	Current level	Increase since 1750	Radiative forcing (W/m <sup>2</sup> )
Carbon dioxide	280 ppm	385 ppm	105 ppm	1.66
Methane	700 ppb	1,741 ppb	1,045 ppb	0.48
Nitrous oxide	270 ppb	321 ppb	51 ppb	0.16
Ozone	25	34 ppb	9 ppb	0.35
CFC-12	0	533 ppt	533 ppt	0.17

Source: [7].

For EVs of various types that are fueled with electricity and/or H<sub>2</sub>, the GHGs of most interest are CO<sub>2</sub>, CH<sub>4</sub>, N<sub>2</sub>O, the latest automotive refrigerants (e.g., hydrofluorocarbon (HFC)-134a, HFO-1234yf, etc.), ozone, and secondary particulates from power production. Some other gases with apparently lesser significance (due in part to their relatively weak “global warming potentials [GWPs]”) but that also contribute are CO and various nonmethane hydrocarbons (NMHCs) (apart from their contribution to ozone formation).

Table 5.1 above summarizes the preindustrial and current levels of atmospheric concentration of four principal GHGs, as well as their total increase and the corresponding level of increased radiative forcing in units of watts per square meter. The increased concentrations of CO<sub>2</sub> have provided the majority of the increases in radiative forcing of these four gases, but the others have also made significant contributions.

## 2.1 Overview of previous research

Research on the GHG emissions from fuel cycles related to EV use dates back to at least the early 1990s, when the introduction of BEVs by major automakers and a growing concern about climate change spurred interest in comparing the GHG emissions from battery and fuel cell EVs with the emissions from conventional vehicles. Most studies focused on criteria air pollutants, but some GHGs were occasionally included. Significant research efforts in the 1990s include those by university and government lab research groups [8–11] and consulting firms [12–14]. The next decade saw major efforts by automakers [15, 16], industry research organizations [17], and other groups. More recently, major efforts have examined the potential GHG impacts of PHEVs in a series of efforts that are discussed later.

This chapter features the LEM (the Life Cycle Emissions Model) and the GREET (Greenhouse gases, Regulated Emissions, and Energy use in Transportation) model as they are both well developed with long histories, and also are relatively well documented. They therefore are relatively “transparent” tools for analyzing emissions from a wide range of vehicle and fuel combinations. Along with other efforts, these models are



described below as being among the key sources of information for comparing emissions of different types of EVs. Other studies have examined more specific vehicle and fuel pathways involving EVs with regard to their GHG emissions, but that still have yielded interesting insights. Several of these are also discussed in this chapter.



### 3. FORMATION OF GHG EMISSIONS FROM EV FUEL CYCLES

A key feature of GHG emissions from the production of transportation fuels and electricity is that emissions of  $\text{CO}_2$  are comparatively easy to estimate: they can be approximated as the carbon content of the fuel multiplied by 3.66 (the ratio of the molecular mass of  $\text{CO}_2$  to the molecular mass of carbon), on the assumption that virtually all of the carbon in fuel oxidizes to  $\text{CO}_2$ .

In contrast, combustion emissions of all the other GHGs are a function of many complex aspects of combustion dynamics (such as temperature, pressure, and air-to-fuel ratio) and of the type of emission control systems used, and hence cannot be derived from one or two basic characteristics of a fuel. Instead, one must use published emission factors for each combination of fuel, end-use technology, combustion conditions, and emission control system. Likewise, noncombustion emissions of GHGs (e.g., gas flared at oil fields or  $\text{N}_2\text{O}$  produced and emitted from fertilized soils), cannot be derived from basic fuel properties, and instead must be measured and estimated source-by-source and gas-by-gas. Lipman and Delucchi [18] provide a compendium of many of these emission factors, but we note that some of them have been updated based on more recent data than were available at the time that study was published.

As indicated above, GHG emissions from the life cycle of fuels for BEVs and  $\text{H}_2$  fuel cell EVs are entirely in the form of upstream emissions, with no emission from the vehicles themselves (except for water vapor in the case of FCVs). As such, the GHG emissions from battery and fuel cell EVs are entirely related to the production of electricity or  $\text{H}_2$ . Emissions from electricity generation processes are generally well known and well studied; this is less true for  $\text{H}_2$  production but in most cases these emissions are well understood as well. Some novel  $\text{H}_2$  production methods, and those that are based on conversion from biofuels, have somewhat complex and certainly not completely understood and established levels of emissions of GHGs.

In contrast, for PHEVs, emissions are a complex combination of upstream and in-use emissions. Emissions from these vehicles are more complex than for conventional vehicles or EVs, because these vehicles combine features of internal combustion engine vehicles (ICEVs) with those of EVs. Various vehicle design and operational strategies are available for PHEVs, and these can have important emissions implications. For example, PHEVs can be designed to be either “charge depleting (CD)” or “charge sustaining (CS)” and this affects the relative levels of electricity and gasoline used. (See Gonder and Markel [19] and Katrasnik [20] for further discussion of operating strategies for PHEVs.)

### 3.1 Upstream emissions

The emissions associated with fuel production or “upstream” emissions dominate the fuel cycles associated with BEVs and FCVs. Other emissions are possible—for example, FCVs produce water vapor, which is a weak GHG but produced in amounts by FCVs that are very small in a relative sense to the global hydrologic cycle and not unlike water vapor emissions as a combustion product from conventional vehicles.

For BEVs, upstream emissions consist of emissions from the production and delivery of electricity for vehicle charging. These emissions vary regionally, due to the fuels and types of power plants used to generate electricity. For PHEVs, total emissions consist of a mix of upstream emissions from electricity generation (proportional to the extent that the vehicle is recharged with electricity) and both upstream and in-use emissions from fuel combustion. Finally, for FCVs, emissions are again entirely upstream from the production, delivery, and dispensing of gaseous or liquid H<sub>2</sub> (again with the exception of small amounts of water vapor that are emitted directly from FCVs exhaust systems).

#### 3.1.1 Overview of estimates of upstream emissions

Various studies have examined the upstream emissions from vehicle fuels production, especially from gasoline and diesel fuel and electricity production but also for other fuels such as compressed natural gas, ethanol and methanol, H<sub>2</sub>, and biodiesel among others. These have been conducted in various regions (mainly in the USA and Europe) and with various emphases (i.e., various vehicle type/technology combinations, CO<sub>2</sub> or a whole suite of gases, sometimes including criteria pollutants as well as GHGs, etc.).

Efforts to analyze upstream emissions became important especially when the introduction of BEVs and FCVs was contemplated. These early efforts, some of which are mentioned above, have been superseded by more sophisticated efforts based on further developments in EV technology and the concept of PHEVs as well as BEVs and FCVs. Several of these more recent efforts are reviewed and compared below, following further discussion of the nature and character of GHG emissions from EV fuel cycles.

### 3.2 Combustion or “in-use” emissions

Emissions of GHGs from engine combustion processes result from a complex combination of combustion dynamics and emission controls, and vary widely by fuel type, engine operation, and emission control system applied (if any). For EVs, combustion emissions from the vehicle are limited to PHEVs that either use a combustion engine and generator as a “range extended” for what is fundamentally an EV driveline, or where the engine is connected in parallel to the driveline with the electric motor. Either way, the combustion engine operates periodically to supplement the electric motor operation, and thereby produces GHG emissions. The only other combustion emissions that might be expected from EVs are from those that might include a supplemental fuel-fired heater for the passenger cabin, for occasional use in colder climates. For BEVs and FCVs,

combustion emissions are upstream only because these vehicles operate entirely on electric propulsion.

Key GHG emission products from combustion engines include CO<sub>2</sub>, CH<sub>4</sub>, N<sub>2</sub>O, CO, NO<sub>x</sub>, soot, and various air toxics and other trace chemicals that can play roles in the formation of secondary particulates and other gases (such as ozone [O<sub>3</sub>]) that are known to have climatic effects. Additional in-use emissions include those that can occur from vehicle air-conditioning systems, where GHGs are often used as refrigerants.

### **3.2.1 Combustion emissions of carbon dioxide—overview**

CO<sub>2</sub> is emitted directly from combustion engine vehicles and from electricity-generating power plants. Compared with other GHGs that are formed through complex combustion processes (e.g., N<sub>2</sub>O, NO<sub>x</sub>, and CO) emissions of CO<sub>2</sub> are easier to estimate because most fuel carbon oxidizes to CO<sub>2</sub> and emissions are thus closely related to fuel carbon levels.

### **3.2.2 Emissions of carbon dioxide from combustion engines**

Combustion engine-based motor vehicles emit CO<sub>2</sub> directly from their vehicle tailpipes. These emissions are closely correlated with the total carbon in the vehicle fuel. The U.S. Environmental Protection Agency (EPA) uses a carbon content estimate of 2,421 g of carbon per gallon of gasoline and 2,778 g of carbon per gallon of diesel fuel for purposes of estimating CO<sub>2</sub> emissions from combustion of these fuels [21].

To calculate the CO<sub>2</sub> emissions resulting from combustion of these fuels, one can closely approximate this by multiplying the fuel carbon content by an “oxidization factor” and by the ratio of molecular weights of CO<sub>2</sub> (44) to elemental carbon (12). This results in the following sample calculations, assuming a 99% oxidization factor (the value used by the EPA):

CO<sub>2</sub> emissions from a gallon (liter) of gasoline = 2,421 g × 0.99 × (44/12) = 8,788 g

Thus: 8.8 kg CO<sub>2</sub>/gallon or 2.3 kg CO<sub>2</sub>/liter

CO<sub>2</sub> emissions from a gallon (liter) of diesel = 2,778 g × 0.99 × (44/12) = 10,084 g

Thus: 10.1 kg CO<sub>2</sub>/gallon or 2.7 kg CO<sub>2</sub>/liter

These factors can be used for reasonable first order approximations of the direct tailpipe emissions of CO<sub>2</sub> from ICEV vehicles using gasoline and diesel fuel. For further discussion (see, e.g. [3, 9, 22]).

### **3.2.3 Combustion emissions of carbon dioxide from electricity generation**

CO<sub>2</sub> is emitted directly from energy generation facilities, particularly those that are fossil fuel powered or biomass powered. In the case of biomass-powered facilities, the CO<sub>2</sub> emitted represents a partial or full “closed loop” as biomass removes CO<sub>2</sub> from the atmosphere as it is grown. Biomass cofiring with coal power plants has also been shown to reduce emissions of sulfur dioxide (SO<sub>2</sub>) and nitrogen oxides [23].

Renewable and nuclear facilities emit little to no CO<sub>2</sub> directly, but may have significant emissions through other parts of their full fuel cycle (e.g., the construction of nuclear plants, activities from uranium mining, construction of wind turbine systems). In general these emissions are much lower than the lifetime emissions of especially coal-fired power plants, that are used for up to 50 years and that represent a large amount of “locked-in” emissions with each new plant built. For example, an estimated 100 million tons of CO<sub>2</sub> are generated from the fuel burned by a 500 MW coal-fired power plant over a 40-year lifetime [24]. For purposes of comparison, a recent study reports that coal-fired power plants in the United States emit about 1,200 kg per MWh while natural gas combined cycle plants emit about 700 kg per MWh and renewable and nuclear sources emit much lower levels, on the order of 25–75 kg per MWh [25].

### **3.2.4 Emissions of methane from combustion engines**

CH<sub>4</sub> is emitted directly from combustion-engine vehicles, along with other unburned hydrocarbons. CH<sub>4</sub> emissions from combustion engines are a function of the type of fuel used, the design and tuning of the engine, the type of emission control system, the age of the vehicle, and other factors. CH<sub>4</sub> has a 100-year GWP value of 25, meaning that each molecule has 25 times the radiative-forcing impact of a CO<sub>2</sub> molecule over that time period [26].

Although CH<sub>4</sub> emissions *per se* are not regulated in the United States, the systems used to control emissions of NMHCs and total hydrocarbons from combustion engines do to some extent control CH<sub>4</sub> emissions. As with N<sub>2</sub>O emissions from gasoline light-duty vehicles (LDVs), discussed below, CH<sub>4</sub> emissions also seem to increase somewhat as a function of catalyst age. However, there are few data for high-mileage LDVs, particularly for Tier 1 light-duty automobiles and light-duty trucks (LDTs), and this makes the estimation of deterioration rates difficult. When regression analyses were performed on the available data, emission trend lines slope upward, but with very low associated coefficient of determination (“*r*<sup>2</sup>”) values [18]. This suggests that CH<sub>4</sub> emissions also tend to increase with higher age vehicles.

There are many CH<sub>4</sub> emissions tests for gasoline vehicles, but comparatively few for diesel and alternative-fuel ones. Various emission factors and deterioration rates for CH<sub>4</sub> were estimated in Lipman and Delucchi [18], along with emission factors for some AFVs.

### **3.2.5 Emissions of methane from power plants**

Power plants also produce relatively small amounts of CH<sub>4</sub> as unburned hydrocarbons, with emission factors that are available in comprehensive databases from the U.S. EPA [23] and the Intergovernmental Panel on Climate Change (IPCC) [26]. With natural gas power plants, there also can be fugitive CH<sub>4</sub> emissions from pipelines, purging, and venting procedures (see [3] for estimates). These can add to the total CH<sub>4</sub> emissions from natural gas power plant fuel cycles.

### **3.2.6 Formation and emissions of nitrous oxide from combustion engines**

$\text{N}_2\text{O}$  is a potent GHG with a 100-year GWP value of 298 [27] that is emitted directly from motor vehicles.  $\text{N}_2\text{O}$  emissions from catalyst-equipped gasoline LDVs depend significantly on the type and temperature of catalyst, rather than total oxide of nitrogen ( $\text{NO}_x$ ) levels or fuel nitrogen content. This is because gasoline contains relatively little nitrogen and therefore fuel  $\text{NO}_x$  and  $\text{N}_2\text{O}$  emissions from autos are low. Furthermore, the high temperatures and pressures of the internal combustion engine are sufficient to form  $\text{NO}_x$  thermally, but evidently are inefficient for production of  $\text{N}_2\text{O}$ .

As a result, cars without catalytic converters produce essentially no net  $\text{N}_2\text{O}$ . However, cars with catalytic converters can produce significant  $\text{N}_2\text{O}$  when the catalyst starts out cold. Essentially, as a vehicle warms up and the catalyst temperature increases, a “pulse” of  $\text{N}_2\text{O}$  is released. This occurs until the catalyst temperature increases beyond the temperature “window” for  $\text{N}_2\text{O}$  formation, after which emissions of  $\text{N}_2\text{O}$  are minimal. Older catalysts have a wider window for formation, hence older three-way catalyzed equipped vehicles tend to emit more  $\text{N}_2\text{O}$  than younger vehicles.

This temperature dependence of  $\text{N}_2\text{O}$  formation has important implications regarding potential emissions from PHEVs. If the combustion engine in a PHEV is cycling on and off, then the catalyst may be cooling off and reheating multiple times during a trip instead of a single time, which could result in increased emissions of  $\text{N}_2\text{O}$ . One concept to mitigate this would be to electrically heat the catalyst to keep it from cooling off, but this would come at some (perhaps small) net energy penalty for the vehicle. This issue of potentially increased emissions of  $\text{N}_2\text{O}$  from PHEVs appears to be a significant issue for further study.

Emissions of  $\text{N}_2\text{O}$  from combustion engines have been estimated by the EPA, the IPCC [26], and other research centers. Primary  $\text{N}_2\text{O}$  emissions testing studies from vehicles and other sources have been conducted at U.S. EPA test facilities in Michigan, and at the National Renewable Energy Laboratory, among other places. Estimates prior to and circa 1999 were reviewed in Lipman and Delucchi [18]. For a more recent testing and analysis study of these emissions, see Behrentz et al. [28] and the IPCC [26].

### **3.2.7 Emissions of nitrous oxide from power plants**

Power plants also emit  $\text{N}_2\text{O}$ . Although the power plant combustion chemistry of  $\text{N}_2\text{O}$  is quite complex, several general trends are apparent. Higher  $\text{N}_2\text{O}$  emissions are generally associated with lower combustion temperatures, higher rank fuels, lower ratios of fuel oxygen to fuel nitrogen, higher levels of excess air, and higher fuel carbon contents [29]. Explanations for the temperature dependence of  $\text{N}_2\text{O}$  formation include lower catalytic decomposition activity at lower temperatures, lower availability of NCO free radical (needed for one route of  $\text{N}_2\text{O}$  formation) at higher temperatures due to oxidation to NO, and higher rates of removal of  $\text{N}_2\text{O}$  through reaction with atomic  $\text{H}_2$  at higher temperatures [29].

N<sub>2</sub>O emission factors for power plants are provided by EPA [23] and the IPCC [26]. Generally, N<sub>2</sub>O emissions from power plants are a small fraction of total fuel cycle CO<sub>2</sub> equivalent (CO<sub>2</sub>e) GHG emissions from power plants [3].

### **3.2.8 Emissions of other greenhouse gases from EV fuel cycles**

Emissions of other GHGs from the production and use of EVs include criteria pollutants, such as CO, NMHCs, NO<sub>x</sub>, and SO<sub>x</sub>, and automotive refrigerants such as chlorofluorocarbon (CFC) and HFC-134a. Criteria pollutants typically have weak direct-forcing GWP values and are emitted in much lower quantities than CO<sub>2</sub>, but can contribute to the formation of compounds that do have a strong radiative forcing effect, such as ozone and sulfate aerosol. As an example of how these other pollutants can affect overall results, relative levels of the sulfate aerosols that are produced by coal power plants can affect their overall climate impacts. As shown in Table 5.4 (in Section 4.1.1) that compares emissions for BEVs from China, Germany, Japan, and the USA, the overall GHG reductions of BEVs running on coal-produced electricity are greater for China than for the United States. Since the sulfate aerosols formed by SO<sub>x</sub> emissions have a “cooling” rather than a “warming” effect, the emissions from coal-fired power plants in China to power BEVs can actually have less of a warming effect than those in the United States. This is the case even though the plants are on average more efficient in the United States.

Also potentially important are the refrigerants used in automotive air conditioners, which can be released during accidents or improper maintenance procedures, and which can have very high GWP values. Refrigerant use in automotive air conditioners has evolved from the use of R-12 throughout the 1970s and 1980s to a transition to HFC-134a in the 1990s primarily to help protect the earth’s ozone layer. HFC-134a is still a potent GHG however, with a 100-year GWP value of 1,430 [27]. Other nonozone-depleting refrigerants such as HFO-1234yf and CO<sub>2</sub> are being investigated as lower GWP options that can still be effective in automotive applications.

## **3.3 Emissions of CO<sub>2</sub> and other GHGs from the vehicle life cycle**

What we call “the vehicle life cycle” includes the life cycle of the materials that compose a vehicle and the life cycle of the vehicle itself. The life cycle of automotive materials, such as steel, aluminum, and plastics, extends from production of raw ore to delivery of finished materials to assembly plants, and includes recycled materials as well as materials made from “virgin” ore. The life cycle of the vehicle itself includes vehicle assembly, transportation of finished motor vehicles and motor-vehicle parts, and vehicle disposal.

In the vehicle life cycle there are two broad sources of GHG emissions, similar to the emissions sources in the industrial sector in general: emissions related to the use of process energy (e.g., fuels burned in industrial boilers to provide process heat), and noncombustion emissions from process areas (e.g., emissions from the chemical reduction of alumina to aluminum, or NMHC emissions from painting auto bodies). Energy

use and process areas can produce CO<sub>2</sub>, CH<sub>4</sub>, N<sub>2</sub>O, CO, NMHCs, SO<sub>x</sub>, NO<sub>x</sub>, particulate matter (PM), and other pollutants relevant to life cycle analysis (LCA) of CO<sub>2</sub> GHG emissions. The most extensive of the vehicle life cycle assessment models, including the LEM and GREET models, include characterization of these vehicle manufacturing emissions and their contribution to the overall emissions from various vehicle/fuel life cycles. In general, manufacturing emissions can be somewhat higher for some types of EVs than for conventional vehicles (e.g., those that use large nickel-based batteries). The vehicle manufacturing emissions for EVs are often *proportionately* larger than for conventional vehicles because of their lower life cycle emissions. A key point is that because vehicle operational emissions dominate, EVs are often much cleaner than conventional vehicles in an overall sense even if they have slightly to somewhat higher vehicle manufacturing emissions.



## 4. ESTIMATES OF GHG EMISSIONS FROM EV FUEL CYCLES

Various efforts have examined the emissions of GHGs from EV fuel cycles, but looking at different types of vehicles, with one or more fuel feedstock options, and at varying levels of detail. See the appendix to this chapter for a compilation and “typology” of sorts of several of these studies and their scope. Here we briefly describe a few of the major modeling efforts, emphasizing the well-developed LEM and GREET models that are most familiar, and compare their results below.

### 4.1 LEM—overview

An extensive effort to assess GHG emissions from motor vehicle fuels and electricity production and use, and that we feature in this chapter, is the LEM project at UC Davis. The LEM uses LCA to estimate energy use, criteria air-pollutant emissions, and CO<sub>2</sub>e GHG emissions from a wide range of energy and material life cycles. It includes life cycles for passenger transport modes, freight transport modes, electricity, materials, heating and cooling, and more. For transport modes, it represents the life cycle of fuels, vehicles, materials, and infrastructure. It calculates energy use and life cycle emissions of all regulated air pollutants plus so-called GHGs. It includes input data for up to 30 countries, for the years 1970–2050, and is fully specified for the United States.

For motor vehicles, the LEM calculates life cycle emissions for a variety of combinations of end-use fuel (e.g., methanol, H<sub>2</sub>, electricity, etc.), fuel feedstocks (e.g., petroleum, coal, corn, etc.), and vehicle types (e.g., internal combustion engine vehicle, FCV, etc.). For LDVs, the fuel and feedstock combinations included in the LEM are shown in [Table 5.2](#).

The LEM estimates emissions of CO<sub>2</sub>, CH<sub>4</sub>, N<sub>2</sub>O, CO, total PM, PM less than 10 μm diameter (PM<sub>10</sub>), PM from dust, H<sub>2</sub>, oxides of nitrogen (NO<sub>x</sub>), CFCs (CFC-12), nonmethane organic compounds (NMOCs), (weighted by their ozone-forming

**Table 5.2** Fuel and feedstock pathways and vehicle types analyzed in the LEM

Feedstock	Fuel							
	Gasoline	Diesel	Methanol	Ethanol	Methane (CNG, LNG)	Propane (LPG)	Hydrogen (CH2) (LH2)	Electric
Petroleum	ICEV, FCV	ICEV	–	–	–	ICEV	–	BEV
Coal	ICEV	ICEV	ICEV, FCV	–	–	–	FCV	BEV
Natural gas	–	ICEV	ICEV, FCV	–	ICEV	ICEV	ICEV, FCV	BEV
Wood or grass	–	–	ICEV, FCV	ICEV, FCV	ICEV	–	FCV	BEV
Soybeans	–	ICEV	–	–	–	–	–	–
Corn	–	–	–	ICEV	–	–	–	–
Solar power	–	–	–	–	–	–	ICEV, FCV	BEV
Nuclear power	–	–	–	–	–	–	ICEV, FCV	BEV

*Note:* ICEV = internal combustion engine vehicle, FCV = fuel cell vehicle; BEV = battery electric vehicle.



**Table 5.3** LEM CEFs versus IPCC GWPs

Pollutant	LEM CEFs (year 2030)	IPCC 100-year GWPs
NMOC-C	3.664	3.664
NMOC-O <sub>3</sub> /CH <sub>4</sub>	3	Not estimated
CH <sub>4</sub>	14	23
CO	10	1.6
N <sub>2</sub> O	300	296
NO <sub>2</sub>	-4	Not estimated
SO <sub>2</sub>	-50	Not estimated
PM (black carbon)	2,770	Not estimated
CFC-12	13,000	8,600
HFC-134a	1,400	1,300
PM (organic matter)	-240	Not estimated
PM (dust)	-22	Not estimated
H <sub>2</sub>	42	Not estimated
CF <sub>4</sub>	41,000	5,700
C <sub>2</sub> F <sub>6</sub>	92,000	11,900
HF	2,000	not estimated

Source: LEM CEFs from the year 2005 version of the LEM. IPCC GWPs from the IPCC [30]. CEF = CO<sub>2</sub> equivalency factor; GWP = global warming potential.

potential), HFC-134a, and SO<sub>2</sub> (Table 5.3). These species are reported individually, and aggregated together weighted by CO<sub>2</sub> equivalency factors (CEFs).

These CEFs are applied in the LEM the same way that GWPs are applied in other LCA models, but are conceptually and mathematically different from GWPs. Whereas GWPs are based on simple estimates of years of radiative forcing integrated over a time horizon, the CEFs in the LEM are based on sophisticated estimates of the present value of damages due to climate change. Moreover, whereas all other LCA models apply GWPs to only CH<sub>4</sub> and N<sub>2</sub>O, the LEM applies CEFs to all of the pollutants listed above. Thus, the LEM is unique for having original CEFs for a wide range of pollutants.

#### 4.1.1 LEM—emission results for BEVs and FCVs

As noted above, BEVs and FCVs fueled with onboard H<sub>2</sub> are unique among motor vehicle options in that their emissions are entirely upstream. They are often called “zero emission” vehicles, when in fact this means an absence of tailpipe emissions (which is important from a human health/exposure perspective, to be sure). Most BEV and FCV fuel options do entail significant reductions in GHG and criteria pollutant emissions compared with conventional gasoline vehicles, but this is not always the case (e.g., if coal without carbon capture is the sole feedstock for the electricity for BEV charging).

Table 5.4 presents the final gram-per-km emission results by vehicle/fuel/feedstock, and percentage changes relative to conventional gasoline vehicles, for the USA, China,

**Table 5.4a** Gram-per-kilometer emissions and percentage changes vs. gasoline ICEV (LEM CEFs)

<b>USA 2010 and 2050</b>								
<b>Battery EVs—by type of power plant fuel</b>								
	<b>Coal</b>	<b>Fuel oil</b>	<b>NG boiler</b>	<b>NG turbine</b>	<b>Nuclear</b>	<b>Biomass</b>	<b>Hydro</b>	<b>Other</b>
<b>Year 2010</b>								
Fuel life cycle (g/km)	266.0	231.9	141.3	143.6	14.6	24.2	10.4	7.7
Fuel life cycle (% change)	-20.0%	-30.2%	-57.5%	-56.8%	-95.6%	-92.7%	-96.9%	-97.7%
Fuel and vehicle life cycle <sup>a</sup> (g/km)	365.9	331.8	241.2	243.5	114.5	124.0	110.3	107.6
Fuel and vehicle life cycle <sup>a</sup> (% change)	-6.9%	-15.5%	-38.6%	-38.0%	-70.9%	-68.4%	-71.9%	-72.6%
<b>Year 2050</b>								
Fuel life cycle (g/km)	227.5	197.2	105.9	107.8	7.8	(-3.2)	5.2	3.0
Fuel life cycle (% changes)	-18.7%	-29.6%	-62.2%	-61.5%	-97.2%	-101.1%	-98.1%	-98.9%
Fuel and vehicle life cycle <sup>a</sup> (g/km)	262.4	232.1	140.8	142.7	42.7	31.7	40.1	37.9
Fuel and vehicle life cycle <sup>a</sup> (% change)	-17.1%	-26.7%	-55.5%	-54.9%	-86.5%	-90.0%	-87.3%	-88.0%
<b>Fuel cell EVs—by fuel and feedstock</b>								
<b>General fuel</b>	<b>Gasoline</b>	<b>Methanol</b>	<b>Methanol</b>	<b>Ethanol</b>	<b>Hydrogen</b>	<b>Hydrogen</b>	<b>Hydrogen</b>	<b>Hydrogen</b>
<b>Fuel specification</b>	RFG-Ox10	M100	M100	E100	CH2	CH2	CH2	CH2
<b>Feedstock</b>	<i>Crude oil</i>	<i>NG</i>	<i>Wood</i>	<i>Grass</i>	<i>Water</i>	<i>NG</i>	<i>Wood</i>	<i>Coal</i>
<b>Year 2010</b>								
Fuel life cycle (g/km)	163.9	164.1	47.9	85.4	35.7	135.1	47.8	83.6
Fuel life cycle (% changes)	-50.7%	-50.7%	-85.6%	-74.3%	-89.3%	-59.4%	-85.6%	-74.8%
Fuel and vehicle life cycle <sup>a</sup> (g/km)	223.6	224.1	107.9	145.3	96.6	196.0	108.7	144.6
Fuel and vehicle life cycle <sup>a</sup> (% change)	-43.1%	-43.0%	-72.5%	-63.0%	-75.4%	-50.1%	-72.3%	-63.2%

(Continued)

**Table 5.4a (Continued)**

**Year 2050**

Fuel life cycle (g/km)	134.0	122.6	18.3	13.2	27.5	113.3	24.3	61.6
Fuel life cycle (% changes)	-52.1%	-56.2%	-93.5%	-95.3%	-90.2%	-59.5%	-91.3%	-78.0%
Fuel and vehicle life cycle <sup>a</sup> (g/km)	163.7	152.5	48.1	43.0	59.7	145.6	56.6	93.9
Fuel and vehicle life cycle <sup>a</sup> (% change)	-48.3%	-51.8%	-84.8%	-86.4%	-81.1%	-54.0%	-82.1%	-70.3%

**Japan 2010 and 2050**

**Battery EVs—by type of power plant fuel**

	<b>Coal</b>	<b>Fuel oil</b>	<b>NG boiler</b>	<b>NG turbine</b>	<b>Nuclear</b>	<b>Biomass</b>	<b>Hydro</b>	<b>Other</b>
<b>Year 2010</b>								
Fuel life cycle (g/km)	215.2	185.0	175.8	140.0	11.2	17.7	10.3	7.8
Fuel life cycle (% changes)	-34.7%	-43.8%	-46.6%	-57.5%	-96.6%	-94.6%	-96.9%	-97.7%
Fuel and vehicle life cycle <sup>a</sup> (g/km)	305.6	275.4	266.2	230.5	101.7	108.1	100.7	98.2
Fuel and vehicle life cycle <sup>a</sup> (% change)	-21.6%	-29.3%	-31.7%	-40.9%	-73.9%	-72.3%	-74.2%	-74.8%
<b>Year 2050</b>								
Fuel life cycle (g/km)	175.4	142.0	130.5	111.8	5.4	(-1.0)	5.2	3.0
Fuel life cycle (% changes)	-35.8%	-48.1%	-52.2%	-59.1%	-98.0%	-100.4%	-98.1%	-98.9%
Fuel and vehicle life cycle <sup>a</sup> (g/km)	207.3	173.8	162.4	143.7	37.3	30.9	37.1	34.9
Fuel and vehicle life cycle <sup>a</sup> (% change)	-32.6%	-43.5%	-47.2%	-53.3%	-87.9%	-90.0%	-88.0%	-88.7%

### Fuel cell EVs—by fuel and feedstock

General fuel	Gasoline	Methanol	Methanol	Ethanol	Hydrogen	Hydrogen	Hydrogen	Hydrogen
<b>Fuel specification</b>	RFG-Ox10	M100	M100	E100	CH2	CH2	CH2	CH2
<b>Feedstock</b>	<i>Crude oil</i>	<i>NG</i>	<i>Wood</i>	<i>Grass</i>	<i>Water</i>	<i>NG</i>	<i>Wood</i>	<i>Coal</i>
<b>Year 2010</b>								
Fuel life cycle (g/km)	161.6	169.9	45.0	106.4	27.3	138.8	39.2	79.4
Fuel life cycle (% changes)	-50.9%	-48.4%	-86.3%	-67.7%	-91.7%	-57.9%	-88.1%	-75.9%
Fuel and vehicle life cycle <sup>a</sup> (g/km)	221.0	229.5	104.6	165.9	87.9	199.5	99.9	140.1
Fuel and vehicle life cycle <sup>a</sup> (% change)	-43.3%	-41.1%	-73.2%	-57.4%	-77.4%	-48.8%	-74.4%	-64.1%
<b>Year 2050</b>								
Fuel life cycle (g/km)	130.3	126.1	10.6	36.8	17.1	111.9	12.0	51.2
Fuel life cycle (% changes)	-52.3%	-53.8%	-96.1%	-86.5%	-93.7%	-59.1%	-95.6%	-81.3%
Fuel and vehicle life cycle <sup>a</sup> (g/km)	158.2	154.2	38.6	64.8	47.7	142.5	42.5	81.7
Fuel and vehicle life cycle <sup>a</sup> (% change)	-48.6%	-49.9%	-87.5%	-78.9%	-84.5%	-53.7%	-86.2%	-73.5%
<b>China 2010 and 2050</b>								
<b>Battery EVs—by type of power plant fuel</b>								
	<b>Coal</b>	<b>Fuel oil</b>	<b>NG boiler</b>	<b>NG turbine</b>	<b>Nuclear</b>	<b>Biomass</b>	<b>Hydro</b>	<b>Other</b>
<b>Year 2010</b>								
Fuel life cycle (g/km)	216.2	217.5	183.0	133.5	15.3	55.5	9.8	7.3
Fuel life cycle (% changes)	-37.2%	-36.8%	-46.8%	-61.2%	-95.5%	-83.9%	-97.1%	-97.9%
Fuel and vehicle life cycle <sup>a</sup> (g/km)	321.2	322.5	288.1	238.5	120.3	160.5	114.9	112.3
Fuel and vehicle life cycle <sup>a</sup> (% change)	-21.4%	-21.1%	-29.5%	-41.6%	-70.5%	-60.7%	-71.9%	-72.5%

(Continued)

**Table 5.4a (Continued)**

**Year 2050**

Fuel life cycle (g/km)	201.9	155.4	132.9	97.2	7.3	3.9	4.9	2.8
Fuel life cycle (% changes)	-28.1%	-44.7%	-52.7%	-65.4%	-97.4%	-98.6%	-98.3%	-99.0%
Fuel and vehicle life cycle <sup>a</sup> (g/km)	240.6	194.1	171.6	135.8	46.0	42.5	43.5	41.4
Fuel and vehicle life cycle <sup>a</sup> (% change)	-25.2%	-39.6%	-46.6%	-57.7%	-85.7%	-86.8%	-86.5%	-87.1%

**Fuel cell EVs—by fuel and feedstock**

<b>General fuel</b>	<b>Gasoline</b>	<b>Methanol</b>	<b>Methanol</b>	<b>Ethanol</b>	<b>Hydrogen</b>	<b>Hydrogen</b>	<b>Hydrogen</b>	<b>Hydrogen</b>
<b>Fuel specification</b>	RFG-Ox10	M100	M100	E100	CH2	CH2	CH2	CH2
<b>Feedstock</b>	<i>Crude oil</i>	<i>NG</i>	<i>Wood</i>	<i>Grass</i>	<i>Water</i>	<i>NG</i>	<i>Wood</i>	<i>Coal</i>

**Year 2010**

Fuel life cycle (g/km)	151.3	151.6	65.8	117.9	44.6	124.1	62.0	82.2
Fuel life cycle (% changes)	-56.0%	-55.9%	-80.9%	-65.7%	-87.0%	-63.9%	-82.0%	-76.1%
Fuel and vehicle life cycle <sup>a</sup> (g/km)	215.7	216.5	130.6	182.5	109.9	189.4	127.4	147.5
Fuel and vehicle life cycle <sup>a</sup> (% change)	-47.2%	-47.0%	-68.0%	-55.3%	-73.1%	-53.6%	-68.8%	-63.9%

**Year 2050**

Fuel life cycle (g/km)	122.0	114.1	23.6	27.8	31.0	106.2	29.4	60.9
Fuel life cycle (% changes)	-56.6%	-59.4%	-91.6%	-90.1%	-89.0%	-62.2%	-89.5%	-78.3%
Fuel and vehicle life cycle <sup>a</sup> (g/km)	155.2	147.5	57.1	61.1	66.8	142.0	65.1	96.6
Fuel and vehicle life cycle <sup>a</sup> (% change)	-51.7%	-54.1%	-82.3%	-81.0%	-79.2%	-55.8%	-79.7%	-69.9%

## Germany 2010 and 2050

### Battery EVs—by type of power plant fuel

	Coal	Fuel oil	NG boiler	NG turbine	Nuclear	Biomass	Hydro	Other
<b>Year 2010</b>								
Fuel life cycle (g/km)	239.5	188.0	164.3	131.1	28.3	23.3	10.4	7.8
Fuel life cycle (% changes)	-28.1%	-43.5%	-50.7%	-60.6%	-91.5%	-93.0%	-96.9%	-97.7%
Fuel and vehicle life cycle <sup>a</sup> (g/km)	333.8	282.4	258.6	225.4	122.6	117.6	104.7	102.0
Fuel and vehicle life cycle <sup>a</sup> (% change)	-14.9%	-28.0%	-34.1%	-42.6%	-68.8%	-70.0%	-73.3%	-74.0%
<b>Year 2050</b>								
Fuel life cycle (g/km)	200.5	144.7	121.5	104.2	15.3	(-0.3)	5.2	3.0
Fuel life cycle (% changes)	-26.7%	-47.1%	-55.6%	-61.9%	-94.4%	-100.1%	-98.1%	-98.9%
Fuel and vehicle life cycle <sup>a</sup> (g/km)	230.7	174.9	151.7	134.4	45.5	29.9	35.5	33.2
Fuel and vehicle life cycle <sup>a</sup> (% change)	-24.8%	-43.0%	-50.6%	-56.2%	-85.2%	-90.3%	-88.5%	-89.2%

### Fuel cell EVs—by fuel and feedstock

General fuel	Gasoline	Methanol	Methanol	Ethanol	Hydrogen	Hydrogen	Hydrogen	Hydrogen
<b>Fuel specification</b>	RFG-Ox10	M100	M100	E100	CH2	CH2	CH2	CH2
<b>Feedstock</b>	<i>Crude oil</i>	<i>NG</i>	<i>Wood</i>	<i>Grass</i>	<i>Water</i>	<i>NG</i>	<i>Wood</i>	<i>Coal</i>
<b>Year 2010</b>								
Fuel life cycle (g/km)	163.8	168.7	48.9	100.5	65.5	134.2	49.0	80.9
Fuel life cycle (% changes)	-50.8%	-49.3%	-85.3%	-69.8%	-80.3%	-59.7%	-85.3%	-75.7%
Fuel and vehicle life cycle <sup>a</sup> (g/km)	222.2	227.5	107.7	159.1	125.1	193.9	108.7	140.6
Fuel and vehicle life cycle <sup>a</sup> (% change)	-43.4%	-42.0%	-72.5%	-59.5%	-68.1%	-50.6%	-72.3%	-64.2%

(Continued)

**Table 5.4a (Continued)**

<b>Year 2050</b>								
Fuel life cycle (g/km)	130.4	125.1	9.7	45.7	31.8	96.9	11.8	37.3
Fuel life cycle (% changes)	-52.3%	-54.3%	-96.4%	-83.3%	-88.4%	-64.6%	-95.7%	-86.4%
Fuel and vehicle life cycle <sup>a</sup> (g/km)	157.2	152.0	36.8	72.6	61.0	126.1	41.1	66.6
Fuel and vehicle life cycle <sup>a</sup> (% change)	-48.8%	-50.5%	-88.0%	-76.3%	-80.1%	-58.9%	-86.6%	-78.3%

Notes: "LEM CEFs" are the CO<sub>2</sub> equivalency factors developed for the LEM, as distinguished from the IPCC GWPs (Table 3); ICEV = internal combustion engine vehicle; EV = electric vehicle; NG = natural gas; Hydro = hydropower; Other = solar, geothermal power; RFG = reformulated gasoline; Ox = oxygenate (ETBE, MTBE, ethanol, methanol) (volume % in active gasoline); M = methanol (volume % in fuel for methanol vehicle; remainder is gasoline); CNG = compressed natural gas; LNG = liquefied natural gas; CH<sub>2</sub> = compressed hydrogen; E = ethanol (volume % in fuel for ethanol vehicle; remainder is gasoline).

<sup>a</sup>The vehicle life cycle includes emissions from: the life cycle of materials used in vehicles, vehicle assembly and transport, the life cycle of refrigerants, the production and use of lube oil, and brake wear, tire wear, and road dust.

**Table 5.4b** Gram-per-kilometer emissions for the baseline conventional vehicle

	USA	Japan	China	Germany
Year 2010				
Fuel life cycle (g/km)	332.5	329.4	337.8	333.0
Fuel and vehicle life cycle <sup>a</sup> (g/km)	392.9	389.8	408.6	392.3
Year 2050				
Fuel life cycle (g/km)	280.0	273.3	281.0	273.4
Fuel and vehicle life cycle <sup>a</sup> (g/km)	316.5	307.8	321.5	306.9

Japan, and Germany, for the years 2010 and 2050. In the United States in the year 2010, BEVs reduce fuel life cycle GHG emissions by 20% (in the case of coal) to almost 100% (in the case of hydro and other renewable sources of power). If the vehicle life cycle is included, the reduction is less, in the range of 7–70%, because emissions from the battery vehicle life cycle are larger than emissions from the gasoline ICEV life cycle, on account of the materials in the battery. The emission reduction percentages generally are larger in the year 2050, mainly because of the improved efficiency of vehicles and power plants. The emission reductions in Japan, China, and Germany are similar to those in the United States, except that in those cases the reduction using coal power is larger, due the greater efficiency of coal plants in Germany and Japan, and to high SO<sub>2</sub> emissions from coal plants in China (recall that SO<sub>2</sub> has a negative CEF [Table 5.3]).

In the United States in 2010, FCVs using gasoline or methanol made from natural gas offer roughly 50% reductions in fuel life cycle GHG emissions. FCVs using methanol or H<sub>2</sub> made from wood reduce fuel life cycle GHG emissions by about 85%; FCVs using H<sub>2</sub> made from water reduce emissions by about 60%, and FCVs using H<sub>2</sub> made from water (using clean electricity) reduce fuel life cycle GHG emissions by almost 90%. Again, the reductions are slightly less if the vehicle life cycle is included, and slightly larger in the year 2050. The patterns in Japan, China, and Germany are essentially the same, because the vehicle technology and the fuel production processes are assumed to be the same as in the United States.

## 4.2 GREET model—overview

The GREET model has been under development at Argonne National Laboratory (ANL) for about 15 years. The model assesses over 100 fuel production pathways and about 75 different vehicle technology/fuel system types, for hundreds of possible permutations of combinations of vehicles and fuels. It is used by over 10,000 users worldwide and has been adapted for use in various countries around the world [4, 9, 15, 16, 22]. GREET estimates CO<sub>2</sub>e emissions of CO<sub>2</sub>, CH<sub>4</sub>, and N<sub>2</sub>O from the life cycle of fuels and the life cycle of vehicles, using the IPCC's GWPs to convert CH<sub>4</sub> and N<sub>2</sub>O into CO<sub>2</sub>es.



The latest version of GREET (GREET 1.8c released in 2009) is noteworthy for its much expanded treatment of PHEVs along with updated projections of electricity grid mixes in the United States based on the latest projections by the Energy Information Administration (EIA). This latest version of the model analyzes PHEVs running on various fuels along with electricity, not just gasoline and diesel.

Additional fuels analyzed for use in PHEVs and other vehicle types include corn-based ethanol (E85—85% blend with gasoline), biomass-derived ethanol (E85), and H<sub>2</sub> produced from three different methods: (i) steam CH<sub>4</sub> reforming of natural gas (distributed, small scale); (ii) electrolysis of water using grid power (distributed, small scale); and (iii) biomass-based H<sub>2</sub> (larger scale). The analysis also examines different regions of the United States, and the United States on average, for power plant mixes and emission factors for BEV and PHEV charging and other electricity demands.

#### **4.2.1 GREET—GHG emission results for BEVs and FCVs**

The GREET model results for BEVs and FCVs are broadly similar to the LEM results discussed above. These results are briefly reviewed here. Recent GREET results for various types of PHEVs are discussed in Section 4.4.3 below along with the results of other studies of PHEV emissions.

GREET shows that emission reductions of about 40% can be expected from BEVs using the average electricity grid mix in the United States, compared with emissions from conventional vehicles. In comparison, GREET results suggest that BEVs using a California electricity grid mix would produce reductions of about 60%. Meanwhile FCVs using H<sub>2</sub> derived from natural gas would reduce emissions by just over 50%. FCVs using the average grid mix of U.S. electricity to produce H<sub>2</sub> through the electrolysis process would result in an *increase* in emissions by about 20%. As shown in LEM as well, BEVs and FCVs using entirely renewable fuels to produce electricity and H<sub>2</sub> would nearly eliminate GHGs [31].

### **4.3 Other EV GHG emission modeling efforts**

Various other studies of the relative GHG emission benefits of different types of EVs have been done by other university and national laboratory research groups, consulting firms, government agencies, nongovernment organizations, and industry research groups. Many of these are discussed and compared in the sections that follow.

Key organizations that have been involved in previous efforts include many in the United States (some listed below), the Japanese Ministry of Economy, Trade, and Industry, Japanese research universities including the University of Tokyo, the International Energy Agency, the European Union, Natural Resources Canada, and many other government and research organizations around the world. In the United States, in addition to the national laboratories and the University of California, key efforts have been led by the Massachusetts Institute of Technology, Carnegie Mellon University,

Stanford University, the Pacific Northwest Laboratory, the National Renewable Energy Laboratory, General Motors, and the Electric Power Research Institute (EPRI), among others. Once again, several of these efforts are discussed and compared below.

#### **4.4 Comparison of major modeling efforts**

The various LCA modeling efforts around fuel cycles for EVs are challenging to compare because of the many different dimensions that they encompass, and because they rarely overlap very well in that regard. Hence there is often the challenge of trying to make “apples to apples” versus “apples to oranges” comparisons. Below we include a figure that does compare the results from a few of the most detailed studies; however, we caution that no attempt has been made to correct for key differences in their underlying assumptions (e.g., assumed vehicle driveline efficiencies, etc.). We also include [Table 5. A-1](#) in an appendix to this chapter that compares the key features of eight other LCA efforts compared with the LEM. This table gives a good sense of the types of key aspects that are included in these models, and the extent to which each of them encompasses or addresses them.

As shown in the table, various studies focus on different sets of vehicle and fuel combinations. In our review above we emphasize the most extensive studies that included BEVs and FCVs as well as PHEVs, but we note that there are carefully performed studies that look at a narrower range of vehicle technologies (e.g., that only compare BEVs to ICEVs, for example). We feature recent LEM results for BEVs and FCVs because the results that we present here draw out some interesting regional differences.

##### **4.4.1 Comparison of GHG emissions estimates for BEVs and FCVs**

The study of emissions from BEVs dates back to the 1990s and even earlier, and several studies were performed on emissions from FCV fuel cycles starting in the late 1990s and through the early 2000s. Early BEV emission studies tended to emphasize criteria pollutants, while later studies have also included CO<sub>2</sub>, CH<sub>4</sub>, and N<sub>2</sub>O. Of course we note that the criteria air pollutants are also GHGs, or go on to help form them through secondary atmospheric chemistry processes (e.g., in the case of ozone and secondary particulates).

With regard to estimates of GHG from BEVs, the emissions of course depend strongly on the mix of power plants that is in use in a region, and the specific power plant (or alternately average emission factor) that is assumed to be applicable during the assumed period of vehicle charging. Several studies were conducted for California in the 1990s when the introduction of BEVs was being mandated by the state. These included studies by consulting firms conducted for the California Air Resources Board and other efforts such as the “Total Energy Cycle Assessment of Electric and Conventional Vehicles” (or EVTECA) effort in the late 1990s that combined the efforts of three U.S. national

laboratories to examine the LCA of BEVs compared with conventional vehicles. These studies generally found significant benefits from BEVs in terms of GHG emission reductions, along with the more mixed results for the criteria pollutants that were the main focus of the studies [32, 33]. However the studies were often limited to CO<sub>2</sub> only as far as the GHGs examined, sometimes along with CH<sub>4</sub> and several air pollutants that were more of concern at the time.

Other studies have been done in the past several years comparing BEVs and FCVs as alternatives to ICEVs, with results based on more “modern” assumptions that are better comparisons to the recent work on emissions from PHEVs. One such study by MIT concludes that conventional ICEVs emit about 252 g of CO<sub>2</sub>e/km and that by 2,030 this might be reduced to about 156 g/km. In comparison, 2030 FCVs could emit about 89 g/km, BEVs could emit 116 g/km, and a PHEV-30 (with a 30 mile/50 km AER) might emit about 86 g of CO<sub>2</sub>e/km. Thus, the study finds that the PHEV-30s and FCVs have the largest emission reductions relative to the 2030 ICEV (44 and 42%), followed closely by the BEVs (26%). Hence, all three options (as well as a 2030 advanced conventional hybrid in this analysis) are significantly better than the advanced 2030 ICEV [34].

Another recent such comparison of BEVs and FCVs found that GHG emissions from lithium-ion BEVs were much lower than from either nickel-metal hydride or lead-acid-battery-based vehicles, ranging from about 235 g/km for a 100 km range vehicle to about 375 g/km for a 600 km range vehicle. Meanwhile, FCV emissions are relatively unchanged by driving range, at about 180 g/km. This assumes the electricity is from the U.S. marginal grid mix and that H<sub>2</sub> for the FCVs is made from natural gas. Hence this study suggests that FCVs operating on H<sub>2</sub> from natural gas can have lower GHG emissions than even relatively low-range BEVs in the United States [35], a finding that is consistent with most other studies.

A major, ongoing European study makes detailed estimates of life cycle GHG emissions from alternative-fuel ICEVs, hybrid vehicles, and FCVs [36]. The study uses the Advisor model to simulate vehicle energy use, and a detailed original analysis by L-B-Systemtechnik (LBST) (which also worked on the GM/ANL [16] analysis for Europe) to estimate upstream or “well to tank” emissions. The EUCAR study [36] estimated life cycle emissions for methanol FCVs, using wood, coal, and natural gas as feedstocks, and for compressed-H<sub>2</sub> vehicles, using wood and natural gas as feedstocks. FCVs using H<sub>2</sub> made from natural gas had about 55% lower well-to-wheel GHG emissions than a conventional gasoline ICEV, and FCVs using H<sub>2</sub> made from wood had about 90% lower emissions.

The results of various studies with regard to GHG emissions reductions from BEVs and FCVs, including LEM, GREET, and the studies mentioned above, are compared with several PHEV studies in Section 4.5. These results should be interpreted with some caution because of the many different assumptions made in the studies, but do provide some sense of the relative emission benefits that EV types can provide.

#### 4.4.2 Overview of GHG emissions estimates for PHEVs

PHEVs generate GHG emissions from three distinct sources: the life cycle of fuels used in the ICE, the life cycle of electricity used to power the electric drivetrain, and the life cycle of the vehicle and its materials. A number of studies, reviewed below, have estimated GHG emission reductions from PHEVs relative to conventional ICEVs considering the life cycle of fuels and the life cycle of electricity generation. Because energy use and emissions for the vehicle life cycle are an order of magnitude smaller than energy use and emissions for the fuel and electricity life cycle [37–40], and because there are relatively few studies of emissions from the PHEV vehicle life cycle, once again we do not consider the vehicle life cycle in much detail here, but point interested readers to the efforts referenced above for more details.

With regard to GHG emissions from the life cycle of petroleum fuels used in ICEs for PHEVs, these depend mainly of the fuel use of the engine and the energy inputs and emission factors for the production of crude oil and finished petroleum products. A number of studies estimate the fuel use of ICEs in PHEVs, for example, Table 5.2 of Bradly and Frank [41] reports the gasoline consumption reduction (%) and the gasoline consumption of the conventional ICEV (l/100 km) for a variety of simulated and tested PHEVs. The PHEVs were found to reduce gasoline consumption by 50–90%. To estimate the GHG emissions from the petroleum fuel life cycle, many studies use the ANL GREET model, discussed elsewhere in this chapter.

GHG emissions from the use of electricity by PHEVs depend mainly on the energy use of the electric drivetrain, the efficiency of electricity generation, and the mix of fuels used to generate electricity. The energy use of the electric drivetrain in a PHEV is a function of the size and technical characteristics of the electric components (battery, motor, and controller), the vehicle driving and charging patterns, and the control strategy that determines when the vehicle is powered by the battery and when it is powered by the ICE. The studies reviewed here and tabulated in Table 5.5 consider two basic control strategies, discussed earlier in the chapter: “all-electric” or “blended.” In the all-electric strategy, the PHEV is designed to have a significant AER over a specified drive cycle, and the vehicle runs on the battery until the battery’s state of charge (SOC) drops to some threshold value (e.g., 40%), at which point the engine turns on and the vehicle operates as a CS hybrid (e.g., the Prius) until the next recharging.

In a PHEV with a large AER, the electric drivetrain is sized to have enough power to be able to satisfy all power demands over the drive cycle without any power input from the engine. By contrast, in the blended strategy, the electric drivetrain and the engine work together to supply the power over the drive cycle. The blended strategy can be either “engine dominant,” in which case the battery is used to keep the engine running at its most efficient torque/rpm points, or “electric dominant,” in which case the engine turns on only when the power demand exceeds the capacity of the electricity drivetrain

**Table 5.5** Projected PHEV GHG emissions impacts

Report	Emissions estimation <sup>a</sup>	CD range (km)	Control Strategy	Year	Grid GHGs (gCO <sub>2</sub> e/kWh) <sup>b</sup>	PHEV GHGs (gCO <sub>2</sub> e/km) <sup>b</sup>	ICEV GHGs (gCO <sub>2</sub> e/km) <sup>b</sup>	% reduction (vs. ICEV)
EPRI 2001 [17]	Average	32.2 <sup>c</sup>	AE	2010	427	144	257	44%
		96	AE	2010	427	112	257	57%
Samaras and Meisterling [42]	Scenario	30	AE	NR	200	126	257	51%
					670	183	269	32%
					950	217	276	21%
		90	AE	NR	200	96	257	63%
					670	183	269	32%
950	235	276	15%					
Kromer and Heywood [34]	Average	48	Blended	2030	769	86.2	156	45%
		96	Blended	2030	769	89.8	156	43%
Silva et al. [43]	Average	~57 <sup>d</sup>	AE	n.s. <sup>e</sup>	543 (USA)	~110 <sup>d</sup>	n.s.	n.e.
					387 (Europe)	~105 <sup>d</sup>	n.s.	n.e.
					428 (Japan)	~108 <sup>d</sup>	n.s.	n.e.
					883 (coal)	~125 to 220 <sup>d</sup>	~230 <sup>d</sup>	~4~46%
Jaramillo et al. [44] PNNL [45]	Scenario Simplified dispatch	60	AE	n.s. <sup>e</sup>	94% NG/6% C	n.s.	n.s.	40%
		53	n.s. <sup>f</sup>	2002	1% NG/99% C	n.s.	n.s.	-1%
					U.S. average	n.s.	n.s.	27%

Stephan and Sullivan [46]	Scenario	63	n.s. <sup>f</sup>	Current/long term	598 (current NG)	184/119 <sup>g</sup>	432	57%/72% <sup>g</sup>			
					954 (current coal)	274/192 <sup>g</sup>	432	37%/56% <sup>g</sup>			
					608 (U.S. average)	177	432	59%			
Parks et al. [47] ANL [48]	Dispatch Dispatch/ scenario	32	Blended	2004	454	154	251	39%			
					2020	U.S. average	146	233	37%		
						California	140	233	40%		
						Illinois	162	233	30%		
						Renewable	115	233	51%		
EPRI and NRDC [49]	Dispatch/ scenario	16	AE	2050	97	140	233	40%			
					199	143	39%				
					412	147	37%				
					32.2	AE	2050	97	103	233	56%
								199	109	53%	
			412	119	49%						

Notes: CD = charge depleting; GHG = greenhouse gas; CO<sub>2e</sub> = CO<sub>2</sub> equivalent; ICEV = internal combustion engine vehicle; PHEV = plug-in hybrid electric vehicle; AE = all electric (meaning the vehicle operates solely on the battery until a certain SOC is reached); blended = vehicle is designed to use both the engine and battery over the drive cycle; n.s. = not specified; n.e. = not estimated; NG = natural gas; C = coal.

<sup>a</sup> “Average” means annual-average emissions from the entire national electric grid. “Scenario” means the study considered different fuel mix and hence emission scenarios for the electric grid. “Dispatch” means the study estimated marginal fuel mixes and emissions for PHEV charging based on a dispatch model.

<sup>b</sup> GHG emissions and CO<sub>2</sub> equivalency are estimated as follows: EPRI 2001, Parks et al., Silva et al., and Stephan and Sullivan: CO<sub>2</sub> only. ANL: 2007 IPCC [29] GWPs for CH<sub>4</sub> and N<sub>2</sub>O. Samaras and Meisterling, EPRI/NRDC, and Jaramillo et al.: 2001 IPCC [30] 100-year GWPs for CH<sub>4</sub> and N<sub>2</sub>O. Kromer and Heywood and PNNL: IPCC 1995 GWPs for CH<sub>4</sub> and N<sub>2</sub>O. Note that Samaras and Meisterling and Jaramillo et al. do not explicitly state which GHGs they include in their CO<sub>2e</sub> measure; however, they refer to CO<sub>2e</sub> estimates from the GREET model, which considers CH<sub>4</sub> and N<sub>2</sub>O. Similarly, PNNL does not state which CO<sub>2e</sub> measure they use, but they do state that they use GREET version 1.6, with year 2001 documentation, so we assume that the 1995 IPCC GWPs apply.

<sup>c</sup> Using the “unlimited” case, which allows the maximum amount of electric miles.

<sup>d</sup> We estimated these from a graph: Figs. 5.2 and 5.4 of Silva et al., and Fig. 5.4 of Jaramillo et al.

<sup>e</sup> Year of analysis not specified, but appears to be roughly current.

<sup>f</sup> PNNL and Stephan and Sullivan estimate emissions from electric operation only; they do not estimate emissions from the ICE in a PHEV.

<sup>g</sup> The number before the slash is the result for “current technology” electricity generation, and the number after the slash is the result for “new technology” electricity generation, in the long term. The new technology is more efficient than the current technology

[19]. (See Katrasnik [20] for a comprehensive formal framework for analyzing energy flows in hybrid electric vehicle [HEV] systems.)

The efficiency of electricity generation can be estimated straightforwardly on the basis of data and projections in national energy information systems, such as those maintained by the EIA (for the United States) ([www.eia.doe.gov/fuelectric.html](http://www.eia.doe.gov/fuelectric.html)) or the International Energy Agency (for the world) ([www.iea.org](http://www.iea.org)). Life cycle models, such as GREET and the LEM, also have comprehensive estimates of GHG emissions from the life cycle of electricity generation for individual types of fuels.

However, it is not straightforward to estimate the mix of fuels used to generate the electricity that actually will be used to charge batteries in PHEVs. The “marginal” generation fuel mix depends on the interaction of supply-side factors, such as cost, availability, and reliability, with anticipated hourly demand patterns, and can vary widely from region to region [50]. This supply–demand interaction can be represented formally with models that attempt to replicate how utilities actually dispatch electricity to meet demand. A few studies, reviewed below, have used dispatch models to estimate the mix of fuels used to generate electricity for charging PHEVs. However, as dispatch models generally are not readily available, most researchers either have assumed that the actual marginal mix of fuels is the year-round average mix, or else have reported results for different fuel mix scenarios.

#### **4.4.3 Review of estimates of GHG emissions from PHEVs**

In this section we review several recent comprehensive studies of GHG emission reductions with PHEVs. Table 5.5 summarizes the studies and the results, for the studies that can be reasonably compared directly.

First, as noted above, the ANL GREET model has been widely used and adjusted for various settings, and has recently expanded capabilities for analysis of life cycle GHG emissions from PHEVs. As an example of recent GREET model results, one ANL study [48] focused on three regions (Illinois, New York, and California) that provide a wide range of marginal electricity generation mixes, plus a U.S. average generation case and an all-renewable generation case. To estimate the marginal mix of fuels used to generate electricity in the regions, the study used the results of the region-specific dispatch modeling of Hadley and Tsvetkova [51]. They examined a nighttime charging scenario, in which charging was in the late evening in the year 2020 and there was an assumed 2 kW charging rate.

ANL estimated that the GHG emissions of a petroleum PHEV are 30–50% lower than an ICEV, with the greater reduction corresponding to lower grid emissions. ANL also estimated the impacts of the grid GHG intensity on the overall emissions of PHEVs powered by other fuels, including biofuels and H<sub>2</sub>. They found that while the California generation mix reduced CO<sub>2</sub> emissions from all PHEVs relative to the U.S. average mix, PHEVs powered by biomass-based fuels were not affected as greatly. The study also

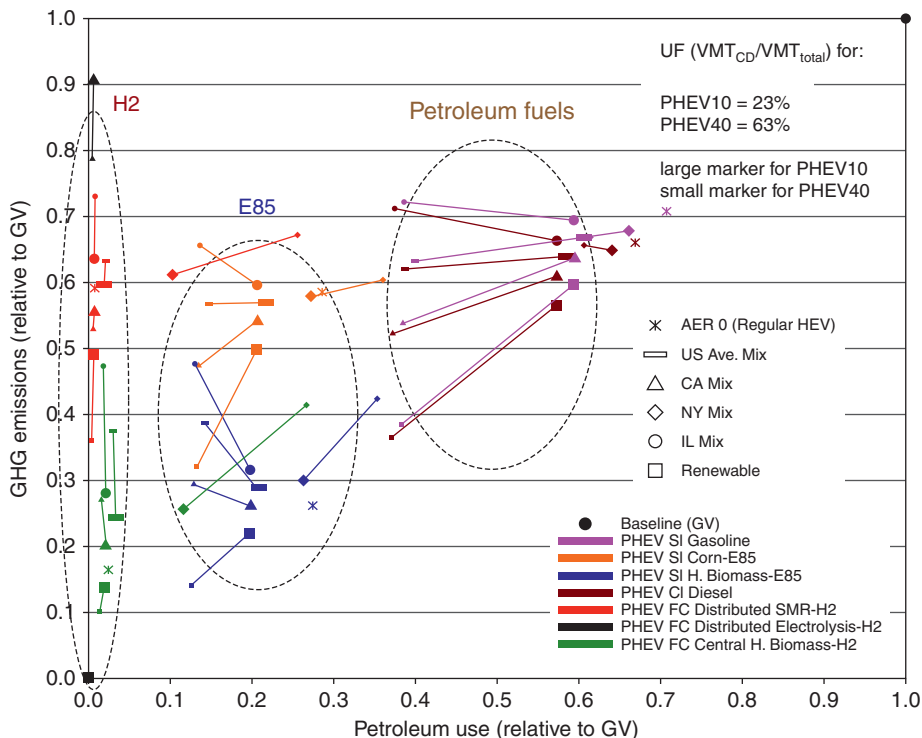


**Figure 5.2** Relative GHG emission and petroleum use impacts of PHEVs from various fuels using the GREET model [48] (see color plate 1).

shows that PHEVs charged on a GHG-intensive electricity grid can have greater well-to-wheels GHG emissions than regular HEVs and that this is exacerbated by increasing the amount of battery capacity [52].

Another set of ANL/GREET results for various types of PHEVs—fueled by gasoline, ethanol, or H<sub>2</sub> fuel cells—are presented in Fig. 5.2. As shown in the figure, renewable H<sub>2</sub> used in fuel cells and biomass-derived ethanol have the largest reductions in both GHG emissions and petroleum use. Fuel cell PHEVs using natural gas-derived H<sub>2</sub> can also offer significant benefits, along with those using petroleum fuels but with relatively clean electricity, for example, from renewables or the California grid mix.

Also, Samaras and Meisterling [42] performed a hybrid LCA of PHEV GHG emissions using GREET 1.7 along with results from the Economic Input–Output Life Cycle Assessment Model developed at Carnegie Mellon University ([www.eiolca.net](http://www.eiolca.net)). They defined the low, average, and high electricity grid GHG intensities as 200, 670, and 950 g of CO<sub>2</sub>e/kWh, respectively. They estimated that PHEVs had only 15% lower GHG emissions than a comparable ICEV in the high-grid emissions case, but 63% lower emissions in the low-grid emissions case.



Parks et al. [47] used the characteristics of Colorado's Xcel Energy System in 2004 for their analysis of CO<sub>2</sub> emissions from PHEV charging and use. They used a chronological dispatch model called PROSYM, developed by Global Energy Decisions, to model the operation of the electricity grid. The Xcel region's electricity grid is primarily fossil fuel based and had an average CO<sub>2</sub> emissions intensity of 884.5 g of CO<sub>2</sub>/kWh (1,950 lb/MWh) in 2004. Parks et al. [47] calculated CO<sub>2</sub> emissions under four charging scenarios:

- Uncontrolled—no time restrictions, peak around 4–6 pm, 1.4 kW rate.
- Delayed—charging starts at 10 pm, 1.4 kW rate.
- Off-peak—controlled charging starts after 10 pm and ends by 7 am, 3.2 kW rate.
- Continuous charging—charging allowed all day, charging stations available, 1.4 kW rate.

They found that the CO<sub>2</sub> emissions from PHEV-32 charging were about 454 g/kWh (1,000 lbs/MWh) under all of the above scenarios, which is about 40% less than the estimated ICEV emissions (251 g CO<sub>2</sub>/km).

Kromer and Heywood [34] forecasted that the average GHG intensity of the 2030 U.S. electricity grid will be 769 g of CO<sub>2e</sub> GHGs/kWh, based on energy projections from the EIA (2006) and emissions calculations from Groode [53]. Gasoline “well-to-tank” emissions of 21.2 g CO<sub>2e</sub>/MJ were taken from a GM/ANL study [54], and “tank-to-wheels” emissions were modeled in the vehicle simulation program ADVISOR, over standard EPA driving cycles. With these assumptions, PHEVs were estimated to have about 45% lower GHG emissions than ICEVs.

A 2001 report by the EPRI assumed that the marginal electricity load for PHEVs would be met by combined cycle natural gas plants. The study estimated a grid GHG intensity of 427 g of CO<sub>2</sub>/kWh, which is the average of the high and low estimates of marginal emissions estimates made by consulting firm AD Little Inc. for the California Air Resources Board in 2000. In EPRI's average-driving-schedule case with nightly charging, the PHEV-32 emits 144 g of CO<sub>2</sub>/km and the PHEV-96 emits 112 g of CO<sub>2</sub>/km, both of which are much lower than the estimated ICEV CO<sub>2</sub> emissions of 257 g/km [17].

Analysts at Pacific Northwest National Laboratory (PNNL) [45] used a simplified dispatch model to estimate the impacts of PHEV charging on GHG emissions. PNNL estimated the average hourly demand for an average winter day and an average summer day in each of 12 electricity-generating regions of the United States, with no PHEV recharging. They then assumed that the difference between the available hourly electricity generating capacity and the estimated hourly electricity demand without PHEVs would be used to charge PHEVs. They assumed that only natural gas and coal power would be available to supply this “marginal” electricity demand. They used version 1.6 of ANL's GREET model to estimate fuel cycle GHG emissions for the gasoline vehicle and for electricity generation. With these assumptions

and methods, they estimated that PHEVs operating in all-electric mode would have 0–40% lower fuel cycle GHG emissions than gasoline vehicles, with the reduction depending on the share of coal in the regional available capacity mix (PNNL did not model emissions from operation of the ICE in a PHEV). For the whole United States, the average reduction was 27%.

The approach of Stephan and Sullivan [46] is similar to that of PNNL. They assumed that PHEVs would be supported by “spare utility capacity,” which they defined as the difference between 90% of peak generating capacity and the actual nighttime demand. However, rather than use a simplified dispatch approach to estimate electricity fuel mix and emissions by region, the authors used what they called “empirical” estimates of CO<sub>2</sub> emission rates in various regions developed. They estimated that fuel cycle CO<sub>2</sub> emissions from PHEVs operating in electric mode would be 40–75% lower than emissions from gasoline vehicles, in the 12 electricity-generating regions of the United States. With the U.S. average electricity generation fuel mix, the reduction would be about 60%. They also reported CO<sub>2</sub> emission impacts for current- and new-technology coal and natural gas plants.

A 2007 report by EPRI and the Natural Resources Defense Council (NRDC) combines dispatch modeling with the scenario analysis to estimate PHEV GHG emissions for the years 2010 and 2050 [49]. A selection of their results for the year 2050 is presented in Table 5.5 and additional fleet-wide results for 2050 are shown in Table 5.6. Note that the grid emissions in this study—97, 199, and 412 g /kWh in 2050—are much lower than the emissions estimated in the other studies in Table 5.5, on account of EPRI and NRDC assuming that grid emissions will decrease over time as older plants are retired and are replaced by more efficient ones. Their analysis shows that life cycle GHG emissions decrease as the CD range of the PHEV increases, even in the high-grid emissions case. This is different from the result of (for example) Samaras and Meisterling [42], who estimate that increased CD range results in higher emissions in their high-grid emissions case. This difference is due to the large difference in the grid GHG intensities assumed in the two studies.

**Table 5.6** Annual GHG reduction from PHEVs in the year 2050

2050 annual GHG reduction (million metric tons)		Electric sector CO <sub>2</sub> intensity		
		High	Medium	Low
PHEV fleet penetration	Low	163	177	193
	Medium	394	468	478
	High	474	517	612

Source: NRDC/EPRI [49].

Another study of PHEVs by Silva et al. [43] concludes that for the United States, CD PHEVs with 15 kWh of battery capacity can have GHG emissions on the order of 70–80 g/km, or about 40% less than a conventional baseline vehicle (not shown in Table 5.5). The reductions would be greater in Japan and Europe, which have a lower carbon fuel mix for electricity generation than the United States does (Table 5.4). CS PHEVs were found to have considerably higher emissions than the CD designs, in fact higher than baseline vehicles in the study for the USA and Europe. The study also found that the proportion of emissions attributable to vehicle fueling versus “cradle to grave” manufacturing and maintenance varies strongly with distance driven, where, for example, for a CS PHEV driving a total of 300,000 km the emissions are 15% for the vehicle manufacturing and maintenance and 85% for fuel use, where for lower total mileage of 150,000 km the proportion is 25% (manufacturing and maintenance) to 75% (fuel use). Silva et al. assumed NiMH batteries and used ADVISOR to do the simulation modeling and GREET for emissions estimates.

In another recent study, Jaramillo et al. [44] compare the GHG emissions impacts of PHEVs with FCVs and conventional vehicles, assuming that PHEVs are operated either on conventional gasoline or “coal to liquids” (CTL) fuels and electricity and that FCVs use H<sub>2</sub> made from coal gasification. Under varying assumptions about the level of carbon capture and sequestration from the CTL and gasification processes, they find that PHEVs could reduce emissions by up to 46% compared with conventional vehicles (Table 5.5) and by up to 31% compared with hybrid vehicles. FCVs could decrease GHG emissions by up to 50% compared with conventional vehicles or could increase them considerably depending on the level of carbon capture and the source for electricity needed for H<sub>2</sub> compression. Meanwhile, CTL fuels used in conventional and hybrid vehicles would significantly increase emissions compared with conventional gasoline and diesel vehicles.

#### **4.4.4 Comparison of GHG emissions reductions from PHEVs**

The studies summarized in Table 5.5 indicate that PHEVs have 20–60% lower GHG emissions than their counterparts ICEV counterparts, with the lower-end reductions corresponding mainly to relatively low-carbon fuel mixes for electricity generation. To put the grid GHG emission numbers of Table 5.6 into perspective, the LEM estimates that in the United States in the year 2020, life cycle emissions from coal-fired plants are 1,030 g of CO<sub>2</sub>e/kWh-generated, and life cycle emissions from gas-fired plants are 520 g of CO<sub>2</sub>e/kWh-generated, using IPCC GWPs. Studies using dispatch modeling of the electricity grid indicate a narrower range of reductions, 30–50%. By comparison, studies tabulated by Bradley and Frank [41] indicate slightly greater reductions, about 40–60%

Some of the results of Table 5.5 merit further explanation. For example, Kromer and Heywood [34] report a higher grid GHG intensity than several other cases, but

lower emissions per kilometer than Samaras and Meisterling [42] and Graham/EPRI [17]. The high-grid GHG intensity comes from DOE–EIA projections, and the lower emissions per kilometer is likely due to the assumed improvement in efficiency and emissions in the 2030 ICEV. The relatively large reductions estimated by Stephan and Sullivan [46] are due to several factors: (i) they start with a relatively high-emitting gasoline vehicle; (ii) they consider electric operation of the PHEV only; (iii) they assume relatively efficient power plants in the long term; and (iv) they consider only CO<sub>2</sub> emissions.

In sum, PHEVs promise significant reductions in GHG emissions in most regions and conditions. This is especially the case in the longer term, when the electricity grid is likely to be cleaner, and vehicles are likely to have higher battery storage capacities.

#### 4.5 Comparison of GHG emissions reductions from EV types

By way of an overall comparison of the emission reductions estimated for the various types of EVs, see Figs. 5.3 and 5.4. As shown in Fig. 5.3, BEVs have the potential to reduce well-to-wheels GHG emissions by about 55–60% using either natural gas power plants or the California grid mix (which is heavily dependent on natural gas).

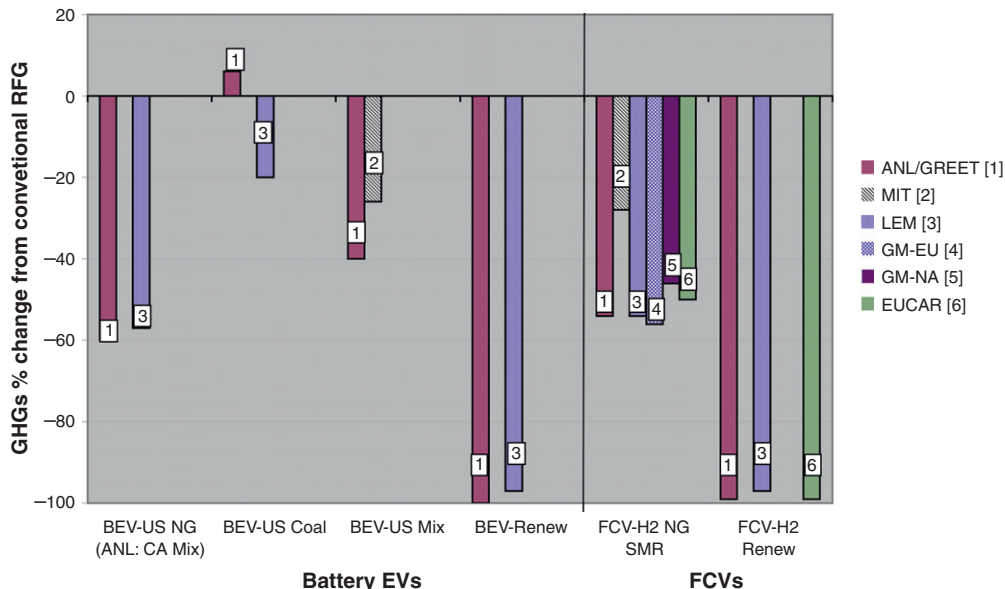


**Figure 5.3** Comparison of well-to-wheels GHG emission reduction estimates from BEVs and FCVs. (Sources: (1) ANL/GREET [22, 31]; (2) MIT [34]; (3) LEM [Table 5.4]; (4) GM-EU [16]; (5) GM-NA [15]; (6) EUCAR [36]). (Notes: BEV = battery electric vehicle; CA = California; FCV = fuel cell vehicle; H<sub>2</sub> = hydrogen; NG = natural gas; renew = renewable fuel; SMR = steam methane reforming).

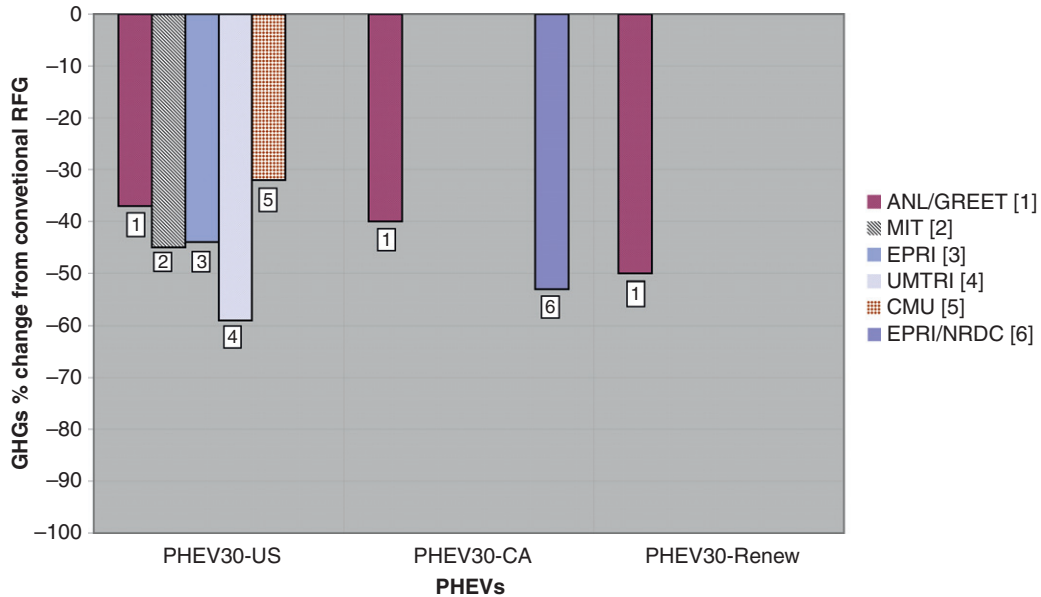


**Figure 5.4** Comparison of well-to-wheels GHG emission reduction estimates from PHEVs. (Sources: (1) ANL/GREET [22,52]; (2) MIT [34]; (3) EPRI [17]; (4) EPRI/NRDC [49]; (5) UMTRI [46]; (6) CMU [42]). (Notes: CA = California; PHEV30 = plug in hybrid vehicle with 30 mi (50 km) electric range; renew = renewable fuel).

Using coal-based power, BEVs may reduce emissions by about 20% or slightly increase them (i.e., model results vary somewhat), and using the U.S. grid mix (which is about half coal-based) emission reductions on the order of 25–40% appear possible. For FCVs using H<sub>2</sub> produced from natural gas steam reformation, GHG emissions can be reduced by 30–55% according to the various studies. Once again, when entirely or nearly entirely powered by completely renewable fuels such as wind, solar, and hydropower, GHG emissions from both BEVs and FCVs can be almost entirely eliminated.

As shown in Fig. 5.4, emission reductions possible from PHEVs are somewhat more modest than for some BEV and FCV configurations. For a PHEV type considered in several studies that has a 30 mile (50 km) electric range, GHG emission reductions compared with a conventional vehicle are estimated to be in the range of 30–60% using the U.S. grid mix. For the California electricity mix, a range of 40–55% has been estimated. Also, one estimate shown in the figure finds a 50% reduction potential with PHEV30s running on renewables-based electricity. We note that for PHEVs in particular, these relative emission reduction results vary by assumed driving patterns and distances as well as underlying emission factors for electricity and gasoline used. This leads to further sources of potential variation amongst the studies, along with other

variables such as the assumed driveline efficiencies, upstream emission factors, and the type and size of the vehicle itself.



## **5. MAGNITUDE OF POSSIBLE GHG REDUCTIONS—SCALING UP THE EV INDUSTRY**

As shown above, EVs can offer significant GHG benefits when compared on a one-to-one basis with conventional vehicles. However, a major issue with a rapid scale-up of EVs is the availability of advanced electric vehicle battery packs in the numbers needed for a major commercial launch of vehicles by several automakers at once. The need to scale up battery production in the cell sizes and configurations needed for different types of EVs is accompanied by several other needs to support the introduction of EVs into consumer households. These include (i) improving the procedures for installing recharging facilities for EVs at household and other sites; (ii) better understanding of the utility grid impacts of significant numbers of grid-connected vehicles; (iii) better understanding the consumer and utility economics of EV ownership (and/or leasing of car or battery); and (iv) better education for consumers and tools to assist them to determine if their driving habits would be good “fits” for the characteristics of the different types of EVs. These and other related issues are being explored by the University of California and other groups as new EVs are being introduced into the market [55, 56].

Additional issues related to vehicle scale-up include provision of H<sub>2</sub> for FCVs, currently an expensive proposition for low volumes of dispensed fuel, development and dissemination of appropriate safety procedures for first responders in dealing with accidents with vehicles having high-voltage electrical systems and/or H<sub>2</sub> fuel storage, and additional education and outreach programs for mechanics and fleet managers [57]. These measures will be needed to help EVs become more established and acceptable to consumers in various market segments.

### **5.1 Scaling up the EV industry—how fast can it be done?**

A recent analysis examined the potential of various options to scale up to become a “Gigaton solution” by 2020, meaning that it could account for a gigaton of CO<sub>2</sub> reduction on a global annual basis by 2020 [58]. The study found that achieving “Gigaton Scale” with a strategy based largely on a massive introduction of grid-connected EVs would require about 1,000 times as many batteries in the near term as are expected to be available (i.e., tens of millions globally rather than tens of thousands), growing to needs for hundreds of millions of battery packs by 2020. This implies a massive investment in battery production capacity at a time when battery designs are still being improved and perfected to the point where commercially acceptable PHEVs and BEVs can be produced. This suggests that achieving

Gigaton Scale with EVs is not possible by 2020. However, much larger gains are possible by 2030 and especially 2050, given the relatively slow dynamics of motor vehicle fleet stock turnover [59].

The EPRI/NRDC study noted above includes scenario estimates of future GHG reductions from vehicles fleets in the United States, and finds that reductions of up to about 500 megatons per year are possible by 2050, depending on the level of PHEV fleet penetration and the CO<sub>2</sub> intensity of the electricity sector. Table 5.6 in the following section presents some of the key results of the study.

It is important to note, however, that more generally PHEVs and other EVs are technologies that can scale fairly rapidly. Typical automotive volumes run to several hundred thousand units per year for individual popular models (e.g., the combined United States and Japanese sales of the Toyota Prius are around 275,000–300,000 per year), and there is the potential to incorporate electric drive technology into many vehicle models. The rate of scaling is mainly limited by the growth of supplier networks and supply chains, and by the dynamics of introducing new vehicles with 15-year lives into regional motor vehicle fleets, along with economic and market response constraints on the demand side.

## 5.2 GHG reductions from a scaled up fleet of EVs

Given the entire transportation sector dynamics described above, it is much easier to see large reductions in emissions in LDV emissions by 2030, 2040, and 2050 than by 2020, given that a significant percentage of new vehicles sold today will still be on the road in the next 10 years. For example, as shown in Table 5.6 the EPRI/NRDC study [40] concludes that under the most optimistic U.S. scenario assessed—high PHEV fleet penetration and low electric sector CO<sub>2</sub> intensity—612 million megatons of emissions could be reduced annually by 2050. Extrapolated globally, these emission reductions could be on the order of 2–3 gigatons annually, based on optimistic assumptions about fleet penetration and GHG intensity in the electric power sector.



## 6. KEY UNCERTAINTIES AND AREAS FOR FURTHER RESEARCH

The analysis of life cycle CO<sub>2</sub>e GHG emissions from advanced electric vehicles involves many uncertainties. Some of these are relatively clear (e.g., what exactly are the driveline efficiencies of various types of alternative fuel vehicles, what efficiencies are involved in key upstream fuel production processes, and so on) and many others are subtler but potentially of significance. These include secondary impacts of fuel cycles, such as the “indirect land use change” impacts of biofuels, where production of biofuels implies cultivation of land that in some cases can



displace its use for other purposes, and how emissions from power plants and other combustion sources actually result in exposures and potential harm to humans and the environment.

Exploring these uncertainties in much detail is beyond the scope of this chapter, but is discussed in some of the studies referenced here. However below we briefly mention a few key sources of remaining uncertainty in LCA of EV fuel cycles. We also note that the GREET model in particular now includes the ability to include estimates of the levels of uncertainty in key input variables, and incorporates this capability through a graphical user interface version of the model interface that runs in a PC Windows environment. This can be useful but of course still can benefit from additional efforts to characterize and attempt to narrow the remaining uncertainties themselves.

### 6.1 Key uncertainties in LCA analysis of GHGs from EV fuel cycles

Because GHGs are produced in myriad ways from EV fuel cycles, including both upstream and vehicle-based emissions (in the case of PHEVs and HEVs), and because EV technologies are still evolving, there are considerable uncertainties involved in present-day or prospective analysis of their impacts. Over the course of the past 20 years many of these uncertainties have been narrowed—for example, the manufacturing cost and performance of electric vehicle motors and motor controllers has become better established—but many still remain.

Some of the key remaining uncertainties include the following:

- uncertainties in the emission rates of high GWP value gases (e.g., N<sub>2</sub>O, CH<sub>4</sub>, refrigerants, etc.) that are emitted in lower quantities than CO<sub>2</sub> from vehicle fuel cycles, but that can still be significant;
- secondary impacts such as indirect land use change and macroeconomics;
- climate impacts of emissions of typically overlooked but potentially important pollutants such as oxides of sulfur, ozone precursors, and PM;
- rate of future vehicle and fueling system performance improvements;
- potential “wild cards” in future fuels production processes, such as the successful introduction of carbon capture and sequestration; and
- breakthroughs in electricity, advanced biofuel, or H<sub>2</sub> production.

As time goes on, we can expect more to be learned about these key areas, and for the remaining uncertainties to be narrowed. At the same time, new fuel cycles based on evolving technology are likely to become available but with potentially significant uncertainties until more is learned about them in turn (e.g., diesel-type fuels from algae, new types of PHEVs running on various fuels, other new types of synthetic Fischer–Tropsch process and bio-based fuels, etc.). The significant amount of research currently underway is encouraging, but given the pressing nature of the energy and



climate challenges facing many nations, one could argue that more attention should be paid to this critical area.



## 7. CONCLUSIONS

Various types of hybrid and all-electric EVs can offer significant GHG reductions when compared to conventional vehicles on a full fuel cycle basis. In fact, most EVs used under most conditions are expected to significantly reduce life cycle CO<sub>2e</sub> GHG emissions. Under certain conditions, EVs can even have very low to zero emissions of GHGs when based on renewable fuels. However, at present, this is more expensive than other options that offer significant reductions at lower costs based on the use of more conventional fuels. It is important to note that when coal is heavily used to produce electricity or H<sub>2</sub> (e.g., with the U.S. grid mix that is about half composed of coal), GHG emissions tend to increase significantly compared with conventional fuel alternatives. Unless carbon capture and sequestration becomes a reality, using coal-based fuels even in conjunction with electric drive systems offers little or no benefit.

In general, various studies show that BEVs reduce GHGs by a widely disparate amount depending on the type of power plant used and the particular region involved, among other factors. Reductions typical of the U.S. would be on the order of 20–50%, depending on the relative level of coal versus natural gas and renewables in the power plant feedstock mix. However, much deeper reductions of over 90% are possible for BEVs running on renewable or nuclear power sources. PHEVs running on gasoline reduce emissions by 20–60%, and fuel cell EVs reduce GHGs by 30–50% when running on natural gas-derived H<sub>2</sub> and up to 95% or more when the H<sub>2</sub> is made (and potentially compressed) using renewable feedstocks. These are all in comparison to what is usually assumed to be a more advanced gasoline vehicle “baseline” of comparison, with some incremental improvements by 2020 or 2030. It is important to note once again, however, that emissions from all of these EV types are widely depending on the details of how the electric fuel or H<sub>2</sub> is produced. This is true despite the fact that GHG and air pollutant emissions are typically mostly or entirely “upstream” rather than from the vehicle’s tailpipe. This makes these emissions in principle easier to control but also may mean that they are far removed from where the fuel is actually used in the vehicle.

Overall, EVs offer the potential for significant and even dramatic reductions in GHGs from transportation fuel cycles. Pursuing further development of this promising set of more efficient technologies would thus seem to be of paramount importance, given the rapidly spiraling growth in motor vehicle ownership and use around the globe and the declining natural resource base remaining to support it.

## ACKNOWLEDGMENTS

The authors would like to thank Andy Lentz and Anthony Kwong for helping to compile information useful for the preparation of this chapter. We acknowledge the UC Berkeley Institute of Transportation Studies, the UC Davis Plug-In Hybrid Electric Vehicle Center, and the National Science Foundation MUSES Program for partial support for the research upon which this chapter is based. We would also like to thank Michael Wang, Joan Ogden, Stefan Unnasch, and Robert Williams for many years of useful and productive discussions and information sharing on the topic of the emissions from motor vehicle fuel cycles.

## REFERENCES

1. S.A. Shaheen, T.E. Lipman, *Int. Assoc. Traffic Safety Sci.* 31 (2007) 6.
2. P.M. Forster, V. Ramaswamy, In *climate change 2007: The Physical Science Basis*, S. Solomon, D. Qin, M. Manning, Z. Chen, M. Marquis, K.B. Avery, M. Tignor and H.L. Miller (Eds.), Cambridge University Press (2007).
3. M.A. Delucchi, *A Lifecycle Emissions Model (LEM): Lifecycle Emissions from Transportation Fuels, Motor Vehicles, Transportation Modes, Electricity Use, Heating and Cooking Fuels, and Materials*, UCD-ITS-RR-03-17 (2003).
4. M. Wang, *J. Power Sources* 112 (2002) 307.
5. R.F. Weiss, S.E. Craig, *Geophys. Res. Lett.* 3 (1976) 751.
6. M. Prigent, G.D. de Soete, *SAE Tech Paper Series #8904922* (1989).
7. Oak Ridge National Laboratory, Carbon Dioxide Information Analysis Center. <http://cdiac.ornl.gov>, 2009.
8. M.A. Delucchi, *Emissions of Greenhouse Gases from the Use of Transportation Fuels and Electricity*, ANL/ESD/TM-22, Argonne National Laboratory, 1991.
9. M.Q. Wang, *REET 1.0—Transportation Fuel Cycles Model: Methodology and Use*, ANL/ESD-33, Argonne National Laboratory, 1996.
10. M.A. Delucchi, *Emissions of non-CO<sub>2</sub> Greenhouse Gases from the Production and Use of Transportation Fuels and Electricity*, UCD-ITS-RR-97-05, 1997.
11. J.M. Ogden, R.H. Williams, *Solar Hydrogen*, 1989.
12. Acurex Environmental Corporation, *Evaluation of Fuel-Cycle Emissions on a Reactivity Basis: Volume 1, Main Report*, FR-96-114, 1996.
13. S. Unnasch, *Greenhouse Gas Analysis for Fuel Cell Vehicles*, 2006 Fuel Cell Seminar, 2006.
14. C.E. Thomas, B.D. James, F. Lomax, *J. Power Sources* 25 (2000) 551.
15. General Motors, Argonne National Laboratories, BP, ExxonMobil, and Shell, *GM Well-to-Wheel Energy Use and Greenhouse Gas Emissions of Advanced Fuel/Vehicle Systems – North American Analysis*, General Motors, Argonne, USA, 2001.
16. General Motors, L-B-Systemtechnik GmbH, BP, ExxonMobil, and Total-FinaElf, *GM Well-to-Wheel Energy Use and Greenhouse Gas Emissions of Advanced Fuel/Vehicle Systems – European Analysis*, General Motors, Ottobrun, Germany, 2002.
17. R. Graham, *Comparing the Benefits and Impacts of Hybrid Electric Vehicle Options*, Electric Power Research Institute Report 1000349, 2001.
18. T.E. Lipman, M.A. Delucchi, *Climatic Change* 53 (2002) 477.
19. J. Gonder, T. Markel, *SAE Technical Paper Series, #2007-01-0290*, Society of Automotive Engineers, 2007.
20. T. Katrasnik, *Energy Convers. Manage.* 50 (2009) 1924.
21. U.S. Environmental Protection Agency, EPA420-F-05-001, 2005.
22. M. Wang, Y. Wu, A. Elgowainy, *REET1.7 Fuel-Cycle Model for Transportation Fuels and Vehicle Technologies*, Argonne National Laboratory, 2007.
23. U.S. Environmental Protection Agency, *Compilation of Air Pollutant Emission Factors (AP-42)*, 2009.
24. M.C. Bohm, H.J. Herzog, J.E. Parsons, J.E. Sekar, *Int. J. Greenhouse Gas Control* 1 (2007) 113.
25. R. Dones, T. Heck, S. Hirschberg, *Encyclopedia of Energy* 3 (2004) 77–95.

26. Intergovernmental Panel on Climate Change, 2006 IPCC Guidelines For National Greenhouse Gas Inventories, H.S. Eggleston, L. Buendia et al. (Eds.), Institute for Global Environmental Strategies, Japan, 2006.
27. J.C. Kramlich, W.P. Linak, *Prog. Energy Combust. Sci.* 20 (1994) 149.
28. E. Behrentz, R. Ling, P. Rieger, A.M. Winer, *Atmos. Environ.* 38 (2004) 4291.
29. Intergovernmental Panel on Climate Change, *Climate Change 2007: The Physical Science Basis*, Contribution of Working Group I to the Fourth Assessment Report of the IPCC, S. Solomon, D. Qin, et al. (Eds.), Cambridge University Press, 2007.
30. Intergovernmental Panel on Climate Change, *Climate Change 2001: The Scientific Basis*, J.T. Houghton, Y. Ding et al. (Eds), 2001.
31. M. Wang, *Well-to-Wheels Energy Use Greenhouse Gas Emissions and Criteria Pollutant Emissions—Hybrid Electric and Fuel Cell Vehicles*, SAE Future Transp. Tech. Conf., 2003.
32. Acurex Environmental Corporation, *Evaluation of Fuel-Cycle Emissions on a Reactivity Basis: Volume 1, Main Report*, FR-96-114, 1996.
33. N.S. Rau, S.T. Adelman, D.M. Kline, *EVTECA—Utility Analysis Volume 1: Utility Dispatch and Emissions Simulations*, TP-462-7899, National Renewable Energy Laboratory, 1996.
34. M.A. Kromer, J.B. Heywood, *Electric Powertrains: Opportunities and Challenges in the U.S. Light-duty Vehicle Fleet*, MIT Pub. No. LFEE 2007-03 RP, 2007.
35. C.E. Thomas, *Int. J. Hydrogen Energy* 34 (2009) 6005.
36. EUCAR and ECJRC, *Well-to-Wheels Analysis of Future Automotive Fuels and Powertrains in the European Context*, 2007.
37. G.A. Keoleian et al., SAE Technical Paper Series, #982169, Society of Automotive Engineers, 1998.
38. J.L. Sullivan et al., *Life Cycle Inventory of a Generic U.S. Family Sedan: Overview of Results*, UsCAR Amp Project, SAE Technical Paper Series #982160, 1998.
39. M.A. Delucchi, *World Resources Review* 13 (1) (2001) 25–51.
40. A. Burnham, M. Wang, Y. Wu, *Development and Applications of GREET 2.7—The Transportation Vehicle-Cycle Model*, ANL/ESD/06-5, Argonne National Laboratory, 2006.
41. T.H. Bradley, A.A. Frank, *Renew. Sustain. Energy Reviews* 13 (2009) 115.
42. C. Samaras, K. Meisterling, *Environ. Sci. Technol.* 42 (2008) 3170.
43. C. Silva, M. Ross, T. Farias, *Energy Convers. Manage.* 50 (2009) 1635.
44. P. Jaramillo, C. Samaras, H. Wakeley, K. Meisterling, *Energy Policy* 37 (2009) 2689.
45. M. Kintner-Meyer, K. Schneider, R. Pratt, *Impact Assessment of Plug-in Hybrid Vehicles on Electric Utilities and Regional U. S. Power Grids*, Pacific Northwest National Laboratory, 2006.
46. C.H. Stephan, J. Sullivan, *Environ. Sci. Technol.* 42 (2008) 1185.
47. K. Parks, P. Denholm, T. Markel, *Costs and Emissions Associated with Plug-In Hybrid Electric Vehicle Charging in the Xcel Energy Colorado Service Territory*, NREL/TP-640-41410, 2007.
48. A. Elgowainy, A. Burnham, M. Wang, J. Molburg, A. Rousseau, *Well-To-Wheels Energy Use and Greenhouse Gas Emissions Analysis of Plug-In Hybrid Electric Vehicles*, ANL/ESD/09-2, Argonne National Laboratory, 2009.
49. Electric Policy Research Institute and National Resources Defense Council, *Environmental Assessment of Plug-In Hybrid Electric Vehicles, Volume 1: Nationwide Greenhouse Gas Emissions*, Report No. 1015325, 2007.
50. Edison Electric Institute (EEI), *Diversity Map*, <http://www.eei.org> 2009.
51. S. Hadley, A. Tsvetkova, *Potential Impacts of Plug-In Hybrid Electric Vehicles on Regional Power Generation*, ORNL/TM-2007/150, Oak Ridge National Laboratory, 2008.
52. M. Wang, *Well-to-Wheels Analysis of Biofuels and Plug-In Hybrids*, Presentation at Argonne National Laboratory, June 3 2009.
53. T.A. Groode, *A Methodology for Assessing Mit's Energy Use and Greenhouse Gas Emissions*, Master of Science Thesis, Massachusetts Institute of Technology, 2004.
54. N. Brinkman, M. Wang, T. Weber, T. Darlington, *Well-to-Wheels Analysis of Advanced Fuel/Vehicle Systems—A North American Study of Energy Use, Greenhouse Gas Emissions, and Criteria Pollutant Emissions*, Argonne National Laboratory, 2005.
55. E. Martin, S.A. Shaheen, T.E. Lipman, J. Lidicker, *Int. J. Hydrogen Energy* 34 (2009) 8670.

56. K.S. Kurani, T.S. Turrentine, D. Sperling, *Transport. Res. Part D* 1 (1996) 13.
57. California Environmental Protection Agency, *Hydrogen Blueprint Plan: Volume 1* (2005).
58. S. Paul and C. Tompkins (Eds.), *Gigaton Throwdown: Redefining What's Possible for Clean Energy by 2020*, 2009.
59. T. Lipman, *Plug-in Hybrid Electric Vehicles*, in S. Paul and C. Tompkins (Eds.), *Gigaton Throwdown: Redefining What's Possible for Clean Energy by 2020*, 2009.
60. General Motors et al., "Annex "Full Background Report"—Methodology, Assumptions, Descriptions, Calculations, Results—To the GM Well-to-Wheel Analysis of Energy Use and Greenhouse Gas Emissions of Advanced Fuel/Vehicle Systems—A European Study", L-B-Systemtechnik GmbH, Ottobrunn, Germany, September 27 (2002b). Available from: [www.lbst.de/gm-wtw](http://www.lbst.de/gm-wtw).
61. M.A. Weiss et al., *On the road in 2020: A Lifecycle Analysis of New Automotive Technologies*, MIT Energy Laboratory Report EL 00-003, Massachusetts Institute of Technology, October (2000). [http://web.mit.edu/sloan-auto-lab/research/beforeh2/files/weiss\\_otr2020.pdf](http://web.mit.edu/sloan-auto-lab/research/beforeh2/files/weiss_otr2020.pdf).
62. A. Bandivadekar, K. Bodek, L. Cheah, C. Evans, T. Groode, J. Heywood et al., *On the Road in 2035: Reducing Transportation's Petroleum Consumption and GHG Emissions*, Laboratory for Energy and the Environment, Report No. LFEE 2008-05 RP, 2008 Massachusetts Institute of Technology, July 2008, <http://web.mit.edu/sloan-auto-lab/research/beforeh2/otr2035/>
63. EUCAR (European Council for Automotive Research and Development), CONCAWE, and ECJRC (European Commission Joint Research Centre), *Well-to-Wheels Analysis of Future Automotive Fuels and Powertrains in the European Context, Well-to-Wheels Report, Version 1b*, January 2004. Version 2c, March 2007 update, and version 3, November 2008. Available from: <http://ies.jrc.ec.europa.eu/our-activities/support-for-eu-policies/well-to-wheels-analysis/WTW.html>.
64. J. Hackney, R. de Neufville, *Life Cycle Model of Alternative Fuel Vehicles: Emissions, Energy, and Cost Trade-Offs*, *Transport. Res. Part A* 35 (2001) 243.
65. P. Ahlvik, A. Brandberg, *Well to Wheels Efficiency for Alternative Fuels from Natural Gas or Biomass*, Publication 2001:85, Swedish National Road Administration, October (2001).
66. H.L. Maclean, L.B. Lave, R. Lankey, S. Joshi, *A Lifecycle Comparison of Alternative Automobile Fuels*, *J. Air Waste Manage. Assoc.* 50 (2000) 1769.
67. K. Tahara, et al., *Comparison of CO<sub>2</sub> Emissions from Alternative and Conventional Vehicles*, *World Resources Review* 13 (1) 52–60 (2001).



## APPENDIX

In the following table, the structure and coverage of the LEM are compared with that of several other recent transportation fuel cycle or life cycle modeling efforts.

**Table 5.A-1** Comparison of the LEM with other recent life cycle modeling efforts

Project	GM—ANL USA	GM—LBST Europe	MIT 2020	EUCAR	LEM
Region	North America	Europe	Based on U.S. data	Europe	Multicountry (primary data for USA; other data for up to 30 countries)
Time frame	Near term (about 2010)	2010	2020	2010 and beyond	Any year from 1970–2050
Transport modes	LDV (LDT)	LDV (European minivan)	LDV (midsize family passenger car)	LDVs (compact five-seat European sedan)	LDVs, HDVs, buses, light-rail transit, heavy-rail transit, minicars, scooters, off-road vehicles
Vehicle drivetrain type	ICEVs, HEVs, BEVs, FCEVs	ICEVs, HEVs, FCEVs	ICEVs, HEVs, BEVs, FCEVs	ICEVs, HEVs, FCEVs	ICEVs, BEVs, FCEVs
Motor fuels	Gasoline, diesel, naphtha, FTD, CNG, methanol, ethanol, CH <sub>2</sub> , LH <sub>2</sub> , electricity	Gasoline, diesel, naphtha, FTD, CNG, LNG, methanol, ethanol, CH <sub>2</sub> , LH <sub>2</sub>	Gasoline, diesel, FTD, methanol, CNG, CH <sub>2</sub> , electricity	Gasoline, diesel, FTD, CNG, ethanol, FAME, DME, naphtha, methanol, CH <sub>2</sub> , LH <sub>2</sub>	Gasoline, diesel, LPG, FTD, CNG, LNG, methanol, ethanol, CH <sub>2</sub> , LH <sub>2</sub> , electricity
Fuel feedstocks	Crude oil, natural gas, coal, crops, lignocellulosic biomass, renewable and nuclear power	Crude oil, natural gas, coal, crops, lignocellulosic biomass, waste, renewable and nuclear power	Crude oil, natural gas, renewable and nuclear power	Crude oil, natural gas, coal, nuclear, wind, sugar beets, wheat, oil seeds, wood	Crude oil, natural gas, coal, crops, lignocellulosic biomass, renewable and nuclear power

Vehicle energy-use modeling, including drive cycle	GM simulator, U.S. combined city/highway driving	GM simulator, European Drive Cycle (urban and extra-urban driving)	MIT simulator, U.S. combined city/highway driving	Advisor (NREL simulator), New European Drive Cycle	simple model based on SIMPLEV-like simulator, U.S. combined city/highway driving
Fuel life cycle	GREET model	LBST E <sup>2</sup> I-O model and database	Literature review	LBST E <sup>2</sup> I-O model and data base (review & update of GM et al. [16])	Detailed internal model
Vehicle and material life cycle	Not included	Not included	Detailed literature review and analysis	Not included	Internal model based on detailed literature review and analysis
GHGs (CEFs)	CO <sub>2</sub> , CH <sub>4</sub> , N <sub>2</sub> O (IPCC) (other pollutants included as non-GHGs)	CO <sub>2</sub> , CH <sub>4</sub> , N <sub>2</sub> O (IPCC)	CO <sub>2</sub> , CH <sub>4</sub> (IPCC)	CO <sub>2</sub> , CH <sub>4</sub> , N <sub>2</sub> O (IPCC)	CO <sub>2</sub> , CH <sub>4</sub> , N <sub>2</sub> O, NO <sub>x</sub> , VOC, SO <sub>x</sub> , PM, CO, H <sub>2</sub> , HFCs, CFCs (own CEFs, also IPCC CEFs)
Infrastructure Price effects	Not included Not included	Not included Not included	Not included Not included	Not included Not included	Crude representation A few simple quasi-elasticities
Reference	GM, ANL et al. [15]	GM et al. [16, 60]	Weiss et al. [61] Bandivadekar et al. [62]	Concawe et al. [63]	Delucchi [3]

---

*(Continued)*

**Table 5.A-1 (Continued)**

<b>Project</b>	<b>ADL AFV LCA</b>	<b>EcoTraffic</b>	<b>CMU I-O LCA</b>	<b>Japan CO2 from AFVs</b>	<b>LEM</b>
Region	USA	Generic, but weighted toward European conditions	USA	Japan	Multicountry (primary data for USA; other data for up to 30 countries)
Time frame	1996 baseline, future scenarios	Between 2010 and 2015	Near term	Near term?	Any year from 1970 to 2050
Transport modes	Subcompact cars	LDVs (generic small passenger car)	LDVs (midsize sedan)	LDVs (generic small passenger car)	LDVs, HDVs, buses, light-rail transit, heavy-rail transit, minicars, scooters, offroad vehicles
Vehicle drivetrain type	ICEVs, BEVs, FCEVs	ICEVs, HEVs, FCEVs	ICEVs	ICEVs, HEVs, BEVs	ICEVs, BEVs, FCEVs
Motor fuels	Gasoline, diesel, LPG, CNG, LNG, methanol, ethanol, CH <sub>2</sub> , LH <sub>2</sub> , electricity	Gasoline, diesel, FTD, CNG, LNG, methanol, DME, ethanol, CH <sub>2</sub> , LH <sub>2</sub>	Gasoline, diesel, biodiesel, CNG, methanol, ethanol	Gasoline, diesel, electricity	Gasoline, diesel, LPG, FTD, CNG, LNG, methanol, ethanol, CH <sub>2</sub> , LH <sub>2</sub> , electricity
Fuel feedstocks	Crude oil, natural gas, coal, corn, lignocellulosic biomass, renewable and nuclear power	Crude oil, natural gas, lignocellulosic biomass, waste	Crude oil, natural gas, crops, lignocellulosic biomass	Crude oil, natural gas, coal, renewable and nuclear power	Crude oil, natural gas, coal, crops, lignocellulosic biomass, renewable and nuclear power
Vehicle energy-use modeling, including drive cycle	Gasoline fuel economy assumed; AFV efficiency estimated relative to this	Advisor (NREL simulator), New European Drive Cycle	Gasoline fuel economy assumed; AFV efficiency estimated relative to this	None; fuel economy assumed	Simple model based on SIMPLEV-like simulator, U.S. combined city/highway driving

Fuel life cycle	Arthur D. Little emissions model, revised	Literature review	Own calculations based on other models (LEM, GREET, etc.)	Values from another study	Detailed internal model
Vehicle and material life cycle	Not included	Not included	Economic Input–Output Life Cycle Analysis software (except end-of-life)	Detailed part-by-part analysis	Internal model based on detailed literature review and analysis
GHGs (CEFs)	CO <sub>2</sub> , CH <sub>4</sub> , (partial GWP) (other pollutants included as non-GHGs)	None (energy efficiency study only)	CO <sub>2</sub> , CH <sub>4</sub> , N <sub>2</sub> O? (IPCC) (other pollutants included as non-GHGs)	CO <sub>2</sub>	CO <sub>2</sub> , CH <sub>4</sub> , N <sub>2</sub> O, NO <sub>x</sub> , VOC, SO <sub>x</sub> , PM, CO, H <sub>2</sub> , HFCs, CFCs (own CEFs, also IPCC CEFs)
Infrastructure Price effects	not included Not included	not included Not included	not included Not included (fixed-price I-O model)	not included Not included	crude representation A few simple quasielasticities
Reference	[64]	[65]	[66]	[67]	[3]

---



The terms are defined as follows:

---

Region	The countries or regions covered by the analysis.
Time frame	The target year of the analysis.
Transport modes	The types of passenger transport modes included. LDVs = light-duty vehicles, HDVs = heavy-duty vehicles.
Vehicle drivetrain type	ICEVs = internal combustion-engine vehicles, HEVs = hybrid electric vehicles (vehicles with an electric and an ICE drivetrain), BEVs = battery electric vehicles, FCEVs = fuel cell electric vehicles.
Motor fuels	Fuels carried and used by motor vehicles. FTD = Fischer–Tropsch diesel, CNG = compressed natural gas, LNG = liquefied natural gas, CH <sub>2</sub> = compressed hydrogen, LH <sub>2</sub> = liquefied hydrogen, DME = dimethyl ether, FAME = fatty acid methyl esters.
Fuel feedstocks	The feedstocks from which the fuels are made.
Vehicle Energy-use modeling	The models or assumptions used to estimate vehicular energy use (which is a key part of fuel cycle CO <sub>2</sub> emissions), and the drive cycle over which fuel usage is estimated (if applicable).
Fuel life cycle	The models, assumptions, and data used to estimate emissions from the life cycle of fuels.
Vehicle and materials life cycle	The life cycle of materials and vehicles, apart from vehicle fuel. The life cycle includes raw material production and transport, manufacture of finished materials, assembly of parts and vehicles, maintenance and repair, and disposal.
GHGs and CEFs	The pollutants (greenhouse gases or GHGs) that are included in the analysis of CO <sub>2</sub> equivalent emissions, and the CO <sub>2</sub> equivalency factors (CEFs) used to convert non-CO <sub>2</sub> GHGs to equivalent amount of CO <sub>2</sub> (IPCC = factors approved by the Intergovernmental Panel on Climate Change [IPCC]).
Infrastructure	The life cycle of energy and materials used to make and maintain infrastructure, such as roads, buildings, equipment, rail lines, and so on. (In most cases, emissions and energy use associated with the construction of infrastructure are smaller compared with emissions and energy use from the end use of transportation fuels.)
Price effects	This refers to the relationships between prices and equilibrium final consumption of a commodity (e.g., crude oil) and an “initial” change in supply of or demand for the commodity or its substitutes, due to the hypothetical introduction of a new technology or fuel.

---



# Analysis of Design Tradeoffs for Plug-in Hybrid Vehicles

Benjamin Geller, Casey Quinn, and Thomas H. Bradley<sup>1</sup>

Department of Mechanical Engineering, Colorado State University, Fort Collins, CO 80523-1374, USA

## Contents

1. Introduction	160
2. Methods for Studying PHEV Design	161
2.1 Model of PHEV design process	161
2.2 Review of PHEV design literature	162
2.3 Methods for analysis of PHEV design process	163
3. PHEV Subsystem Description and Tradeoff Analysis	164
3.1 Drivetrain architecture	164
3.1.1 <i>State of the art for drivetrain architecture</i>	164
3.1.2 <i>Requirements of drivetrain architecture design based on PHEV vehicle-level attributes</i>	165
3.1.3 <i>Constraints on vehicle-level design based on drivetrain architecture attributes</i>	166
3.1.4 <i>Constraints on system-level design based on vehicle architecture attributes</i>	167
3.2 Energy storage systems	168
3.2.1 <i>State of the art for PHEV ESS</i>	168
3.2.2 <i>Requirements of ESS design based on PHEV vehicle-level attributes</i>	168
3.2.3 <i>Constraints on vehicle-level design based on ESS attributes</i>	169
3.2.4 <i>Constraints on system-level design based on ESS attributes</i>	169
3.3 Secondary power sources	170
3.3.1 <i>State of the art for secondary power sources</i>	170
3.3.2 <i>Requirements of secondary power source design based on PHEV vehicle-level attributes</i>	170
3.3.3 <i>Constraints on vehicle-level design based on secondary power source attributes</i>	171
3.3.4 <i>Constraints on system-level design based on secondary power source attributes</i>	172
3.4 Energy management strategies	173
3.4.1 <i>State of the art for energy management strategies</i>	173
3.4.2 <i>Requirements of energy management strategy design based on PHEV vehicle-level attributes</i>	174
3.4.3 <i>Constraints on vehicle-level design based on energy management strategy attributes</i>	175
3.4.4 <i>Constraints on system-level design based on energy management strategy attributes</i>	175
3.5 Accessory systems	177
3.5.1 <i>State of the art for vehicle accessory systems</i>	177
3.5.2 <i>Requirements of accessory system design based on PHEV vehicle-level attributes</i>	178
3.5.3 <i>Constraints on vehicle-level design based on accessory system attributes</i>	178
3.5.4 <i>Constraints on system-level design based on accessory system attributes</i>	179
3.6 ESS charging system	179

<sup>1</sup> Corresponding author: [Thomas.bradley@colostate.edu](mailto:Thomas.bradley@colostate.edu)

3.6.1	<i>State of the art for ESS charging systems</i>	180
3.6.2	<i>Requirements of the ESS charging system design based on PHEV vehicle-level attributes</i>	181
3.6.3	<i>Constraints on vehicle-level design based on ESS charging characteristic attributes</i>	181
3.6.4	<i>Constraints on system-level design based on ESS charging characteristic attributes</i>	181
4.	Case Studies	182
4.1	Hymotion Prius and Escape PHEV conversions	185
4.2	Daimler-Chrysler Sprinter PHEV	185
4.3	Chevrolet Volt	186
5.	Concluding Remarks	186
	References	187



## 1. INTRODUCTION

Plug-in hybrid vehicles (PHEVs) are hybrid electric vehicles (HEVs) that can store and use energy from the electric grid to provide tractive power.

As implemented in a variety of demonstration, concept, and production vehicles, this simple functional change to the components of an HEV can provide a variety of personal and societal benefits. Relative to conventional HEVs, these benefits may include reduced vehicle and societal greenhouse gas emissions, reduced vehicle and societal petroleum consumption, reduced regional criteria emissions, improved national energy security, reduced vehicle fueling costs, improved transportation system robustness to fuel price and supply volatility, and the consumer benefits of home refueling.

In many cases, the benefits of PHEVs have been shown to justify the additional functional, monetary, environmental, and infrastructural costs of their production and use. Relative to conventional hybrid vehicles, these costs may include reduced vehicle utility and performance, increased vehicle life cycle costs, increased local criteria emissions, an increased rate consumption of resources for PHEV production and fueling, costs associated with new charging infrastructure, and increases in local and national peak electrical loads.

The effectiveness with which PHEVs can achieve a balance between the benefits and the costs of their implementation is highly dependent on the detailed design, function, and conditions of use of the individual vehicle. At present, there exists no universally agreed upon or optimum design for PHEVs. Every PHEV design that has been proposed or constructed represents a distillation of the designer's philosophy for maximizing the benefits and minimizing the costs of the PHEV. This chapter provides a systematic analysis of the design tradeoffs present in PHEVs. Section 2 presents a model of PHEV design and a review of how PHEV design studies in literature can fit into the PHEV design model. Section 3 summarizes the state of the art for PHEV subsystems and presents some of the most relevant requirements and constraints that affect the design of those subsystems. Section 4 uses contemporary PHEV production and demonstration vehicles as case studies to understand the design objectives and cost-benefit weightings that are implicit in a variety of PHEV designs.

## 2. METHODS FOR STUDYING PHEV DESIGN

The design of any complicated system including PHEVs is complex, multiobjective, and iterative. Further complicating the analysis of design of these commercial products is that the details of commercial design processes are generally not published. Research into design methods is therefore necessarily reductionist; we cannot describe the entire complexity of the design process, instead we must understand and describe the inputs and outputs of the design process and its primary elements.

### 2.1 Model of PHEV design process

This chapter proposes a model which can be analyzed to build an understanding of the PHEV design process. This model is shown conceptually in Fig. 6.1.

The PHEV design process is broken down into three steps which proceed from left to right. Design objectives provide input to the design tradeoff space. The results of the design tradeoffs are the attributes of the design. Example design objectives and example attributes are shown in Fig. 6.1. A hierarchy of design objectives, contributing analyses, and design attributes is also represented in the PHEV design model.

At the lowest level are the objectives, analyses, and attributes of subsystem-level design. Subsystem-level design objectives are concerned with the performance, specification, and sizing of individual components or subsystems of a PHEV. These design objectives might include minimizing engine size, using advanced battery chemistry, or achieving a specific engine turn-on speed. Subsystem-level analyses might include models of engine performance, motor dynamics, or battery lifetime. The subsystem-level design attributes are component specifications and sizes.

At the next higher level are the objectives, analyses, and attributes of vehicle-level design. Vehicle-level design objectives guide the design process to achieve vehicle attributes. These may include objectives for vehicle cost, tested fuel economy, and

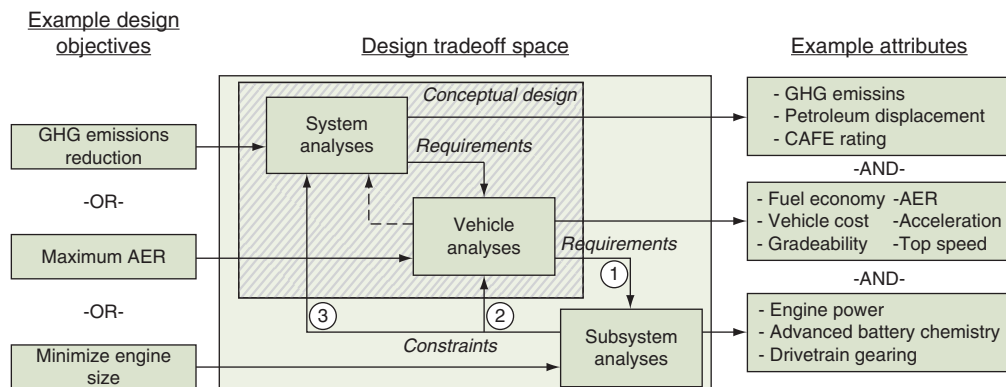


Figure 6.1 PHEV design process methodology diagram.

all-electric vehicle range. Vehicle-level analyses include fuel economy simulation, models of cost to manufacture, and vehicle dynamic performance models. Vehicle-level design attributes are determined solely by the function of the vehicle and its subsystems. Vehicle-level design attributes include many of the conventional metrics of PHEV performance including 0–100 kph time, all-electric range (AER), and retail price.

At the highest level are the objectives, analyses, and attributes of system-level design. System-level objectives, analyses, and attributes describe the function of the PHEV as an element in a larger system over which the vehicle designer may have only limited control. The systems to be considered might be the transportation energy sector, the electric grid, an air quality management district, or a transportation policy. System-level design objectives might include goals for greenhouse gas (GHG) emissions, petroleum displacement, or Corporate Average Fuel Economy (CAFE) rating. Analyses to determine the attributes of a design relative to system-level design objectives are generally outside of the scope of conventional vehicle engineering.

Treating these blocks as elements of the PHEV design process, we can begin to understand the connections between them. Information is exchanged between the contributing analyses through the mechanisms of requirements and constraints. The requirements are passed from the higher level contributing analyses to the lower level contributing analyses. For example, a system-level design objective such as net GHG emissions reduction may be transmitted to the vehicle-level contributing analysis as a requirement for high vehicle fuel economy. In order to achieve the vehicle-level requirement on fuel economy, the engine subsystem will be issued a requirement for a low brake-specific fuel consumption engine. In a similar way, information can be passed from the lower level to the higher level contributing analyses as constraints. For example, a particular battery chemistry may constrain the PHEV's vehicle-level performance by increasing vehicle weight relative to another design option. The battery chemistry will also provide a constraint to the achievable system-level attribute of petroleum displacement by providing a limitation on energy storage capacity.

## 2.2 Review of PHEV design literature

With the classification of design objectives proposed above, we can understand the PHEV design methods that have been proposed in literature on the basis of the conceptual level of their design objectives. Each method has a set of primary design objectives that are inputs to the design process. These objectives are the qualities that are to be met by the resulting vehicle design. For this study, we divide these design objectives into subsystem-, vehicle-, and system-level categories.

The primary groups who have documented a PHEV design process with subsystem-level design objectives are PHEV conversion companies. These companies have the design objective of using their particular battery chemistry or battery system design. Because these PHEVs are conversions, the designers have no control over the other

systems of the PHEV. Battery systems are often shared between PHEV platforms, regardless of the effect on vehicle-level performance attributes. Ronning [1] treads the line between component-level and vehicle-level design objectives by proposing engine size minimization as a design objective, subject to vehicle-level constraints on performance including acceleration times.

PHEV design processes with vehicle-level design objectives have been proposed by a number of researchers. Wong et al. [2] propose that minimization of cost and maximization of all-electric vehicle range should be dual vehicle-level design objectives. Balch et al. [3] seek to maximize all-electric vehicle range subject to vehicle cost and vehicle performance constraints. The design process used in Ref. [4] seeks to achieve certain all-electric vehicle ranges subject to performance constraints.

PHEV design objectives that are posed at the system level are less common. An et al. [5] propose a design process with objectives of compliance with California Zero Emission Vehicle (ZEV) regulations. Meyr et al. [6] propose a design objective of net GHG reductions.

Overall, a majority of published PHEV design studies have design objectives that are posed at the vehicle level and below. On the basis of this review of design objectives from the literature, it becomes evident that only through integrating component design, vehicle design, and system design can system-level design objectives be posed. Expressing design objectives at the system level is necessary to achieve the beneficial system-level vehicle attributes that have been proposed for PHEVs. To date, the system-level vehicle characteristics that have been attributed to PHEVs are not the result of a direct design process, they are by-products of a vehicle-level design process. In order to be able to improve the system-level attributes of PHEVs, we must understand the connections between the PHEV design processes at the three proposed levels.

### 2.3 Methods for analysis of PHEV design process

The stage of conceptual design is highlighted within the design process shown in Fig. 6.1. Conceptual design involves the interaction of the vehicle-level objectives, analyses, and attributes with the system-level objectives, analyses, and attributes. These connections have been studied in detail in the existing literature on PHEVs describing sustainability assessments, net GHG analyses, grid impacts assessments, and conceptual comparisons [29,32,37,38,44–50].

Instead of reviewing this previous work, this study will concentrate on the connections that lead to and from the subsystem-level contributing analyses. To provide justification and structure for a multilevel PHEV design process that can include information exchange between all three levels of analysis, this work will describe the design tradeoffs that result from inclusion of the subsystem analyses in the design process. These connections are labeled in Fig. 6.1 according to the following: signal 1 represents the requirements that are placed on the design of each subsystem by the vehicle-level

operation of the PHEV, signal 2 represents the constraints on the vehicle-level performance that are a result of subsystem design choices, and signal 3 represents the constraints on the system-level attributes of the PHEV that are a result of subsystem design choices.



### 3. PHEV SUBSYSTEM DESCRIPTION AND TRADEOFF ANALYSIS

The subsystems to be analyzed in this study are vehicle architecture, energy storage, secondary energy storage (engine), energy management strategy, accessory systems, and charging systems. For each of these PHEV subsystems, this section will describe the state of the art in design and function of that subsystem, the requirements of the subsystem design that are derived from PHEV vehicle-level attributes, the constraints on vehicle-level design that are based on the attributes of the subsystems, and the constraints on system-level performance that are based on the attributes of the subsystems.

#### 3.1 Drivetrain architecture

The PHEV drivetrain architecture subsystem consists of all of the powertrain components that transmit power from the primary and secondary energy sources to the wheels of the vehicle. The design of the drivetrain architecture subsystem includes design of the transmission, motor/generators, and final drive.

##### 3.1.1 State of the art for drivetrain architecture

PHEV drivetrain architecture is an extension of standard HEV architecture and can be classified into three main categories: series, parallel, and power-split.

Series HEVs consist of a secondary power source, such as an internal combustion engine (ICE) or fuel cell (FC), which is connected to a generator that charges the primary energy source (batteries). The main subsystem components used in PHEVs can be seen in Fig. 6.2. The batteries then power a traction motor to drive the wheels, as can be seen in Fig. 6.3. Parallel HEVs consist of an ICE which is mechanically coupled with a traction motor. The coupling allows for torque addition between the two units but

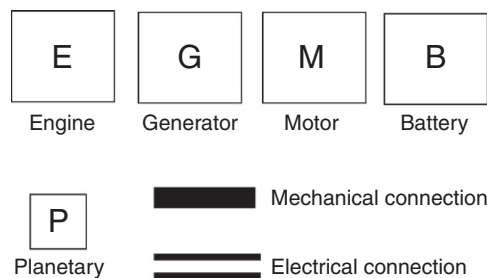


**Figure 6.2** Subsystem component key for PHEV architectures.

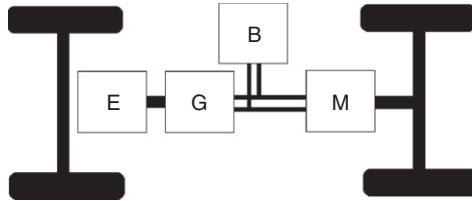


**Figure 6.3** Series PHEV architecture.

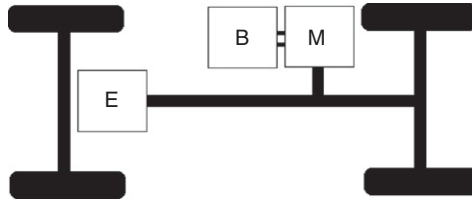


**Figure 6.4** Parallel PHEV architecture.

creates other limiting factors. In most applications, parallel systems are more efficient and have fewer components than series PHEVs (one engine and one motor as opposed to an engine, generator, and motor in series systems) as shown in Fig. 6.4. Power-split (or series-parallel) HEVs are the most complicated of the three systems and combine the positive aspects of both the series and parallel drivetrains. Power-split vehicles are most commonly composed of an ICE coupled with a motor and generator through a speed coupling device such as a planetary (epicyclic) gear set. This configuration offers high efficiency but with more complicated powertrain design and control. An example of a power-split drivetrain is shown in Fig. 6.5.

Each type of drivetrain architecture has costs and benefits, but to date there is no clear optimum configuration for PHEVs.

### **3.1.2 Requirements of drivetrain architecture design based on PHEV vehicle-level attributes**

The function and attributes of the PHEV being designed determines the types of drivetrain architectures that can meet the vehicle-level performance criteria.

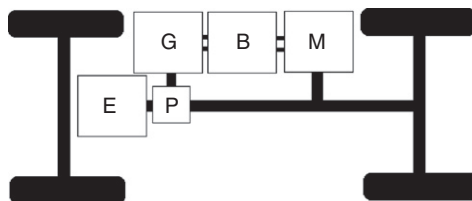


**Figure 6.5** Power-split PHEV architecture.



For PHEVs with significant AER, both parallel- and series-type drivetrain architectures can be successful. In either case, because the traction motor is the only source to drive the wheels, it must be large enough to supply the speed and torque necessary to propel the vehicle throughout the vehicle's entire speed range. Power-split architectures based on epicyclic gears can be more problematic because the speed ratios between the engine, the motors, and the wheels are fixed in relation to one another. In Toyota Prius and Ford Escape transmissions, the maximum speed attainable under all-electric operation is limited by the torque and speed limits of the generator.

The intermittent engine operation that is characteristic of PHEVs provides additional requirements to the drivetrain and its subcomponents. For example, in parallel drivetrains, the electric motor must be multifunctional to achieve the vehicle-level objective of HEV operation. It provides torque for driving the vehicle, and it must be capable of providing torque to compensate for the stopping and starting of the engine which occurs during normal PHEV operation. The traction motors in series and power-split drivetrains are not as multifunctional as in parallel drivetrains, but the generator control in both of these architectures can be complicated by PHEV-type operation.

### ***3.1.3 Constraints on vehicle-level design based on drivetrain architecture attributes***

The primary characteristics of the drivetrain architecture decisions that affect the vehicle-level attributes of the PHEV are packaging and cost constraints. The cost of electric motors, power electronics, and batteries increases with increasing torque output, thereby leading the PHEV designer toward using smaller electronic components with more complicated mechanical connections. These smaller components also contribute to decreased vehicle mass, thereby improving PHEV fuel economy and performance. In general, series hybrid vehicles require larger electronic components including both motor and generator, resulting in a more weighty and expensive drivetrain system. Parallel vehicles require fewer power electronic components, which in general results in a drivetrain that is more compact, lighter, and less costly than that of series vehicles.

Because there are more electrical connections instead of mechanical connections, component location and orientation is the least limited in series PHEVs. Series powertrains are understood to be most suited to medium- and heavy-duty PHEVs because of the additional space that is available for the components and the vehicle platform's increased tolerance for vehicle weight. Series systems also exhibit their highest efficiency gains at low speed, urban-type driving [8, 9].

Power-split hybrids can be specified so as to perform in the continuum of design space between series and parallel drivetrains.

### 3.1.4 Constraints on system-level design based on vehicle architecture attributes

Although all of the PHEV architectures offer improvement on efficiency and reduced emissions compared to conventional vehicles, there are slight variations in their environmental impacts. Series vehicles have increased losses because of the additional energy conversion (mechanical to electrical and vice versa) that are present in the system, contributing to an overall lower efficiency than a comparable parallel or power-split system [12]. Series hybrid vehicles do have the advantage of being able to operate their ICE in an optimum range at all times which leads to fewer emissions. Series vehicles are also capable of being powered by a FC which turns the vehicle into a complete zero emissions vehicle (ZEV). Although both parallel and power-split benefit from reduced engine sizing and enlarged electro-chemical capacity, they still must operate their engines through a wider range, which is not ideal for emissions. Within this comparison between parallel and power-split though, power-splits have more control over their operational ICE range because they are not directly connected to the drive wheels such as parallel hybrid vehicles [13].

Depending on the design goals for the overall vehicle, the different architectures satisfy aspects unequally. If environmental impact and simplicity are the main goals with less emphasis on performance, range, and cost, then series architectures may be optimal. If drivability and performance are key, and more resources available to cover design complexity and controls, then the power-split architecture may be optimal. Finally, if environmental impact and cost are the leading design criteria, then parallel drivetrains may be optimal. These design decisions can be observed and compared in Table 6.1. The weightings of these performance attributes have not been assigned because their relative value must be determined from the vehicle design criteria.

**Table 6.1** Comparison of vehicle architecture

Battery system	Series	Parallel	Power-split	References
Weight	0	+	–	[8, 10, 12]
Cost	0	+	–	[8–10, 12, 22]
Controls	+	0	–	[8, 9, 12, 22, 61, 62]
Number of components	0	+	–	[8–10, 12, 22]
Volume	–	+	–	[8, 10, 12]
Performance	–	+	+	[8, 10, 12]
Drivability	0	0	+	[8, 11, 12, 63]
Efficiency	–	+	+	[8, 12, 22]
Design freedom	–	0	+	[8–10, 12]
Total	–3	+6	–1	

## 3.2 Energy storage systems

Usually electrochemical energy storage for PHEVs consists of batteries, although battery/ultracapacitor [14] and regenerative FC [15–17] PHEVs have been proposed. The energy storage system (ESS) consist of the battery modules and their support systems including thermal management, electrical management, and safety subsystems. The functions of the ESS for PHEVs are to store electric energy for propulsion and to meet some short-term power demands of the vehicle. These short-term power demands can be charging the ESS in the case of regenerative braking, or they can be discharging the ESS, in the case of vehicle accelerations. The batteries of PHEVs must perform these functions at a variety of states of charge (SOC). Depending on the characteristics of the vehicle, the electrical energy stored can commonly be as large as 19 kWh with power transients of >75 kW for a mid-sized sedan [18], or 30 kWh and >150 kW for a full-size sport utility vehicle (SUV) [19].

### 3.2.1 State of the art for PHEV ESS

The consensus of recent meetings and publications on battery systems for PHEVs is that lithium ion (Li ion) battery systems will be the battery system of choice for near- and long-term PHEVs. Other technologies, including lead-acid and nickel-metal hydride will not meet the performance and cost points required for mass market PHEV applications [7].

Within the design space of Li ion battery technology, there is still significant debate over what the characteristics of PHEV ESSs should be such as chemistry, size, cooling method, and depth of discharge. Li ion batteries are available in a variety of dopings and chemistries, all of which exhibit different characteristics in terms of energy density, lifetime, overcharge tolerance, cost, and manufacturability. Also, no consensus exists on what level of depth of discharge is appropriate for Li ion battery systems to achieve design lifetimes, or even what the primary cause of battery end-of-life will be. When sizing ESS, some PHEVs have been designed with nearly zero charge depleting range (RCD). Also, a variety of studies dismiss ESS sized for more than 100 miles of electric range as economically unoptimized.

### 3.2.2 Requirements of ESS design based on PHEV vehicle-level attributes

The function of a PHEV ESS is central to the vehicle's design function and operation. PHEV operation places special requirements on the battery systems that are not present in other types of electrified vehicles.

A PHEV ESS must be able to tolerate unique types of charge–discharge cycles. Whereas BEVs engage in approximately one deep charge–discharge cycle per trip, and HEVs engage in a number of shallow charge–discharge cycles per trip, PHEVs engage in both one deep charge–discharge cycle and a number of shallow charge–discharge cycles per trip. The effects of this type of cycling are difficult to predict although it is expected

that PHEV-type charge–discharge cycles will be more deleterious to Li ion battery lifetime than either EV- or HEV-type discharge cycles [7, 20]. Despite this, experimental measurements of battery degradation under a PHEV-type charge–discharge cycle have shown acceptable lifetime and performance [21].

Energy output from the ESS is often dictated by the vehicle-level requirement for charge-depleting range. Power output from the ESS is dictated by the power required for high-performance driving including 0–100 kph tests, off-road, and gradeability tests. Because PHEV batteries must be specified to meet both the energy and power requirements of the vehicle, they generally require higher power to energy (PE) ratios than EV batteries and lower PE ratios than HEV batteries. Thus, there are requirements on the battery system that are PHEV specific, and the costs, performance, and lifetime of PHEV batteries cannot directly be extrapolated from the data from either EV or HEV applications.

### ***3.2.3 Constraints on vehicle-level design based on ESS attributes***

The ESS of PHEVs provides many constraints on vehicle-level design attributes. Unavoidable design tradeoffs exist between the ESS specifications and the vehicle-level design attributes such as passenger space, performance, and vehicle costs.

The ESS of PHEVs is generally heavier and more bulky than those of HEVs. Whereas HEVs have been designed with the ESS integrated into the chassis, body, or trunk of the conventional vehicle, PHEVs may require a vehicle redesign to accommodate the increased weight and bulk of the PHEV ESS. PHEV conversions require significant compromises to vehicle handling and interior volume to package the battery system. For example, the GM Volt uses a custom vehicle chassis with an integrated battery tunnel. This configuration centers the mass of the battery system to improve vehicle dynamics, reduces the lost interior volume, and protects the pack from accidental impact.

The increased mass of PHEV ESS elicits a cost in terms of vehicle fuel economy and performance. Because of the dynamic nature of vehicle fuel economy and performance testing, vehicle-level attributes such as tested fuel economy, 0–100 kph times, and dynamic handling are very sensitive to vehicle mass. As a result, PHEVs generally have slightly lower charge sustaining fuel economy and slightly worse dynamic performance when compared to conventional HEVs.

Finally, a PHEV ESS is intrinsically more costly than a conventional HEV ESS due to its increased capacity and power. PHEV studies agree that the manufacturer cost and purchase price of PHEVs will be significantly higher than comparable HEVs due to the costs of the PHEV ESS.

### ***3.2.4 Constraints on system-level design based on ESS attributes***

The system-level attributes of a PHEV design are in large part determined by the attributes of the ESS subsystems. Relative to conventional HEVs, PHEVs have a large ESS that can more significantly affect the system-level attributes of the vehicle.

Numerous studies have examined the effect of battery sizing on system-level design attributes for PHEVs. These studies have focused on system-level design attributes such as GHG emissions, petroleum consumption, and sustainability assessments. In another example, in PHEVs, the production of the ESS can represent a significant portion of the lifecycle energy consumption of the vehicle. The production of a Li ion battery ESS in conventional HEVs consumes approximately 6.1% of life cycle energy. In PHEVs, the production of a 114 kg Li ion battery [22] can consume 22.9% of the vehicle life cycle energy [23]. Oversizing the ESS, as may be required to ensure battery lifetime [24], will only increase the vehicle life cycle energy embedded in the ESS production. With increasing ESS capacity, there exists a tradeoff between the increasing life cycle energy required for ESS production and the decreasing life cycle energy consumed during vehicle operation.

### **3.3 Secondary power sources**

PHEVs have a secondary energy source to supply tractive energy to the vehicle and to meet instantaneous power demands. Secondary power sources can be classified according to fuel-type and fuel conversion method. The leading fuel types are gasoline (including reformulated gasoline and ethanol blends), diesel (including biodiesels), natural gas, and hydrogen. Within these, there are fuel conversion methods including port injection spark ignition (PISI), direct injection spark ignition (DISI), and direct injection compression ignition (DICI) engines. FCs are also considered as another method although their specific fuel conversion method only applies for the hydrogen and hydrocarbon fuel types [25].

#### ***3.3.1 State of the art for secondary power sources***

Currently, gasoline–electric HEVs dominate the US hybrid market because of stringent light-duty vehicle emissions regulations. Diesel tends to take a slight advantage in European countries based on fuel cost, fuel availability, and customer base. Technology in the FC field has developed enough recently though to make them more feasible. Many automakers have announced production plans for hydrogen FCs. Hydrogen ICEs have been proposed as an intermittent stepping stone between gasoline and FCs but will most likely not become necessary because of the rate at which FCs are currently advancing [26]. Although they have been proposed for use in PHEVs, solid oxide fuel cell (SOFC)s and hydrogen combustion engines are not widely accepted as viable technologies in the short term.

#### ***3.3.2 Requirements of secondary power source design based on PHEV vehicle-level attributes***

The vehicle-level design attributes will dictate the sizing, fuel conversion method, emissions system function, and range for the secondary power source.

In parallel PHEVs, the sizing of the secondary power source can be determined from the torque requirements of the vehicle [10]. Larger vehicles with more torque requirement such as medium- and heavy-duty vehicles can benefit from larger displacement engines or diesel engines. Light-duty vehicles that require less torque can use gasoline engines and operate them primarily at high loading conditions where the engines operate most efficiently.

More turn on/off cycles are required in parallel PHEVs than the other two, and series PHEVs require the least of the three. It has been shown that by minimizing or deducing engine idle through turn offs, overall consumption can be reduced by about 7.5% over a standard cycle [25]. This affects choices because gasoline engines are more adapted to this function than either the diesel or hydrogen ICE. This also brings up the issue of hot and cold starts with regards to emissions. Hot and cold starts are affected by the frequency of engine cycles and if there are any systems in place to maintain engine temperature when it is not operational. The most commonly considered aspect of engine turn-on/off operation is that if a vehicle has been designed to operate in a blended mode with frequent on/off cycles, then a diesel ICE should not be used because of the large increase in emissions in comparison to gasoline engines associated with cold starts.

Another consideration that designers must make is the desired range of the vehicle, although the specifics of range will be discussed further in Section 3.4. Hydrogen use increases fuel economy and reduces emissions dramatically for FCs but they are limited in range by the hydrogen storage tank. Pressure trends tend to be near 700 bar for most applications but some prefer 350 bar for safety and reliability. These tanks also cost roughly \$10,000 and offer a somewhat limited range of 200–300 miles. This would require more frequent refueling than with a conventional gasoline vehicle [7]. In comparison, the energy content of gasoline and diesel power sources are limited primarily by volume and mass restrictions because their storage tanks are relatively cheap and simple to scale in size.

### ***3.3.3 Constraints on vehicle-level design based on secondary power source attributes***

The secondary power source attributes will dictate the design constraints of the vehicle-level design by determining available power, energy, and control strategy methods.

If an FC is chosen as the secondary power source, the series PHEV architecture is the only architecture capable of supporting it. FCs can be used as a third power source in parallel/power-split PHEVs, but the added costs currently outweigh any potential performance gains.

In Ref. [25], vehicle-level design attribute of energy consumption per unit distance traveled was compared for multiple fuel types and combustion methods. For HEV applications, hydrogen PISI and diesel DICl showed the best values (FCs were not considered). Gasoline PISI and diesel DISI followed behind with fuel consumption values that are comparable to one another.

Based on the distance to a refueling station, fuel supply capacity can be determined. Longer distances between stations require vehicles to have a larger supply tank or battery capacity [27]. Gasoline and electricity have the shortest average distance to refuel, followed closely by diesel. Natural gas has the furthest average refueling distance, over 30 times further than gasoline. Biodiesel and ethanol are in the mid range with between 10 and 15 times the distance of gas or standard diesel. Hydrogen has not been compared here because of the limited availability, although a study by Ogden [28] shows that depending on current market penetration hydrogen refueling could be feasible with average distances either the same or up to 2 times further than current gasoline/diesel stations, allowing for possibly half as many total stations.

The same considerations made for secondary power source turn-on/off must also be applied here. For example, if a diesel engine is chosen, then it would be appropriate to choose a control strategy that limits turn-on/off cycles and cold starts, more so than if a comparable gasoline engine is chosen.

Although diesel engines are currently more efficient (lower consumption) and produce low levels of GHG, their mass market appeal is lower than gasoline engines in the United States and capital costs tend to be several tens of percent higher than spark ignition gasoline engines. These higher costs must be considered as a tradeoff for power and efficiency when choosing vehicle components such that the overall cost of design is not too high. For example, combining a diesel DICI engine with a power-split architecture would be relatively expensive [25].

### ***3.3.4 Constraints on system-level design based on secondary power source attributes***

System-level design constraints and requirements can be split into two categories that help us further refine our choice: well-to-wheel (WTW) emissions assessments and fuel source renewability.

Of the secondary energy sources available for PHEVs, there are tradeoffs between cost and renewability. Currently, the cheapest source to design and implement is gasoline HEVs because of the world's standardized dependence and familiarity. As this source is known to be nonrenewable, it will eventually run out, with prices increasing continuously in the long term up to this point. Ethanol has shown to be an expensive supplement to reduce dependence on pure gasoline and currently still heavily depends on gasoline. Diesel engines used also fit into this category of nonrenewable, but have become decreasingly so with the introduction of advanced biodiesels. Hydrogen for use in IC engines and FCs can be made from renewable electricity, but it carries a higher price tag for refinement and implementation.

In a recent study by Argonne National Lab (ANL) [29], WTW emissions were compared for nine different fuels each with five different parameters. The fuel types cover variations in diesel, ethanol, electricity, gasoline, and hydrogen with parameters of

**Table 6.2** Comparison of fuel well-to-wheel emissions

Emission	Gasoline	Diesel	Ethanol	Hydrogen	Electricity
VOC	0	+	–	+	+
NO <sub>x</sub>	0	0	–	+	0
PM <sub>10</sub>	+	+	–	+	–
PM <sub>2.5</sub>	+	+	–	0	–
CO	+	0	+	+	+
Total	+3	+3	–3	+4	0

Source: Ref. [29].

volatile organic compounds (VOCs), mono-nitrogen oxides (NO<sub>x</sub>), particulate matter based on diameter (PM<sub>10</sub> and PM<sub>2.5</sub> where subscripts represent micrometer (μm)), and carbon monoxide (CO). The emissions studies were split into the different stages of production such as mining, processing, and exhaust but only the overall totals will be presented here. The last parameter of the study was to compare both urban and total emissions for each fuel because different driving cycles contribute to varying emissions characteristics. Without weighting any of the emissions contributors, based on the study by ANL, hydrogen appears to have the least amount of WTW emissions, closely followed by gasoline and diesel. Ethanol has the highest total emissions of the group. Additional notes for the comparison include that gasoline and diesel emissions are listed for hybrid applications (conventional applications would be scaled higher) and the high particulate emissions from electricity production are created in the coal mining process which would not affect the general public as much as tailpipe emissions do. An unweighted comparison of the various fuel types and their respective emissions has been presented in [Table 6.2](#).

### 3.4 Energy management strategies

PHEVs are unique in that they have two possible energy sources that can be used to propel the vehicle. The objective of the energy management strategy in PHEVs is to optimize the types and quantity of energy used so as to meet vehicle performance goals. The design of energy management strategies requires significant tradeoffs between the subsystem-, vehicle-, and system-level functions of PHEVs.

#### 3.4.1 State of the art for energy management strategies

The energy management strategy defines the control logic that governs how the electric motor and secondary power source will be controlled to provide the PHEV's tractive energy. PHEV control strategies utilize different combinations of vehicle operational modes. The most prevalent PHEV operational modes are listed and described below [30, 31]:



- Electric vehicle (EV) mode – Allows the PHEV to operate as an electric vehicle. Therefore, in the EV mode, the PHEV’s engine is not permitted to operate and only utilizes the electric motor to provide the tractive force.
- Charge depleting (CD) mode – Prioritizes the use of the electric motor over the engine. However, if the demanded tractive power exceeds the limits of the electric motor, the engine assists the electric motor to meet the vehicle’s power demands. The goal of the CD mode is to fully deplete the usable ESS energy.
- Charge sustaining (CS) mode – Utilizes a combination of engine and motor management to try and maintain the ESS SOC at a specified level. This mode is equivalent to conventional HEV operation.
- Engine only mode – Prioritizes the use of the engine over the motor.

The PHEV control mode can either be manually selected by the driver or automatically be selected based upon feedback signals from various vehicle systems such as the ESS SOC, ESS temperature, tractive power requirements, vehicle location, and expected trip length [5, 31, 32]. PHEVs can be classified based on the ways that the energy management strategy uses the operational modes described above. Reference [33] classifies PHEVs into blended, AER-capable, and range-extended categories. Blended PHEVs are incapable of running an entire urban dynamometer driving schedule (UDDS) cycle in EV mode, AER-capable PHEVs are able to drive an entire UDDS cycle in EV mode, and range-extended PHEVs are capable of driving an entire US06 cycle in EV mode.

Blended PHEVs operate in a mixture of EV, CD, and engine only modes, while the ESS’s SOC remains above the CS SOC threshold. Once the SOC reaches the specified threshold, the PHEV operates in CS mode until the batteries are recharged. AER-capable and extended range electric vehicle (EREV) PHEVs have the ability to operate in the EV mode until a control threshold, such as a maximum vehicle power required, is crossed. Upon crossing the control threshold, the engine assists the traction motor. In general, AER-capable PHEVs are more likely than range-extended PHEVs to operate in blended mode under normal driving conditions. PHEVs have been successfully designed and demonstrated within all of these categories, and no universally preferred strategy exists.

#### ***3.4.2 Requirements of energy management strategy design based on PHEV vehicle-level attributes***

PHEV-specific vehicle-level design objectives can set requirements for operation of the energy management subsystem that are different than the requirements from conventional HEVs.

For example, AER-capable and range-extended PHEVs operate in an extended-duration EV mode that does not require an engine start with the starting of the vehicle. When the PHEV designer sets a vehicle-level objective to achieve a certain 0–100 kph acceleration time, the energy management strategy must decide whether or not to turn on the engine or to perform the acceleration in EV mode. Whereas a conventional HEV

engine and emissions system can be maintained at operating temperature, many types of PHEV operation do not require the engine to operate regularly. The PHEV energy management strategy must weigh the costs of full throttle cold-start emissions against the costs of missing the 0–100 kph acceleration time design objective.

### ***3.4.3 Constraints on vehicle-level design based on energy management strategy attributes***

There exists a stark tradeoff between the type of energy management strategy that is employed by the PHEV and its performance against vehicle-level design objectives. PHEVs that use an AER or EREV strategy are less capable of effectively meeting driver demands and vehicle-level performance objectives such as sustained top speed, gradeability, passing performance, and standing acceleration. A blended PHEV can meet these performance requirements more cost effectively due to the fact that AER and EREV PHEVs require larger and more expensive components to achieve equivalent performances while operating in EV mode [32, 34–37].

In addition, studies have shown that PHEV fuel economy is sensitive to the rate of charge depletion, independent of the energy management strategy type. Ideally, the ESS is fully depleted between charges and is recharged upon completion of each trip. Researchers have proposed that an optimum ESS depletion rate can be calculated based on trip length, the distance from the next expected recharge point, and the amount of energy remaining in the ESS [38]. A PHEV using a blended control strategy may provide the most fuel economy benefit if the driver will exceed the AER capability of the PHEV on a regular basis.

### ***3.4.4 Constraints on system-level design based on energy management strategy attributes***

The energy management strategy for PHEVs can greatly affect its ability to meet system-level design objectives. Potential system-level design objectives for PHEVs might include compliance with the ZEV regulations, and targeted reductions in real-world fuel consumption, criteria emissions, and GHGs.

Compliance with ZEV regulations is an important goal for large automakers because of the potential for exclusion from the California auto market. The ZEV program requires OEMs to design vehicles that have reduced emissions and improved fuel economies. This program requires OEMs to achieve a certain number of credits each year which are awarded based upon a vehicle's ability to utilize other energy sources besides petroleum, improved fuel economy, and vehicle emissions. Under the ZEV program, all PHEVs are classified as Enhanced Advanced Technology Partial Zero Emission Vehicles (PZEV<sub>E.AT</sub>) and receive a minimum ZEV credit of 0.2. The remainder of a PHEV's ZEV credit rating is derived utilizing the zero emission vehicle miles traveled (VMT), advanced componentry (AC), and the low fuel cycle emissions (LFCE)

factors. The zero emissions VMT is derived in [6.1] and incorporates the vehicle's equivalent all-electric range (EAER)<sup>1</sup> and the utility factor (UF) based upon the charge depletion range actual (RCDA).

$$\text{VMT} = \frac{\text{EAER}(1 - \text{UF}_{\text{RCDA}})}{11.028} \quad [6.1]$$

The AC portion of the ZEV credit is based on the PHEV's peak power output, traction voltage, and the EV mode capability. The LFCE is based on the use of compressed natural gas (CNG) and hydrogen. The total ZEV credit allotted to a PHEV platform is the summation of these four factors [39].

$$\text{ZEV}_{\text{PHEV}} = \text{VMT} + \text{AC} + \text{LFCE} + \text{PZEV}_{\text{E.AT}} \quad [6.2]$$

Based on the requirements of the ZEV program, the credits available for a vehicle are dependent on the energy management strategy through the EAER, UF, and AC factors. The value of the PHEV as a component of the ZEV program is dependent on optimization of the energy management subsystem toward ZEV program goals.

To model the performance of PHEVs as they will be used during real-world operation, UF analyses have been developed based on the driving statistics of the US population. SAE J2841 uses data from National Household Transportation Survey (NHTS) to define a UF which is a national statistical probability that a vehicle will be driven less than or equal to its AER during an average driving day. To construct this UF, the distance traveled by each household automobile during the surveyed travel day can be extracted from the NHTS dataset. For a single day ( $k$ ), the distance-based UF of a PHEV with an RCD, over a travel day covering distance  $d(k)$ , can be calculated as the ratio of the RCD to the distance-traveled RCD/ $d(k)$  if  $d(k) < \text{RCD}$ , or 1.0 if  $d(k) > \text{RCD}$ . For  $N$  travel days, a composite UF can be calculated as a function of RCD [100]:

$$\text{UF}(\text{RCD}) = \frac{\sum_{k=1}^N \min(d(k), \text{RCD})}{\sum_{k=1}^N d(k)} \quad [6.3]$$

The UF defines the dependence between the energy management strategy and the modeled real-world petroleum displacement, criteria emissions, or GHG emissions. These quantities can be calculated in units of quantity per unit distance using  $X$ , where  $C_{\text{CD}}$  is the consumption (or emission) during charge depleting operation and  $C_{\text{CS}}$  is the

<sup>1</sup>The EAER is a blended PHEV's equivalent AER [31].

consumption (or emission)  $C_{UF\text{weighted}} = UF \cdot C_{CD} + (1 - UF)C_{CS}$  during charge sustaining operation:

$$C_{UF\text{weighted}} = UF \cdot C_{CD} + (1 - UF)C_{CS} \quad [6.4]$$

This formula shows that the higher the rate of charge depletion, the higher the UF applied to the CD operating mode, and the more improved the PHEV petroleum displacement, criteria emissions, or GHG emissions will be. In summary, the system-level attributes of the PHEV are highly dependent on the subsystem-level attributes of the energy management strategy. Changes in the energy management strategy have been shown to have large impacts on the large-scale performance of the PHEV.

### 3.5 Accessory systems

Accessory systems are all of the systems of a vehicle that service the functions of the car unrelated to propulsion. This can include power steering, braking, passenger comfort, lighting, and so forth. As implemented today, PHEVs leverage many of the accessory systems present in conventional vehicles. Some of the vehicle accessory systems such as passenger comfort systems, structures, safety systems, and fueling systems are virtually unchanged from their conventional counterparts. In a variety of other accessory systems, the function and form must be entirely changed in order to preserve vehicle performance and consumer acceptability. Because of the high degree of energy flow optimization that goes into the design of PHEVs, the design of PHEV accessory systems can have a strong effect on the vehicle-level and system-level performance of the vehicle.

#### 3.5.1 State of the art for vehicle accessory systems

At present, a number of vehicle accessory systems are entirely compatible with the requirements of PHEVs. Systems that had been expensive, limited production items, such as electric power steering and hydraulically boosted power brakes, are now mass production systems available on both conventional and hybrid vehicles. The primary accessory system that drives vehicle design compromises is the heating, ventilation, and air-conditioning (HVAC) systems. The three primary functions of the HVAC system are cabin heating, cooling, and defogging.

At present, most PHEVs use an HVAC system that is at least partially electrically powered. In demonstration and research vehicles, this can be as simple as a resistance heater and an air conditioning compressor driven by electric motor [74, 98]. Although these retrofit systems are simple to implement and control, the increased parts count and low coefficient of performance of the resistance heater (CoP = 1) make them more expensive and massive than conventional HVAC systems. Air conditioning compressors that can be driven by both electric motors and the engine have been developed [40].

The highest efficiency and performance is delivered by heat pump systems that can heat, cool, and defog the vehicle interior [83, 99]. These systems use vapor compression

cycles powered by an electric motor to achieve high coefficients of performance ( $\text{CoP} > 3$ ) [99]. Heating, cooling, and defogging functions are performed using shared components, thereby limiting the cost and mass of the HVAC system. In these heat pump systems, waste heat from the engine coolant loop can also be injected into the heating ducts via a coolant-to-air heat exchanger.

### ***3.5.2 Requirements of accessory system design based on PHEV vehicle-level attributes***

The functional requirements of accessory systems for PHEVs are the same as for conventional vehicles. Consumer acceptability will not accept performance at less than full function. PHEV operation applies new constraints to the design of the vehicle accessory systems because of the intermittent engine operation that is intrinsic to many PHEV control strategies. Because the engine in many PHEVs is operated intermittently, there is no consistent source of waste heat available for cabin heating. The higher efficiency of the electric drive system of a PHEV makes the waste heat from the electric drive system of low quality; it is not generally usable for cabin heating. Because of these constraints, accessory systems that allow for fully functional operation of the HVAC during engine-off driving must be electrically powered. This constraint complicates the design of the accessory systems.

For electrically powered air conditioning systems, the refrigerant compressor is powered by a high power ( $\sim 2.5$  kW) electric motor which has high cost, weight, and bulk relative to conventional compressors which are driven by the front engine accessory drive (FEAD). For air conditioning compressors which are dual driven (by the FEAD during engine operation and by an electric motor during all-electric operation), the cost weight and bulk are increased again. These dual-driven compressors incorporate two-stage compressors for optimized operation at both engine and electric motor speeds [40]. Heat pump air conditioning systems can meet the requirements for all-electric operation as the compression stage of the vapor compression cycle is powered by an electrically driven compressor.

For cabin heating systems, the requirement for all-electric operation requires a complete reengineering of the heating systems. Electric resistance heaters can be integrated into the cabin heating ducts and powered by the high-voltage battery bus. As an alternative, heat pump systems can be designed to meet the requirements for cabin heating during all-electric operation.

### ***3.5.3 Constraints on vehicle-level design based on accessory system attributes***

Even with the best available technologies, the accessory systems provide a variety of constraints on the vehicle-level performance of PHEVs. One of the main differences between the design of conventional vehicles and PHEVs is the vehicle-level performance sensitivity to increased demands from accessory systems. Conventional vehicle designs can be considered robust in terms of the vehicles' ability to maintain vehicle-level

performance with varying accessory system loads. PHEV vehicle-level performance however is extremely sensitive to changes in accessory system loads.

For PHEVs which operate in a mode where engine operation is prohibited (in compliance with the ZEV mandate), the energy for operation of the passenger heating system must come from the conversion of stored electrical energy to heat. In many climates, this can be a multi-kilowatt load [41] which can significantly reduce the energy efficiency of the vehicle. Preconditioning can reduce the heating energy required by preheating the passenger compartment while the vehicle is still connected to the electric grid. Preconditioning does not significantly improve the total energy efficiency of the vehicle, but it may improve the consumer acceptance and ZEV-range capability of the vehicle. Preconditioning using a heat pump system is more energetically efficient than preconditioning with a resistive heater, but the heat pump system comes with significant complications including frosting of the evaporator during operation [42]. To address these challenges, it may be advantageous for PHEVs to turn on the ICE to generate waste heat when cabin heating is demanded by the driver, but engine operation and idling can represent a significant compromise to the fuel economy attributes of the vehicle [43].

#### ***3.5.4 Constraints on system-level design based on accessory system attributes***

Based on the constraints that the accessory systems place on the vehicle-level performance, it is possible to understand the compromises to PHEV system-level attributes that are caused by the accessory systems. First, PHEVs that seek to maximize their effectiveness under the California ZEV regulations must have electrically driven accessories to avoid engine starts during both the UDDS and US06 test cycles. For these vehicles, the energy consumption of the accessory system exacts a cost on its real-world performance. A 2 kW electrical accessory load can increase the charge-sustaining GHG emissions of a PHEV by a factor of 2 [41]. The compromise of turning on the engine to produce and use waste heat to meet the accessory heating loads can reduce the value of the PHEV according to the ZEV program.

In summary, the design of the vehicle accessory systems requires a stark tradeoff between the requirements for passenger comfort and various vehicle and system-level design goals. Even fully functional all-electric heat pump systems that allow PHEVs to operate under both all-electric and charge sustaining modes exact a large fuel economy cost that is not accounted for in PHEV sustainability impacts to date.

### **3.6 ESS charging system**

A fundamental characteristic of PHEVs is their ability to recharge their ESS from the electric grid. The charging system is the set of controls, communication, power electronics, and power transfer equipment that makes the recharging of PHEVs possible. The design of charging systems for PHEVs consists of both the specification of the physical hardware for charging and the specification of the control system which controls the charging strategy for the vehicle.

### **3.6.1 State of the art for ESS charging systems**

PHEV ESS charging can be constrained or unconstrained. Unconstrained charging is the simplest form of PHEV charging and allows the PHEV owner to plug in at any time of the day without any limitations [44]. Constrained charging is defined as any charging strategy in which the electric utility and vehicle are able to cooperatively implement charging strategies. These constrained charging strategies will aim to limit PHEV charging loads so that they are not coincident with the peak loads of the day. The first generation of PHEVs will use unconstrained opportunity charging due to the initial low volume of vehicles and low impact on the electric grid [45–47]. However, most research to date has shown that as PHEVs penetrate the market, unconstrained charging will need to be replaced with some level of constrained charging to reduce the possibility of exacerbating peak electric demands [48–50]. Constrained charging behavior can potentially permit up to 50% PHEV market penetration without an increase in generation capacity and also presents the possibility for the electric utility to regulate the system more effectively resulting in more uniform daily load profiles and reduced operational costs [48]. Due to the long-term risks involved in allowing unconstrained charging to occur, this section will only focus on how controlled charging impacts the design of PHEVs. The most prevalent strategies currently being pursued to implement constrained charging are labeled as valley filling, demand response, vehicle-to-grid (V2G), real-time price charging, and delayed charging [47–54].

The SAE J1772 standard has been developed to provide design guidance for PHEV power transfer connections. The standard requires PHEV power transfer connections to be able to operate on single phase 120 V or 240 V and also support communication. The power transfer equipment can either be a separate component or be integrated into the windings and power electronics of the traction motor and motor drive. In order for PHEVs to be capable of V2G, either an inverter must be added to the PHEV's power electronics or equipment capable of utilizing the on-board charger as both an inverter and a rectifier would need to be used [51]. Although various power levels of charging have been proposed, level 1 charging (110 V, 15 A) is most common. Level 2 and level 3 quick chargers have increased power ratings, but the installation of level 2 and level 3 chargers can be a slow and costly process, especially for residential installations [52].

All of the constrained charging strategies require some level of communication between the PHEV or PHEV owner and the electric utility or grid system operator. For demand response, real-time pricing, and delayed charging, the PHEV or PHEV owner must be able to receive and process pricing and/or power interrupt signals sent by the electric utility [48]. The remaining charging strategies, valley filling and V2G charging, require electronic two-way communication between the PHEV and the electric utility or the grid system operator [45, 53]. Two-way communication is required because the electric utility or the grid system operator needs to know the SOC of all the PHEVs connected in order to forecast the expected charging load for the valley-filling



algorithm and the availability of PHEVs for providing V2G frequency control. Research has shown that the communication task can be achieved by integrating Broadband over Powerline and HomePlug™, Zigbee™, or cellular communication technologies into a stationary charger or into the PHEV's power electronics [54].

### ***3.6.2 Requirements of the ESS charging system design based on PHEV vehicle-level attributes***

Vehicle-level attributes such as fuel economy and AER transmit design requirements to PHEV ESS charging systems. These vehicle-level attributes impact the decision of what power rating is most appropriate for PHEV power transfer equipment. For example, if the design of a PHEV is aimed at increasing the vehicle's AER, the PHEV's ESS will need to be augmented to store more energy. This increased capacity of the ESS will require longer charging times [55], which can be reduced through the utilization of level 2 or level 3 power transfer equipment. However, power transfer equipment with higher power ratings increases the cost and complexity of the ESS charging system.

### ***3.6.3 Constraints on vehicle-level design based on ESS charging characteristic attributes***

Studies have stated that constrained charging can provide the electric utility an opportunity to improve resource utilization. As a result of this, the electric utilities will be able to provide reduced rates to PHEV owners who comply with the regulations of the constrained charging program [56]. These reduced rates help improve vehicle performance in terms of operating cost. However, constrained charging programs can lead to reductions in fuel economy and AER since the permitted charging time or time with reduced electric charging rates would be limited and decrease the number of hours which PHEVs are able to charge each day. As the allowable charging hours are decreased, the ability of a PHEV to fully recharge begins to decline. PHEVs utilizing level 1 charging can be significantly impacted since it takes approximately 8 hours to charge a vehicle with an ESS usable capacity similar to a Chevrolet Volt [52, 55]. If a PHEV is incapable of fully recharging the ESS, the AER/EAER of the vehicle will be reduced and could decrease the fuel economy of the vehicle if the PHEV is forced to operate in CS mode more frequently. Increased operation in CS mode reduces PHEV performance in terms of fuel economy, which is one of the major vehicle attributes being considered to justify the higher cost of PHEVs in comparison to conventional vehicles and HEVs.

### ***3.6.4 Constraints on system-level design based on ESS charging characteristic attributes***

Regardless of the type of constrained charging strategy utilized, the ESS charging components and strategies will impose constraints on the electric grid. The largest impact controlled charging will have on the electric grid is associated with the



communication requirements needed between PHEVs and PHEV owners and the electric utility or grid system operator. The simplest way in terms of communication that an electric utility can control charging behaviors is with time of use (TOU) rates. TOU rates can be relayed to PHEV owners through rate plans that only change based on time of day and year and require the installation of an electric meter capable of metering energy transfer in real time for billing purposes. However, it is yet to be determined if TOU rates are strong enough motivators to affect the charging habits of the majority of PHEV owners. The next level of complexity available for the electric utility is the use of real-time data communication. One of the problems associated with using real-time data transfer to centrally monitor and control a large number of PHEVs is that it has been seen as an overwhelming task [57]. Constrained charging of PHEVs will require a large investment in electric grid infrastructure and will significantly increase the workload of the electric utility.

Another large concern currently being expressed by electric utilities is the expected increased loads on residential transformers and other electric grid components. Studies have shown that the acceptance of HEVs has typically occurred nonuniformly throughout a geographic area, and they are expecting the adoption of PHEVs to follow a similar pattern [58]. This poses a problem for the utilities especially with respect to the loading of residential transformers because most residential transformers are already approaching their recommended use capacities. Another concern is that although constrained charging of PHEVs will help the electric utility keep from exacerbating their peak demands, constrained charging may force transformers especially in residential areas and other grid infrastructure to be fully utilized for the majority of the day. This increased use would reduce the amount of rest and cooling time the equipment would experience which could shorten the operational life of the transformers and other electric grid equipment [59, 60].



---

## 4. CASE STUDIES

Now that the main components of state-of-the-art design have been covered it is possible to take a look at a few of the leading PHEVs in production. By comparing vehicles that were created to meet a range of design constraints, we can make critical remarks regarding decisions that were made and what possible alternatives could have been implemented. The vehicles that will be compared in depth are two production HEVs that have been modified with commercially available plug-in kits (Hymotion), the Toyota Prius and Ford Escape, and two vehicles that have been designed as OEM PHEVs, the Chevrolet Volt and Chrysler Sprinter. For each of these vehicles, this section describes the requirements and constraints that dictate the vehicle attributes at the system, vehicle, and component levels, which can be seen in Table 6.3.

**Table 6.3** PHEV case study comparisons

	Attribute	Specification	Toyota Prius	Chevrolet Volt	Ford Escape	Chrysler Sprinter
<b>Vehicle level</b>	Configuration	Body type	Sedan	Sedan	SUV	Cargo van
		Seating	4–5	4–5	5	8
		Drive Wheels	2	2	4	2
		Drivetrain	Power-Split	Series	Power-Split	Parallel
		Weight (lbs)	3,408	~3,500	4,174	8,550
	Cost	\$	24,000 + 10,000 (kit)	40,000	32,000 + 10,000 (kit)	33,000+? <sup>a</sup>
	EV range	EAER (mi)	29.7	40	15.9	20
		UF	0.683	0.625	0.580	
	Fuel efficiency	(mpg)	100	100–230	60	
		Total range (mi)	635	640	530	
		Fuel capacity (gal)	11.9	12	15	26
Performance	Acceleration (0–60 mph)	9.8	8.5	12.4	22	
	Top speed (mph)	110	120	100	100	
<b>Subsystem level</b>	Battery	Type	Li ion	Li ion	Li ion	Li ion
		Weight (lb)	187	400	325	400
		Energy capacity (kWh)	5	16	8.5	15.1
	Charging	Time (h)	5.5	8 (3)	6–8	6–8
		Current (A)	10	15	15	15
		Voltage (V)	120	120 (240)	120	120
	Electric motor	Power (hp)	79	150	94	131
		Torque (lb-ft)	153	236		280
		Type	Permanent magnet		Permanent magnet	Permanent magnet
	Generator	kW		53		
	ICE	Capacity (l)	1.8	1.4	2.3	2.3
		Power (hp)	97	100	155	140
		Torque (lb-ft)	105		136	160
		Fuel type	Gasoline	Gasoline/E85	Gasoline	Gasoline/diesel

(Continued)

**Table 6.3** (Continued)

	Attribute	Specification	Toyota Prius	Chevrolet Volt	Ford Escape	Chrysler Sprinter
<b>System level</b>	Greenhouse gasses	NO <sub>x</sub> (g/mile)	0.006		0.004	
	Petroleum displacement	Factor	0.606	1 <sup>b</sup>	0.458	
	Sales volume	Total since 2005	<5,000 (600,000 HEVs)	~60,000 <sup>c</sup>	<2,000 (75,000 HEVs)	~50
	Approximate ZEV	Credits	1.5537	2.50	1.3055	

Source: From Refs. [64–97].

<sup>a</sup> Cost listed is for a conventional Sprinter; specific additional costs value are undetermined but known to be higher than the other vehicles included in the case study.

<sup>b</sup> Petroleum displacement is based on one UDDS driving cycle.

<sup>c</sup> Sales volume is approximated; the Chevrolet Volt is expected to go on sale in the 2011 model year.

## 4.1 Hymotion Prius and Escape PHEV conversions

The Hymotion Prius and Escape PHEVs are aftermarket conversions of the Toyota Prius and the Ford Escape hybrids into PHEVs. Hymotion replaces the OEM NiMH battery pack with a higher capacity Li ion pack, adds a battery charging inverter, and changes some aspects of the vehicle controller. These changes allow the Hymotion Prius and Escape PHEVs to function as a blended-type PHEV.

The attributes of the conversion PHEVs show a design tradeoff between the subsystem optimized for HEV operation and those required for PHEV operation. The Prius and Hybrid Escape are originally designed and optimized for HEV operation. As such, components such as the traction motor, ICE, and generator have been chosen by the OEM according to the requirements of HEV operation and are not specifically designed for AER capabilities. The aftermarket designers have to specify the new battery pack and charging to operate correctly with the current vehicle components instead of being able to design the system for optimal function as a PHEV. For example, the powertrain architectures of both conversion vehicles are power-split. The Toyota/Aisin Seiki powersplit transmissions are designed for efficient HEV operation. The transmission gear ratios allow the vehicle to operate from the electric motor at low speed and from the gasoline engine at higher speed. Although this is an acceptable solution for HEV operation, PHEV operation ideally requires a higher engine turn-on speed, a longer AER, and more electric motor usage than these powertrains are designed to allow. The powertrain architecture constrains the vehicle to operate in a blended-type operating mode, thereby limiting the fuel economy of the PHEV conversions relative to a more ideal powertrain. The design tradeoffs have impact at all levels of vehicle performance. Blended operation limits the petroleum displacement and GHG emissions reductions that are available from the conversion vehicles.

## 4.2 Daimler-Chrysler Sprinter PHEV

The Daimler-Chrysler Sprinter PHEV is a limited production PHEV based on the Sprinter cargo van platform. The vehicle was designed and constructed by Daimler-Chrysler KEN group to function as a limited AER PHEV. The target customers were utilities, commercial delivery services, and transit.

The design of the PHEV Sprinter shows stark compromises between vehicle performance and cost. Analyzing the results of the Sprinter design can help explain why a large, expensive vehicle resulted. Because of the highly utilitarian role of medium-duty vehicles, the Sprinter design objectives seem to have prioritized vehicle-level performance over system-level objectives such as petroleum displacement. Unlike the conversion vehicles, the Sprinter PHEV powertrain systems have all been designed for PHEV operation. The Sprinter's parallel drivetrain allows the vehicle to preserve performance appropriate for medium-duty applications by allowing the ICE to assist the traction motor under heavy loads. The Sprinter PHEV is capable of operating in EV

mode with an AER of ~20 miles, but because of the small power output of the traction motor, a high-torque ICE had to be included to meet practical power requirements. The larger engine reduces the Sprinter PHEV fuel economy and decreases the magnitude of the system-level benefits that a PHEV might be expected to achieve. The Sprinter also has an available diesel ICE option, which is the much preferred engine technology in Europe. Even with its relatively low-power electric powertrain, the PHEV Sprinter's low production volume made it the most expensive vehicle reviewed.

### 4.3 Chevrolet Volt

The Chevrolet Volt is the first mass production PHEV from a major US automaker. It is scheduled for release in the 2011 model year. The Volt powertrain and chassis are unique to the model and the attributes of the vehicle can be used to understand the design objectives that motivate the development of this advanced vehicle.

Because the Chevrolet Volt is a full production vehicle from General Motors, it can contribute to many of General Motors' system-level objectives including compliance with the California Air Resource Board (CARB) ZEV program. The Volt was designed to have a minimum AER goal of 40 miles to try and meet the daily driving requirements of most American drivers and to maximize the ZEV credits awarded in the VMT category explained in Section 3.4.4. Advanced accessories including heat pump HVAC, battery thermal management systems, and a series architecture allow the Volt to drive with full performance without requiring engine turn-on during acceleration events, providing the Volt with true ZEV capability. Although this has benefits for compliance of the Volt with the CARB ZEV regulations, this design decision requires that the Volt use a larger traction motor, larger battery pack, and more advanced electric components than any of the other three vehicles compared here. These component-level decisions help to make the mass-produced Volt an expensive vehicle, more expensive even than the hand-built Hymotion Prius. The design of the Volt shows that there exists a tradeoff between achieving system-level design objectives (such as ZEV regulation compliance) and vehicle-level design objectives (such as cost).



## 5. CONCLUDING REMARKS

This chapter has presented an analysis of the design methods and tradeoffs that characterize the design of PHEVs. This study proposes a model of the PHEV design process which is broken up into three components: design objectives, analyses, and design attributes. Objectives, analyses, and attributes for the PHEV can exist at system level, vehicle level, and subsystem level. The proposed systematic model of the design process provides PHEV designers with a framework for integrating and organizing design objectives, analyses, and design attributes. For a variety of the PHEV subsystems, this study has investigated and summarized the design tradeoffs that exist between these

three levels of the design process. Finally, a set of PHEV production vehicles was used as a series of case studies to examine the results of these tradeoffs in practice.

This analysis has resulted in several primary findings that can contribute to an improved understanding of PHEV design. First, a majority of PHEV studies to date have used vehicle-level design objectives to guide the design process. Unless PHEV design objectives can be expressed at the system level, the system-level design attributes of PHEVs are merely fortuitous. Only by including system-level design objectives and analyses directly into the PHEV design process, can system level design attributes be achieved.

Second, the design of PHEVs is characterized by strong connections between the characteristics of the vehicles at the subsystem level and the design attributes at the vehicle and system levels. For each of the subsystems described in this study, there are many requirements transmitted from the vehicle to the subsystems and constraints transmitted from the subsystems to the higher levels of design. In future work, conceptual design of PHEVs must become more closely integrated with the embodiment design of PHEV subsystems. PHEV system-level impacts assessments must begin to grapple with the compromises to ideal operation that will come with consideration of the design tradeoffs required by PHEV subsystems.

Finally, from the case studies we can see how PHEV designers have found compromises among these design tradeoffs so as to achieve a set of design objectives. Some case studies showed that subsystem-level design objectives can limit design space, not allowing optimization toward system-level attributes. Others show that system-level design objectives may lead a PHEV designer to compromise vehicle-level performance in pursuit of optimized system-level performance. Only with a unified PHEV design process can PHEV designers create design concepts that can take advantage of the interrelations between PHEV design objectives and attributes.

At present, PHEVs are in a unique position in their product life cycle. The design space around PHEVs is very open and optimal designs have not yet emerged. Because PHEV performance is so sensitive to the relationships between system- and subsystem-level attributes, there exists a significant opportunity to achieve societal and environmental improvements through the advancement of improved PHEV design.

## REFERENCES

1. J.J. Ronning, SAE International Spring Fuels and Lubricants Meeting and Exposition, Dearborn, USA, 1997.
2. Y.S. Wong, K.T. Chau, *J. Asian Electric Vehicles* 4 (2006) 899.
3. R.C. Balch, A. Burk, 16th Annual Battery Conference on Applications and Advances, Long Beach, USA, 2001.
4. EPRI (Electric Power Research Institute), *Comparing the Benefits and Impacts of Hybrid Electric Vehicle Options*, Palo Alto, USA, 2001.
5. F. An, A. Frank, M. Ross, *Meeting Both ZEV and PNGV Goals with a Hybrid Electric Vehicle: An Exploration*, SAE, Warrendale, PA, USA, 1996.
6. N. Meyr, C. Carde, C. Nitta, D. Garas, T. Garrard, J. Parks, *Society of Automotive Engineers World Congress and Exposition*, Detroit, USA, March 2003.

7. F.R. Kalhammer, B.M. Kopf, D.H. Swan, V.P. Roan, M.P. Walsh, Status and Prospects for Zero Emissions Vehicle Technology, Report of the ARB Independent Expert Panel 2007, State of California Air Resources Board, Sacramento, USA, April 13, 2007.
8. M. Ehsani, Y. Gao, J.M. Miller, Proceedings of the IEEE, vol. 95, April 2007.
9. A. Emadi, Y.J. Lee, K. Rajashekara, IEEE Trans. Ind. Electron. 55 (2008) 2237.
10. M. Ehsani, K.M. Rahman, H.A. Toliyat, IEEE Trans. Ind. Electron. 44 (1997) 19.
11. S. Golbuff, Optimization of a Plug-in Hybrid Electric Vehicle, Georgia Institute of Technology, George Woodruff School of Mechanical Engineering, Atlanta, Georgia, USA, 2006.
12. V. Freyermuth, E. Fallas, A. Rousseau, SAE Int. J. Engines 1 (2008) 392.
13. J.Y. Park, Y.K. Park, J.H. Park, Proceedings Institution Mechanical Engineers. Part D – J. Automob. Eng. 222 (2008) 989.
14. EPRI, Analysis of Ultracapacitors for Use in a Grid-Connected Electric Vehicle, Palo Alto, USA, 2002.
15. F. Kalhammer, Plug-in Hybrid Electric Vehicle Workshop at 20th International Electric Vehicle Symposium, Long Beach, USA, November 2003.
16. N. Schofield, H.T. Yap, C.M. Bingham, IEEE (Institute of Electrical and Electronics Engineers) International Conference on Electric Machines and Drives, San Antonio, USA, 2005.
17. G.J. Suppes, S. Lopes, C.W. Chiu, Int. J. Hydrogen Energy 29 (2004) 369.
18. W.R. Warf, M.S. Duvall, B.D. Moran, A.A. Frank, 16th Annual Battery Conference on Applications and Advances, Long Beach, USA, January 2001.
19. M. Duvall, N. Meyer, B.R. Huff, C. Carde, J. Parks, R. Schurhoff, Design and Development of the UC Davis Future Truck, SAE, Warrendale, PA, USA, 2002.
20. M.W. Verbrugge, P. Liu, J. Electrochem. Soc. 153 (2006) A1237.
21. EPRI (Electric Power Research Institute), Test Profile Development for the Evaluation of Battery Cycle Life for Plug-in Hybrid Electric Vehicles, Palo Alto, USA, 2003.
22. R. Graham, Comparing the Benefits and Impacts of Hybrid Electric Vehicle Options, EPRI, Palo Alto, USA, 2001.
23. A. Burnham, M. Wang, Y. Wu, Development and Applications of GREET 2.7 – the Transportation and Vehicle-Cycle Model, Argonne, USA, 2006.
24. EPRI (Electric Power Research Institute), Advanced Batteries for Electric-Drive Vehicles: A Technology and Cost-Effectiveness Assessment for Battery Electric, Power Assist Hybrid Electric, and Plug-in Hybrid Electric Vehicles, Palo Alto, USA, 2003.
25. A. Taylor, Energy Policy 36 (2008) 4657.
26. X. He, Development and Validation of a Hybrid Electric Vehicle with Hydrogen Internal Combustion Engine, Ph. D. Thesis, Electrical Engineering, Texas Tech. University, 2006.
27. H.S. Mohamadabadi, G. Tichkowsky, A. Kumar, Energy 34 (2009) 112.
28. J. Ogden, Hydrogen Delivery Model for H2A Analysis: A Spreadsheet Model for Hydrogen Delivery Scenarios, University of California, Davis Institute of Transportation Studies, Davis, CA, USA, 2004.
29. H. Huo, Y. Wu, M. Wang, Atmos. Environ. 43 (2009) 1796.
30. T.H. Bradley, A.A. Frank, Renew. Sust. Energy Rev. 13 (2009) 115.
31. M. Duoba, R. Carlson, D. Bocci, Calculating Results and Performance Parameters for PHEVs, SAE 2009-01-1328, 2009.
32. EPRI (Electric Power Research Institute), Comparing the Benefits and Impacts of Hybrid Electric Vehicle Options for Compact Sedan and Sport Utility Vehicles, Palo Alto, USA, 2002.
33. M. Duoba, R. Carlson, J. Wu, SAE Int. J. Engines 1 (2009) 359.
34. A.F. Burke, On-off Engine Operation for Hybrid/Electric Vehicles, SAE, Warrendale, PA, USA, 1993.
35. N.D. Struven, Experimental Facilities and Engine Studies for a Parallel Hybrid Electric Vehicle, Department of Mechanical and Aeronautical Engineering, University of California, Davis, 2002.
36. A.A. Frank, Battery Dominant Hybrid Electric Vehicle Systems Development and Evaluation, South Coast Air Quality Management District, Diamond Bar, California, 2002.
37. M. Kromer, J. Heywood, A Comparative Assessment of Electric Propulsion Systems in the 2030 US Light-Duty Vehicle Fleet, SAE 2008-01-0459, 2008.
38. M. O'Keefe, T. Markel, EVS-22 Conference, Yokohama, Japan, 2006.
39. California's Zero Emission Vehicle Program. [http://www.arb.ca.gov/msprog/zevprog/zev\\_tutorial.pdf](http://www.arb.ca.gov/msprog/zevprog/zev_tutorial.pdf), 2009. April 21, 2010.

40. J.M. Miller, *IEEE Trans. Power Electron.* 21 (2006) 756.
41. J.P. Rugh, R.S. Howard, R.B. Farrington, M.R. Cuddy, D.M. Blake, *Innovative Techniques for Decreasing Advanced Vehicle Auxiliary Loads*, National Renewable Energy Laboratory, Golden, CO, USA, 2000.
42. Toyota, *New Features Manual RAV4-EV*, Toyota Motor Corporation, Torrance, CA, USA, 2001.
43. R. Carlson, M. Duoba, D. Bocci, H. Lohse-Busch, *Proceedings of (EVS-23) Electric Vehicle Symposium by (ANL) Argonne National Laboratory*, Anaheim, USA, 2007.
44. L. Gaines, A. Burnham, A. Rousseau, D. Santini, *Sorting Through the Many Total-Energy-Cycle Pathways Possible with Early Plug-in Hybrids*, Center for Transportation Research, Argonne National Laboratory, Argonne, USA, 2007.
45. M.C. Kintner-Meyer, K.P. Schneider, R.G. Pratt, *Impacts Assessment of Plug-in Hybrid Vehicles on Electric Utilities and Regional US Power Grids. Part 1: Technical Analysis*, Pacific Northwest National Laboratory (PNNL), PNNL-SA-61669, 2007.
46. EPRI (Electric Power Research Institute), *Environmental Assessment of Plug-in Hybrid Electric Vehicles. Volume 1: Nationwide Greenhouse Gas Emissions*, Palo Alto, USA, 1015325, 2007.
47. S.W. Hadley, A.A. Tsvetkova, *Potential Impacts of Plug-in Hybrid Electric Vehicles on Regional Power Generation*, Oak Ridge National Laboratory (ORNL), Oak Ridge, TN, USA, ORNL/TM-2007/150, 2007.
48. P. Denholm, W. Short, *Evaluation of Utility System Impacts and Benefits of Optimally Dispatched Plug-in Hybrid Electric Vehicles*, National Renewable Energy Laboratory (NREL), Golden, CO, USA, NREL/TP-620-40293, 2006.
49. K. Parks, P. Denholm, T. Markel, *Costs and Emissions Associated with Plug-in Hybrid Electric Vehicle Charging in the Xcel Energy Colorado Service Territory*, National Renewable Energy Laboratory (NREL), Golden, CO, USA, NREL/TP-640-41410, 2007.
50. W. Short, P. Denholm, *Preliminary Assessment of Plug-in Hybrid Electric Vehicles on Wind Energy Markets*, National Renewable Energy Lab (NREL), Golden, CO, USA, NREL/TP-620-39729, 2006.
51. A. Brooks, *Vehicle-to-Grid Demonstration Project: Grid Regulation Ancillary Service with a Battery Electric Vehicle*, Report prepared by AC Propulsion for the California Air Resources Board and the California Environmental Protection Agency. <http://www.udel.edu/V2G>.
52. K. Morrow, D. Kerner, J. Francfort, *U.S. Department of Energy Vehicle Technologies Program – Advanced Vehicle Testing Activity – Plug-in Hybrid Electric Vehicle Charging Infrastructure Review*, Idaho National Laboratory (INL), Idaho Falls, ID, USA, INL/EXT-08-15058, 2008.
53. W. Kempton, J. Tomic, *J. Power Sources* 144 (2005) 280.
54. T. Markel, *Communication and Control of Electric Vehicles Supporting Renewables*, National Renewable Energy Laboratory (NREL), Golden, CO, USA, 2009.
55. M.S. Duvall, *Battery Evaluation for Plug-in Hybrid Electric Vehicles*, Electric Power Research Institute EPRI, Palo Alto, USA, 2005.
56. M.J. Scott, M. Kintner-Meyer, D.B. Elliot, W.M. Warwick, *Impacts Assessment of Plug-in Hybrid Vehicles on Electrical Utilities and Regional US Power Grids. Part 2: Economic Assessment*, Pacific Northwest National Laboratory, Richland, WA, USA, 2006.
57. B. Kirby, E. Hirst, *Computer-Specific Metrics for the Regulation and Load Following Ancillary Services*, Oak Ridge National Laboratory (ORNL), Oak Ridge, TN, USA, ORNL/CON--474, 2000.
58. M. Rowand, *Plug-in 2009 Conference and Exposition*, Long Beach, USA, 2009.
59. W. Kempton, V. Udo, K. Huber, K. Komara, S. Letendre, S. Baker, et al., *A Test of Vehicle-to-Grid (V2G) for Energy Storage and Frequency Regulation in the PJM System*. <http://www.magicconsortium.org>. April 21, 2010.
60. J. Taylor, A. Maitra, M. Alexander, D. Brooks, M. Duvall, *Evaluation of the Impact of PEV Loading on Distribution System Operations*, IEEE Power Engineering Society, Calgary, Canada, July 2009.
61. J.P. Gao, G.M.G. Zhu, E.G. Strangas, F.C. Sun, *Proceedings Institution Mechanical Engineers. Part D – J. Automob. Eng.* 223 (2009) 1003.
62. N.D. Kim, J.M. Kim, H.S. Kim, *Proceedings Institution Mechanical Engineers. Part D – J. Automob. Eng.* 222 (2008) 1587.
63. S. Kliuzovich, *Transport* 22 (2007) 105.



64. American Ceramic Society, *Am. Ceram. Soc. Bull.* 86 (2007) 21.
65. Ford Motor Company, *Clean Air Environ. Quality* 41 (2007) E1.
66. S. Abuelsamid, Full Specifications on the Chevy Volt. Detroit Auto Show, 2007. <http://green.autoblog.com/2007/01/07/detroit-auto-show-full-specifications-on-the-chevy-volt/> September 28, 2009.
67. E. D. T. A. 2009, Hybrid Sales Figures/Tax Credits for Hybrids. [http://www.electricdrive.org/index.php?ht=d/Articles/cat\\_id/5514/pid/2549](http://www.electricdrive.org/index.php?ht=d/Articles/cat_id/5514/pid/2549). April 21, 2010.
68. Auto123.com. Ford Escape Plug-in Hybrid First Impressions. <http://www.auto123.com/en/ford/escape/2009/review?carid=1091801300&pg=1&artid=108592>, 2009. September 24, 2009.
69. CalCars, DaimlerChrysler Describes its PHEV Sprinter Van. <http://www.calcars.org/calcars-news/83.html> 2005.
70. H. Canada, Product Literature, March 12, Ontario, Canada, 2007.
71. Q. Cao, S. Pagerit, R. Carlson, A. Rousseau, PHEV Hymotion Prius Model Validation and Control Improvements, Argonne National Laboratory, Argonne, USA.
72. R. Carlson, M. Duoba, F. Jehlik, T. Bohn, D. Bocci, Advanced Vehicle Benchmarking of HEV's and PHEV's, Argonne National Laboratory, DOE Hydrogen Program and Vehicle Technologies, Annual Merit Review, Argonne, IL, USA, 2009.
73. M. Duvall, Plug-in Hybrid Electric Sprinter Van Prototype Initial Test Results, Technical Update, Electric Power Research Institute, Palo Alto, USA, 2005.
74. M. Duvall, Plug-in Hybrid Electric Sprinter Van – Final System Design Specification, Phase 1: Prototype Vehicles, Technical Report, Electric Power Research Institute, Palo Alto, USA, 2005.
75. M. Duvall, Zev Technology Symposium, Sacramento, CA, USA, September 2006.
76. EcoHuddle, Plug-in Supply Prius + PHEV Conversion Kit. <http://www.ecohuddle.com/products/plug-in-supply-prius-phev-conversion-kit>. September 24, 2009.
77. EETrex, Plug-in Hybrid Electric Vehicle Conversions – Ford Escape, HybridPlus, Boulder, USA, 2009.
78. USDOE (United States Department of Energy), Plug-in Hybrid Electric Vehicle R&D Plan: External Draft, Washington, DC, USA, 2007.
79. USDOE, North American PHEV Demonstration, in Vehicle Testing Program, USDOE (United States Department of Energy), Washington, DC, USA, 2008.
80. USDOE, Vehicle Technologies Program: PHEV Accelerated Testing Results – Jan. 2009, in Advanced Vehicle Testing Activity, Energy Efficiency and Renewable Energy (EERE), Washington, DC, USA, 2009.
81. Enginer, Products; Prius Plug-in PHEV Conversion Kit with Lithium-Ion, 2009.
82. Suzuki, EV-Sport, Automotive Engineering International Online: Global Concepts (Part 2), Warrendale, PA, October 10, 2000.
83. S. Fletcher, Chevy Volt Prototype Test Drive: Detroit's Great Electric Hope. <http://www.popsoci.com/cars/article/2009-05/test-drive-chevy-volt?page>. September 28, 2009.
84. J. Francfort, L. Slezak, Advanced Vehicle Testing Activity (AVTA) – Vehicle Testing and Demonstration Activities, U.S. Department of Energy – Vehicle Technologies Program 2009, Annual Merit Review, Idaho National Laboratory, Idaho Falls, ID, USA, May 2009.
85. S. Freeman, GM Pledges to Make Plug-in Hybrid Vehicle, The Washington Post (Copyright online LexisNexis), November 30, 2006.
86. GM-Volt, Chevy Volt Specs: Preliminary Specifications: 2011 Chevrolet Volt, 2009. <http://gm-volt.com/full-specifications>. September 24, 2009.
87. GreenCarCongress, Hymotion Unveils Plug-in Hybrid Kits for Toyota and Ford Hybrids, February 21, 2006. [mmillikin@bioagemedia.com](mailto:mmillikin@bioagemedia.com), [GreenCarCongress.com](http://GreenCarCongress.com).
88. HybridCars.com., Chevrolet Volt. <http://www.hybridcars.com/vehicle/chevy-volt.html>. September 25, 2009.
89. Hymotion, L5 Plug-in Conversion Module (PCM) Owner's Manual, A123Systems, Watertown, MA, 2008.
90. M. Krebs, General Motors' First Plug-in Hybrid, the Chevrolet Volt Concept, Introduces GM's New Family of Electric-Drive Propulsion Systems. <http://www.edmunds.com/insideline/do/Features/articleId=119088?mktcat=volt-performance&kw=volt+performance&mktid=ga27908020>. September 24, 2009.

91. J. Loposer, Chevy Finally Releases Official Volt Specs. <http://www.greendaily.com/2008/09/16/chevy-finally-releases-official-volt-specs>. September 24, 2009.
92. M. General, GM Announces Intention to Produce Plug-in Hybrid SUV, General Motors Press Release, Detroit, USA, November 29, 2006.
93. M. General, Chevrolet Volt – GM’s Concept Electric Vehicle – Could Nearly Eliminate Trips to the Gas Station, General Motors Press Release, Detroit, USA, 2007.
94. General Motors, Chevrolet Volt Expects 230 mpg in City Driving. <http://media.gm.com/servlet/GatewayServlet?target=http://image.emerald.gm.com/gmnews/viewpressreldetail.do?domain=12&docid=56132>. September 28, 2009.
95. P.H.E.V. America, U.S. Department of Energy Advanced Vehicle Testing Activity, Electric Transportation Applications, 2008.
96. T. Quiroga, 2011 Chevrolet Volt First Drive – Car News. [http://www.caranddriver.com/news/car/09q2/2011\\_chevrolet\\_volt\\_first\\_drive-car\\_news](http://www.caranddriver.com/news/car/09q2/2011_chevrolet_volt_first_drive-car_news). September 28, 2009.
97. WorldCarFans.com., DaimlerChrysler is Only Manufacturer Building Plug-in Hybrid Vehicles. <http://www.worldcarfans.com/10603317412/dodge-sprinter-plug-in-hybrid-electric-vehicle-phev>. September 24, 2009.
98. B. Johnston, T. McGoldrick, D. Funston, H. Kwan, M. Alexander, F. Alioto, The Continued Design and Development of the University of California, Davis Futurecar, University of California, Davis, 1997.
99. A. Frank, B.D. Johnston, T. McGoldrick, D. Funston, H. Kwan, M. Alexander, Society of Automotive Engineers International Congress and Exposition, Detroit, USA, 1998.
100. SAE International, Utility Factor Definitions for Plug-in Hybrid Electric Vehicles Using 2001 U.S. DOT National Household Travel Survey Data, SAE J2841. [www.sae.org/technical/standards/J2841\\_200903](http://www.sae.org/technical/standards/J2841_200903), 2009. April 21, 2010.



# Evaluation of Energy Consumption, Emissions, and Costs of Plug-in Hybrid Vehicles

Carla Silva<sup>1</sup> and Tiago Farias

Department of Mechanical Engineering, IDMEC/IST, Instituto Superior Técnico, Technical University of Lisbon, Av. Rovisco Pais, 1 Pav. Mecânica I, 1049-001 Lisboa, Portugal

## Contents

1. Introduction	193
2. Factors Affecting Plug-In Hybrid Fuel Consumption and Emissions	195
3. SAE J1711 Recommended Practice	196
3.1 Points to be considered	198
4. Methodology	198
5. United States, Europe, and Japan Analysis	200
5.1 Fuel consumption and regulated emission factors	200
5.2 CO <sub>2</sub> global emissions	203
5.3 Impact on the electric grid	205
5.4 Costs	206
6. Conclusions	206
Acknowledgments	208
Nomenclature	209
References	209



## 1. INTRODUCTION

Plug-in hybrid electric vehicles (PHEVs) are gaining attention due to their ability to reduce gasoline/diesel consumption by using electricity from the grid as an alternative energy source. A PHEV differs from a pure electric vehicle (EV) because it uses other energy sources besides electricity, and the battery usually has a lower capacity. A PHEV differs from a conventional hybrid electric vehicle (HEV) due to its higher battery capacity, the existence of an appropriate electrical outlet (“plug”) to recharge the battery from the electric grid, and the different battery state of charge (SOC) management strategy. Most HEVs use the battery pack in a charge-sustaining (CS) mode (maintaining their SOC nearly constant through discharging and charging from

<sup>1</sup> Corresponding author: carla.silva@ist.utl.pt

the vehicle engine and the regenerative braking system), while PHEVs can operate in either charge-depleting (CD, similar to EV vehicles) or CS mode. In CD mode, the battery is discharged until a minimum SOC is reached (30–45% depending on battery and powertrain configuration); afterward, CS mode is set up, just as for conventional hybrids sustaining strategy. The distance traveled before the designed minimum SOC is reached can be a measure of the all-electric range (AER), despite the internal combustion engine (ICE) being used occasionally to help the propulsion. However some authors define it as the distance covered until the ICE is turned on for the first time or as the distance that displaces petroleum consumption on the standard test cycle. AER is also highly dependent on the driving cycle. For example, the California Air Resources Board uses the designation of PHEV20 meaning 20 miles of AER in the urban dynamometer driving schedule (UDDS) driving cycle.

PHEV design has been studied since the 1970s [1] mainly at the University of California, Davis (UCDavis) [1]. Since the 1990s, the Hybrid Electric Vehicle Working Group (WG) convened by the Electric Power Research Institute (EPRI), has been active in plug-in research by comparing vehicles fuel consumption (FC) and emissions in a well-to-wheels perspective (fuel life cycle), as well as customer preferences and analyzing the operating costs [2]. The US National Renewable Energy Laboratory has also been active in modeling PHEVs [3], component sizing [4], and fuel economy calculation [5]. The MIT's Laboratory for Energy and the Environment is also concerned with comparing vehicle technologies in terms of fuel and vehicle life cycle [6]. Recently, the UCDavis Plug-in Hybrid Electric Vehicle Research Center has been very active in analyzing the consumer behavior when using PHEVs [7]. However, these studies are US market oriented and no reference is made to other markets such as the European and Japanese. At IDMEC/IST a research team on Transports, Energy, and Environment is studying PHEV full life cycle, including materials cradle-to-grave life cycle and fuel production–distribution–storage life cycle, for several fuel pathways such as gasoline, diesel, hydrogen, electricity, and biofuels [8]. The same research team has an onboard laboratory to monitor driver behavior, FC, and tailpipe emissions from such vehicles [9].

This chapter presents a broader methodology of FC and emissions determination that can be applied more generally, thus including US, European, and Japanese legislations. The factors affecting PHEV FC and emissions are discussed and whenever possible reference to consumer surveys is made. The SAE J1711 recommended practice is described and disadvantages of the methodology are pointed out. Based on this, a different methodology is proposed and applied to two PHEVs in US, European, and Japanese driving cycles. CO<sub>2</sub> total emissions are estimated for both fuel life cycle and cradle-to-grave materials cycle. Based on the electricity consumption, the impact of these vehicles on the electric grid is estimated. Finally, a cost assessment on production and use (maintenance and fuel price) is made.



## 2. FACTORS AFFECTING PLUG-IN HYBRID FUEL CONSUMPTION AND EMISSIONS

PHEVs have two sources of energy for propulsion: electricity (from the grid and from energy recovery during braking for battery recharging) and chemical energy from hydrocarbon-based fuel stored in the tank. Just like HEVs, the electrical drivetrain and internal combustion drivetrain can be arranged so that the energy paths to the wheels are in parallel, in series or in combination of the two (full hybrid).

The manufacturer's energy management strategy adopted will dictate how each energy source is going to be used [10]. The so-called range extender PHEVs run primarily on electricity discharging the battery, and after the SOC reaches a minimum, operate in CS mode. Blended PHEVs are similar to range extender but in CD mode may turn on the ICE whenever needed.

Charging frequency and charging time depend on the driver and the availability of recharging sites at the vehicle parking. The performance of a PHEV is maximized if each trip is started with the battery fully charged, that is, the more often the battery is charged, the better is the performance. Recent surveys indicate that people may prefer plugging in a vehicle instead of fuelling it at the gas station. In the EPRI study of Ref [2], interviewed people were very interested in saving money due to price difference between electricity and gasoline, and in the possibility for an extended range without having to stop to a refueling station. In the UC Davis study [7], interviewed people that drove Toyota Prius converted in 2007 to plug-in, also wanted to take the maximum advantage of driving in electrical mode. Most of interviewed people plug vehicles in whenever possible in multiple locations that they visited regularly such as their workplaces and homes; reduced running cost by using electricity instead of gasoline was also pointed out. Even with off-peak recharging being cheaper and sometimes "less pollutant" at the electricity generation, people usually are not exclusively night rechargers. The results of both studies suggest that it is more likely that people would drive in CD operation mode than in CS mode as long as electricity prices are lower than gasoline prices.

Similarly to other vehicle technologies, the driving cycle will dictate the power management of the propulsion system, and, consequently will dictate the amount of FC, electricity consumption and tailpipe emissions. Additionally, the distance traveled in each journey will also dictate the use of CD or CS mode. Average daily commuting distances between home and work are 30 km for USA [11], between 5 and 30 km for Europe [12], and 20 km for Japan [13]. So, worldwide, a 20 km daily trip is common and this distance can be used as a reference for general analysis.

Electricity use by PHEVs is locally free of emissions, which is a good thing when air quality of driving surroundings is the main issue to be accounted for. However, the electricity to recharge their batteries is being produced elsewhere and usually not from renewable sources. Combustion-based power plants will produce emissions that will harm local air quality and, in particular, will produce CO<sub>2</sub> emissions that will add to the

global CO<sub>2</sub> impact of the PHEV. Similar reasoning should be applied to the other fuel in use, this time regarding origin, production, and distribution to the filling station. This analysis is the so called fuel life cycle (well-to-tank).

Summarizing, the factors that affect FC and emissions of PHEVs are as follows:

- manufacturer powertrain management;
- charging frequency;
- driving cycle;
- energy source (fuel and electricity) well-to-tank life cycle.

In order to make comparisons with other vehicle technologies possible, a fair methodology for the calculation of FC and emissions must be derived for PHEVs.



### 3. SAE J1711 RECOMMENDED PRACTICE

Regarding vehicle technology comparison, the Society of Automotive Engineers (SAE) J1711 Recommended Practice for Measuring the Exhaust Emissions and Fuel Economy of Hybrid-Electric Vehicles [14] has been used for US light-duty vehicle technology comparison studies, including PHEVs and HEVs.

SAE J1711 document seeks to provide a technical foundation for reporting procedures applied to a range of HEVs designs including PHEVs. US UDDS cycle, US Highway Fuel Economy Test (HWFET) and US Corporate Average Fuel Economy (CAFE, FC weighted as 55% UDDS + 45% HWFET) cycle are considered (see Table 7.1). For FC estimation, the CAFE driving cycle is applied but with some modifications for PHEVs. The following steps are considered (also refer to Fig. 7.1):

For UDDS:

1. The cycle is performed with an initial SOC of 100% and repeated four times or more if no engine turn on occurs; battery is fully recharged; electric consumption is converted to gasoline equivalent (based on gasoline energy content); gasoline consumption is recorded and added to gasoline equivalent electric consumption (this corresponds to the full charge test, FCT);

**Table 7.1** Driving cycles specifications

Country	USA		Europe	Japan
	UDDS	HWFET	NEDC	JC08
Maximum speed (km/h)	91	96	120	82
Average speed (km/h)	32	78	34	24
Distance (km)	12	17	11	8
Time (s/min)	1369/23	765/13	1180/20	1204/20
Maximum acceleration (m/s <sup>2</sup> )	1.48	1.43	1.06	1.69
Idle (s)	259	6	298	358

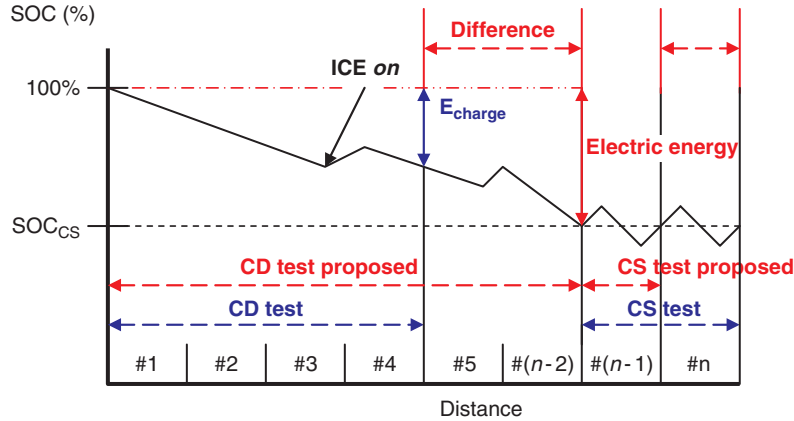


**Figure 7.1** Existing full charge test and partial charge test for PHEV according to SAEJ1711 (CD test, CS test) and proposed base methodology (CD test proposed, CS test proposed). #*n* means number of cycle runs.

2. the cycle is performed with an initial SOC equal to CS level and repeated two times; gasoline consumption is recorded (this corresponds to the partial charge test, PCT);
3. CD gasoline consumption is taken to be a fraction of FCT (in CD mode) and a fraction of the PCT (in CS mode); the fraction is based on US driving statistics that determine on aggregate how much of a vehicle's driving is expected to occur in CD or CS;
4. final gasoline consumption is calculated applying a 50% weighting factor to the CD and CS gasoline consumption, that is similar to assume that the vehicle is equally likely to be charged daily as to never be charged at all, or that the vehicle is charged on average once every 2 days [5].

For HWFET:

1. The cycle is performed with an initial SOC of 100% and repeated three times or more if no engine turn-on occurs; the rest is the same as point 1 for UDDS. Points 2, 3, and 4 are the same as points 2, 3, and 4 for UDDS.

CAFE gasoline consumption is 55/45% weighted harmonic average to UDDS and HWFET final results.

FC of each driving cycle is calculated by

$$\begin{aligned}
 FC_{CS} &= \frac{V_{\text{fuelCS}}}{D_{CS}} \\
 FC_{CD} &= \frac{V_{\text{fuelCD}} + \frac{E_{\text{charge}}}{E_{\text{gasoline}}}}{D_{CD}} \\
 FC_{CD,UF} &= UF \times FC_{CD} + (1-UF) \times FC_{CS} \\
 FC_{\text{cycle}} &= 0.5 \times FC_{CD,UF} + 0.5 \times FC_{CS}
 \end{aligned} \tag{7.1}$$

where the volume of gasoline consumed in each operating mode (CS or CD) is registered ( $V_{\text{fuel}}$ ), electric energy consumed ( $E_{\text{charge}}$ ) converted to gasoline equivalent by using gasoline lower heating value ( $E_{\text{gasoline}} = 8.83 \text{ kWh/l}$ ) and utility factor (UF) used to weigh how much of the driving is expected to occur in CD mode versus CS mode, based on US driving statistics.  $D$  stands for distance.

For regulated emissions, the Federal Test Procedure (FTP, i.e., cold start UDDS bag 1 and bag 2 + hot start UDDS bag 3 and 4) is used for PHEVs in CS operation mode that is the “worst-case” scenario for emissions. So UDDS bag 1 and bag 2 are collected. Bag 3 and bag 4 equivalent to hot start UDDS are collected and the 21, 25, 29, and 25% weighting factors are applied to measured emissions in each bag. Usually, in conventional vehicles bag 4 test is not performed and is assumed equal to bag 2 emission results.

### 3.1 Points to be considered

Some modifications to the SAE J1711 have been reported. For example, the report of Ref. [2] uses the FCT for all drive cycles ending when the engine turns on regardless of distance traveled. Gonder and Simpson [5] propose the following modifications: report electricity separately, extend the CD distance till the SOC reaches the CS level, and change the charging frequency assumption from once any other day to once daily. SAE J1711 is currently being revised [15] and some changes are being considered, for example, eliminate the requirement to be compatible with EV procedures by not converting the electric energy consumption into equivalent units of consumable fuel; change the baseline assumption for a driver’s battery charge frequency from once every other day to once a day; and include US06/SC03 additional emission test cycles, again considering the “worst-case” of CS only operation.



## 4. METHODOLOGY

This chapter will present a broader methodology allowing a fair comparison between vehicles, based on SAE J1711 recommended practice and additional recommended modifications that were suggested so far.

The base assumptions are (see Fig. 7.1 for the proposed operating mode division):

- separate fuel and electricity consumption;
- avoid a predefined repetition of the standard driving cycle for CD operation mode by repeating the cycle until the SOC reaches the CS level for CS mode;
- avoid a predefined repetition of the standard driving cycle for CS operation (one cycle may be sufficient to guarantee a final SOC within 5% of CS SOC);
- avoid a detailed knowledge of driving statistics, skipping the UF weighting based on it;
- consider that the probability to be in CD or CS is equal;
- calculate regulated emissions based on the same premises.



FC of each driving cycle in this way is calculated by

$$\begin{aligned} FC_{CS} &= \frac{V_{\text{fuelCS}}}{D_{CS}} \\ FC_{CD} &= \frac{V_{\text{fuelCD}}}{D_{CD}} \\ FC_{\text{cycle}} &= 0.5 \times FC_{CD} + 0.5 \times FC_{CS} \end{aligned} \quad (7.2)$$

Note the difference from this set of equations and SAEJ1711 set of Eqs. 7.1, and the distinct division in CD and CS operating modes shown in Fig. 7.1. Emissions follow the same logic of FC calculation, i.e. they have to be determined for each operating mode.

Extreme scenarios of battery recharge and commuting distances (always driving in CS mode; always driving in CD mode; 20 km travel in CD) are also analyzed and should be accounted for. Always driving in CS mode means the PHEV operation is similar to a HEV with the battery state-of-charge kept around a specified minimum (30–45% depending on battery and powertrain configuration). FC in this case is only chemical. Always driving in CD mode means the initial SOC is always 100%. 20 km travel in CD means the driver recharges the battery nightly and drives the average daily commuting distance in CD mode starting the home-to-work distance with the battery fully charged, and starting the way back home with the battery in a state between full charge and minimum charge.

Two idealized PHEVs configurations were considered as an example: a series hybrid with gasoline feed (such as GM Volt configuration) and a parallel hybrid, also with gasoline feed (such as Mercedes Sprinter configuration). PHEVs technical specifications are described in Table 7.2.

ADVISOR software [16] is used to simulate these PHEVs for the US, European, and Japanese driving cycles.

FC, electricity consumption and regulated emissions are calculated using base assumptions described above and additionally SAEJ1711 for the US case.

**Table 7.2** PHEVs specifications

Configuration	Series (range extender)	Parallel (blended)
Weight (kg)	1323	1234
ICE Power (kW)	53	41
Chemical fuel	gasoline	gasoline
Electrical motor power (kW)	75	30
Generator power (kW)	53	–
Battery type/capacity (kWh)	NiMH/15	NiMH/15
SOC <sub>CS</sub> (%)	45	30
Power/weight (W/kg)	57	59

CO<sub>2</sub> emissions are calculated for the following:

- chemical FC (based on combustion carbon balance) and life cycle until reaching the filling station;
- electricity generation and distribution losses to the consumer;
- cradle-to-grave cycle of vehicle materials.

Impact on the electric grid in terms of required power is assessed based on “worst-case” scenario, namely:

- maximum battery discharge and recharging equivalent energy per vehicle;
- minimum recharging time of 3 h and equivalent power requirements per vehicle;
- simultaneous recharging.

Cost calculations take into account utilization of the vehicle (assuming chemical fuel and electricity prices and maintenance additional cost) and manufacturers’ additional costs.



## 5. UNITED STATES, EUROPE, AND JAPAN ANALYSIS

Most countries worldwide have certain light-duty emission standards and respective driving cycles for measuring emissions/FC in a dynamometer. Table 7.1 shows the standard drive cycle specifications for USA, Europe, and Japan. In the United States the FTP is used for HC, CO, NO<sub>x</sub>, and PM emissions, while CAFE is used for FC. Europe uses the NEDC (New European Driving Cycle). Japan currently uses two driving cycles: Japanese new urban driving cycle (JC08) and 10–15 weighted as 25% of JC08 mode cold start + 75% of 10–15 mode hot start. However in 2011, the 10–15 mode hot start will be replaced by JC08 hot start, so for the present study only the JC08 driving cycle was considered. Most of the other countries use their own emission/FC regulations based on the European or US driving cycles [17].

### 5.1 Fuel consumption and regulated emission factors

Tables 7.3–7.5 show FC and regulated emissions obtained with ADVISOR for the developed methodology, for a user that: (a) never recharges the battery (100% CS), (b) always recharges the battery and drives daily distances that explore all the CD mode (100% CD), and (c) always recharges the battery but drives only 20 km daily in CD. SAEJ1711 results are presented for the United States. Base results represent our proposed methodology (see Eq. 7.2). Concerning the exploitation of CD and CS modes of operation, for series PHEV about 5 NEDC runs were required to complete the CD mode (7 for Japan cycle, 5 for UDDS, and 4 for HWFET), and it had the possibility of 50 km all electric in all cycles. For parallel PHEV, 13 NEDC, 13 JC08 cycles, 9 UDDS, and 20 HWFET were required. Parallel PHEV runs all electric for nearly 20 km in all cycles. Fig. 7.2 shows simulated instantaneous FC for both PHEVs configurations in JC08 (hot start) driving cycles.

**Table 7.3** PHEVs FC and regulated emissions for the United States—series/parallel configuration values

Methodology/value	Chemical FC (l/100 km)	Electrical FC (Wh/km)	HC (g/km)	CO (g/km)	NO <sub>x</sub> (g/km)
SAE J1711	4.4/4.8	–	0.34/0.23	1.12/1.02	0.31/0.28
Base (proposed)	2.6/4.2	62/35	0.17/0.14	0.60/0.71	0.16/0.18
100% CS	5.3/5.7	0	0.34/0.23	1.12/1.02	0.31/0.28
100% CD	0/2.7	123/70	0/0.06	0/0.40	0/0.08
20 km CD	0/0.8	123/117	0/0.09	0/0.37	0/0.06

**Table 7.4** PHEVs FC and regulated emissions for Europe—series/parallel configuration values

Methodology/value	FC chemical (l/100 km)	FC electrical (Wh/km)	HC (g/km)	CO (g/km)	NO <sub>x</sub> (g/km)
Base (proposed)	2.8/4.8	62/36	0.32/0.25	1.06/1.10	0.25/0.26
100% CS	5.6/6.8	0	0.65/0.43	2.11/1.69	0.50/0.41
100% CD	0/2.8	123/72	0/0.08	0/0.49	0/0.10
20 km CD	0/0.02	123/110	0/0.19	0/1.31	0/0.20

**Table 7.5** PHEVs, FC, and regulated emissions for Japan—series/parallel configuration values

Methodology/Value	Chemical FC (l/100 km)	Electrical FC (Wh/km)	HC (g/km)	CO (g/km)	NO <sub>x</sub> (g/km)
Base (proposed)	2.8/3.9	62/37	0.16/0.13	0.49/0.58	0.14/0.18
100% CS	5.8/6.5	0	0.68/0.43	2.18/1.96	0.52/0.45
100% CD	0/1.6	123/73	0/0.07	0/0.31	0/0.07
20 km CD	0/0	123/130	0/0	0/0	0/0

In terms of dynamometer driving cycles, the repetitions could represent as much as 5–8 h testing per vehicle. This extensive measurement time is a disadvantage of this methodology, but, currently, minimum test methods for PHEVs are being discussed [15].

It is interesting to note that, for the United States, SAEJ1711 FC and emissions are similar to those obtained in 100% CS mode, except for electric consumption that is not considered separately in SAEJ1711. Base results, representing the proposed methodology, present halved values for both fuel and regulated emissions vs. SAEJ1711. Extreme scenarios reveal that gasoline consumption can be near zero in all driving cycles if a commuting distance of 20 km is considered. If 100% CD operation is considered, series configuration will remain with zero gasoline

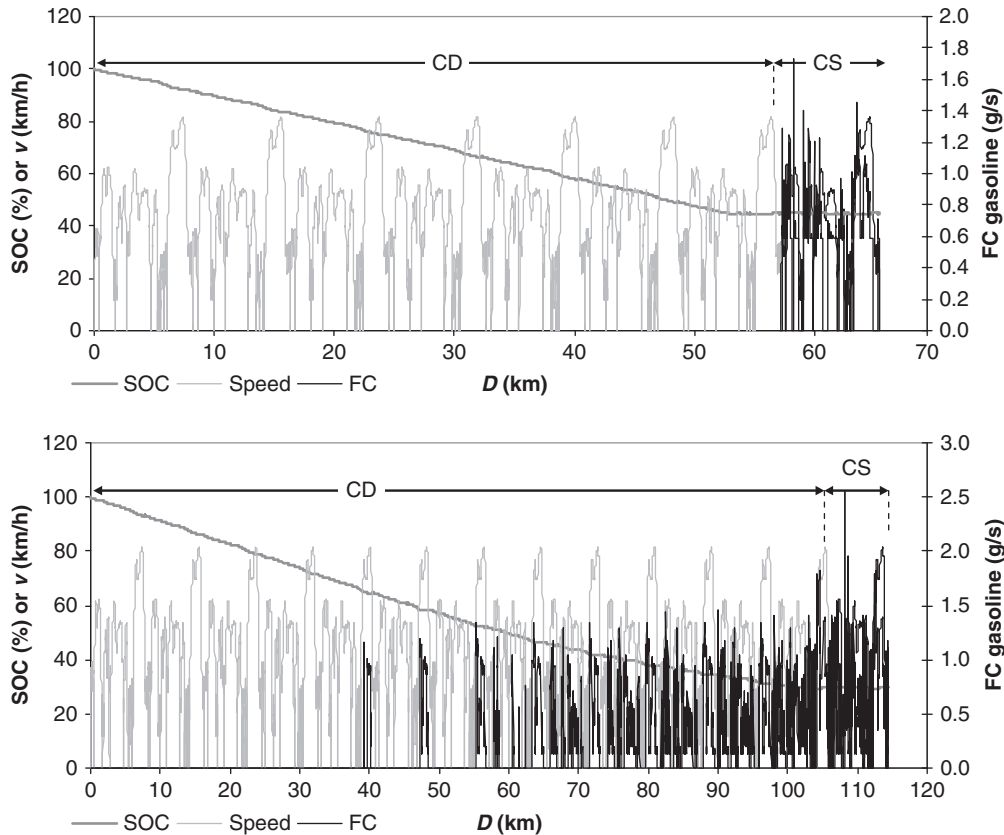


**Figure 7.2** (Up) Series PHEV FC for JC08 Japan (7 runs in CD, 1 run in CS). (Down) Parallel PHEV FC for JC08 Japan (13 runs in CD, 1 in CS).

consumption in all driving cycles. The same is not true for parallel configuration than can have as much as 140 times higher gasoline consumption in 100% CD compared to 20 km CD mode. Electric consumption is obviously higher in CD modes, and these extreme scenarios should be considered for estimations of the impact on the electric grid. Series configuration has lower FC in the US driving cycle versus the other cycles. Parallel configuration in base scenario has lower FC in the USA versus Europe but higher versus Japan.

Summarizing, these results show the variations in energy consumption and emissions when considering both base and extreme scenarios, for the same driving cycle, considering the same scenarios among different driving cycles and considering different powertrain configurations. AER (considered the distance covered before the first ICE turning on), is nearly the same for each technology among different driving cycles.

## 5.2 CO<sub>2</sub> global emissions

Because CO<sub>2</sub> emissions are not a local air quality issue but instead a global environmental issue, a true comparison among different technologies should consider their fuel life cycle analyses and also materials cradle-to-grave contribution along the vehicle mileage.

CO<sub>2</sub> emissions were calculated for the following:

- chemical FC (based on combustion carbon balance) and life cycle from production to storage in the filling station;
- electricity generation and distribution losses to the consumer;
- materials cradle-to-grave life cycle.

CO<sub>2</sub> emissions during fuel life cycle are presented in Figs. 7.3 and 7.4 for each standard driving cycle. The authors assume that CO<sub>2</sub> emissions produced from electricity generation derived from coal-fired power stations, from oil-fired power stations and from combined cycle natural gas power stations, are 887, 704, and 443 g/kWh, respectively ([18–20]). Emissions associated with construction and operation of power plants represent about 2–5% of total CO<sub>2</sub> and were not considered. Nuclear power, biomass-fired power, wind power, solar power, hydropower, and geothermal power are considered to be CO<sub>2</sub> emission free versus combustion power plants despite the emissions associated with transportation of raw material, processing and extraction, and construction of the power plant that represents about 15 g/kWh of CO<sub>2</sub>. Distribution to the consumer is considered to have 92% efficiency [18]. US electric mix was assumed to be 50% coal, 17% natural gas, 3% oil, 19% nuclear, 7% hydro, and 4% others (leading to a combined

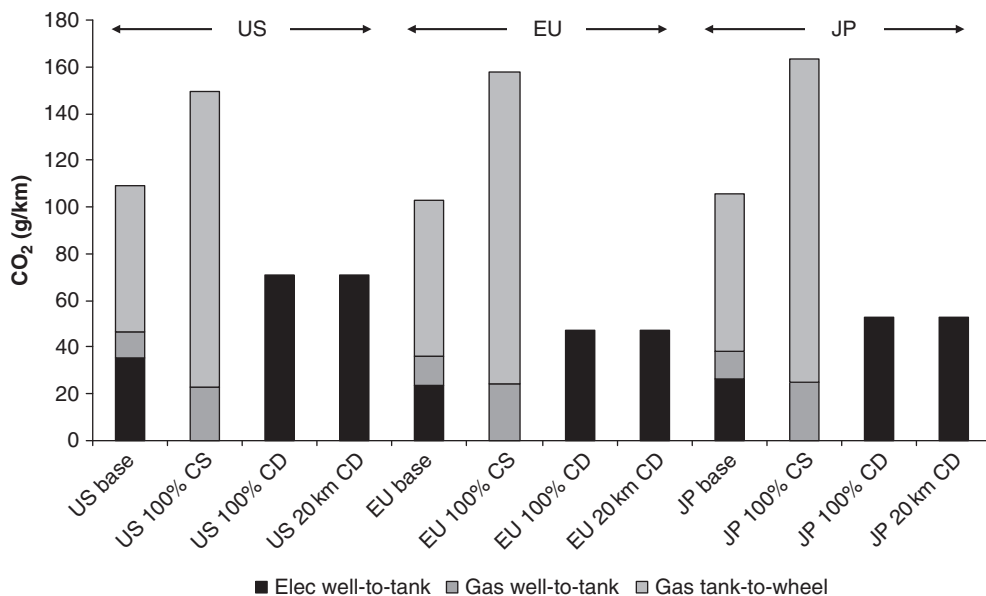


**Figure 7.3** Series PHEV fuel life cycle CO<sub>2</sub> emissions for USA, Europe, and Japan.

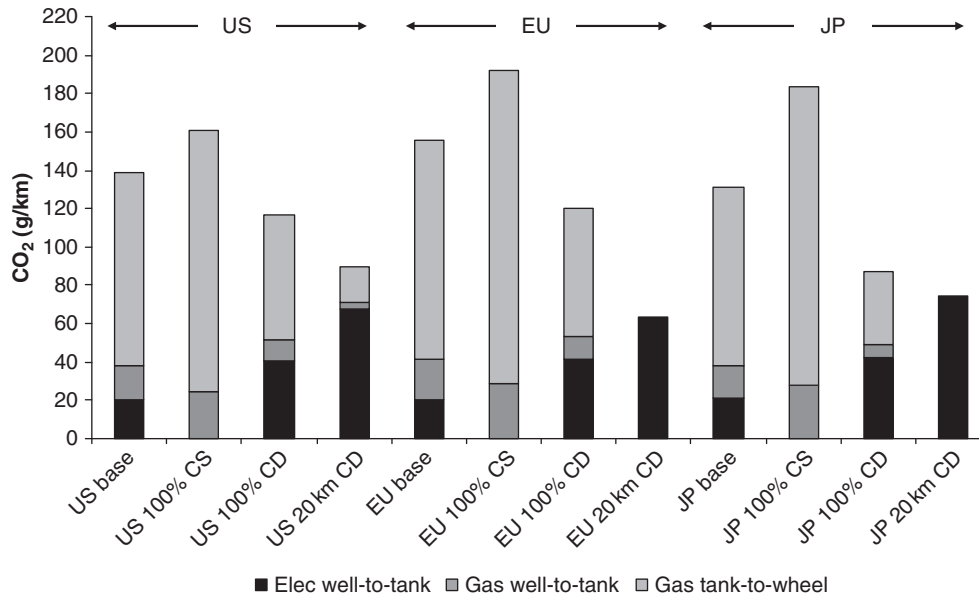


**Figure 7.4** Parallel PHEV fuel life cycle CO<sub>2</sub> emissions for USA, Europe, and Japan.

value of 543 g/kWh), Europe electric mix was assumed to be 31% coal, 19% natural gas, 4% oil, 31% nuclear, 11% hydro, and 4% others (combined value: 387 g/kWh) and Japan electric mix was assumed to be 27% coal, 23% natural gas, 12% oil, 26% nuclear, 10% hydro, and 2% others (combined value: 428 g/kWh).

While it is not the main objective of this chapter to compare PHEVs with other technologies in terms of CO<sub>2</sub> emitted, a cradle-to-grave analysis for the distance covered was made using the GREET software ([21,22]) for the different electric mixes (USA, Europe, and Japan) and powertrain configurations (series or parallel).

Note that the CO<sub>2</sub> from fuel life cycle contribution can be as much as 150 g/km if no advantage is taken from plug-in configuration (no battery external recharge, 100% CS). This value can be at least halved if CD is the main operation mode (100% CD, or 20 km CD), independently of the driving cycle considered.

Fig. 7.5 shows the case of a series PHEV in Europe covering a typical commuting distance of 20 km per day always in CD operation mode. In this case the total CO<sub>2</sub> emitted to the atmosphere can reach roughly 25 tons for 300,000 km (~80 g/km), 40% coming from the cradle-to-grave materials production/recycling/maintenance, and the rest from electricity consumption when recharging the battery. If the total driving distance is only 150,000 km, 60% of the CO<sub>2</sub> emitted comes from materials cycle, and the rest from electricity consumption.

Maximum CO<sub>2</sub> impact occurs, for the European case, for a PHEV always in CS operation mode (battery never externally recharged), emitting 67 tons of CO<sub>2</sub> for

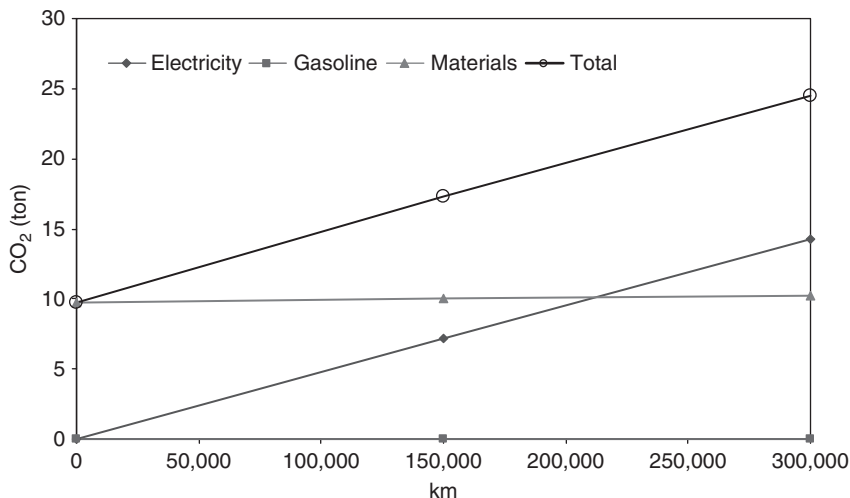


**Figure 7.5** Series PHEV CO<sub>2</sub> contribution along its usage, for a typical daily distance of 20 km (in CD operation mode) and for Europe.

300,000 km (15% from materials cycle, 85% from gasoline use). For 150,000 km, 39 tons of CO<sub>2</sub> are emitted (75% from gasoline use and the rest from materials cycle).

### 5.3 Impact on the electric grid

The power demand on the grid will be a function of the voltage and amperage of the connection to the grid. The capacity of the battery to be recharged will then determine the recharging time.

From the simulations of several electricity consumption factors (see Section 5.1), the most extended use of this energy source occurs in 100% CD regimes, where the battery discharges about 55–70% of maximum SOC. Series configuration will imply an 8.25 kWh recharge (55% of 15 kWh) to refill the battery. Parallel configuration requires 10.5 kWh (70% of 15 kWh). The grid voltage is 110 V/60 Hz in the United States, 230 V/50 Hz in Europe, and 100 V/50–60 Hz in Japan. For a 30 A circuit, a parallel PHEV would take 3–4 h in the United States (maximum load 3.3 kW) and Japan (maximum load 3 kW) and 1–2 hours in Europe (maximum load 6.9 kW) for recharging from 30 to 100% SOC.

The electric infrastructure at home must be prepared to recharge the PHEV simultaneously with other electric devices. Parking lots must be prepared to recharge a large amount of vehicles, and finally the national electric grid must have available power to simultaneous recharge a fleet of PHEVs.

Hypothetically, if all plug-in vehicles recharge their batteries at the same time, 1 million plug-in would require a maximum 3.8 GW (considering 8% losses in the distribution and 3 hour recharging). If 20 km CD is considered, nearly 1 GW is required for the same number of vehicles. Again, these different extreme scenarios should be considered.

## 5.4 Costs

We can identify four types of costs for the users: acquisition, maintenance and fuel cost (both electricity and gasoline), and circulation tax. Acquisition and circulation costs are highly dependent on incentives and eventually can make more advantageous to have a plug-in “environmentally friendly” vehicle than a conventional one. In terms of manufacturers’ additional costs, these are estimated to be \$4,000–\$10,000 versus conventional equivalent gasoline vehicles [2,6]. Concerning maintenance, the main differences comes from battery replacements: every 80,000 km in conventional vehicles (lead-acid) and every 160,000 km for Ni-MH or Li-ion batteries [2]. For vehicles covering 150,000 km, maintenance of a PHEV is nearly the same as for a conventional vehicle. If vehicle mileage goes up to 300,000 km, maintenance of a PHEV is about \$2,000–\$7,000 more expensive than an equivalent conventional vehicle. Finally, fuel cost is presented in Table 7.6, while Figs. 7.6 and 7.7 present the cost of vehicle use in €/km for the different scenarios evaluated and for series and parallel PHEV solutions, respectively. Equivalent conventional gasoline vehicles have a higher cost than the 100% CS one (about 20–30% higher). It is important to note that fuel cell, plug-in hybrid, and pure EVs usually compensate in terms of cost only if long distances are driven (higher than 150,000 km) [23]. This is important when calculating possible tax incentives to purchase these kinds of technologies, and when applying fuel price incentives, having in mind that the final consumer is extremely sensitive to the driving distance breakeven of their investment in acquiring an alternative technology vehicle.



## 6. CONCLUSIONS

A broader methodology based on SAE J1711 should be adopted for PHEVs, aiming at a fair comparison among vehicle technologies regarding emission/FC standards.

Total CO<sub>2</sub> emissions calculation, required electric grid power per plug-in vehicle and maintenance and use cost as a function of the travelled distance should also be computed.

The methodology presented is as follows for the different operating modes:

**Table 7.6** Fuel prices (conversion: €1 for \$1.47 and 157.23 yen)

Country	USA	Europe	Japan
Electricity (€/kWh) <sup>a</sup>	0.057	0.088	0.104
Gasoline (€/l) <sup>b</sup>	0.540	1.348	0.992

<sup>a</sup> OECD 2007, Energy Prices and Taxes—Quarterly Statistics.

<sup>b</sup> IEA, End-User Petroleum Product Prices and average crude oil import costs, December 2007.



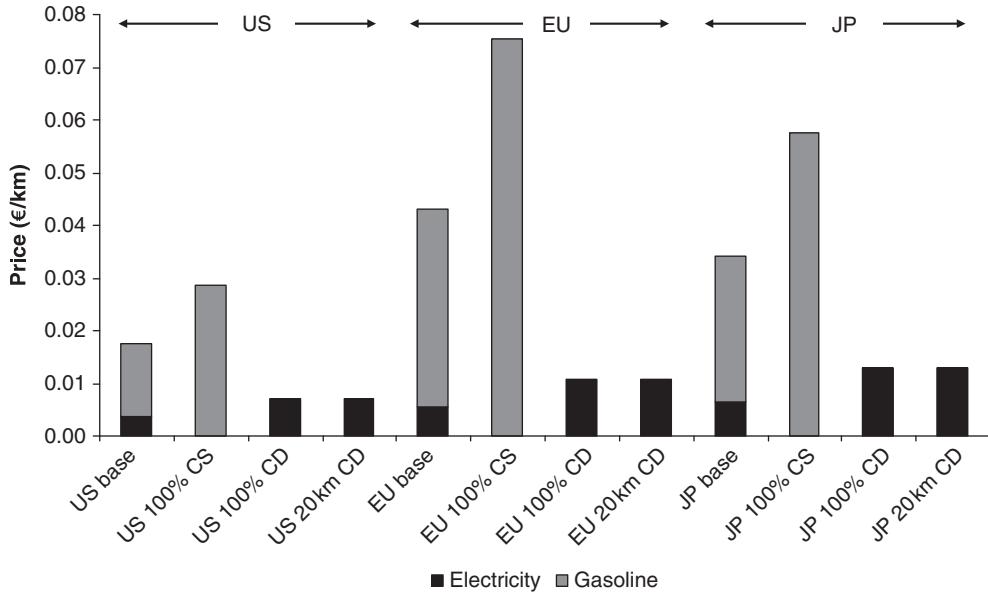


**Figure 7.6** Series PHEV utilization prices for USA, Europe and Japan.

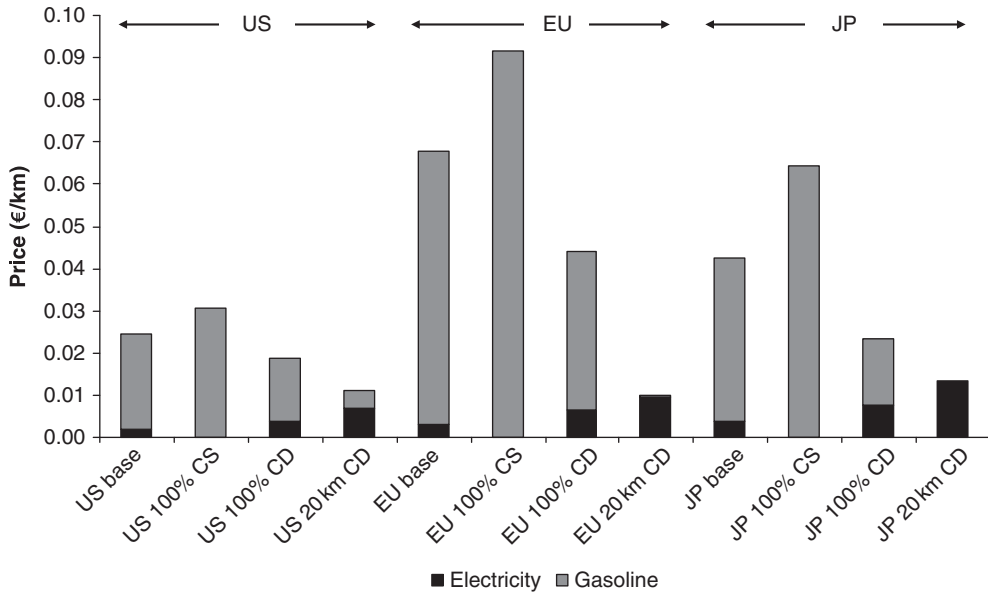


**Figure 7.7** Parallel PHEV utilization prices for USA, Europe, and Japan.

- explore the CD mode: repeat the standard driving cycle with the battery starting fully charged and ending with the CS state-of-charge;
- calculate CD emissions (g/km), FC (l/100 km) and electricity consumption (kWh/km);
- explore the CS mode: perform the standard driving cycle with the battery starting and ending with the CS level (one cycle is enough to guarantee a final SOC within 5% of CS SOC);
- consider that the probability to be in CD or CS is equal, so apply a 50% weight to CD and CS emissions, FC, and electricity consumption results.

Additional extreme scenarios of always travelling in CS or CD modes can be derived from previous calculations and should be included when reporting data for FC (both chemical and electrical) and for emissions.

The methodology was applied to one plug-in range extender gasoline vehicle and a blended plug-in gasoline vehicle, along US, European, and Japanese driving cycles. Chemical FC, electrical FC, and regulated emission factors are presented, obtained from direct simulations using the ADVISOR code.

CO<sub>2</sub> emissions were calculated for chemical FC, electricity generation, and cradle-to-grave materials production/recycling. Total driven kilometers greatly affects total CO<sub>2</sub> contribution of the vehicle: for a series PHEV covering 20 km daily, always in CD operation mode, total CO<sub>2</sub> emitted to the atmosphere can reach ~25 tons for 300,000 km (40% from materials cycle and the rest from electricity consumption when refilling the battery). If the driving distance along the vehicle's life is only 150,000 km, 60% of the CO<sub>2</sub> emitted comes from materials cycle, and the rest from electricity consumption.

The CO<sub>2</sub> impact is maximum, for the European cycle, for a PHEV always in CS operation mode (see Figs. 7.6 and 7.7), with the battery never recharged: it emits 67 tons of CO<sub>2</sub> for 300,000 km (15% from materials cycle, 85% from gasoline use) and 39 tons for 150,000 km (75% from gasoline use and the rest from materials cycle).

Maximum impact on the electric grid for the electrical consumption of these PHEVs was estimated. If fast recharging is required (3 hours) about 3 kW/vehicle are needed. The total vehicle mileage will affect greatly not only use costs (electric CD operation being up to 70–90% cheaper than conventional hybrid operation), but also maintenance additional costs (about the same for 150,000 km, and \$2,000–\$7,000 greater than a conventional vehicle for 300,000 km).

## ACKNOWLEDGMENTS

The authors would like to acknowledge FCT-Fundação para a Ciência e Tecnologia through the national project “MMSAFU-Microsimulation Model to Simulate Alternative Fuel Usage” (POCI/ENR/57450/2004) and through the MIT-Portugal project “Power demand estimation and power system impacts resulting from fleet penetration of electric/plug-in vehicles” (MIT-Pt/SES-GI/0008/2008). Also thanks to Professor Marc Ross, and to the following graduate students, Jean Marc, Mário Tomás, and Patrícia Baptista whose research is directly related to the subject of this chapter.

## NOMENCLATURE

CAFE	US corporate average fuel economy
CD	charge depleting
CS	charge sustaining
EV	electric vehicle
FC	fuel consumption
FCT	full charge test
HEV	hybrid electric vehicle
HWFET	highway fuel economy cycle
ICE	internal combustion engine
JC08	Japanese new urban driving cycle
NEDC	New European Driving Cycle
PHEV	plug-in hybrid electric vehicle
PCT	partial charge test
SOC	state of charge
UDDS	urban dynamometer driving schedule

## REFERENCES

1. A.A. Frank, *Am. Sci.* 95 (2007) 156.
2. Electrical Power Research Institute (EPRI), Comparing the Benefits and Impacts of Hybrid Vehicle Options, EPRI, Palo Alto, USA, July 2001, Report 1000349.
3. T. Markel, K. Wipke, 16th Annual Battery Conference on Applications and Advances, January 9–12, Long Beach, USA, 2001 (NREL/CP–540–30601).
4. T. Markel, A. Simpson, SAE Future Transportation Technology and IEEE Vehicle Power and Propulsion, Joint Conferences, Chicago, USA, September 7–9, 2005 (NREL/CP–540–38538).
5. J. Gonder, A. Simpson, 22nd International Battery, Hybrid and Fuel Cell Electric Vehicle Symposium and Exhibition (EVS–22), Yokohama, Japan, 2006 (NREL/CP–540–40377).
6. M.A. Kromer, J.B. Heywood, Electric Powertrains: Opportunities and Challenges in the U.S. Light-duty Fleet, MIT Report No. LFEE 2007–03 RP, May 2007.
7. K.S. Kurani, R.R. Heffner, T.S. Turrentine, Driving Plug-in Hybrid Electric Vehicles: Reports from U.S. Drivers of HEVs Converted to PHEVs, Circa 2006–07, Institute of Transportation Studies, University of California, Davis, October 16, 2007.
8. P. Baptista, C.M. Silva, G. Gonçalves, T.L. Farias, Proceedings of EVS–24, Stavanger, Norway, May 2009.
9. H. Zhai, H.C. Frey, N.M. Roupail, G.A. Gonçalves, T.L. Farias, *J. Air Waste Manage. Assoc.* 59 (2009) 912.
10. T.H. Bradley, A.A. Frank, *Renew. Sustain. Energy Rev.* 13 (2009) 115.
11. P.S. Hu, T.R. Reuscher, Summary of Travel Trends: 2001 National Household Travel Survey, US Department of Transportation and Federal Highway Administration, Oak Ridge, USA, December 2004.
12. V. Helminen, M. Ristimäki, *J. Transp. Geogr.* 15 (2007) 331.
13. H. Ueda, K. Nakazawa, H. Takafumi, Reducing the Environmental Load by Encouraging a Modal Shift in Commuting, Proceedings of Environmental Modeling and Simulation, Report No. 432, 2004.
14. SAE J1711–MAR1999, Recommended Practice for Measuring the Exhaust Emissions and Fuel Economy of Hybrid Electric Vehicles, SAE International, March 1999.
15. M. Duoba, R. Carlson, J. Wu, Proceedings of EVS–23, Anaheim, USA, December 2007.
16. K. Wipke, M. Cuddy, S. Burch, *IEEE Trans. Veh. Technol.* 48 (1999) 1751.
17. F. An, A. Sauer, Comparison of Passenger Vehicle Fuel Economy and Greenhouse Gas Emission Standards Around the World, Pew Centre on Global Climate Change, Arlington, USA, December 2004.

18. C.A. Lewis, MEET Project: Methodologies for Estimating Air Pollutant Emissions from Transport, European Project, Contract n. ST-96-SC.204>, 1997.
19. H. Hondo, *Energy* 30 (2005) 2042.
20. International Energy Agency (IEA), Electricity Statistics. <http://www.iea.org/Textbase/stats/prodresult.asp?PRODUCT=Electricity/Heat>, 2004 (accessed 12.07.2009).
21. M.Q. Wang, Y. Wu, A. Elgowainy, Operating Manual for GREET: Version 1.7, ANL/ESD/05-3, Center for Transportation Research, Argonne National Laboratory, Argonne, Ill., November 2005.
22. A. Burnham, M. Wang, Y. Wu, Development and Applications of GREET 2.7—The Transportation Vehicle-Cycle Model, Energy Systems Division, Argonne National Laboratory, Argonne, USA, 2006.
23. P. Baptista, M. Tomás, C.M. Silva, Hydrogen Power Theoretical and Engineering Solutions—International Symposium, Lisbon, April 2009.



# Improving Petroleum Displacement Potential of PHEVs Using Enhanced Charging Scenarios

Tony Markel, Kandler Smith and Ahmad A. Pesaran<sup>1</sup>

National Renewable Energy Laboratory, 1617 Cole Blvd., Golden, CO 80401, USA

## Contents

1. Introduction	211
1.1 Review of previous results	212
1.2 Review of battery life modeling	214
2. Approach	214
2.1 Vehicle simulation model	215
2.2 Driving profile database	216
2.3 Battery aging model	217
3. Results	218
3.1 Driving profile impact	219
3.2 Battery aging with different charging scenarios	220
4. Conclusions	224
Acknowledgments	224
References	225



## 1. INTRODUCTION

The United States faces a serious transportation energy problem. The transportation sector depends almost entirely on a single fuel – petroleum. The future of the petroleum supply and its use as the primary transportation fuel threaten both personal mobility and economic stability. For example, the United States currently imports nearly 60% of the petroleum it consumes and dedicates more than 60% of its petroleum consumption to transportation [1]. As U.S. petroleum consumption continues to climb despite steadily declining domestic production, the percentage of petroleum imports will grow. Also, international pressures continue to increase as the growing economies of China and India consume petroleum at rapidly increasing rates. Many experts now predict that world petroleum production will peak within the next 5–10 years, greatly straining the petroleum supply and demand balance in the international market [2].

<sup>1</sup> Corresponding author: ahmad.pesaran@nrel.gov

Hybrid electric vehicle (HEV) technology presents an excellent way to reduce petroleum consumption through efficiency improvements. HEVs use energy storage systems (ESSs) combined with electric motors to improve vehicle efficiency by enabling the use of smaller sized engines and by recapturing energy normally lost during braking events. A typical HEV can reduce gasoline consumption by about 30–45% over that of a comparable conventional vehicle [3]. However, even aggressive introductions of efficient and affordable HEVs to the market will only slow the increase in petroleum demand due to vehicle life and annual travel trends. Reducing U.S. petroleum dependence below current levels requires vehicle innovations beyond today's HEV technology.

Plug-in hybrid electric vehicle (PHEV) technology provides the potential to displace a significant portion of transportation petroleum consumption by using electricity for portions of trips. A PHEV is an HEV with the ability to “plug-in” so as to recharge its ESS with electricity from the utility grid. With a fully charged ESS, the vehicle will tend to use electricity rather than liquid fuels. A key benefit of plug-in hybrid technology is that the vehicle no longer depends on a single fuel source. The primary energy carrier would be electricity generated from a diverse mix of domestic resources, including coal, nuclear, natural gas, wind, hydroelectric, and solar energy. The secondary energy carrier would be a chemical fuel stored on the vehicle (e.g., gasoline, diesel, ethanol, or even hydrogen). Although PHEVs must still overcome technical challenges related to ESS cost, size, and life, the technology nevertheless provides a relatively near-term petroleum displacement option [4]. The combination of fuel savings potential, consumer usage patterns, charging scenarios, battery life attributes, and battery costs all need to be balanced and optimized to find the best low-cost solution for displacing fuel using PHEV technology. This work integrates a recently developed battery life assessment method into sets of PHEV simulations to better understand the impacts of charge management scenario options and the potential to reduce battery size while providing equivalent or greater fuel savings.

The National Renewable Energy Laboratory (NREL) is involved in significant PHEV-related research and development, including PHEV batteries and their interactions with the electricity grid. NREL has simulated the performance of PHEVs, performed cost/benefit analyses, developed PHEV batteries requirements for the U.S. Department of Energy and the United States Advanced Battery Consortium, performed thermal testing of PHEV batteries, used its PHEV test bed (a Prius converted to a plug-in with EnergyCS or Hymotion conversion kits) for field testing, studied grid interaction with PHEVs, and developed models for PHEV battery cost, life, and performance trade-off studies. This chapter uses the results and insights from these parallel studies to explore charging scenarios and environmental conditions that strike a balance among cost, life, and fuel savings.

## 1.1 Review of previous results

Markel and Simpson [5] presented the cost/benefit ratio of several PHEV design scenarios relative to conventional and hybrid vehicles, and Gonder et al. [6] have

presented a comparison of the fuel savings benefit variability over real-world driving profiles. ADVISOR<sup>TM</sup>, a vehicle systems simulation package, was used along with 227 unique real-world driving profiles to demonstrate the spectrum of fuel savings benefits that result from a broad distribution of driving behaviors. Although differences exist across driving profiles, when evaluated as a fleet, the simulations showed a savings of  $\sim 0.9$  gallons of gasoline per day per vehicle, or 66% for the PHEV-40 and 55% for the PHEV-20 design. Under long-term cost assumptions, the PHEV-20 was estimated to cost  $\sim \$3,000$  less than the PHEV-40 design scenario [5].

In a study conducted in collaboration with Xcel Energy, the real-world simulation results [6] were used to generate estimates of the utility load profile from charging PHEVs under several scenarios [7]. The utility integration study included four scenarios: “baseline,” with one unmanaged charge per day; “delayed,” with all charging delayed until after 10 p.m.; “utility load valley filling,” in which all charging is optimally controlled to occur during the lowest utility demand period; and “opportunity,” in which charging occurs anytime the vehicle is parked. In NREL’s publications [4,6,8], the expected performance of PHEVs over real driving profiles based on travel survey data was presented (Fig. 8.1), and they show that although consumer driving is more aggressive than standard test and design profiles, there is still significant potential for fuel savings with plug-in hybrid technology.

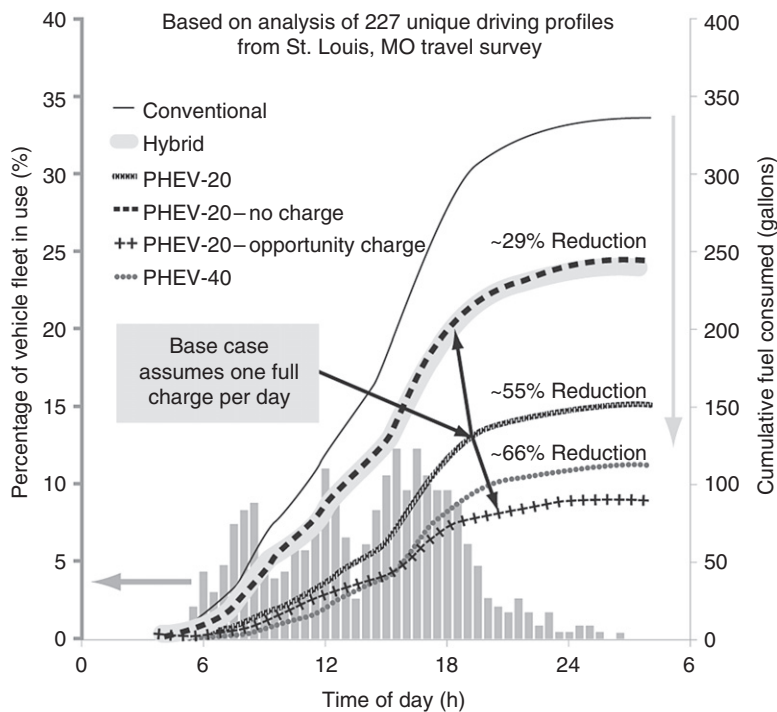


**Figure 8.1** Plug-in hybrid simulations over real driving profiles lead to greater than 50% petroleum displacement.

The opportunity charge scenario proved to provide the greatest vehicle petroleum displacement, while other scenarios provided a potentially more desirable scenario from a utility operation's perspective because of lower operating costs and emissions impacts. The vehicle ESS encounters very different operating characteristics under each scenario. The battery life impacts of differences in usage profiles were not quantified. Research now focuses on the impact factors and opportunities for cost reduction of the plug-in hybrid system.

## 1.2 Review of battery life modeling

Battery life modeling is complicated, because life is affected by many factors, including the temperature and state of charge (SOC) during storage, the depth of each discharge cycle, the frequency of cycling, and the rate of cycling. For automotive applications, the battery is often deemed to be at the end of its useful life when it has degraded to 80% of its original power or energy capacity [9]. The PHEV duty cycle may be the most difficult that a battery may see. In HEV usage, the ESS is maintained in a medium to high SOC level, and cycling is quite shallow. In electric vehicle (EV) applications, the ESS is cycled deeply; however, this cycling may occur only every few days rather than daily, as it does in a PHEV. If a PHEV is charged more than once a day, the duty cycle may be even more severe. Battery life modeling coupled with vehicle systems simulations provides an opportunity for quantifying these differences.

Most commonly, battery cycle life is projected by extrapolating degradation-per-cycle data measured during accelerated cycling tests [10]. Battery calendar life, or years in life, is projected by extrapolating a model fit to degradation measured with time during storage at normal and elevated temperatures [11]. True battery life, however, is dependent upon both storage and cycling, and it is important when exploring real-world scenarios that the battery aging model combine both cycling and storage effects.

Hall et al. [12] recently demonstrated the importance of collecting real-time cycling data as well as accelerated cycling data for a lithium ion battery with a nickel-cobalt-aluminum (NCA) cathode. They found that accelerated cycling results (4 cycles/day) tended to overpredict actual NCA battery life when compared with 5 years of real-time cycling data (1 cycle/day) for a geosynchronous orbit satellite application. Differences between accelerated cycling and real-time cycling degradation could not be wholly explained by correcting for calendar effects.



---

## 2. APPROACH

Vehicle systems simulation enables the rapid exploration of vehicle design and control options. Battery life models provide the ability to quantify differences in battery usage scenarios. Real-world driving profiles are extremely valuable for understanding the real fuel savings potential of PHEVs and highlighting the design challenges of incorporating sufficient power capability, energy storage sizing, and fleet charging strategies. This study uses all three modeling and data resources to compare two PHEV scenarios:



1. PHEV-40 with a single evening charge
2. PHEV-20 with opportunity charging throughout the day.

## 2.1 Vehicle simulation model

Vehicle system simulation enables modeling and evaluation of many vehicle powertrain and control scenarios. ADVISOR was used to simulate the operation of conventional, hybrid, and PHEV options for this study. Inputs to this model include details about the powertrain components, the vehicle attributes, the control strategy, and the driving profile. Results provide detailed information on the time-dependent operation of all of the components and the overall performance of the vehicle. For this study, of primary interest are the fuel consumption and the ESS operational details. Table 8.1 shows the attributes of the vehicle simulated.

Key assumptions were as follows:

- The baseline vehicle is based on a Malibu/Camry-like mid-size vehicle.
- The PHEV has the ability to operate on the electric drivetrain alone during urban driving.
- Controls operate the PHEV in charge depletion mode between 95 and 30% SOC.
- The strategy implements a charge sustaining operation between 25 and 35% SOC.
- The baseline scenario begins to recharge the battery after the end of the last driving trip.
- The opportunity scenario begins to recharge any time the vehicle key is turned off.
- The battery is recharged at a constant 1.4 kW utility load with an 85% efficient charger.

The battery life impacts of two PHEV scenarios were considered: one with 40 miles of range and a single daily charge and the other with 20 miles of range and the ability to charge

**Table 8.1** Simulated vehicle attributes

	Units	Conventional	Hybrid	PHEV-20	PHEV-40
Engine power	kW	121.7	82	79.4	81.9
Motor power	kW	n/a	39	43.6	48
ESS power	kW	n/a	50	47	51.8
ESS energy (total)	kWh	n/a	1.9	9.4	18.5
Curb mass	Kg	1,429	1,399	1,488	1,567
Fuel economy (urban/highway)	Mpg	26	39.2	54	67.4
Electric consumption (urban/highway)	Wh/mi	n/a	n/a	95	157
All-electric range (urban)	Miles	n/a	n/a	22.3	35.8

n/a, not available.

at all parked times. A PHEV-40 is designed to provide  $\sim 40$  miles of electric drive capability on an urban driving profile. On driving profiles requiring more power than that encountered in urban driving or for distances longer than 40 miles, the petroleum-fueled engine supplements the battery power and energy capability. Likewise, the PHEV-20 has  $\sim 20$  miles of urban electric drive capability. Based on an assessment of 2001 National Household Travel Survey (NHTS) data, a 40-mile vehicle satisfies 68% of consumers' daily driving needs with a single daily charge. A 20-mile range would cover 42% of consumers' daily needs [13]. With additional recharge opportunities, the 20-mile PHEV should provide equal or greater fuel displacement, depending on the driving profile attributes.

## 2.2 Driving profile database

The driving profile database for this study includes one full day of driving data for 227 unique vehicles that were collected using Global Positioning System (GPS) data loggers as part of a metropolitan travel survey in St. Louis, Missouri, in 2002. Expansion factors to weight these cycles to be representative of the entire survey population were not applied. A typical driving profile includes several individual driving trips defined by elapsed time and vehicle speed. Parked times and durations are also included. Fig. 8.2 shows the distribution of daily distances in this dataset.

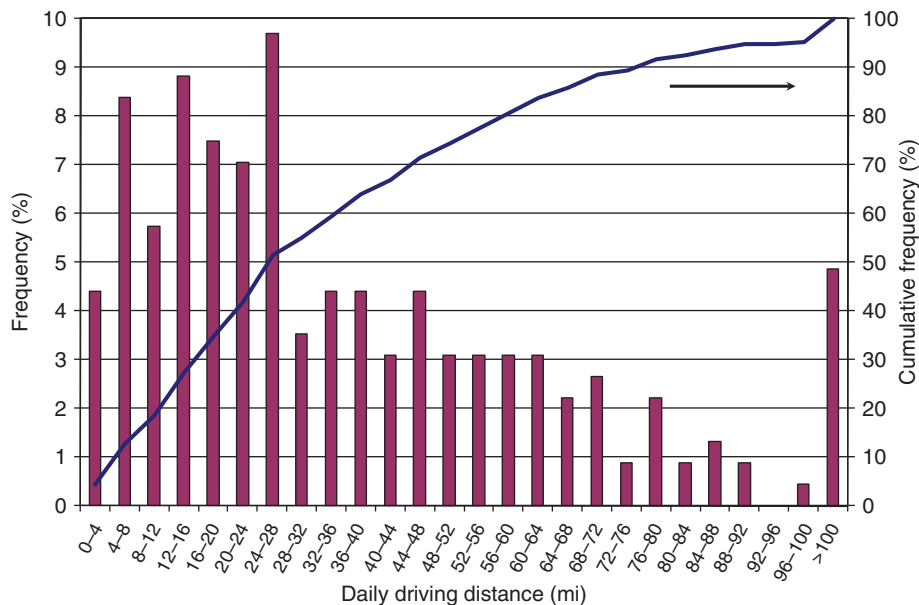


**Figure 8.2** St. Louis driving profile dataset: daily driving distance distribution.

### 2.3 Battery aging model

Battery performance degradation has been shown to be dependent on a number of operational parameters, including number of cycles  $N_i$  at a given SOC swing  $\Delta SOC_i$ , time  $t$ , voltage exposure  $V(t)$ , temperature exposure  $T(t)$ , and charge current rate  $I(t)$ . With sufficient data, the dependency of capacity fade and resistance growth on each operational parameter can be established. Physical or empirical models can be fit to data to interpolate/extrapolate results for different scenarios.

In order to explore the impact of PHEV consumer use scenarios on battery performance degradation, the present work uses an empirical model [14] fit to data from Hall et al. for a Saft VES-140 Li ion cell with carbon/NCA chemistry [12,15,16]. Operational parameters explored in that study included end of charge voltage, depth of discharge, temperature, and number of cycles per day. Cycling conditions included the aforementioned real-time and accelerated cycling conditions as well as storage.

Hall et al. found that storage degradation time dependency could be well described by a  $t^{1/2}$  model, consistent with a diffusion-limited corrosion reaction mechanism that builds a film layer at the electrode surface. They also found that small  $\Delta SOC$  cycles tended to suppress the film layer growth somewhat, while large  $\Delta SOC$  cycles tended to degrade the positive electrode active material and cause additional resistance growth and capacity loss. The addition of cycling degradation was well correlated by adding a  $t$  or  $N$  dependency to the  $t^{1/2}$  storage model.

Full details of the present carbon/NCA chemistry degradation model may be found in Ref. [14]. The model captures both storage- and cycling-induced resistance growth with

$$R = a_1 t^{1/2} + a_{2,t} t + a_{2,N} N \quad [8.1]$$

Results of various storage and cycling tests were used to fit coefficients  $a_1$  ( $\Delta SOC$ ,  $T$ ,  $V$ ) and  $a_2$  ( $\Delta SOC$ ,  $T$ ,  $V$ ) and capture  $\Delta SOC$ ,  $T(t)$ , and  $V(t)$  dependencies. Depth of discharge dependency was fit using empirical formulas. Temperature and voltage dependencies were fit with physically justifiable Arrhenius and Tafel relationships, respectively. Separate  $t$ - and  $N$ -dependent terms (rather than  $t$ -only or  $N$ -only) in [8.1] are necessary to describe degradation under both real-time and accelerated cycling conditions.

To describe capacity fade, the model assumes Li loss to be the dominant mechanism on storage and active site loss to be the dominant mechanism on cycling [17]. Available Li capacity  $C_{Li}$  is described as

$$C_{Li} = d_0 + d_1 a_1 t^{1/2} \quad [8.2]$$

while active site capacity is described as

$$C_{sites} = e_0 + e_1 (a_{2,t} t + a_{2,N} N) \quad [8.3]$$

Actual measured or usable capacity is taken as the lesser of [8.2] or [8.3]:

$$C = \min (C_{Li}, C_{sites}) \quad [8.4]$$

The Saft VES-140 cells [12,15,16] are nearly a decade old and might not reflect the life capability of present-day PHEV battery technology. It is also possible that these cells, intended for aerospace application, use more expensive materials and last longer than present-day PHEV cells. In order to account for both of these possibilities, several battery degradation model parameters were adjusted to match recent published data for vehicle electric drive batteries also with carbon/NCA chemistry.

The model used for scenario analysis matches the following actual measured aging results. After 4.5 years of storage at 40°C and 50% SOC, the battery will have lost 10% capacity [11]. After 13.7 years at 35°C, the resistance will have grown 110% [18]. Following 2700 PHEV power profile cycles consisting of  $\Delta SOC = 75\%$  deep discharge and numerous shallow cycles at 25°C, the battery resistance will have grown 50% and capacity will have faded 8% [10,19].



### 3. RESULTS

Vehicle simulations were conducted for five vehicles and charge scenarios. These included conventional, HEV, PHEV-20 baseline charge, PHEV-40 baseline charge, and PHEV-20 opportunity charge. The total fleet fuel savings relative to the conventional case are shown in Fig. 8.3.

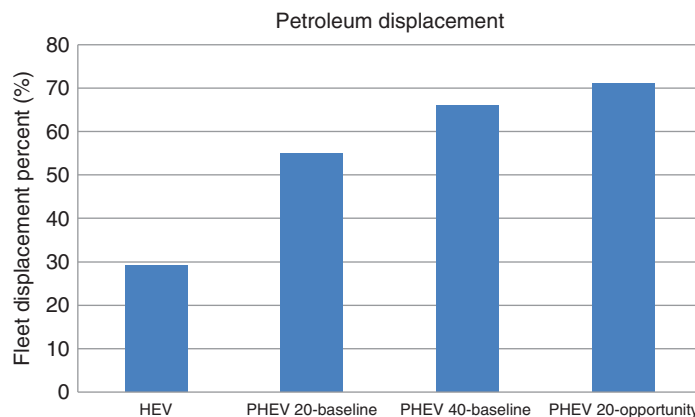


**Figure 8.3** Fuel displacement potential of various hybrid scenarios relative to conventional vehicle fuel use.

### 3.1 Driving profile impact

The driving profile characteristics can affect the relative benefits of the PHEV-20 opportunity charging scenario in comparison to the PHEV-40 baseline charge scenario. Cycles with more short trips and parked time between trips provide more opportunity for recharging the depleted battery, while cycles with only a few long trips provide less overall benefit of opportunity charging.

Fig. 8.4 provides an example of the simulation details for a single driving profile simulation. The chart shows the vehicle speed profile, the cumulative fuel consumption, and the varying battery SOC for each of the vehicle and charge scenarios. This specific vehicle traveled  $\sim 55$  miles over the course of one day. The opportunity charge capability extended the electric-only range on this driving profile by over 30 miles for the PHEV-20. Fuel savings relative to the HEV for the opportunity charge case were 1.5 gallons, while the fuel savings for the single charge per day PHEV-40 case were  $\sim 1$  gallon. The ESS SOC history for each of the three scenarios is also provided. The HEV SOC scenario varies along a very narrow range. The PHEV-40 with a single evening charge incurs a single full discharge and charge. The PHEV-20 with opportunity charge

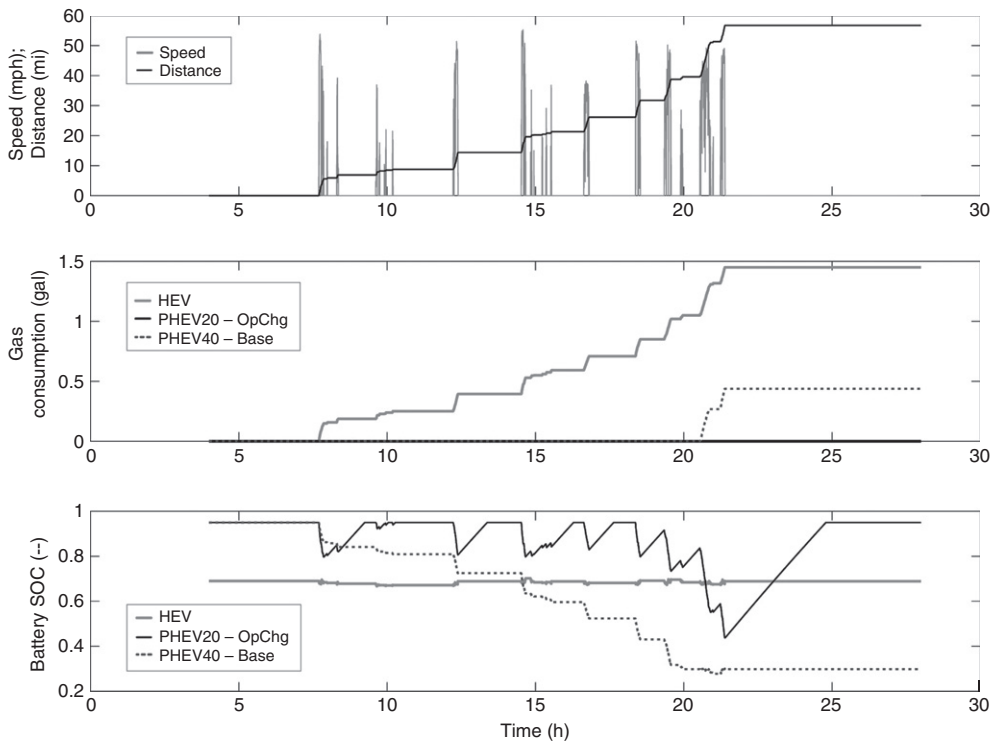


**Figure 8.4** Gasoline consumption and state of charge behavior greatly impacted by battery size and charging scenario.

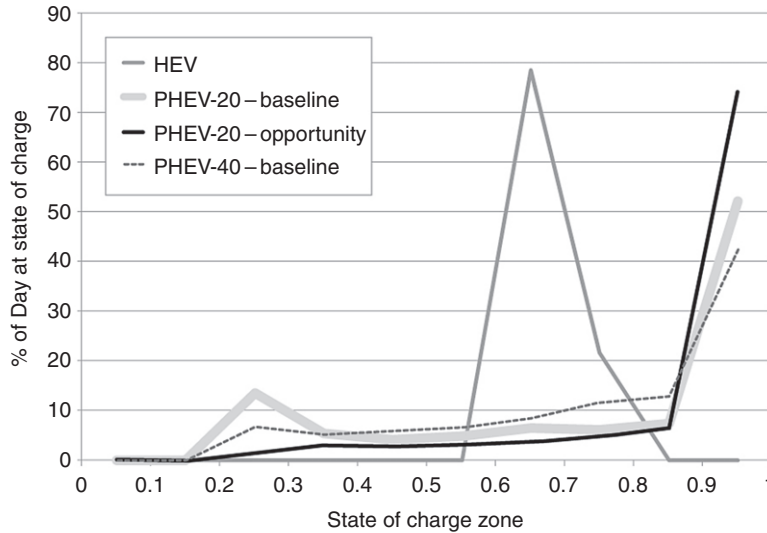


**Figure 8.5** State of charge (SOC) for several PHEV and charge scenarios.

capability incurs multiple cycles. These cycling scenarios will have very different impacts on battery life. In addition, this is only a sample, a single cycle selected from the 227 unique driving profiles. Relative benefits will vary with driving profile attributes.

The SOC characteristics of the entire fleet can also be assessed. Fig. 8.5 shows the ESS SOC information for all of the vehicle driving profiles in the dataset. The amount of time spent in each SOC range is compared for each charge scenario. The opportunity charge scenario results in more time in the highest SOC range of any of the scenarios. The PHEV-40 baseline spends time in both low SOC and high SOC ranges. The battery in the HEV scenario spends nearly all of its time in the mid-range SOC. The battery operating characteristics resulting from these simulations provide input information for the evaluation of the cycling impacts on battery life.

### 3.2 Battery aging with different charging scenarios

The battery aging model is used to simulate resistance growth and capacity fade for the 227 different one-day vehicle driving profiles. Vehicle simulations were performed for the two different vehicle/charging scenarios to generate battery cycling profiles: PHEV-40 with a single evening charge and PHEV-20 with opportunity charging throughout the day.

For a given vehicle driving profile, the two cases above impose very different cycles on the battery. The PHEV-20 battery is quickly cycled to its maximum  $\Delta$ SOC depth because of its smaller capacity. Under the opportunity charging scenario, it is also charged/discharged with more cycles per day. A constant temperature of 30°C is used for all simulations. Previous work [14] found that this condition closely matches ambient

temperature fluctuations in Phoenix, Arizona, commonly used as a worst-case climate for vehicle design.

It is important to note that all Li ion batteries have different characteristics and will degrade differently depending on chemistry, materials, and manufacturing techniques. Furthermore, the 15-year scenarios explored using the model are significantly extrapolated forward in time compared with datasets used to fit the model. The present battery degradation projections are not meant to represent definitive outcomes for a particular Li ion battery, but instead are intended to illustrate differences between the two different charging scenarios and demonstrate a variety of possible end-of-life outcomes. The results may aid the interpretation of battery degradation measured for actual vehicle fleets.

Fig. 8.6 shows the model-projected battery resistance growth and capacity fade at the end of 15 years of cycling for the 227 different vehicle driving profiles. Resistance

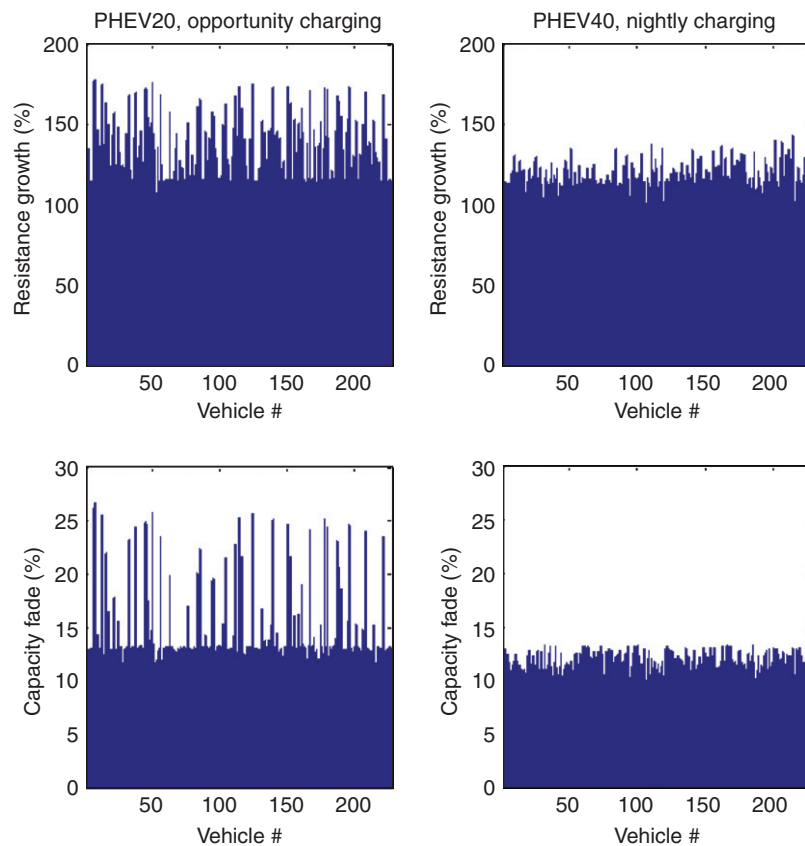


**Figure 8.6** Capacity fade and resistance growth for PHEV-20 opportunity charging (left column) and PHEV-40 nightly charging (right column) scenarios for various vehicle driving cycles. Results are at the end of 15 years at 30°C (comparable to Phoenix, Arizona, conditions) for each of the 227 different drive cycle profiles.

growth generally exceeds 100%, consistent with the model parameter assumptions discussed in Section 2.3. The large resistance growth indicates that these batteries would need to be sized with substantial excess power at the beginning of life in order to maintain usable energy and thus electric driving range for 15 years at this high-temperature condition of 30°C. Capacity fade ranges from 10 to 15% in most cases. Approximately 25% of the PHEV-20/opportunity charge cases experience severe capacity fade, greater than 13.5%. These most severe PHEV cases, however, encounter two to three deep discharges per day and over the 15 years accumulate far more cycles than the typical goal of 5,000 deep discharge cycles for PHEV batteries [9].

Fig. 8.7 shows battery degradation versus average daily SOC. All results are at the end of 15 years of cycling per each of 227 different vehicle driving cycles. A generally increasing trend in degradation is observed with average SOC, consistent with the increased voltage exposure for those batteries. For both the PHEV-20/opportunity charge and the PHEV-40/nightly charge cases, a minimum line of degradation with average SOC is observed. This line corresponds to shallowly or infrequently cycled batteries in which the storage degradation effect dominates. For the PHEV-40, the dominant cycle is once per day. This cycling is benign enough so that, in all but one PHEV-40 case, Li loss at 30°C controls capacity fade [8.2] rather than active site loss [8.3]. For the PHEV-20, with much

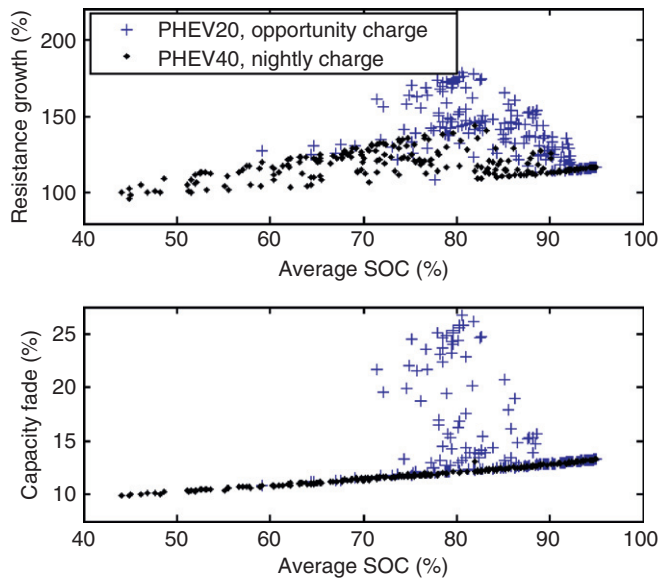


**Figure 8.7** Resistance growth and capacity fade at the end of 15 years at 30°C for 227 different vehicle driving cycles. The increasing trend with average SOC is due to the generally higher voltage exposure for those cases.



more frequent daily cycling, capacity fade is more often controlled by active site loss, indicated by the large variability in the possible capacity fade outcomes.

Resistance growth, rather than being controlled by either storage or cycling, is affected by both storage and cycling. In Fig. 8.7, a minimum line of resistance growth versus average SOC is again observed in the 227 different vehicle driving profiles. These are all cases in which storage effects dominate. For both PHEV-20/opportunity charge and PHEV-40/nightly charge cases, cycling further increases resistance growth in comparison to the storage-dominated cases. The PHEV-20 case shows roughly double the variability in resistance growth at the end of 15 years when compared with the PHEV-40 case.

Fig. 8.8 displays resistance growth and capacity fade at the end of 15 years at 30°C versus the maximum daily  $\Delta$ SOC, that is, the deepest discharge encountered each day for the 227 different cycles. Both resistance growth and capacity fade can either increase or decrease with maximum daily  $\Delta$ SOC swing, depending on the severity of the cycling. The increasing trend is due to the higher severity of cycling degradation caused by increasing  $\Delta$ SOC. This cycling-dominated degradation is much more common for the PHEV-20/opportunity charge case in comparison to the PHEV-40/nightly charge case.

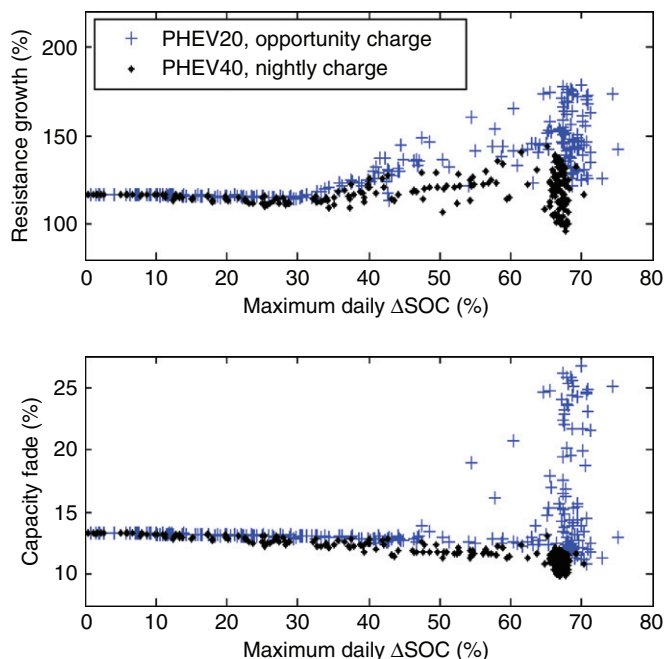


**Figure 8.8** Resistance growth and capacity fade at the end of 15 years at 30°C for 227 different vehicle driving cycles. Resistance growth and capacity fade can either increase or decrease with maximum daily  $\Delta$ SOC swing because of competing degradation mechanisms of voltage exposure and cycling stress.

The decreasing trend with  $\Delta\text{SOC}$  seen for other simulation results is due to the higher voltage exposure experienced by batteries that are cycled very little and instead spend much of their life near full charge. For these cycles, degradation is largely storage dominated.



## 4. CONCLUSIONS

The PHEV duty cycle of a full discharge on a daily basis for 10–15 years in an automotive environment may be one of the most difficult life performance challenges for batteries. Both cycling and calendar aging affect the power and capacity fade rates of a battery. A model has been developed to estimate the combined impacts of cycling and calendar aging influences, including time spent at high SOC, time spent at high temperature, and depth of discharge and frequency of cycling.

Batteries account for a significant portion of the initial cost of a PHEV. The long-term manufacturing cost of a PHEV-20 is expected to be on the order of \$3,000 less than that of a PHEV-40 because of its smaller battery. While a PHEV-20 may seem to have less potential for petroleum displacement as a result of its smaller electric range, recharging between trips can enable greater utilization of its smaller battery. Vehicle simulations for 227 different real-world driving profiles find that a PHEV-20, charged at every opportunity, can displace 5% more fuel than a PHEV-40 that is charged only once each night. This PHEV-20 opportunity charging scenario, however, places more frequent deep discharge cycles on the battery in comparison to the PHEV-40 nightly charging scenario and can be expected to degrade the PHEV-20 battery at a faster rate.

Simulations of battery aging for PHEV-20 opportunity charge and PHEV-40 nightly charge scenarios for 227 driving cycles illustrate a large variety of possible outcomes, depending on the manner in which a battery is cycled and stored. With more severe cycling, 25% of the simulated PHEV-20 opportunity-charged fleet experiences substantially greater degradation than the PHEV-40 nightly charged fleet after 15 years of cycling at 30°C (NCA chemistry). In some situations, cycling can reduce degradation by reducing time spent at high SOC; however, this effect is generally small when compared with the cumulative stress of multiple deep discharge cycles per day. Both storage- and cycling-dominated degradation outcomes are possible, depending on how the battery is used.

## ACKNOWLEDGMENTS

This work was sponsored by the United States Department of Energy, Office of Renewable Energy and Energy Efficiency, Vehicle Technologies Program. We would like to thank David Howell of Energy Storage for his support.

## REFERENCES

1. U.S. Energy Information Administration, 2006. <http://www.eia.doe.gov>.(accessed 10.07.06).
2. R. Hirsch, R. Bezdek, R. Wendling, Peaking of World Oil Production: Impacts, Risks, and Mitigation, U.S. Department of Energy, 2005. [http://www.netl.doe.gov/energyanalyses/pubs/Oil\\_Peaking\\_NETL.pdf](http://www.netl.doe.gov/energyanalyses/pubs/Oil_Peaking_NETL.pdf) (accessed 10.07.06)
3. T. Markel, Platform Engineering Applied to Plug-in Hybrid Electric Vehicles, 2007 SAE Congress, SAE International, Detroit, MI, 2007.
4. T. Markel, M. O'Keefe, A. Simpson, J. Gonder, A. Brooker, Plug-in HEVs: A Near-Term Option to Reduce Petroleum Consumption, NREL/540-MP-39415, 2005.
5. T. Markel, A. Simpson, Cost-Benefit Analysis of Plug-in Hybrid Electric Vehicle Technology, 22nd Electric Vehicle Symposium, Yokohama, Japan, 2006.
6. J. Gonder, T. Markel, A. Simpson, M. Thornton, Using GPS Travel Data to Assess the Real World Driving Energy Use of Plug-in Hybrid Electric Vehicles (PHEVs), NREL Report No. CP-540-40858, 2007.
7. K. Parks, P. Denholm, T. Markel, Costs and Emissions Associated with Plug-in Hybrid Electric Vehicle Charging in the Xcel Energy Colorado, NREL/TP-640-41410, 2007.
8. T. Markel, A. Pesaran, PHEV Energy Storage and Drive Cycle Impacts, NREL Report No. PR-540-42026, 2007.
9. A. Pesaran, T. Markel, Battery Requirements for Plug-in Hybrid Electric Vehicles: Analysis and Rationale, 23rd International Electric Vehicles Symposium (EVS 23), Anaheim, CA, 2007.
10. L. Gaillac, 23rd International Electric Vehicle Symposium and Exposition, Anaheim, CA, 2007.
11. M.C. Smart, K.B. Chin, L.D. Whitcanack, B.V. Ratnakumar, Storage Characteristics of Li-Ion Batteries, NASA Aerospace Battery Workshop, Huntsville, AL, November 14-16, 2006.
12. J.C. Hall, T. Lin, G. Brown, Decay Processes and Life Predictions for Lithium Ion Satellite Cells, 4th International Energy Conversion Engineering Conference and Exhibit, San Diego, CA, 2006.
13. A.D. Vyas, D.J. Santini, L.R. Johnson, Plug-in Hybrid Electric Vehicles' Potential for Petroleum Use Reduction, Transportation Research Board 88<sup>th</sup> Annual Meeting, Washington, D.C., 2009.
14. A. Pesaran, T. Markel, K. Smith, PHEV Battery Trade-off Study and Standby Thermal Control, 26th International Battery Seminar, Fort Lauderdale, FL, 2009.
15. J.C. Hall, A. Schoen, A. Powers, P. Liu, K. Kirby, Resistance Growth in Lithium Ion Satellite Cells. I. Non Destructive Data Analysis, 208<sup>th</sup> Electrochemical Society Meeting, Los Angeles, CA, 2005.
16. J.C. Hall, A. Schoen, A. Powers, P. Liu, K. Kirby, P. Biensan et al., Resistance Growth in Lithium Ion Satellite Cells. II. Electrode Characterization After Cell Wear Out, 208<sup>th</sup> Electrochemical Society Meeting, Los Angeles, CA, 2005.
17. R. Spotnitz, Symposium on Large Lithium Ion Battery Technology at 8th Advanced Automotive Battery Conference, Tampa, FL, 2008.
18. P. Biensan, Y. Borthomieu, Saft Li-Ion Space Batteries Roadmap, NASA Aerospace Battery Workshop, Huntsville, AL, 2007.
19. T. Markel, K. Smith, A. Pesaran, PHEV Energy Storage Performance/Life/Cost Tradeoff Analysis, 8th Advanced Automotive Battery Conference, Tampa, FL, 2008.



# Fuel Cell Electric Vehicles, Battery Electric Vehicles, and their Impact on Energy Storage Technologies: An Overview

Ulrich Eberle<sup>1</sup> and Rittmar von Helmolt

Hydrogen, Fuel Cell & Electric Propulsion Research Strategy, GM Alternative Propulsion Center Europe, Adam Opel GmbH, IPC MK-01, 65423 Rüsselsheim, Germany

## Contents

1. Introduction	227
2. The Boundary Conditions for Automotive Technology Development	228
3. Fuel Cell Electric and Battery Electric Vehicles — Two Competing Concepts?	230
4. Fuel Cell Electric Vehicles	232
5. Extended-Range Electric Vehicles	237
6. Infrastructure Issues	242
7. Conclusions	244
Acknowledgements	244
List of abbreviations	244
References	245



## 1. INTRODUCTION

In contrast to vehicles powered by a conventional fossil fuel- or biofuel-based ICE, the energy storage system is of crucial importance for electric vehicles (EVs). Two major options exist: one is the storage of electrical energy using batteries, the other one is the storage of energy in form of hydrogen.

The development of such EV concepts has a very long tradition at General Motors (GM) and Opel, regardless whether fuel cell electric vehicles (FCEVs), pure battery electric vehicles (BEVs), or hybrid variants are concerned. For instance, the world's first fuel cell EV, the GM Electrovan of 1966 was developed and designed by GM. Over the course of the late 1990s, this technology was revived and reintroduced within the framework of a large-scale development program. These efforts have led to the development of the current GM HydroGen4 fuel cell car, a mid-sized crossover vehicle based on the Chevrolet Equinox.

<sup>1</sup> Corresponding author: Ulrich.Eberle@de.opel.com

Also during the 1990s, a large development effort on pure BEVs was initiated. These automobiles were deployed to large-scale demonstration projects (e.g., the Opel Impuls to the so-called “Rügen-Projekt” on the German island of Rügen in the Baltic Sea, and to the Aachen area [1]). But also mass-produced EVs were designed and brought to the market on a lease basis, namely, the GM EV1.

The depletion of the fossil resources and the climatic change caused by anthropogenic CO<sub>2</sub> emissions have again made the development of zero-emission vehicles more and more important in the last few years. For all projects carried out by Opel and GM in this field, the GM Alternative Propulsion Center Europe in Mainz-Kastel (Germany) played an important and central role [2]. In the framework of this chapter, the latest vehicle projects like the GM HydroGen4 and the Chevrolet Volt (as well as the respective VOLTEC powertrain system) are introduced and discussed. The effects on the fuel infrastructure will also be evaluated.



## **2. THE BOUNDARY CONDITIONS FOR AUTOMOTIVE TECHNOLOGY DEVELOPMENT**

Approximately 900 million vehicles worldwide are on the roads today. About 96% of the fuel used for propulsion purposes is thereby produced from fossil sources of energy. There are estimates for the year 2020 that the number mentioned above will increase to approximately 1.1 billion vehicles, in particular due to the economic expansion and industrial development of China and India. This will inevitably have consequences for global crude oil demand and for the worldwide CO<sub>2</sub> emissions. Since an increase in demand of oil and CO<sub>2</sub> production proportional to the projected number of vehicles is not sustainable for financial, ecological, and political reasons, every implementation strategy must aim at the replacement of fossil fuels as a source of energy for automotive applications.

Therefore, a key element of GM’s advanced propulsion strategy is the electrification of the automobile, respectively, the displacement of gasoline by alternative energy carriers (see [Figure 9.1](#)). That leads to reduced fuel consumption, reduced emissions, and also to increased energy security via geographic diversification of the available energy sources. At GM, this strategy has its roots with the introduction of the first modern EV, the 1996 GM EV1. The EV1 was a pure BEV produced in small series for the “average Joe” driver. Unfortunately, the market experience with the EV1 and its initial lessees indicated that further significant improvements in BEV technology were needed. Some EV1 drivers coined the term “range anxiety” describing their omnipresent concern or even fear of becoming stranded with a discharged battery in a limited-range vehicle, away from the electric infrastructure. Hence, improvements in onboard energy storage (directly proportional to vehicle range) and, in particular,

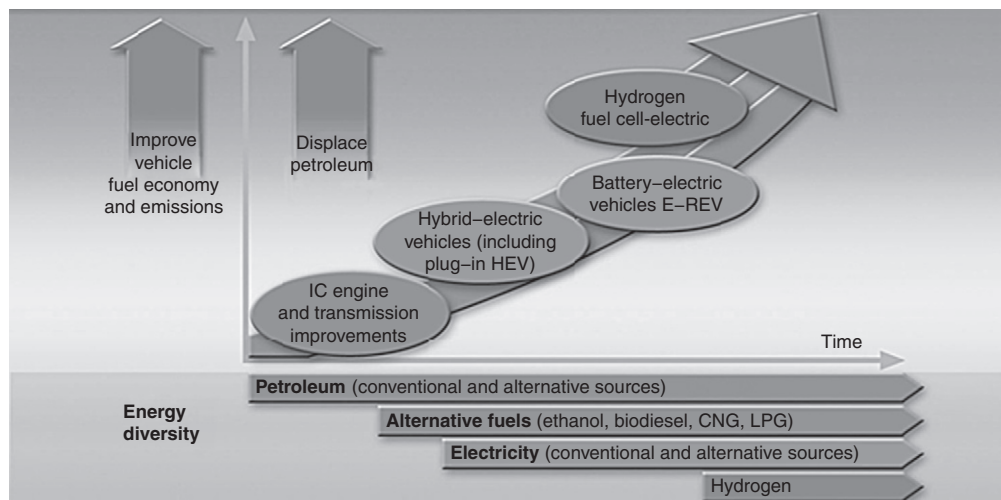


**Figure 9.1** GM's advanced propulsion strategy.

charging time were assessed to be essential for a more widespread deployment of BEVs. Due to these constraints, pure BEVs have not reached the commercial mass market until now. Nevertheless, most of the EV-enabling electric components and systems have found utility in the meantime by adapting them for the usage in mild and full hybrid electric vehicles (HEVs). Such vehicles do not provide full power by exclusively using the electric motor. Therefore, the power and energy level requirements for the system components are reduced in comparison to a conventional BEV. In addition, while conventional hybrids (both mild and full HEVs) improve vehicle efficiency (thus reduce gasoline consumption, and thereby, CO<sub>2</sub> emissions), all the energy they consume is generated from an onboard liquid medium. The onboard electrical engine and the storage system are only used to shift the operating point of the ICE to a more favorable point on the efficiency map and to enable recuperation. Thus, HEVs provide unfortunately not any additional pathways to utilize CO<sub>2</sub>-neutral renewable energy sources. Partially, these drawbacks may be resolved by introducing so-called extended-range electric vehicles (E-REVs) that are discussed in the following sections.

Zero-emission vehicles using an electric powertrain system based on hydrogen fuel cells or purely battery-electric systems that are fully competitive to conventional vehicles regarding performance and ease-of-use represent the ultimate target of the GM strategy (see Figure 9.1). A further important step into this direction is the start of mass production of the Chevrolet Volt at the end of 2010, as well as the introduction of other vehicles (e.g. the Opel Ampera) which are also based on the VOLTEC technology [2].

### 3. FUEL CELL ELECTRIC AND BATTERY ELECTRIC VEHICLES — TWO COMPETING CONCEPTS?

Within the general public and also within the automotive and fuels community very often the impression is created that an exclusive decision has to be made between fuel cell electric and battery electric vehicles, as question of either/or. However, this is definitely not the case since these technologies address different areas of the vehicle market. This is due to the extremely different energy densities of the applied energy carriers (see Figure 9.2).

To realize a vehicle with a range of 500 km, using today's diesel technology, a tank system that weighs approximately 43 kg and requires a volume of just less than 50 l is needed. To realize a corresponding zero-emission vehicle using hydrogen technology, one has to build on a system weighing about 125 kg (based on a 700 bar compressed gaseous hydrogen vessel). The energy storage gets even heavier if a future highly advanced lithium-ion (Li-ion) battery system (usable system energy density: 120 Wh/kg; current technology is closer to 90 Wh/kg) would be implemented (see Figure 9.2): To provide a vehicle range of 500 km, the weight of the energy storage system would be just below one metric ton. Furthermore, a hydrogen tank can be refilled completely within 3–5 min, very similar to a conventional diesel tank. In contrast, recharging a battery can take—depending on the available infrastructure and battery size—from hours (considering a 50 kW fast charging point) up to many hours or even to a whole day (conventional 230 V/16 A electrical outlet).

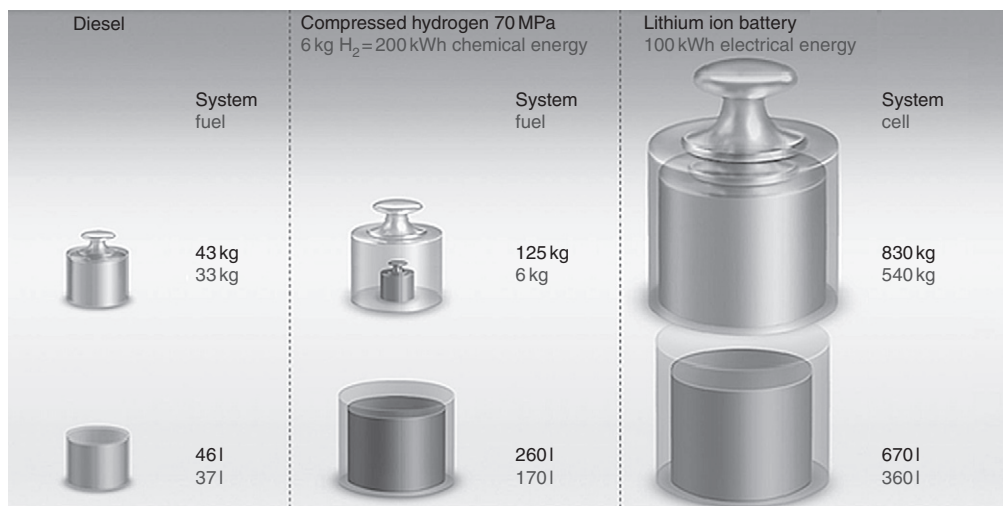


**Figure 9.2** Energy storage system weight and volumes for various energy carriers (considering a vehicle range of 500 km).



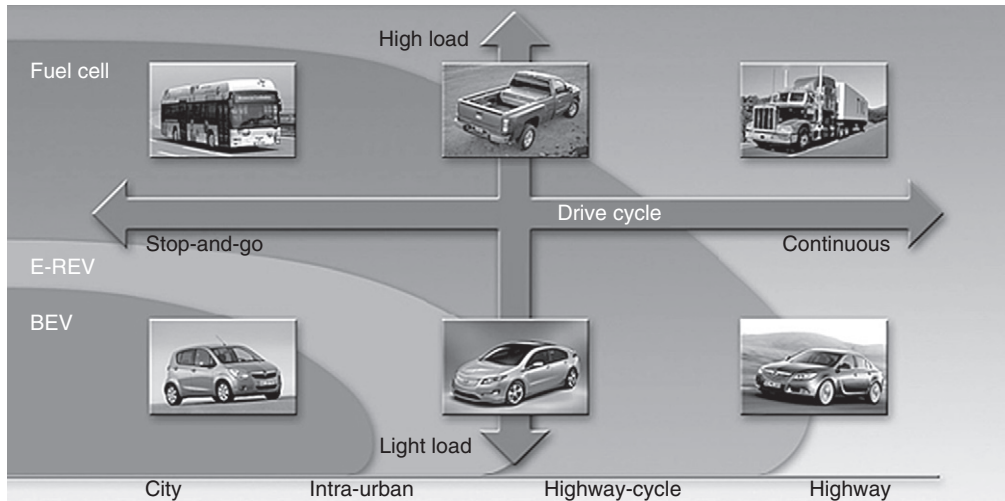


**Figure 9.3** Application map for various EV technologies.

Projections show that a hydrogen tank system for a vehicle range of 500 km could be manufactured for approximately US\$ 3,000 at high-volume production; on the other hand, a comparable 100 kWh battery would cost approximately US\$ 50,000.

Therefore, it makes sense to develop and use a BEV for a driving and duty cycle for which a smaller battery and a lower range is sufficient and viable. The impact of the energy storage densities and drive cycles, respectively, duty cycles on an appropriate propulsion technology is shown in Figure 9.3. The pure battery vehicle is the technology of choice for small urban vehicles with ranges up to 150 km. A so-called E-REV such as the Chevrolet Volt or the Opel Ampera is perfectly suited for those customers who need sometimes—but not too often—longer ranges of up to 500 km; and for those who are willing to accept a small ICE in order to ensure the range beyond the initial 60 km of pure EV operation. On the other hand, hydrogen fuel cell vehicles offer a different kind of advantage: they are always operated as zero-emission vehicles, can be refueled within 3–5 min, and offer a long range of about 500 km at full performance, even for family-sized cars.

Due to its comparatively high-energy density of 1600 Wh/kg of tank system weight, hydrogen is the ideal energy carrier to serve as intermediate store of fluctuating renewable energy such as solar and wind power, and to enable the usage of this green energy as transportation fuel. Early commercialization of the automotive fuel cell technology is expected to start sometime in between 2015 and 2020.

Hence, depending on the required operating range, a future electric powertrain will either be combined with just a battery (BEV), or the needed energy for longer ranges will be provided by an ICE-generator set (E-REV) or by a high-performance fuel cell (FCEV). These two latter concepts will be introduced and discussed in detail in Sections 4 and 5.



## 4. FUEL CELL ELECTRIC VEHICLES

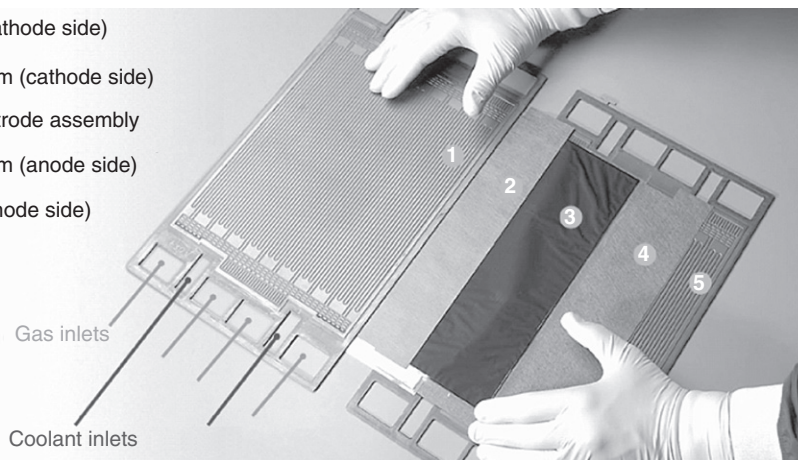
As already mentioned, General Motors has a long history of innovations within the field of hydrogen technology: the world's first fuel cell car, the Electrovan (1966), was developed by GM. This vehicle was equipped with an alkaline fuel cell (AFC) and two cryogenic tank vessels for liquid hydrogen and liquid oxygen [3,4,5].

The fuel cell stack represents the core component of the complete fuel cell power system. There is a wide range of fuel cell types available, including mid- and high-temperature fuel cells. However, only low-temperature fuel cells working with a proton-conducting polymer membrane (proton exchange membrane, PEM) are viable for automotive applications. PEM fuel cells combine a comparatively low operating temperature, typically between 60 and 80°C, with a high-power density, the option of conventional air operation, and the potential of being manufactured at low cost. PEM fuel cell-based power systems provide similar performance features as ICEs, with which they are competing. The fuel cell stack is built up from hundreds of single cells (see Figure 9.4a) and—like a battery—it directly converts chemical energy into electrical energy.

The “fuel,” however, is not contained in the electrode, but supplied to the electrode from a separate subsystem. As long as fuel and oxidant are provided to the fuel cell at

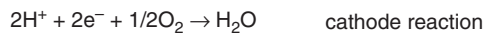
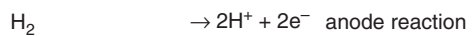
(A)

- 1 Bipolar plate (cathode side)
- 2 Diffusion medium (cathode side)
- 3 Membrane electrode assembly
- 4 Diffusion medium (anode side)
- 5 Bipolar plate (anode side)



(B)

1) Acidic electrolyte, e.g.  
in case of a PEMFC:



2) Alkaline electrolyte, e.g.,  
in case of an AFC:

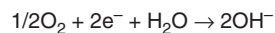


**Figure 9.4** (A) Setup of PEM fuel cell; (B) chemical reactions at the electrodes.

sufficient quantities, the generation of electrical energy is ensured. The challenge consists in evenly supplying all single cells of the stack with fuel and also in removing the reaction (or waste) products properly. In the case of a hydrogen PEM fuel cell, the waste product is just pure water.

After the technology transition from AFC to PEM fuel cells, the various generations of HydroGen1 to HydroGen4 were developed. The integration of the fuel cell system into vehicles can be done similarly to the integration of ICEs. It has been demonstrated that sufficiently powerful and compact drivetrains could be realized. The fuel cell system and the electric traction system of the GM HydroGen3 were packaged in a way that they fitted into the same volume as an ICE propulsion module; even the same mounts could be used. Such an integrated fuel cell module (population dress-up module, PDU) allows the simple and cost efficient vehicle assembly in existing vehicle plants. Thus, PDUs are a reasonable technology scenario for the introduction of large-volume production on the basis of existing platforms. There is, however, no technical restriction that would rule out a completely different configuration of the fuel cell powertrain components on board of the vehicle.

The scalability of fuel cell systems also facilitates the adaptation of such a drivetrain to different vehicle sizes (see Figure 9.5). One example is the fuel cell system that was originally developed for the GM HydroGen3 van, and afterward was adapted to a small vehicle, the Suzuki MR Wagon FCV, using a shorter fuel cell stack with reduced cell count. Eventually, it was adapted to a GMT800 truck by doubling the stack and some other components.

Here 70 MPa CGH<sub>2</sub> (compressed gaseous hydrogen) storage systems are state of the art since the public presentation of the HydroGen3 in 2002 [3]. As shown in Figure 9.2, 1,600 Wh/kg can be achieved for such a single-vessel tank system. Typically, 4–7 kg of hydrogen have to be stored onboard. That remains to be a significant issue for the vehicle integration. Furthermore, cylindrical vessels are required for CGH<sub>2</sub> fuel storage. In existing vehicles, without any modifications, there is not enough space for hydrogen storage devices that could provide a range comparable to conventional vehicles. Hence, rear body modifications are necessary to integrate the hydrogen storage vessel(s). In an extreme case, one could imagine concepts where the car is built around the hydrogen storage. Vehicle designers at GM have developed the Chevrolet Sequel concept car (see Figure 9.6a)



**Figure 9.5** The GM HydroGen3 system architecture (60 kW at the wheels) has been scaled down for the integration into a Suzuki MR Wagon FCV (38 kW at the wheels), and scaled up for the propulsion of a Chevrolet Silverado military truck (120 kW at the wheels).

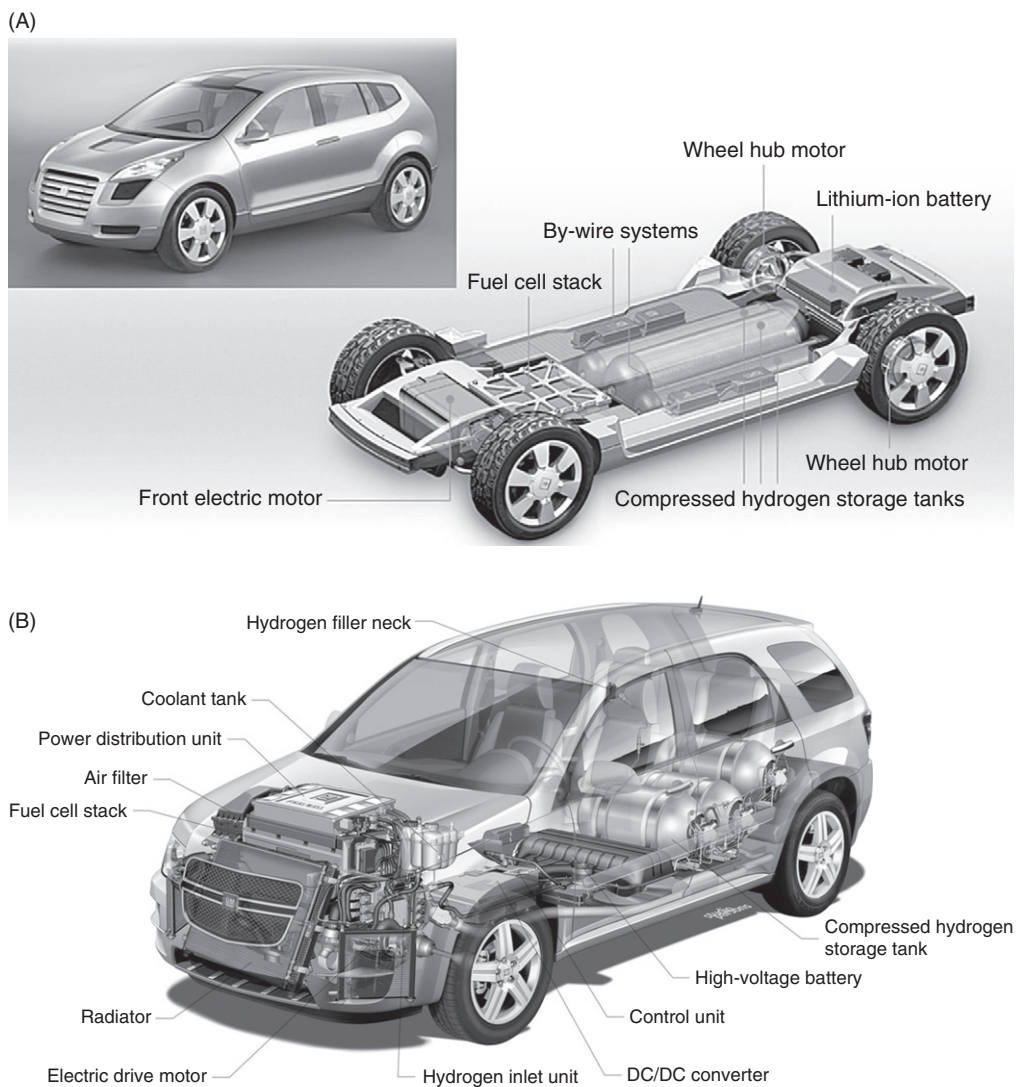


**Figure 9.6** (A) GM Sequel and the skateboard chassis; (B) GM HydroGen4 vehicle.

providing enough space for three large 70 MPa CGH<sub>2</sub> vessels (total fuel capacity: 8 kg of hydrogen). By doing so, for the very first time, an FCEV operating range of significantly more than 300 miles could be achieved and demonstrated on public roads between suburban Rochester and New York City in May 2007. The fuel cell system of the Sequel has been packaged into the vehicle underbody as well, offering flexibility for the interior design. Although the Sequel is only a concept vehicle with no production intent at this time, one may imagine that vehicles one day will be developed and optimized for the specific characteristics and opportunities that fuel cells and H<sub>2</sub> can offer.

Since autumn 2007, within the framework of “Project Driveway”, more than 100 cars of the current generation HydroGen4 (Figure 9.6b) were deployed to demonstration projects all over the world (e.g., in the United States and in Germany). These vehicles offer an improved everyday capability and a higher performance than their predecessors (see Table 9.1). For instance, the cars can be both operated and started at very low temperatures, down to  $-25^{\circ}\text{C}$ .

**Table 9.1** Technical specifications of the GM HydroGen4

Vehicle type	Five-door, crossover vehicle, front-wheel drive, based on the Chevrolet Equinox
Dimensions	
Length	4,796 mm
Width	1,814 mm
Height	1,760 mm
Wheelbase	2,858 mm
Trunk space	906 Liter
Weight	2,010 kg
Payload	340 kg
Hydrogen storage system	
Type	3 Type IV CGH <sub>2</sub> vessels
Operating pressure	70 MPa
Capacity	4.2 kg
Fuel cell system	
Type	PEM
Cells	440
Power	93 kW
Battery system	
Type	Ni-MH
Power	35 kW
Energy content	1.8 kWh
Electric propulsion system	
Type	Three-phase, synchronous motor
Continuous power	73 kW
Maximum power	94 kW
Maximum torque	320 Nm
Performance	
Top speed	160 km/h
Acceleration (0–100 km/h)	<12 s
Range	320 km
Operating temperature	$-25^{\circ}\text{C}$ to $+45^{\circ}\text{C}$ , vehicle can be parked at ambient temperature $<0^{\circ}\text{C}$ (without external heating)

The electrical propulsion system provides a maximum torque of 320 Nm at the motor and accelerates the HydroGen4 in less than 12 s from 0 to 100 km/h. The continuous power output of the electric motor of 73 kW is sufficient for a maximum

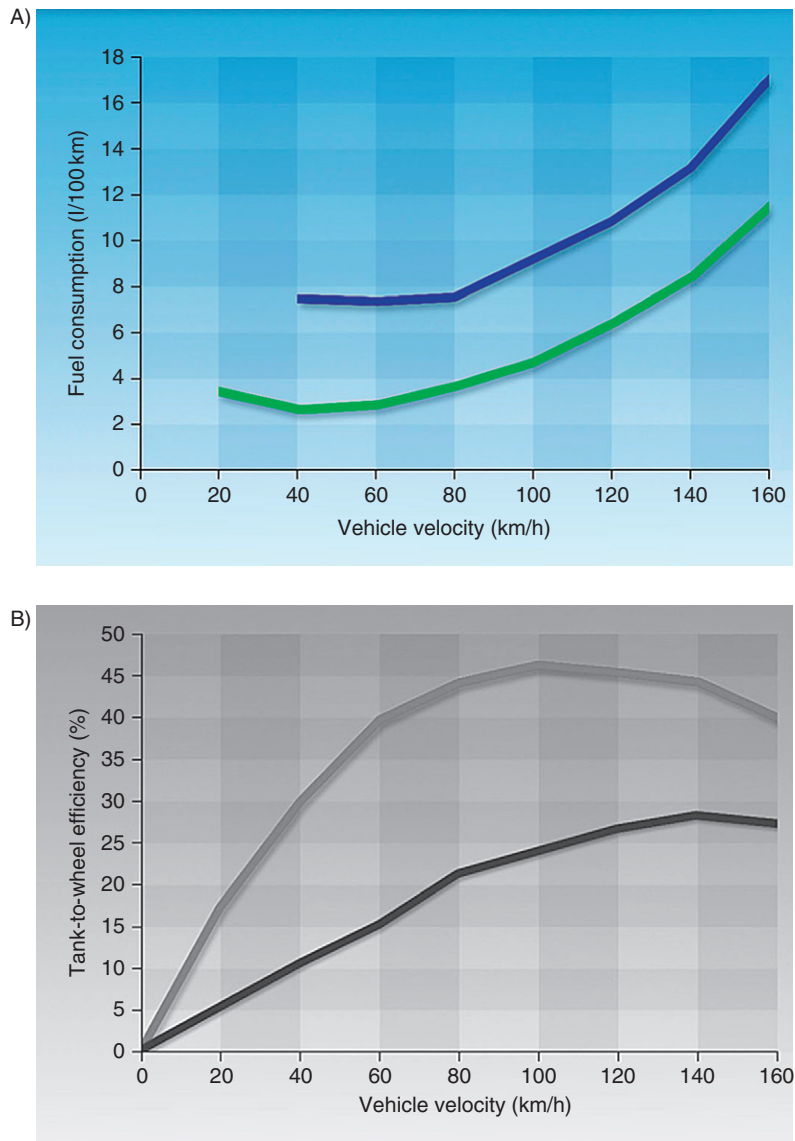


**Figure 9.7** (A) Fuel consumption versus vehicle speed for the GM HydroGen4 (lower line, hydrogen consumption converted to gasoline equivalent) and the conventional ICE version of the Chevrolet Equinox (upper line); (B) efficiency versus vehicle speed for HydroGen4 (upper line) and Equinox (lower line).



speed of 160 km/h; the maximum performance is 93 kW. Three carbon-fiber tanks onboard store 4.2 kg of hydrogen and enable a range of 320 km. The empty hydrogen storage system can be completely refilled within 3 min (according to SAE J2601 and SAE J2799). To further improve the agility of the vehicle and to increase the efficiency by enabling recuperation, a nickel metal-hydride battery (Ni-MH) with an energy content of 1.8 kWh is also installed onboard.

More than 10,000 customers in four countries drove the 115 HydroGen4 vehicles (10 of these are operated within the “Clean Energy Partnership” in Berlin); more than 80 mainstream drivers have used vehicles for extended periods of 2–3 months. The vehicles went through a total road performance of over 1,600,000 km (status: September 2009). A fuel cell system durability of about 30,000 miles has been demonstrated within Project Driveway, and an updated HydroGen4 system is projected to reach 80,000 miles. Further improvements will be achieved for the 2015–2020 early commercialization timeframe.

The vehicles proved to be more efficient than the comparable conventional Chevrolet Equinox vehicle with gasoline engine by a factor of 2 (EPA Composite cycle, 4.6 l/100 km of gasoline equivalent in comparison with 9.6 l/100 km of gasoline for the Equinox, see Figure 9.7). Particularly passenger vehicles are mostly operated at loads significantly below their rated power: for such operating conditions, the gain in efficiency offered by fuel cells is maximum. However, at very low-power output, even the fuel cell system efficiency sharply drops, while the fuel consumption increases. This is attributed to many balance-of-plant components, such as the air compressor, as they have to be operated even at idle power. At full load, similar to ICEs, the fuel consumption is significantly higher, but the relative drop in efficiency is stronger than for ICEs.

For a detailed discussion of the fuel cell vehicle efficiency and the corresponding values for key components, the authors recommend Ref. [3]. Many aspects of hydrogen storage technology (including alternative storage options) are summarized in Ref. [4].



## 5. EXTENDED-RANGE ELECTRIC VEHICLES

On the occasion of the North American International Auto Show in 2007 the Chevrolet Volt (see Figure 9.8 and Table 9.2) and the VOLTEC technology were presented for the first time [2,3]. The Volt is an EV equipped with an additional gasoline engine that is just used to extend the vehicle range beyond the electric range when required (E-REV). Main energy storage is a Li-ion battery with a nominal energy content of 16 kWh (depth-of-discharge is about 50%, i.e., 8 kWh are usable) and a pure battery-electric range of 60 km. The T-shaped battery (see Figure 9.8c and Table 9.2) consists of four modules containing more than 220 cells and the complete automotive battery pack weighs approximately 180 kg. That energy storage system was developed by GM in cooperation with the Korean battery cell manufacturer LG Chem.

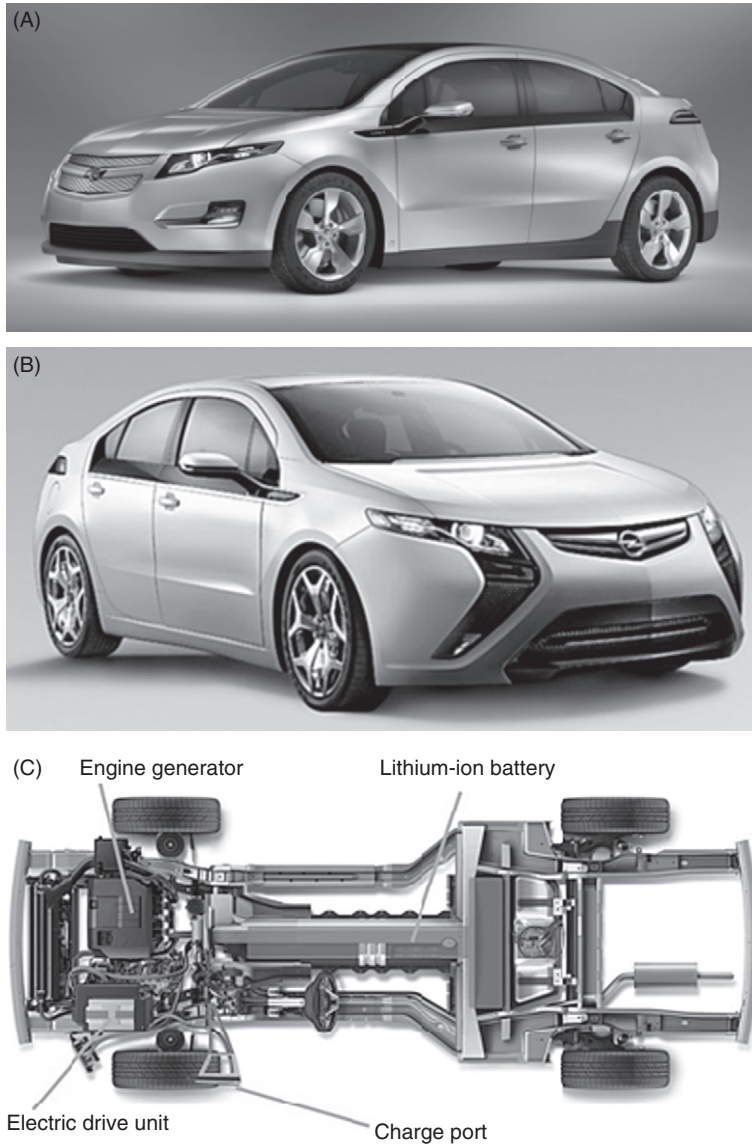


**Figure 9.8** (A) Chevrolet Volt, (B) Opel Ampera (based on the VOLTEC system), and (C) T-shaped battery.

The electric powertrain offers a maximum power output of 111 kW and a maximum torque of 370 N m at the motor. This is sufficient to accelerate the Volt from 0 to 100 km/h in less than 9 s and the VOLTEC powertrain enables a top speed of 160 km/h. The nominal size of the battery of 16 kWh was derived from the fact that a vehicle range of about 50–60 km is needed to cover at least 80% of the daily driving profiles of regular

**Table 9.2** Technical specifications of the Chevrolet Volt

Vehicle type	Electric vehicle, front-wheel drive; range extender; charging via electrical grid using a standard wall outlet
Dimensions	
Length	4,404 mm
Width	1,798 mm
Height	1,430 mm
Wheelbase	2,685 mm
Battery system	
Type	Li-ion battery
Cells	>220
Weight	180 kg
Length	1.8 m, T-shaped
Power	Provides full performance
Energy content	16 kWh (ca. 8 kWh usable)
Electric propulsion system	
Type	Three-phase induction motor
Maximum Power	111 kW
Maximum Torque	370 N m
Range extender	
Type	Gasoline, naturally aspirated, 1.4l displacement, family 0-derivative
Power	53 kW
Performance	
Maximum speed	160 km/h
Acceleration (0–100 km/h)	9 s
Range	Electric range: up to 60 km; approximately 500 km with range extender

customers in many countries (as an example data for Germany is given in [Figure 9.9](#)). For these distances, the vehicle is operated as a pure electric car and therefore as a zero-emission vehicle. This operating mode is, hence, called “charge-depleting” mode or “EV mode.” By limiting the battery size, it is possible to integrate such an extended-range drivetrain concept into GM’s global compact architecture (see [Figures 9.8](#) and [9.10](#)). Doing so, also the total battery costs can be limited since these costs are more or less proportional to the nominal energy content (see [Section 3](#)).

An additional advantage of a battery of such dimensions is that the usable 8 kWh of electrical energy could be recharged in just a few hours in Europe, but also in the United States (US standard wall outlet 110 V/16 A: about 6 h; European standard wall outlet 230 V/16 A: about 3 h). On the vehicle side, both Volt and Ampera are equipped with a socket according to SAE J1772. The required cord-set (SAE J1772 plug on the vehicle



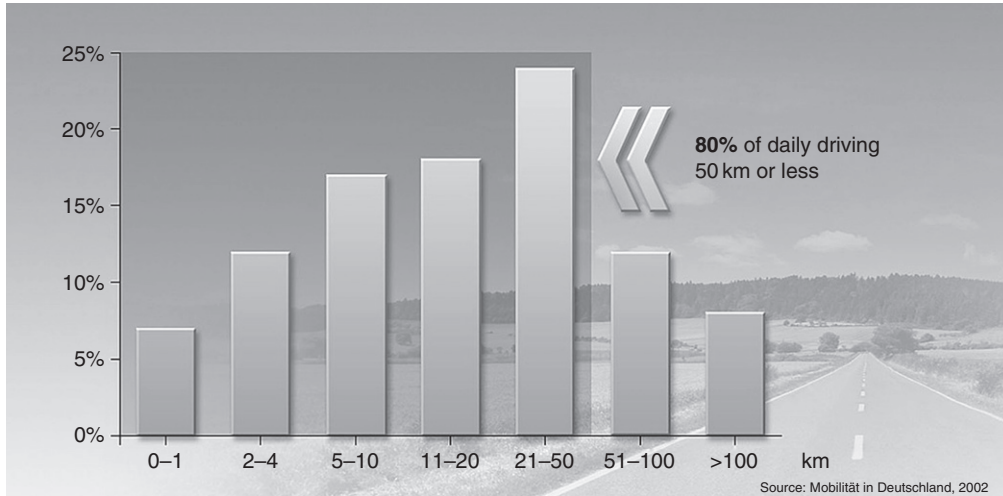


**Figure 9.9** Daily driving distances in Germany.

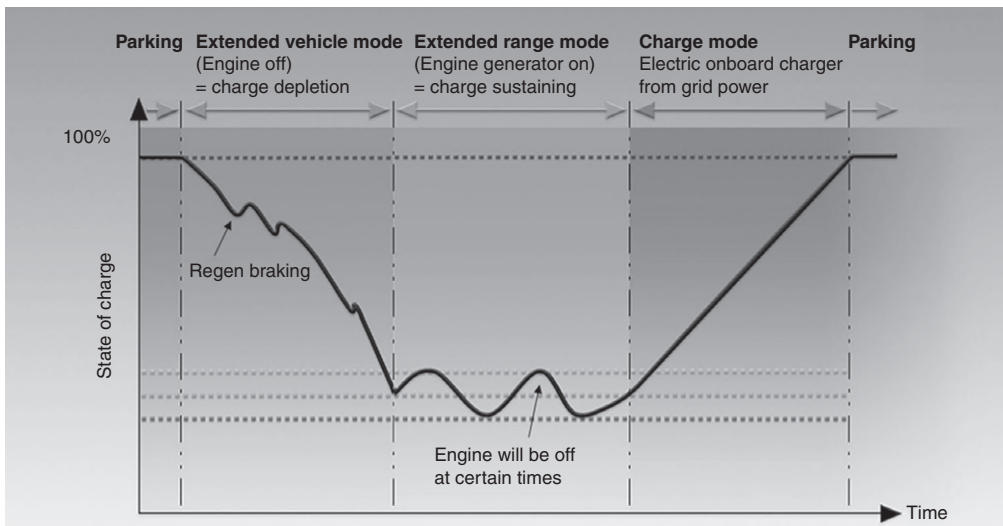


**Figure 9.10** E-REV operating concept, approximately 50% of the nominal battery energy content is used.

side → country-specific home plug) is carried in the vehicle. In contrast, due to their bigger batteries, pure battery EVs would be dependent on off-board chargers (or even quick-charging stations) applying higher voltage and current levels in order to achieve such acceptable recharging times.

A naturally aspirated family-0 gasoline engine with a displacement of 1.4l generates 53 kW of power that can be utilized when the state of charge drops below a certain

value: this operating mode is called “charge-sustaining” or “extended-range” mode (see Figure 9.10). By adding the ranges of both charge-depleting and charge-sustaining modes, a total vehicle range of more than 500 km can be achieved. For the normal daily driving profiles, it is nevertheless ensured that the VOLTEC vehicles are driven without any fossil fuel consumption and the related issues. For an annual electric driving distance of 13,000 km, the Chevrolet Volt or an Opel Ampera would require only 1730 kWh of electrical energy. This value corresponds to a level of just about 40% of the annual energy consumption of an average four-person household in Germany [6] (4500 kWh). Considering the New European Driving Cycle (defined in the ECE R101 document, see also the respective appendices for EV operation), less than 40 g CO<sub>2</sub>/km would be emitted by an Opel Ampera.

As mentioned before, the Chevrolet Volt and the VOLTEC propulsion technology have been presented for the first time in January 2007. In the same year, the decision was made to initiate the product engineering and to introduce the Volt as a volume production vehicle. The first battery packs were already assembled in late 2007, and the first components in vehicle tests were started. In 2008, the first packs were mounted on mule vehicles for early tests of the production-intent propulsion system, and the first vehicle crash tests were successfully performed (see Figure 9.11). Till early summer 2009 about 80 Volt prototypes were built. The series production of the Chevy Volt will start at the end of 2010 at a GM plant in Michigan, USA; the volume production of the Opel Ampera with the same VOLTEC powertrain technology is set to begin about 1 year later.

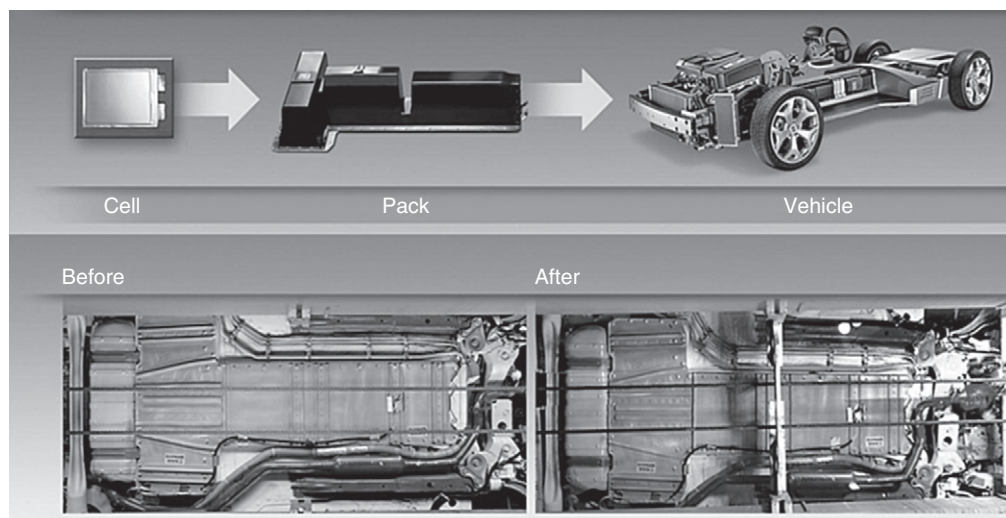


**Figure 9.11** (Up) Integration of battery cells into modules and vehicle; (down) first crash test: the T-shaped battery is visible.

## 6. INFRASTRUCTURE ISSUES

To set up a sufficiently dense (and sufficiently consumer-friendly) hydrogen filling station infrastructure, for example, in the United States, approximately 12,000 gas stations need to be built. The underlying model [7] assumes that in the 100 biggest metropolitan areas of the United States (comprising about 70% of the total population) the maximum distance between two filling stations would not exceed 2 miles, resulting in 6,500 intraurban stations.

On the freeways connecting these large conurbations, a filling station would have to be installed every 25 miles [7]. This highway network would correspond to 5,500 additional stations. Such a comprehensive filling station network (see Figure 9.12) could serve about 1 million hydrogen vehicles and would cost approximately US\$10–15 billion over a time period of 10 years.

Similar to today's gasoline infrastructure, a hydrogen gas station would be able to serve hundreds of vehicles per day, since just 3–5 min are needed to refill a hydrogen car. This is not the case for pure BEVs: for battery technology and electric grid stability reasons, charging times of at least one to several hours or even longer periods are required, that is, a standard public charging point becomes blocked for hours by just one customer. Hence, such a station could only serve a few vehicles per day. For EVs, there exists a strong interdependency between two normally completely distinct activities, namely “parking” and “refueling.” Furthermore, the typical customer does not want to wait at the vehicle until it is recharged. On the other hand, the charging points are comparatively cheap even at low volumes (US\$4,000–8,000 including installation)

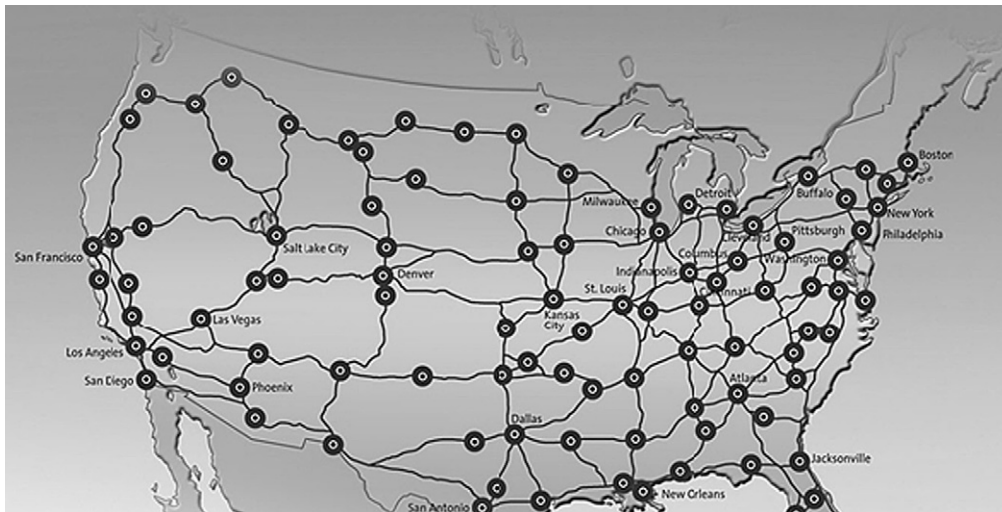


**Figure 9.12** 100 largest US metropolitan areas and interconnecting corridors.

leading to low initial costs for early fleet demonstrations. This is in particular valid when the conventional 230V/16A technology (e.g., chargers, connectors, and wall outlets) can be used.

Although a single charging point is much less expensive than an H<sub>2</sub> fueling station, considering an ultimate scenario with an increasing penetration of the vehicle fleet with EVs (i.e., >1 million zero-emission vehicles in Germany), the cost for the implementation of a local battery recharging infrastructure under these assumptions approaches the initially much higher cost of a more centralized hydrogen infrastructure. This is caused by the high number of required charging pole installations: in fact, the ratio of public charging points per vehicle needs to be close to 1 or even higher. However, for small- to mid-sized fleets of zero-emission vehicles, the infrastructure for pure battery or E-REVs can be set up more simply due to the better scalability and the lower initial cost for a sufficiently dense network.

On the other hand, hydrogen offers a different and very important advantage: due to its high-energy density, hydrogen as an energy carrier is the ideal partner for the intermediate storage of fluctuating, renewable energies. Doing so, excess amounts of sustainable energy sources such as solar and wind power can be made available not only for stationary but also for automotive applications. Let us consider, for example, the North German electric power grid, the so-called “E.ON Kontrollzone Nord”: in October 2008, the power fed into the grid by wind turbines fluctuated (sometimes within a few hours, sometimes within days) between a maximum of approximately 8,000 MW and virtually zero. It is evident that it would be very helpful to “buffer” energy in intermediate stores to handle these fluctuations, that is, to absorb energy during a certain time period from the grid or, vice versa, to provide the required energy back to the grid.

Today, this “buffer” is realized as pumped hydro stores (the largest facility in Germany, Goldisthal, offers a maximum storage capacity of 8,000 MWh [8]) or in compressed air reservoirs (typically a salt cavern, with a volume of 2 million cubic meters, and a maximum storage capacity of 4,000 MWh). If hydrogen would be used as medium instead of compressed air, up to 600,000 MWh energy could be stored in the identical salt cavern. Unlike conventional technology, hydrogen therefore offers not only a buffer store for short time periods ranging from a few minutes to hours. Such a large-scale hydrogen store could absorb the excess wind energy of several days. The stored gas eventually could be either converted back into electric energy or could simply be used as a fuel for hydrogen vehicles. In contrast, even large fleets of pure battery EVs are not able to provide a competitive energy storage dimension: if 5 kWh of the usable energy content of an EV battery (for operating lifetime and customer ease-of-use considerations, 10% of the total nominal energy content should not be exceeded) could be subscribed to and utilized by the electric utility, just to replace the pumped hydro store of Goldisthal, 1.6 million EVs would be needed.



## 7. CONCLUSIONS

GM's long-term advanced propulsion strategy consists in displacing gasoline and diesel fuel as energy sources for the automotive application. This will be achieved by a continuously increasing electrification of the powertrain. However, the energy density of current and future automotive batteries unfortunately provides limitations for the development of pure battery electrical vehicles as soon as longer vehicle ranges significantly beyond 100 miles are required. Therefore, GM and Opel pursue the E-REV and FCEV concepts for this application field. Ranges of 500 km can be achieved with hydrogen fuel cell vehicles and 700 bar CGH<sub>2</sub> tanks; moreover, hydrogen can be produced at large scale at competitive prices. In the area of longer-range sustainable mobility, the future of automotive propulsion seems to rely mostly upon E-REV and FCEV vehicles and for some urban applications also upon small-sized BEV. During the early commercialization phases, all of these vehicles will be more expensive than comparable conventional vehicles; therefore, the support and cooperation of all involved stakeholders is indispensable during this initial phase. The most important players thereby are primarily car manufacturers, energy companies, and the governments. But also the end consumer needs to accept and buy these innovative vehicles despite the remaining incremental cost compared to conventional vehicles.

## ACKNOWLEDGEMENTS

The authors appreciate fruitful discussions and valuable input from D. Hasenauer, S. Berger, and L.P. Thiesen on sustainable energy and transportation technologies.

## LIST OF ABBREVIATIONS

AFC	alkaline fuel cell
BEV	battery electric vehicle
CNG	compressed natural gas
CGH <sub>2</sub>	compressed gaseous hydrogen
DC	direct current
ECE	Economic Commission for Europe
E-REV	extended-range electric vehicle
EV	electric vehicle
EPA	Environmental Protection Agency
FCEV	fuel cell electric vehicle
GM	General Motors
HEV	hybrid electric vehicle
ICE	internal combustion engine
Li-ion	lithium-ion
LPG	liquefied petroleum gas
NEDC	New European Driving Cycle
Ni-MH	nickel metal-hydride battery
PEM	proton exchange membrane

PEMFC	proton exchange membrane fuel cell
PDU	propulsion dress-up module
SAE	Society of Automotive Engineers

## REFERENCES

1. R. Bady, J.W. Biermann, B. Kaufmann, H. Hacker, European Electric Vehicle Fleet Demonstration with ZEBRA Batteries, US, *SAE* paper 1999-01-1156. <http://www.sae.org/technical/papers/>
2. T. Johnen, R. von Helmolt, U. Eberle, Conference Proceedings Volume of Technischer Kongress 2009, German Automotive Industry Association VDA.
3. R. von Helmolt, U. Eberle, Hydrogen Technology, A. Leon (Ed.), Springer, Berlin and Heidelberg (both Germany) 2008, pp. 273–290, ISBN 978-3-540-79027-3.
4. M. Felderhoff, C. Weidenthaler, R. von Helmolt, U. Eberle, *Phys. Chem. Chem. Phys.* 9 (2007) 2643.
5. C. Marks, E.A. Rishavy, F.A. Wyczalek, SAE Congress, January 1967, Detroit, USA, SAE paper 670176.
6. EnergieAgentur.NRW (Energy Agency of the German state of North Rhine-Westphalia), [http://www.ea-nrw.de/\\_database/\\_data/datainfopool/prozentuale\\_anteile\\_tabelle.pdf](http://www.ea-nrw.de/_database/_data/datainfopool/prozentuale_anteile_tabelle.pdf), information retrieved on September 1, 2009.
7. B.K. Gross, I.J. Sutherland, H. Mooiweer, GM/shell study 2007, Hydrogen Fueling Infrastructure Assessment. <http://www.h2andyou.org/pdf/10Things.pdf>; information retrieved on September 1, 2009.
8. Pumped Hydro Store Goldisthal, Technical Specifications. [http://www.vattenfall.de/www/vf/vf\\_de/Gemeinsame\\_Inhalte/DOCUMENT/154192vatt/Bergbau\\_und\\_Kraftwerke/P02115223.pdf](http://www.vattenfall.de/www/vf/vf_de/Gemeinsame_Inhalte/DOCUMENT/154192vatt/Bergbau_und_Kraftwerke/P02115223.pdf); information retrieved on September 1, 2009.

# On the Road Performance Simulation of Battery, Hydrogen, and Hybrid Cars

Bent Sørensen<sup>1</sup>

Department of Environmental, Social and Spatial Change, Bld. 11.1, Universitetsvej 1, Roskilde University, PO Box 260, DK-4000 Roskilde, Denmark

## Contents

1. Introduction	247
2. Simulation of Efficient Internal Combustion Vehicle	249
3. Simulation of Fuel Cell Vehicle	257
4. Simulation of Battery Vehicle	260
5. Simulation of Hybrid Vehicles	267
6. Optimization of Hybrid Configuration	268
7. Conclusions	271
References	272
Appendix: Performance Measures	273



## 1. INTRODUCTION

While batteries and fuel cells are related technologies, one storing the energy-containing agents inside and the other outside the electrochemical device, this does not necessarily mean that they develop in parallel, cost- or performance-wise. During the 1970s and 1980s, batteries received much more R&D attention than fuel cells, in the hope that lead-acid batteries could be replaced by battery types with better power and energy densities, both for small and large-scale applications, and with a tolerable cost level. This development went disappointingly much slower than anticipated, although finally new battery types such as lithium-ion based ones did take over the market for small consumer items (first watches, calculators, and similar devices of very low-energy requirements, later—at the end of the 1990s—stepping up to portable computers, drilling machines, and lawn mowers). However, the development has now regained momentum and although prices are still too high, there are hopes for the next steps moving into the markets for automobile traction and main power plant energy management.

During the early 1990s, when the disappointment over the battery progress was largest, R&D in fuel cells increased dramatically, both for high-temperature and

---

<sup>1</sup> Corresponding author: boson@ruc.dk



especially for low-temperature fuel cell types such as the proton exchange membrane (PEM) fuel cell, and the collaboration between fuel cell manufacturers and car companies was stepped up. One such alliance announced that a fuel-cell-driven automobile would be put on the market by 2004, that is a production-line vehicle rather than an experimental or demonstration type “zero-series” version. This did not happen, presumably because neither price nor durability had reached the minimum goals considered necessary for market entry.

As then pointed out by a few observers, there is an alternative strategy, involving a gradual introduction of both batteries and fuel cells into the automobile sector, through a smoothly developing transition involving a range of hybrid concepts [1]. Central in this argumentation is the fact that the average power requirement during nearly all driving cycles is 10–20 times lower than the maximum power need during a few, exceptional driving situations. This suggests having two power sources in the vehicle, one delivering the average power and the other the peak power. The first can be rated much lower than the power-conversion devices currently installed in vehicles, and thus it allows the use of technology with a high price per unit of rated power.

Current hybrid cars available in the marketplace are combining internal combustion (IC) engines (using fossil fuels such as gasoline or diesel oil) with electric motors fed by batteries of various types. Two concepts are available: either a stand-alone model using the fuel IC engine and a generator to charge the batteries or a plug-in hybrid being charged during parking from the general power grid. The main advantage is in both cases that electric motor operation can be used in urban environments to reduce emissions causing air pollution. The next step would be to reduce the engine rated power and increase battery size, so that the IC engine is only used to charge batteries, while all driving is using the electric motor. The rationale is that the efficiency of electric motors do not drop with part-load as much as is the case for IC combustion engines.

The IC engine plus battery concept allows a start configuration with largely acceptable consumer cost in the current economic context, by limiting the use of batteries alone to an urban driving range of 30–50 km, and only to increase this range if/when advanced batteries become less expensive. The batteries have to be advanced, for example, of lithium-ion type, because otherwise the weight of conventional lead-acid batteries or even advanced metal hydride batteries will eat up most of the hybrid concept’s efficiency gain.

As the next step, the IC engine can be replaced by a fuel cell, rated only near the average rate of energy use rather than at the maximum, in the interest of keeping cost down. A further transition to a pure fuel cell vehicle is unlikely, because it would require a cost reduction for fuel cells exceeding that achieved for the battery component. The mentioned similarity in technology makes this an improbable development.

In any case, one has to consider not only initial cost, but also lifetime costs of operating the vehicle. The trend in vehicle construction has over the two recent decades been one of



prolonging the lifetime of a vehicle, for several reasons, including the consideration of environmental impacts, which of course include those associated with energy used in manufacture and in the treatment associated with recycling and reuse of materials. Today, many passenger cars are built to have an average lifetime of about 20 years. Since the goal lifetime of both batteries and fuel cells are set at 5 years, this means replacing these components 3 times during the operational life of the vehicle. Furthermore, even a 5-year lifetime is high for an electrochemical device. It took a long time for lead-acid batteries to reach this level. The cost of these replacements, involving garage-level work that is typically much more expensive than production-line operation, could pose a limitation hard to overcome. The future of battery and fuel cell vehicles is therefore still highly uncertain, but acceptance may be helped when resource depletion and environmental concern over pollution and greenhouse warming make energy prices generally go up.



## 2. SIMULATION OF EFFICIENT INTERNAL COMBUSTION VEHICLE

As a reference, the performance of conventional vehicles with IC engines will be looked at, using the same model tools as will be used for the subsequent simulations of battery, hydrogen, and hybrid vehicles. The modeling is based on a superstructure of application routines added on top of the mathematical modeling software [2]. The original set of application routines was developed at the National Renewable Energy Laboratory [3] and subsequently augmented with modules for the specific investigations made here. The basic simulation approach is that of a time-wise progressing calculation in iterative steps forward and backward, trying to meet the driving speed prescription of a specified driving cycle time series.

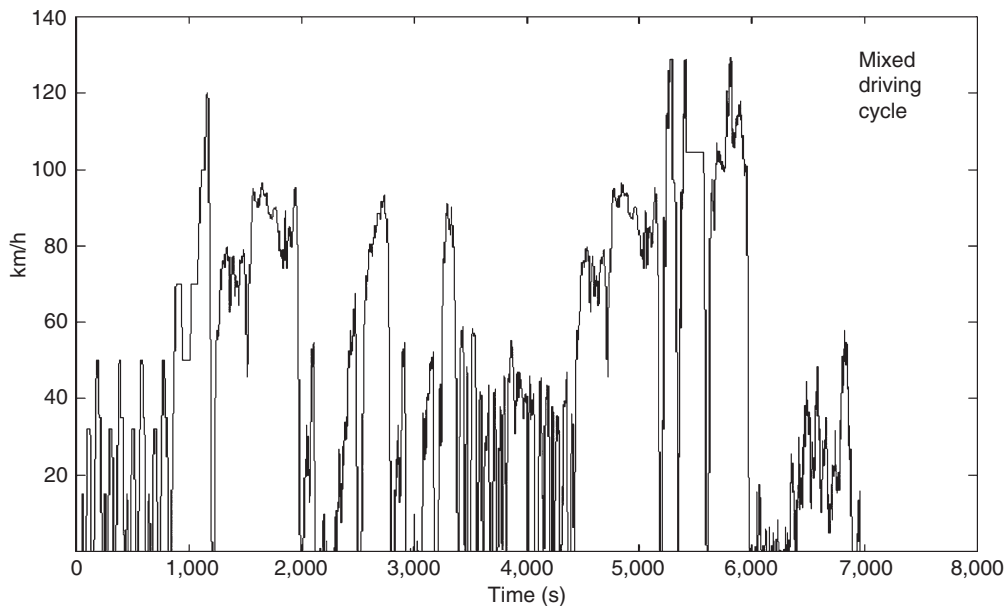
The IC vehicle simulation modeling takes departure in data for a commercial four- to five-passenger car, the Volkswagen Lupo TDI-3L that was in production from 1999 to 2004<sup>1</sup>. It accepts both mineral diesel oil and biodiesel fuels in a 45 kW common-rail diesel engine and has a fuel efficiency ensuring 33 km/l of diesel fuel (1.08 MJ/km or 31 of diesel per 100 km, equivalent to 3.4l of gasoline per 100 km) for the standard European driving cycle [4]. Among its energy efficiency-promoting features is a computer-controlled five-speed automatic transmission, causing the average energy loss to be 20% lower than that of a typical five-speed manual transmission.

The common-rail diesel engines dominating the market today are of the generation of advanced compression ignition diesel engines, where the air is compressed before being mixed with a controlled amount of fuel. This is a key reason for achieving higher efficiency than the Otto engines. The high temperature associated with the compression allows ignition without spark creation. The high-pressure common-rail injection principle has

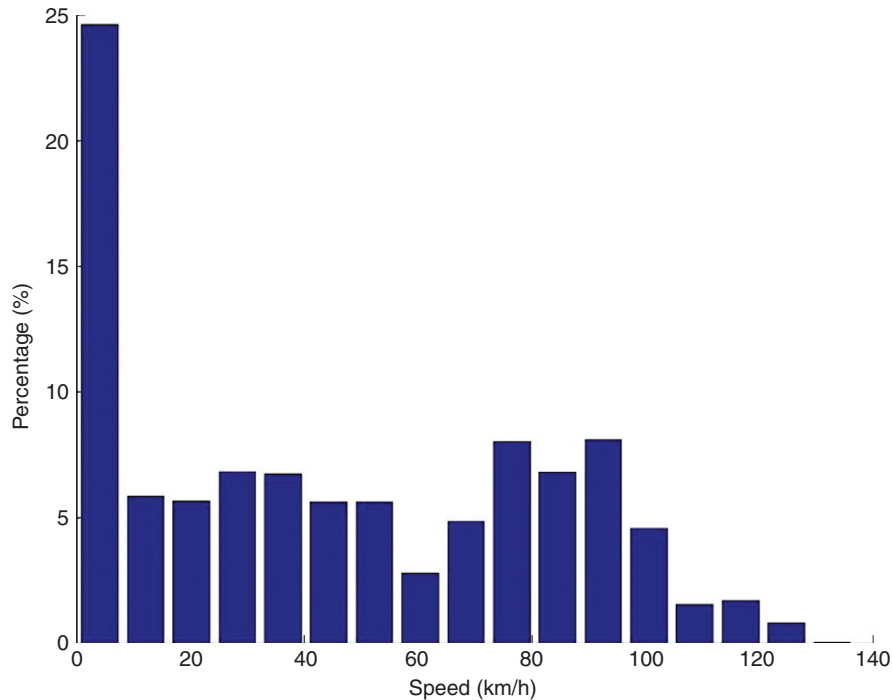
<sup>1</sup> The reason for abandoning production was the appointment of a new management that did not have energy efficiency in its business strategy. Leadership in efficient passenger vehicles has now been taken over by companies such as Citroën (cf [5, 6]).

increased the energy efficiency of diesel vehicles by some 30% relative to comparable Otto engines using gasoline as a fuel. This is interesting because diesel has traditionally been considered an inferior fuel relative to gasoline, with lower efficiency and more undesirable emissions. However, the introduction of turbocharged direct injection (TDI) and electronic control changed that in favor of diesel engine operation. The high-pressure (currently around 140 MPa) common-rail principle solved the problem of pulverizing diesel droplets to a small particle size and thereby reducing the amount of unburned fuel. Computerized control allows a rapid injection with the main stage surrounded by two minor injection stages serving to reduce noise and reduce unburned fuel while increasing exit flow temperature, which again reduces pollutant emissions.

The driving cycle adopted for the comparison of different vehicles' performance is a mixture of the driving cycles used in the United States and in Europe for providing unbiased consumer information and in some cases for automobile taxation purposes. It is difficult to construct a driving cycle that would not be slightly "unfair" to some car models, for example, by specifying driving speeds that would force some cars to change gear level more frequently than others. The 89 km driving cycle used in the simulations is shown in Fig. 10.1, and the frequency distribution of the driving speeds it contains in Fig. 10.2. It alternates between highway driving, suburban driving with occasional red-light stops, and city-core driving with many stops and idling. The European driving cycle (appearing as the first 2,000 s in Fig. 10.1) has been criticized for not containing a realistic proportion of motorway driving. This has been remedied by the motorway portion of the

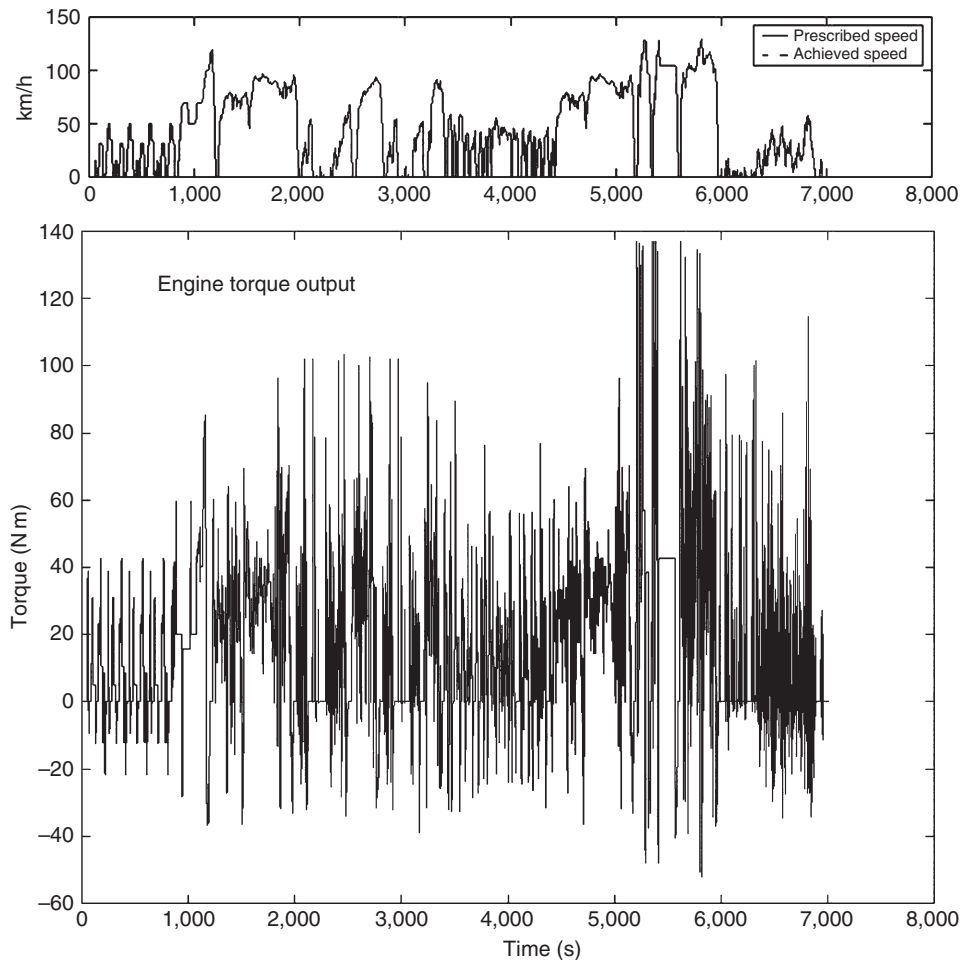


**Figure 10.1** Driving cycle used in simulations.



**Figure 10.2** Frequency distribution of driving speeds in the mixed driving cycle used in the simulations.

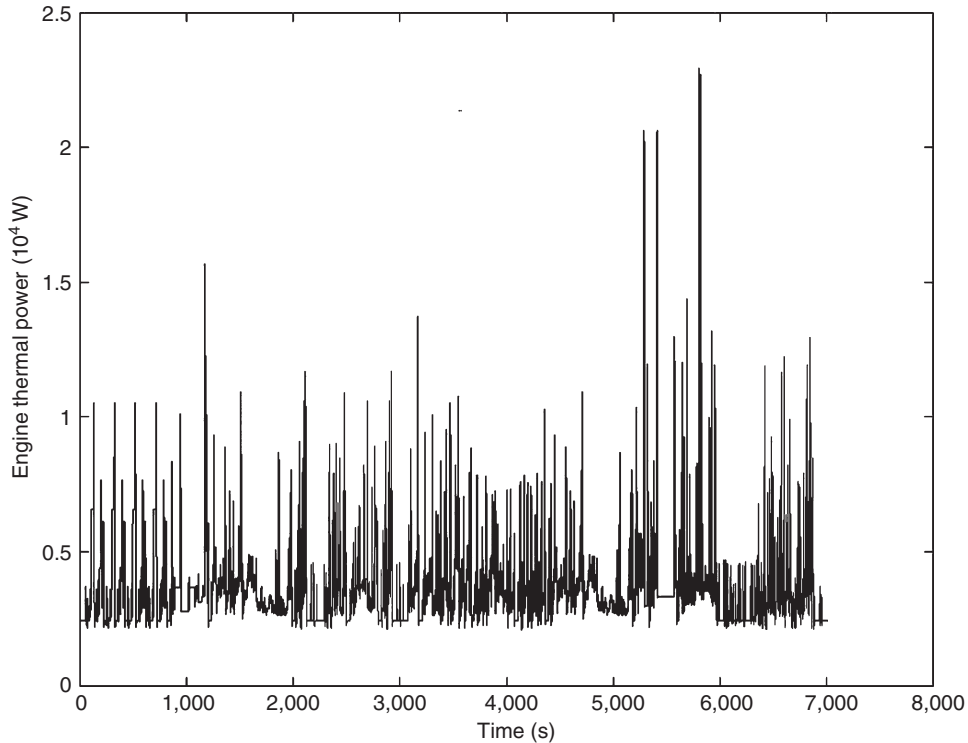
cycle in Fig. 10.1, appearing from 5,200 to 6,000 s. For the Lupo, the simulation described below gives an average fuel-to-wheel efficiency identical to the 31 of diesel per 100 km accepted for regulatory purposes. In Denmark, annual car taxation is inversely proportional to the fuel efficiency. The driving cycle used for the purposes mentioned here is unrealistic in not having any grades included. The rationale behind this is that presence of grades in actual road driving is very different from region to region and therefore not inviting the common approach that, for example, for the European Union is a political goal. The same is true for the temperature dependence of measured performance. Regions with cold winters have additional fuel use, partly in periods following cold starts and partly due to cabin heating throughout the trip. The official performance data are normally obtained at a prescribed ambient temperature of 20°C. As a result, the experience of most drivers is that actual performance is lower than the regulatory numbers, by amounts on the order of 10%. Poor driving with unnecessary accelerations and braking, depressing the gas pedal unnecessarily during cruising and not releasing it when a red light is spotted can degrade performance by another 10–20%. Interestingly, there are technical ways of diminishing these negative effects, for example, by careful selection of the exchange ratios of multilevel transmissions, and the driver dependence of energy performance therefore varies considerably from one car make to another.



**Figure 10.3** Diesel car simulation. Lower panel: engine torque delivery during the driving cycle of Figure 1. Upper panel: Time-aligned vehicle driving speed, which is identical to that prescribed by the driving cycle to within 1%.

Fig. 10.3 gives the diesel engine torque delivered through the driving cycle, aligned with the time development of achieved vehicle speed, which is very close to the prescribed speed. The highest torque demands are associated with motorway accelerations. The engine modeling is based on measured fuel use as function of shaft revolutions (“engine speed”) and torque output, but for a 60 kW engine used earlier by Volkswagen and Mercedes, for which complete fuel and environmental performance measurements have been made [7]. Only the overall scaling is modified to agree with the measured total fuel use and total emissions of the Lupo [8, 9].

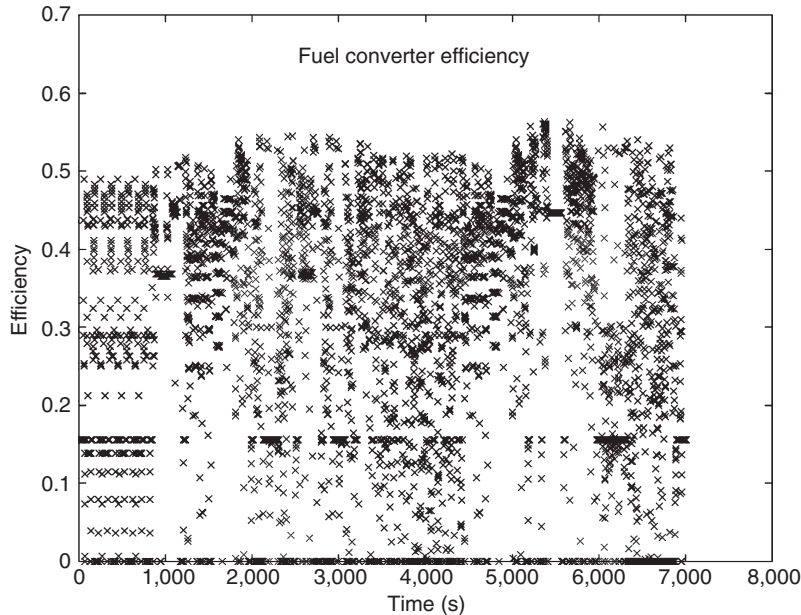
The simulated performance of the Lupo during the mixed driving cycle is given in Fig. 10.4, in the form of the total thermal power output from the engine, through the



**Figure 10.4** Diesel car simulation. Engine thermal power output during the simulated driving cycle.

driving cycle. A lower limiting power value during idling is seen. The real Lupo has an idling control that closes down the engine after some 20 s of idling (under the condition that the car is not moving and that a foot is firmly depressing the brake) and restarts it when the foot is removed from the brake. This is not modeled but is believed to be of minor importance for the driving cycle prescribed, because the extra energy used to restart the engine eats up part of the gain obtained by reducing idling time to 20 s. This does not imply that the idling control is superfluous, because it prevents long-time idling, which is a bad habit of some drivers. In some countries, over 1 min of idling is forbidden by law. The mixed driving cycle has a number of stops at red light. If the duration of red lights is 1 min, a random arrival hypothesis would give average waiting times of 30 s, only 10 s more than the Lupo limit, consistent with the remark that the idling control of the Lupo is of minor importance for the mixed driving cycle simulation. Green-wave control of traffic lights will further reduce the idling problem, so preventing prolonged driver-decided idling is really the main advantage of the Lupo system.

The course of engine efficiency with driving time along the prescribed cycle is shown in Fig. 10.5. It reveals the well-known fact that IC engines are not operating efficiently under part-load. In particular, the low efficiency associated with driving in the lowest gear level stands out by the clustering of data at its maximum 15% efficiency.



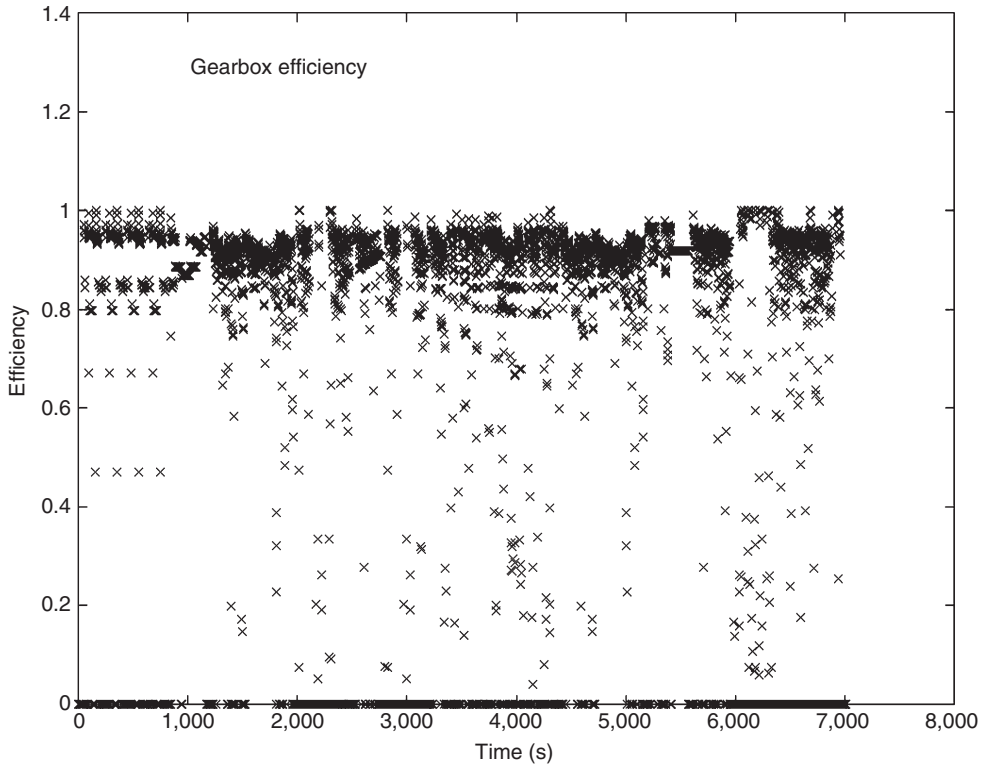
**Figure 10.5** Diesel car simulation. Engine conversion efficiency during the simulated driving cycle.

Fig. 10.6 finds that the transmission has an efficiency over 90% during most of the time. The origins of energy losses are summarized in Fig. 10.7.

A main concern over vehicles using fossil or biofuels is the air pollution associated with the combustion cycle. The emission data scaled from those of [7] to represent a Lupo operated by mineral diesel oil were subjected to driving cycle simulation for Lupo conventional diesel operation, giving overall emissions generally consistent with other studies of similar cars [8, 10,11] The fuel characteristics were subsequently changed to those of biodiesel (using current European norm specifications for the composition), which relative to the fossil-based diesel fuel is assumed to have 25% less CO emissions, 10% higher  $\text{NO}_x$  emissions, 40% less particulate emissions, and 80% less hydrocarbon carry-through [12]. The fuel efficiency is assumed unchanged.

Engine emissions during the mixed driving cycle are shown in Fig. 10.8, while Fig. 10.9 presents the tailpipe emissions at the end of the exhaust control path that involves catalyst action and electrostatic filters to reduce particulate matter dispersal, but not  $\text{NO}_x$  emission reduction. Comparing Figs. 10.8 and 10.9, one observes the little change in  $\text{NO}_x$  emissions, but up to an order of magnitude reduction in the other pollutants.  $\text{CO}_2$  is not mentioned here, as it directly proportional to the carbon content of the fuel combusted.

Unlike some more recent common-rail diesel cars, the Lupo catalyst exhaust control has modest particulate and  $\text{NO}_x$  reduction capability. Still, it meets the 2005 emission requirements of the European Union (the “Euro4 requirements”).



**Figure 10.6** Diesel car simulation. Energy efficiency of transmission unit during the simulated driving cycle.

Current state-of-the-art diesel passenger vehicles have particulate filters installed. The increased use of biodiesel and other biofuels is currently debated. They are largely CO<sub>2</sub> neutral when viewed in a life-cycle perspective, and vehicle emissions are lower than those of both gasoline and mineral diesel fuels, except for higher NO<sub>x</sub> emissions, which could soon be removable by techniques already being used in large power plants of environmental lead countries. Negative comments are usually directed at the availability of biomass feedstock and competition with food production. In evaluating these critical comments, a distinction should be made between biofuels using grains of food crops as basis for the fuel production, and those that only use residues. The latter type not only avoids food competition, but the resources of feedstock biomass residues for these “second-generation biofuels” are ten times larger than for grain-based biofuels.

In a global renewable energy scenario [1, 13], future production of biofuels would be from agricultural and forestry residues. The efficiency advantage of current diesel engines over Otto engines suggests that efforts be directed toward biodiesel.

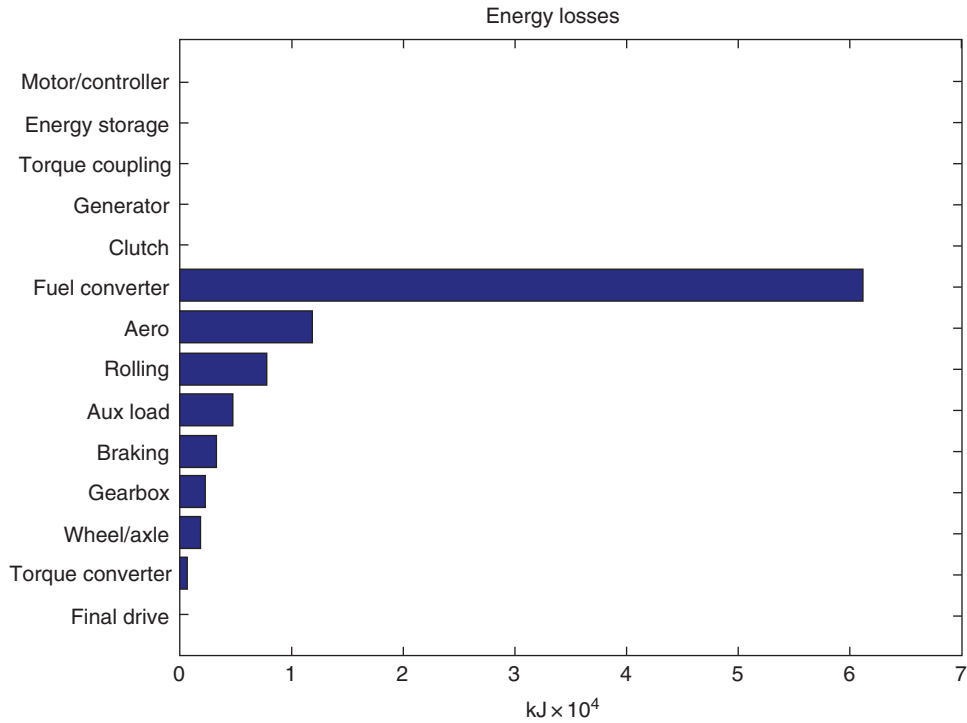


**Figure 10.7** Diesel car simulation. Distribution of energy losses during the simulated driving cycle.

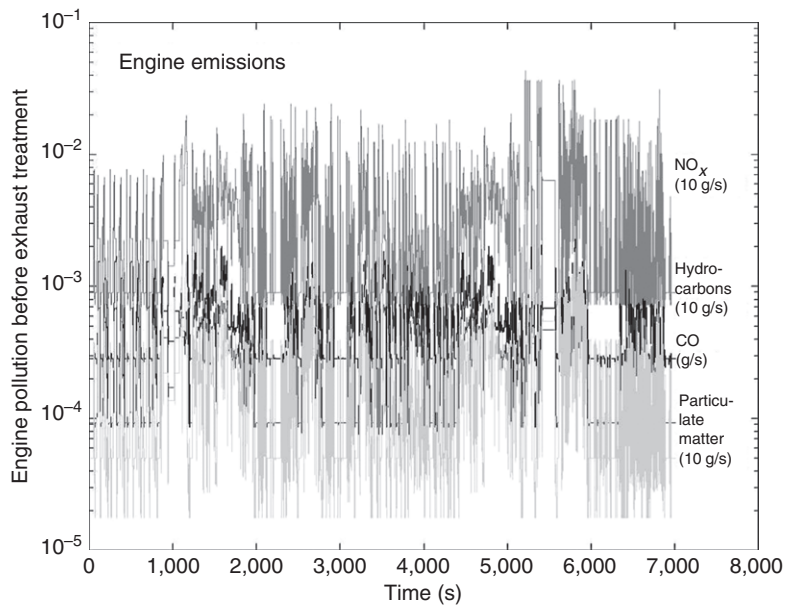


**Figure 10.8** Diesel car simulation. Emissions from the engine during the simulated driving cycle.



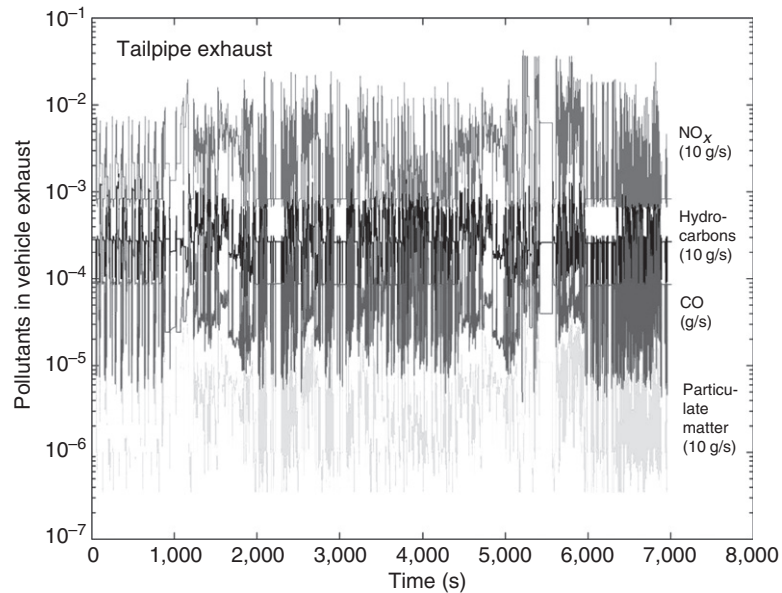


**Figure 10.9** Diesel car simulation. External emissions from the vehicle tailpipe during the simulated driving cycle.

Average biodiesel Lupo emissions for the entire trip is found to be 0.029 g/km unburned hydrocarbons, 0.075 g/km CO and 0.278 g/km  $\text{NO}_x$ , plus negligible amounts of particulates. The corresponding figures for the mineral-diesel Lupo are 0.03, 0.10, 0.25, and 0.02 g/km particulates [1, 14].



### 3. SIMULATION OF FUEL CELL VEHICLE

A “pure” fuel cell automobile is simulated by use of a series connection, that is, all electricity generated is passed through a traction battery rather than directly to the motor. This is the same mode as used for the hybrid vehicles discussed in Section 5. The battery is just chosen small enough (1.25 MJ capacity) to perform only smoothing operations and not act like an independent power source.

The basic vehicle is still the same Volkswagen Lupo as used in Section 2. The basic mass of the vehicle is 564 kg, to which comes an exhaust catalyst treatment system of mass 10 kg, a transmission system of 50 kg, and an assumed average passenger and freight load of 136 kg. The lithium-ion traction battery weighs 6 kg, the motor/controller system 60 kg, and the 40 kW fuel cell system 130 kg, including hydrogen fuel onboard storage and handling, leading to a total mass of 961 kg. The performance data for the fuel cell used in the simulation correspond to

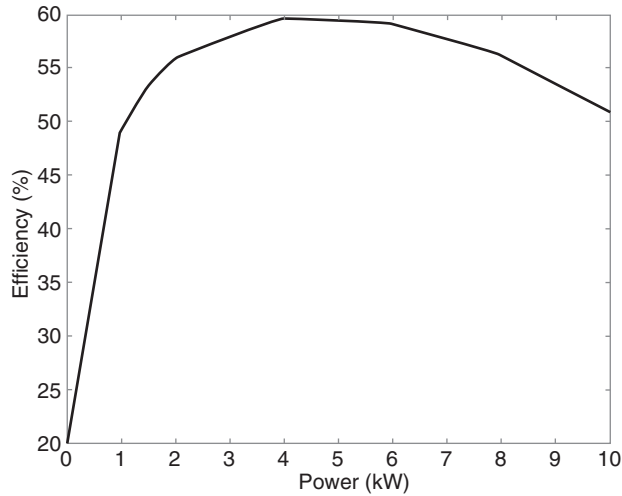


**Figure 10.10** Fuel cell car simulation. Assumed efficiency curve for modeled fuel cells.

that of a “goal” technology rather than that of the currently available demonstration cars. Fig. 10.10 shows the efficiency of the fuel cell, reaching 59% and being high for part-loads except for the smallest ones. The same is borne out by the hydrogen consumption curve of Fig. 10.11.

The results of simulating this vehicle are shown in Figs. 10.12 and 10.13. The car would have a range of 675 km with 4 kg of hydrogen stored onboard, under conditions

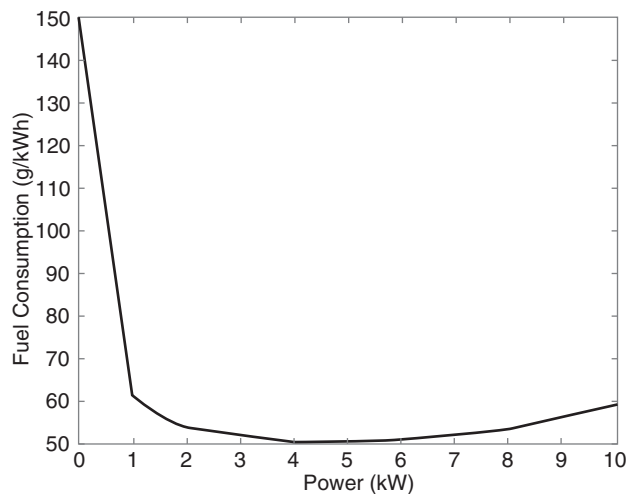


**Figure 10.11** Fuel cell car simulation. Fuel consumption curve for modeled fuel cells.

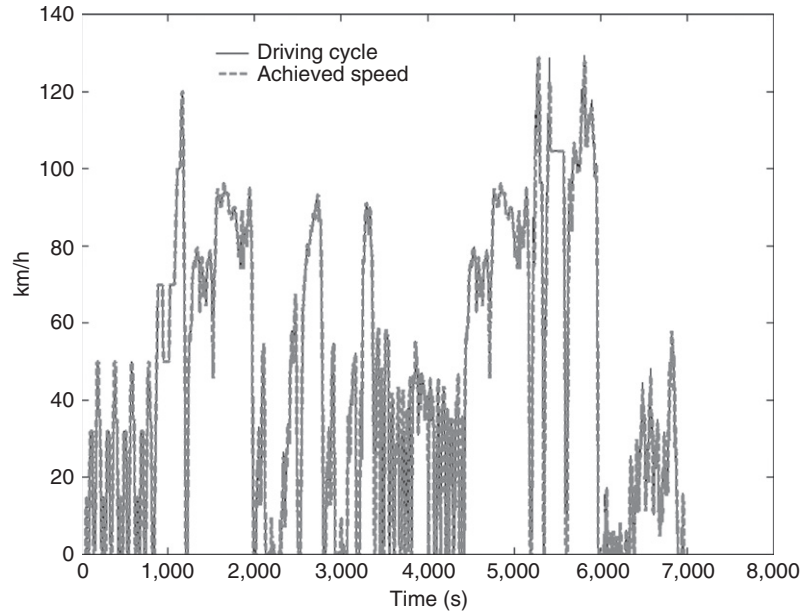


**Figure 10.12** Fuel cell car simulation. Prescribed (full line) and achieved (dashed line) speed along the mixed driving cycle, the latter for a 40 kW pure fuel cell vehicle.

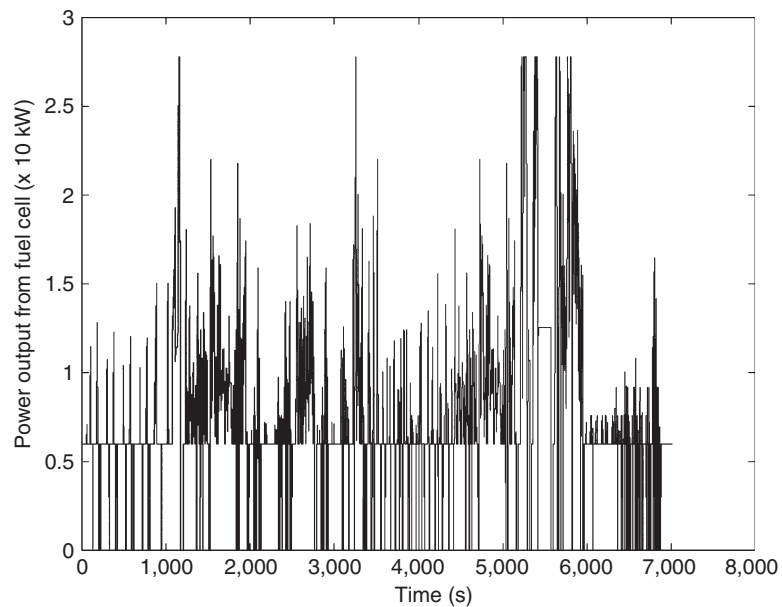


**Figure 10.13** Fuel cell car simulation. Power output from fuel cell along the mixed driving cycle, for a 40 kW pure fuel cell vehicle.

such as the assumed driving cycle. Fig. 10.12 indicates the actual time series of driving speeds obtained according to the simulation, as well as the prescribed driving cycle. Only in a few instants is there 1–3% difference, and the performance is as good as that of the diesel Lupo modelled in Section 2. Fig. 10.13 shows the fuel cell power output along the driving cycle. The average energy use of the fuel cell during the trip is 1.138 MJ/km (equivalent to 3.5 l of gasoline per 100 km).



#### 4. SIMULATION OF BATTERY VEHICLE

A purely electrical vehicle based on the Lupo concept would for comparison with the diesel and fuel cell cars have to be an all-purpose passenger vehicle rather than a dedicated city vehicle. This means achieving a range between recharging of batteries that ideally matches that of the diesel version (900 km) or the fuel cell version (675 km), but which, considering that several cars sold today have lower ranges between refilling, might be acceptable to customers with a range of only 400 km. The electric vehicle modeled here has a range of 455 km, requiring 1,000 modules of a model lithium-ion battery [15], storing up to 250 MJ and weighing 1,134 kg, which more than doubles the vehicle mass and is unlikely to be acceptable. If lead-acid or NiMeH batteries had been used, the battery weight would have been over 2.5 metric tons. The point is of course, that mass increases of this size has a noticeable negative impact of efficiency performance. For instance, the range of a Lupo with only half as many lithium battery modules is about 240 km, suggesting that even this new generation of batteries will likely be reserved for special vehicles only aiming to penetrate part of today's passenger car market.

The implications for power delivery are illustrated in Fig. 10.14, suggesting that the best performance is ensured if the battery is never discharged much under 40%. The roundtrip efficiency of the battery at 25°C, as a function of current and state of charge, is high at low currents and declines with increasing currents drawn, but still stays above 70% for currents up to 100 A.

In Figs. 10.15, 10.16, and 10.17 the simulated performance of the pure electric vehicle is given for a trip through the mixed driving cycle. Fig. 10.15 shows that the electric motor is capable of delivering a higher torque than the diesel engine of Fig. 10.3. Fig. 10.16 indicates that the state of battery charge drops by 22% during the 89 km driving cycle and Fig. 10.17 shows the power output from the battery, during discharge to motor and during braking regeneration. Prescribed driving cycle speeds are reached and the battery–motor system performs as well or better than that of the IC engine system of Section 2. The drawback of pure electric vehicles for mixed city highway use lies in the compromise between range and battery mass that has to be made.

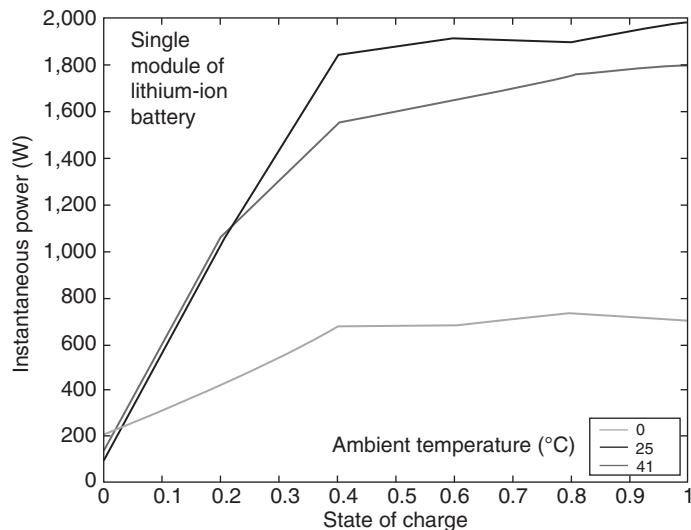


**Figure 10.14** Electric vehicle simulation. Instantaneous power delivered by a 6 Ah module of lithium-ion battery (Saft) as a function of temperature [15].

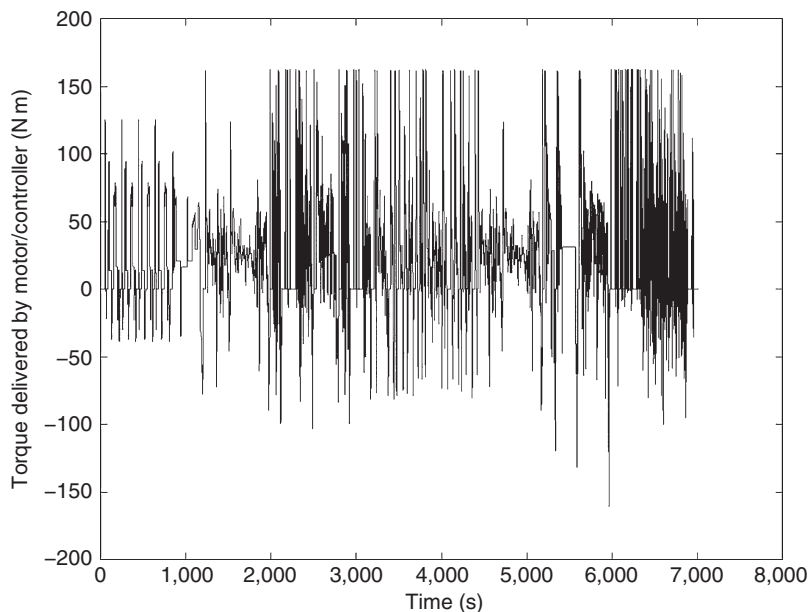


**Figure 10.15** Electric vehicle simulation. Simulated torque delivered by motor over the mixed driving cycle (negative during braking regeneration).

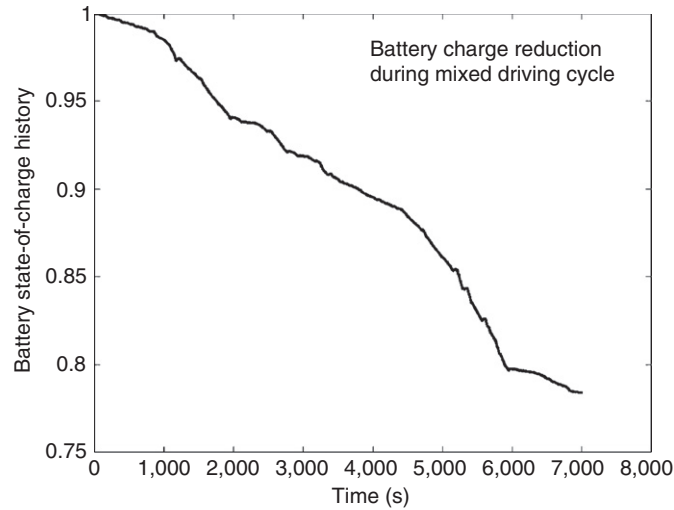


**Figure 10.16** Electric vehicle simulation. Lithium-ion battery charge state along the mixed driving cycle.

The characteristics of the 50 kW motor used in all the simulations is shown in [Fig. 10.18](#), giving maximum torque and efficiencies as function of motor revolutions, both for motoring and for generating (recharging batteries). The operating points indicated are for the hybrid configuration used in the following [Figs. 10.19–10.26](#).

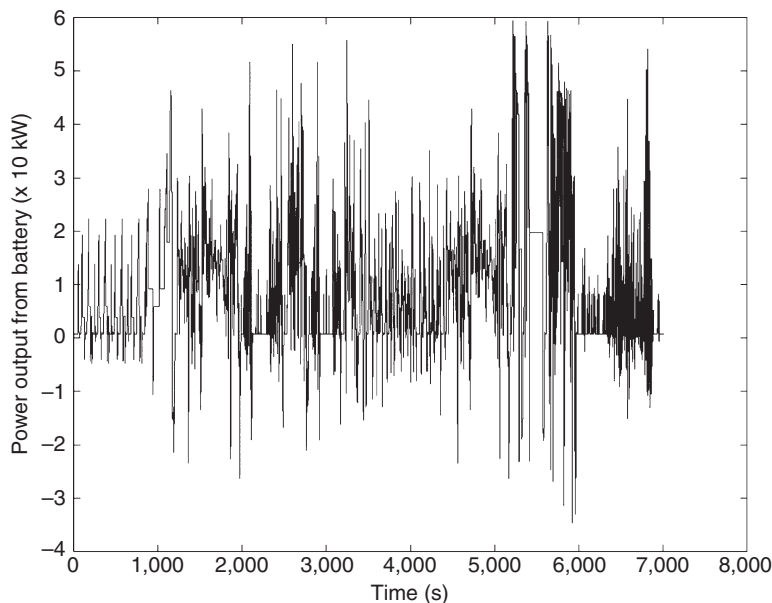


**Figure 10.17** Electric vehicle simulation. Power output from lithium-ion battery during the mixed driving cycle. Negative values represent brake energy recovery.

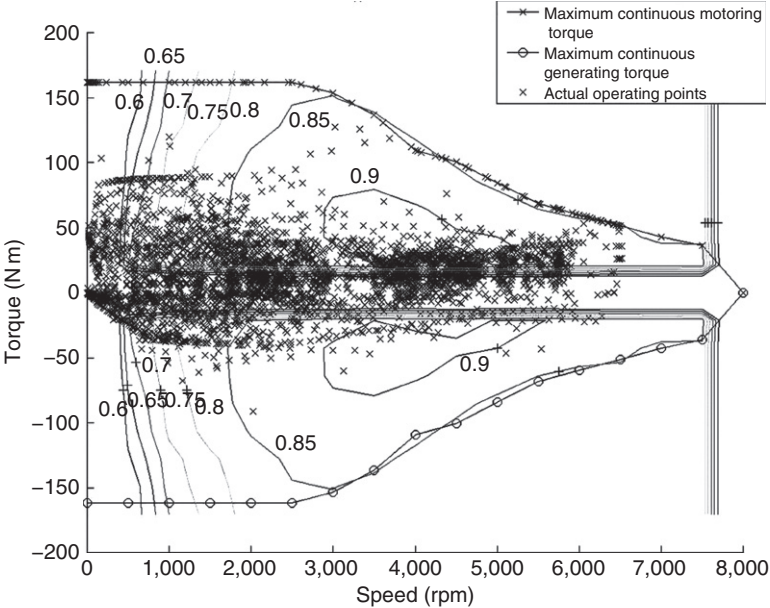


**Figure 10.18** Electric and fuel cell vehicle simulations. All simulations of battery and fuel cell vehicles assume the use of a 50 kW motor. The picture gives its torque characteristics during continuous motoring and generating (limiting curves with crosses or circles) and the motor efficiencies (lines with numbers attached). Finally, the operating points for the mixed driving cycle are indicated (free-standing crosses) for the hybrid vehicle discussed in Section 5 (20 kW fuel cell, 15 MJ lithium-ion battery).

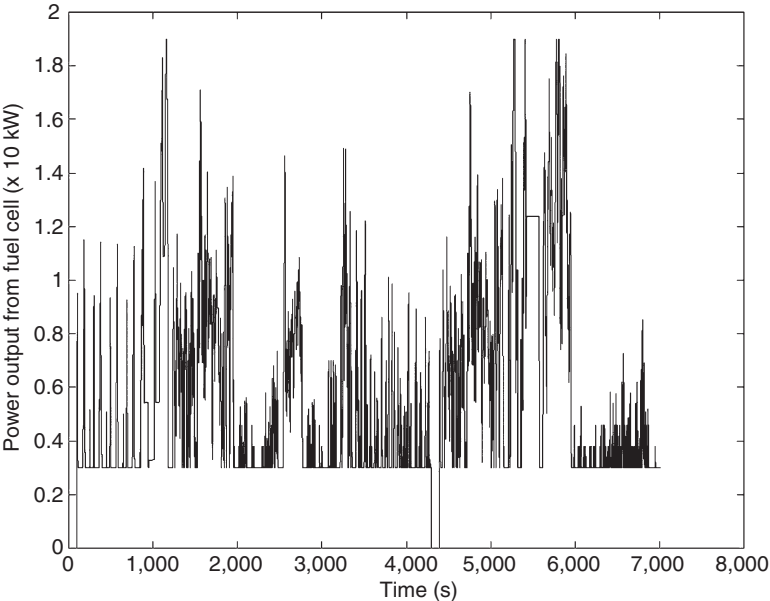


**Figure 10.19** Hybrid car simulation. Fuel cell power output during the simulated driving cycle.

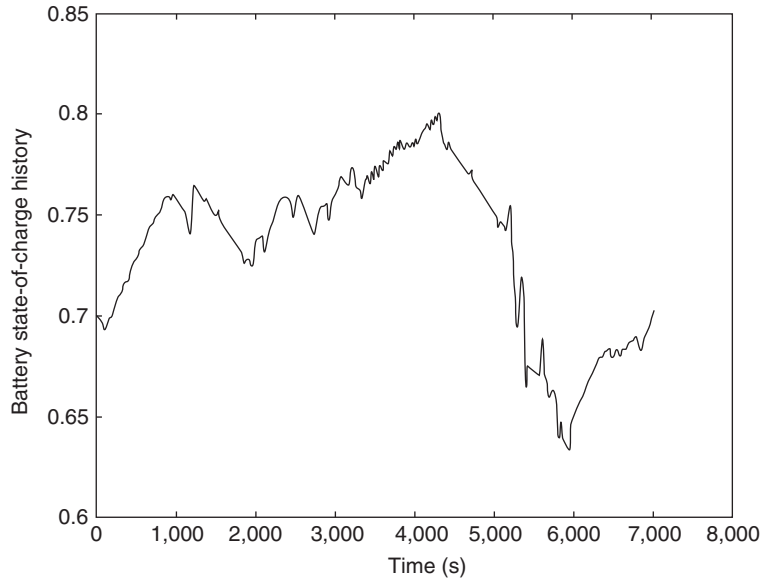


**Figure 10.20** Hybrid car simulation. Lithium-ion battery charge state during the simulated driving cycle (the identity of charge state at beginning and end of trip has been used to determine battery size for a given fuel cell rating).

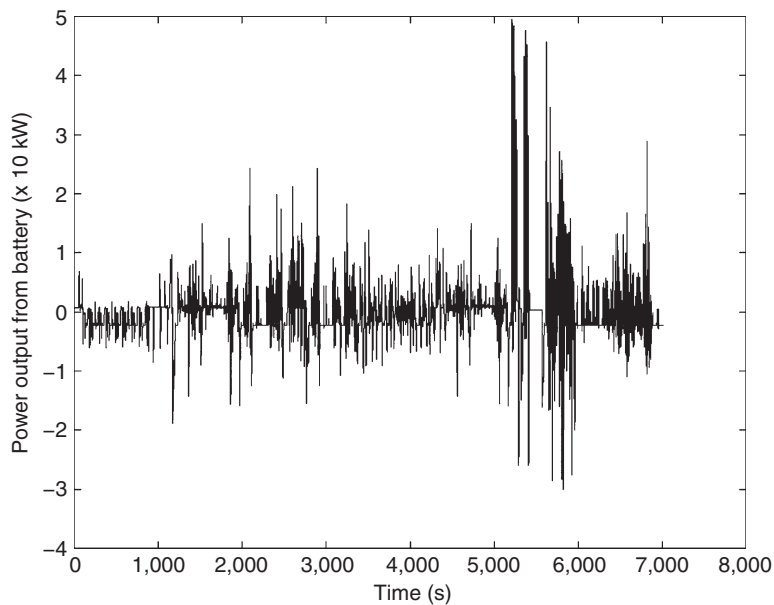


**Figure 10.21** Hybrid car simulation. Battery power output during the simulated driving cycle (negative when recuperating deceleration energy).



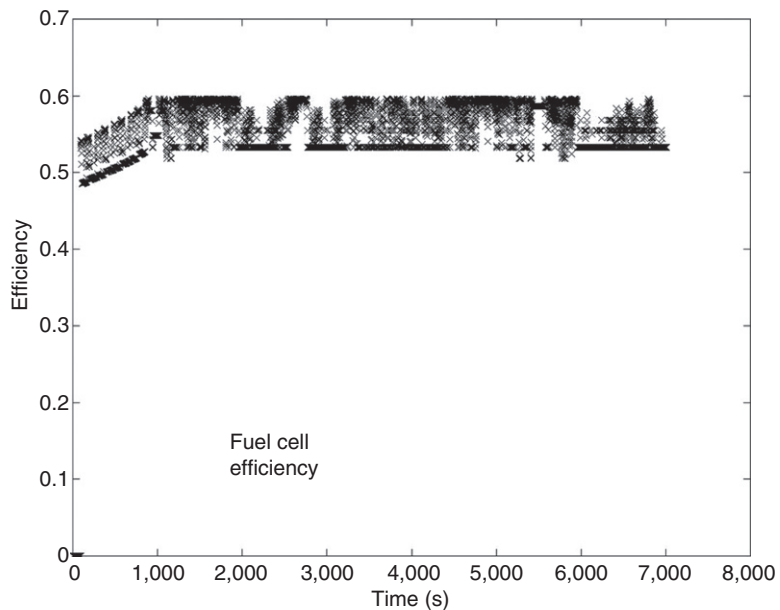


**Figure 10.22** Hybrid car simulation. Fuel cell conversion efficiency during the simulated driving cycle.

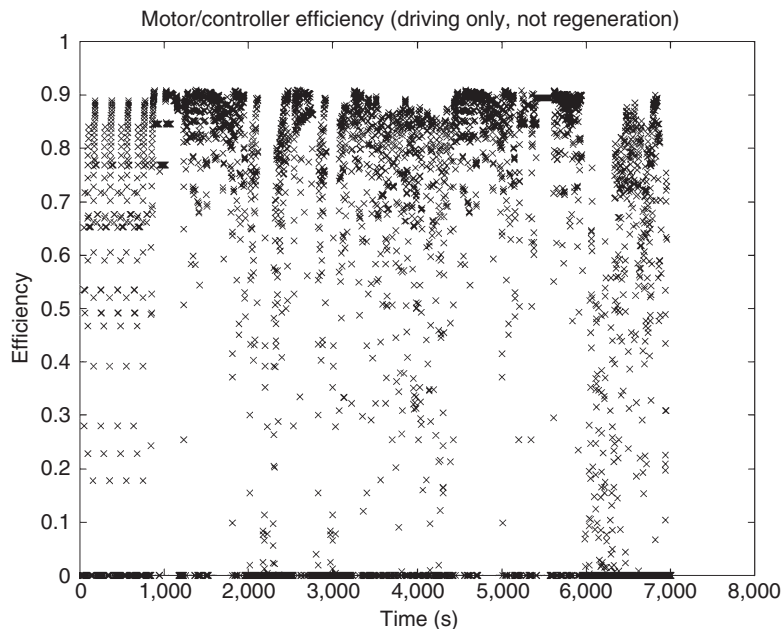


**Figure 10.23** Hybrid car simulation. Efficiency of motor-controller system during the simulated driving cycle.

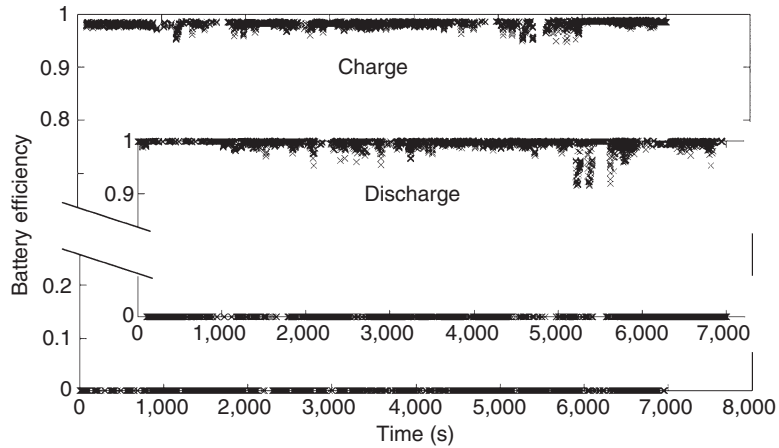


**Figure 10.24** Hybrid car simulation. Battery efficiency during charge and discharge operations along the simulated driving cycle.

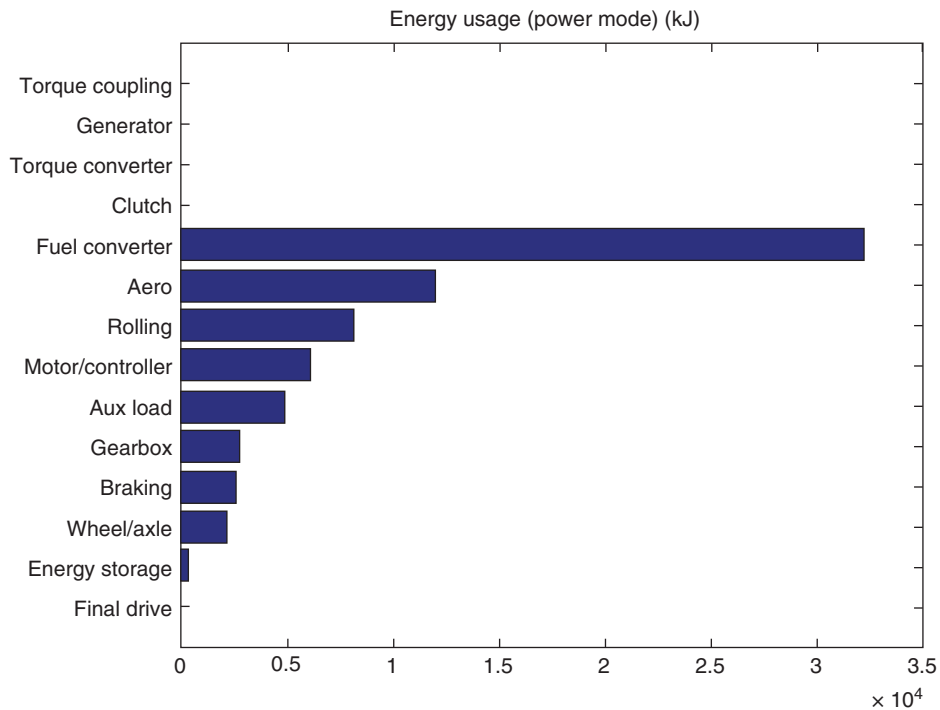


**Figure 10.25** Hybrid car simulation. Distribution of total losses during the generating sections of the simulated driving cycle.

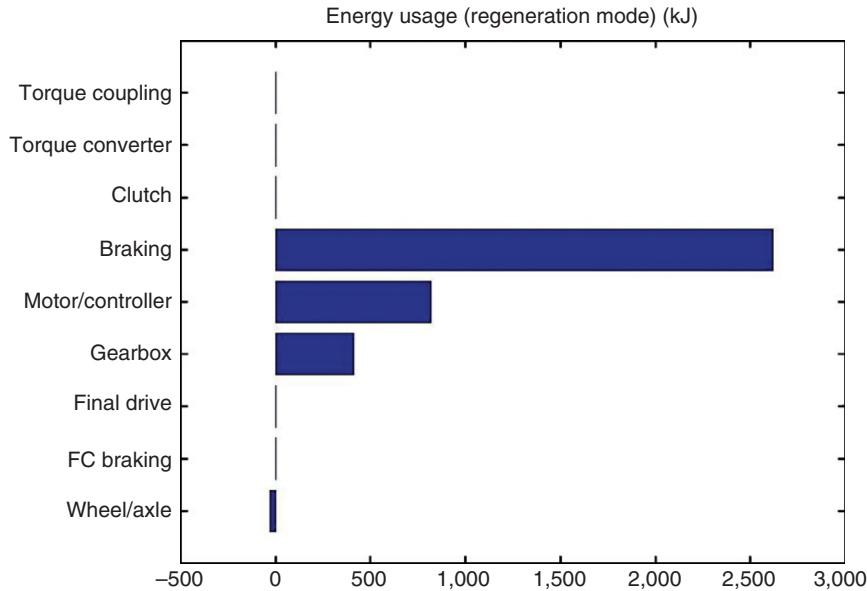


**Figure 10.26** Hybrid car simulation. Distribution of total losses during the regenerating sections of the simulated driving cycle (note the expanded scale relative to Figure 25).



## 5. SIMULATION OF HYBRID VEHICLES

Hybrids between battery and fuel cell vehicles may be of two kinds. In one, the batteries are exclusively recharged by hydrogen fuel through the fuel cell. For a selected fuel cell rated power, the battery size is determined that will render the battery in the same charge state at the end of the prescribed mixed driving cycle as at the beginning. This turns out for the modeled class of vehicles to be possible only with a fuel cell rating of 20 kW or higher. The other kind of hybrid (plug-in vehicle) would allow batteries to be charged from external sources. It would require charging stations at parking spaces or garages similar to those for pure electric vehicles. To allow charging at home or working place, the additional cost of these charging facilities must be considered. It is, however, very small compared to the cost of hydrogen filling stations.

In this section, the detailed operation of the smallest self-recharging hybrid vehicle will be discussed. In addition to a 20 kW fuel cell, it must have a 15 MJ lithium-ion battery, as well as the 50 kW motor used for all the simulations (cf. Fig. 10.18). Fig. 10.19 shows the fuel cell power output and Fig. 10.20 the state of charge for the battery along the mixed driving cycle. Although the initial and final charge states are identical (by choice of battery size), there are excursions of  $\pm 10\%$  during the trip, with the lowest value occurring after the freeway part of the driving cycle. The battery power output and input are shown in Fig. 10.21. It is seen that the maximum power derived from the

battery occurs on the freeway section, whereas the particular driving pattern in the urban sections determines whether fuel cell or battery contribute most to operating power. This is contrary to the often-voiced opinion that battery operation takes place during urban driving and fuel cell operation during highway driving. Of course, this depends on control strategy, but since neither electric nor hydrogen operation cause detrimental local emissions, there is no reason to insist on excluding fuel cell use during urban driving.

The fuel cell conversion efficiency along the driving cycle is shown in Fig. 10.22 and that of the motor-controller system in Fig. 10.23. The first is uniformly high, as the control operation excludes use of the fuel cells for propulsion when the power required is under some 10% of the rated power (see Fig. 10.19). The battery efficiency is over 90% (Fig. 10.24), with the lowest values occurring during freeway accelerations. Figs. 10.25 and 10.26 give a survey of total losses distributed on devices for driving and for deceleration recharging modes.



## 6. OPTIMIZATION OF HYBRID CONFIGURATION

For the hybrid vehicles with enough fuel cell rated power to ensure recharging of the batteries, the fuel use is rather similar. However, as the fuel cell rating goes up and the needed battery capacity down, there are larger excursions in the battery state of charge during the driving cycle. This is illustrated in the lower part of Fig. 10.27, where two state of charge curves are shown, for fuel cell rating 25 and 35 kW, that is, between the minimum stand-along rating of 20 kW used in the discussion of Section 5 and the 40 kW rating (Section 3) that makes storage batteries unnecessary, except for the smoothing function of a very small traction battery. However, none of the two battery charge-state curves reach values significantly below the 40% where, according to the discussion of Section 4, the battery performance begins to degrade.

The top part of Fig. 10.27 shows similar state of charge curves for two plug-in configurations. The 5 kW fuel cell and 125 MJ battery behavior exhibit a continuous drop similar to that of the pure battery-based electric vehicle. For 15 kW fuel cell and a 25 MJ lithium-ion battery, there are situations within the driving cycle that lead to recharging of the batteries, but still the final charge state is 13% lower than the initial one, indicating a need for power grid recharging, however only at 890 km intervals, as shown in Table 10.1.

Table 10.1 also gives the masses of equipment parts, in addition to the distances between recharging for the plug-in alternatives. The division of total energy uses between grid electricity and fuel cell hydrogen is further illustrated in Fig. 10.28, along with the energy use of the diesel (or biodiesel) Lupo vehicle. One notes that the lowest total energy use is obtained for the purely battery-based electrical vehicle, then for the hybrids with the ones having small fuel cell rating lowest, and finally the pure fuel

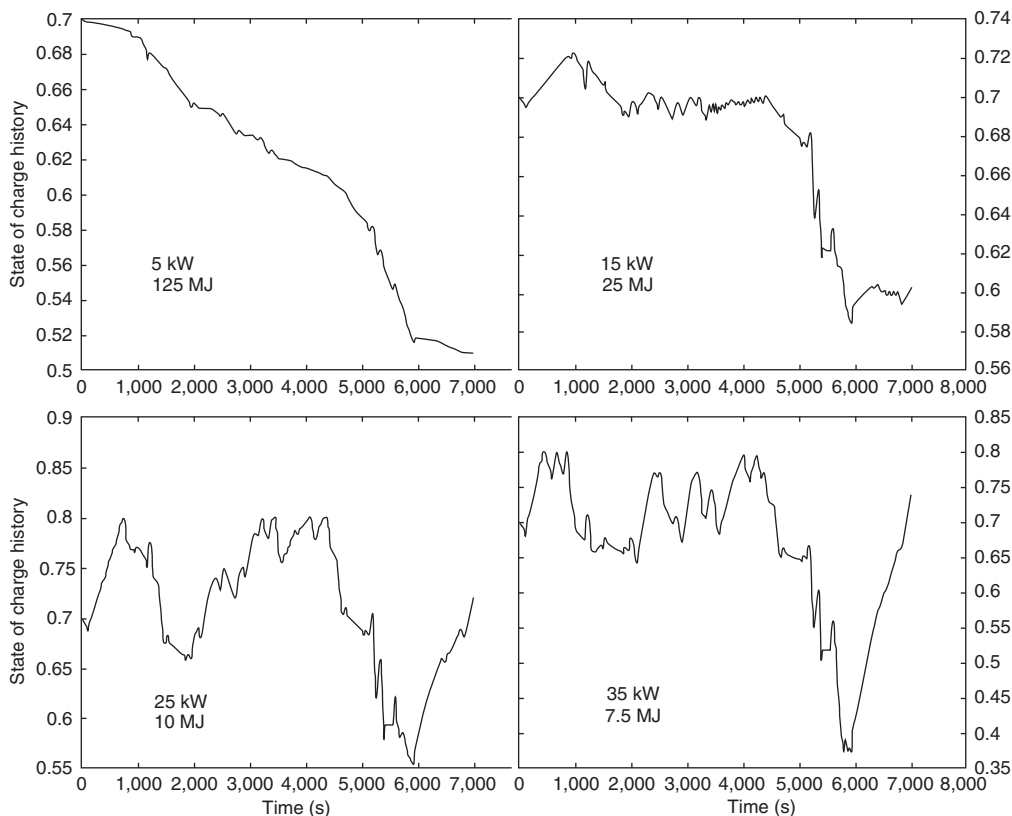


**Figure 10.27** Hybrid car simulation. Lithium-ion battery charge state during the simulated driving cycle, for four hybrid configurations: Upper windows: Plug-in hybrids with 5 and 15 kW fuel cells (corresponding battery rating 125 and 25 MJ). Lower windows: Grid-independent hybrid vehicles with 25 and 35 kW fuel cells (battery rating 10 and 7.5 MJ). Note that vertical scale for each window is different.

**Table 10.1** Summary of data for hybrid configurations of the Lupo-based vehicles

<b>Plug-in hybrids</b>					
Fuel cell rating (kW)	0	5	10	15	—
Fuel cell system mass (kg)	0	43	55	68	—
Fuel cell energy use (MJ/km)	<b>0</b>	<b>0.435</b>	<b>0.666</b>	<b>0.751</b>	—
Battery capacity (MJ)	250	125	57.5	25	—
Battery system mass (kg)	1136	567	261	113	—
Battery fuel use (MJ/km)	<b>0.617</b>	<b>0.263</b>	<b>0.1</b>	<b>0.028</b>	—
Battery recharging range (km)	405	468	574	890	—
<b>Self-recharging hybrids</b>					
Fuel cell rating (kW)	20	25	30	35	40
Fuel cell system mass (kg)	80	93	105	118	130
Fuel cell energy use (MJ/km)	<b>0.796</b>	<b>0.809</b>	<b>0.818</b>	<b>0.842</b>	<b>1.138</b>
Battery capacity (MJ)	15	10	10	7.5	0
Battery system mass (kg)	68	45	45	34	—

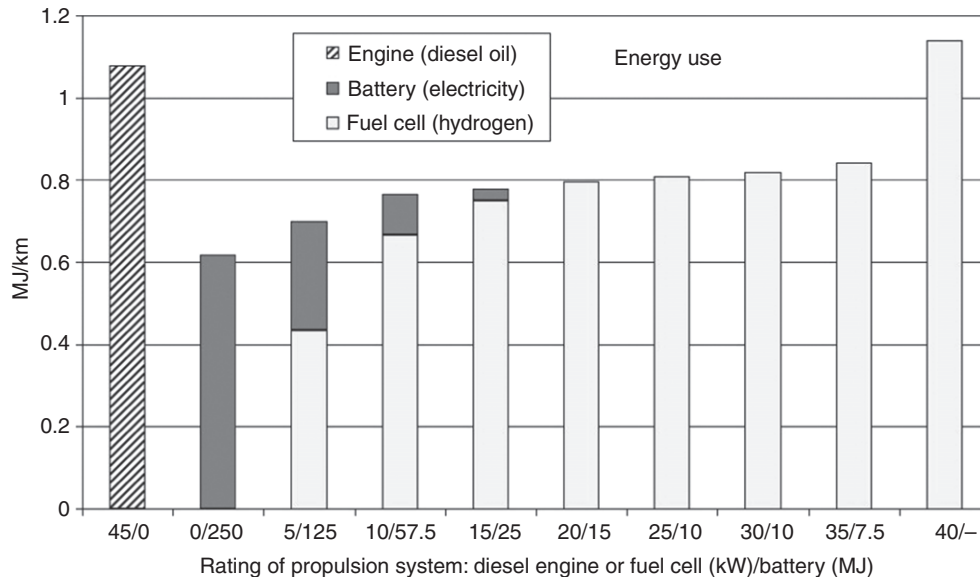


**Figure 10.28** Comparison of energy use for different vehicle configurations: Diesel Lupo, plug-in hybrids, self-recharging hybrids, and pure fuel cell vehicle.

cell vehicle, which has the highest energy use, higher than that of the diesel Lupo. The reason for this is that the model has to assume the use of the fuel cell system with poor efficiency at very low loads (Fig. 10.10), and already the 35 kW hybrid has a 30% better efficiency, because even the small 7.5 MJ battery is capable of taking care of the situations where the fuel cell operation would have been most inefficient.

In looking at the efficiency comparison of Fig. 10.28, one should keep in mind, that these are vehicle efficiencies. In a life-cycle view, one should add the losses occurring during the production of either electricity for charging batteries, or the hydrogen in the vehicle container system. The losses in hydrogen production and storage container compression may be 30–50%, using conventional steam reforming methods for obtaining hydrogen. If produced from electricity there are different losses, depending on the source of electricity. Electricity production from fossil fuels has an efficiency of 30–50%, the latter requiring multistage power extraction, but if the primary source is renewable energy such as wind power, it is customary not to include the losses in conversion from air motion to electricity. Despite all these qualifications, it is interesting that even the “goal” fuel cell of Fig. 10.10 will not be able to beat the diesel Lupo efficiency, unless hybrid configurations taking advantage of the unique characteristics of traction batteries is employed. That a pure electric vehicle has the highest efficiency is not surprising, but this has to be weighed with considerations of driving range and cost.

## 7. CONCLUSIONS

One conclusion that is obvious from playing with the composition of propulsion systems for passenger vehicles is that all components that may influence efficiency, whether part of the power supply system or not, must be made as energy efficient as possible, before expensive components such as lithium batteries or PEM fuel cells are brought in play. The cost of using advanced low-weight but high-strength materials and designing the vehicle with the smallest practical air and rolling resistance is far below the cost of the new power systems. This has been clearly proven by the VW Lupo and a corresponding Audi A4, which compensated for adding more luxury equipment by replacing all steel-based components with ones made of advanced low-weight materials, in order to achieve the same fuel efficiency as the Lupo. No compromise on safety was made, as both vehicles reached the top levels regarding safety in collision test ratings.

Many fuel cell prototypes have put 60–100 kW of fuel cells into a basic car of poor efficiency, which makes no sense considering that the fuel cell cost is the most difficult obstacle to such cars becoming economic, even with steeply rising fossil fuel prices. After all there are back-stop technologies such as the biodiesel vehicles, which at little or no cost increase could replace a large part of the current fleet of passenger cars, provided that the efficiency is similar to that of the Lupo. It seems unlikely that pure fuel cell or pure electric vehicles could ever reach competitiveness relative to efficient biodiesel cars, but there is a possibility that hybrids could.

Fig. 10.29 gives some rough estimate of the relative cost of different hybrid configurations. The basic guess of prices for PEM fuel cells and lithium-ion traction batteries is highly uncertain, as it is based on rumors from an industry (understandably) unwilling to quote real prices for prototype vehicle components. However, the relative behavior is more reliable, and Fig. 10.29 offers a parametric study of reducing either the fuel cell cost or the battery cost by 50%. The results thus may have more than academic interest: in the reference case, the pure electric vehicle is the most expensive, followed by the pure fuel cell vehicle, and the least expensive one is the plug-in vehicle with modest battery capacity (25 MJ) combined with a modest fuel cell rating (15 kW). If prices are changed in favor of fuel cells, this vehicle is still the best buy, but rivaled by the lowest fuel cell rated (20 kW) self-recharging version (15 MJ battery capacity). On the other hand, if prices are tilted in favor of batteries, the plug-in vehicle with 58 MJ battery-capacity and only 10 kW of fuel cells has the lowest cost.

One should remember the effect of the shorter life expectancy for batteries and fuel cells, compared to lifetime of the vehicle itself, that was mentioned in Section 1. When discussing cost in a generic sense, life-cycle assessment should be used, especially when comparing polluting vehicles with nonpolluting ones. This has been done in several studies for fuel cell vehicles as well as for comparable vehicles with competing forms of traction [1, 10, 11, 14, 16, 17].

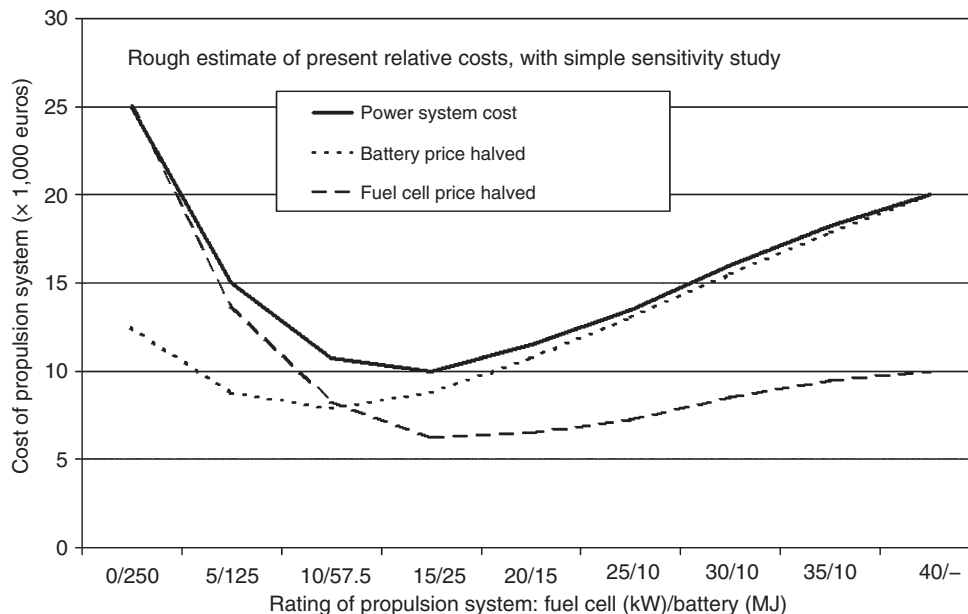


**Figure 10.29** Estimate of power system costs for fuel cell-battery hybrids, based on a cost of 500 €/kW of fuel cell and 100 €/MJ of lithium-ion battery. The sensitivity to these assumed unit costs is investigated by halving one or the other.

## REFERENCES

1. B. Sørensen, *Hydrogen and Fuel Cells*, Elsevier Academic Press, Burlington, MA, USA, 2005.
2. Matlab, a collection of mathematical modeling software, originally in the public domain. Various upgraded commercial versions available from the MathWorks, Natick, MA, USA, 2002.
3. T. Markel, A. Brooker, T. Hendricks, K. Kelly, B. Kramer, M. O'Keefe, et al., *J. Power Sources* 110 (2002) 255. (Recently, a commercial version of the software has been developed by AVL, Graz, Austria. The calculations used as a basis for the present discussions were performed by the author during 2002 and 2003. Most of the figures appeared previously, e.g., in Refs. [8, 13, 14]).
4. Danish Traffic Agency, *New Passenger Car Energy Classification*. Website <http://www.hvorlangtpaa-literen.dk>, (accessed 1.12.2005).
5. B. Sørensen, *Proceedings of the World Hydrogen Technology Conference, Singapore 2005*, paper A16-230. IESE Nanyang University. *Int. J. Hydrogen Energy* 32 (2007) 683.
6. B. Sørensen, *Proceedings of the 2nd European Hydrogen Energy Conference, Zaragoza, Spain, 2005*, paper 4c-3. IDEA Madrid. *Int. J. Hydrogen Energy* 32 (2007) 1597.
7. S. Studer, R. Wagner, *Measurements made at Oak Ridge National Laboratory, TN, USA, and described in Advisor program documentation file for module FC\_CI60* written by V. Johnson at National Renewable Energy Laboratory, Golden, CO, USA, 2001.
8. G. Schweimer, M. Levin, *Life Cycle Inventory for the Golf A4* (internal report Volkswagen AG, 2001, used in VW Environmental Report 2001/2002: Mobility and Sustainability, 2002).
9. VW, *Lupo 3 litre TDI Technical Data*, Volkswagen AG, Wolfsburg, Germany, 2001.
10. S. Weiss, J. Heywood, A. Schafer, F. AuYeung, *On the Road 2020*. Massachusetts Institute of Technology Report EL 00-003. Lab. Energy & Environment, MIT Cambridge, MA, USA, 2000.
11. S. Weiss, J. Heywood, A. Schafer, V. Natarayan, *Comparative Assessment of Fuel Cell Cars*. Lab. Energy & Environment, Report 2003-001 RP, MIT, Cambridge, MA, USA, 2003.



12. L. Pelkmans, S. Hultén, R. Cowan, G. Azkarate, A. Christidis, Institute for Prospective Technology Studies, JCR Report EUR 20746 EN, Sevilla, Spain, 2003.
13. B. Sørensen, *Renewable Energy*, third ed., Elsevier Academic Press, Burlington, MA, USA, 2004.
14. B. Sørensen, Proceedings of the 15th World Hydrogen Energy Conference, Yokohama, Japan, paper 3-1189, World Hydrogen Energy Association, 2004.
15. V. Johnson, in Advisor Program Documentation File for Module Ess\_LI7\_Temp, National Renewable Energy Laboratory, Golden, CO, USA, 2001.
16. M. Pehnt, *Int. J. Hydrogen Energy* 26 (2001) 91.
17. M. Pehnt, in *Handbook of Fuel Cells. Fundamentals, Technology and Applications*, Vol. 4, W. Vielstick, H. Gasteiger, A. Lamm (Eds.), John Wiley & Sons, Chichester, UK, 2003 (Chapter 94).



## APPENDIX: PERFORMANCE MEASURES

It is conventional to specify the performance of road vehicles by giving kilometers driven per liter of fuel, or liters of fuel per 100 km, or MJ/km. The latter is used in this chapter, as it is meaningful no matter what kind of fuel is used. If different vehicles are compared, this kind of measure is less suitable, because different vehicles have different purposes, as demonstrated, for example, by different capabilities for carrying a payload of passengers or freight. I have earlier proposed to employ a measure of the capability to perform “transport work,” defined as the product of kilometers driven and the mass of persons and goods being moved by that number of kilometers [6, 14]. The performance would thus be described by the MJ/(km × kg) required to move a unit of payload by a unit of distance, or by the inverse, km × kg/MJ. I suggest that the transport work-related performance should be used in comparative assessments (including the establishment of a basis for taxation), because it treats small and large passenger cars, freight movement by vans, lorries, ships, or airplanes, etc., on the same footing.



# Life Cycle Assessment of Hydrogen Fuel Cell and Gasoline Vehicles

Mohammed M. Hussain\* and Ibrahim Dincer<sup>1\*\*</sup>

\*National Research Council – Institute of Fuel Cell Innovation, Vancouver, British Columbia, Canada

\*\*Faculty of Engineering and Applied Science, Institute of Technology (UOIT), University of Ontario, Oshawa, Ontario, Canada

## Contents

1. Introduction	275
2. Methodology	278
3. Scope	279
4. Limitations	280
5. Results and Discussion	280
6. Concluding Remarks	284
References	285



## 1. INTRODUCTION

The transportation sector is a significant contributor to major environmental concerns such as global warming, greenhouse gas (GHG) emissions, and climate change. According to the US Environmental Protection Agency (EPA) estimates, in 2006, approximately 28% of total US GHG emissions came from the transportation sector [1]. The technology which provides a potential solution to major environmental concerns arising from the transportation sector is often referred to as polymer electrolyte membrane (PEM) fuel cell. PEM fuel cell-powered vehicles using hydrogen have many advantages, such as energy efficient and environmentally benign operation, compatible with renewable energy sources and carriers of future energy security, economic growth, and sustainable development.

However, to validly assess an emerging technology like PEM fuel cell-powered vehicle, the methodology must consider the total system over its entire life cycle. The life cycle of a vehicle technology must include all the steps required to produce a fuel, to manufacture a vehicle, and to operate and maintain the vehicle throughout its lifetime including disposal and recycling at the end. A typical life cycle of a vehicle is shown in Fig. 11.1. Utilizing a life cycle approach is essential in better understanding the relative importance of one technology over other [2]. On the other hand, without a life cycle

<sup>1</sup> Corresponding author: Ibrahim.Dincer@uoit.ca

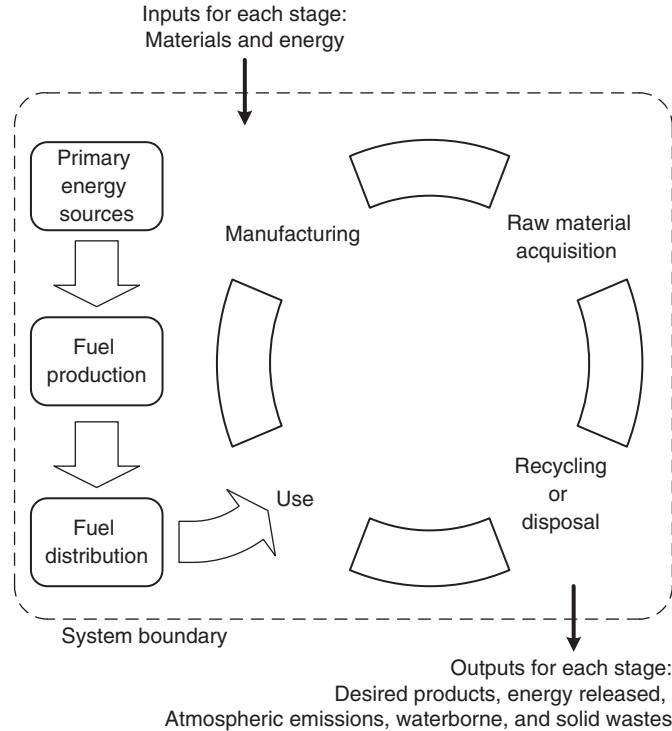


**Figure 11.1** Typical life cycle stages of a vehicle.

approach, false conclusions can be drawn [3]. Therefore, many North American and European companies have incorporated life cycle-based methodologies into their business and decision making processes.

One such approach which assesses or evaluates the technologies over their entire life cycle is often referred to as life cycle assessment (LCA). LCA is a “cradle-to-grave” approach, which sets a systematic procedure for compiling and examining the inputs and outputs of materials and energy and associated environmental impacts of a product or technology along its entire life cycle [4,5]. According to the International Organization for Standardization (ISO), an LCA involves four major steps, as illustrated in Fig. 11.2. The first major step of an LCA is to define the goal and scope of an investigated system or product, wherein the intended application of the study, the data sources, and the system boundaries are described and the criteria for selecting input and output flows or processes are specified. The second major step is referred to as the “inventory analysis,” which involves collection of data and calculation or quantification of relevant inputs and outputs over the entire life cycle stages of an investigated system. Typically, data collection follows a process chain, involving extraction, conversion, transport, production, use and disposal or recycling. Then, the potential impacts of all the relevant input

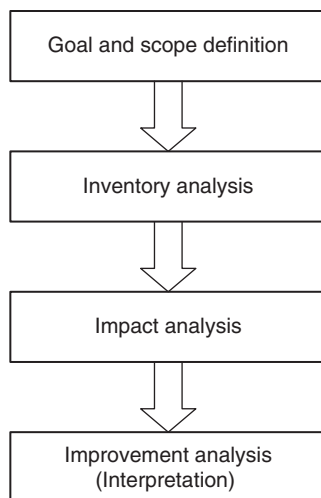


**Figure 11.2** Steps involved in an LCA [4].

and output flows considered in the inventory analysis are determined in the third major step of an LCA, which is referred to as the “impact analysis.” Finally, in the last step of an LCA, the findings from the inventory and impact analyses are combined to draw conclusions and to provide future directions for improving the design and performance of the investigated system [6].

Numerous LCA studies on hydrogen fuel cell technology in relation to conventional and other alternative transport solutions have been reported in the literature, mainly focusing on different stages of vehicle life cycle with different fuel options and variable degrees of details and impacts [7–19]. Weiss et al. [8] assessed the technologies for new passenger cars that will be developed and commercialized by the year 2020. It was reported that their quantitative results are subject to the uncertainties due to projections into the future and those uncertainties are larger for rapidly developing technologies, such as fuel cells and new batteries. In another assessment from Weiss et al. [11], it was concluded that hydrogen is the only promising fuel option for automobile systems with much lower GHG emissions only if it is produced from nonfossil sources of primary energy (such as nuclear, wind, or solar) or from fossil primary energy with carbon sequestration.

Colella et al. [14] conducted an LCA to estimate the net change in emissions and energy use from an instantaneous change to a hydrogen fuel cell vehicle (HFCV) fleet. Granovskii et al. [15] also conducted life cycle analysis of hydrogen fuel cell and gasoline vehicles using a first principle methodology. Similarly, Zamel and Li [16,17] performed life cycle studies of hydrogen fuel cell and internal combustion engine gasoline vehicles in Canada and the United States, with fuel cycle calculations carried out using GREET [20] and vehicle cycle data obtained from the published literature. General Motors (GM) also conducted two well-to-wheels (WTW) analysis [18,19], one based in North

America and the other in Europe. A total of 88 fuel supply pathways including 14 hydrogen-based pathways were examined in the GM's European WTW analysis.

The objective of this chapter is to present an LCA of HFCV which includes not only the operation stage of the vehicle on the road but also the manufacture and distribution of both the vehicle and the fuel during the vehicle's entire lifetime and to compare it with the conventional gasoline internal combustion engine vehicle (ICEV).

## 2. METHODOLOGY

The LCA of a vehicle technology is the comprehensive evaluation of all the major steps required to make up the life cycle of a vehicle and is shown in Fig. 11.3. It can be classified into two major cycles, referred to as the "fuel cycle" and the "vehicle cycle". The "fuel cycle" involves the following stages:

- *Feedstock production*: Energy consumption and GHG emissions during the production of primary energy sources (natural gas and crude oil) are quantified in this stage.
- *Feedstock transport*: The primary energy sources for hydrogen and gasoline have to be transported to the refineries and reforming plants. Energy consumption and GHG emissions during the transport of primary energy sources are counted in this stage.
- *Fuel production*: Energy consumption and GHG emissions during processing of primary energy sources (refining crude oil for gasoline and reforming natural gas for hydrogen) are quantified in this stage.

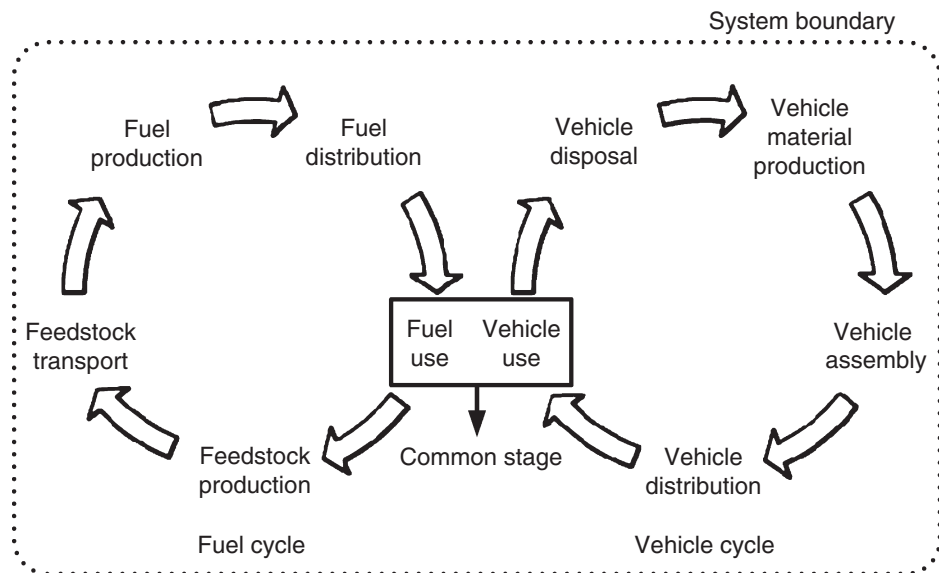


Figure 11.3 Vehicle life cycle stages described in Section 2.

- *Fuel distribution*: Energy consumption and GHG emissions during distribution of hydrogen and gasoline to the tanks of the vehicles are counted in this stage. Typically, distribution of gasoline follows a supply chain: from refineries to terminals by ship or pipeline, transfer to road tankers, to service stations, and finally to vehicle tank. Similarly, natural gas is transported through pipeline or road tankers to decentralized refueling stations, where hydrogen is produced through steam reforming.

On the other hand, the “vehicle cycle” consists of the following stages:

- *Vehicle material production*: Energy use and GHG emissions from vehicle materials production are counted in this stage. Typically, vehicle incorporates nearly 890 kg of ferrous metals, 100 kg of different types of plastics, roughly 80 kg of aluminum, and about 200 kg of other materials [8]. And for PEM fuel cell-powered automobile, we need the materials for fuel cell components such as polymer membrane, platinum as catalyst, graphite, etc.
- *Vehicle assembly*: The energy required and GHG emissions for transport of vehicles during assembly are quantified here. Because of the complex supply chain in the automobile industry and the associated difficulty in estimating vehicle assembly energy requirements, assembly energy is typically estimated as a linear function of vehicle mass [21].
- *Vehicle distribution*: The energy needed and GHG emissions during the transport of a vehicle from the assembly line to the dealership are counted in this stage.
- *Vehicle use*: It coincides with the fuel use stage of the “fuel cycle.” It includes energy consumption and GHG emissions during maintenance and repair over the lifetime, which is typically assumed to be 300,000 km [13].
- *Vehicle disposal*: After a vehicle’s life, the vehicle is shredded. The disposal energy is the sum of energy needed to move the bulk from the dismantler to a shredder and the shredding energy [22].

The assessment of energy consumption and GHG emissions during the life cycle stages of fuel and vehicle cycles is based on various sources reported in the published literature. The analyses of different stages of both cycles (fuel and vehicle) are then combined to obtain the total life cycle energy consumption and GHG emissions of a vehicle.

---



### 3. SCOPE

In this chapter, the following fuel and vehicle technologies are assessed based on the methodology described in the above section.

*Fuels considered:*

- Hydrogen from natural gas reforming in hydrogen refueling stations
- Gasoline from crude oil

*Vehicle technologies considered:*

- PEM fuel cell-powered vehicle using hydrogen as fuel
- Spark ignition internal combustion (IC) engine-powered vehicle using gasoline as fuel

---

## 4. LIMITATIONS

The assessment presented in this chapter is based on various data sources published in the open literature, and like any other assessment or analysis has some limitations. The major boundaries and assumptions considered in the present assessment are stated below:

- The boundaries of the physical system are such that secondary energy and environmental effects are not quantified. For instance, energy consumption and GHG emissions during the operation of a steam reforming plant of natural gas are quantified, but the energy and emissions involved in making the steel, concrete or other elements embodied in the plant itself are not counted.
- Data used for assessment is from mid-size family passenger cars (average vehicle weight is 1,300 kg).
- Data used is based on North American experience.
- Other production methods (e.g., electrolysis, nuclear, hydro, etc.) of hydrogen are not considered in the present assessment: only large-scale production methods are considered. For instance, hydrogen is mostly produced via steam reforming of natural gas at present; similarly, gasoline is mostly produced via crude oil refining.

---

## 5. RESULTS AND DISCUSSION

We begin the assessment from fuel cycles, which include recovery of the raw material for each (such as natural gas for hydrogen or crude oil for gasoline) through conversion to the final fuel (such as hydrogen or gasoline) and delivery into the tank of the passenger car. The two characteristics of the fuel cycles assessed in the present study include the following:

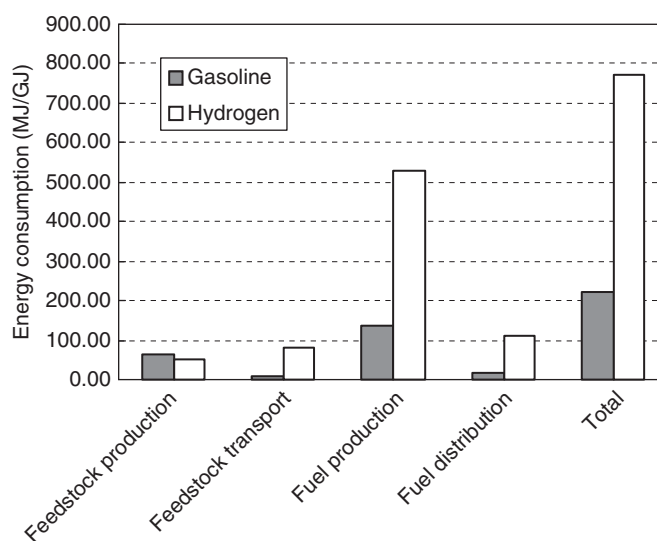
- Total energy consumed originating from raw materials or other energy sources
- Total GHG emitted from raw materials or other sources

The GHG emissions assessed in the present study are CO<sub>2</sub> and CH<sub>4</sub>. N<sub>2</sub>O is neglected since its greenhouse contribution for each of the fuel cycles accounts for less than 1% of the other gas emissions [23,24].

The energy consumption and GHG emissions during fuel cycles for hydrogen and gasoline are listed in Table 11.1. Figs. 11.4 and 11.5 show the comparison of energy consumption and GHG emissions during the fuel cycles of hydrogen and gasoline, respectively. It can be seen from the figures that both energy consumption and GHG

**Table 11.1** Energy consumption and GHG emissions during fuel cycles [8,25,26]

	Energy consumption (MJ/GJ)		GHG emissions (kg CO <sub>2</sub> /GJ)	
	Hydrogen	Gasoline	Hydrogen	Gasoline
Feedstock production	50.0	62.40	23.52	3.40
Feedstock transport	80.0	8.20	1.23	0.60
Fuel production	530.0	135.00	99.00	12.00
Fuel distribution	110.0	15.00	8.25	0.70
Total	770.0	220.60	132.00	16.70

**Figure 11.4** Energy consumption during fuel cycles of hydrogen and gasoline [8,25,26].

emissions during the fuel cycle of hydrogen are higher when compared to the gasoline fuel cycle. Fuel production stage of hydrogen cycle is the major contributor to the total energy consumption and GHG emissions. The other significant contribution comes from the fuel distribution stage which includes the primary energy in the form of the electric power used for compressing hydrogen.

Table 11.2 lists the energy consumption and GHG emissions during vehicle cycle of HFCV and ICEV. The comparison of energy consumption and GHG emissions during the vehicle cycle of HFCV and ICEV is shown in Figs. 11.6 and 11.7, respectively. The greatest contributor to energy consumption and GHG emissions for the ICEV is the vehicle use stage (coincides with fuel use stage). The energy consumption of ICEV is



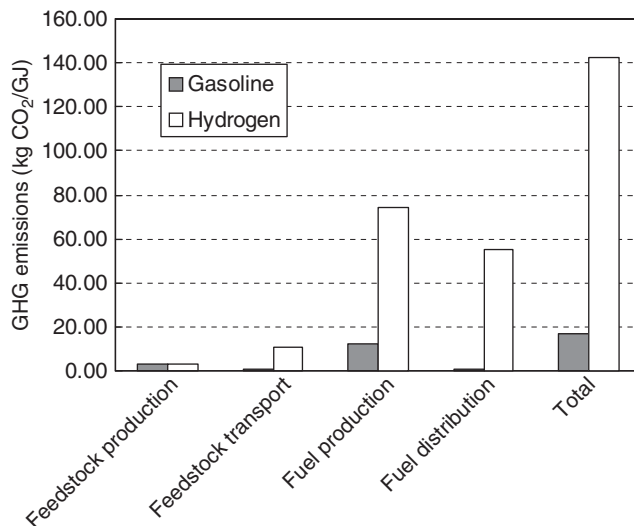


**Figure 11.5** GHG emissions during fuel cycles of hydrogen and gasoline [8,25,26].

**Table 11.2** Energy consumption and GHG emissions during vehicle cycles [8,13]

	Energy consumption (MJ)		GHG emissions (kg CO <sub>2</sub> )	
	HFCV	ICEV	HFCV	ICEV
Vehicle materials production	54,600.0	49,800.0	3,630.0	3520.0
Vehicle assembly	24,300.0	25,500.0	1,650.0	1,760.0
Vehicle distribution	2,100.0	2,100.0	110.0	110.0
Vehicle use	195,000.0	819,000.0	0.0	5,903.3
Vehicle disposal	300.0	300.0	0.0	0.0
Total	276,300.0	896,700.0	5,390.0	64,423.3

about 3 times higher than that of HFCV. Moreover, GHG emissions during the vehicle cycle of HFCV are around 8% of the GHG emissions of the ICEV, which clearly indicates the environmental friendliness of HFCV.

Figs. 11.8 and 11.9 show the comparison of life cycle energy consumption and life cycle GHG emissions of the two vehicle technologies considered in the present assessment. Although the fuel cycle energy consumption of HFCV is about 3.5 times higher than that of ICEV, the overall life cycle energy consumption of HFCV is about 2.3 times less than that of ICEV. This is due to high efficiency of HFCV as compared to ICEV during the vehicle use stage of the vehicle cycle. Similarly, the

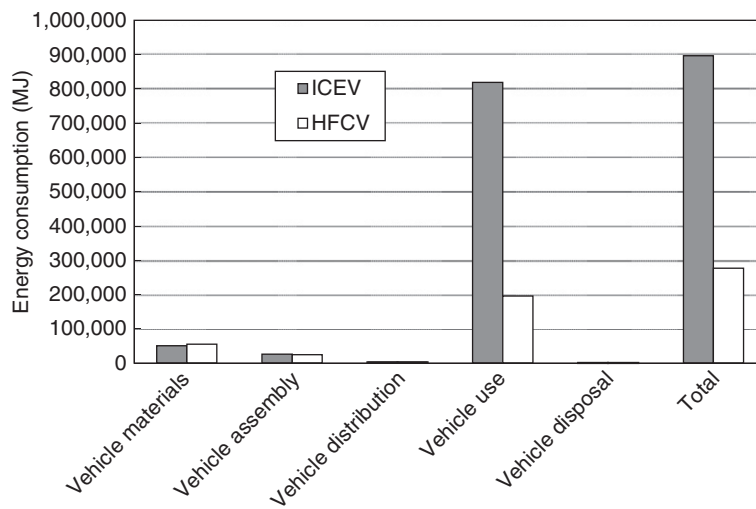


**Figure 11.6** Energy consumption during vehicle cycles of HFCV and ICEV [8,13].

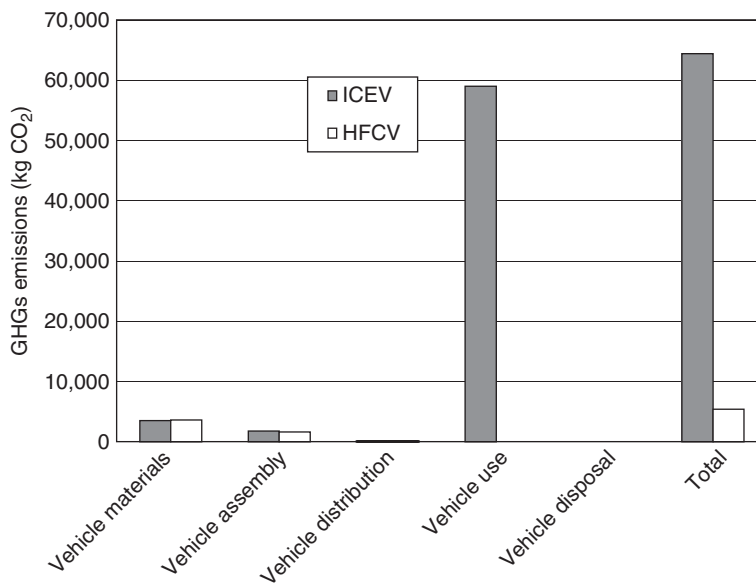


**Figure 11.7** GHG emissions during vehicle cycles of HFCV and ICEV [8,13].

GHG emissions of HCFV is 8.5 times higher than that of ICEV during the fuel cycle; however, the overall life cycle GHG emissions of an HFCV are about 2.6 times lower than that of ICEV, which is due to zero GHG emissions during the vehicle use stage of the vehicle cycle.

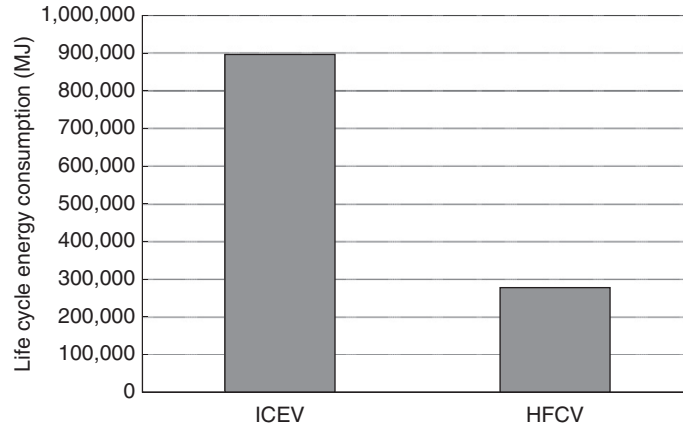


**Figure 11.8** Life cycle energy consumption of vehicle technologies.

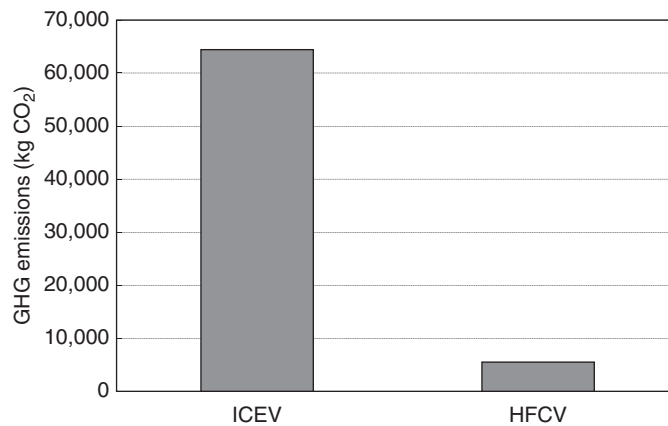


**Figure 11.9** Life cycle GHG emissions of vehicle technologies.



## 6. CONCLUDING REMARKS

An LCA of HFCV and ICEV has been presented in this chapter. An LCA is a technique to assess the energy and associated environmental impact of a system or product. The assessment presented in this chapter is based on various sources available in the published literature. The characteristics of the vehicles (HFCV and ICEV) assessed are energy consumption and GHG emissions during their entire life cycles.

It is found that the energy consumption and GHG emissions during the fuel cycle of hydrogen are higher than the fuel cycle of gasoline, and fuel production stage of the hydrogen fuel cycle is the major contributor to the total energy consumption and GHG emissions.

However, during the vehicle cycle, the energy consumption and GHG emissions of ICEV are higher than that of HFCV, and the greatest contributor to the energy consumption and GHG emissions is the vehicle use stage of the ICEV. Moreover, it is found that the overall life cycle energy consumption of HFCV is about 2.3 times less than that of ICEV and overall GHG emissions of HFCV are about 2.6 times lower than that of ICEV.

## REFERENCES

1. EPA, Inventory of US Greenhouse Gas Emission and Sinks: 1990–2006, Office of Global Warming, Washington, D.C., 2008.
2. M. Pehnt, *Int. J. Life Cycle Ass.* 8 (2003) 283.
3. I. Pembina, *Life-cycle Value Assessment (LCVA) of Fuel Supply Options for Fuel Cell Vehicles in Canada*, Calgary, Canada, 2002.
4. ISO 14040, *Environmental Management – Life Cycle Assessment – Principles and Framework*, International Organisation for Standardisation, Geneva, Switzerland, 1997.
5. M. Pehnt, *Int. J. Hydrogen Energy* 26 (2001) 91.
6. M. Pehnt, *Handbook of Fuel Cells – Fundamentals, Technology and Applications*, John Wiley and Sons, Ltd, Chichester, UK, 2003.
7. M. Singh, R. Cuenca, J. Formento, L. Gaines, B. Marr, D. Santini, et al., *Total Energy Cycle Assessment of Electric and Conventional Vehicles: An Energy and Environmental Analysis*, Argonne National Laboratory, ANL/ES/RP-96387, Springfield, VA 22161, 1998.
8. M.A. Weiss, J.B. Heywood, A. Schafer, F.F. AuYeung, *On the Road in 2020*, MIT EL 00-003, Energy Laboratory, Massachusetts Institute of Technology, Cambridge, 2000.
9. A. Bauen, D. Hart, *J. Power Sources* 86 (2000) 482.
10. C. Handley, N.P. Brandon, R. van der Vorst, *J. Power Sources* 106 (2002) 344.
11. M.A. Weiss, J.B. Heywood, A. Schafer, V.K. Natarajan, *Comparative Assessment of Fuel Cell Cars*, MIT LFEE 2003-001, Laboratory of Energy and the Environment, Massachusetts Institute of Technology, Cambridge, 2003.
12. H.L. MacLean, L.B. Lave, *Environ. Sci. Technol.* 37 (2003) 5445.
13. B. Sorensen, *Total Life-Cycle Assessment of PEM Fuel Cell Car*, Energy and Environment Group, Roskilde University, Denmark, 2004.
14. W.G. Collela, M.Z. Jacobson, D.M. Golden, *J. Power Sources* 150 (2005) 150.
15. M. Granovskii, I. Dincer, M. Rosen, *Int. J. Hydrogen Energy* 31 (2005) 337.
16. N. Zamel, X. Li, *J. Power Sources* 155 (2006) 297.
17. N. Zamel, X. Li, *J. Power Sources* 162 (2006) 1241.
18. General Motors, Argonne National Laboratories, BP, ExxonMobil, and Shell, *GM Well-to-Wheel Energy Use and Greenhouse Gas Emissions of Advanced Fuel/Vehicle Systems – North American Analysis*, General Motors, Argonne, USA, 2001.
19. General Motors, L-B-Systemtechnik GmbH, BP, ExxonMobil, and Total-FinaElf, *GM Well-to-Wheel Energy Use and Greenhouse Gas Emissions of Advanced Fuel/Vehicle Systems – European Analysis*, General Motors, Ottobrun, Germany, 2002.
20. M. Wang, *REET 1.5 – Transportation Fuel-Cycle Model*, vol. 1: Methodology, Development, Use and Results, Center for Transportation Research, Argonne National Laboratory, Argonne, USA, 1999.
21. *Automotive Engineering, Life Cycle Analysis: Getting the Total Picture on Vehicle Engineering Alternatives*, SAE International, Troy MI 48084 USA, 1996.
22. *Automotive Engineering, Progress in Recycling Specific Materials from Automobiles*, SAE International, Troy MI 48084 USA, 1997.
23. M. Wang, H.S. Huang, *A Full Fuel Cycle Analysis of Energy and Emissions Impacts of Transportation Fuel Produced from Natural Gas*, Report ANL/EDSs-40, prepared by Argonne National Laboratory, The Center for Transportation Research, Energy Systems Division for US DOE, 1999.
24. Energy Information Administration (EIA), US DOE, *Emissions of Greenhouse Gases in the United States 1996*, DOE/EIA-0573(96), 1997.

25. IEA (International Energy Agency), *Automotive Fuels for the Future: The Search for Alternatives*, IEA-AFIS, Paris, 1999.
26. P.L. Spath, M.K. Mann, *Life Cycle Assessment of Hydrogen Production Via Natural Gas Steam Reforming*, NREL (National Renewable Energy Laboratory), Colorado, NREL/TP-570-27637, 2001.



# DOE’s National Fuel Cell Vehicle Learning Demonstration Project — NREL’s Data Analysis Results

Keith Wipke<sup>1\*</sup>, Sam Sprik<sup>\*</sup>, Jennifer Kurtz<sup>\*</sup>, Todd Ramsden<sup>\*</sup>, and John Garbak<sup>\*\*</sup>

<sup>\*</sup>National Renewable Energy Laboratory, Golden, CO 80401, USA

<sup>\*\*</sup>U.S. Department of Energy, Washington, DC 20585, USA

## Contents

1. Introduction	288
2. Approach and Industry Partners	288
3. Demonstration Logistics	289
3.1 Geographic regions	289
3.2 Vehicle rollout	289
3.3 Hydrogen production technologies	290
3.4 Process for publishing results	290
4. Results	291
4.1 Vehicle fuel economy	291
4.2 Vehicle driving range	291
4.3 Fuel cell efficiency	292
4.4 Fuel cell system specific power and power density	293
4.5 Fuel cell durability	293
4.6 Factors affecting fuel cell durability	297
4.7 Vehicle maintenance	298
4.8 Infrastructure maintenance	298
4.9 Vehicle refueling rates	298
4.10 Fueling rate comparison between fills for 350 and 700 bar	298
4.11 On-site production efficiency from natural gas reformation and electrolysis	299
4.12 Vehicle greenhouse gas emissions	300
4.13 Fuel cell vehicle freeze capability	301
5. Concluding Remarks	302
Acknowledgements	303
Definitions, Acronyms, Abbreviations	303
References	303

<sup>1</sup> Corresponding author: Keith.Wipke@nrel.gov



## 1. INTRODUCTION

The primary goal of this project is to validate vehicle and infrastructure systems using hydrogen as a transportation fuel for light-duty vehicles. This means validating the use of fuel cell vehicles (FCVs) and hydrogen refueling infrastructure under real-world conditions using multiple sites, varying climates, and a variety of sources for hydrogen. Specific objectives include validating hydrogen vehicles with more than a 250-mile range, 2,000 h fuel cell durability, and a \$3 per gasoline gallon equivalent (\$3/gge [gallon of gasoline equivalent], U.S. dollars) hydrogen production cost (based on modeling for volume production). We are identifying the current status of the technology and tracking its evolution over the duration of the 5-year project, particularly between first- and second-generation FCVs.

The role of the National Renewable Energy Laboratory (NREL) in this project is to generate the maximum value for the U.S. Department of Energy (DOE) and industry from the data produced by this “learning demonstration.” We seek to understand the progress being made toward achieving our technical targets and to provide information that will help move the program’s research and development (R&D) activities toward more quickly developing cost-effective, reliable hydrogen FCVs and supporting refueling infrastructure.



## 2. APPROACH AND INDUSTRY PARTNERS

Our approach to accomplishing the project’s objectives is structured around a highly collaborative relationship with each of the four industry teams, which includes Chevron/Hyundai-Kia, Daimler/BP, Ford/BP, and GM/Shell. We are receiving raw technical data for both the hydrogen vehicles and the refueling infrastructure that enable us to perform unique and valuable analyses across all four teams. This allows us to feed the current technical challenges and opportunities back into the DOE Fuel Cell Technologies R&D Program (FCT) and assess the current status and progress toward targets.

To protect the commercial value of these data for each company, we established the Hydrogen Secure Data Center (HSDC) in 2004 to house the data and perform our analysis, as shown in Fig. 12.1. To ensure that value is fed back to the hydrogen community, we publish composite data products (CDPs) twice a year at technical conferences to report on the progress of the technology and the project, focusing on the most significant and recent results [1–4]. Additional CDPs are being conceived as additional trends and results of interest are identified, and as we receive requests from DOE, industry, and codes and standards committees. We also provide detailed analyses (which are not public) of data for each individual company back to them to maximize the benefit to industry of NREL’s analysis work and to obtain

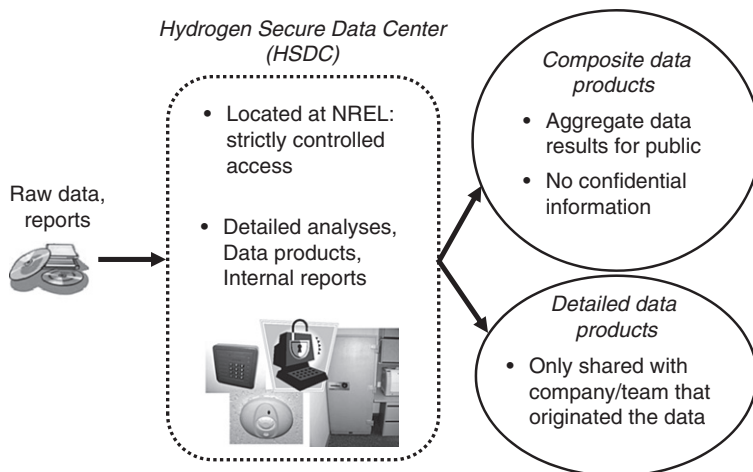


**Figure 12.1** Data flow into NREL's Hydrogen Secure Data Center, resulting in public Composite Data Products and nonpublic Detailed Data Products.

feedback on our methodologies and results. These nonpublic results are known as detailed data products.



## 3. DEMONSTRATION LOGISTICS

### 3.1 Geographic regions

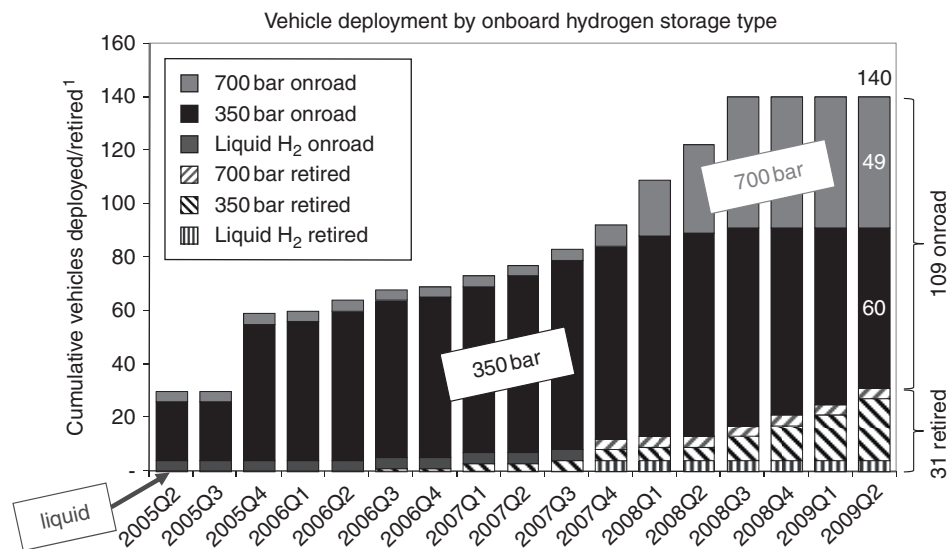
This project focuses on five geographic regions in the United States, in part to include climatic differences—cold, hot, humid, or dry—in the study as well as to include different driving patterns:

1. San Francisco to Sacramento region (California)
2. Los Angeles metropolitan area (California)
3. Detroit metropolitan area (Michigan)
4. Washington, D.C., to New York region (Northeast U.S.)
5. Orlando metropolitan area (Florida)

### 3.2 Vehicle rollout

Beginning in 2005, the automotive companies in the study deployed vehicles in the five geographic regions listed above, and full deployment of both first- and second-generation vehicles occurred by the third quarter (Q) of 2008, as shown in Fig. 12.2. The total number of vehicles deployed was 140. The graph also shows that three onboard hydrogen storage systems were used: liquid hydrogen, 350 bar compressed hydrogen, and 700 bar compressed hydrogen. As discussed later, the 700 bar compressed hydrogen was necessary to achieve the >250-mile driving range target for 2008.





(1) Retired vehicles have left DOE fleet and are no longer providing data to NREL.

**Figure 12.2** Vehicle deployment by onboard hydrogen storage type.

This figure also shows that as the vehicles age and specific customers complete the usage planned for them, some of the vehicles are being retired or returned to the manufacturers (as indicated by hatched bars). Of the total of 140 vehicles deployed, 31 have been retired (or otherwise removed from the set of vehicles provided to NREL) and 109 are still on the road (as of June 2009).

### 3.3 Hydrogen production technologies

To support these vehicles, four different types of hydrogen refueling stations were installed. Of the 20 stations, just over half featured on-site production of hydrogen from either reforming natural gas (four stations) or electrolyzing water (seven stations). The remaining stations used hydrogen that was delivered to the site, either as compressed gas cylinders (six stations) or as liquid hydrogen (three stations). As of June 2009, three of the 20 stations had been retired, with more stations being retired as the project approaches completion.

### 3.4 Process for publishing results

The most recent public results were generated by analyzing all of the data received since the inception of the project and creating a total of 72 new or updated CDPs [5]. The analyses include second-by-second data from every one of the 140 vehicles and data from each refueling event, along with monthly data on hydrogen production efficiencies. To accomplish such a massive data analysis activity, we developed and revised an

in-house analysis tool—the Fleet Analysis Toolkit, or “FAT.” Because there are now so many technical results from this project, they cannot all be discussed in any individual paper or presentation. Therefore, in 2007 NREL launched a new page on the Internet at [http://www.nrel.gov/hydrogen/cdp\\_topic.html](http://www.nrel.gov/hydrogen/cdp_topic.html) to provide the public with direct access to the latest published results. Since all 72 CDPs are now available on the Internet, this discussion will include just some of the highlights and key findings.



## 4. RESULTS

### 4.1 Vehicle fuel economy

Vehicle fuel economy was measured using city and highway drive-cycle tests on a chassis dynamometer according to the draft SAE J2572 standard. These raw test results were then adjusted according to U.S. Environmental Protection Agency (EPA) methods to create the fuel economy that consumers would see on window stickers when purchasing a vehicle (22% reduction for Hwy, 10% reduction for City). Since the project began in 2005, the EPA adjustments were made using the pre-2007 model year algorithms. We acknowledge that new vehicles sold today use a new set of cycles and adjustment algorithms; however, these were not retroactively implemented on the project vehicles or their previously generated results. We will likely add another set of results using the new EPA algorithms to see how well they capture the real-world fuel economy that we have observed.

Generation 1 vehicles had an adjusted fuel-economy range of 42–57 miles/kg hydrogen for the four teams, and generation 2 vehicles showed a slight improvement in fuel economy, to 43–58 miles/kg. Onroad fuel economy from first-generation vehicles was 31–45 miles/kg; from second-generation vehicles, it was 35–52 miles/kg. All of the Learning Demonstration vehicles were built using existing vehicle platforms that were originally designed for gasoline combustion engines.

### 4.2 Vehicle driving range

Vehicle driving range was calculated using the fuel economy results discussed above and multiplying them by the usable hydrogen stored onboard each vehicle. Generation 1 vehicles had a range from just over 100 miles up to 190 miles from the four teams, whereas generation 2 vehicles using 700 bar pressure hydrogen tanks showed a significantly improved window-sticker driving range of 196–254 miles, as shown in Fig. 12.3. This demonstrated that DOE's September 2008 milestone of 250 miles had been achieved. As mentioned earlier, all of the Learning Demonstration vehicles are based on existing platforms, and higher driving ranges are expected when the vehicles are designed around hydrogen, which allows larger quantities of hydrogen to be stored as well as an optimized vehicle structure, mass, aerodynamics, and layout.

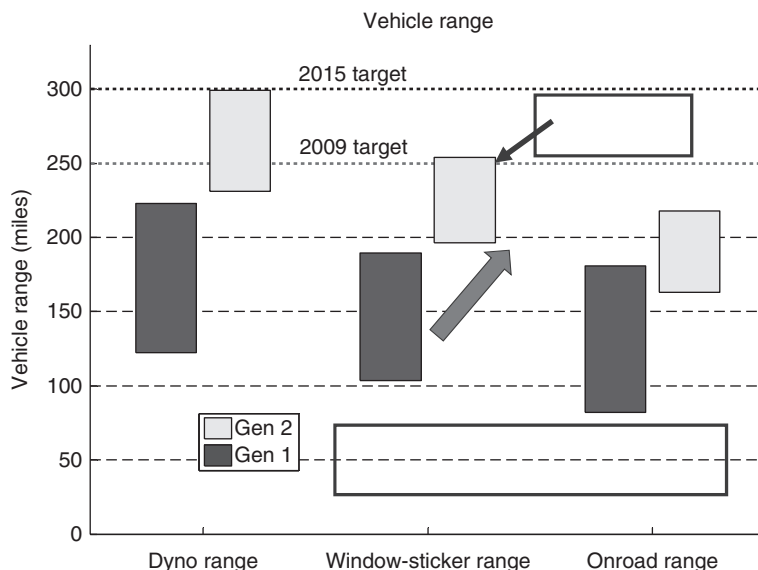
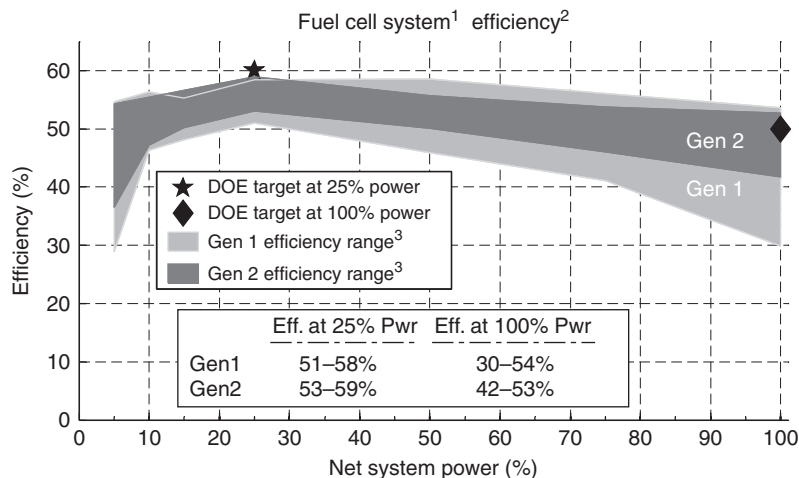


**Figure 12.3** Vehicle driving range for first- and second-generation vehicles, based on fuel economy and usable hydrogen.

### 4.3 Fuel cell efficiency

The baseline fuel cell system efficiency was measured from selected vehicles on a vehicle chassis dynamometer at several steady-state points of operation. The system, as defined here, includes any parasitic loads responsible for the care and feeding of the stack, including air compressors, water pumps, fans, and the like. DOE's technical target for net system efficiency at  $\frac{1}{4}$  power is 60%; the target at full power is 50% efficiency. Results that we had published earlier showed efficiency data at only  $\frac{1}{4}$  power, but the new results, shown in Fig. 12.4, show the span of efficiency data from all four teams over the entire power range, from 5% up to 100% for both first- and second-generation systems. At  $\frac{1}{4}$  power, first-generation systems were 51–58% efficient, while second-generation systems were 53–59% efficient; this is compared with DOE's ultimate 60% efficiency target. At full power, where the target is 50% efficiency, the first-generation systems were 30–54% efficient and second-generation systems were 42–53% efficient. So the efficiency target at 100% power has been met, and the target at  $\frac{1}{4}$  power is within one percentage point of being met.

Perhaps the most important finding relative to fuel cell system efficiency is that these high efficiencies were maintained while simultaneously improving stack durability and cold-start freeze tolerance. This demonstrates a significant achievement resulting from the project. The improvements in both stack durability and cold-start tolerance are discussed later.



1. Gross stack power minus fuel cell system auxiliaries, per DRAFT SAE J2615. Excludes power electronics and electric drive.
2. Ratio of DC output energy to the lower heating value of the input fuel (hydrogen).
3. Individual test data linearly interpolated at 5,10,15,25,50,75, and 100% of max net power. Values at high power linearly extrapolated due to steady state dynamometer cooling limitations.

**Figure 12.4** Fuel system efficiency as a function of power.

#### 4.4 Fuel cell system specific power and power density

Data were received on total fuel cell system mass, volume, and power. Both the specific power (W/kg) and the power density (W/L) were evaluated for generation 1 and compared with generation 2 fuel cell systems. We found that while the fuel cell system power density stayed about the same between the two generations (ranging from 300 to 400 W/L), there were significant improvements in fuel cell system specific power, improving from generation 1 results of 200–300 W/kg up to generation 2 results of 300–400 W/kg. It appears as though it may take another generation or two before the fuel cell systems achieve DOE's 2010 and 2015 target of 650 W/kg.

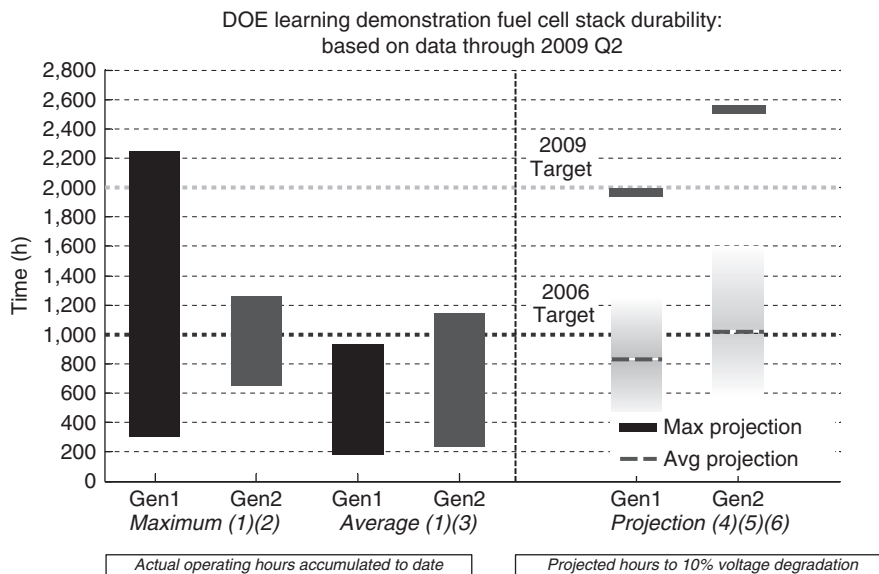
When the fuel cell system is combined with the hydrogen storage system, we can compare that result with DOE 2010 and 2015 R&D goals to allow comparisons with other energy and power systems, such as batteries. We found that the system, which includes the fuel cell and the hydrogen storage, can be over 200 W/L, just shy of the target of 220 W/L. The combined system specific power was as high as 250 W/kg from generation 2 vehicles, compared with the target of 325 W/kg.

#### 4.5 Fuel cell durability

Fuel cell stacks will need roughly a 5,000 h life to compete in the light-duty vehicle market. Preliminary durability estimates were first published on this project in the fall of 2006 when most stacks only had a few hundred hours or less of on-road operation

accumulated. NREL developed a methodology for projecting the gradual degradation of the voltage based on the data received to date. This involved creating periodic fuel cell polarization curve fits from the on-road stack voltage and current data, and calculating the voltage under high current. This enabled us to track the gradual degradation of the stacks with time and do a linear fit through each team's data. We then compared these results to the first-generation target of 1,000 h for 2006.

In the past 3 years, many more hours have been accumulated on the first-generation fuel cell stacks (consistent with a staged rollout), and the range of fleet average hours accumulated is now ~200–900 hours. The range of fleet maximum hours accumulated spans ~300–2,200 hours, as shown in Fig. 12.5. This is the first time, to our knowledge,



- (1) Range bars created using one data point for each OEM. Some stacks have accumulated hours beyond 10% voltage degradation.
- (2) Range (highest and lowest) of the maximum operating hours accumulated to date of any OEM's individual stack in "real-world" operation.
- (3) Range (highest and lowest) of the average operating hours accumulated to date of all stacks in each OEM's fleet.
- (4) Projection using on-road data—degradation calculated at high stack current. This criterion is used for assessing progress against DOE targets, may differ from OEM's end-of-life criterion, and does not address "catastrophic" failure modes, such as membrane failure.
- (5) Using one nominal projection per OEM: "Max Projection" = highest nominal projection, "Avg Projection" = average nominal projection. The shaded projection bars represents an engineering judgment of the uncertainty on the "Avg Projection" due to data and methodology limitations. Projections will change as additional data are accumulated.
- (6) Projection method was modified beginning with 2009 Q2 data, includes an upper projection limit based on demonstrated op hours.

**Figure 12.5** Stack hours accumulated and projected hours to 10% voltage degradation.

that a light-duty passenger fuel cell car has accumulated over 2,000 h in real-world operation without the need to repair the fuel cell stack, which is a significant project accomplishment. We now also have sufficient data on second-generation stacks, and we found that the range of average hours accumulated was 200–1150 h, while the span of maximum hours accumulated was 600–1,250 h.

The amount of data extrapolation we have to make using the slope of the linear voltage degradation method (10% voltage drop target divided by the mV/hour slope) continues to decrease as we receive additional data. However, with the additional data we have also found that the accuracy of the 10% voltage degradation projection could be improved by using a nonlinear fit to account for the more rapid degradation that occurs within the first few hundred hours [6]. Fuel cell stack degradation results for this project in 2008 began using a two-segment linear fit and a weighting algorithm to come up with a more robust fleet average that was less sensitive to an individual stack. Note that the 10% criterion, which is used for assessing progress toward DOE targets, may differ from the manufacturer's end-of-life criterion and does not address "catastrophic" failures such as membrane failure. One of the results not included here (CDP number 73) varies this percentage from 10% up to 30% to show the sensitivity to this threshold. The projected times to 10% fuel cell stack voltage degradation from the four teams using this two-step linear fit technique have an average of 833 h for first-generation stacks and 1,020 h from second-generation stacks.

In addition to this voltage degradation technique, five new CDPs have been generated to flesh out the complete picture of the performance and durability of the stacks. Specifically, relative to fuel cell stack durability, the following new results have been created:

- Histogram of fuel cell stack operating hours for first- and second-generation stacks separately, identifying how many of these stacks are (1) still in operation, (2) have been retired, or (3) are not currently accumulating hours (but not removed because of low performance).
- Histogram of power drop during fuel cell stack operation period with the same classifications described above.
- Graphs of the drop in the maximum power capability of the stacks as a function of their operational hours: separate results for first-generation and second-generation stacks.
- Histogram of projected hours to low power operation limit.

Fig. 12.6 shows a histogram of the hours accumulated on each stack for both first- and second-generation stacks. It shows that many first-generation stacks have been retired with <400 h, while a few have very high hours. Second-generation stacks have lower accumulated hours, but very few stacks have been retired because of low performance and most are still in operation. Based on the shape of the power drop shown in Fig. 12.7 for first-generation stacks (which follows a similar pattern so far for second-generation stacks),

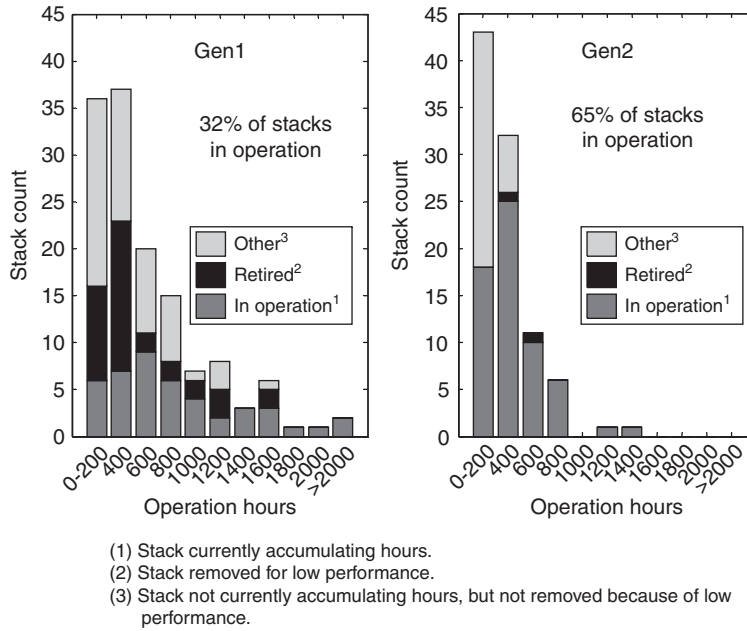
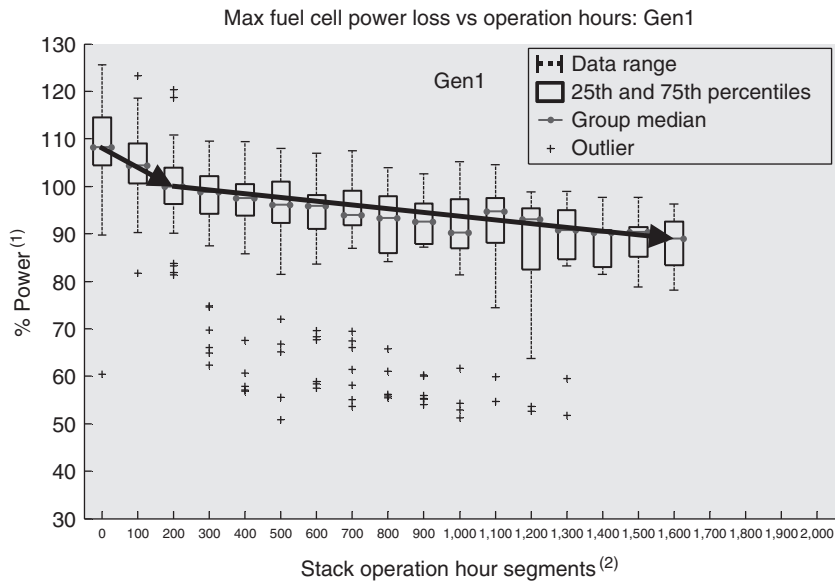


**Figure 12.6** Histogram of operating hours for first- and second-generation stacks.



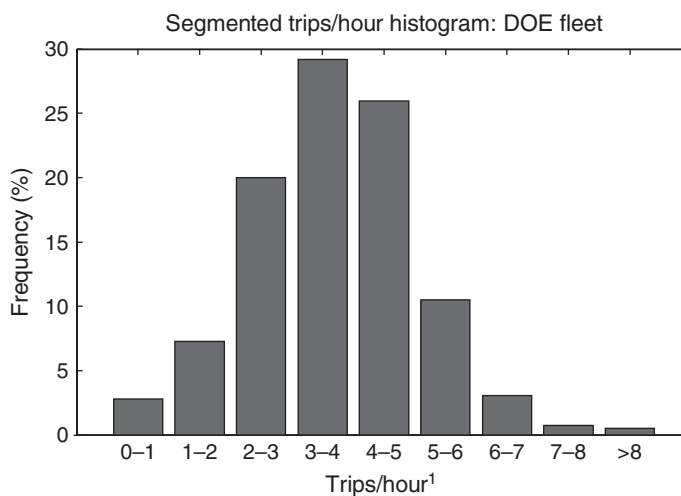
(1) Normalized by fleet median value at 200 h.  
 (2) Each segment point is median FC power (+/-50 h).  
 Box not drawn if fewer than 4 points in segment.

**Figure 12.7** Power loss as a function of operating time for first-generation stacks.

we conclude that there is an initial power drop in roughly the first 200 h and that afterward a much lower degradation rate is observed. Therefore, with much fewer hours accumulated to date on second-generation stacks, current durability projections are expected to be lower than they will be after more data are accumulated (making this a conservative estimate). These stack durability results will be updated as additional data are accumulated.

#### 4.6 Factors affecting fuel cell durability

We continued investigating factors that are affecting the rates of fuel cell stack degradation. Two of these factors that our industry partners asked us to examine were the amount of time the fuel cell spends at various voltage levels and the average number of trips per operating hour. We found that about 15% of the time was spent at roughly the open-circuit voltage and very low current, while only 17% of the time was spent at <70% of the maximum voltage (corresponding to high load). We examined the average number of trips per hour, shown in Fig. 12.8, and found a relatively normal distribution around the median of roughly four trips per hour. This information was also provided to an international fuel cell durability task force that was formulating durability test protocols, as they wanted to make sure they knew the actual number of average trips per operating hour from real stacks in everyday use. We also examined whether there was a trend of average trips per hour as a function of stack operating hours, and we found that the stacks that have demonstrated long hours (to date) show lower average trips per hour. We need to accumulate more data before we can attribute a causal relationship between the two.



(1) Trips/hour based on 50 h segments spanning stack operating period.

**Figure 12.8** Histogram of average trips per hour.



## 4.7 Vehicle maintenance

Over the 4 years of vehicle operation, a large set of data has been collected on all of the vehicle maintenance events. There were a total of 11,075 maintenance events consuming 11,849 h. We found that 33% of the vehicle maintenance events were associated with the fuel cell system, consuming 49% of the maintenance labor. Over half (58%) of the vehicle maintenance events were not related to the power train. Breaking down the details of the fuel cell system into all of its subsystems, we found a surprising result: only 10% of the fuel cell system events were associated with the fuel cell stack, while the most frequently serviced parts of the fuel cell system were the thermal management system (38%); the air system (24%); controls, electronics, or sensors (13%); the fuel system (11%); and then the fuel cell stack (number 5 on the list). This indicates that other components in the fuel cell system rather than the fuel cell stack itself need more attention and potentially more R&D before these vehicles reach the point of commercialization.

## 4.8 Infrastructure maintenance

Like vehicle maintenance, the hydrogen fueling station maintenance data were also analyzed. There were a total of 2,291 infrastructure maintenance events, requiring 11,119 h. While we assumed that one of the production components would top the list, it was actually the system control and safety systems that accounted for the most maintenance events (21%) and labor (20%). The four major components of the system—compressor, electrolyzer, reformer, and dispenser—were roughly equal in terms of maintenance requirements. The hydrogen storage system required the least maintenance, just a few percent.

## 4.9 Vehicle refueling rates

More than 21,000 refueling events have been analyzed to date, and the refueling amount, time, and rate have been quantified. The average time to refuel was 3.26 min, and 86% of the refueling events took less than 5 min. The average amount per fill was 2.14 kg, reflecting both the limited storage capacity of these vehicles (~4 kg, maximum) and drivers' comfort level with letting the fuel gauge get close to empty. DOE's target refueling rate is 1 kg/min, and these Learning Demonstration results indicate an average of 0.78 kg/min, with 24% of the refueling events exceeding 1 kg/min.

## 4.10 Fueling rate comparison between fills for 350 and 700 bar

The previously discussed refueling rates included all types of refueling events that occurred within the project. There has been much interest from industry and from the codes and standards community on the effect of communication versus noncommunication and 350 bar versus 700 bar pressure on fill rates. A communication fill means that the vehicle communicates data about the state of its hydrogen storage tank(s), such as tank

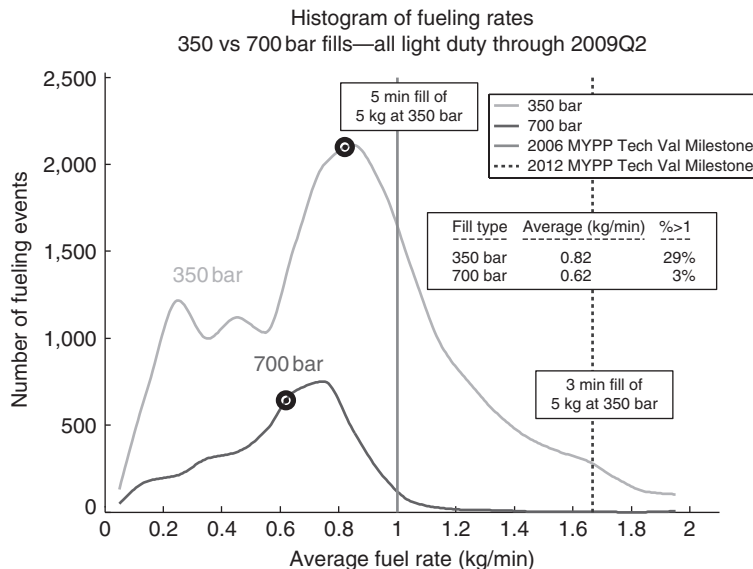


**Figure 12.9** Comparison of fueling rates for 350 and 700 bar pressure refueling rates.

temperature, pressure, and maximum pressure rating, to the refueling station. We found that communication fills are capable of having higher average fill rates (0.82 kg/min) than noncommunication fills (0.62 kg/min). We also examined the difference in fill rates based on fill pressure, as shown in Fig. 12.9, and found that 700 bar fills were currently 24% slower than 350 bar fills. The average 350 bar fill rate was 0.82 kg/min, while the average 700 bar fill rate was only 0.62 kg/min.

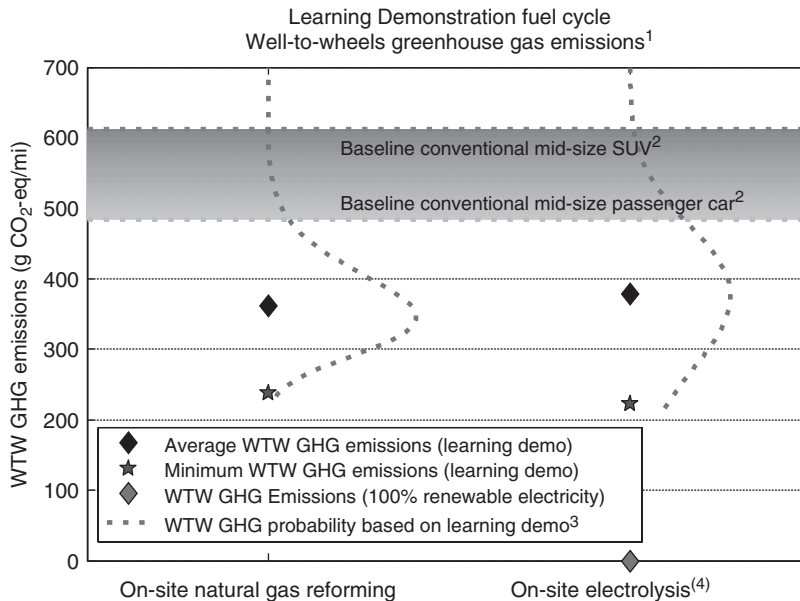
#### 4.11 On-site production efficiency from natural gas reformation and electrolysis

Detailed data on all of the energy inputs required to produce hydrogen on site were gathered and analyzed and compared with DOE's 2010 program targets for natural gas reformation and 2012 targets for water electrolysis. The results indicate that natural gas reformation efficiency was demonstrated close to the 2010 target of 72% through achieving a best quarterly efficiency of 67.7% and a best monthly efficiency of 69.8%. The best quarterly efficiency for water electrolysis was 61.9%, with a best monthly efficiency also of 61.9% (compared with the 2012 target of 69%). Note that targets for both of these technologies are for future years (2010 and 2012) and results from the Learning Demonstration time frame (2005–2009) were not expected to have achieved future targets. Additionally, the targets are set for significantly larger stations (1500 kg/day of H<sub>2</sub>) and much higher utilization (70% capacity factor) than we have in the Learning Demonstration. The purpose of comparing our actual results to these future targets is to benchmark demonstrated progress toward the targets while technical R&D

development continues to improve the state of the art. Note that the on-site hydrogen production costs have also been evaluated but the results are still under review.

## 4.12 Vehicle greenhouse gas emissions

Greenhouse gas emissions from the Learning Demonstration fleet have been assessed and compared to greenhouse gas emission estimates for conventional gasoline vehicles. The results shown in Fig. 12.10 indicate that when using hydrogen produced on site via



- (1) Well-to-Wheels greenhouse gas emissions based on DOE's GREET model, version 1.8b. Analysis uses default GREET values except for FCV fuel economy, hydrogen production conversion efficiency, and electricity grid mix. Fuel economy values are the Gen1 and Gen 2 window-sticker fuel economy data for all teams (as used in CDP #6); conversion efficiency values are the production efficiency data used in CDP #13.
- (2) Baseline conventional passenger car and light duty truck GHG emissions are determined by GREET 1.8b, based on the EPA window-sticker fuel economy of a conventional gasoline mid-size passenger car and mid-size SUV, respectively. The Learning Demonstration fleet includes both passenger cars and SUVs.
- (3) The Well-to-Wheels GHG probability distribution represents the range and likelihood of GHG emissions resulting from the hydrogen FCV fleet based on window-sticker fuel economy data and monthly conversion efficiency data from the Learning Demonstration.
- (4) On-site electrolysis GHG emissions are based on the average mix of electricity production used by the Learning Demonstration production sites, which includes both grid-based electricity and renewable on-site solar electricity. GHG emissions associated with on-site production of hydrogen from electrolysis are highly dependent on electricity source. GHG emissions from a 100% renewable electricity mix would be zero, as shown. If electricity were supplied from the U.S. average grid mix, average GHG emissions would be 1245 g/mile.

**Figure 12.10** WTW greenhouse gas emissions results from Learning Demonstration vehicles using hydrogen produced through natural gas reformation and water electrolysis.

either natural gas reformation or water electrolysis, Learning Demonstration hydrogen FCVs offer significant reductions of greenhouse gas emissions relative to conventional gasoline vehicles. Conventional gasoline mid-sized passenger vehicles emit 484 g CO<sub>2</sub>-eq/mi (grams CO<sub>2</sub> equivalent per mile) on a well-to-wheels (WTW) basis and conventional mid-size sport utility vehicles (SUVs) emit 612 g CO<sub>2</sub>-eq/mi on a WTW basis. The WTW greenhouse gas emissions for the Learning Demonstration FCV fleet (which includes both passenger cars and SUVs) were analyzed based on the window sticker fuel economy of the Learning Demonstration fleet and the actual distribution of hydrogen production conversion efficiencies from on-site hydrogen production. Average WTW greenhouse gas emissions for the Learning Demonstration fleet operating on hydrogen produced from on-site natural gas reformation were 362 g CO<sub>2</sub>-eq/mi, and the lowest WTW GHG emissions for on-site natural gas reformation were 237 g CO<sub>2</sub>-eq/mi. For the Learning Demonstration fleet operating on hydrogen produced from on-site water electrolysis (including some renewable sources of electricity), average WTW GHG emissions were 378 g CO<sub>2</sub>-eq/mi, and the lowest emissions were estimated to be 222 g CO<sub>2</sub>-eq/mi for the month with the best electrolysis production conversion efficiency.

### 4.13 Fuel cell vehicle freeze capability

First-generation FCVs in this project were not freeze capable. They were either limited to warm climates only or were stored indoors during freezing conditions in colder climates. Second-generation vehicles, however, were freeze capable and able to be deployed in places like New York and Detroit without special compensation for the overnight soak temperatures.

As part of this project, the industry partners performed special start-up tests to measure the time required to both drive the vehicle away from being parked overnight and the time to reach maximum fuel cell power. They performed this test using both a 12 h soak (simulating an overnight soak) and an equilibrium soak (in which all parts of the vehicle reach ambient conditions, simulating being parked at the airport) at -20°C. The results are shown in Fig. 12.11. It should be noted that DOE's target was for a start-up time of 30 s to 50% of rated power from -20°C. Since this is a metric that the consumer would not be able to observe directly, we chose the time from key-on to drive-away and time to full power, which the consumer would be much more conscious of.

We found a large spread in the start-up results, with one team having around 20 s to drive-away and one having almost 5 min. For the time to maximum power, the best team was around 1.5 min while the longest was almost 9 min. Therefore, we can conclude that the fuel cell systems have now been made freeze-tolerant, but more work is needed to provide the level of cold-start convenience that consumers will expect.

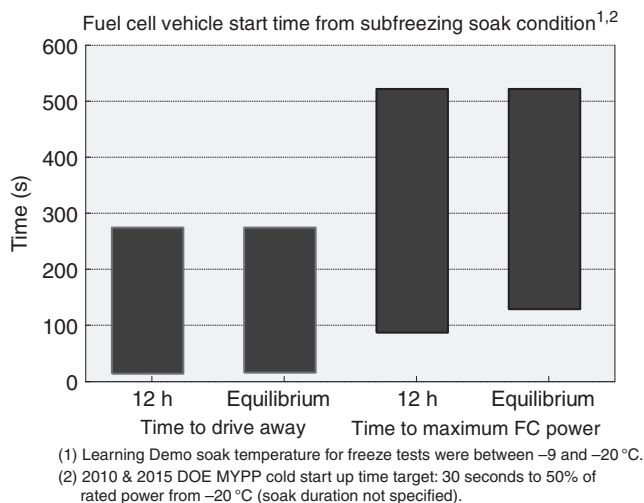


**Figure 12.11** FCV start time from subfreezing soak condition.



## 5. CONCLUDING REMARKS

We have now completed the first 4 years of the project with 140 FCVs and 20 project refueling stations deployed. This allowed us to analyze data from over 400,000 individual vehicle trips covering 2.3 million miles traveled and 115,000 kg H<sub>2</sub> produced or dispensed. We have published 72 CDPs to date and made them directly accessible to the public from NREL's Internet site. Thirty-one of the vehicles and three of the stations have now been retired, with more to be retired soon as the project begins to wind down.

We found that the fuel cell system efficiency for both first- and second-generation systems was very close to or exceeded the targets at  $\frac{1}{4}$  power and full power. This impressive performance was maintained while the stacks improved in both durability and freeze capability.

On the key topic of fuel cell durability, we found that the best performing first- and second-generation teams' vehicles met DOE's 1,000 and 2,000 h durability targets, respectively. Second-generation stack durability results should be considered preliminary because, although some of the projections are above 2,000 h, most stacks have not yet accumulated 1,000 h.

NREL will continue to identify opportunities to send findings from the project back to the DOE programs and industry R&D activities to maintain the project as a "learning demonstration." As the last deliverable from this project, we will write a final comprehensive summary report for publication that summarizes the final analysis results.

## ACKNOWLEDGMENTS

The Technology Validation part of the U.S. Department of Energy Fuel Cell Technologies Program funded this project. In addition, the authors wish to thank the auto industry and energy companies for their contributions of detailed raw data provided to NREL as well as their valuable feedback on our methodologies and results.

## DEFINITIONS, ACRONYMS, ABBREVIATIONS

CDP	composite data product
FAT	Fleet Analysis Toolkit (software tool developed at NREL)
FCV	fuel cell vehicle
Gge	gallon of gasoline equivalent
FCT	Fuel Cell Technologies Program (DOE program)
HSDC	Hydrogen Secure Data Center (at NREL)
NREL	National Renewable Energy Laboratory
Q	quarter
R&D	research and development
WTW	well-to-wheels

## REFERENCES

1. K. Wipke, S. Sprik, J. Kurtz, J. Garbak, Fuel Cell Vehicle Infrastructure Learning Demonstration: Status and Results, Proton Exchange Membrane Fuel Cells 8 (ECS Transactions Vol. 16, No.2), September 2008.
2. K. Wipke, S. Sprik, J. Kurtz, H. Thomas, J. Garbak, FCV Learning Demonstration: Project Midpoint Status and First-Generation Vehicle Results, World Electric Vehicle J. 2 (3) NREL/JA-560-45468 (November 2008).
3. K. Wipke, S. Sprik, J. Kurtz, J. Garbak, Field Experience with Fuel Cell Vehicles, Handbook of Fuel Cells — Fundamentals, Technology, and Applications, Volume 6: Advances in Electrocatalysis, Materials, Diagnostics and Durability, NREL/CH-560-43589, John Wiley & Sons, Ltd., Chichester, U.K, March 2009 (Chapter 60).
4. K. Wipke, S. Sprik, J. Kurtz, T. Ramsden, J. Garbak, U.S. Fuel Cell Vehicle Learning Demonstration: Status Update and Early Second-Generation Vehicle Results, 24th International Battery, Hybrid and Fuel Cell Electric Vehicle Symposium, Stavanger, Norway, May 2009.
5. K. Wipke, S. Sprik, J. Kurtz, T. Ramsden, Composite Data Products for the Controlled Hydrogen Fleet and Infrastructure Demonstration and Validation Project, Fall 2009, National Renewable Energy Laboratory, Golden, CO, USA, September 2009.
6. J. Kurtz, K. Wipke, S. Sprik, Fuel Cell Vehicle Learning Demonstration: Study of Factors Affecting Fuel Cell Degradation, 6th International Fuel Cell Science, Engineering and Technology Conference (ASME Fuel Cell Conference), Denver, USA, June 2008.



# Battery Requirements for HEVs, PHEVs, and EVs: An Overview

Michel Broussely<sup>1</sup>

Formerly Scientific Director of Specialty Battery Division at Saft, France, 53 Avenue de Poitiers, 86240 Ligugé, France

## Contents

1. Introduction	305
2. General Requirements	306
2.1 Energy/Power	306
2.2 Cost	307
2.3 Battery life	310
2.3.1 Cycle life	311
2.3.2 Calendar life	312
2.4 Temperature control	313
2.5 Safety	314
2.6 Recycling and environmental issues	315
3. Specific Requirements and Examples	316
3.1 Microhybrids (idling start/stop)	316
3.2 Soft hybrids (stop and go)	317
3.3 Full hybrids (power assist HEVs)	319
3.3.1 Example of existing HEV battery systems: NiMH batteries	320
3.3.2 Example of incoming HEV battery systems: Li ion batteries	322
3.4 Plug-in hybrids	326
3.4.1 Li ion batteries for PHEVs	328
3.5 Electric vehicles	329
3.5.1 Examples of recent EV battery systems: Li ion	334
3.5.2 Examples of recent EV battery systems: lithium metal polymer	337
3.5.3 Examples of recent EV battery systems: sodium/nickel chloride (ZEBRA)	338
4. Fuel Cell Hybrid Vehicles	340
5. Summary of the Different Li ion Chemistries Existing at Present, and to be Used in HEVs, PHEVs, or EVs	340
6. The Future	342
References	344



## 1. INTRODUCTION

The poor properties of batteries compared to the requirements are the main limiting factor for the development of all types of electric vehicles in the last decades.

<sup>1</sup> Corresponding author: [broussely@libertysurf.fr](mailto:broussely@libertysurf.fr)

The power source is indeed the most critical component, and large R&D efforts have been devoted in the last 20 years to answer an increasing and urging need for vehicles consuming less fossil fuel. Thanks to these efforts, recent battery improvements have made the future much more promising.

This chapter intends to describe the battery properties in different electric vehicles configurations and to give some example of the most recent developments. A previous analysis by the same author for hybrid electric vehicles (HEVs) and electric vehicles (EVs) can be found in Ref. [1].

Very important programs for batteries development started about 15 years ago, supported by a strong financial effort of governmental institutions and car manufacturers associations all over the world: European commission and state governments in Europe, DOE/USABC (United States Advanced Battery Consortium) in the USA, and CRIEPI/LIBES in Japan. Thanks to this, huge improvements have been achieved in battery technology, notably with the introduction of non aqueous systems based on lithium (Li). Fuel cells have also progressed very much, but not yet to the point of becoming affordable in terms of cost and longevity.

However, no real industrial development could have been expected until the necessity to reduce both CO<sub>2</sub> emission and oil consumption was recognized and accepted by the customers, pushed by financial incentives of the governments. An important step was achieved about 10 years ago with the launch of the hybrid “Prius” by Toyota, which demonstrated the feasibility of this concept and acceptance by the market. Today, most of the car manufacturers are developing or commercializing several types of hybrid cars, and pure EVs are the subject of a spectacular interest never seen before, which should lead to their actual commercialization in the next few years.

Although no real worldwide standards exist today for the batteries powering these vehicles, there are general requirements established by the car manufacturers associations during this long battery development phase. However, detailed specifications of batteries for the cars under development are usually confidentially established between car and battery makers.



---

## 2. GENERAL REQUIREMENTS

### 2.1 Energy/Power

From small hybrid to full electric vehicles, the specific electric properties required and battery size vary considerably with the vehicle type and size. Pure EV needs the largest amount of energy in the dedicated volume available in the car with the smallest weight possible, whereas the batteries for HEV should provide the maximum power in a minimum size. Fig. 13.1 and Table 13.1 describe the general power and energy ranges required from the battery by different types of electric vehicles. These electric properties will be described in more detail in further sections devoted to specific vehicle types.



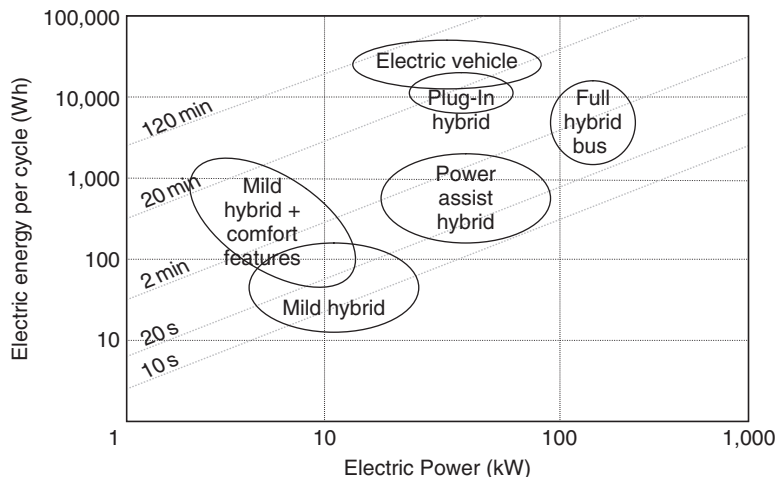


**Figure 13.1** Description of the power/energy characteristics required from the battery by different types of electric vehicles.

**Table 13.1** The different types of EVs/HEVs and approximate energy/power requirements

EV type	Power range (kW)	Energy range (kWh)	Voltage range (V)
Micro-HEV	2.5–5	0.5	12–36
Mild HEV	15–20	1	120–160
Full HEV	30–50	2–3	200–350
FCHEV	25–30	1–2	220
Plug-in HEV	30–100 (Van)	5–15	200–350
EV	35–70 (Van)	25–40	200–350

## 2.2 Cost

The battery appears as the most expensive component in electric vehicles, and a significant part of the components cost in hybrids. Therefore, there is a strong pressure to reduce its costs. At the same time, the requirements of longevity, reliability, and safety are very high, making this goal difficult to achieve for battery manufacturers.

Depending on the type of vehicle, the price is related to energy (kWh, for EVs) or power (kW, for HEVs). Literature values vary significantly and are generally more related to future goals than present selling prices, which anyway remain generally confidential between car and battery manufacturers. USABC has set cost goals for the different types of vehicles for the development programs (Table 13.2).

The battery price is particularly critical for EVs, because the amount of energy required for achieving a sufficient range, and hence the battery size, is important. As can be noted in Table 13.2, the initial goal for the selling price was aggressively low, but

**Table 13.2** Cost objectives defined by USABC for several vehicle types

Vehicle type (year of goals setting)	Price goals per kW or kWh	Average battery cost goal
EV (selling price at 25 ku/y) (about 1995)	150 \$/kWh	\$6,000 (40 kWh)
Power Assist HEV (production price at 100 ku/year) (2002)	20 \$/kW	\$800 (40 kW)
Plug-in HEV short range (10 miles) (production price at 100 ku/year) (2007)	470 \$/kWh (38 \$/kW)	\$1,600 (45 kW–3.4 kWh)
Plug-in HEV long range (40 miles) (production price at 100 ku/year) (2007)	290 \$/kWh (90 \$/kW)	\$3,400 (38 kW–11.6 kWh)

the real battery cost is still high. New Li batteries can provide the minimum distance of 150–200 km required for EVs, but their price represents a hurdle to the commercialization of these vehicles.

The price of high-power batteries used in HEVs is more affordable, because their energy, and therefore the size, is much smaller. However, the very high-power density requires larger surface area of thinner electrodes, current collectors, and separator, which increases the manufacturing cost. As a reference example, the retail price of a replacement NiMH battery for Prius II HEV was 128 K JPY in 2007 (~US\$1500 at the present exchange rate, twice the goal of USABC). But this value was estimated close to the production cost [2], with a high nickel price at that time.

The batteries for plug-in HEVs (PHEVs), needing both the high power of power assist HEVs, and enough energy to provide a car range from 30 to 60 km depending on design choice, have a medium power/energy ratio. They are bigger than HEV batteries, and therefore more expensive. The increased cost due to the battery compared to a power assist HEV should be compensated by the savings in fuel consumption while the car is used on pure electric mode. Present battery price is ~\$1,000/kWh, and should therefore be reduced 2–3 times to reach the USABC goals.

A rough estimate of the composition of the cost of a complete battery system produced at industrial level in large quantities is 75–85% for the electrochemical cells and 15–25% for the battery system assembly, and thermal and electrical management. Within the cell, 80–90% is material cost and 10–20% labor cost. Because the raw materials are the most expensive part of the price, the cost of the cells constituting the battery system is more or less proportional to the size.

Cost is therefore an important parameter to take into account in the choice of new materials to be studied to make new battery systems. However the bare cost (per kg for example) must always be related to other major properties such as energy density and life. A lower price of the positive material (which is the most expensive active component) may ultimately lead to a more expensive battery system if the resulting energy density is too low.

**Table 13.3** Cost breaking down when the positive of a Li ion battery is replaced by one of lower price and energy density

	Cells relative cost				Energy coefficient (Wh)	Total cost (per Wh)	Battery assembly and electronics	Full system
	Positive	Others	Labor	Total				
Reference	28	40	12	80	1	80	20	100
New system	14	40	12	66	0.85	77.6	20	97.6

For example, Table 13.3 describes the relative price breaking down of a Li ion battery systems using a half-price positive material, price but inducing a 15% energy density reduction, compared to a reference typical cost distribution. This example leads to less than 3% cost reduction of a larger and heavier battery system.

The manufacturing cost decreases when the production volumes increase. Fig. 13.2 shows the steady increase since 2002 of the number of NiMH and Li ion cells (except for the period 2008–2009) [3]. As shown in Fig. 13.3, an analogous trend can be found for the market of these two batteries for HEVs [3]. The chemistries like Li ion, that are suitable to build both types of batteries for EVs (energy) and HEVs (power), so cumulating the production volumes, have a potential cost evolution advantage for the future, compared to chemistries that are specific to energy only and still using expensive components, such as LMP (Li metal polymer) or Na/NiCl<sub>2</sub> (ZEBRA) batteries for EVs.

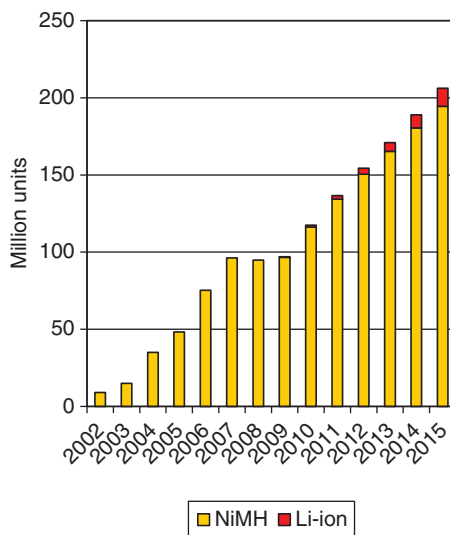


**Figure 13.2** NiMH and Li ion cells sold per year in the period 2002–2015 (from Ref. [3]).

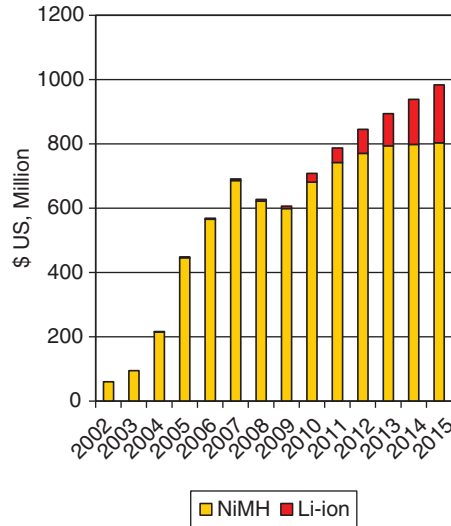


**Figure 13.3** NiMH and Li ion market for HEVs in the period 2002–2015 (million US\$) (from Ref. [3]).

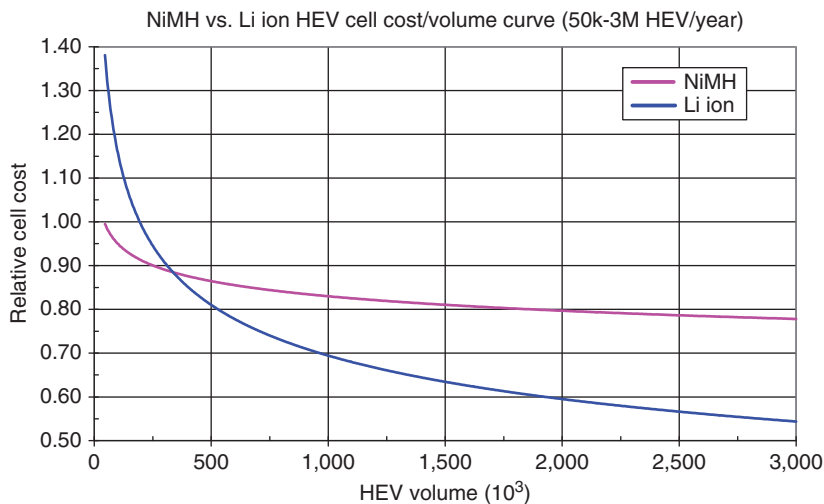
The second important contribution to the total cost is the battery assembly and management system that is required to insure the correct monitoring of the multiple cells assembly during discharge and charge. In turn, this is essential to insure the required reliability and safety of the system. The use of electronic components and systems already utilized in the car industry should allow reducing significantly this cost, compared to other battery systems.

Fig. 13.4 describes the expected evolution of the relative cost for the two battery systems competing for HEVs [4]. A very important price drop is expected for the Li ion batteries with increasing production volume, becoming in the future cheaper than the NiMH, today less expensive and almost exclusively used.

In fact, life cycle cost, rather than selling price, is the really significant number to be taken into account. Therefore, other properties of the battery such as aging on rest and cycling are of utmost importance on the actual cost over the car life. These properties and the reliability are particularly important for the EV fleets, or to establish an affordable leasing price of the battery for an individual EV customer.

## 2.3 Battery life

A limited battery life has small consequences for portable equipment but becomes a serious concern for large battery systems and is a critical requirement for EV large batteries. It has a direct impact on the life cycle cost [5], and therefore, the battery should not be replaced during the average lifetime of the car, that is, more than 10 years. Besides the heavy weight and low-energy density of lead acid batteries, their life has been the biggest drawback that impaired in the past the development of EVs



**Figure 13.4** Expected relative cell cost evolution with production volumes of NiMH and Li ion batteries for HEVs (from Ref. [4]).

using these batteries, whose deep discharge cycle life is limited to several hundreds of cycles only.

In fact, a battery is the seat of complex chemical reactions while being on charge or discharge, or even being on rest, when side reactions can still occur between the active materials in contact. This is one of the main concerns when creating a new battery system, and a quite difficult property to assess on a long time frame. It requires long-term experiments before allowing an accurate prediction of the actual life of a battery. The maturity of an electrochemical system is therefore an important parameter to take into consideration.

### 2.3.1 Cycle life

The number of cycles expected from a battery during its life is of course very dependent on the usage profile. A full EV requires deep discharge cycling, that is, using the maximum available energy stored during one charge, whereas a HEV only uses a small part of its energy, being constantly recharged by the internal combustion engine (ICE). In the first case, the battery is generally charged overnight for utilization over the next day. Therefore, the number of cycles required corresponds to more or less one cycle/day of use up to 80% of the stored energy, and 3,500 such cycles would represent about a 10-year life. The total cumulated driving distance depends on the battery size and energy density determining the car range. NiCd batteries, used in commercially available EVs during the last 25 years, usually provided ~70 km average range, leading to a cumulated driving distance of more than 200,000 km, that is, an 8-year daily utilization

or ~3,000 cycles, while generally less than 1,000 cycles were obtained with lead acid batteries.

The required cycle life of advanced EV Li ion batteries, at 80% depth of discharge (DOD), is usually around 3,000 cycles, which represents as much as 360,000 km for an average 120 km range. It can be seen from these figures that the life requirement of an EV battery is more demanding than that of most of the conventional ICE cars.

In the case of HEVs, the battery is subjected to thousands of very short cycles per day, using a very small amount of the total battery energy at ~50% state of charge (SOC). Because the energy involved in each cycle (corresponding to each power peak required from the electric power train) may largely vary, average values have been set to define a cycle life. A typical requirement for a full hybrid car battery is ~300,000 cycles of 25 Wh, representing 8% of a 0.33 kWh battery [6].

The electrochemical reactions occurring at each electrode during cycling produce very important changes in the active materials. Aging may be the result of these modifications occurring at different levels: in the molecular/crystalline structure of the materials due to ion insertion/deinsertion or in the electrode bulk stressed by important volume changes between charged and discharged state. Side reactions between the active materials and the electrolyte may also occur, especially in high-energy density and high voltage systems. In fact, each battery system has its own degradation mechanisms, which must be carefully studied when developing a battery system. Many factors must be considered to assess the cycle life, that is, depth of charge/discharge, current drain, temperature, and voltage limits, each of them having more or less importance as regards the battery system. Therefore, the precise cycle life of a battery depends on the application, and it must be assessed on a case-by-case basis.

Examples of cycle life tests and results will be discussed in the following sections describing the specific requirements of vehicle types.

### **2.3.2 Calendar life**

Calendar life is defined as the battery life on rest, that is, without occurrence of electrochemical reactions. During rest, batteries are also aging, and both utilization and rest time must be considered to assess the global lifetime. This is mainly due to interactions between the active materials in contact with the electrolyte. When charged, a battery includes reactive materials in both positive and negative electrodes, respectively, oxidizing and reducing agents. The electrolyte, in contact with both electrodes, is ideally chemically stable, but this is never completely true, and slow reactions occur with time, this leading to capacity or power loss.

Therefore, to comply with a lifetime requirement, both components of aging have to be taken into account by the battery maker. Long lifetime assessment of a battery is even more difficult than cycle life prediction, because anticipation by aging

acceleration is always a difficult exercise. Temperature increase is the only way to accelerate side reaction rates, but the acceleration coefficient factor to assess the ambient temperature aging rate is never a trivial number, and long and expensive experimentation must be performed before being able to give a reasonable warranty for the battery life. Of course, the impact of any change in the battery chemistry on the calendar life must be verified, and consequently extends the time for qualification. It is therefore difficult to introduce rapidly new battery systems or important changes into existing systems. Typically, 10–15 years calendar life are required for EV or HEV batteries, at an average temperature including the rest periods (typically 25°C) and working periods (up to 45°C).

Very important R&D efforts are presently carried out by many laboratories to address the calendar and cycle life of the new battery systems developed for EVs or HEVs [7]. The ultimate goal is to build aging models, taking into account all the utilization parameters, in order to verify the battery behavior during its use, and anticipate possible premature aging or failure. This is for example the goal of the SIMSTOCK cooperative European program being carried out in Europe [8].

## 2.4 Temperature control

Because the temperature is very influent on aging rate, it should be maintained as low as possible during use, and a temperature management system must be included in the battery. Maximum operating temperature in usual conditions should preferably be ~40°C, which can be achieved either by liquid or air cooling systems, associated to the car heat management system, or the air conditioning system. In addition, the temperature should be as much as possible evenly distributed. Indeed, the battery systems are built by association of many single cells, in parallel or series assembly. Uneven temperature distribution would result in uneven power distribution and SOC misbalance between cells. In addition, this misbalance may produce accelerated local cell aging which would impair the life of the complete battery.

The source of heat in a battery comes primarily from its electric resistance, and heat is produced proportionally to the square of the current drain, either on charge or discharge. In addition, the aqueous systems of sealed design, that is, lead acid, nickel cadmium, or nickel/metal hydride, produce some heat at the end of charge, when water of the electrolyte is involved in the electrochemical reactions. Water recombination occurs, and some of the energy provided to the battery is converted into heat. This reaction does not occur in the nonaqueous systems (i.e., Li, or Li ion, and ZEBRA batteries), which makes the thermal management easier and gives them also the advantage of a better energy efficiency.

A particular mention should be made of “hot” systems, for example, Li polymer or ZEBRA, which must be maintained permanently at elevated temperatures (80–90°C and 270–350°C, respectively). This is obtained by appropriate insulation design and heat

transfer monitoring. When the battery is neither discharged nor charged, some of its energy should be used to maintain the temperature at the required level.

## 2.5 Safety

As a high-energy containing system, a battery represents a danger, just as the fuel tank of a conventional car. Although the equivalent energy stored in a battery is much smaller, it is perceived as a greater risk, because electricity is involved and because of the complexity of the system, inducing more potential failures.

The highest hazard considered is the sudden release as heat of the electrical energy stored. Indeed, battery charging produces oxidizing and reducing compounds at the positive and negative electrodes, respectively, which might, under certain circumstances, chemically react together to produce heat. The worst consequences would be a fire or explosion, which is in fact the battery container bursting due to large and fast release of gases. Triggering of this ultimate reaction is always a local overheating that leads the chemicals to react together, producing themselves heat and therefore inducing a thermal runaway. The local overheating might itself have several causes, such as internal or external short circuit and battery overcharge.

There are various factors that make this possible sketch more or less dramatic or likely to occur. The main factor is the nature of the chemicals contained in the battery. The new high-energy systems contain nonaqueous flammable solvents as electrolytes, whereas the conventional batteries use water which has on the contrary a beneficial effect on heat propagation. The second factor is the energy density of the battery. The highest the energy density, the largest the amount of heat to be released out of a given volume, and the highest the temperature reached and/or amount of gas produced. Third factor is the kinetic of the chemical degradation reaction, and rate of propagation through the battery, that is, the rate of heat release.

During battery development, safety consideration is always a major concern, which governs the choice of materials and battery design to prevent such a drastic situation. Many studies are being devoted to this topic, either to search for less reactive materials, for example, nonflammable electrolytes, or to understand the degradation mechanisms, this helping with battery design [9].

Drastic safety requirements of batteries for EVs or HEVs are set by the car manufacturers, and passing a bench of severe tests reproducing the use and abuse conditions is a prerequisite for the qualification. The most frequent abuse conditions explored are external short circuits that can results from an electrical system failure or crash, internal short circuits resulting form crash, overvoltage or overcurrent coming from battery system or charger failure, heating from an outside heat source such as a fire, and strong mechanical stress due to vibrations and shocks.



While a battery should not produce high safety hazard when abused, it must always remain totally safe during normal utilization, which nevertheless can produce external stress.

## 2.6 Recycling and environmental issues

Used cars have been for long time recycled, but mostly for steel and other metals. However, the percentage of recycled components has been recently increased by regulations. For example, the European Parliament and the Council promulgated the Directive 2000/53/EC on September 2000 [10], defining the end-of-life of vehicles. According to this directive,

*no later than 1 January 2006, for all end-of-life vehicles, the reuse<sup>1</sup> and recovery<sup>1</sup> shall be increased to a minimum of 85% by an average weight per vehicle and year. Within the same time limit the reuse<sup>1</sup> and recycling<sup>1</sup> shall be increased to a minimum of 80% by an average weight per vehicle and year.*

And

*no later than 1 January 2015, for all end-of-life vehicles, the reuse<sup>1</sup> and recovery<sup>1</sup> shall be increased to a minimum of 95% by an average weight per vehicle and year. Within the same time limit, the reuse<sup>1</sup> and recycling<sup>1</sup> shall be increased to a minimum of 85% by an average weight per vehicle and year.*

In the same directive,

*In order to promote the prevention of waste, Member States shall encourage, in particular (...) vehicle manufacturers, in liaison with material and equipment manufacturers, to limit the use of hazardous substances in vehicles and to reduce them as far as possible from the conception of the vehicle onwards, so as in particular to prevent their release into the environment, make recycling easier, and avoid the need to dispose of hazardous waste,*

and

*Member States shall ensure that materials and components of vehicles put on the market after 1 July 2003 do not contain lead, mercury, cadmium or hexavalent chromium other than in cases listed in Annex II...*

The SLI (starting, lighting, ignition) lead acid batteries are part of the exceptions listed, because no other battery system is able yet to compete with them in terms of

<sup>1</sup> Definitions: “reuse means any operation by which components of end-of-life vehicles are used for the same purpose for which they were conceived,” “recovery means the use of combustible waste as a means to generate energy through direct incineration with or without other waste but with recovery of the heat,” and “recycling means the reprocessing in a production process of the waste materials for the original purpose or for other purposes but excluding energy recovery.”

price. In the same way, the use of cadmium in batteries for EVs was part of the exemption, because no other battery commercially available up to now could be replaced in existing vehicles. However, this exemption is not definitive, as follows:

*in accordance with the procedure laid down in Article 11 the Commission shall on a regular basis, according to technical and scientific progress, amend Annex II, in order to: (...) delete materials and components of vehicles from Annex II if the use of these substances is avoidable*

Therefore, as a major component of the electric vehicles, batteries must comply with these regulations, do not contain hazardous materials, and must be collected and recycled accordingly. In fact, the collection and recycling are already established for long time in the car industry for lead acid batteries, mainly because of the toxicity of lead. Indeed, manufacturers could demonstrate a real “closed loop” solution, with 80–95% of used car batteries collected and recycled at the end of their life (and with collection figures even reaching ~100% in industrial countries). More than 70% of the lead produced in the world (out of ~6 billion tons) is used for battery applications and ~65% is originated from recycled lead.

Because a battery is composed of many different chemical compounds, recycling process is not trivial, and many innovative and diverse processes have been developed over the years by several companies worldwide [11]. The economical and environmental aspects of recycling depend greatly on the components, their value, toxicity, etc., and this is an important major parameter in the choice of materials during the R&D phase.

The recycling of the new battery systems recently developed for electric vehicles are required to follow these rules, and processes and equipments must be established to insure future treatment at the end of life. For example, the Belgian company Umicore [12] has developed a process (VAL'EAS™) dedicated to the recycling of rechargeable Li ion and NiMH batteries and battery packs [13, 14].



### 3. SPECIFIC REQUIREMENTS AND EXAMPLES

#### 3.1 Microhybrids (idling start/stop)

In these cars, the combustion engine is stopped as soon as the car stops. The starter–alternator is only used to start the engine. No regenerative energy is recovered on braking, and a few hundred watt-hours of energy is required (with a power of 2.5–5 kW). Therefore 12 V SLI lead acid batteries of the largest size can supply the required power. The same battery provides the energy for onboard equipment and starting. The battery is usually maintained at full SOC, but much more frequently and more deeply discharged than the conventional SLI. Table 13.4 describes a typical cycle life test for “stop and start” application [15]. Therefore, battery aging is the challenge, the projected lifetime

**Table 13.4** Typical cycle life test for Stop and Start applications (from Ref. [15])

Sequences	
1	Charge during 20 h at 14.4 V + 4 h at $I_{20} \times 0.5$ (100%SOC)
2	10,000 cycles at 40°C, 1.3% DOD; charge: 3 min at 14 V (maximum current: 50 A); discharge: 1 min at $I_{20} \times 16$
3	Recharge during 20 h at 14.4 V + 4 h at $I_{20} \times 0.5$
4	Capacity test: Discharge at C/20 at 25°C to 10.5 V (>10 h)
5	Recharge during 20 h at 14.4 V + 4 h at $I_{20} \times 0.5$
6	Cold cranking test: high rate 10 s pulse at -18°C to 7.2 V
7	Back to 1

**Table 13.5** Typical idling stop rate description in city drive (Kyoto) (from Ref. [16])

Driving course	Units	Kyoto city
Driving time/day	min	140
Driving distance/day	km	30
Average discharge current	A	22
Number of stops	times	38
Accumulated stops duration	min	35.2
Total idling stop rate	%	25.1%

being generally about 1–2 years less than SLI batteries in conventional cars. As a consequence, the battery cost has to be as low as possible, and the replacement cost should be compensated by increased fuel economy. This fuel consumption reduction is obviously very dependent on the driving mode; in true urban configuration, with many stops, fuel saving can be more than 15%. Table 13.5 describes a typical utilization in urban conditions [16], recorded in Kyoto.

The valve-regulated adsorbed glass mat (AGM) technology is the most appropriate and offers the best cost/performance ratio, because of an improved cycle life [15], as for example described in Fig. 13.5.

Flooded type batteries with improved cycle life are also being developed, as evidenced in Fig. 13.6. UltraBattery is a new concept comprising a lead acid battery and an asymmetrical capacitor [17].

### 3.2 Soft hybrids (stop and go)

The main difference with the former concept is that some energy is saved by regenerative electric power produced on braking (50–60% braking energy is converted to electricity), and more electric energy is used on starting because the car starts in an electric mode, while the ICE is being started. Compared to “stop and

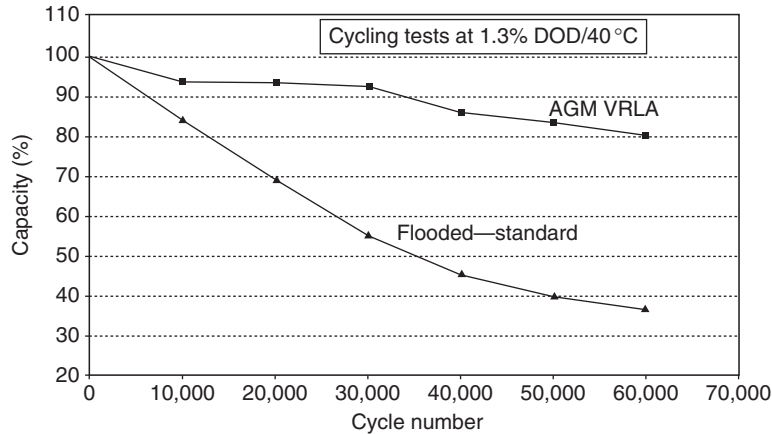


**Figure 13.5** Capacity evolution of an AGM VRLA cell during start and stop cycling test, compared to a conventional flooded cell (from Ref [15]).

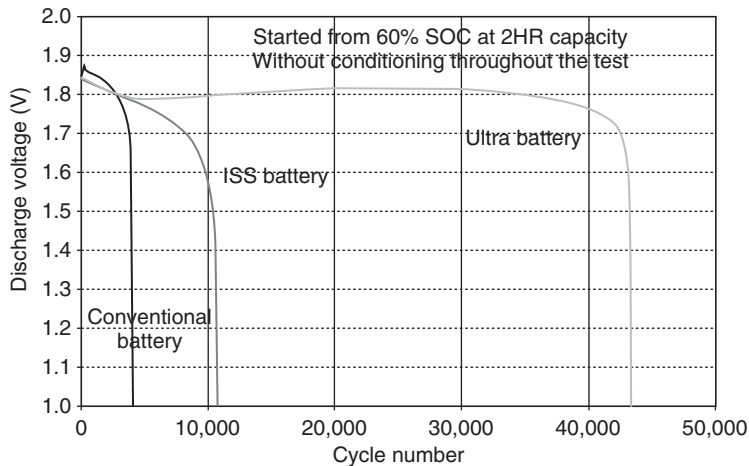


**Figure 13.6** Cycling performance of improved flooded lead acid battery (UltraBattery). ISS stands for idling start stop (from Ref [17]).

start,” the gain in fuel consumption can be almost doubled in the same driving conditions (from 5 to 25%).

There is a strong impact on the energy storage system that must be able to sustain high charge peak power, and provide more power and energy during the starting phase. The average power required during car start and average regeneration power is  $\sim 6$  kW. The lead acid battery provides the energy required during start, and all onboard electric energy needs. Because the battery provides more energy, the SOC will vary more than

in the “stop and start,” and typical depth of cycling range is 20% DOD, between 100 and 80% SOC, for a battery of similar size to the “stop and start” hybrid. The conventional lead acid battery design with flat plates is not well suited for this working mode and lifetime is reduced. The solution would be to increase the battery size, but volume and weight would become a burden. A better technical solution is the advanced high-power lead acid technology of spirally wound design. Another solution considered today is an association of conventional SLI lead acid battery and supercapacitors. The role of the capacitors is to accommodate and store the high peaks of regenerative power and help on starting, while the battery provides energy.

High-power Li ion batteries possess both power and energy requirements and can be considered as a future longer life solution as soon as the cost becomes compatible.

### 3.3 Full hybrids (power assist HEVs)

Power assist hybrid cars have been commercialized since 1997, when the Toyota Prius was introduced. Since then, many other car manufacturers have proposed these vehicles or are being developing them. More than 15 new models have been announced to be produced before 2013. The battery business is consequently deeply involved in this evolution, leading to large efforts of R&D, which should end in significant battery improvements.

In this configuration, both the engine and electric motor contribute to powering the car, with electric power being used for starting and acceleration. A limited range of a few kilometers in pure EV mode is possible. The energy required to the battery is still small, but the power has to be high (see Table 13.1). The battery is permanently either on discharge or charge, and the SOC has to be maintained at an intermediate level, so that the battery can deliver peak power to the drivetrain, and accept power from the engine or regenerative braking. The main requirement of the battery is therefore its ability to sustain a very large number of high drain and shallow cycles, and store this energy efficiently. Table 13.6 describes the performance goals set by the FreedomCAR project (2002) for power assist vehicles [6]. Particularly important points still constituting a challenge for improving the present batteries are cost, calendar life, and cycle life, which are actually linked.

Other features which are not listed in this table are also important to insure a correct behavior on use and long life, such as SOC monitoring and cell balancing. Indeed, the SOC of the battery must be kept within predefined limits, to ensure the battery ability to deliver discharge power on demand, and accept charge regen power when braking. This SOC must be equally distributed within the cells of the battery assembly. Cell balancing strategy must be set to allow the charge equilibration all over the battery service life. This is obtained in the battery pack through the BMS, battery monitoring system, and is more or less easy and efficient depending on the battery electrochemistry.

**Table 13.6** FreedomCAR energy storage system performance goals for power assist hybrid electric vehicles (November 2002)

Characteristics	Units	Power assist (minimum)	Power assist (maximum)
Pulse discharge power (10 s)	kW	25	40
Peak regenerative pulse power (10 s)	kW	20 (55 Wh pulse)	35 (7 Wh pulse)
Total available energy (over DOD range where power goals are met)	kWh	0.3 (at C1/1 rate)	0.5 (at C1/1 rate)
Minimum round-trip energy efficiency	%	90 (25 Wh cycle)	90 (50 Wh cycle)
Cold cranking power at $-30^{\circ}\text{C}$ (three 2 s pulses, 10 s rest between)	kW	5	7
Cycle life, for specified SOC increments	Cycles	300,000 25 Wh cycles (=7.5 MWh)	300,000 50 Wh cycles (=15 MWh)
Calendar life	Years	15	15
Maximum weight	kg	40	60
Maximum volume	l	32	45
Operating voltage limits	$V_{dc}$	Max < 400, Min > $(0.55 \times V_{max})$	Max < 400, Min > $(0.55 \times V_{max})$
Maximum allowable self-discharge rate	Wh/day	50	50
Temperature range: equipment operation	$^{\circ}\text{C}$	$-30$ to $+52$	$-30$ to $+52$
Temperature range: equipment survival	$^{\circ}\text{C}$	$-46$ to $+66$	$-46$ to $+66$
Production price at 100,000 units/year	\$	500	800

### 3.3.1 Example of existing HEV battery systems: NiMH batteries

At present, the battery system mostly used in HEVs is NiMH, made by PEVE (Toyota/Panasonic joint venture); Fig. 13.7 shows an example of battery pack for this application. The NiMH battery was introduced by Toyota since 1997 for the Prius (Fig. 13.8). The first cars used a battery system with cylindrical cells, while the recent models are using a prismatic design. The unit cell characteristics of the different generations are described in Table 13.7. Several other manufacturers are also producing NiMH battery systems for HEVs, for example, Sanyo and Johnson-Controls-Saft.

The specific power of the battery module, measured during 2 and 10 s pulses as a function of SOC, exceeds 1,000 W/kg as described in Fig. 13.9 [19].

Fig. 13.10 describes the power evolution during a cycling test of two battery generations at  $40^{\circ}\text{C}$ , showing that the cell resistance remains stable up to an equivalent driving distance of at least 300,000 km, this demonstrating the excellent cycle life of the NiMH system.

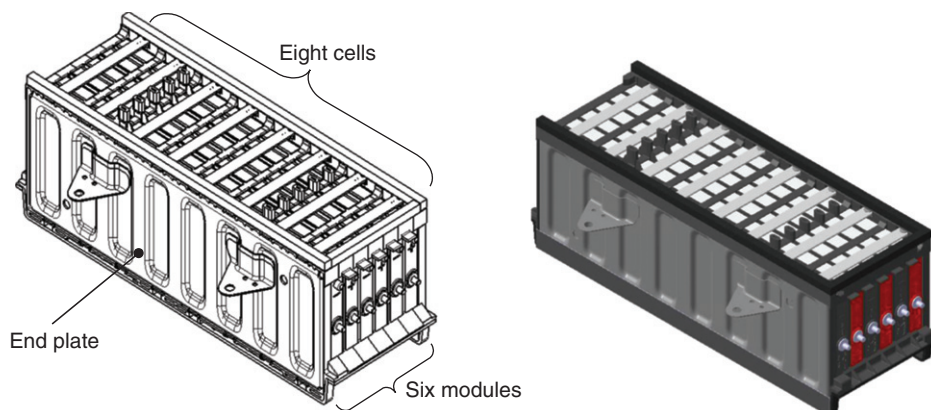


**Figure 13.7** Example of a NiMH battery pack for HEV (PEVE, from Ref. [18]).



**Figure 13.8** Battery system of the Toyota Prius (2006); sealed NiMH, power output: 28 kW, voltage: 201.6V. Expected life based on lab testing: 150,000 miles.

**Table 13.7** Main characteristics of PEVE NiMH high-power cells modules for HEVs (from Ref. [18])

	1st Gen cylindrical	Prismatic Gen1	Prismatic Gen2	New model
Nominal voltage (V)	7.2	7.2	7.2	7.2
Nominal capacity	6 Ah	6.5 Ah	6.5 Ah	6.5 Ah
Output power (six cells module) (W)	872	1,050	1,352	1,352
Mass (g)	1090	1050	1040	1197
Dimension (mm)	19.6 (W) 106 (H) 285 (L)	19.6 106 285	19.6 106 271.5	18.4 96 279
Battery pack height (mm)	–	174	176	142

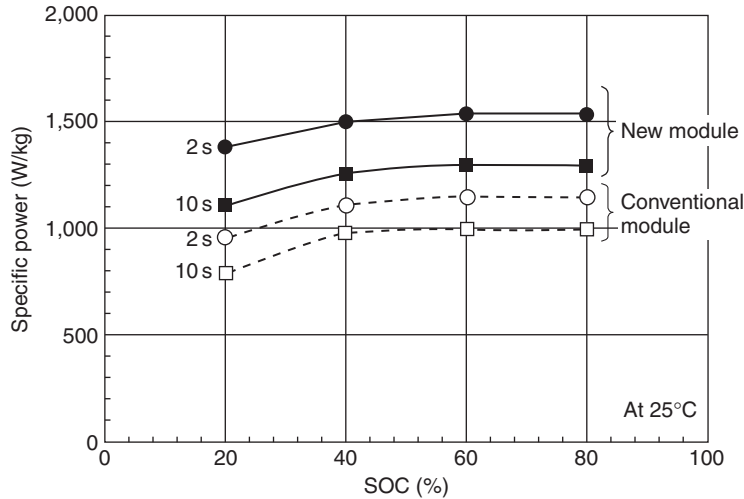


**Figure 13.9** Specific power variation of a NiMH module for HEV battery as a function of SOC, at 25°C (from Ref [19]).

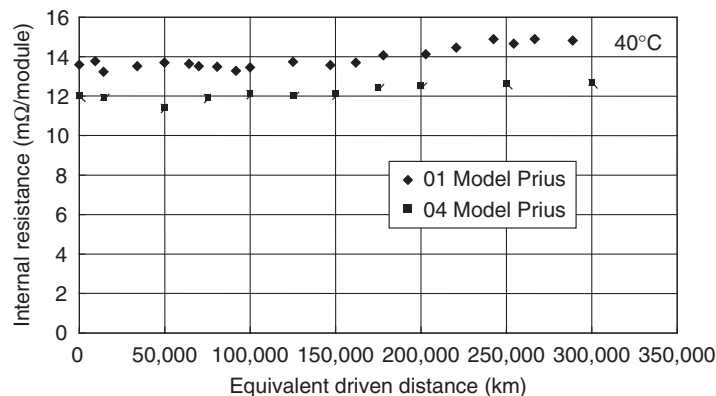


**Figure 13.10** Cycle life characteristics of NiMH PEVE batteries for HEVs: internal resistance variation versus equivalent driven distance.

### 3.3.2 Example of incoming HEV battery systems: Li ion batteries

The main advantages of Li ion in HEVs are power density, life, and potentially lower cost in large volumes. High-power batteries have been manufactured for several years for industrial applications as well as consumer applications, for example, power tools. They have proven able to deliver several thousands of W/kg, a level usually provided so far by ultracapacitors. Their use in HEVs has been long considered and much R&D efforts have been devoted to this goal. However, only recently they have been introduced in the commercial market, for example, by Daimler in the Class S400 hybrid car. Fig. 13.11



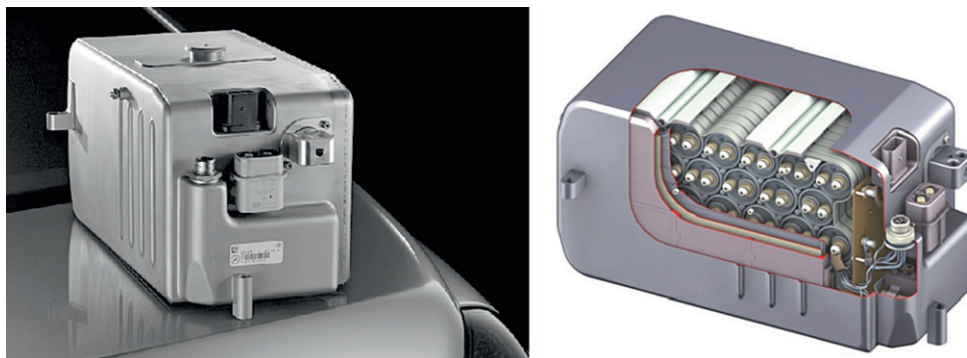


**Figure 13.11** Picture and schematic view of the Li ion battery used in Mercedes-Benz S400 Hybrid.

**Table 13.8** Main characteristics of the Li ion battery used in Mercedes-Benz S400 Hybrid

Battery voltage	126 V
Energy	0.8 kWh
Power	19 kW
Cell capacity	0.65 Ah
Weight	25 kg

shows the picture and schematic view of a battery pack composed of 35 cylindrical Li ion cells in series. The cells are manufactured by Johnson–Controls–Saft in France and the battery pack assembly by Continental in Germany. The main electrical characteristics of the battery are summarized in Table 13.8. The size of the battery, located near the engine, is not larger than that of a regular lead acid battery (H8 format). The lifetime is 10 years, with 600,000 shallow cycles corresponding to ~160,000 km. The cell picture and its main characteristics are reported in Fig. 13.12.

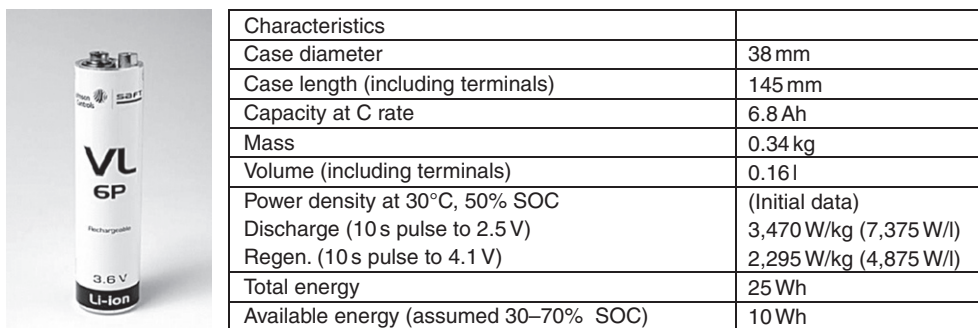


**Figure 13.12** Li ion VL6P for HEV batteries (JCS) (from Ref. [20]).

A particular attention has been given to the cell and battery designs to insure a safe operation, whatever the possible abuse conditions. The battery is connected to the vehicle air conditioning circuit so it can be cooled independently from the engine. By maintaining the battery at ambient temperatures always below 50°C, this thermal management insures the best conditions to extend the battery life.

Fig. 13.13 shows the discharge and regenerative power characteristics calculated at various DOD and at 25°C following the FreedomCar Low-HHPC procedure [20]. At 50% DOD, the voltage limited discharge power is 1180 W/cell at +30°C and 90 W/cell at -35°C. Short-pulse recharge during regenerative operation can also be performed at high rates in a wide temperature range.

This cell benefits from the excellent calendar and cycle life already demonstrated with this chemistry (positive electrode based on LiNiCoAl oxide) [21]. Fig. 13.14 shows the results of accelerated aging tests performed on the VL6P cell. This figure compares actual VL6P impedance increase versus data obtained by the Idaho National Laboratory in a previous program with cells using similar chemistry. These results show that the projected calendar life for the VL6P cell matches the vehicle life span.

Fig. 13.15 gives an example of the Li ion cell ability to deliver a satisfactory power during an extended cycle life in HEV conditions. VL6P used in the described battery for Mercedes S400 is compared to a previously developed VL7P of similar design.

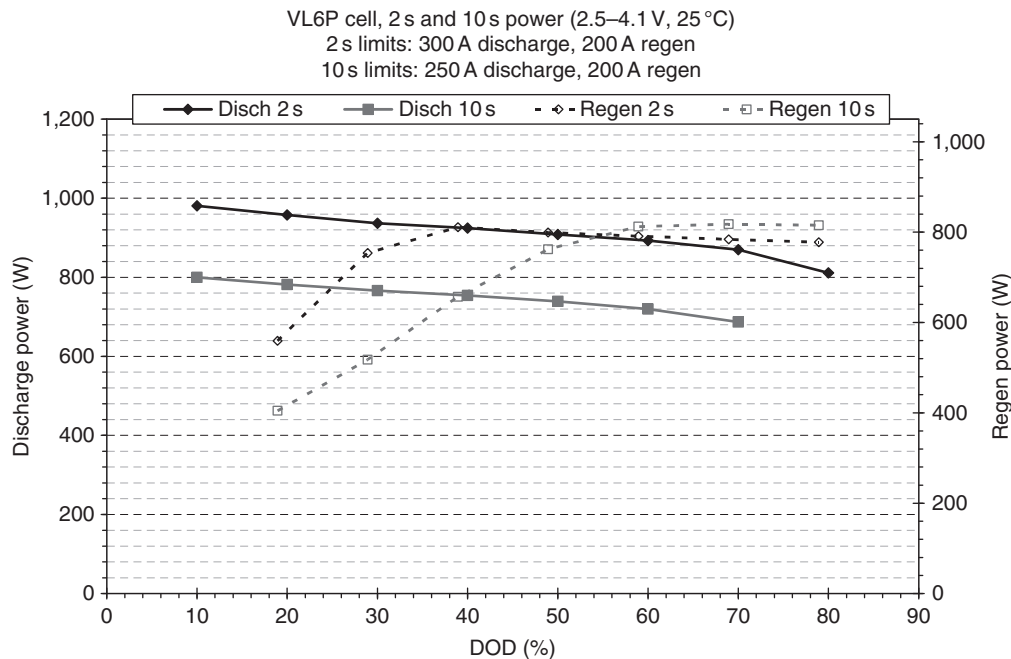


**Figure 13.13** VL6P power as a function of DOD. Discharge and regen, 10 and 2 s pulses at 25°C.

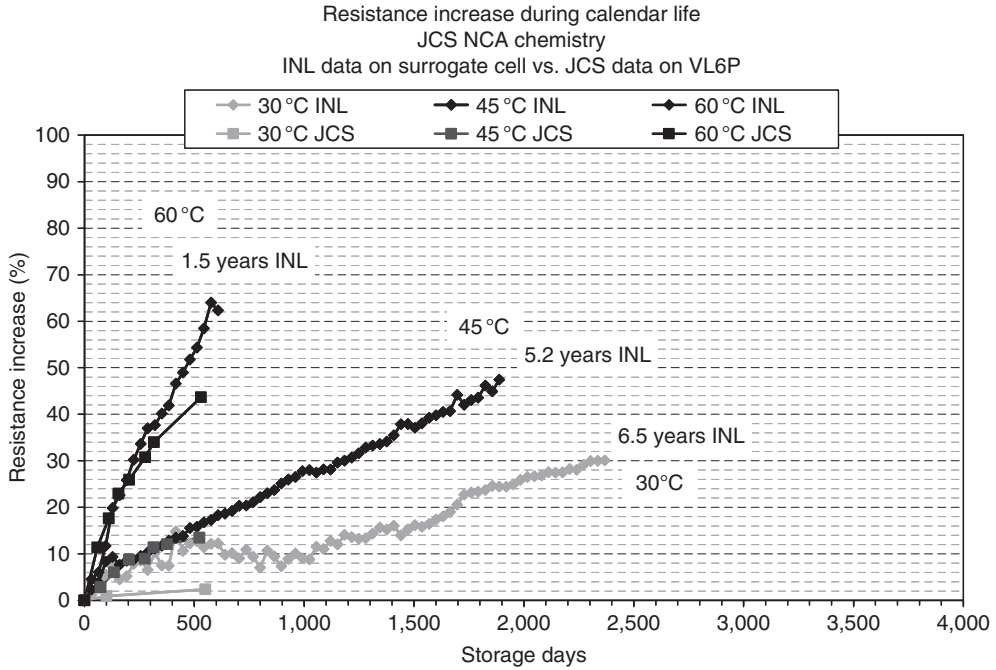


**Figure 13.14** VL6P resistance evolution after storage at various temperatures.

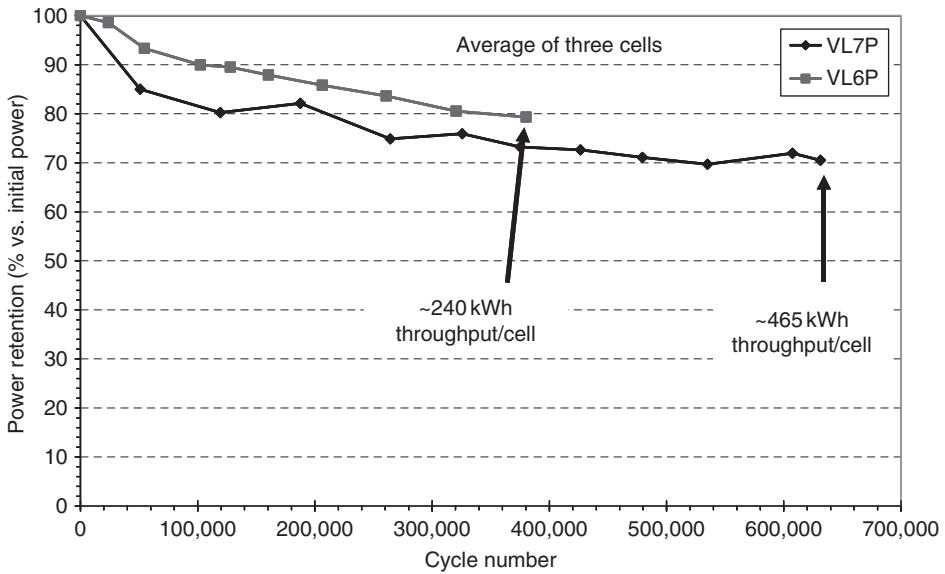


**Figure 13.15** Power retention during cycle life tests of VL6P and VL7P high power JCS Lion cells under HEV load profile. Cycling conditions:  $T = 30^{\circ}\text{C}$ ;  $\text{SOC} = 60\%$ ;  $\Delta\text{SOC} = 3\%$ ; rate = 20C. Power measured with 18 s pulses at 60% SOC down to 2.3 V, at 25°C.



Cell characteristics	
Voltage	3.7 V
Dimensions ( $H \times W \times L$ )	82.6 × 21 × 112 mm
Mass	0.331 kg
Nominal capacity	6 Ah
Specific energy	67.1 Wh/kg
Specific discharge power (10 s, 50% SOC)	3,600 W/kg
Specific charge power (1 s, 20–70% SOC)	3,000 W/kg

**Figure 13.16** EH6 Li ion cell for HEV (GS-Yuasa, from Ref. [22]).

An example of prismatic design manufactured by GS-Yuasa [22] is described in Fig. 13.16. Predicted retention of power and capacity were 78 and 65%, respectively, at the end of life after 15 years (131,400 h) of usage under the conditions presumed by GS Yuasa, consisting of 10,000 h cycling mode (150,000 miles drive) between 20 and 70% SOC at 45°C and 121,400 h storage mode at 50% SOC at 25°C.

Many other Li ion batteries are under development and/or industrialization to power several new HEV programs. Unlike NiMH, there are several “families” of Li ion batteries, depending on the electrochemistry used; a summary is made in Section 5.

### 3.4 Plug-in hybrids

The battery size required for PHEVs is an intermediate between those of pure EVs and HEVs. The most important modification compared to the HEV is that the battery can be charged from an external source, and should store enough energy to grant a significant driving distance in pure EV mode. The car is usually charged overnight, so the battery is fully charged when starting operation, at variance with the HEV battery which is practically never at the full charge state. Many scenarios are then possible to manage the energy, between full electric CD (charge depleting) mode, until a given SOC (~50%) is reached and hybrid CS (charge sustaining) mode, the goal being to save as much fuel as possible. The SOC utilization during driving of PHEVs and HEVs is schematically compared in Fig. 13.17.

The size (energy) of the battery depends on the minimum full electric drive range required, but it should still provide about the same minimum power. Therefore, the energy to power ratio varies with the optimum cell design.

Many modeling studies have been carried out to define the best scenarios for fuel saving. National Renewable Energy Laboratory [24] in the United States has, for example, studied the comparison between a pure electric charge-depleting mode (EV in Fig. 13.17) and a hybrid charge-depleting mode (EV/HEV in Fig. 13.17). In the latter case, high-power

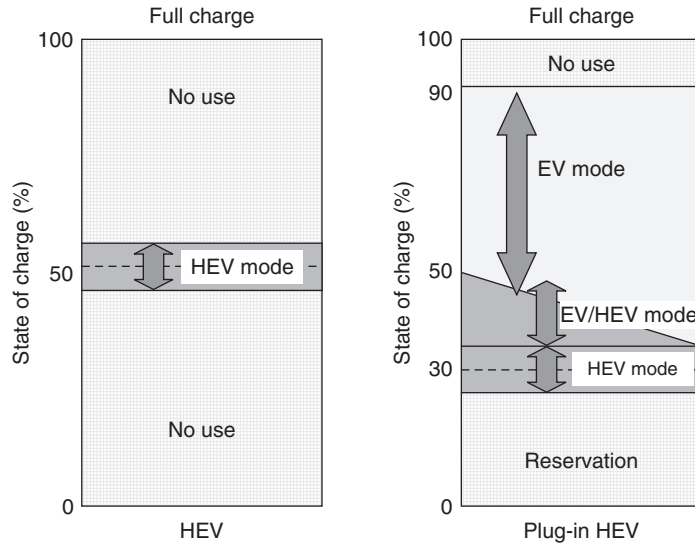


**Figure 13.17** Schematic comparison of the SOC during battery utilization in HEV and PHEV (from Ref. [23]).

pulses are provided by the engine, this leading to less expensive battery designs with lower power/energy ratio.

Fig. 13.18 describes, for example, the power-to-energy ratio as a function of the required electric range for several PHEV sizes. These simulations studies are made, for example, at Argonne National Lab in the United States within the FreedomCar program [25].

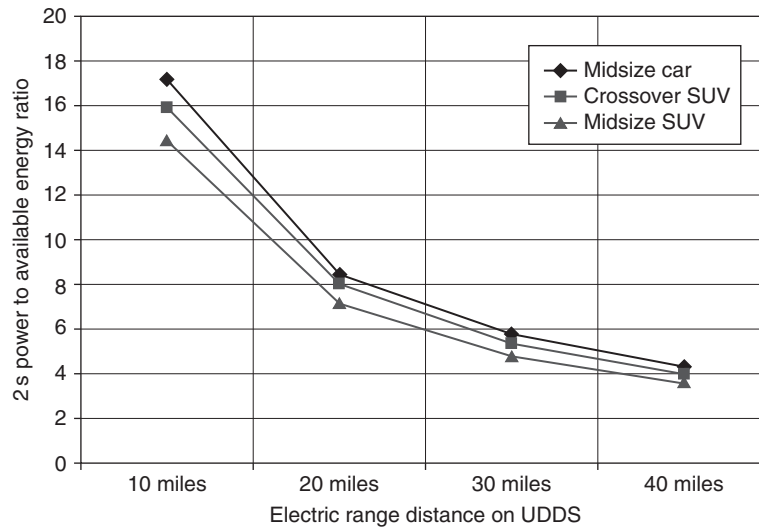


**Figure 13.18** Power to energy ratio simulations as function of AER for several car sizes (from Ref [25]).

**Table 13.9** USABC's goals for advanced batteries for PHEVs

Characteristics at EOL (End of Life)	Units	High power-to-energy ratio	High energy-to-power ratio
Reference equivalent electric range	Miles	10	40
Peak pulse discharge power—2 s/10 s	kW	50/45	46/38
Peak regen pulse power (10 s)	kW	30	25
Available energy for CD (charge depleting) mode, 10 kW rate	kWh	3.4	11.6
Available energy for CS (charge sustaining) mode	kWh	0.5	0.3
Minimum round-trip energy efficiency (USABC HEV cycle)	%	90	90
Cold cranking power at -30°C, 2 s—three pulses	kW	7	7
CD life/discharge throughput	Cycles/MWh	5,000/17	5,000/58
CS HEV cycle life, 50 Wh profile	Cycles	300,000	300,000
Calendar life, 35°C	Year	15	15
Maximum system weight	kg	60	120
Maximum system volume	l	40	80
Maximum operating voltage	V <sub>dc</sub>	400	400
Minimum operating voltage	V <sub>dc</sub>	$>0.55 \times V_{\max}$	$>0.55 \times V_{\max}$
Maximum self-discharge	Wh/day	50	50
System recharge rate at 30°C	kW	1.4 (120 V/15 A)	1.4 (120 V/15 A)
Unassisted operating and charging temperature range	°C	-30 to +52°C	30 to +52°C
Survival temperature range	°C	-46 to 66°C	-46 to 66°C
Maximum system production price at 100 ku/year	\$	1,700	3,400

Larger, and more expensive, batteries will produce less fuel consumption providing that the all-electric range (AER) allowed by the battery energy is actually mostly used. If not, the weight excess due to the battery size would induce less fuel saving during the use in the charge-sustaining hybrid mode. Li ion batteries reduce this constraint thanks to their high specific energy. Modeling fuel saving as a function of battery parameters such as energy density, power density, and operating temperature is necessary to define the best vehicle characteristics in normalized driving cycles [26, 27]. Table 13.9 describes the goals set by USABC for PHEVs with two power/energy ratio limits [6, 28].

### 3.4.1 Li ion batteries for PHEVs

Because of its high specific energy and energy density, Li ion is today the only system being considered for powering PHEVs, although its properties are still considered insufficient. Table 13.10 is a summary of PHEV Li ion battery main attributes to be

**Table 13.10** Summary of main battery characteristics to be improved in a short term for PHEV batteries (from Ref. [29])

Battery attribute	Current status	Goals	
		2012	2014
Available energy	3.4 kWh	3.4 kWh (10 miles)	11.6 kWh (40 miles)
Cost	\$1,000+/kWh	\$500/kWh	\$300/kWh
Cycle life (EV cycles)	1,000 <sup>a</sup>	5,000	3,000–5,000
Cycle life (HEV cycles)	300,000	300,000	200,000–300,000
Calendar life	3+ years <sup>a</sup>	10+ years	10+ years
System weight (kg)	80	60	120
System volume (l)	70	40	80

<sup>a</sup> The present status varies with electrochemistries, some systems have proven > 4000 EV cycles and 10 years calendar life.

**Table 13.11** Main characteristics of a Li ion battery pack designed for PHEV (JCS)

Unit cell capacity	41 Ah
Average cell voltage	3.6 V
Number of cells	12 modules of 6 cells
Operating voltage	194.4–288 V
Energy	10.5 kWh
Power (30 s, 50% SOC)	61 kW
Weight (approx.)	105 kg

improved in a short term, as defined by US DOE [29] for the PHEV program. The goal is a PHEV battery that enables a 40 mile AER and costs \$3,400.

The main challenges are cost, cycle life in EV mode, calendar life, and energy density for the long range PHEV. Several Li ion chemistries are challenging for this application. They are not at the same level of maturity, but some of them have already demonstrated satisfactory EV cycle life and calendar life. A summary of the particular properties of each chemistry can be found in Section 5. Although some HEVs can be adapted as plug-in, no real PHEV was commercially available at the end of 2009. Several car makers have announced their forthcoming production and batteries are being developed in collaboration with battery manufacturers.

Table 13.11 describes a Li ion battery pack designed for PHEV, which should provide a ~40 km range in EV mode to a mid size car, for a 0.9–0.3 SOC variation of the battery. It is formed by high-energy/medium power 41-Ah cylindrical cells.

### 3.5 Electric vehicles

Although the development programs launched to help R&D of batteries for electric vehicles focused at the beginning on pure EVs (e.g., USABC in the early 1990s), actual

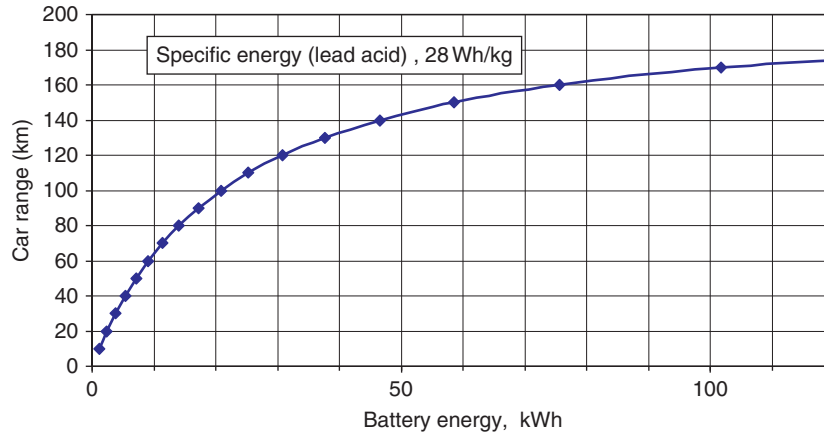


**Figure 13.19** Example of the calculated midsize EV range as a function of battery energy.

industrial developments were up to now very limited. The situation has very recently changed spectacularly, as more than 18 models are announced to be commercialized before 2012! This is not only due to incentive actions of governments and demand from customers, but also recognition that new battery systems are now complying with a minimum of requirements. However, further significant improvements are still required to allow a real wide diffusion of these cars.

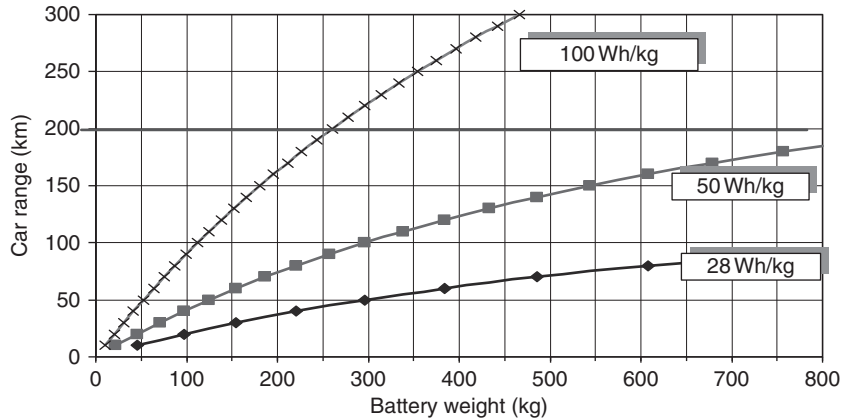
The main property to be considered for an EV battery is the specific weight. Indeed, the weight of the large batteries required to provide a minimum car range is a limiting factor. The car range is not proportional to the battery energy, because of the energy consumption due to the battery weight excess. This is illustrated in Fig. 13.19, which represents the calculated range of an 800 kg midsize car using a low-energy density battery, assuming an average consumption of 135 Wh/ton/km.

Fig. 13.20 describes for the same conditions the calculated range as a function of the weight of batteries with different specific energies. Tables 13.12 and 13.13 summarize examples of comparative characteristics of different batteries weighing 250 kg or having a volume of 200 l, respectively, to power a typical midsize car [30].

The calculated power characteristics are reported in Table 13.14, showing the superiority of the Li ion technology also in terms of power. These results clearly demonstrate that advanced Li battery systems only can fulfill the minimum range requirements for EVs, still having weight and volume compatible with the car.

The initial goals for the main parameters were fixed by the USABC [6] more than 10 years ago, and are still valid. They are described in table Table 13.15. This means that, although intense R&D work has been carried out during this period, some of the goals are still to be reached. The power capability is sufficient, and energy density allows a reasonable car range, although future improvements are highly desired.





**Figure 13.20** Calculated car range as a function of battery weight for several specific energies.

**Table 13.12** Comparison of different technologies of EV batteries for a typical size of 250 kg

Technology	Pb-Acid	Ni-Cd	Ni-MH	Li-Ion
Vehicle curb weight		1200 kg		
Battery weight allocation (typ.)		250 kg		
Battery structure, cooling, etc.		55 kg		
Module weight allocation		195 kg		
Energy density (module) (Wh/kg)	33	45	70	120
Onboard energy (kWh)	6.4	8.8	13.0	23.4
Range at 120 Wh/ton/km (km)	53	73	114	195

**Table 13.13** Comparison of different technologies of EV batteries for a typical size of 200 l

Technology	Pb-Acid	Ni-Cd	Ni-MH	Li-Ion
Battery volume allocation (typ.)		200 l		
Battery structure, cooling, etc.		70 l		
Module volume allocation		130 l		
Volumetric energy (module) (Wh/l)	75	80	160	190
Onboard energy (kWh)	9.8	10.4	20.8	24.7
Range at 120 Wh/ton/km (km)	81	87	173	206

The main challenges are cost, which actually limits the present diffusion (see Section 2.2), cycle and calendar life, and safety. This last property is critical, especially because of the size of the batteries, containing a large amount of active materials and

**Table 13.14** Power characteristics comparison for a 250 kg battery using different chemistries

Technology	Pb-Acid	Ni-Cd	Ni-MH	Li-Ion
Vehicle curb weight		1200 kg		
Battery weight allocation (typ.)		250 kg		
Battery structure, cooling, etc.		55 kg		
Module weight allocation		195 kg		
Power density (module) (W/kg)	75	120	170	370
Battery power (kW)	15	24	33	72

**Table 13.15** USABC's goals for advanced batteries for EVs (from Ref. [6])

Parameter (units) of fully burdened system	Minimum goals for commercialization	Long-term goal
Power density (W/l)	460	600
Specific power (discharge, 80% DOD/30 sec) (W/kg)	300	400
Specific power (regen, 20% DOD/10 sec) (W/kg)	150	200
Energy density (C/3 discharge rate) (Wh/L)	230	300
Specific energy (C/3 discharge rate) (Wh/kg)	150	200
Specific power/specific energy ratio	2:1	2:1
Total pack size (kWh)	40	40
Life (years)	10	10
Power and capacity degradation (% of rated spec)	20	20
Cycle life (80% DOD) (cycles)	1,000, 20% performance loss (10% desired)	1,000
Selling price (25,000 units at 40 kWh) (\$/kWh)	<150	100
Operating environment (°C)	-40 to +50°C	-40 to +85°C
Normal recharge time	6 h (4 h desired)	3–6 h
High rate charge	20–70% SOC in <30 min at 150 W/kg (<20 min at 270 W/kg desired)	40–80% SOC in 15 min
Continuous discharge in 1 hour (no failure) (% of rated energy capacity)	75	75

energy (see Section 2.5). Cycle life and calendar life have been well demonstrated for some nickel oxide-based positive materials, as shown, for example, in Figs. 13.21 and 13.22.

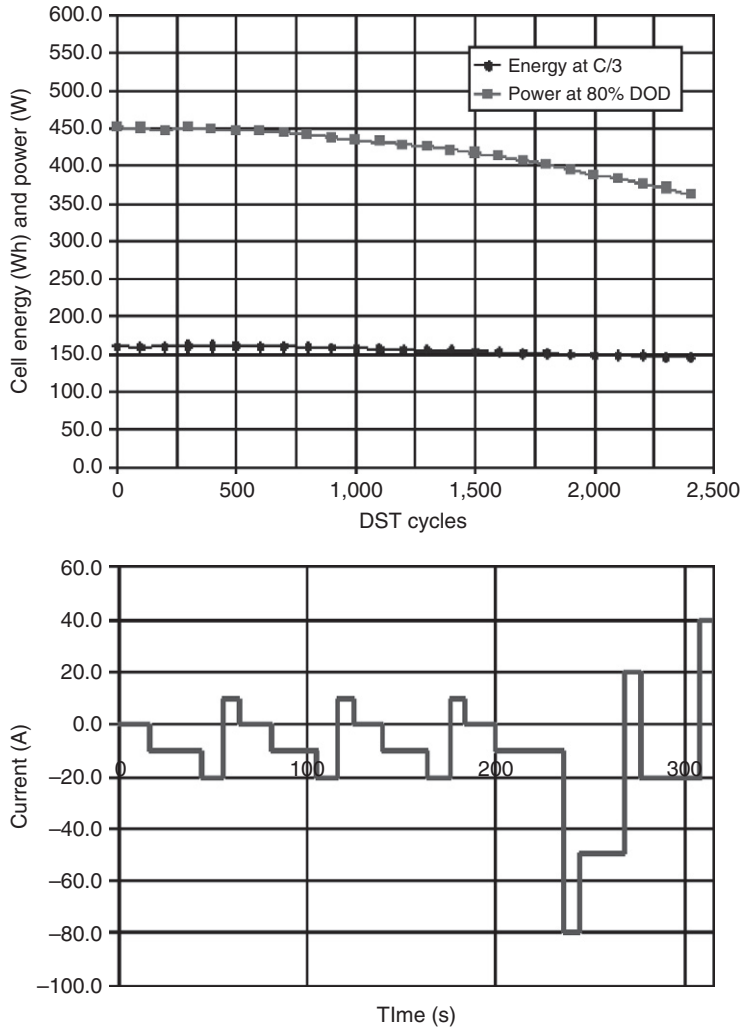


**Figure 13.21** (Up) Energy and power evolution of Saft VL45E cells during cycling at 80% DOD, DST cycle. Every 50 cycles, energy measured at 100% DOD—C/3, power measured at 80% DOD, 300 A–5min pulse. (Down) DST cycle profile: microcycle duration = 16 s; maximum power = 240 W/kg; 1 cycle = continuous cycling up to 80% DOD.

The peculiarity of cycle life testing for EV is a large DOD, which represents a full utilization of the stored energy per day of usage. This is obviously the worst condition, as the active materials inside the electrodes are subjected to a large transformation at each cycle.

Charging time is normally ~6 h. Increasing the charge rate capability (i.e., power of the battery) is possible, but to the detriment of the energy density. There is therefore a trade-off between the maximum range without recharge and the time to recharge (besides the constraint of power capability of charge terminals).

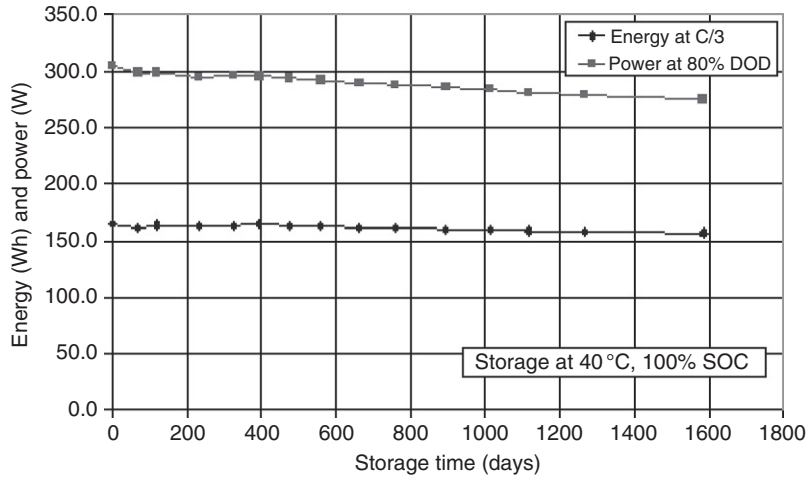


**Figure 13.22** High-energy Saft VL45E cells: power and energy retention during storage at 4.0V (100% SOC) and 40°C.

Because of the large size of these batteries, the cost acts today as the major hurdle to their expansion, and battery leasing is considered a feasible option to commercialize new EVs. It is expected that increasing production volumes of batteries using the same chemistries of HEVs will help decreasing their cost (see Section 2.2).

### 3.5.1 Examples of recent EV battery systems: Li ion

The Mitsubishi “iMiEV” car recently introduced in Japan uses a GS Yuasa Li ion battery, whose electrochemistry is based on a LiNiMnCo mixed oxide positive electrode. The prismatic shape cell and module characteristics are shown in Fig. 13.23, while the battery pack characteristics are described in Table 13.16.

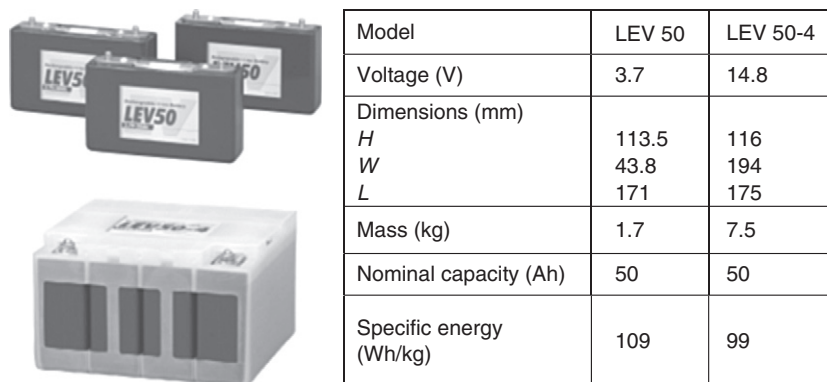


**Figure 13.23** Li ion cell (LEV 50) and module (LEV 50-4) for EV battery (GS-Yuasa, from Ref [22]).

**Table 13.16** Specifications of the battery pack of iMiEV

Dimensions (mm)	1400 × 700 × 200
Weight	200 kg
Nominal voltage	330 V (88 cells in series)
Energy	16 kWh
Specific energy	80 Wh/kg
Maximum output power	60 kW
Continuous current for quick charge	125 A



Cell type	VL45E	VL41M	VL22M
Capacity (Ah) C/3 @ 4V	45	41	22
Diameter (mm)	54	54	54
Length (mm)	222	222	145
Weight (kg)	1.07	1.07	0.65
Volume (dm <sup>3</sup> )	0.51	0.51	0.33
Energy (Wh)	160	146	78
Power (W) 30s – 50%SOC	710	850	700

**Figure 13.24** Li ion cells and module for EV battery (JCS). Characteristics of these cells are in the accompanying table.

Cylindrical high-energy Li ion cells, with a LiNiCoAl mixed oxide positive electrode, are used by JCS in the module for EV batteries described in Fig. 13.24.

Renault-Nissan announced recently the introduction in Europe by 2012 of several EV models using a battery manufactured by AES (Automotive Energy Supply), a joint venture between Nissan and NEC. The 32 Ah, 3.6 V cell (~1 kg) has a flat prismatic polymer case (Fig. 13.25). The electrochemistry is based on lithiated manganese spinel as a positive material. Modules made with these cells are assembled into a 170 V, 12 kWh battery pack including electronics (Fig. 13.26), used to build complete EV battery systems (Table 13.17).

The US company A123Systems [31] is also developing a similar flat cell design, using LiFePO<sub>4</sub> as a positive electrode; a cell and module for EV/PHEV are shown in Fig. 13.27.

All these batteries use relatively large cells, assembled in series (modules/pack) to produce the required voltage. A different concept is used by Tesla Motors [32], whose EV battery is composed of a large number of <2 Ah small cylindrical 18,650 cells in

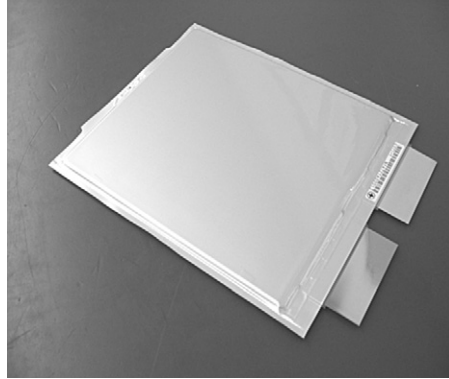


**Figure 13.25** Prismatic polymer case Li ion cell for EV (AES).

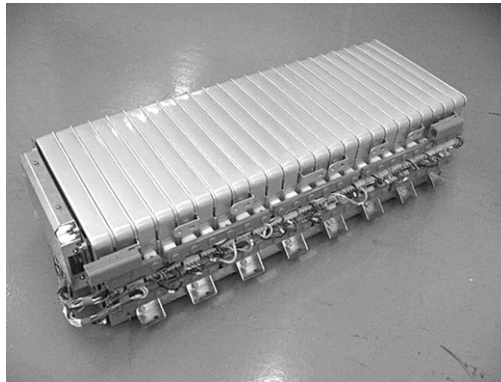


**Figure 13.26** 170 V, 12 kWh pack for EV battery (AES).

**Table 13.17** Example of EV battery system characteristics (AES)

<b>Complete battery system characteristics</b>	
Voltage	340 V
Energy	24 kWh
Dimensions ( $L, W, H$ ) (mm)	1200 × 750 × 250
Weight	230 kg

series/parallel assembly. These cells are manufactured by Sony primarily for portable computers. The 6,831 cells constituting the battery pack provide 53 kWh for a weight of 450 kg, and have a specific energy of  $\sim 120$  Wh/kg in the 366 V system. This pack gives the \$190,000 “Roadster 2008” car a range of  $\sim 350$  km.

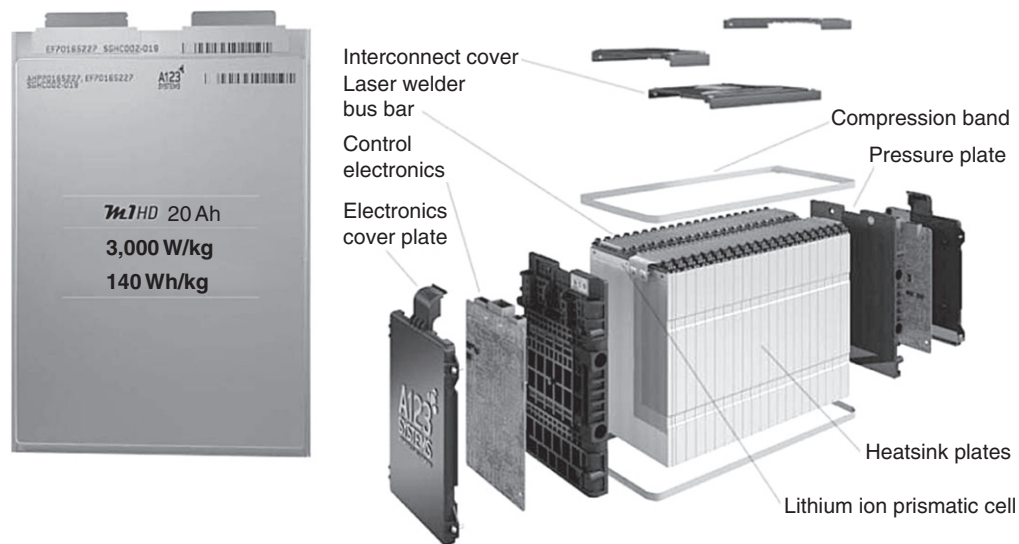


**Figure 13.27** Li ion cell and module for EV/PHEV battery (A123Systems, from Ref [31]).

### 3.5.2 Examples of recent EV battery systems: lithium metal polymer

Contrary to the Li ion, the LMP battery uses metallic Li as a negative electrode. A polymeric electrolyte allows obtaining a better Li cycling efficiency, very bad in liquid electrolytes. Invented by Armand and Duclot [33] at the end of the 1970s, this concept has been first applied by HydroQuebec in Canada to develop Li batteries.

EV application was considered in the 1990s by the Canadian company Argotech (a joint venture between Hydro Quebec and 3M) under the USABC R&D program, and battery prototypes were built and integrated in demonstration vehicles. Avestor (HydroQuebec-Kerr MacGee) restarted the program until 2005 when it was stopped. The French company Batscap (Bolloré group) has been developing this type of batteries for EV since 1998, and started recently an industrial production to equip a small size EV (the Bluecar), build jointly by Bolloré and Pininfarina and to be launched commercially in 2010. At the production start, the car will only be rent.

Because the conductivity of the polymer electrolyte is very low, the battery must be operated at a temperature above ambient, typically 80°C. Battery modules are made by series connected flat prismatic stacks placed in a single stainless-steel box. Several flat heater devices are placed between the cells to heat the battery and maintain the appropriate working temperature. The battery module is also thermally insulated. A battery management system maintains the temperature between 60 and 80°C. Depending on operating conditions it may be required to cool or heat the battery.

Because its power capability is lower than that of Li ion, the use of LMP in HEVs is not anticipated, and would be limited to pure EVs. In the Bluecar, the battery is



**Figure 13.28** Picture and schematic view of a LMP battery (from Ref [34]).

associated to a supercapacitor, manufactured by the same company, to provide the high peak power and store the regenerative power on braking [34]. The challenge of LMP batteries is to match the demonstrated long cycle life of Li ion batteries. Because it does not contain flammable liquid organic solvent, its behavior under abuse conditions is reported to be safer. However, the large amount of Li that may burn violently at high temperature still creates serious safety concerns, and appropriate safety features must be implemented to avoid this overheating.

Limited information is available today on the battery internal design. The main electrical characteristics of the pack, shown in Fig. 13.28, are reported in Table 13.18 [34]. Its energy density is similar to that of Li ion. The battery will provide the car with a range of 250 km, and has an expected life of 200,000 km (i.e., 1,000 cycles at 80% DOD).

### 3.5.3 Examples of recent EV battery systems: sodium/nickel chloride (ZEBRA)

The high-temperature ( $\sim 300^\circ\text{C}$ ) battery system known as ZEBRA has been studied since mid-1980s as an improvement of the sodium sulfur battery. The active materials are liquid Na and  $\text{NiCl}_2$ . The main features are the use of a solid electrolyte,  $\beta$ -alumina, and a liquid electrolyte,  $\text{NaAlCl}_4$ , the latter being placed in the positive compartment. ZEBRA batteries are now manufactured by the Swiss company MES-DEA. This system has reached a mature development and has been manufactured in several battery systems

**Table 13.18** Main electrical characteristics of the LMP battery system (from Ref. [34])

Energy	30 kWh
Operating voltage	435/300 V
Peak power (30s)	45 kW
Specific energy	100 Wh/kg
Energy density	100 Wh/l
Weight	300 kg
Volume	300 l



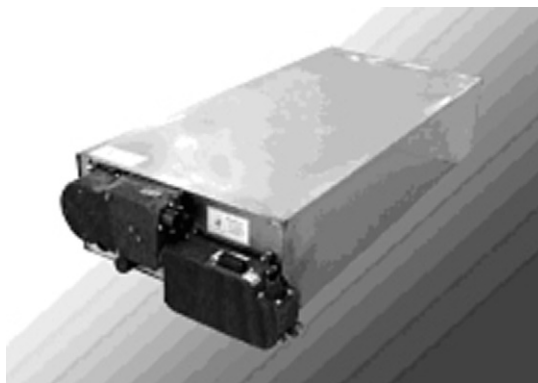


**Figure 13.29** Z21 ZEBRA battery (from Ref. [36]).

to power different types of vehicles, from EVs to buses, although not yet commercially available passenger cars.

Specifications of the Z21 battery system (Fig. 13.29) are reported in Table 13.19. Integration in a THINK City car has been recently described [35]. For this car, the battery is the “Z36-371-ml3x-76” with a voltage of 371 V, a nominal capacity of 76 Ah, and a complete energy of  $\sim 28.2$  kWh. A typical charge time is 8 h.

The energy density is similar to that of Li ion batteries, but the power density is much lower. Like LMP, this technology does not allow a high-power version to be used in HEVs. The battery should be maintained during rest at its operating temperature by electric resistance heaters, while during discharge the temperature is mainly maintained by the energy generated by ohmic losses and polarization. The heat loss of a Z21 battery

**Table 13.19** Example of ZEBRA battery specifications (from MES-DEA data sheet, Ref. [36])

Battery type	Z21
Cell type/number	ML/8, 240 cells
Rated energy (kWh)	15.5
Weight with BMS (kg)	134
Dimensions ( $W \times L \times H$ ) (mm)	444 $\times$ 962 $\times$ 206
OCV (V)	310
Max regen voltage (V)	372
Minimum discharge voltage (V)	206
Specific energy (Wh/kg)	115
Peak power (kW)	24
Specific power (W/kg)	180
Thermal loss (W)	<90
Cooling	Air
Heating time (h)	24 at 230 Vac
Ambient temperature ( $^{\circ}\text{C}$ )	-40 to +50

type is less than 90 W at 270°C, which represents a maximum of ~7 days storage capability without external power source for a 15.5 kWh battery. Although cooling down to ambient temperature and reheating is not convenient, it was demonstrated that >40 freeze/thaw cycles had no detrimental effect on the performance [37].



#### 4. FUEL CELL HYBRID VEHICLES

In order to optimize (downsize) as much as possible the fuel cell, the vehicle has to be of hybrid design, where the battery may be used for the following:

- Traction power during fuel cell start-up.
- Acceleration performance.
- Power assist during drive cycles.
- Electrical accessory loads.
- Regenerative braking energy recapture.
- Fuel cell start up and shutdown.

Today there is no precise goal for specific battery requirements. A study by NREL [38] concluded that these requirements would range from 55–85 kW and up to 7 kWh depending on the fuel cell system size and the intended roles of the energy storage system. It was concluded that significant fuel cell downsizing leads to increased energy storage system requirements, and that downsizing beyond the power level required for continuous gradeability should be avoided since it leads to dramatically increased energy requirements.

It can be anticipated that the size and properties of the battery should be similar to those required from a battery of equivalent size for power assist HEVs.



#### 5. SUMMARY OF THE DIFFERENT LI ION CHEMISTRIES EXISTING AT PRESENT, AND TO BE USED IN HEV<sub>S</sub>, PHEV<sub>S</sub>, OR EV<sub>S</sub>

Born in 1990, the Li ion battery concept is the achievement of more than 40 years of research and development on rechargeable Li batteries. As shown in Fig. 13.30, Li ion batteries can surpass all other batteries in specific energy (and energy density) as well as specific power. A variety of materials have been studied, from the carbon type for the negative to the oxidizing compounds for the positive electrode. Of the many systems studied, a few are now presently used or will be used in vehicles applications [39].

LiNi<sub>x</sub>M<sub>y</sub>O<sub>2</sub> materials, so-called Ni-based, where M can be several metal ions, have similar structure to LiCoO<sub>2</sub>. These materials are less expensive as they use less cobalt, while having higher or similar energy density. One of these, LiNi<sub>x</sub>Co<sub>y</sub>Al<sub>z</sub>O<sub>2</sub>, also called NCA, has been studied and commercialized by Saft in industrial batteries, especially for space applications. It exhibits excellent cycling and long calendar life properties, with the best figures that Li ion chemistries can show today [40]. It has been chosen by JCS and Toyota for electric vehicles. Nickel/cobalt/manganese oxides, NMC, are also used and

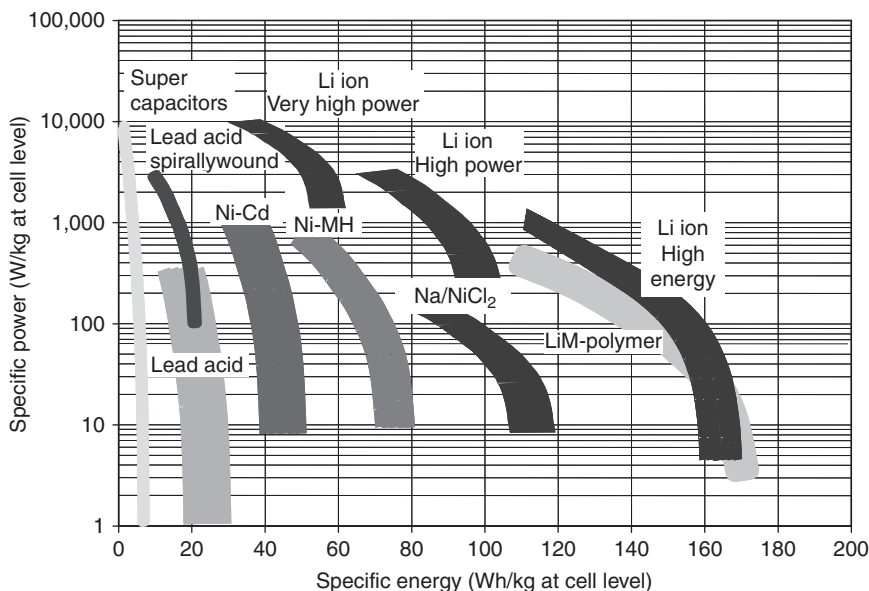


**Figure 13.30** General comparison of main rechargeable systems used in industrial batteries. Pseudo-Ragone diagram, W/kg/Wh/kg.

have similar properties, but little less industrial experience. NMC is more and more used to replace  $\text{LiCoO}_2$  in small batteries to reduce their cost, and has been selected by GS-Yuasa and Hitachi Vehicle Energy in Japan.

These layered oxides suffer from low chemical stability when they are overcharged (totally delithiated), and therefore induce a potential safety hazard in this abuse condition, thus necessitating appropriate safety features in cell and battery design.

$\text{LiMn}_2\text{O}_4$  spinel and derived materials are safer because their fully charge state,  $\text{MnO}_2$ , is stable. They have a potentially lower cost, but their energy density is lower than the Ni-based oxides. The power capability is excellent, but the batteries suffer from shorter life due to the slight solubility of manganese that destroys the long-term stability of the negative electrode, especially at high temperature. This material, with design features that mitigate this drawback, has been chosen by NEC.

$\text{LiFePO}_4$  has been more recently introduced [41]. It has an excellent stability on overcharge, this giving an improved safety, and the potential for low cost due to the use of iron. Its energy density is, however, significantly lower than the other materials, because of the lower voltage operation and lower material density. Contrary to other positive materials, its voltage is almost constant with DOD. It has therefore a larger useful SOC range, but the SOC monitoring and cell balancing is more challenging. It may be more suitable for high-power applications (HEV) than high energy (EV, PHEV). This material is used by A123Systems and Valence Technology in the United States.

**Table 13.20** Schematic summary of pro/con properties of the main Li ion chemistries for EV/HEV applications

Positive material	LiNi <sub>x</sub> M <sub>y</sub> O <sub>2</sub>	LiMn <sub>2</sub> O <sub>4</sub>	LiFePO <sub>4</sub>
Energy density	++	+	–
Power	+	++	+
Cost	--	–	–
Life	++	–	? <sup>a</sup>
Abuse tolerance	–	+	+
SOC monitoring and cell balancing	++	+	–

<sup>a</sup> Less mature system, conflicting reports.

The negative active material consists of carbon powder, in which Li ions are inserted during charge. The initial carbon material when Li ion was first introduced was a disordered carbon (hard carbon), which is still used in some cases. Most Li ion designs now use graphitized carbons featuring higher capacity density and lower voltage. Their stability on charge/discharge cycling is excellent due to a passivation layer formed in contact with the electrolyte. This is a key property that enables the existence of Li ion batteries, and is a challenge to replacing graphite with higher energy materials. The main attributes of these systems are schematically summarized in [Table 13.20](#)



## 6. THE FUTURE

Although very important improvements have been achieved in batteries in the last decade, allowing the present industrial introduction in all types of electric vehicles, there is no doubt that this trend will continue in the future. Fundamental research in advanced materials is the key for success, as it has been the case for 20 years, with the introduction of Li ion batteries. Many research organizations and networks have been set all over the world to reach this goal, with huge investments for personnel and equipment.

Governmental financial supports are granted to help this work. For example, NEDO (New Energy and Industrial Technology Development Organization) started since 2007 in Japan a new project called “Development of High-Performance Battery System for Next-Generation Vehicles (Li-EAD project)” [42]. The targets of this 5-year project, which groups together a variety of organizations including national research centers, battery developers, universities, and automobile manufacturers, are summarized on [Fig. 13.31](#).

Specific energy of 100 Wh/kg and specific power of 2,000 W/kg are the targets for the technological development of battery modules for plug-in hybrid vehicles, while development of battery materials should upgrade these numbers to 200 Wh/kg and 2,500 W/kg. For future electric vehicles an energy density of 500 Wh/kg is targeted.

An ambitious R&D plan for the batteries of the next generation vehicles was proposed in Japan in 2006 by METI—Direction of Vehicle Battery Development—as schematized in [Fig. 13.32](#)

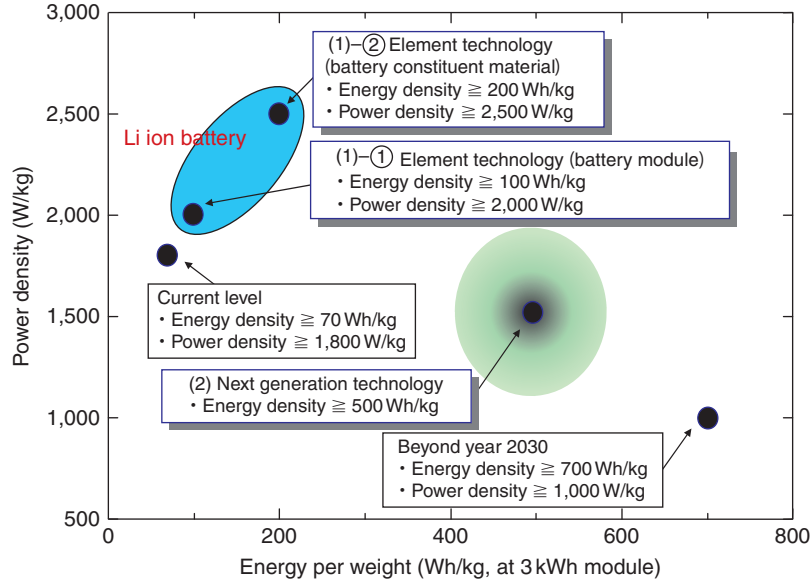


Figure 13.31 Target of Li-EAD project, NEDO (from Ref. [42]).

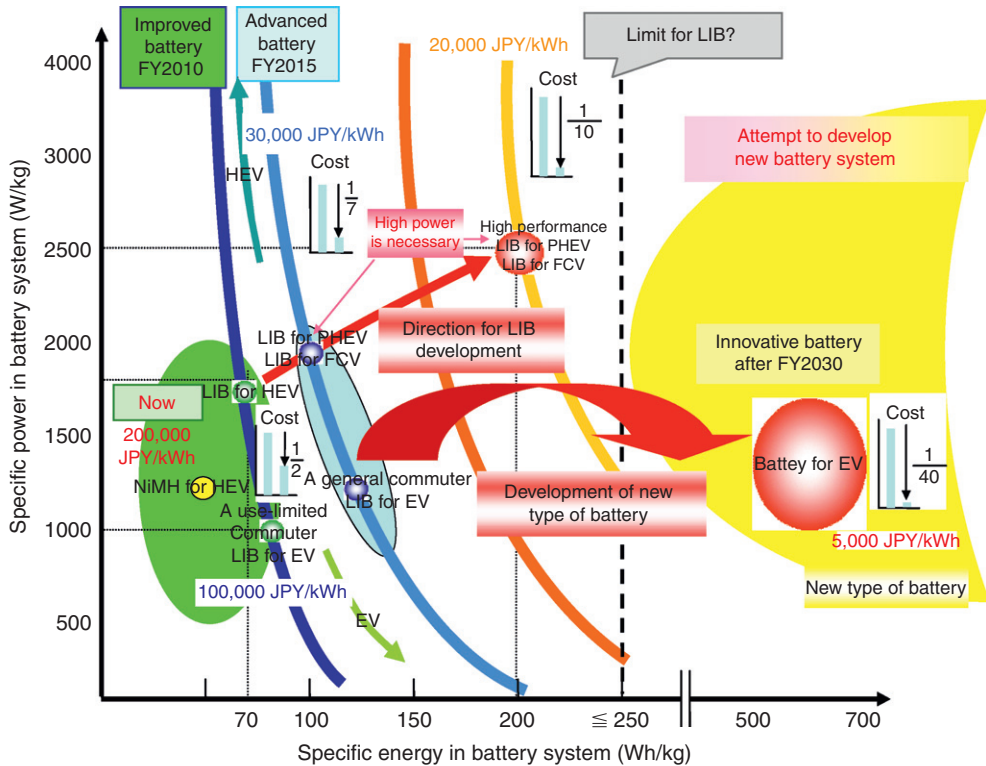


Figure 13.32 Schematic R&D plan for the batteries of future generation vehicles (METI, Japan, 2006) (from Ref. [23]) (see color plate 2).

## REFERENCES

1. M. Broussely, Traction Batteries. EV and HEV, In *Industrial Applications of Batteries from Cars to Aerospace and Energy Storage*, M. Broussely and G. Pistoia (Eds.), Elsevier, Amsterdam, 4 (2007) 203–271.
2. H. Takeshita, 24th International Battery Seminar, Ft Lauderdale, USA, 2007.
3. C. Pillot, Proceedings of EVS-24, Stavanger, Norway, 2009.
4. T. Miller, I.M. Lithium Supply & Markets Conference Santiago 2009, Santiago, Chile, 2009.
5. A. Pesaran, K. Smith, T. Markel, Proceedings of the 9th AABC Conference, Long Beach, USA, 2009.
6. US DOE website, URL: [http://www.uscar.org/guest/article\\_view.php?articles\\_id=85](http://www.uscar.org/guest/article_view.php?articles_id=85), 2009 (accessed 10.09).
7. M. Broussely, Aging Mechanism in Li ion Batteries and Calendar Life Predictions, In *Advances In Lithium-Ion Batteries*, W. van Schalkwijk and B. Scrosati (Eds.), Kluwer Academic Pub., Boston, 4 (2003) 393–432.
8. F. Badin, Proceedings of EVS-24, Stavanger, Norway, 2009.
9. P. Roth, Proceedings of the 1st Conference on Advanced Lithium Batteries for Automobile Applications, Chicago, USA, 2008.
10. Official Journal of the European Communities, 21.10.2000, L269/34.
11. D. Cheret, Battery Collection and Recycling, In *Industrial Applications of Batteries. From Cars to Aerospace and Energy Storage*, M. Broussely and G. Pistoia (Eds.), Elsevier, Amsterdam, 14 (2007) 691–736.
12. Website <http://www.batteryrecycling.unicore.com/valeasProcess/>, 2009 (accessed 10.09).
13. D. Cheret, G. Van Damme, Proceedings of EVS-22, Yokohama, Japan, 2006.
14. W. Ghyoot, S. Levasseur, E. Put, K. Vandeputte, J. Tytgat, Proceedings of the 2nd International Congress Advanced Battery Technologies 2009, Frankfurt, Germany, 2009.
15. F. Trinidad, C. Hernandez, M. Lacadena, B. Jacq, G. Fossati, R. Johnson, Proceedings of the 5th AABC Conference, Honolulu, USA, 2005.
16. T. Kameda, Proceedings of the 5th AABC Conference, Honolulu, USA, 2005.
17. K. Nakano, S. Takeshima, J. Furukawa, *Furukawa Rev.* 32 (2007) 49.
18. H. Miyamoto, T. Asahina, T. Matsuura, S. Hamada, T. Eto, Proceedings of EVS-21, Monaco, 2005.
19. K. Ito, M. Ohnishi, Proceedings of EVS-20, Long Beach, USA, 2003.
20. F. Bonhomme, J. Symanski, J.-L. Liska, P. Blanchard, S. Bourlot, G. Houchin-Miller, Proceedings of the 1st Conference on Advanced Lithium Batteries for Automobile Applications, Chicago, USA, 2008.
21. M. Broussely, P. Biensan, S. Herreyre, F. Bonhomme, K. Nechev, R. Staniewicz, *J. Power Sources* 146 (2005) 90.
22. T. Murata, Proceedings of the 1st Conference on Advanced Lithium Batteries for Automobile Applications, Chicago, USA, 2008.
23. H. Kobayashi, FC Expo 2009, Tokyo, 2009.
24. T. Markel, A. Pesaran, Proceedings of the 7th AABC Conference, Long Beach, USA, 2007.
25. A. Rousseau, N. Shidore, R. Carlson, P. Nelson, Proceedings of the 7th AABC Conference, Long Beach, USA, 2007.
26. A. Rousseau, N. Shidore, R. Carlson, D. Karbowski, Proceedings of the 1st Conference on Advanced Lithium Batteries for Automobile Applications, Chicago, USA, 2008.
27. A. Moawad, G. Singh, S. Hagspiel, M. Fella, A. Rousseau, Proceedings of EVS-24, Stavanger, Norway, 2009.
28. A. Pesaran, T. Markel, H.S. Tataria, D. Howell, Proceedings of EVS-23, Anaheim, USA, 2007.
29. D. Howell, Proceedings of the 9th AABC Conference, Long Beach, USA, 2009.
30. M. Broussely, Li Ion batteries for EV, HEV and other industrial applications, In *Lithium Batteries. Science and Technology*, G.A. Nazri and G. Pistoia (Eds.), Kluwer Academic Publishers, Boston, 21 (2004) 645–685.
31. A. Chu, Proceedings of the 9th AABC Conference, Long Beach, USA, 2009.
32. J.B. Straubel, Proceedings of the 9th AABC Conference, Long Beach, USA, 2009.
33. M. Armand, M. Duclot, French Patent FR 7832976 (1978).
34. From website <http://www.bluecar.fr>, 2009 (accessed 10.09).
35. F. Resmini, J. Ohlson, Proceedings of EVS-24, Stavanger, Norway, 2009.

36. From website <http://www.cebi.com>, 2009 (accessed 10.09).
37. J. Gaub, A. van Zyl, Proceedings of EVS-14, Orlando, USA, 1997.
38. T. Markel, M. Zolot, K.B. Wipke, A. Pesaran, Proceedings of the 3rd AABC Conference, Nice, France, 2003.
39. D. Tien, Proceedings of the 1st International Conference on Advanced Lithium Batteries for Automobile Applications, Chicago, USA, 2008.
40. M. Broussely, Proceedings of the 1st International Symposium on Large Lithium Ion Battery Technology and Application (LLIBTA), Honolulu, USA, 2005.
41. J.B. Goodenough, A. Phadi, K.S. Nanjundaswamy, C. Masquelier, WO9740541 patent, University of Texas, 1997.
42. H. Kobayashi, Proceedings of the 1st Conference on Advanced Lithium Batteries for Automobile Applications, Chicago, USA, 2008.



# Battery Environmental Analysis

Peter Van den Bossche<sup>1\*</sup>, Julien Matheys<sup>\*\*</sup> and Joeri Van Mierlo<sup>\*\*</sup>

\*Erasmus Hogeschool Brussel, Nijverheidskaai 170, Anderlecht, Belgium

\*\*Department of Electrical Engineering and Energy Technology (ETEC), Vrije Universiteit Brussel, Pleinlaan 2, Brussels, Belgium

## Contents

1. Introduction	348
2. Quantitative analyses: LCA	348
2.1 Methodology	348
2.2 Life cycle impact assessment method	349
2.2.1 Selection of impact assessment method	349
2.2.2 Impact categories	351
2.2.3 Damage categories	351
2.2.4 Weighting	351
2.2.5 Eco-indicator points	352
3. Model	352
3.1 Composition	353
3.2 Assembly	355
3.3 Use of the battery in the vehicle	355
3.4 Recycling	355
3.5 Electricity production	356
3.6 Reliability of the Results	356
4. Impact of the Different Battery Technologies	357
4.1 Assembly and recycling of the battery	357
5. Electric Vehicles Traction Batteries	358
5.1 Battery technical characteristics	358
5.2 Reference vehicle	359
5.3 Functional unit	359
5.3.1 FU constant battery energy content and constant lifetime range of the vehicle	359
5.3.2 FU constant battery mass and constant lifetime range of the vehicle	360
5.3.3 FU constant range and constant lifetime distance covered by the vehicle	361
5.3.4 Overview	362
5.4 Results	362
5.4.1 Impact of the different stages	362
5.4.2 Reliability of the data	364
5.4.3 Boundary conditions	364
5.4.4 Limitations of the impact assessment method used	365
5.4.5 Sensitivity analysis	365
5.5 Discussion of the results	369

<sup>1</sup> Corresponding author: peter.van.den.bossche@ehb.be



5.5.1 Importance of recycling	369
5.5.2 Impact per kilogram for the different battery technologies	369
5.5.3 Impact of the application	369
5.5.4 Impact of the batteries	370
5.5.5 General conclusion of the quantitative analysis	370
6. Qualitative Analysis	371
6.1 Overview	371
6.1.1 Nickel-Zinc	371
6.1.2 Lithium-ion-polymer and lithium-metal	372
6.1.3 Zinc-air	372
6.1.4 Vanadium redox, zinc-bromine, polysulfide-bromine	373
6.1.5 Nickel-iron	373
6.2 Discussion of the qualitative analysis	373
References	374



## 1. INTRODUCTION

Battery and hybrid electric vehicles, in substitution of internal combustion engine (ICE) vehicles, are a part of the solution to problems such as urban air pollution, fossil fuel depletion and global warming [1–3]. When analysing electric vehicles, the battery is often considered to be the main environmental concern, be it pertinent or not. Anyhow, the environmental impact of the battery should be assessed. Many batteries contain heavy metals, each with their specific toxic properties to environment and human health (HH).

The impacts of the different battery technologies should be analysed individually to allow the comparison of the different chemistries and to enable the definition of the most environmental friendly battery technology for electrically propelled vehicles. This can be done in a qualitative or a quantitative way. Provided that the necessary data are available (often the most challenging task of an exhaustive environmental study), life cycle assessment (LCA) is the most appropriate method for quantitative comparisons of products or services. Therefore a significant part of this chapter is dedicated to the LCA of traction batteries for electric vehicles [4].

The first step of the environmental analysis presented in this chapter was to list the available battery technologies for electric vehicle applications. Afterwards, a model for the different battery types has been developed and introduced in an LCA software tool. This model allows an individual comparison of the different phases of the life cycle of traction batteries. This makes it possible to identify the heaviest burden on the environment for each life phase of each battery.



## 2. QUANTITATIVE ANALYSES: LCA

### 2.1 Methodology

LCA studies the environmental aspects and potential impacts of a product throughout its life from raw material acquisition through production, use and disposal [5]. Other

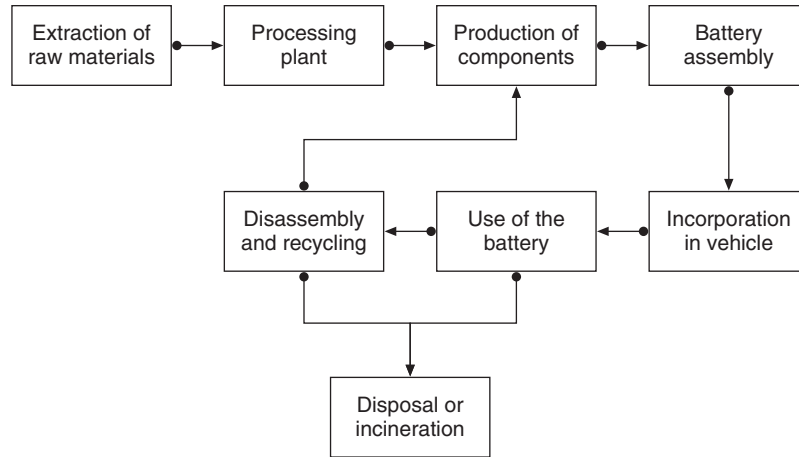


**Figure 14.1** The schematized life cycle of a battery.

instruments exist to assess some environmental impacts of products or services. But its so-called cradle-to-grave approach makes LCA unique. A schematized overview of the life cycle of a battery is shown in Fig. 14.1.

An overall approach is a must when wanting to compare different products in an appropriate way, therefore it was decided to use an LCA approach. The advantage of LCA can be explained by the fact that different products may have burdens in different parts of their life cycle. For example, one product may use less resources (e.g. energy) compared to another product during the use phase, but this may be at the cost of more resources used in its production phase [6].

The LCA of a product will probably never be completely exhaustive; as a consequence the analyst has the freedom to choose to which degree of detail he or she will try to model the assessed life cycle. However, it should be clear that the choice of a more or less detailed model determines the degree of precision and correctness of a study to a certain extent [7].

There are four ISO standards specifically designed for LCA applications:

- ISO 14040: Principles and Framework [8]
- ISO 14041: Goal and Scope Definition and Inventory Analysis [9]
- ISO 14042: Life Cycle Impact Assessment [10]
- ISO 14043: Interpretation [11]

## 2.2 Life cycle impact assessment method

### 2.2.1 Selection of impact assessment method

Life cycle impact assessment (LCIA) methods try to link each life cycle inventory (LCI) result (elementary flow or other intervention) to its environmental impact(s) [12]. According to ISO 14042, LCI results are classified into impact categories, each with a category indicator [10].

Often the impact assessment methodologies differ and the choice of one of the methods remains a difficult decision. Previous studies demonstrated that, in some cases, this choice actually has affected the results of the study [13].

In the past, two classic schools of methods have been used [12]:

- Classical impact assessment methods (e.g. CML, EDIP), which restrict (quantitative) modelling to relatively early stages in the cause–effect chain (or environmental mechanism) to limit uncertainties and which group LCI results in the so-called midpoint categories, according to themes. (Themes are common mechanisms, such as climate change, or are generally accepted groupings, such as ecotoxicity.)
  - Damage-oriented methods (e.g. Eco-indicator 99, EPS), which try to model the cause–effect chain up to the endpoint (damage), sometimes with high uncertainties.
- LCIA aims to evaluate the significance of potential environmental impacts using the results originating from the LCI phase. The ISO 14040 standard suggests dividing this phase of an LCA into the following steps [8]:

- *Classification*: once the different impact categories are defined, the LCI results have to be assigned to these impact categories. For example, CO<sub>2</sub> and CH<sub>4</sub> can be allocated to the impact category ‘Global Warming’, while SO<sub>2</sub> and NH<sub>3</sub> are assigned to the impact category ‘Acidification’.
- *Characterization*: once the different LCI results are assigned to the different impact categories, one should define the characterization factors. These factors define the relative contribution of the different LCI results to the impact category. For example, the contribution of CH<sub>4</sub> to global warming is 21 times higher than the contribution of CO<sub>2</sub>; this means that if the characterization factor of CO<sub>2</sub> is 1, the characterization factor of CH<sub>4</sub> would be 21. Characterization can be shortly described as the conversion of LCI results to common units within each impact category, so that results can be aggregated into category indicator results.

The following elements are optional:

- *Normalization*: the magnitude of indicator results is calculated relatively to reference information.
- *Weighting*: indicator results coming from the different impact categories are converted to a common unit by using factors based on value choices.
- *Grouping*: impact categories are assigned to one or more sets (on a nominal or a hierarchical basis).
- *Sensitivity analysis*: in order to be able to evaluate the influence of the most important assumptions, it is strongly recommended to perform a sensitivity analysis during and at the end of the LCA.

Several LCIA methods can be used. A typical choice for this study is Eco-indicator 99, a quite standard and widespread methodology. In this LCIA method, three types of models are basically used [14]:

- Modelling of the Technosphere in the inventory phase (modelling of all processes in the life cycle). The inventory result divides the impact of the processes in impact on resources, land use and emissions).
- Modelling of the Ecosphere in the impact assessment phase ((modelling of the effects and damages of these events to obtain three categories of effects and damages: resources (R), ecosystem quality (EQ) and human health (HH)).
- Modelling of the Value sphere in the weighting and ranking phase. As different types of (environmental) impacts need to be combined to obtain a comparable overall score (or indicator), value choices (weightings) have to be made.

### **2.2.2 Impact categories**

All the inventory results are linked with one or more of the impact categories: i.e. emissions, land use or resources.

As in all other impact assessment methods, in Eco-indicator 99 it is not possible to take all the impacts (for every impact category) into account. This is due to the huge number of small impacts caused by virtually every human activity. It is important to know which components are included in the different impact categories and which are not. This is required to evaluate the eventual influence on the results when including and/or excluding them. For example, the category 'Resources' is determined by 13 different components.

### **2.2.3 Damage categories**

The results of the impact categories are used to quantify the damages in each of the three damage categories: HH, EQ and R. This is done by fate analysis, exposure analysis, effect analysis, damage analysis, etc.

- HH: this category includes the number and duration of diseases, as well as the life years lost due to premature death caused by environmental pollution. Following effects are included: climate change, ozone layer depletion, carcinogenic effects, respiratory effects and ionizing (nuclear) radiation.
- EQ: this category includes the effect on species diversity, especially vascular plants and lower organisms. Following effects are included: ecotoxicity, acidification, eutrophication and land use.
- R: this category includes the surplus energy needed in the future to extract lower quantities of mineral and fossil resources. The depletion of agricultural and bulk resources, such as sand and gravel, is considered under land use.

### **2.2.4 Weighting**

In the Eco-indicator 99 method, the weighting step is performed by a panel, which has been selected according to a series of strict criteria. In debates about the significance of environmental effects opinions are usually very diverse. This may be due to varying knowledge, but fundamental differences in attitude and perspective play an important

**Table 14.1** The three archetypes of the Eco-indicator 99

	<b>Time perspective</b>	<b>Manageability</b>	<b>Required level of evidence</b>
Hierarchist (H)	Balance between short and long term	Proper policy can avoid many problems	Inclusion based on consensus
Individualist (I)	Short time	Technology can avoid many problems	Only proven effects
Egalitarian (E)	Very long term	Problems can lead to catastrophes	All possible effects

role too. To take these differences into account, three archetypes/perspectives were defined: hierarchist, individualist and egalitarian. The main characteristics of these perspectives are summarized in Table 14.1.

In general, value choices made in the hierarchist perspective are politically and scientifically accepted. As a consequence, the LCA for this application will be performed using Eco-indicator 99 from a hierarchist perspective.

### 2.2.5 Eco-indicator points

The data of the different stages of the life cycle are linked, processed and weighted in the impact assessment and Eco-indicator points are obtained. The standard Eco-indicator values, the *Eco-indicator points* (Pt), can be regarded as dimensionless figures. As the size of the milli-point (mPt) is more convenient, Eco-indicator lists usually use this unit.

The scale has been chosen in such a way that the value of 1 Pt is representative for one thousandth of the yearly environmental load of one average European inhabitant. However, the absolute value of an Eco-indicator point is not very relevant as the main purpose is to compare relative differences between products or components.



## 3. MODEL

Before assessing the environmental impact, the analyst has to possess a clear view of the object under study. Therefore an analysis of the composition of the product, its production, use, recycling and disposal processes must be undertaken. The battery technologies assessed in the present LCA are lead-acid (Pb-acid), nickel-cadmium (NiCd), nickel-metal hydride (NiMH), sodium-nickel chloride (NaNiCl) and lithium-ion (Li-ion).

The data were obtained through enquiries among battery manufacturers and by examination of the literature available [15–21].

To obtain an objective result, the system boundaries of the LCA must be defined. The area considered is the western world, while for the time period the current state of the technology was taken into account. The related other life cycles (trucks, industrial

buildings, electric power plants, roads, etc.) have not been considered, since they will not influence the results significantly. Other boundary conditions will be described further in this chapter.

### 3.1 Composition

Each substance or compound can be allocated to one of the major components of the battery: electrode, electrolyte, separator, case and other components. Lists of the substances with major importance, as well as their assumed mass (in percentage), are given in Tables 14.2–14.6. These tables are subdivided into components. The Battery Management Systems are not taken into account in the present compositions of the different batteries.

**Table 14.2** Typical composition of the different parts of a Lead-Acid battery

	Substance	Weight percentage
Electrodes	Antimony	0.7
	Arsenic	<0.1
	Copper	<0.1
	Lead	61.0
	Oxygen	2.3
Electrolyte	Sulphuric acid	10.3
	Water	16.9
	Separator	Glass
Separator	Plastic	1.8
	Case	Plastic

**Table 14.3** Typical composition of the different parts of a Nickel-Metal Hydride battery

	Substance	Weight percentage
Electrodes	Nickel	20.6
	Rare earth metals	10.1
	Nickel hydroxide	21.5
	Cobalt	4.8
Electrolyte	Potassium hydroxide	3.3
	Sodium hydroxide	0.9
	Water	11.7
Separator	Plastic	2.6
Case	Plastic	9.0
Other	Copper	1.2
	Steel	8.0
	Other	6.3

**Table 14.4** Typical composition of the different parts of a Nickel-Cadmium battery

	<b>Substance</b>	<b>Weight percentage</b>
Electrodes	Nickel	13.2
	Nickel hydroxide	15.4
	Cadmium hydroxide	20.7
	Cobalt hydroxide	1.4
Electrolyte	Potassium hydroxide	4.9
	Sodium hydroxide	0.3
	Lithium hydroxide	0.6
	Water	16.5
Separator	Plastic	4.5
Case	Steel	14.8
	Plastic	7.6

**Table 14.5** Typical composition of the different parts of a Sodium-Nickel Chloride battery

	<b>Substance</b>	<b>Weight percentage</b>
Electrodes	Nickel	17.6
	Sodium chloride	11.6
	Copper	3.5
	Iron	16.5
Electrolyte	Potassium hydroxide	4.9
	Aluminium oxide	16.5
	Sodium aluminium chloride	14.3
Case	Steel	9.8
Other	Steel	4.1
	Plastic	2.2
	Other	4.0

**Table 14.6** Typical composition of the different parts of a Lithium-ion battery

	<b>Substance</b>	<b>Weight percentage</b>
Electrodes	Carbon	15
	Lithium metal oxide	23.6
	Plastics & rubber	2.4
Electrolyte	Organic carbonates	12.6
	Lithium hexafluorophosphate	3.2
Case	Other	21.2
Other	Aluminium	12.6
	Copper	9.5

### 3.2 Assembly

The raw materials or the components are purchased by the manufacturers and are processed in the factory to form the battery components.

The energy consumption for assembling the different batteries is shown in [Table 14.7](#). The electricity production mix used in this study is the European Mix (EU-25) in the year 2002.

The data regarding the energy needed to assemble the batteries were provided by battery producers and were compared with data found in the literature. The emissions of the energy production are the only emissions taken into account in the assembly stage. No other air and water emissions are assumed in this stage of the life cycle, because these data are not available for all the technologies. This allows comparing the different technologies in an unbiased way.

### 3.3 Use of the battery in the vehicle

To determine the environmental impacts of the different battery technologies during the use phase, some assumptions have been made. Concerning the use phase of the battery electric vehicle, the only environmental impact to be considered comes from the electricity losses of the batteries due to the battery masses and their efficiencies.

### 3.4 Recycling

An equivalent recycling level is considered for each battery technology. As an illustration, this means that if the plastic is recycled for one battery, the case is assumed to be recycled for each battery technology. It is assumed that the recycled materials (prime metals) have the same quality as the original materials. The impact of the produced slags and other by-product is not taken into account, because the influence of these slags on the Eco-indicator points of the battery is negligible. A collection rate of 100% was assumed, which means that all the spent batteries are recycled at the end of life. These data are realistic for the widespread use of the battery considering the weight and volume of the battery electric vehicle (BEV) and heavy electric vehicle (HEV) batteries and considering the answers of various stakeholders to our questionnaires. A recycling rate of

**Table 14.7** Energy for the assembly of batteries

	Assembly (MJ/kg)
Lead-Acid	10.7
Nickel-Metal Hydride	9.8
Nickel-Cadmium	19.6
Sodium-Nickel Chloride	20.9
Lithium-ion	42.8



**Table 14.8** Energy for the recycling of batteries

	Recycling (MJ/kg)
Lead-Acid	2.9–4.1
Nickel-Metal Hydride	4.7
Nickel-Cadmium	3.3–4.7
Sodium-Nickel Chloride	4.7
Lithium-ion	4.7

95% of the retrieved materials (mainly metals) was assumed for the different technologies (except for lead because of the high maturity of lead recycling; recycling rate = 98.3%). It is assumed the electrolyte is neutralized before disposal. The only exception is the sulphuric acid of Pb-acid batteries, of which 90% is recuperated. The energy consumption (European Mix) for the recycling process for the different technologies is presented in Table 14.8.

Two recycling processes have been assessed for the Pb-acid and for the NiCd batteries. In the first scenario, the complete battery is fed into a furnace and the burning of the plastics is used as a kind of heat supply. This implies reduced energy consumption compared to the second scenario, in which (a part of) the plastic is separated before the rest of the battery is sent to the furnace. The plastics are recycled in this scenario. This explains why two values are displayed in the table for these two technologies.

NiMH and NaNiCl batteries can be recycled in a similar way as the NiCd batteries [22]. As a consequence, the same energy consumption is assumed. This is due to the fact that no data are available eventually for recycling plants dedicated solely to one of these technologies.

At present there is not yet a large-scale recycling process available for Li-ion traction batteries; therefore, equivalent energy consumption is assumed for these batteries.

### 3.5 Electricity production

The electricity production mix used in this study (European Mix) is a proportional mix of the different electricity production methods of the 25 EU member states in 2002. The different electricity production methods have varying impacts on the environment. As a consequence, the choice of one specific method or one specific country mix would potentially influence the results of the study, and should thus be avoided. Consequently, the results of this study can be seen as a reflection of the European situation.

### 3.6 Reliability of the Results

To perform a reliable study, the relevant process parameters (emissions, used resources, energy consumption, etc.) have to be imported for all the different substances (e.g. raw materials) and energy sources. These parameters are often not very well known. These

data can be found in commercially available databases or can be estimated if there is no appropriate database available. The reliability of the data can thus vary and influence the results. For base metals and common materials, reliable data are accessible easily, whereas for more exotic substances, such as the organic carbonates used in Li-ion batteries, data are harder to find.



## 4. IMPACT OF THE DIFFERENT BATTERY TECHNOLOGIES

### 4.1 Assembly and recycling of the battery

The environmental impact is expected to be the highest for the electrodes, which can be explained by the important mass of this component and in some cases by the toxic properties of the used materials (metals) compared to the other components (electrolyte, separator and cases).

The global environmental impact of the assembly and recycling for 1 kg of the different battery technologies is illustrated in Fig. 14.2. It shows that the recycling phase allows compensating the environmental impacts of the production phase to a great extent. For battery technologies where a recycling infrastructure is available, at least 70% of the impact of the assembly phase is compensated during the recycling phase. Metals tend to be recycled more massively than many other components, which compensates for an important part of the impact they have during production. For instance, when a large part of the impact is due to energy consumption, this contribution to the impact cannot be recovered during the recycling.

A substantial part of the potential damage to human health and to the ecosystems can be avoided thanks to recycling processes. On the other hand, the damage to non-renewable resources seems to be reduced in a less important way. This can be

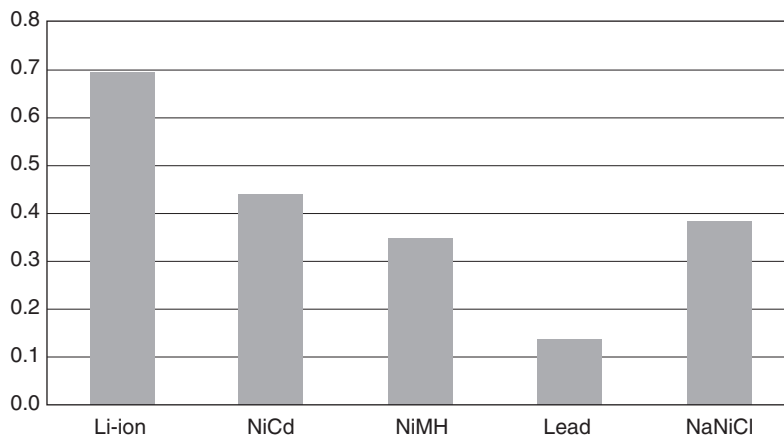


**Figure 14.2** Impact of assembly and recycling.

explained by the fact that fossil energy sources are included in the depletion of resources. Of course, the energy put into the process of producing metals cannot be recovered and additionally the recycling processes consume a certain amount of energy too. Both last *raisons* explain the lower proportions of the compensations of resource depletion thanks to recycling compared to the other damage categories. The depletion of minerals and metals on the other hand is diminished drastically thanks to recycling.



## 5. ELECTRIC VEHICLES TRACTION BATTERIES

In order to assess the environmental impact of the batteries when used as traction batteries for electric vehicles, the actual use of the batteries has to be taken into account and the different batteries compared based on a reference scenario.

### 5.1 Battery technical characteristics

The technical parameters (specific energy, number of cycles, energy efficiency) of the different technologies are shown in Table 14.9. These data have been obtained through contacts with the battery industry and through literature research. The technical performances play an important role in the environmental impact of the batteries as these parameters determine the required quantities of batteries for each technology as well as the frequency in which the batteries are replaced during the vehicle's lifetime.

The environmental impact of the maintenance has been assumed to be negligible. The depth of discharge (DOD) of the battery is assumed to reach 80% for each cycle. The self-discharge of the batteries is neglected for all the technologies.

The NaNiCl battery is the only high-temperature battery amongst the assessed technologies. As a consequence, extra energy (typical power 85 W) is needed to keep the battery at an appropriate temperature. The additional energy consumption needed for heating the battery has been estimated to be 7.2% of the capacity. This assumption is based on a daily use of the vehicle, except on weekends.

**Table 14.9** Technical characteristics of traction batteries

	Specific energy (Wh/kg)	Number of cycles	Energy efficiency (%)	Heating losses (%)
Lead	40	500	82.5	
NiMH	70	1,350	70.0	
NiCd	60	1,350	72.5	
Li-ion	125	1,000	90.0	
NaNiCl	125	1,000	92.5	7.2

## 5.2 Reference vehicle

The model is based on a typical small urban electric vehicle, with a net weight of 888 kg (including the driver, excluding the battery). The energy consumptions during driving are calculated for the Economic Commission for Europe (ECE) cycle [23]. As the battery weight depends on the applied technology, this implies different energy consumptions for each battery technology. These different energy consumptions were simulated and calculated by the Vehicle Simulation Programme [24]. These simulations lead to the following equation, which allows us to determine the specific energy consumption for each battery technology:

$$E_c = m_b \cdot \alpha + \beta \quad [14.1]$$

where  $E_c$  is the electricity consumption in Wh/km and  $m_b$  the battery mass in kg, assuming the energy consumption is related to the weight of the vehicle (including the battery), this allows to define the coefficients  $\alpha$  and  $\beta$  ( $\alpha = 0.054$  Wh/kg·km and  $\beta = 133$  Wh/km). This gives a linear relationship between battery weight and electricity consumption, where also the efficiencies of the various battery types have to be taken into account.

## 5.3 Functional unit

The functional unit (FU) is the core of any LCA, since it provides the reference to which all other data in the assessment are normalized. Basically, an FU is the basis on which different products are to be compared.

The FU has to be chosen in a way that the different batteries can be compared in an objective way: amongst others, the lifetime range of the car has to be identical for all the technologies. Different technical parameters play a key role when defining the FU, e.g. cycle number, range, energy content of the battery, specific energy.

There are different possibilities to define an FU, but not all of them are appropriate. The following FU can be discerned:

- FU constant energy content of battery + constant lifetime range of the vehicle
- FU constant battery mass + constant lifetime range of the vehicle
- FU constant range + constant lifetime range of the vehicle.

### 5.3.1 FU constant battery energy content and constant lifetime range of the vehicle

Pros:

- The same global energy content.

Cons:

- The useful energy output can differ from one technology to another (because of the battery efficiencies)
- Ranges differ from one technology to another (because of the different battery masses and battery efficiencies)

- Energy consumption differs from one technology to another (because of the different masses of the batteries)
- The number of cycles required to cover the total distance differs from one technology to another (because of the varying energy consumptions).

This FU corresponds to an equal energy content of the different batteries. The output energy, however, can be different for each technology, due to the different energy efficiencies of the different batteries.

A 12-kWh energy content and a lifetime distance  $D$  of 160,000 km (more precisely 159,292 km) to be covered by the car have been taken as a reference for the FU. About 160,000 km is the distance covered during the lifetime of the vehicle when using Pb-acid batteries (200 cycles a year, during 15 years, with the batteries replaced when reaching end-of-life).

The number of cycles  $n$  required for the other technologies is a function of the total distance and the range per cycle ( $R$ ):

$$n = \frac{D}{R} \quad [14.2]$$

with the range dependent on battery efficiency, DOD, energy content  $E_b$  and energy consumption  $E_c$ , the latter given by Eq. [14.1], as shown by the following equation:

$$R = \frac{\eta_b \times DOD \times E_b}{E_c} \quad [14.3]$$

The number of batteries ( $N_b$ ) needed to cover the total distance then follows from the total number of cycles ( $N_c$ ) divided by the cycle life ( $t_b$ ) of the battery:

$$N_b = \frac{N_c}{C_b} \quad [14.4]$$

The required number of batteries will always be an integer in real life. However, we have chosen to perform this study using the number of batteries obtained in our calculations. This allows obtaining results that are not dependent on the arbitrary choice of a lifetime car range. Characteristics of the FU assuming constant energy content and constant lifetime range can be found in [Table 14.10](#).

### 5.3.2 FU constant battery mass and constant lifetime range of the vehicle

Pros:

- The energy consumption of the vehicles is the same for the different battery technologies
- The most appropriate battery mass can be selected as a function of the size and the energy consumption of the vehicle.

**Table 14.10** FU constant energy

	$m_b$ (kg)	$E_s$ (Wh/kg)	$c_b$	$E_b$ (kWh)	$R$ (km)	$N_c$	$N_b$	$D$ (km)
Lead	300	40	500	12	53	3,000	6.00	159,292
NiMH	171	70	1,350	12	47	3,371	2.50	159,292
NiCd	200	60	1,350	12	48	3,290	2.44	159,292
Li-ion	96	125	1,000	12	63	2,547	2.55	159,292
NaNiCl	96	125	1,000	12	60	2,670	2.67	159,292

Cons:

- Ranges differ from one technology to another
- The energy contents of the batteries differ from one technology to another
- The number of cycles required to cover the total distance differ from one technology to another.

For this, the weight of the reference battery is set to 300 kg and the lifetime distance to 159,292 km. The choice of the lifetime distance, as well as the calculations related to the different parameters, is similar to the ones explained in the previous section. Characteristics are given in [Table 14.11](#).

### 5.3.3 FU constant range and constant lifetime distance covered by the vehicle

Pros:

- The vehicle is able to cover the same distance independently of the technology. As a consequence, the same number of cycles is needed to cover the lifetime distance of the vehicle.
- The payload delivered by every battery technology is exactly the same (the driver gets exactly the same ‘service’ out of each battery technology).

Cons:

- The masses and energy contents differ from one battery technology to another
- The assumptions are conceptually more complicated compared to the other FU.

When using the third FU, the battery enables the vehicle to cover a determined range with a single charge. This range was chosen to be 60 km.

**Table 14.11** FU constant mass

	$m_b$ (kg)	$E_s$ (Wh/kg)	$c_b$	$E_b$ (kWh)	$R$ (km)	$N_c$	$N_b$	$D$ (km)
Lead	300	40	500	12.0	53	3,000	6.00	159,292
NiMH	300	70	1,350	21.0	79	2,020	1.50	159,292
NiCd	300	60	1,350	18.0	70	2,276	1.69	159,292
Li-ion	300	125	1,000	37.5	181	880	0.88	159,292
NaNiCl	300	125	1,000	37.5	173	923	0.92	159,292

**Table 14.12** FU constant range

	$m_b$ (kg)	$E_s$ (Wh/kg)	$c_b$	$E_b$ (kWh)	$R$ (km)	$N_c$	$N_b$	$D$ (km)
Lead	344	40	500	13.8	60	3,000	6.0	180,000
NiMH	222	70	1,350	15.5	60	3,000	2.2	180,000
NiCd	253	60	1,350	15.2	60	3,000	2.2	180,000
Li-ion	92	125	1,000	11.5	60	3,000	3.0	180,000
NaNiCl	97	125	1,000	12.1	60	3,000	3.0	180,000

The mass of the battery follows from the following relationship:

$$R = \frac{E_d}{E_c} = \frac{DOD \cdot E_s \cdot m_b \cdot \eta_b}{m_b \cdot \alpha + \beta} \quad [14.5]$$

where  $E_d$  is the energy delivered to the battery and  $E_c$  the energy consumption derived from Eq. [14.1]. The lifetime distance  $D$  was chosen as 180,000 km, corresponding to 3,000 charge–discharge cycles. Depending on the technology, the required number of batteries needed for the FU was determined, as shown in Table 14.12.

### 5.3.4 Overview

Only three FUs seemed to form an appropriate choice to compare the different battery technologies. Each of these FUs (constant energy content, constant mass or constant range, all coupled to a constant lifetime distance) implies some advantages and disadvantages. The importance allocated to these advantages and disadvantages by the investigators will obviously be determinant when having to decide which FU to choose. The total environmental impact calculated using each of these three FUs is shown in Fig. 14.3 for all the technologies.

This figure clearly shows that similar results are obtained for the three different FUs and that the choice amongst these FUs has no significant impact on the result. The FU assuming a constant range seems to be the most appropriate, as it compares the batteries on the basis of the same delivered performances (all the vehicles can deliver exactly the same payload). As a consequence, the discussion concerning the environmental impacts is dedicated to this FU.

## 5.4 Results

### 5.4.1 Impact of the different stages

The impacts of the different stages of the battery life cycle (assembly + recycling, use due to the battery mass and use due to the energy efficiency), calculated with the constant range FU, are shown in Fig. 14.4.

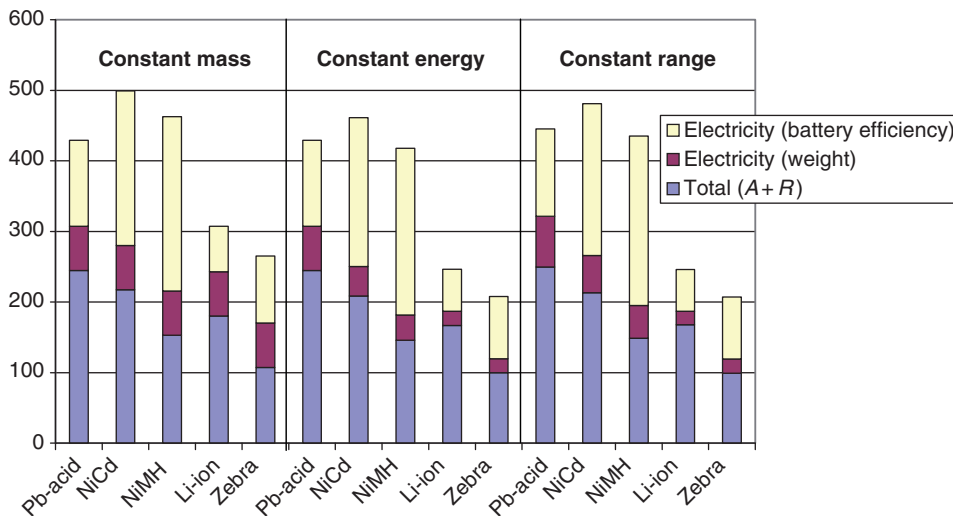


**Figure 14.3** Environmental impact of different FU (rescaled to  $D = 160,000$  km).  $A + R$  = assembly + recycling.

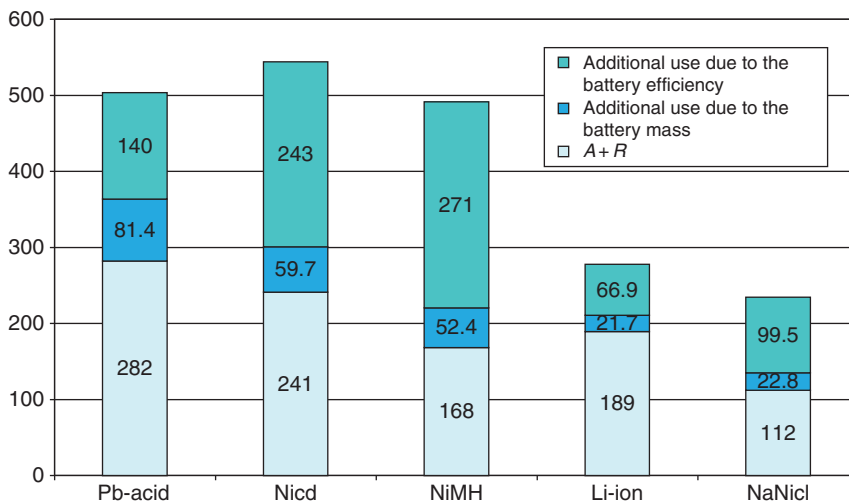


**Figure 14.4** Environmental impact of the assessed technologies, including the losses due to the battery during its use.

When considering the life cycle of the batteries, it appears that the energy losses have a very significant impact on the environment. However, this impact is strongly dependent on the way electricity is produced. As already mentioned, in this study the European electricity production mix has been used, but the impact would be much lower if



renewable energy sources were used more intensively. In the future, the electricity production will most probably imply less emissions and thus a lesser impact on the environment. However, these issues should be assessed by a specific electricity production policy and cannot be handled through battery-specific policies only.

When looking at the environmental impact of the battery (excluding the losses due to battery efficiency and battery mass), it appears that the Pb-acid battery has the highest impact, followed by NiCd, Li-ion, NiMH and NaNiCl. Note however that these results were obtained without complete environmental data concerning the electrolyte of the Li-ion technology, as detailed data were unavailable at the time of calculation. As a consequence, the environmental rating of Li-ion could be considered an optimistic value.

When including the effects of the losses due to the battery (battery efficiency and battery mass), three battery technologies appear to have a somewhat higher environmental impact compared to the other two. The inclusion of the battery efficiencies results in a higher environmental impact for NiCd and NiMH batteries and a lower one for Li-ion batteries compared to the others.

#### **5.4.2 Reliability of the data**

Ideally, to perform an LCA, reliable data are needed for every single component used in the batteries and for all the process parameters involved in the manufacturing of these components.

For four of the five discussed technologies (Pb-acid, NiMH, NiCd and NaNiCl), data concerning over 80% of the mass of the battery are considered to be accurate. Concerning Li-ion batteries, data regarding over 60% of the mass of systems with different compositions are accurate. The proportionally lower accuracy for Li-ion batteries can be explained by the use of very specific chemicals and metal alloys in this technology. For the Li-ion electrolyte however, virtually no environmental data are available.

As these electrolytes are quite complex, it is not unrealistic to consider they have a relatively high score per kilogram compared to the other electrolytes. As a consequence, it can be assumed that the real environmental score of the Li-ion battery will be slightly worse than the score obtained with these calculations.

#### **5.4.3 Boundary conditions**

The system boundaries were defined. The interaction of the FU with nature is assessed considering the following life stages of the battery:

- The extraction of raw materials
- The processing activities of the materials and components
- The use of the battery in the vehicle
- The recycling of discarded batteries
- The final disposal or incineration.

Self-discharge of the battery was not included for any of the assessed technologies because of the great dependence of this parameter on the way of using the vehicle. Maintenance of the batteries was not included either, as this impact is expected to be relatively small. Regarding electricity consumption, the European (EU-25) electricity production mix was considered [25]. It was assumed that the recycled materials have the same quality as the original ones. A collection rate of 100% and a recycling rate of 95% were assumed (see Section 3.4 for more details).

#### **5.4.4 Limitations of the impact assessment method used**

Each impact assessment method implies some advantages and disadvantages. The hierarchist version of Eco-indicator 99 was chosen as it is a quite standard and widespread methodology.

It should be noted that, just as for the other impact assessment methods, not all of the emissions and used resources are included in Eco-indicator. It is also important to know which damage models are included and excluded in the model.

#### **5.4.5 Sensitivity analysis**

As LCA studies are based on numerous assumptions (concerning average battery composition, energy consumption, etc.), important variations may be found in the final results. A sensitivity analysis is used to assess the robustness of the results obtained. To this end, the assumptions made during the development of the model were modified and the consequences on the results were analysed.

##### **Sensitivity analysis for assembly and recycling**

The variations included calculations making use of different relative sizes of the components of the battery (10% more weight of one component, compensated by an equivalent decrease of another component). The proportional masses of electrodes, electrolytes and cases have thus been altered.

For battery assembly and recycling, the sensitivity analysis showed that the assumptions did not have any significant impact on the results, as the conclusions regarding the environmental impact of 1 kg of each battery type remain the same.

##### **Sensitivity analysis for different scenarios**

The recycling rates and efficiencies have been modified as well as the amounts of energy required to produce and recycle the different types of batteries. Moreover, other ranges allowed by one charge have been assumed (50 or 70 km instead of 60 km).

Some data cannot be altered in a sensitivity analysis without implying the assessment of a different FU. As a consequence, number of cycles, specific energy, DOD, energy efficiency and different consumption of the vehicle have not been altered in the current sensitivity analysis.

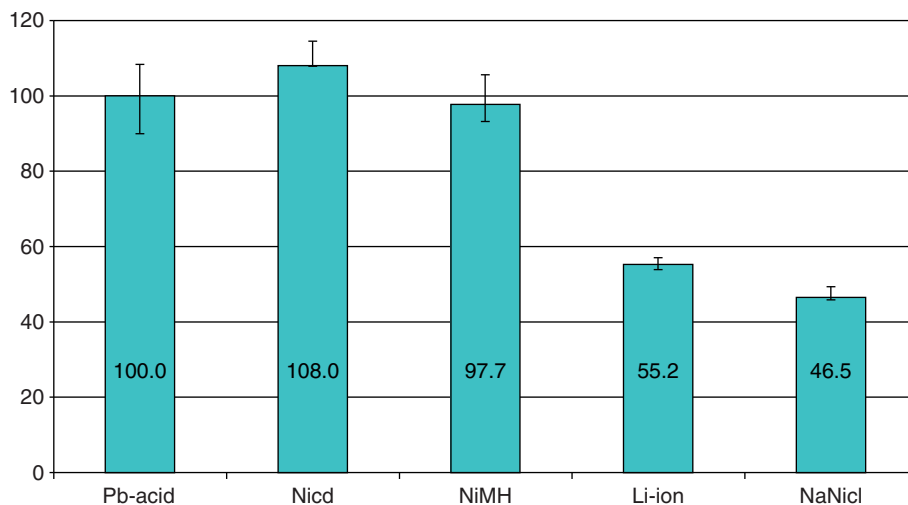


**Figure 14.5** Overview of the relative environmental scores (including the sensitivity analysis).

Fig. 14.5 demonstrates that the assumptions previously mentioned (except for the different one-charge ranges) did not have any significant impact on the results, as the conclusions remain the same (compare Figs. 14.4 and 14.5). This demonstrates that the results of this study are reliable and illustrates the robustness of the model.

The bars in the figure represent the relative environmental impact of every battery type, taking the Pb-acid technology as a reference (score equal to 100). The error bars represent the intervals containing all the results obtained during the sensitivity analysis.

Fig. 14.5 summarizes the battery sensitivity analysis. It should be mentioned that it includes the results originating from production, recycling and energy losses due to the battery mass and efficiency.

#### Sensitivity analysis for different ranges

In the constant range FU, the standard range was set to 60 km. The impacts of other ranges (50 or 70 km) have been investigated and the results are shown in Fig. 14.6.

The results of the changes in the range are discussed separately from the other results of the sensitivity analysis, because they implicitly lead to the creation of new and different FUs.

The absolute environmental impacts are different from the ones obtained using the 60-km range, but the main trends and thus the conclusions stay the same for each range value for the assessed batteries.

#### Sensitivity analysis for electricity production

The environmental impact of the production of 1,000 MJ of electricity using the European Mix is summarized in Table 14.13. It should be mentioned that in these calculations the impact of the capital goods is included. Otherwise the impact of renewable energy sources (wind and water) would be zero.

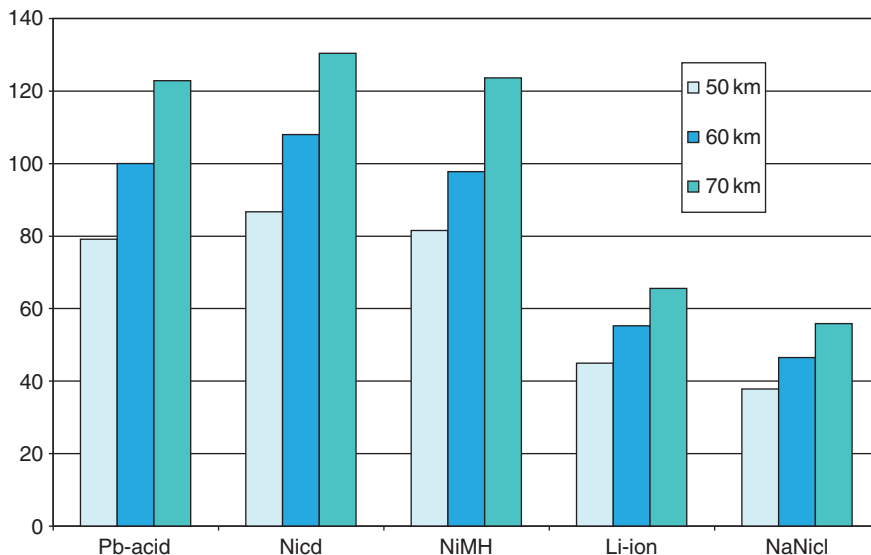


**Figure 14.6** Environmental burden when the range is modified to 50 or 70 km.

**Table 14.13** Environmental impact of the production of electricity (1,000 MJ)

Type of power plant	Eco-indicator points
Wind	0.68
Hydro	0.10
Nuclear	1.59
Coal	7.08
Gas	13.50
Lignite	7.96
Oil	22.40

These figures show that the number of Eco-indicator points induced by the production of 1,000 MJ is the highest when using oil-powered plants. The Eco-indicator points allocated to the electricity production using lignite- or coal-powered plants are almost three times less than when using an oil-powered plant and almost two times less when using the gas-powered plants compared to the oil-powered plant. This is also due to the fact that the reserves of the different fossil fuels are taken into account. The more important the world reserves, the lower impact (the number of Eco-indicator points) when consuming the fossil fuel. The impact of nuclear power plants (in Eco-indicator points) is five times less than the average of the European Mix. It is important to mention that the nuclear waste is not taken into account in the Eco-indicator methodology. The impact of the renewable sources is not zero, as the capital goods are included.

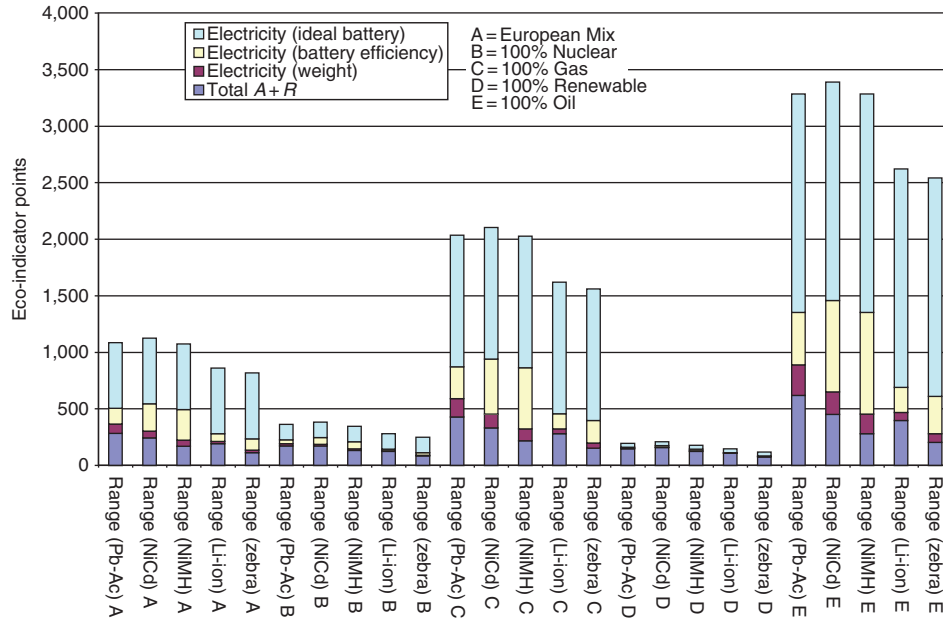


**Figure 14.7** Impact of the electricity production method on the global results (see color plate 3).

Fig. 14.7 clearly shows the important influence of the electricity production method on the global results. The ranking of the different technologies remains unchanged, but the overall, specific impact of the different batteries varies strongly depending on the electricity production method.

These results show that sometimes it is more important to improve the environmental impact of the energy production method as it can probably be improved more significantly than the environmental impact of the battery itself.

Fig. 14.8 confirms this statement. The three right-hand bars represent the environmental impacts of electric vehicles using different electricity production methods. The EVs using electricity produced by renewable technologies presents a much lower environmental impact than the EVs using electricity obtained from the combined cycle gas turbines (CGT) or the Belgian electricity production mix.

Fig. 14.8 also shows that EVs are much more environmental friendly than all the other vehicles, as assessed in the Ecoscore study [26]. In the Ecoscore methodology, a high score corresponds to a low environmental impact.

#### Conclusion of the sensitivity analysis

The sensitivity analysis demonstrated that the non-technical assumptions (the ones not intrinsically defining the FU) did not have any significant impact on the results and the conclusions remain the same.

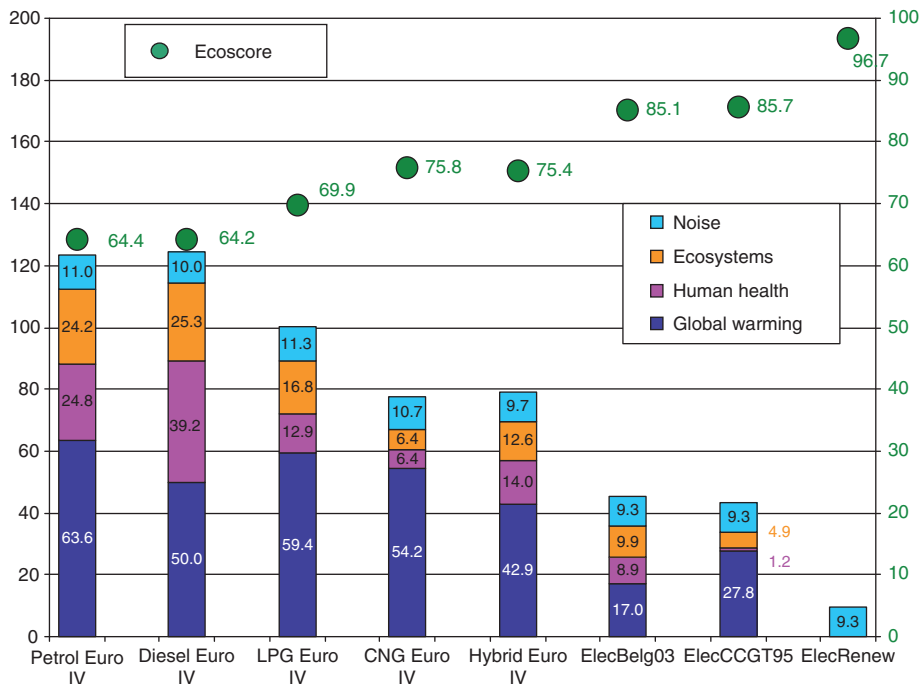


Figure 14.8 Rankings of several vehicle types [26] (see color plate 4).

## 5.5 Discussion of the results

### 5.5.1 Importance of recycling

A key conclusion is that the impacts of the assembly and production phases can be compensated to a large extent when the collection and recycling of the batteries is efficient and performed on a large scale.

### 5.5.2 Impact per kilogram for the different battery technologies

When analysing the environmental impacts of the different technologies per kilogram, one could get the (wrong) impression that the technology having the lowest impact per kilogram is the most environment friendly. However, several technical aspects play a significant role in the overall environmental impact of the batteries. As an example, a battery with a high specific energy (or a high specific power in the case of HEVs) and a high number of cycles will involve a lower amount of batteries to allow identical performance.

### 5.5.3 Impact of the application

The global environmental rating of a specific battery technology will also differ depending on the application. This implies that it is incorrect to state that a certain technology is

more environmental friendly compared to another. As a consequence, conclusions have to be drawn for batteries in each specific application.

#### **5.5.4 Impact of the batteries**

When excluding the additional energy consumption due to the battery efficiencies and the additional masses of the batteries, the following environmental ranking is obtained (decreasing environmental impact): Pb-acid, NiCd, Li-ion, NiMH and NaNiCl.

Looking at the global results, the following environmental ranking is obtained (decreasing environmental impact): NiCd, Pb-acid, NiMH, Li-ion and NaNiCl. Globally three battery technologies, Pb-acid, NiCd and NiMH, appear to have very comparable impacts on the environment. It can thus be stated that, taking sensitivity analysis into account, these technologies have a higher environmental impact than the Li-ion and the NaNiCl technologies.

When the calculations are performed with batteries that have higher or lower energy storage capacities (batteries allowing to cover a more extended or a more limited range with a single charge), the main conclusions remain valid. In other words, three of the assessed technologies (Pb-acid, NiCd and NiMH) have a comparable environmental burden, and this burden is higher than the ones of the other two technologies (Li-ion and NaNiCl). However these results have to be considered with care because environmental data concerning some aspects of the Li-ion and NaNiCl batteries (e.g. the electrolyte) are quite rare.

When analysing the results of this study, it should be kept in mind that the environmental impacts of the batteries of electric vehicles are small (whatever the battery technology used) compared to the environmental burden caused by vehicles equipped with ICEs. Therefore, the results of this study should be seen as an indication of how to further enhance the environmental friendliness of electric vehicles.

#### **5.5.5 General conclusion of the quantitative analysis**

It is important to define the boundary conditions, the technical characteristics and the field of application of the different technologies when describing and discussing the impact of battery technologies on the environment. Indeed, the results of the LCA are strongly influenced by the performance characteristics of the battery.

A FU was chosen as a reference to compare the different technologies in an objective way. Similar analyses performed for hybrid electric vehicle batteries (high-power batteries with a relatively lower energy density) are likely to result in quite different trends.

The three possible FUs for battery electric vehicle resulted in similar conclusions. Pb-acid, NiCd and NiMH batteries have a comparable and larger environmental impact than Li-ion and NaNiCl batteries.



## 6. QUALITATIVE ANALYSIS

### 6.1 Overview

The most common battery technologies are discussed in the first part of this chapter in a quantitative way. In this section, some other interesting but less-widespread battery technologies are considered and described in a qualitative way. These technologies include

- Nickel-zinc
- Li-ion polymer and lithium metal
- Zinc-air
- Vanadium redox, zinc-bromine, polysulfide-bromine
- Nickel-iron.

Not all the data necessary to perform a full quantitative LCA study are available for these technologies. In terms of development, most of them have not yet reached a commercially viable stage and are still under further development. As a consequence, some of the (laboratory) technical data remain to be confirmed in real-world experiments. Some of the data described below are not yet generally accepted and can change in the future.

A rough evaluation of the potential environmental impact for electric vehicle applications of these technologies is as follows:

#### 6.1.1 Nickel-Zinc

This battery consists of a nickel electrode (mainly nickel hydroxide) (20%), a zinc electrode (zinc oxide and calcium oxide) (30%), separators (6%), electrolyte (24%) and casting/connectors (~20%) [21].

No detailed recycling plan has yet been formulated, but the battery does not contain any particularly hazardous materials. The untreated batteries would probably be considered as hazardous waste due to the corrosive (alkaline) electrolyte, but this could be recovered to eliminate that problem.

The NiZn battery contains valuable raw materials, such as nickel, and is highly recyclable. Reclaiming and recycling NiZn batteries is straightforward and makes sense from both an environmental and an economical point of view. NiZn batteries can be recycled using similar methods as for the recycling of NiMH and NiCd batteries.

The relatively high specific energy (70–80 Wh/kg) makes it possible to use a relatively small battery pack to reach a sufficient energy content. On the other hand, the limited number of cycles (300–500 deep cycles) is clearly a disadvantage when wanting to use these batteries for electric vehicle applications and reduces the environmental performance of the battery.

In addition, the relatively low specific power (200 W/kg) results in the fact that NiZn batteries currently do not form an optimal solution for HEV applications, also from an environmental viewpoint.



### 6.1.2 Lithium-ion-polymer and lithium-metal

Li-ion -polymer batteries have positive electrodes consisting of Li-metal oxides, where the metal can be cobalt, nickel or manganese. They have carbon/graphite negatives and a gel polymer electrolyte.

Li-metal batteries have a positive consisting of vanadium oxide and a negative formed by a lithium foil, while their electrolyte is a solid polymer [21].

Li-polymer battery recycling is an area where progress is still needed. It seems that some work is underway to process the Li-polymer batteries in an appropriate way, but no data were available for this study. This technology and the Li-ion technology have many constituents in common, but the use of a solid polymer could complicate the dismantling and recovery as new materials with new properties are introduced.

The technical performances (specific power, specific energy and number of cycles) of Li-polymer and Li-metal are a bit lower than the performances of Li-ion batteries [27].

These cells may be used in electrically propelled vehicles in the future as the polymer technology mitigates the safety issues related to Li-ion. The technical characteristics involve that the environmental impacts of the Li-polymer and Li-metal batteries are expected to be somewhat higher than the environmental impact of the Li-ion ones. This is due to the higher amount of material needed to assemble these batteries.

### 6.1.3 Zinc-air

Zn-air batteries can be mechanically recharged by replacing their zinc anodes (39% of the weight of the battery). They have carbon (air) cathodes (12%) and potassium hydroxide as an electrolyte (28%) [24].

Recharging is done in a plant where spent anodes are taken out of the vehicles and replaced with fresh ones. The spent zinc electrodes are processed electrochemically for regeneration.

The battery materials are non-toxic and should be quite easy to handle although no recycling scheme has been proposed yet. The electrolyte should be neutralized but, apart from the zinc anodes which are recycled during the lifetime of the battery, the materials are steel, carbon, plastic, copper and nickel. All these materials can be processed relatively simply in the current recycling system.

A complete environmental impact assessment of the Zn-air system should take into account the emissions and waste due to battery mechanical recharging (direct environmental impact).

Due to its relatively low specific power (70–100 W/kg), the Zn-air technology is not suitable for hybrid vehicle applications. Nevertheless, thanks to their high energy densities (200 Wh/kg), these batteries are suitable for battery-electric applications. Theoretically, the number of cycles of the Zn-air battery is very high, as the Zn electrode can be cycled to nearly 100% of its capacity and the positive electrode uses oxygen from air. A major disadvantage, however, is the need for mechanical recharging.

Zn-air batteries can be a good choice for fleet applications, because in this case it is possible to use a centralized plant for zinc anodes regeneration. From an environmental point of view, there are no crucial concerns, as the components of the Zn-air battery do not present any major toxicity. However, the specificity of this technology (mechanical recharging) implies a difficult comparison of this kind of batteries with the others.

#### **6.1.4 Vanadium redox, zinc-bromine, polysulfide-bromine**

A synonym for these batteries is flow batteries, as they have a circulating system for the electrolyte. In the vanadium redox and polysulfide-bromine systems, the reactants and products of the electrode reactions remain in solution.

Prototypes of the zinc-bromine battery have a specific energy of 80 Wh/kg and a specific power of 100 W/kg. Reliable data on its lifetime are not available due to the fact that this system has only been tested on a prototype scale in vehicle applications; furthermore, research activities for motive power applications have been abandoned. Because of the low specific power this battery seems inadequate for hybrid applications. The other flow batteries have similar characteristics and, accordingly, similar conclusions can be drawn.

The amount of data concerning these technologies is too low to discuss their potential environmental impact in more detail.

#### **6.1.5 Nickel-iron**

Nickel-iron (NiFe) batteries have performance characteristics similar to NiCd batteries and, therefore, could be a substitute for them. However, their low energy efficiency (50–60%) causes excessive water consumption. This disadvantage makes these batteries less attractive for commercial electric vehicle use. Their electrodes can easily be recycled and the recycled materials can be used in the steel industry.

## **6.2 Discussion of the qualitative analysis**

Just like for the technologies discussed quantitatively, it is important to define the application where the battery is going to be used and to choose an appropriate reference basis before comparing the different technologies. The comparison based on an equal mass is an inappropriate option. As previously discussed in the sections dedicated to the quantitative analyses, the technical parameters (specific energy, specific power, energy efficiency, number of cycles, etc.) strongly influence the required battery mass and number of batteries needed for the FU.

As has been shown in the previous sections of this study, recycling of the spent batteries is important, because it can save resources and lower the total environmental impact of the life cycle of the batteries. This conclusion remains valid for the batteries discussed in this section too.

## REFERENCES

1. L. Gaines, M. Singh, Impacts of EV Battery Production and Recycling, in: Technical Women's Symposium, Argonne National Laboratory, Argonne, USA, April 1996.
2. G. Maggetto, J. Van Mierlo, *Ann. Chim. – Sci. Mat.* 26 (2001) 9.
3. J. Van Mierlo, J. Timmermans, G. Maggetto, P. Van den Bossche, S. Meyer, W. Hecq et al., *Transport. Res. D – Transport Environ.* 9 (2004) 387.
4. P. Van den Bossche, F. Vergels, J. Van Mierlo, J. Matheys, W. Van Autenboer, *J. Power Sources* 162 (2006) 913.
5. ISO 10440, Environmental Management — Life Cycle Assessment — Principles and Framework, ISO, 1997.
6. G. Finnveden, *Int. J. Life Cycle Ass.* 5 (2000) 229.
7. A. Burgess, D. Brennan, *Chem. Eng. Sci.* 56 (2001) 2589.
8. ISO 14040, Environmental Management — Life Cycle Assessment — Principles and Framework, ISO, 1997.
9. ISO 14041, Environmental Management — Life Cycle Assessment – Goal and Scope Definition and Inventory Analysis, ISO, 1998.
10. ISO 14042, Environmental Management – Life Cycle Assessment – Life Cycle Impact Assessment, ISO, 2000.
11. ISO 14043, Environmental Management – Life Cycle Assessment – Life Cycle Interpretation, ISO, 2000.
12. O. Jolliet, M. Margni, R. Charles, S. Humbert, J. Payet, G. Rebitzer et al., *Int. J. Life Cycle Ass.* 8 (2003) 324.
13. L. Dryer, A. Niemann, M. Hauschild, *Int. J. Life Cycle Ass.* 8 (2003) 191.
14. VROM, The Eco-indicator 99: A Damage Oriented Method for Life Cycle Impact Assessment. Methodology Report, Vol. 36A of Publicatiereeks productenbeleid, Ministerie van Volkshuisvesting, Ruimtelijke Ordening en Milieubeheer, 1999.
15. M. Garcia, F. Schlüter, Life-cycle Assessment for Batteries of Electric Vehicles, Master's thesis, Chalmers University of Technology (1996).
16. A. Kertes, Life Cycle Assessment of Three Available Battery Technologies for Electric Vehicles in a Swedish Perspective, Master's thesis, Royal Institute of Technology, Stockholm (1996).
17. M. Rantik, Life Cycle Assessment of Five Batteries for Electric Vehicles Under Different Charging Regimes, KFB-Meddelande 28.
18. European Commission, Integrated Pollution Prevention and Control (IPPC). Reference Document on Best Available Techniques in the Non-Ferrous Metals Industries, Tech. Rep., EC, 2001.
19. G. Tsoufas, C. Pappis, S. Minner, *Resour. Cons. Recycl.* 36 (2002) 135.
20. S. Daniel, C. Pappis, T. Voutsinas, *Resour. Cons. Recycl.* 37 (2003) 251.
21. Investire, Investigations on Storage Technologies for Intermittent Renewable Energies, Tech. Rep., European Project, 2003.
22. R.G. Jungst, Recycling of Electric Vehicle Batteries, in: G. Pistoia, J.-P. Wiaux and S. Wolsky, Eds., *Used Battery Collection and Recycling*, Elsevier Science B.V., Amsterdam, 2001.
23. P. Van den Bossche, The Electric Vehicle: Raising the Standards, Ph.D. thesis, Vrije Universiteit Brussel, 2003.
24. J. Van Mierlo, G. Maggetto, *IEEE Trans. Veh. Technol.* 53 (2004) 401.
25. Eurostat, Energy Statistics, [http://epp.eurostat.ec.europa.eu/portal/page/portal/statistics/search\\_database](http://epp.eurostat.ec.europa.eu/portal/page/portal/statistics/search_database), 2005 (accessed 07.05)
26. J. Van Mierlo, J. Timmermans, G. Maggetto, P. Van den Bossche, S. Meyer, W. Hecq et al., Final Report: Bepalen Van Een Ecoscore Voor Voertuigen En Toepassing Van Deze Ecoscore Ter Bevordering Van Het Gebruik Van Milieuvriendelijke Voertuigen, Tech. Rep., Vrije Universiteit Brussel, 2005.
27. S. Dhameja, *Electric Vehicle Battery Systems*, Newnes, Boston, 2002, p. 230.



# A Roadmap to Understand Battery Performance in Electric and Hybrid Vehicle Operation

**Bor Yann Liaw<sup>1</sup> and Matthieu Dubarry**

Hawai'i Natural Energy Institute, SOEST, University of Hawai'i at Manoa Honolulu, HI 96822, USA

## Contents

1. Introduction	375
2. Field Test Data Collection and Analysis	378
2.1 Vehicle usage pattern analysis	378
2.2 Representative usage schedule	380
3. Laboratory Battery Tests	382
3.1 Assessing battery performance	384
3.2 Understanding battery degradation mechanisms	385
3.2.1 SOC determination by relaxed cell voltage	387
3.2.2 Incremental capacity analysis	389
3.2.3 Measuring polarization resistance	389
3.2.4 Mapping the degradation	391
3.3 Characterize cell-to-cell variations	393
4. Single Cell and Battery Pack Modeling	394
4.1 Single-cell modeling	395
4.2 Accommodating cell-to-cell variations	397
4.3 Battery pack modeling	398
5. Vehicle Drivetrain Platform Modeling	399
6. Concluding Remarks	400
Acknowledgement	401
References	401



## 1. INTRODUCTION

To date, the automobile industry continues to face difficulties and challenges to understand and manage performance of a battery pack in electric or hybrid vehicle (EHV) operation. To characterize battery performance in vehicle drivetrains, two general practices are performed in the industry. One is to conduct road test to study battery behavior on a vehicle platform. [1–4]. The other is laboratory testing, either with a

<sup>1</sup> Corresponding author: bliaw@hawaii.edu

drivetrain on a dynamometer [5–22] or with a test on the battery alone using special protocols and procedures [23, 24].

The first approach using road test gives close-to-real-life situations to evaluate battery performance and degradation. A major hurdle making this approach less favorable is that it is difficult to justify the value that can be derived from the costly operation. Adequate analysis to derive meaningful information from the field testing has been missing due to sporadic nature of driving cycles and wide distribution of driving conditions, making in-depth understanding unlikely possible. At best, the analyses on field test data only result in statistical summaries [1–4], which offer little help to understand battery behavior due to the lack of explanations of how causes (driving conditions) and consequences (degradation) influence and shape battery behavior. The difficulty in understanding field test results continues to hamper accurate prediction of battery performance in real-life use.

In the second approach, dynamometers or test stands and a set of specific protocols, such as accelerated cycle life tests, are usually used. Dynamometer (or, alternatively, close-track) tests [5–22] are the closest thing to real life, but the approach is limited in scope because of cost, space and time constraints. This limitation raises the issue of how to evaluate battery with the best protocol. One of the difficulties is how to select a driving schedule which is representative of real usage of vehicles. The current approach is limited to a few driving schedules that are commonly used by the industry to perform repeatable tests. The experiences derived from such exercises are useful to some aspects but not truly applicable to all driving conditions. Most tests are designed to evaluate performance characteristics of a battery in average, not particularly focusing on degradation and aging studies with path dependence in mind. Therefore, the validity of accelerated cycle life tests remains a concern and if such tests can reveal real-life situations remains debatable. The same problem remains with battery testing that uses test stands. In these experiments the test stands perform stand-alone tests on batteries to reveal performance characteristics, including life cycle tests to the end-of-life (EOL), using published procedures such as those recommended by the U.S. Department of Energy (U.S. DOE)/U.S. Advanced Battery Consortium (USABC) [23, 24]. These procedures assess the cell or battery pack performance under various load conditions that are considered a close approximation to typical EHV operations. Although those tests are effective in providing a snapshot of typical battery performance, limited sampling by a handful of aging protocols cannot provide an accurate account for battery performance in a vehicle.

To date, limited understanding of battery performance in real life is one of the major obstacles in introducing EHV into marketplace. Very few field studies have been reported to permit more realistic evaluation of battery systems. Fewer studies were reported on combined fleet studies and laboratory tests to yield more comprehensive account of battery performance in real life.

To overcome these obstacles and provide practical solutions, we identified at least three major challenges that, in our opinion, prevent proper understanding of battery performance in real-life usage. The first one is the difficulty in developing suitable protocol and analysis technique to allow collection and interpretation of field test data to extract battery performance in relation to its usage. The second one is the lack of adequate test protocols and analytic techniques to understand the data collected in laboratory for life prediction. The last one is the lack of a high-fidelity battery modeling and simulation tool capable of translating the understanding and experience obtained in the laboratory to real-life situation; therefore, battery performance and life can be predicted for more complex settings in real-life usage.

In this chapter, we intend to describe a roadmap that is rationalized to address these obstacles and provide a pathway to allow better understanding of battery performance in practical EHV applications. The approach comprises the following:

1. Formulating a systematic approach to analyze the driving and duty cycle data recorded from field testing and classify them according to operating condition and usage.
2. Analyzing performance characteristics of batteries from laboratory test results and deriving a proper correlation between duty cycles and performance characteristics via the understanding of degradation mechanisms.
3. Developing an accurate predictive model and simulation tool and methodology to enable prediction of battery performance and life based on both laboratory testing and field operation.

The above approach is summarized in Fig. 15.1. We will use (1) results from field testing of an electric vehicle fleet [28–34], (2) experimental data from laboratory tests of

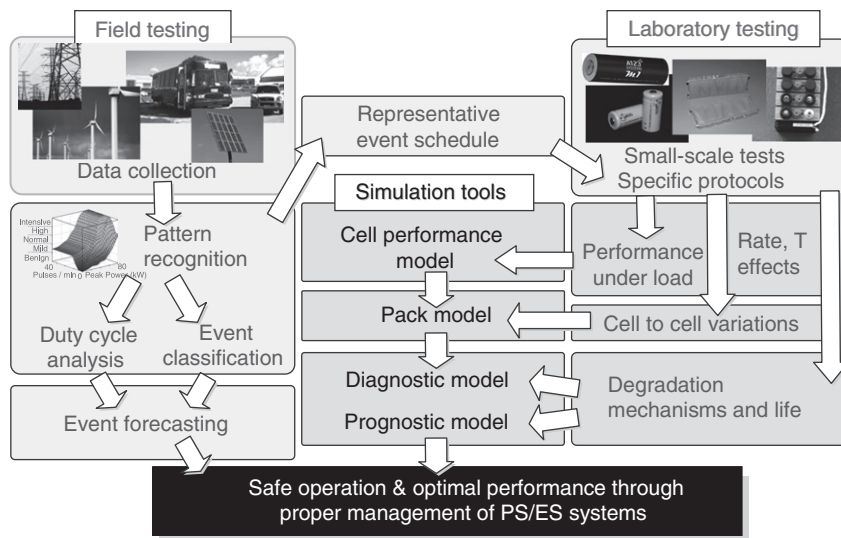


**Figure 15.1** Schematic of a systematic approach in understanding battery performance and developing predictive models and simulation tools for power source (PS) and energy storage (ES) systems.

commercial batteries [36–39], and (3) accurate modeling capability [40–43] derived from the laboratory tests to illustrate the concept of this approach. We will explain how the field data were analyzed, battery performance characteristics yielded from the laboratory tests, and useful correlations derived for the construction of a battery model for performance prediction. More importantly, we will illustrate how to obtain in-depth understanding of battery performance and degradation by a rationalized method to quantify such degradation and to allow prediction of battery service life.



## 2. FIELD TEST DATA COLLECTION AND ANALYSIS

Analysis of trip data collected from EHV operation in real-life usage is difficult and challenging. In fact, no comprehensive approach has been adopted by the industry to date, except for those using standard driving schedules testing on dynamometers or tracks [5–22]. Similar challenges appear when analyzing duty cycle performance of batteries in real-life operations. The best understanding of battery performance should come from its real-life data via comprehensive driving cycle and duty cycle analysis. This direct approach should enhance safety and reliability of a battery system.

Here, we will introduce a methodology that depicts a unique approach to conduct a more comprehensive driving cycle and duty cycle analyses from field test data [28–43]. This approach is based on fuzzy-logic pattern recognition (FL-PR) techniques via the creation of a compositional “driving cycle profile” to represent driving cycle of a trip and a “duty cycle profile” to express battery usage in various driving conditions. The combination of driving and duty cycle analyses enables us to understand EHV and battery performance in a synergistic manner and to assist the formulation of representative usage patterns that depict the average use of vehicle and battery in real-life situations.

### 2.1 Vehicle usage pattern analysis

A unique feature in this approach is the ability to breakdown a driving cycle, a speed time series, into a series of “driving pulses,” which are active driving periods, each between two consecutive stops. Similarly, a duty cycle can be broken down into a time series of “power pulses,” each depicts an active period in which power consumption is above or below the baseline level (which is typically established by the power consumption of auxiliary power units).

Fig. 15.2 illustrates how two conjugated parameters are used in the FL-PR technique to classify driving pulses into driving events. Average speed and distance of a driving pulse are used as a pair of conjugated attributes in pattern recognition of driving events. Membership functions of average speed and distance to depict degree of association in a linguistic expression are used to set up the fuzzy rules to infer the driving event. As a result of the inference, an output fuzzy value representing the driving condition, ranging from “stop-and-go” to “highway” driving, can be assigned to a driving pulse in a driving

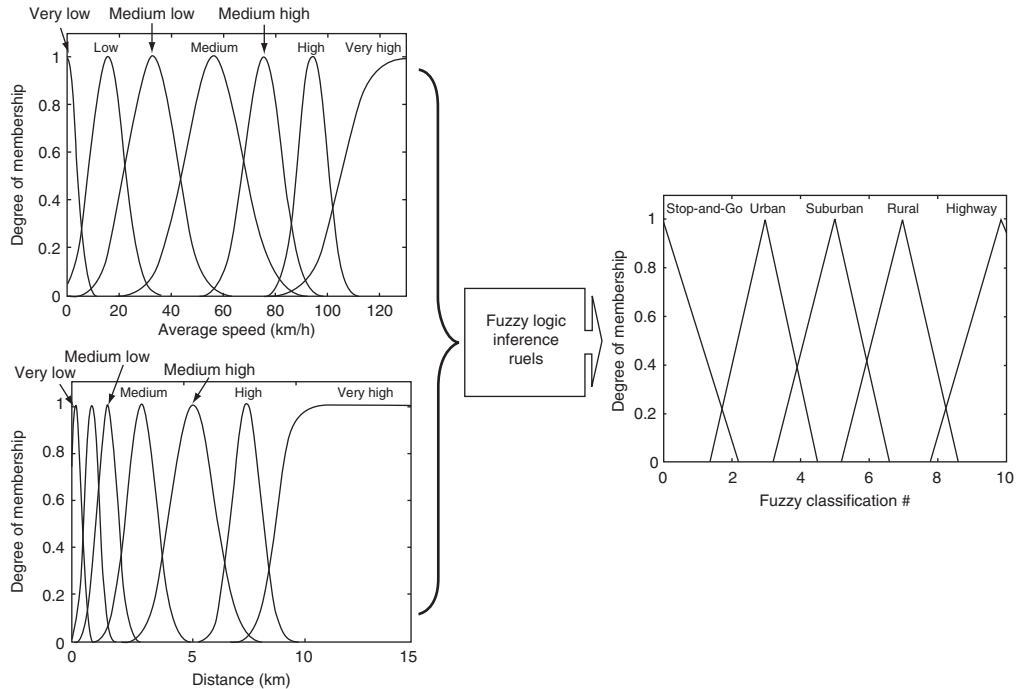


**Figure 15.2** Schematic showing the fuzzy-logic pattern recognition (FL-PR) technique used to classify driving events for a driving cycle.

cycle profile. An analogous approach for classifying the duty pulses can be devised, in which pulse intensity and duration, for instance, are used to determine the extent of stress the battery endures, from benign to intensive.

This classification method provides a convenient way to understand a driving or duty cycle with sufficient details of driving conditions and the associated power consumptions. The merit of this genuine approach is the ability to breakdown trips systematically into a series of events, each assigned with a unique classification.

Combining the knowledge from driving and duty cycle analyses, not only road conditions but also stress levels endured by power source systems can be assessed. Fig. 15.3 shows that such an inference of battery usage can be built upon combining driving and duty cycle analyses into a coherent account of vehicle usage. The correspondence between speed and power in a driving event is not trivial, since driving habit, road condition (including weather), terrain (e.g., grading), and traffic could influence the power consumption at a given speed. Therefore, the additional layer of classification is useful to allow better deciphering of vehicle usage as driving pattern. The term “driving pattern” is supposed to include this inference in describing a vehicle usage event. Such a driving pattern classification will provide a comprehensive assessment of vehicle usage with respect to powertrain (and battery) performance.



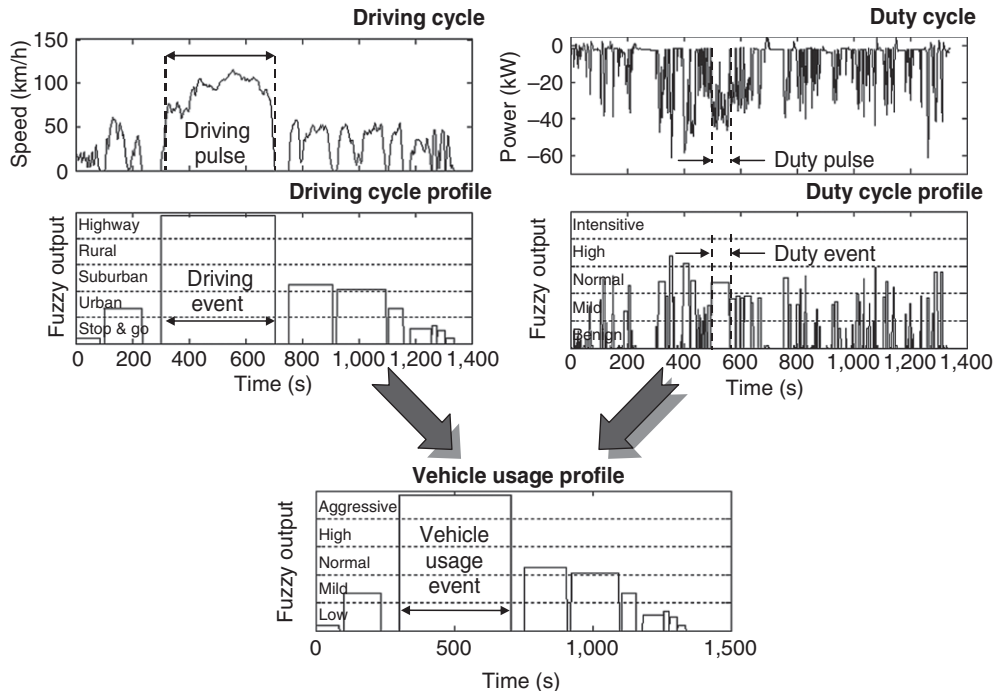


**Figure 15.3** Vehicle usage profile determined by combining driving cycle and duty cycle analyses into a coherent inference method.

## 2.2 Representative usage schedule

With the above approach it is possible to quickly analyze a large set of trip data and, more importantly, to quantify vehicle usage (driving pattern) profiles for trips among vehicles. Fig. 15.4 presents an example of a summary of driving events for two vehicles dispatched to two different locations. One vehicle was used on an air force base (location 1) and the other was operated by the city and county of Honolulu in Hawaii (location 2). The fuzzy classification of the vehicle usage profile can distinctly display the difference in vehicle usage between the two locations. The usage pattern classification shows that the vehicle on the air force base had only been driven on highways occasionally, while the other experienced about 50% of highway driving.

It is possible to derive characteristics of power pulse distribution, the repartition of power pulses at a location, from duty cycle analysis. Fig. 15.5A shows the difference in the characteristics of power pulse distribution (with resolution per kW) summarized from all trips taken at these two locations, revealing the different driving patterns experienced. The vehicle at location 1 shows more frequent use of power events in the 10 kW range in contrast to the other, which exhibits a broader distribution of use in the 10–40 kW range.

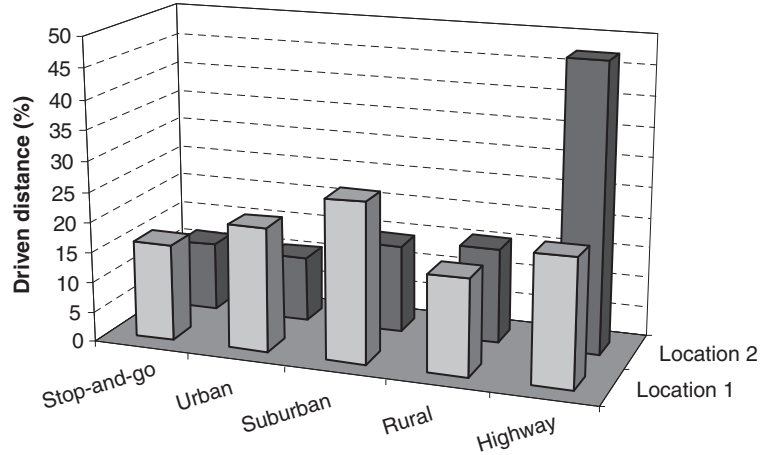


**Figure 15.4** Example of different vehicle usage patterns at two locations.

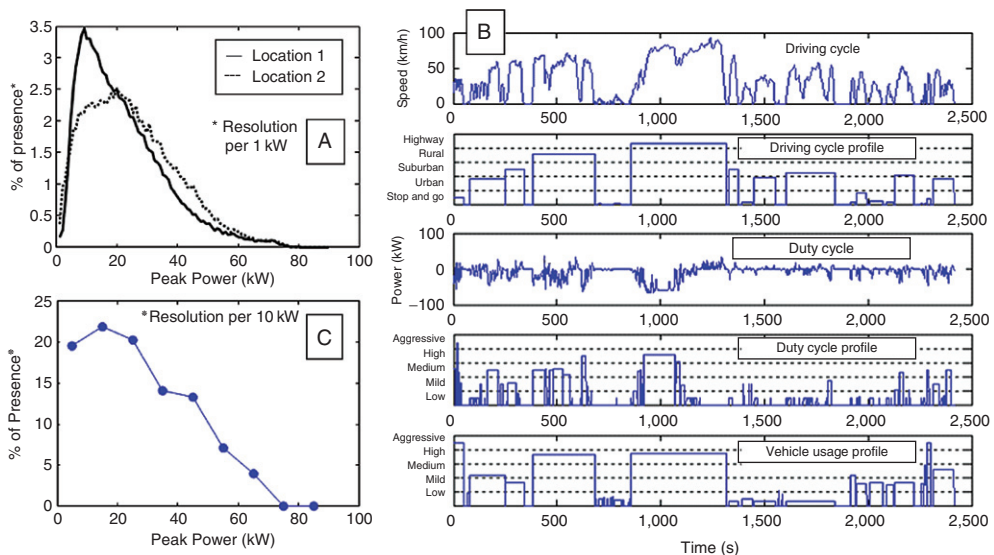


**Figure 15.5** (A) Characteristics of power pulse distribution summarized from the duty cycles collected at two locations, (B) driving pattern analysis of a trip showing how the driving cycle and duty cycle were classified to give driving patterns, and (C) characteristics of power pulse distribution of the trip shown in (B), which resembles the one at location 2 in (A).

Fig. 15.5B further illustrates how the driving cycle and duty cycle are analyzed and classified into driving cycle and duty cycle profiles to reflect a series of driving conditions in a trip and the associated battery power usage and driving pattern. The driving cycle and the classified driving cycle profile show that this trip comprises all five types of

driving events, from stop-and-go to highway. The duty cycle reveals the difference between stop-and-go (around 2,000 s with a series of short and low-intensity pulses) and highway driving (around 1,000 s with a series of long and intense pulses). The duty cycle profile displays the classification of duty pulses into duty events, which are intended to quantify the stress level imposed on the battery system. The profile shows more intensive use of battery power in the beginning of the trip, very mild use in the middle section, and more heavy use again toward the end. The bottom figure displays the vehicle usage profile which summarizes the powertrain usage by the driver in this trip. The vehicle usage revealed the driving patterns, showing the tendency of aggressive driving at first, mellow in the middle section, and medium to high in the end. According to our knowledge of the terrain of the route in this trip, we found that grading plays an important role in the driving patterns. The first part of the trip was uphill, then downhill, and uphill again, as the vehicle moving toward the center of the island. This trip is a good example of a typical driving schedule representing the commute between Mililani and downtown Honolulu, through H-1 and H-2 highway.

Fig. 15.5C presents a characteristic power pulse distribution for the trip analyzed in Fig. 15.5B. Although the number of data points only allowed a rough resolution at 10 kW, the similarity between this curve and the one for location 2 in Fig. 15.5A indicates that the driving and duty schedules shown in Fig. 15.5B could be used as a representative usage schedule for laboratory testing to assess performance and cycle life of a battery system at location 2.



### 3. LABORATORY BATTERY TESTS

Despite the complexity involved in testing vehicles (and drivetrains) either on road or on dynamometer, it is essential to perform laboratory testing on batteries to understand their behavior under load (duty schedule). Due to cost considerations, these tests are often carried out on single cells or small packs with simplified schedules and procedures. The purpose of conducting these tests is to evaluate battery performance to determine if the battery technology can reach a design goal for application. For example, the mid- and long-term goals in the advanced battery criteria have been proposed by the U.S. DOE through the Partnership for a New Generation of Vehicles (PNGV) program with the USABC. To facilitate such testing, the test procedures need to be well-documented, as reported in the USABC *EV Battery Test Procedures Manual* published in 1996 by the U.S. DOE/Argonne National Laboratory, the *PNGV Battery Test Manual* published in 2000 by the U.S. DOE/INEEL, and the *Battery Test Manual For Plug-In Hybrid Electric Vehicles* published in 2008 by the U.S. DOE/Idaho National Laboratory [23, 24].

For most routine testing, the core tests are often recommended, which include constant current (CC) discharge, constant power (CP) discharge, peak power (PP),

and variable power (VP) discharge tests. The CC discharge tests shall provide the information on battery's Peukert behavior, which depicts how capacity varies with discharge rate. The CP discharge tests (mimicking constant speed driving) shall yield cell voltage versus power level relationship at various depths of discharge (DODs). The same set of data can be used to construct the Ragone plot, which depicts battery's specific energy and specific power trade-offs. The peak power tests shall reveal the power capability of a battery for sustaining propulsion at certain DOD, where the value at 80% DOD is typically used in verification against the power goal.

The VP discharge testing is designed to produce the effects of EV driving cycles on the performance and life of a battery. The protocols are based on the industry standard, the federal urban driving schedule (FUDS), which is a complex 1,372 s speed-versus-time profile of an actual driving data, and its derivatives in a simplified format. One cannot use FUDS directly in battery test stand, since it is a driving cycle with a speed-versus-time profile. Modified schedules such as FUDS79, based on 79 W/kg peak power demand for a hypothetical van, are thus recommended by USABC. Similar scaling to different power demand can be used. However, such modified FUDS is still difficult to be executed by most test equipment for battery testing. Therefore, simplified VP schedules such as the dynamic stress test (DST) are often used. This simplified schedule has 360 s sequence of power steps with seven discrete power levels, including three that mimic regenerative braking. The purpose of VP tests is to determine the capacity that can be delivered by a battery with a typical driving schedule, scaled to a power demand goal.

The purpose of these core tests is to understand the average behavior of a battery under different test conditions. Another piece of information that is highly relevant and important from testing is the service life and performance characteristics of a battery in life cycle. This information is usually derived from life-cycle testing, in which either an accelerated aging (such as a DST) or actual use (such as a FUDS) testing regime is applied. Upon completion of a given number of cycles or an extended period of time, a reference performance test (RPT) is launched to assess and quantify battery performance, in terms of power and/or capacity fade, through the evolution of life cycle, to the end-of-life defined by a test plan.

These life-cycle test procedures produce quantitative and well-defined results to determine how long a battery can sustain operation for a specific duty regime. A common drawback from such tests is the inability to extrapolate aging behavior of the battery under a different duty regime that is substantially different from the one used in the tests. The existing aging protocols are not designed to reflect degradation in terms of duty regime variations. To assist better understanding of aging process, in situ techniques that can identify and quantify degradation and its mechanism are desirable.

One additional critical aspect that was not treated openly in literature, or in published procedures, is the cell variations inherent to battery manufacturing process. Such cell variations play an important role in defining battery pack behavior and cell imbalance [39].

In the following section we will elaborate on the results one would expect from the standardized test procedures. We will also describe in situ methods that can be used to monitor battery degradation. Finally, we will discuss the cell-to-cell variations and how they can be characterized with laboratory testing.

### 3.1 Assessing battery performance

The extraction of battery performance information from the RPT through a life-cycle regime to yield battery degradation behavior is the goal of existing test procedures. Fig. 15.6 is an example of results obtained from the USABC test procedures on a commercial  $\text{LiFePO}_4$  cell [38]. Fig. 15.6A shows the evolution of capacity retention upon DST cycling ( $\circ$ ) along with those determined by C/5, C/3, C/2, and C/1 in RPT

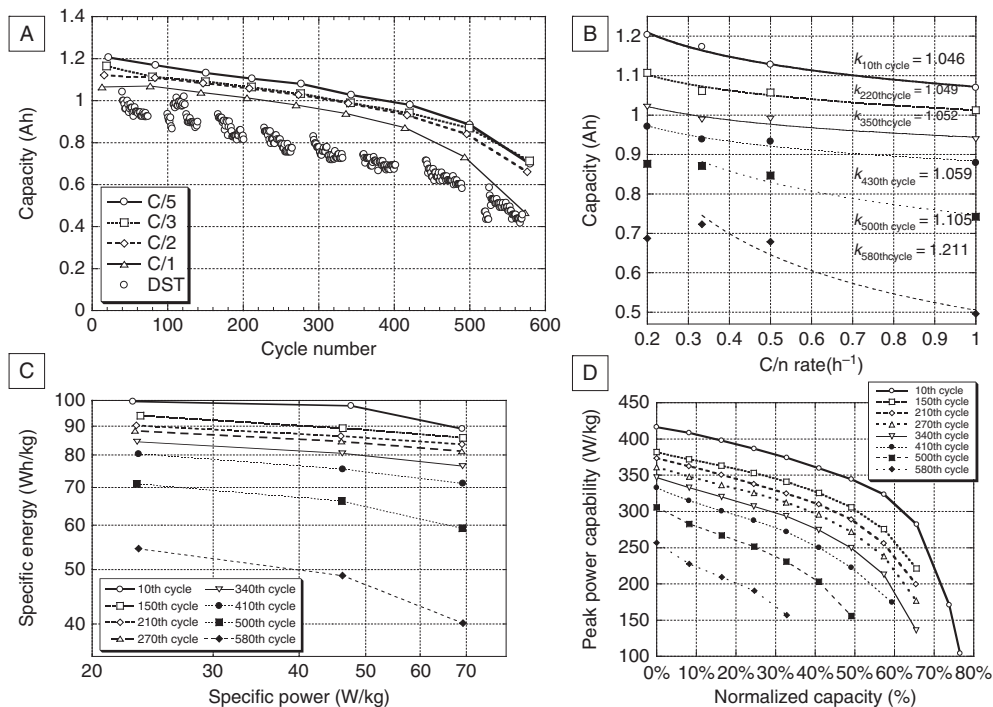


**Figure 15.6** (A) Rate-dependent capacity degradation with cycle number in a commercial  $\text{LiFePO}_4$  cell, (B) an alternate representation of the same rate-dependent capacity degradation with cycle number as shown in (A) with Peukert curves and their respective Peukert coefficient, (C) the Ragone plot of the cell showing the degradation of specific power and specific energy with cycle number, and (D) the peak power capability degradation with cycle number.

through life-cycle test. The USABC procedures specify that the EOL of a battery is reached when it cannot deliver more than 80% of its rated capacity under a specific test regime; thus, the cell reached EOL after 450 cycles. Fig. 15.6B shows the evolution of the associated Peukert curves and coefficients as a function of cycle number. The Peukert coefficients were derived from the Peukert curves as depicted by the Peukert's law,  $C = I^n t$ ; where  $n$  is the Peukert coefficient and  $t$  the nominal discharge time (in hours) for a specific rate  $I$  (in amperes), and  $C$  a dimensionless constant.

The power capability of the cell is presented in two representations (from two different test procedures: CP and VP tests). Fig. 15.6C is the Ragone plot in which the evolution of specific energy (Wh/kg) versus specific power (W/kg) with cycle number is presented. The data used in the Ragone plot are based on the energy attained from CP discharge test regimes, typically at 25, 50, and 75% of the USABC power goal in W/kg. The highest specific power tested was 70 W/kg. The series of Ragone curves follows a downward trend, displaying the specific energy degradation through the life-cycle aging.

The second representation of the power capability is depicted by the peak power capability (PPC) profile of the cell, as described by the ability of the battery to produce 30 s of peak power (roughly at 3.9 C) without lowering the voltage to below 2/3 of the open circuit voltage (OCV) of the battery at the specific DOD. The evolution of PPC as a function of DOD upon cycling is shown in Fig. 15.6D. The PPC decreased slowly in the first 400 cycles. The degradation became severe after that. Only less than 50% of the initial PPC was attainable at 50% DOD after 500 cycles.

### 3.2 Understanding battery degradation mechanisms

The life-cycle test procedures and analyses showed the battery aging and degradation behavior through life cycle, which provide a useful assessment of how long the battery can last under a given duty cycle. Such tests are not sufficient to derive deeper understanding of how battery degrades. For example, many test results have shown a link between capacity (or peak power capability) loss and battery internal resistance increase. Although the evolution of internal resistance in a battery can be estimated from the peak power tests, such information might not provide details on degradation mechanism.

Several issues need to be considered here. First, battery performance degradation may or may not be related to battery internal resistance change. Some degradation mechanisms may not — or at least not in the beginning — be associated with any resistance changes. It is also important to note that the peak power tests refer to DOD, under the assumption that the battery is always recharged to the same SOC. Such an assumption may not be true. In fact, through life-cycle testing, such an assumption is most likely not true. Without a proper reference to SOC, analysis on the degradation may be misleading. Fig. 15.7A illustrates an example where conventional representation of PPC fading as a function of capacity dissipated (i.e., DOD) is presented. Fig. 15.7B presents the same PPC fading data as a function of SOC, where the SOC was determined from

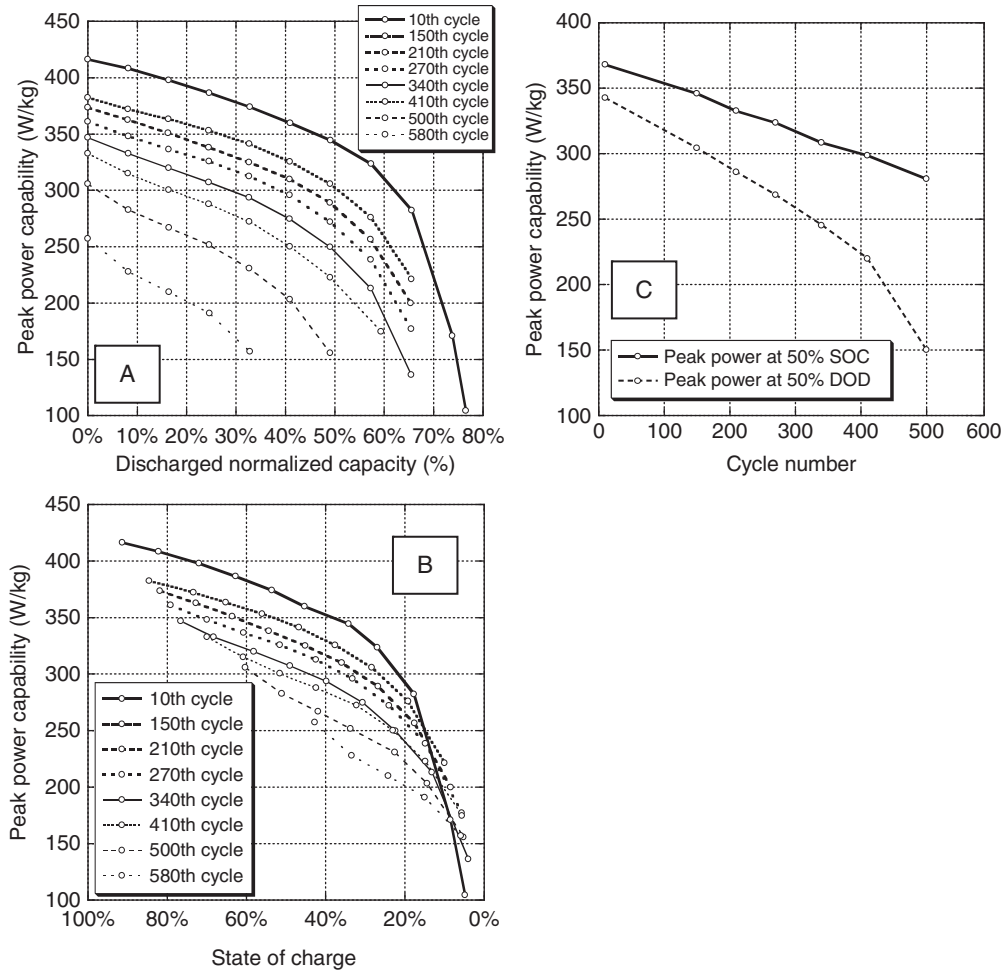


**Figure 15.7** An illustration showing the importance of tracing SOC through aging and degradation in a cell: (A) peak power capability (PPC) versus capacity through cycling, (B) the same PPC as a function of SOC determined by relaxed cell voltages (RCVs), (C) comparison of PPC at 50% DOD and SOC with cycle number.

relaxed cell voltage (RCV), which will be explained below. Fig. 15.7C shows the comparison of the trends of PPC degradation as functions of DOD and SOC, in this case at 50% of each. It is apparent that in DOD the trend line shows an accelerated degradation after 400 cycles, whereas in SOC it remains rather constant. Such difference in the presentations of the degradation behavior could lead to very different understanding on the degradation process. It is therefore important to recognize that the first step in analyzing degradation mechanism is to refer the degradation to a proper thermodynamic state, which is what SOC is for [37]. In contrast to the thermodynamic nature



represented by SOC, DOD is more likely determined by kinetic reasons. The two do not have a universal (or straightforward) relationship. Thus, one should be reminded that the common test procedures can easily determine DOD, but not SOC.

A proper SOC determination relies on thermodynamic conditions. An easy way to reach the thermodynamic equilibrium state is to allow the battery to rest after any test regime and through relaxation to reach equilibrium. The RCV then becomes an indicator of the state of the battery. Tracing the RCV on an OCV versus SOC curve, we can then correctly map the SOC changes. The OCV versus SOC curve can be obtained either by the galvanostatic intermittent titration technique or sometimes by an approximation using a voltage averaging method from charge–discharge curves determined at low rates (e.g., below  $C/25$ ) [37]. Once we properly refer the degradation process to SOC, the evolution of different electrochemical signatures within the cell can be easily inferred. A useful technique to infer electrochemical signatures in a cell is incremental capacity analysis (ICA) using the  $(-dQ/dV)$  curves derived from the charge–discharge curves from testing [35–39, 44–48]. In combination with other pieces of information such as the evolution of internal resistance of the cell, we shall be able to understand the degradation process involved in the cell reactions. Examples have been reported [35–38] in the literature to illustrate how to infer the degradation mechanisms of the cell by such an approach to quantify different contributing factors such as loss of active material, loss of lithium inventory, change of chemistry, as well as resistance or kinetics-induced undercharge and/or underdischarge that affect the cell performance and degradation.

### 3.2.1 SOC determination by relaxed cell voltage

Being aware of the difference between SOC and DOD and the proper method of determining SOC in a cell, in this section we shall discuss an example using a commercial cell for illustration. Understanding the importance of measuring RCV to help the determination of SOC of a cell [35–28], one shall now realize the necessity of imposing a rest period at the end of any test regime in order to facilitate such SOC determination. One should also realize that during a test regime, especially at high rates, the cell voltage reflects only the surface condition of electrodes, while the information on the concentration gradients created inside the electrodes was hidden or skewed. Although with high coulombic efficiency, the amount of charge encountered indeed depicts the extent of reaction in the electrode (the information represented by DOD), without reaching equilibrium we, however, cannot tell the extent of reaction from a state to another (i.e., the information on SOC). Unfortunately, the common practice in managing battery reaction is by voltage and current control; thus, the cutoff conditions are disconnected from SOC. Therefore, a “calibration” is necessary to bring DOD and SOC together on the same scale.

Fig. 15.8 shows an example of how to employ the above approach to a commercial  $\text{LiFePO}_4$  cell. Fig. 15.8A displays four discharge curves, from  $C/25$ ,  $C/5$ ,  $C/3$ , to  $C/1$ . It should be noted that the charge rate prior to each discharge regime is the same as the



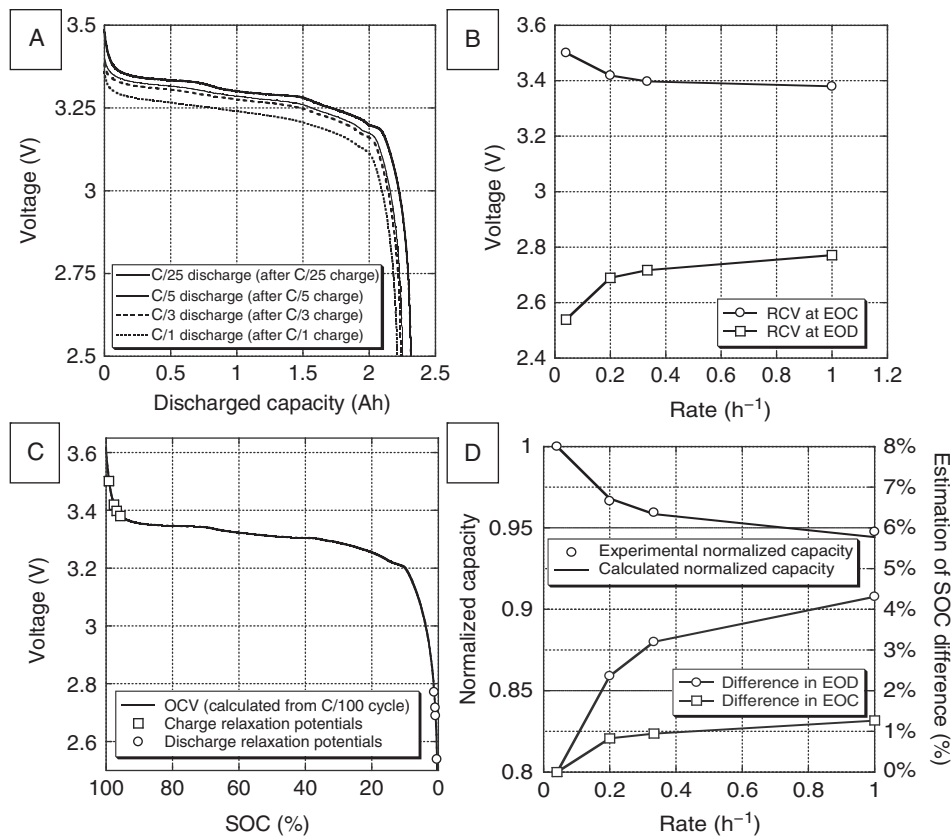


**Figure 15.8** Relevant information for SOC determination in a commercial LiFePO<sub>4</sub> cell. (A) discharge curves at different C rates, (B) relaxed cell voltage at the end of charge and discharge, (C) OCV versus SOC curve estimated from a C/100 cycle regime, and (D) SOC range and the corresponding capacity change at different C rates exhibited by the cell.

discharge rate, which create different end of charge (EOC) conditions. These RCVs are reported in Fig. 15.8B. The squares represent the RCVs in the charge regimes and the circles in the discharge regimes. The OCV versus SOC curve calculated from a C/100 cycle is shown in Fig. 15.8C. By projecting the RCV on the OCV curve, the SOC at the EOC and end of discharge (EOD) in each regime can be determined. The change of SOC range for each regime at a specific rate can also be determined, which should correspond to the respective capacity for that rate. Fig. 15.8D displays the normalized capacity on the left-hand scale and the SOC difference on the right-hand scale versus C rate. The lower curve with squares is the dependence of SOC variations with C rate for the charge regimes at the EOC. The curve above with circles is the dependence of SOC variations with C rate for the discharge regimes at the EOD. The sum of the two curves gives the total SOC variation for each C rate in the charge–discharge cycle. Comparing

the total SOC variation with the capacity determined from the charge–discharge cycle in the experiment, we found the two agree consistently on the normalized capacity scale. Therefore, this is a validation of the SOC range variation as participated in the charge–discharge cycle versus the DOD variations determined in the test at different C rates.

### 3.2.2 Incremental capacity analysis

IC is an increment of capacity associated with a voltage step (i.e.,  $-\Delta Q/\Delta V$ ) [35–38, 44–47]. The IC occurs if a voltage step encounters an electrochemical reaction, leading to a surge of charge being transferred and creating a peak on the IC curve. Each IC peak exhibits a unique shape and intensity, as the electrochemical process progresses with a specific kinetic effect. An ICA can detect a gradual change in cell behavior during a life-cycle test, with greater sensitivity than those based on conventional charge–discharge curves. The sensitivity of ICA is achieved by transforming either a voltage plateau, which is related to a first-order phase transformation, or an inflection point, which is associated with a formation of solid solution, into a clearly identifiable  $-\Delta Q/\Delta V$  peak on the IC curves [35]. By monitoring the evolution of these characteristic  $-\Delta Q/\Delta V$  peaks upon cycling, one can yield key information on the cell behavior (and its change) as reflected by the chemistry.

Fig. 15.9 presents an example of this technique. Fig. 15.9A is a C/25 charge–discharge curve of a commercial  $\text{LiFePO}_4$  cell, while Fig. 15.9B is the associated IC curve with IC peaks labeled for the discharge (as ①, ②, ③, ④, and ⑤) and charge (as ①, ②, ③, ④, and ⑤) regimes. The IC peaks are the convolution of peaks associated with the electrochemical reactions in the active positive and negative electrode materials. We should note that Li intercalation and depletion in  $\text{LiFePO}_4$  involve mainly a single, reversible phase transformation in pseudobinary  $\text{LiFePO}_4\text{--FePO}_4$  system, as a simple crystallographic consideration [47–52] may suggest. This transformation exhibits a single potential plateau near 3.5 V versus  $\text{Li/Li}^+$ . The associated signature for IC should be a sharp single peak, considering its facile kinetics reported in the literature. The presence of Li intercalation in graphite, however, makes this peak convoluted into several peaks corresponding to the Li intercalation and depletion in graphite as staging phenomena [53, 54], as shown in Fig. 15.9C (measured at C/50 versus  $\text{Li/Li}^+$ ). Because of this convolution, all the peaks in Fig. 15.9B correspond to the staging phenomena in the Li–graphite interactions, as shown in Fig. 15.9C. However, we should be mindful that the peaks' position, shape, and intensity are affected by the reaction kinetics. Understanding the convolution of the IC peaks in a cell will help identify the degradation process when the IC peak's position, shape, and intensity change as the cell ages. We shall discuss this aspect later in Section 3.2.4

### 3.2.3 Measuring polarization resistance

Another useful, *in situ* technique that can be used to extract valuable information from RPT test results is the derivation of polarization resistance. Polarization resistance can

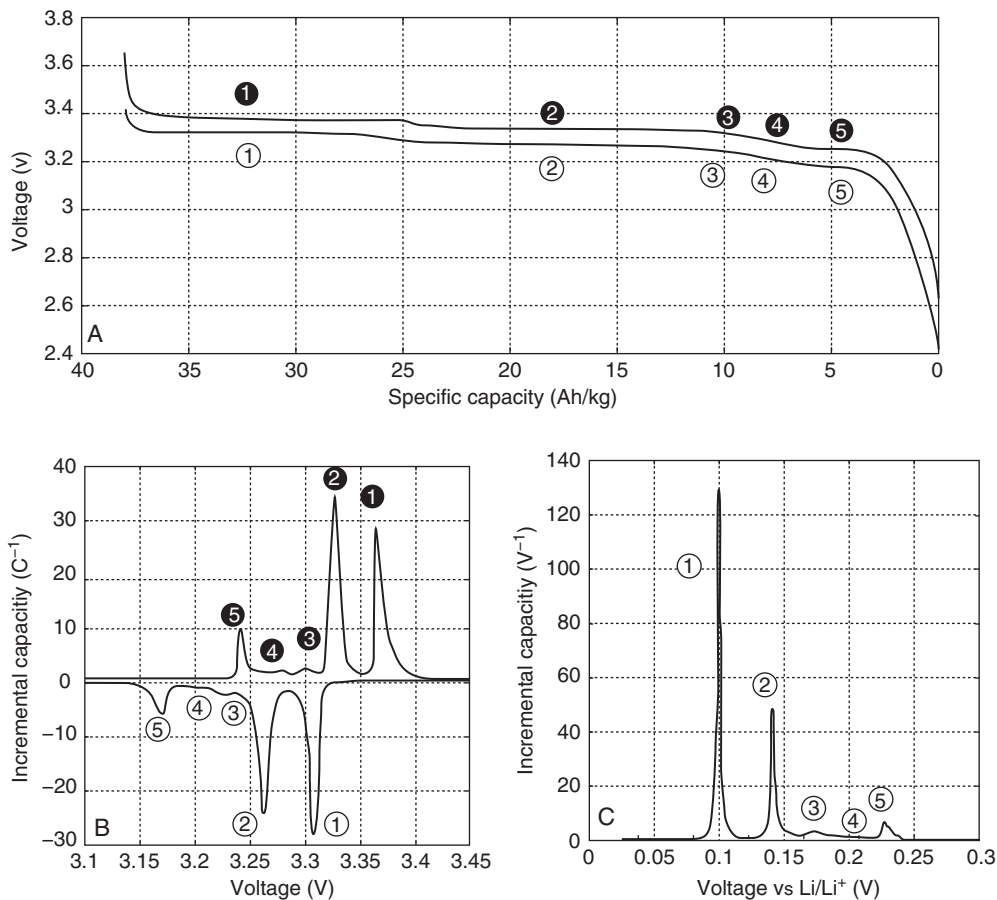


**Figure 15.9** (A) C/25 charge–discharge curve of a commercial LiFePO<sub>4</sub> cell, (B) the corresponding incremental capacity curve, and (C) incremental capacity curve of a graphite electrode versus lithium at C/50.

provide several pieces of information on the cell behavior and degradation. For instance, the resistance value can be an index of the interface property changes often associated with solid electrolyte interphase layer. Practical impacts of polarization resistance on battery performance arise from its influence on the battery voltage, which in turn changes the state of the battery at the cutoff conditions.

To measure polarization resistance, the linear regime of the Tafel behavior can be used, where polarization resistance and current are in proportion, so this measurement can be done in a simple manner. In addition to most conventional approach to use techniques such as electrochemical impedance spectroscopy (EIS), we prefer the method described below to determine the polarization resistance, with in situ monitoring and practical application in mind. Two assumptions were made in this method. The first one

assumes the battery would be recharged to the same SOC (i.e., exhibiting the same RCV) prior to discharge regimes at different rates. We also assume that for those familiar with the ICA one can take the advantage of such technique in providing adequate information using, at least, part of the discharge regime that is common in certain duty cycles of a constant current to allow the determination of the resistance. Fig. 15.10 presents the two methods that allow to utilize the information in a series of IC curves (obtained at different rates, as shown in Fig. 15.10A) to determine the polarization resistance for a commercial LiCoO<sub>2</sub> cell, as shown in Fig. 15.10B.

In the first method, if the cell were charged to the same SOC, the initial IR drop can be used to determine the resistance (as illustrated by the circles and solid line in Fig. 15.10B). If the initial SOC for discharge regime is unavailable, the second method provides an alternative to estimate the polarization resistance using the IC peaks at different rates (as shown by the squares and dashed lines in Fig. 15.10B). In this case, one can depend less on SOC information, as long as the IC peaks can be identified for at least two different rates. In the example shown in Fig. 15.10, the two methods gave the resistance value within a  $\pm 0.5\%$  margin. It should be noted that this approach can be used to characterize the evolution of polarization resistance with temperature and aging.

### 3.2.4 Mapping the degradation

Combining the above three in situ techniques (i.e., using RCV to determine SOC, ICA, and polarization resistance determination), it is possible to identify the signature of all known mechanisms that can contribute to battery capacity fading; namely, loss of active material, loss of lithium inventory, change in chemistry, and undercharge and under-discharge. The distinct signature of an IC change plays a pivotal role in identifying and correlating with a degradation mechanism. How IC changes can be related to degradation mechanisms can be explained as follows:

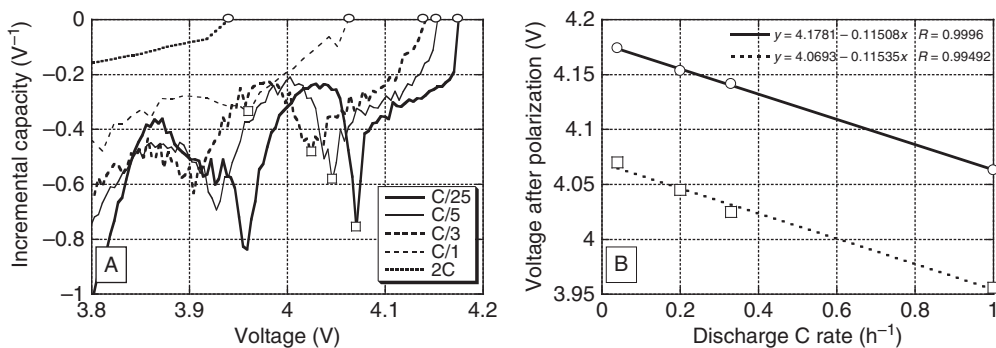


**Figure 15.10** (A) Incremental capacity curves at different discharge regimes, from C/25 to 2C and (B) polarization resistance determined from either the onset voltage of the cell (circles and solid line) or the incremental capacity peak position (squares and dashed lines) at different discharge regimes.

In the case of loss of active material, the intensity of all IC peaks associated with an electrode is supposed to decrease in proportion in both charge and discharge regimes. The RCVs in the regimes shall remain unchanged in most circumstances, as the electrodes with fewer amounts of active materials will still be able to charge or discharge to the same state, unless the disparity in loading between the two electrodes is becoming so substantial and truly disproportional. In such a case, the RCV might be different from what would be expected from the nominal OCV versus SOC curve measured from a healthy cell.

In the case of loss of lithium inventory, although the actual process in various chemistries is still not fully understood yet, our recent test results with  $\text{LiFePO}_4$  cells [38] suggest that some residual lithium ions, which may not encounter in reactions at high rates, may remain in the negative electrode in a healthy, fresh cell. Residual lithium ions are subsequently consumed by the loss of lithium inventory through aging. When such residual lithium ions are consumed, cell capacity will begin to fade as the loss of lithium inventory continues to prevail. This phenomenon could be reflected in the ICA, but may not show any noticeable capacity loss in the initial stage. If there were no capacity loss, IC peaks in discharge regime may not show any fading. On the other hand, in charge regime, because of the loss of lithium inventory the last IC peak may lose its intensity gradually. Subsequently, when the residual lithium ions were gone, on the return to the discharge regime, the first incremental capacity peak will then suffer the same loss in intensity. How quickly such symptom may show up depends on rate and degree of aging.

The symptom from loss of lithium inventory is sometimes difficult to distinguish from undercharge and/or underdischarge. Undercharge and/or underdischarge can be induced by two phenomena. A common one is usually come from an increase of cell's polarization resistance. Increase in polarization resistance will impact the cell voltage under polarization. In the charge regime, this increase will cause the cell to reach the cutoff condition prematurely thus result in undercharge. Vice versa, in the discharge regime, the additional drop in cell voltage will also make the cell prematurely cut off at a higher DOD, leading to underdischarge. The corresponding electrochemical signature is an increase in RCV at the EOD or a decreased RCV at the EOC. Another phenomenon is degradation in reaction kinetics, which results in broadening of the associated incremental capacity peak. If broadening of the peak happens close to the cutoff condition, the reaction might be cut off prematurely before completion. This phenomenon will cause the affected incremental capacity peak(s) to shift the position(s) on the incremental capacity curve, accompanied with intensity decrease. It should be noted that the capacity loss by undercharging and/or underdischarging is usually recoverable if the cutoff condition is properly adjusted.

Finally, any change in the cell chemistry is typically accompanied by an appearance of new incremental capacity peak(s) on the incremental capacity curve. From the increase

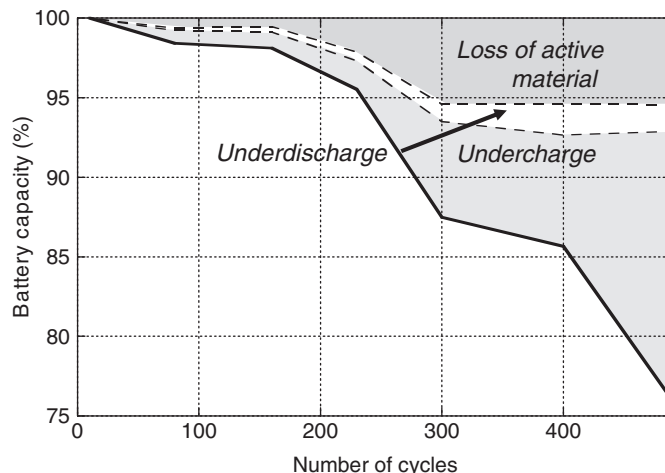


**Figure 15.11** Mapping of degradation attributes in a commercial battery.

of the new incremental capacity peak(s) and the loss of intensity associated with the affected peak(s), we might be able to tell the nature of the chemistry change.

Based on the above descriptions one should be able to identify and quantify cell degradation based on the results obtained from aging and RPT characterizations in the life-cycle tests. One can then construct a map of cell degradation illustrating the temporal evolution of degradation mechanisms through aging. Such a detailed map provides a deeper understanding of cell degradation and shall help predict the end of life condition of the cell. Fig. 15.11 presents an example of a temporal resolution of cell degradation processes deciphered from test results of a prototype  $\text{LiNi}_{0.8}\text{Co}_{0.15}\text{Al}_{0.05}\text{O}_2$  (NCA) cell [35, 36]. The capacity loss mechanisms were determined from the incremental capacity analysis with the help of RCV measurements during cell aging and characterization. It was found that undercharge was the main cause of contribution to the capacity fading. The capacity loss due to undercharge has been verified to be recoverable by further experimenting using a higher voltage cutoff condition at the EOC.

### 3.3 Characterize cell-to-cell variations

It is important to realize that to extend the understanding of battery performance in EHV from cells to assembly of cells as a pack, a critical issue to be addressed is the imbalance among the cells. To address the imbalance issue, one needs to know how cells vary from one to another in their performance characteristics [39].

The imbalance among cells in a pack can be caused by several factors, either extrinsic or intrinsic to the cell properties. For example, extrinsic factors may include current variations in parallel strings or voltage variations in series, which lead to unevenness in

the extent of cell reaction. Extrinsic attributes may come from variations in contact resistance among cells or temperature gradients created by improper thermal management in the pack. Possible intrinsic factors may include variations in cell quality that result from variations in the amount of active material on the electrode, composition, and physical property among cells. As a result of the tolerance margin built into cell processing steps, some intrinsic attributes may be inherent to a manufacturing process. Inhomogeneity in a cell, or among cells, will introduce dissimilarity in certain properties and result in performance variations. How to identify and quantify such variations from cell to cell is a tough challenge.

We have recently demonstrated [39] that using common cell testing procedures and applying electrochemical techniques to analyze the conditioning cycles of 100 cells received from a manufacturer, we could derive three critical attributes: namely, amount of active material in the cell, polarization resistance, and some localized kinetic factors that lead to cell variations. The amount of active material dictates the maximum capacity available in a cell, and it can be quantified from the capacity determined at very slow rates (such as C/25). The polarization resistance dictates the cell voltage under polarization, which in turn influences the portion of capacity deliverable under a certain rate and cutoff condition. Some practical techniques to determine the polarization resistance have been discussed in Section 3.2.3. Finally, the cell's rate capability, which is the ability of the cell to handle the range of rates, is reflected by the localized kinetic factors which dictate a cell's Peukert behavior.



## 4. SINGLE CELL AND BATTERY PACK MODELING

Although battery testing is the best way to derive information that can help understand a battery's electrochemical behavior and performance, it is rather costly, time consuming, and labor intensive. It is therefore desirable to reduce the number of test batteries to minimize the resources required. Battery modeling and simulation, if properly validated, can extend the knowledge from testing to a broader range of conditions.

Unfortunately battery modeling is difficult [40–42, 55–61], and the process not trivial. A battery model only becomes useful when it is adequately validated in order to provide accurate information and high fidelity, truly reflecting the battery behavior. In practical applications, the model should not require intensive computation, if onboard operation is desired. The model should be intuitive to the end users who might not have extensive knowledge about battery behavior. It is certainly desirable to have a model that is adaptive to different chemistries to become a useful predictive tool for virtual prototyping. When a battery model is intended for life prediction, it should be able to handle all degradation processes, both intrinsic and extrinsic to the cell. For a pack simulation, the model also needs to accommodate cell variations to address imbalance issues.

In this section we will discuss an interesting approach towards battery pack modeling by employing a single-cell equivalent circuit model (ECM) that can accommodate cell-to-cell variations and also temperature changes [39–43]. We choose ECM over first-principle electrochemical or empirical models for several reasons. The first-principle models are not favored in our consideration because of the complexity involved in the modeling approach and the extensive experiences and resources required for enabling accurate model computation. More than often a new model has to be developed for a new chemistry or cell design, because new processes may be involved and related parameters need to be determined experimentally or estimated from literature reports. Empirical models may have certain advantages in computation time. However, a simple fit of data using an empirical function may not be sufficient to transcribe complex electrochemical signature into mechanistic understanding of a battery behavior. The lack of such insightful understanding could prevent accurate prediction from experimental assessment if operating or mission profiles change or mutations of the kinetic properties with battery aging vary. Our choice of semiempirical ECM may accommodate these drawbacks and provide the best solution in terms of trade-offs, such as those between accuracy and computation complexity.

#### 4.1 Single-cell modeling

Our approach for single-cell modeling is based on an ECM approach [40–43], as presented in Fig. 15.12. ECM emulates battery behavior using an electrical circuit topology and a layer of electrical components such as resistors and capacitors to mimic chemical and physical processes involved in battery reactions. In the ECM shown in Fig. 15.12,  $V_o$  corresponds to the OCV of the cell as a function of the state of charge (SOC);  $R_1$  is the ohmic contribution to the cell internal resistance, including contact resistance, which is usually constant and can be determined by using the EIS.  $R_2$  is nonlinear, faradaic contributions to the cell internal resistance, mostly due to charge transfer kinetics. Although it is logical to determine  $R_2$  also from the EIS technique, it is time-

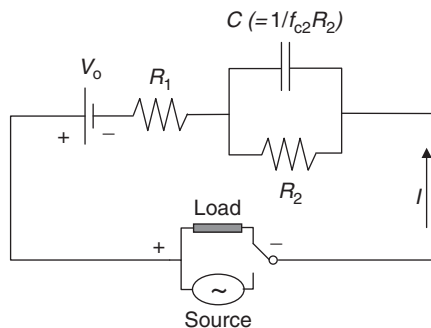


**Figure 15.12** Schematic representation of an ECM for single cell modeling.



consuming and often subjected to human intervention, since the impedance values are SOC and rate dependent.

As an alternative,  $R_2$  can be calculated from experimental data using an approximated Ohm's law by extracting the polarization resistance from cell voltage difference at a given SOC and rate (i.e., C/n) from the OCV.

$$\begin{aligned}\Delta V &= V_{OCV} - V_{C/n} = R_{\text{exp}}(I_{OCV} - I_{C/n}) \\ \text{since } I_{OCV} &= 0, \quad \text{therefore } V_{OCV} - V_{C/n} = -R_{\text{exp}}I_{C/n} \\ \text{and } R_2 &= R_{\text{exp}} - R_1\end{aligned}$$

Based on the above approximation and discrete treatment in deriving polarization resistance as a function of (C/n) rate and SOC, we created a  $R_2$ -C/n-SOC map (Fig. 15.13), from which  $R_2$  can be determined at a given rate and SOC. Applying such a map to the ECM, we can simulate cell performance in the discharge regimes (discharge curves) for a commercial LiCoO<sub>2</sub> cell at various rates as shown in Fig. 15.14. This method may allow extrapolation to higher rates. Fig. 15.14 displays an extrapolation from 2C to 3C. However, we should caution that the accuracy may be compromised when the extrapolation is too far from the experimental data.

To extend the predictive ability of the model for other operating conditions, similar approach can be used to determine variations of  $R_2$  with cell aging process or as a function of temperature. With a complete collection of these maps; for example, a “mapset” in terms of rate, age (under duty cycle aging or thermal aging), and temperature; the ECM can accommodate a wide range of operating conditions with sufficient accuracy and fidelity to simulate cell performance.

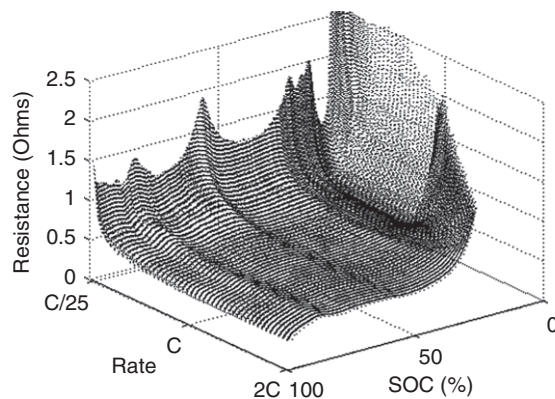


**Figure 15.13** Example of a resistance map associated with a LiCoO<sub>2</sub> Li-ion cell discharge.

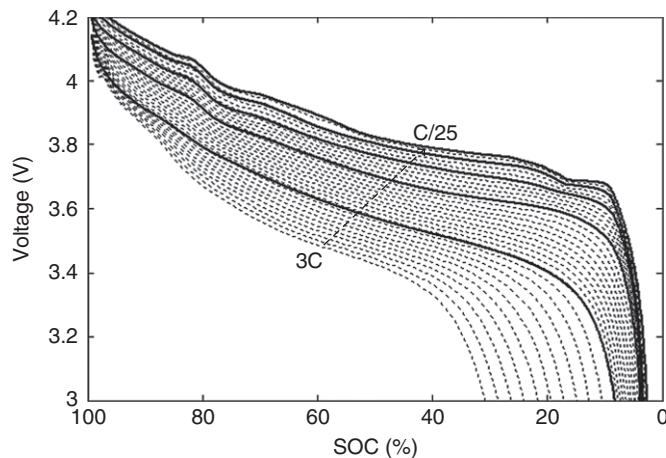


**Figure 15.14** Experimental data (thick lines) vs. simulated discharge curves for a  $\text{LiCoO}_2$  cell from 3C to C/25 with 0.1C steps.

## 4.2 Accommodating cell-to-cell variations

As illustrated in Section 3.3, through laboratory analyses [39, 43], we were able to identify three independent attributes that are relevant and critical to cell variations: (1) amount of active material, (2) polarization resistance, and (3) a lumped contribution from additional kinetic constraints. The amount of active material in a cell can be determined by a charge–discharge cycle running at a low rate such as C/25 to minimize polarization effects and to yield the extent of maximum capacity inherently born by the active material within a set of cutoff conditions. This quantity can be further transcribed into another term we noted as “capacity ration” in Ah/%SOC [39]. To accommodate the cell variations in terms of the amount of active material, as the capacity ration reveals, the single-cell model (SCM) shall use the SOC-based maximum capacity  $Q_{\max}$  available for a given cell (e.g.,  $Q_{25}$ —capacity determined at C/25, in this case, and in most cases where  $Q_{\max}$  can be determined with sufficient confidence) as follows:

$$\text{SOC}(t) = \text{SOC}_{\text{ini}} - \int I \frac{dt}{Q_{\max}}$$

Since the SOC is a universal parameter that is not related to the amount of active material anymore, SOC-based model can thus accommodate the cell variations quantified from proper cell characterization and analysis.

The polarization resistance can be approximated from the linear regime of the IR drop at various discharge rates in each cell, as explained in Section 3.2.3. To accommodate the variations in the polarization resistance, where  $R_p = R_1 + R_2$ , we directly use the  $R_p$  derived from the conditioning cycles in the model to construct the  $R_p$ –C/n–SOC map, similar to that illustrated in Fig. 15.13.

In order to take into account of the lumped contribution from various additional kinetic constraints, we resort to the Peukert behavior. We postulated that these kinetic constraints will influence the effectiveness of active material utilization in general. Thus, we introduced a utilization coefficient to express and adjust the actual amount of active material being involved in the reaction. This utilization adjustment can be performed in the SOC calculation by multiplying  $Q_{\max}$  with a utilization coefficient  $q$  that can be derived from the Peukert coefficient:

$$\text{SOC} = \text{SOC}_{\text{ini}} - \int I \frac{dt}{q Q_{\max}}$$

Taking this approach in accommodating cell variations from the three independent attributes, we virtually can simulate any cell in the batch to reveal its unique characteristic and performance with high fidelity.

### 4.3 Battery pack modeling

Having an accurate SCM is not sufficient to yield a battery pack model with desired accuracy. An accurate account of a battery pack's behavior, and its degradation, has to consider cell variations and incorporate them in the intrinsic property (such as initial, inherent imbalance) of the pack with its topology before any accurate pack simulation can be achieved. It is important to realize that the topology of the battery pack does play an essential role in the modeling, since the topology dictates the physical configuration of multiple cells in the pack, and each cell has a unique characteristic born with its content of active material, polarization resistance, and other kinetic constraints. The two critical components in accommodating cell variations (so each cell is a unique and distinct element in the topology) and pack topology shall determine the success and unique capability of the pack model and simulation. Such a unique capability cannot be achieved easily by other modeling approaches, not even with those employing conventional statistical analysis and empirical fitting with standard deviation.

Another issue related to battery pack modeling is the scale of a pack and the effect of scaling. For a small battery pack, such as that used in a laptop computer or power tool, the individual cell characteristics may play a dominant role in dictating the pack performance. In such a case, the cell variations and accommodating such variations in the pack model may become a significant endeavor in improving pack model accuracy and fidelity. We, however, should be mindful that such a capability is vital to managing pack and cell imbalance issue. On the other hand, when a pack is large in scale, the disparity among the cells may become less critical; thus, the endeavor of managing cell variations may become a daunting effort. In this case, the need for employing statistical method in establishing confidence in error distribution should prevail. One can assess the chance of a bad cell in influencing pack performance and set a sensitivity threshold in the

monitoring system to detect anomalies. The trade-offs in managing the resources and difficulties in a battery pack model in relevance to the scale of operation need to be quantified and assessed.

Another relevant issue in managing battery pack performance is the ability to control pack operating conditions to minimize external influences of cell variations. A common problem faced by the industry today is thermal management, which is supposed to minimize or eliminate thermal gradient within a pack to warrant a consistent pack performance. In addition to the thermal gradient problem in pack thermal management, a pack model needs to address the thermal imbalance on top of the charge imbalance among cells. One advantage of the approach described in this section is the ability to handle individual cell model under the influence of temperature gradients, better than other approaches (considering the complexity involved in the first-principle or empirical models). With this approach and via a thermal convection calculation or temperature monitoring network, we should be able to specify an actual temperature to each cell and therefore increase the accuracy of the pack model simulation.



---

## 5. VEHICLE DRIVETRAIN PLATFORM MODELING

With a successful implementation of a battery pack model, we shall have a tool to address real time-series data with sufficient accuracy. Such a successful implementation remains to be achieved in both field and laboratory testing, so that we will be able to understand the real battery pack behavior and degradation associated with duty cycles. Although a practical implementation is still in progress, there are several aspects worth discussion.

Several vehicle powertrain/drivetrain simulation platforms are readily available to date to allow simulation of vehicle (drivetrain) performance that includes battery performance. Some notable ones such as ADVISOR, PSAT, or VPSET have been reported in the literature [62, 63]. Some of them can be licensed for use. With the aids of these drivetrain simulation platforms, if real battery power usage is available for validation, we can employ these modeling platforms to compare battery performance data. The caveat is that an accurate and high-fidelity battery model needs to be implemented into these platforms to allow realistic comparison.

Another challenge we face today is the lack of a practical method to estimate the SOC (not DOD) during field testing or real-life operation. The conventional coulomb counting method might be useful for DOD estimate. It is not practical for SOC. As we mentioned in Section 3.2.1, there is no straightforward relationship between DOD and SOC. As battery being used and degraded, the situation becomes more complex. Any comparison between the data collected in the field or in laboratory tests and those predicted by the model is going to be extremely difficult. This issue needs to be overcome by developing a reliable battery diagnostic tool that can estimate the SOC or even state of health of a battery pack on the flight to facilitate such comparison.

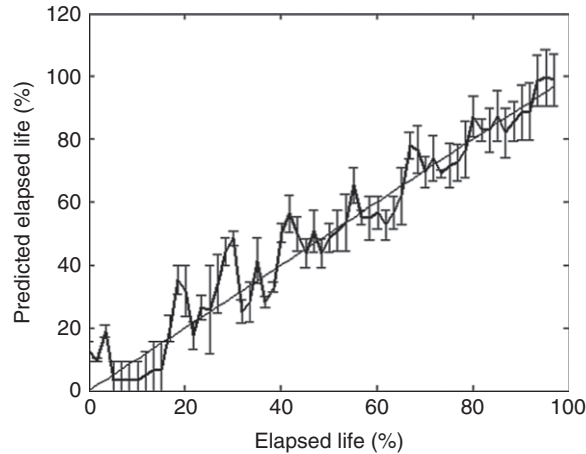


**Figure 15.15** An example of battery life prediction estimated from a battery diagnostic tool.

Fig. 15.15 shows an example of a comparison of state of health (regarding remaining life) predicted for a commercial  $\text{LiFePO}_4$  cell subjected to DST cycling and the predicted elapsed life calculated with a battery diagnostic tool. Each calculation was performed independently from the tool irrelevant to previous or following ones. This technique provides an excellent projection of the remaining life of a cell and at the same time a rather reliable reference point for comparisons between real data in the field and those from laboratory tests.



## 6. CONCLUDING REMARKS

The road map illustrated in Fig. 15.1 summarizes the entire approach to understand battery performance in electric and hybrid vehicle operation. Via field testing (Section 2), proper data collection and analysis should be able to help derive vehicle usage patterns using a FL-PR technique (Section 2.1) as a method to conduct driving cycle and duty cycle analyses. One of the benefits in such a practice is to help understand how drivers in a local community use their vehicles and how such driving habits influence the vehicle powertrain (including battery) performance. Such experiences can also help develop representative driving schedules (Section 2.2) to allow further laboratory tests and characterizations of the powertrain, including battery performance.

In parallel, in laboratory testing conventional test procedures can provide ample amount of information if proper analyses are applied. Section 3.1 illustrates what battery performance information can be obtained and presented to enhance our understanding of battery behavior. Section 3.2 explains how battery degradation information can be yielded from laboratory tests. We further discussed the importance of the SOC determination and how to correctly derive such information (Section 3.2.1) by RCV

measurements. In Section 3.2.2 we explained how to utilize incremental capacity analysis to help us extract battery degradation information to identify degradation mechanisms and quantify the effects (Section 3.2.4). With such understanding of battery behaviors in laboratory tests, we further explain the importance of transcribing such understanding to battery modeling and simulation (Section 4). In Section 4.1, an SCM based on equivalent circuit modeling approach was described, and the advantages of using this approach explained. In the transition from a SCM to a battery pack (Section 4.3), we discussed the importance of understanding cell variations that arise from manufacturing processes (Section 3.3), how such variations can affect our ability to manage battery pack, and how to address them in the modeling approach (Section 4.2). The integral understanding of different aspects in battery behavior and performance will allow us develop a suite of diagnostic tools to control and manage battery pack. At such a stage, vehicle drivetrain performance simulation can be used to integrate the knowledge and utility (Section 5) to aid better understanding of battery pack performance in electric and hybrid vehicle operation.

## ACKNOWLEDGEMENT

This work was conducted under several contracts with the Hawaii Center for Advanced Transportation Technologies (HCATT) with support received from the U.S. Air Force Advanced Power Technology Office (APTO) at the Robins Air Force Base in Georgia. Partial support provided by Expert Microsystems, Inc. (Orangevale, CA) for an STTR project funded by Naval Air Systems Command (Patuxent River, MD) under the contract (Award #N00014-07-M-0414) is also appreciated. We are grateful to the additional support by Idaho National Laboratory under the U.S. Department of Energy Advanced Battery Research program.

## REFERENCES

1. C.J.T. van de Weijer, in: Heavy-Duty Emission Factors—Development of Representative Driving Cycles and Prediction of Emissions in Real-Life, PhD dissertation, Technical University of Graz, Austria, 1997.
2. I.J. Riemersma, P. Hendriksen, N.L.J. Gense, R.T.M. Smokers, Methodology for the Development of Representative Driving Cycles, [http://www.tno.nl/groep.cfm?context=markten&content=markt&laag1=59&item\\_id=59&Taal=2](http://www.tno.nl/groep.cfm?context=markten&content=markt&laag1=59&item_id=59&Taal=2), 2010, (accessed 24.04.10)
3. K.J. Kelly, A. Rajagopalan, Benchmarking of OEM Hybrid Electric Vehicles at NREL, US DOE/ National Renewable Energy Laboratory, Technical Report #NREL/TP-540-31086, August 2001.
4. H.C. Frey, J. Zheng, Environ. Sci. Technol. 36 (2002) 5184.
5. E. Ericsson, Transport. Res. Part D 5 (2000) 337.
6. E. Ericsson, Transport. Res. Part D 6 (2001) 324.
7. F. An, M. Ross, A Model of Fuel Economy and Driving Patterns, Society of Automotive Engineers (SAE), technical paper 93-0328, 1993.
8. F. An, M. Barth, G. Scora, Impacts of Diverse Driving Cycles in Electric and Hybrid Vehicle Performance, Society of Automotive Engineers (SAE), technical paper 97-2646, 1997.
9. F. An, M. Barth, Critical Issues in Quantifying Hybrid Electric Vehicle Emissions and Fuel Consumption, Society of Automotive Engineers (SAE), technical paper 98-1902, 1998.
10. F. An, F. Stodolsky, D. Santini, Hybrid Options for Light-Duty Vehicles, Society of Automotive Engineers (SAE), technical paper 1999-01-2929, 1999.

11. M. Barth, M. Todd, *Transport. Res. Part C* 7 (1999) 237.
12. H.Y. Tong, W.T. Hung, C.S. Cheung, *Atmos. Environ.* 33 (1999) 2323.
13. K.L. Butler, M. Ehsani, P. Kamath, *IEEE Trans. Veh. Technol.* 48 (1999) 1770.
14. Z. Rahman, K. Butler, M. Ehsani, A Study of Design Issues on Electrically Peaking Hybrid Electric Vehicle for Diverse Urban Driving Patterns, Society of Automotive Engineers (SAE), technical paper 1999-01-1151, 1999.
15. C. Young, M.R. Smith, T. Younglove, M.J. Barth, Analysis of Weekday/Weekend Driving Differences in an in-use Vehicle Fleet, Proceedings of the 10th CRC On-Road Vehicle Emissions Workshop, San Diego, CA, 2000.
16. M. Barth, T. Younglove, C. Malcolm, G. Scora, Mobile Source Emissions New Generation Model: Using a Hybrid Database Prediction Technique, Final Report to the U.S. Environmental Protection Agency, 2002.
17. N. Dembski, Y. Guezennec, A. Soliman, Analysis and Experimental Refinement of Real-World Driving Cycles, Society of Automotive Engineers (SAE), technical paper 2002-01-0069, 2002.
18. M. Ergeneman, C. Sorousbay, A. Goktan, *Int. J. Vehicle Des.* 18 (1997) 391.
19. J.H. Kent, G.H. Allen, G. Rule, *Transport. Res.* 12 (1978) 147.
20. D.J. Simanaitis, *Automot. Eng.* 85 (1977) 34.
21. M. André, *Sci. Total Environ.* 334–335 (2004) 73.
22. J.H. Tsai, H.-L. Chiang, Y.-C. Hsu, B.-J. Peng, R.-F. Hung, *Atmos. Environ.* 39 (2005) 6631.
23. [http://www.uscar.org/guest/view\\_team.php?teams\\_id=12](http://www.uscar.org/guest/view_team.php?teams_id=12), 2010, (accessed 24.04.10)
24. <http://avt.inel.gov/>, 2010, (accessed 24.04.10)
25. M. Broussely, S. Herreyre, P. Biensan, P. Kasztejna, K. Nechev, R.J. Staniewicz, *J. Power Sources* 97–98 (2001) 13.
26. R. Spotnitz, *J. Power Sources* 113 (2003) 72.
27. P. Ramadass, B. Haran, P.M. Gomadam, R. White, B.N. Popov, *J. Electrochem. Soc.* 151 (2) (2004) A196.
28. B.Y. Liaw, K.P. Bethune, C.S. Kim, Time-Series Field Trip Data Analysis Using Adaptive Recognition Approach. Analysis on Driving Patterns and Vehicle Usage for Electric Vehicles, 19th Electric Vehicle Symposium (EVS-19), Busan, South Korea, October 2002.
29. B.Y. Liaw, B. Dailliez, A. Teeters, K.-Y. Youn, C.-S. Kim, Vehicle Usage Analysis for Hyundai Santa Fe Fleet in Hawaii, 20th Electric Vehicle Symposium (EVS-20), Long Beach, CA, November 2003.
30. B.Y. Liaw, *J. Asian Elec. Vehicles* 2 (1) (2004) 551.
31. M. Dubarry, M. Bonnet, B. Dailliez, A. Teeters, B.Y. Liaw, *J. Asian Elec. Vehicles* 3 (1) (2005) 657.
32. M. Dubarry, V. Svoboda, R. Hwu, B.Y. Liaw, *J. Power Sources* 174 (2007) 366.
33. B.Y. Liaw, M. Dubarry, *J. Power Sources* 174 (2007) 76.
34. M. Dubarry, N. Vuillaume, B.Y. Liaw, T. Quinn, *J. Asian Elec. Vehicles* 5 (2) (2007) 1033.
35. M. Dubarry, V. Svoboda, R. Hwu, B.Y. Liaw, *Electrochem. Solid State Lett.* 9 (10) (2006) A454.
36. M. Dubarry, V. Svoboda, R. Hwu, B.Y. Liaw, *J. Power Sources* 165 (2007) 566.
37. M. Dubarry, V. Svoboda, R. Hwu, B.Y. Liaw, *J. Power Sources* 174 (2007) 1121.
38. M. Dubarry, B.Y. Liaw, *J. Power Sources* 194 (1) (2009) 541.
39. M. Dubarry, N. Vuillaume, B.Y. Liaw, *Int. J. Energy Res.* 34 (2010) 216.
40. B.Y. Liaw, G. Nagasubramanian, R.G. Jungst, D.H. Doughty, *Solid State Ionics* 175 (2004) 835.
41. B.Y. Liaw, R.G. Jungst, G. Nagasubramanian, H.L. Case, D.H. Doughty, *J. Power Sources* 140 (2005) 157.
42. M. Dubarry, B.Y. Liaw, *J. Power Sources* 174 (2007) 856.
43. M. Dubarry, N. Vuillaume, B.Y. Liaw, *J. Power Sources* 186 (2) (2009) 500.
44. J. Barker, *Electrochim. Acta* 40 (1995) 1603.
45. J. Barker, M.Y. Saidi, R. Koksang, *Electrochim. Acta* 41 (1996) 2639.
46. J. Barker, R. Koksang, M.Y. Saidi, *Solid State Ionics* 89 (1996) 25.
47. K.A. Striebel, A. Guerfi, J. Shim, M. Armand, M. Gauthier, K. Zaghbi, *J. Power Sources* 119–121 (2003) 951.
48. J. Shim, K.A. Striebel, *J. Power Sources* 119–121 (2003) 955.
49. A. Yamada, H. Koizumi, S. Nishimura, N. Sonoyama, R. Kanno, M. Yonemura, et al., *Nat. Mater.* 5 (2006) 357.

50. L. Laffont, C. Delacourt, P. Gibot, M.Y. Wu, P. Kooyman, C. Masquelier, et al., *Chem. Mater.* 18 (2006) 5520.
51. C. Delmas, M. Maccario, L. Croguennec, F. Le Cras, F. Weill, *Nat. Mater.* 7 (2008) 665.
52. T. Ohzuku, Y. Iwakoshi, K. Sawai, *J. Electrochem. Soc.* 140 (1993) 2490.
53. D. Aurbach, B. Markovitsky, I. Weissman, E. Levi, Y. Ein-Eli, *Electrochim. Acta* 45 (1999) 67.
54. H. Buqa, D. Goers, M. Holzapfel, M. Spahr, P. Novak, *J. Electrochem. Soc.* 152 (2005) A474.
55. J. Newman, *Electrochemical Systems*, second ed., Prentice Hall, Englewood Cliffs, NJ, 1991.
56. E. Barsoukov, J.H. Kim, J.H. Kim, C.O. Yoon, H. Lee, *Solid State Ionics* 116 (1999) 249.
57. C. Fellner, J. Newman, *J. Power Sources* 85 (2000) 229.
58. B. Wu, M. Mohammed, D. Brigham, R. Elder, R.E. White, *J. Power Sources* 101 (2001) 149.
59. G.L. Plett, *J. Power Sources* 161 (2006) 1369.
60. R. Spotnitz, *J. Power Sources* 113 (2003) 72.
61. P. Ramadass, B. Haran, P.M. Gomadam, R.E. White, B.N. Popov, *J. Electrochem. Soc.* 151 (2004) A196.
62. [http://www.avl.com/wo/webobsession.servlet/go/encoded/YXBwPWJjbXMmcGFnZ-T12aWV3Jm5vZGVpZD00MDAwMzA0NTk\\_3D.html](http://www.avl.com/wo/webobsession.servlet/go/encoded/YXBwPWJjbXMmcGFnZ-T12aWV3Jm5vZGVpZD00MDAwMzA0NTk_3D.html), 2010, (accessed 24.04.10)
63. A. Nedungadi, M. Pozolo, M. Mimmagh, *A General Purpose Vehicle Powertrain Modeling and Simulation Software—VPSET*, Report No.(s): AD-A479856, Defense Technical Information Center (DTIC) 2008.





# Batteries for PHEVs: Comparing Goals and the State of Technology

Jonn Axsen<sup>1</sup>, Andrew F. Burke, and Kenneth S. Kurani

Institute of Transportation Studies, University of California at Davis, 2028 Academic Surge, One Shields Avenue, Davis, CA 95616, USA

## Contents

1. Introduction	405
2. Basic PHEV Design Concepts	408
3. PHEV Battery Goals	410
3.1 Power	412
3.2 Energy capacity	413
3.3 Life	413
3.4 Safety	415
3.5 Costs	416
3.6 Summary of trade-offs	416
4. Battery Technologies	417
4.1 Nickel-metal hydride	418
4.2 Lithium-ion	419
5. Li-Ion Battery Prospects	420
6. What PHEV Could Be Made With Near-Term Battery Technologies?	423
7. Discussion and Conclusion	425
Acknowledgements	426
References	426



---

## 1. INTRODUCTION

Electric-drive continues to pique imaginations of motorists: clean skies, quiet cars, and plentiful electricity produced from non-polluting domestic sources. So where are our electric automobiles? The answer depends in part on what is an electric automobile. We have seen variations in electric vehicle (EV) size, performance, and definition in efforts to overcome the fundamental challenge of electric-drive – how to store energy and supply power. In short, where are our batteries? This chapter addresses one variation on the definition of an EV and the state of battery development for it – plug-in hybrid electric vehicles (PHEVs).

Much effort and many resources were devoted to the development of electric-drive vehicles over the past three decades. These efforts have been spurred by petroleum supply

---

<sup>1</sup> Corresponding author: [jaxsen@gmail.com](mailto:jaxsen@gmail.com)

and price disruptions, air pollution policy, and climate policy. The US federal government drove initial efforts to develop alternatives to petroleum in the late 1970s and early 1980s. The oil crisis of 1973–1974 prompted funding of research on alternative fuels; perhaps the most important for EVs was the Hybrid and Electric Vehicle Act of 1976, which resulted in long-term projects in the US Department of Energy. Some of these laid the groundwork for the battery, motor, and power and control electronics technologies that emerged during the 1990s [1]. Battery EVs captured renewed attention in the 1990s, stimulated by General Motor’s development of the EV-1 (aka Impact) and California’s Zero-Emissions Vehicle (ZEV) mandate. After years of further technology development and policy debate, policy-makers were convinced by automobile manufacturers in the late 1990s that battery technology was insufficient to meet manufacturers’ EV design goals. However, some battery technologies later proved successful in less-demanding hybrid-electric vehicle (HEV) applications, achieving significant commercial success, typified by the Toyota Prius. Currently, interest has turned to what many claim is the next logical step from the HEV: PHEVs. For example, the California Air Resources Board amended the ZEV mandate in March 2008 to provide incentives for automakers to produce and sell PHEVs [2].

Relative to other electric-drive and conventional gasoline vehicles, one advantage of PHEVs is fuel flexibility. Users could power their vehicle with electricity from the electrical power grid, gasoline (or another fuel), or both. To do so, a PHEV has both an electric motor and a heat engine—usually an internal combustion engine (ICE).<sup>1</sup> This flexibility also complicates vehicle designs and possible ways of using energy from two different systems. Fig. 16.1 shows two simple schematics of possible PHEV architectures, that is, the overall design of the PHEV system to supply power from two different sources. A series drivetrain architecture powers the vehicle only by an electric motor using electricity from a battery. The battery is charged from an electrical outlet, or by the gasoline engine via a generator. A parallel drivetrain adds a direct connection between the engine and the wheels, adding the potential to power the vehicle by electricity and gasoline simultaneously and by gasoline only. While Toyota is currently developing a PHEV with a parallel architecture, i.e. a plug-in version of the Prius, General Motors is working with a series architecture, i.e. the Chevy Volt.

In any PHEV architecture the battery plays a crucial role in storing energy from the electrical grid and from the gasoline engine (through a generator), as well as passing energy back and forth with the electric motor to maximize efficiency.<sup>2</sup> “Pure” EVs only have an electric motor and only run on electricity and thus need batteries that can store large amounts of energy and deliver high power. However, PHEVs can be designed to emphasize energy or power requirements (or both) of batteries.

<sup>1</sup> As the ICE in most conventional vehicles is fueled with gasoline (or diesel), we will refer to gasoline and gasoline engines without precluding the possibility of different future fuels.

<sup>2</sup> During braking and coasting, an electric motor can convert—or regenerate—some of the kinetic energy of the moving vehicle into electrical energy to be stored in the vehicle’s battery.

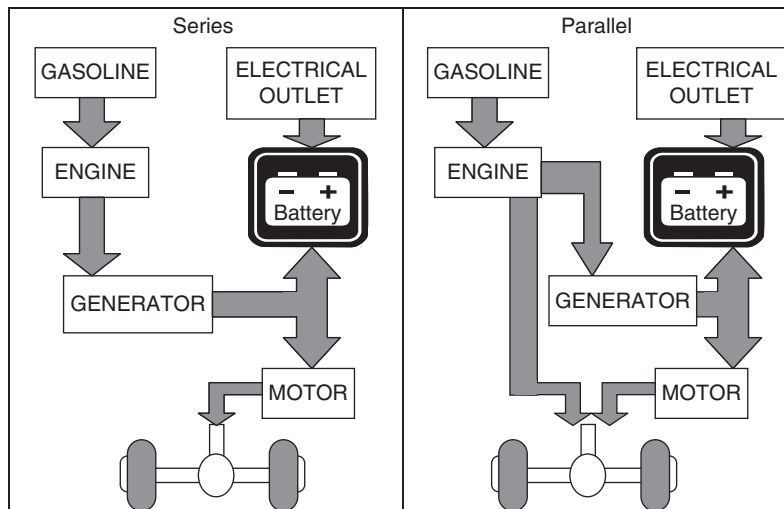


**Figure 16.1** Basic PHEV drivetrain architecture – series vs. parallel design.

Ultimately, the commercial success of the PHEV depends on the development of appropriate battery technologies. There is much uncertainty about both what requirements a battery must meet to produce a successful PHEV and where different battery technologies stand in meeting such requirements. On the one hand, electric-drive advocates claim that battery technology is sufficient to begin the commercial introduction of PHEVs immediately (e.g. [3,4]). On the other hand, critics counter that substantial technological breakthroughs are required before PHEVs should be introduced to the market (e.g. [5]). Anderman [6] states that commercializing PHEVs prior to 2015 would present substantial business risks. Also, as the difference in initial PHEV architectures between automakers shows, there is disagreement on what a PHEV is, or if the concept is flexible enough and the market diverse enough to support multiple incarnations. For their part, policymakers are unsure how to regulate PHEV emissions and “fuel” use under conditions of such technical and market uncertainty.

This chapter intends to help demystify some of the complexities of PHEV battery development. We discuss the basic design concepts of PHEVs, compare three sets of influential technical battery goals, and explain the inherent trade-offs in PHEV battery design. We then discuss the current state of several battery chemistries, comparing their abilities to meet PHEV goals and their potential trajectories for further improvement. Four important conclusions are highlighted. First, PHEV battery “goals” vary according to differing assumptions of PHEV design, performance, use patterns, and consumer demand. Second, battery development is constrained by inherent trade-offs among five main battery attributes: power, energy, longevity, safety, and cost. Third, lithium-ion (Li-ion) battery designs are better suited to meet the demands of more aggressive

PHEV goals than nickel-metal hydride (NiMH) batteries (currently used for HEVs). Fourth, the flexible nature of Li-ion technology, as well as concerns over safety, has prompted several alternate paths of continued technological development. Due to the differences among these development paths, the attributes of one type of Li-ion battery cannot necessarily be generalized to other types.

This chapter is not intended to be a definitive analysis of battery chemistries; instead, it is more of a primer on battery technology, providing the perspective and tools to help readers understand and critically review research on PHEV batteries.

## 2. BASIC PHEV DESIGN CONCEPTS

Before delving into specific technological goals, we first explain four fundamental PHEV concepts. First, for any given architecture, a PHEV can operate in one of two modes: charge sustaining (CS) or charge depleting (CD). Fig. 16.2 (adapted from [5]) illustrates these two modes. In practice, the battery's maximum state of charge (SOC) may be limited to less than 100%, and the minimum SOC constrained to more than 0%, both to preserve battery life and to improve safety. The difference between the maximum and minimum SOC is known as the usable depth of discharge (DOD), which varies across battery and vehicle designs.

In the Fig. 16.2 example, the battery is “fully” charged (from an electrical outlet) to 90% SOC at the beginning of the illustrated cycle. For a distance the PHEV is driven in CD mode – energy stored in the battery is used to power the vehicle, gradually depleting the battery's SOC. Once the battery is depleted to a minimum level, set at around 25% SOC, the vehicle enters CS mode.

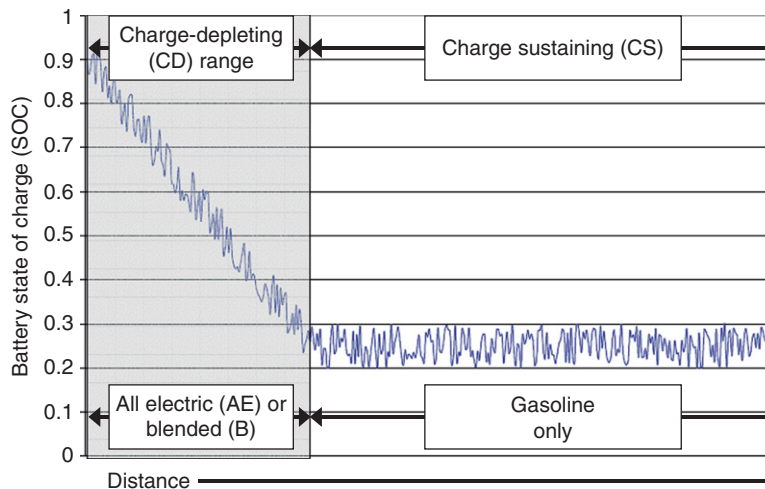


**Figure 16.2** Illustration of typical PHEV discharge cycle – 65% DOD (used with permission from Kromer and Heywood [5]).

in this example, the vehicle switches to CS mode. In CS mode the SOC is sustained by relying primarily on the gasoline engine to drive the vehicle, using the battery and electric motor to increase efficiency and recapture kinetic energy, as is now done in an HEV. Small cycles, or “waves,” can be seen in the SOC during CS operation, where the battery takes on energy from the engine-driven generator or from regenerative braking and uses the energy in the electric motor to improve the efficiency of engine operation. The vehicle remains in CS mode until the battery is plugged in again to recharge.

A second key PHEV concept is that a vehicle can be designed for all-electric (AE) or blended (B) operation in CD mode. A PHEV designed for AE operation can be driven for the CD range using only electricity from the battery, and the engine is not used at all. In contrast, a PHEV designed for B operation will use electricity and gasoline to power the vehicle during the CD range—energy from the engine and the battery are “blended” together through the electro-mechanical drivetrain. Thus, a PHEV designed for AE driving will require a battery capable of delivering more power than a PHEV designed for B driving (as further detailed later) because the battery (and motor and power electronics) must be capable of providing the full power of the vehicle, not just partial power.

Third, PHEV designs are commonly described according to CD range; the common notation is PHEV-X, where X is the distance in miles. For instance, a PHEV-10 can be driven 10 miles in CD mode before switching to CS mode. However, this notation does not distinguish whether a PHEV in CD mode is operating all-electrically or using blending, nor does it specify the driving conditions that would allow CD operation for the stipulated distance. Comparisons of PHEVs, even those sharing the same PHEV-X designation, must reconcile assumptions regarding CD operation and driving behavior.

Kurani, Heffner, and Turrentine [7] discuss how further confusion in PHEV notation can result from two differing concepts of PHEV-X. First, Gondor and Simpson [8] argue that X should be defined as the equivalent number of miles of petroleum displaced by electricity from the battery. This approach makes no distinction between AE and blended operation; a fully charged PHEV-10 could store and use enough electricity to reduce gasoline use by the amount of gasoline required to travel 10 miles, but not necessarily during the first 10 miles. On the other hand, the California Air Resources Board [9] defines X as the total miles that can be driven before the gasoline engine turns on for the first time, also known as AE range (or zero-emissions range).<sup>3</sup> By this definition, a fully charged PHEV-10 could be driven for the first 10 miles without using any petroleum. CARB’s definition requires a more powerful electric motor and battery to avoid engine use during CD mode. Again, these distinctions must be clarified when discussing the battery requirements of a particular PHEV design. In this chapter, we identify CD range and operation with the following notation: AE-X or B-X, where X is the CD range in miles.

<sup>3</sup> As of the writing of this chapter, CARB is considering a proposal to allow PHEVs designed for blended operation to receive credits under the zero-emissions vehicle regulation.

A final point of clarification for PHEV design and notation is the assumed drive cycle used to estimate CD operation and CD range. A drive cycle is a pattern of changing accelerations, speeds, and braking over time used to test fuel economy as well as automotive battery performance. A cycle usually repeats one or more schedules designed by the US Environmental Protection Agency (EPA). The Urban Dynamometer Driving Schedule (UDDS) is most common, established by the EPA to simulate city driving conditions. This schedule includes many accelerations and decelerations over a 23-minute period, with an average speed of 20 miles per hour. The federal highway schedule (HWFET) is typically used to simulate highway driving. Both the UDDS and the HWFET have been criticized for not accurately representing the aggressive nature of US drivers [5], and thus PHEV battery goals based on such schedules may overestimate the performance of a given battery. For instance, if an AE-20 is designed using the UDDS, a more aggressive driving cycle will shorten the CD range, or require engine assistance (blending) during CD mode to achieve the specified range, or both. Thus, in comparing different battery goals, readers must consider drive cycle assumptions and assess how representative such assumption may be of actual driving behavior.



### 3. PHEV BATTERY GOALS

The battery requirements of any given PHEV design are primarily determined by peak power (kW) and energy storage (kWh). As noted, both are dependent on assumptions about CD range, CD operation mode, that is, AE or B, drive cycle, vehicle design, recharge behavior, and other factors.

In this section we present the PHEV battery goals set by the US Advanced Battery Consortium (USABC), as summarized by Pesaran et al [10].<sup>4</sup> Table 16.1 provides a summary that will be referred to throughout this chapter. We focus on USABC goals because these are the most recent and among the most influential goals. The USABC specifies two main PHEV battery types: a high power/energy ratio battery providing 10 miles of AE range (AE-10) and a low power/energy ratio battery providing 40 miles of AE range (AE-40). These categories follow CARB's definition of PHEV-X, where X is the number of miles the vehicle can drive in AE mode during a particular drive cycle, before the gasoline engine turns on. USABC goals are based on the UDDS to be consistent with CARB's testing methods. The USABC AE-10 goals are set for a "crossover utility vehicle" (an automobile-based SUV) weighing 1,950 kg and the AE-40 goals are set for a midsize sedan weighing 1,600 kg. Table 16.1 also specifies weight and volume limits of the battery system. We discuss the five groups of goals below: power, energy capacity, life, safety, and cost, as summarized by [10].

<sup>4</sup>The USABC is a partnership between the US Department of Energy (DOE) and US automobile companies.

**Table 16.1** Comparing PHEV performance goals and battery requirements (refs. [5, 10, 11])

	Units	USABC	MIT		EPRI	
<b>Performance Goals</b>						
CD range	Miles	10	40	30	20	60
CD operation <sup>a</sup>	Type	AE	AE	B	AE	AE
Body type	Type	Cross-over SUV	Mid-size car	Mid-size car	Mid-size car	Mid-size car
Electricity use <sup>b</sup>	kWh/mile	0.42	0.30	0.19	0.24	0.24
Depth of discharge	Percent	70%	70%	70%	80%	80%
Drive schedule	Type	UDDS	UDDS	UDDS, HFWET, US06	UDDS, HFWET	UDDS, HFWET
Battery mass	kg	60	120	60	159	302
Vehicle mass	kg	1,950	1,600	1,350	1,664	1,782
<b>Battery Requirements</b>						
<i>(1) Power</i>						
Peak power	kW	50	46	44	54	99
Peak power density	W/kg	833	383	733	340	328
<i>(2) Energy</i>						
Total energy capacity	kWh	5.6	17.0	8.0	5.8	17.9
Total energy density	Wh/kg	93	142	133	37	59
<i>(3) Life</i>						
Calendar life	Years	15	15	15	10	10
CD cycle life	Cycles	5,000	5,000	2,500	2,400	1,400
CS cycle life	Cycles	300,000	300,000	175,000	200,000	200,000
<i>(4) Cost</i>						
OEM price <sup>c</sup>	\$	1,700	3,400	2,560		
OEM price/total kWh	\$/kWh	300	200	320		

<sup>a</sup> Blended (B) or all-electric (AE) operation.

<sup>b</sup> Grid electricity only—equivalent to total available energy capacity divided by CD range.

<sup>c</sup> Assuming 100,000 units of production per year.

Because USABC goals are highly dependent on various assumptions, we also present alternative assumptions conducted by the Sloan Automotive Laboratory at the Massachusetts Institute of Technology (MIT) and the Electric Power Research Institute (EPRI). Table 16.1 also summarizes the differing assumptions and “goals” of each. We distinguish between PHEV goals—the desired performance level of the vehicle—and PHEV battery requirements—the estimated technical battery specifications required to achieve the stated goals that will be addressed in a later section. Some of the goal categories in Table 16.1 have been explained above; other assumptions and goals are addressed below.

The MIT goals are derived from Kromer and Heywood [5], who used vehicle assumptions that differed from USABC in two important ways. First, MIT set goals for a midsize sedan PHEV with 30 miles of CD range in blended mode (B-30). As a useful side note, MIT illustrates the differences in PHEV goals for different levels of blending versus AE operation. Second, in addition to the UDDS used by the USABC, MIT used the HWFET schedule as well as the US06 schedule, the latter of which is the most aggressive due to longer accelerations and higher top speeds. They explain that this combination of schedules produces a drive cycle that is more representative of actual US driving behavior than the UDDS or HWFET schedules alone, thus allowing more realistic (and stringent) battery goals. Although such a drive cycle requires higher battery performance than USABC’s goals, this is largely offset by their assumptions of CD blending, and a lower vehicle weight. EPRI’s goals are derived from a report conducted by Graham et al. [11], investigating the power requirements of a midsize sedan designed as an AE-20 or AE-60. EPRI’s drive cycle includes the UDDS and HWFET. The primary distinguishing factor of EPRI goals is the higher battery weight assumptions (159–302 kg) compared to USABC and MIT (60–120 kg).

### 3.1 Power

The power of a conventional gasoline vehicle is typically reported in horsepower, where 100 horsepower is equivalent to 75 kW. The USABC’s peak power goals are based on short accelerations (pulses) of 2 and 10 seconds. According to Pesaran et al. [10], the AE-10 requires the ability to provide 50 kW of power (67 horsepower), while the AE-40 requires 46 kW. Power requirements are not typically related to CD range; the AE-10 requires slightly more power due to increased weight (+350 kg), rolling resistance, and frontal area (drag) of the crossover SUV compared to the sedan used for the PHEV-40 analysis.

For comparison, Kromer and Heywood [5] demonstrate how different types of operation in CD mode can influence power requirements for a B-30. While different levels of blended operation require only 23–40 kW of power, a PHEV with AE operation requires a battery that can deliver 60 kW [5]. The latter value is higher than USABC goals due to Kromer and Heywood’s use of more ambitious drive cycles, that is,



HFWET and US06 in addition to the UDDS. In contrast, EPRI's AE-20 requires 54 kW—likely higher than USABC due to the additional use of the HFWET cycle. EPRI's AE-60 goal is much higher—99 kW—in order to optimize overall performance by taking advantage of the heavy battery (302 kg) to allow electric-drive even during aggressive cycles (note that power density is about the same as for EPRI's AE-20).

In comparing battery technologies, analysts typically refer to power density as the power per kilogram of the battery system (W/kg). The USABC's target weight for the AE-40 battery pack is 120 kg, resulting in a power density of 380 W/kg. The target weight for the AE-10 battery pack is 60 kg, resulting in a power density of 830 W/kg—more than double the AE-40 density. In this sense, the power goals of the USABC's AE-10 are more challenging than the AE-40.<sup>5</sup> Of course, these power density goals could be significantly reduced for a blended PHEV design, as with Kromer and Heywood [5], or by allowing a heavier battery, as with EPRI.

### 3.2 Energy capacity

Energy capacity goals relate to the amount of energy stored in the batteries and the batteries' energy density; they determine the distance that can be traveled in CD mode and the mass of the battery system. An important distinction is to be made between available and total energy. A battery with 10 kWh of total energy operating with a 65% DOD would have only 6.5 kWh of available energy.

The USABC's AE-10 requires about 4 kWh of available energy, while the AE-40 requires 12 kWh. With the 70% DOD assumed by USABC, these values correspond to battery systems storing total energy of 5.7 and 17 kWh, respectively. EPRI and MIT estimate similar requirements of available energy for the PHEV designs they analyze, indicating that estimates of energy capacity requirements are not as sensitive to differences in assumption (other than range in CD mode) as are power requirements. A common metric of battery energy is energy density, measured as the total Wh/kg of the battery system. The USABC's energy density goals are 93 Wh/kg for the AE-10 and 142 Wh/kg for the AE-40. MIT's goal is within this range (133 Wh/kg), while EPRI's goals are much lower (37–59 Wh/kg)—the latter difference is again largely due to the much heavier battery mass.

### 3.3 Life

With use and over time, battery performance can substantially degrade, including power, energy capacity, and safety. Table 16.1 portrays three key measures of battery longevity. First, calendar life is the ability of the battery to withstand degradation over time, which

<sup>5</sup> Conceptually, it is possible to combine multiple electricity storage technologies in a single vehicle, for example, batteries with good energy characteristics could be combined with ultracapacitors with good power characteristics. So a PHEV could use batteries primarily to provide energy and ultracapacitors to provide short bursts of power. This possibility is not discussed further in this chapter.

may be independent of how much or how hard the battery is used. The USABC goal for batteries for both their PHEVs is 15 years at a temperature of 35°C, where exposure to hotter temperatures can accelerate degradation. MIT also targets 15 years of calendar life. EPRI uses a less-ambitious target of 10 years, which they cite as being consistent with previous studies, but also consider a 15-year life.<sup>6</sup> Also note that all of the USABC goals are set for the battery's end of life. In other words, the power and energy goals described in the sections above must apply after 15 years of life regardless of use. If these attributes are expected to degrade over time and/or use, initial values will have to be even higher than the stated goals.

Second, deep cycle life is the number of discharge–recharge cycles the battery can perform in CD mode. For example, Fig. 16.2 portrays one complete deep discharge, starting at 90% SOC, ending at 25% SOC; recharging back to 90% SOC would complete one full cycle. The USABC's battery goal is 5,000 deep cycles. This goal assumes one complete deep cycle each day, 330 days of the year, for the 15-year life span of the vehicle. Other studies set less-ambitious targets; MIT states 2,500 deep cycles for the B-30, and EPRI states 2,400 and 1,400 deep cycles for the AE-20 and AE-60, respectively. EPRI's target is lower due to the assumption of shorter life (10 years), whereas MIT's target is based on different assumptions about recharge behavior. One might also consider potential differences in deep cycle goals between different PHEV designs. For example, Kromer and Heywood [5] note that because the charge of a given PHEV-10 will be expended more quickly than that of a given PHEV-30, the PHEV-10 will likely undergo more deep discharge cycles (3,200) than the PHEV-30 (2,500). In considering the USABC goals, an AE-40 may require fewer deep cycles than a comparable AE-10 during the same calendar life.

Third, shallow cycles refer to SOC variations of only a few percent. These smaller variations occur throughout CD and CS mode, as portrayed by the small, rapid fluctuations around the major SOC trend in Fig. 16.2. The battery frequently takes in electric energy from the gasoline engine via a generator and from regenerative braking, and passes energy to the electric motor as needed to power the vehicle. These frequent shallow cycles cause less degradation than deep cycles, but still affect longevity. The USABC longevity target is 300,000 shallow cycles for both PHEV designs, again much higher than the 175,000 set by MIT, or the 200,000 set by EPRI. Although this range of targets (200,000–300,000) is achievable by current HEVs, in a PHEV most of the shallow cycles would likely occur at a relatively low SOC (e.g. 25%), which can cause relatively more wear on the battery. Thus, USABC goals to produce both 5,000 deep discharge cycles and 300,000 shallow cycles at a low SOC present a formidable challenge for battery manufacturers.

<sup>6</sup>Because passenger vehicles typically last longer than 10 years, a battery with this calendar life would have to be replaced during vehicle life; this could substantially increase consumer costs.

A fourth measure of longevity (not shown in Table 16.1) is the range of temperatures the battery can be subjected to while not in operation, neither charging nor discharging. The USABC target range is  $-46^{\circ}\text{C}$  to  $+66^{\circ}\text{C}$ , which more than covers natural conditions of the continental United States. Most studies do not address temperature effects on battery operation, particularly cold climate effects. We do not further address temperature issues in this chapter, but readers should keep in mind the potential importance of this factor.

### 3.4 Safety

Safety is important because batteries store energy and contain chemicals that can be dangerous if discharged in an uncontrolled manner, such as through short circuits, impacts, overcharging, or high heat [12].<sup>7</sup> Public perception of battery safety for automotive application is an especially large concern after millions of laptop computer batteries were recalled in 2005–2006 due to fire hazard, e.g. [13]. However, in automotive applications, batteries use battery management units that provide a higher degree of safety than typical consumer applications, that is, monitoring cell voltage and temperature, and taking corrective action when necessary. As discussed in the following sections, battery safety depends on battery chemistry, design, and manufacturing quality control.

The USABC's battery goals do not include specific safety objectives, although safety is implied in goals of longevity and operation temperature. Safety is typically measured through abuse tolerance tests. Doughty and Crafts [14] outline several abuse tests to be performed on batteries, including mechanical crushing, perforation, external short circuit, overcharging, overheating, fuel fire immersion, and water immersion. In each test, the battery's response is recorded and assessed with regard to longevity and threats to personal safety. Doughty and Crafts [14] state that the magnitude of the response, for example, mild or catastrophic, should be considered in light of the likelihood of the abuse condition to occur in normal operation. For example, Kalhammer et al. [12] outline the results of such abuse tests on one particular battery, where responses range from "no event" to "smoke (venting)" or "flame (low rate combustion)." However, the overall rating of battery safety appears to be subjective, where Doughty and Crafts [14] suggest that the abuse tests they outline can be used to help determine what is "acceptable." Thus, we do not portray safety goals in Table 16.1 – the USABC vaguely state their target as one of "acceptability."

<sup>7</sup> We note that automotive consumers have become habituated to handling toxic, carcinogenic, mutagenic, and highly flammable fuels, i.e., gasoline and diesel. This is not to diminish the safety challenges of batteries, but to note that so far as we know, they are challenges, not insurmountable barriers.

### 3.5 Costs

Battery cost is thought to be one of the most crucial factors affecting the commercial deployment of electric-drive technologies [12]. The USABC cost goals are \$1,700 and \$3,400 for the AE-10 and AE-40 battery packs, respectively, under a scenario where battery production has reached 100,000 units per year [10]. These goals are stated as costs to the original equipment manufacturers (OEMs) and do not include the markup that would be passed on to consumers. (Estimates of the markup on advanced automotive batteries from OEM to consumer range from 25–33% [5].) To facilitate comparison, battery cost is commonly measured in dollars per total kWh (not just available kWh), which equates to \$300/kWh for the AE-10 and \$200/kWh for the AE-40. In the MIT analysis, a value of \$320/kWh is assumed to be required for the commercialization of a B-30. In either analyses, these cost targets are much lower than current prices; the USABC estimates that, in general, current advanced battery costs range from \$800/kWh to \$1,000/kWh or higher.

### 3.6 Summary of trade-offs

This section has described the five main attributes considered by the USABC for PHEV batteries: power, energy capacity, life, safety, and cost. Specific goals used by other analysts for each attribute differ from the USABC's, depending on assumptions about PHEV design, drive cycle, vehicle and battery weight, and recharge behavior. USABC goals are more demanding than most studies, largely due to the stated target of 10 and 40 miles of AE range (with no gasoline use) and restricted battery weight. Many of these goals would be decreased for less-demanding PHEV drivetrain specifications, such as the use of blended operation in CD mode.

There are inherent trade-offs among the attributes discussed above. The USABC presents a combination of goals for battery developers to work toward. Some existing battery technologies can achieve some of these goals. However, meeting all goals simultaneously is far more challenging. For example, higher power, that is, for USABC's AE-10, can be achieved through the use of thinner electrodes. However, these designs tend to reduce cycle life and safety, while increasing material and manufacturing costs. In contrast, high-energy batteries, that is, for USABC's AE-40, use thicker electrodes that increase safety and life, but reduce power density. Thus, it can be very difficult to meet ambitious targets for both power and energy density in the same battery, let alone also meeting the additional considerations of longevity, safety, and cost. Understanding these trade-offs is key to understanding the complexities and challenges of PHEV battery development. Next, we discuss the current state of battery technologies in light of USABC's PHEV goals.

## 4. BATTERY TECHNOLOGIES

In this section we discuss two broad categories of battery chemistries: NiMH and Li-ion. These and other battery chemistries are compared in Fig. 16.3 using Ragone plots modified from Kalhammer et al. [12]. The curves represent the trade-offs inherent in designing batteries for high-energy or high-power applications. Onto these Ragone curves we have plotted USABC, MIT, and EPRI battery requirements presented in the previous section (black circles). The diamonds represent the performance of four PHEV batteries tested at UC Davis: one NiMH and three Li-ion.

To understand Fig. 16.3, we must make an important distinction between the performance attributes of a battery pack and an individual cell. The PHEV goals discussed in Section 3 (USABC, MIT, and EPRI) were reported for a battery pack. However, the values represented by the bands in Fig. 16.3 are for an individual battery cell (which is common practice for Ragone plots). The battery pack (or system) designed for a particular PHEV consists of many individual battery cells, plus a cooling system, inter-cell connectors, cell-monitoring devices, and safety circuits. The added weight and volume of the additional components reduce energy and power density of the pack relative to the cell. In addition, the inter-cell connectors and safety circuits of a battery pack can significantly increase resistance, decreasing the power rating from that

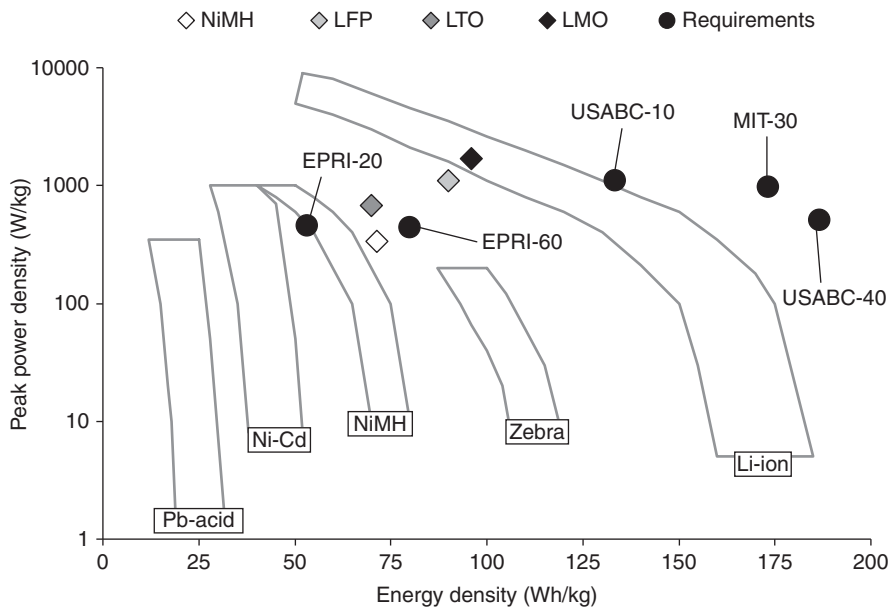


**Figure 16.3** Battery requirements from USABC, MIT, and EPRI, and battery cell potential (Ragone Plots from [12]). See Table 16.3 for acronyms. (Battery specifications are taken from Table 16.1, assuming: (1) motor efficiency of 85%, (2) packaging factor of 0.75, and (3) 80% battery DOD).

achievable by a single cell. Thus, when applying cell-based ratings to a battery pack, and vice versa, a packaging factor conversion must be applied. The packaging factor for energy density is the ratio between the combined weights of the cells to the weight of the entire battery pack. This factor varies across battery designs in the range of 0.6–0.8. There is typically a larger reduction for power density—and thus a smaller packaging factor—than energy density due to added resistance, in addition to the added weight. We assume an optimistic packaging factor of 0.75 for each conversion. Although we have taken efforts to clarify these distinctions, readers are cautioned that in much of the battery literature, cell and pack level values are not clearly distinguished.

The various PHEV requirements in Fig. 16.3 illustrate the implications for differing vehicle assumptions on battery performance goals and resulting conclusions about capabilities of broad classes of battery chemistries to meet those goals. Whereas EPRI's analysis suggests the performance goals for an AE-20 is achievable by current NiMH technology, the goals of the USABC and MIT are beyond even current Li-ion technology capabilities. In any case, it is clear that lead-acid, nickel-cadmium (NiCd), and sodium-nickel chloride (ZEBRA) technologies are not likely to meet requirements for even less-ambitious PHEVs. In contrast, Li-ion battery technologies hold promise for achieving higher power and energy density requirements. Thus, it appears that while NiMH could be used for lower performance PHEV designs (e.g. blended operation with lower CD range), only a battery chemistry with the energy and power density capabilities of Li-ion can meet USABC requirements for PHEVs with AE range. NiMH and Li-ion chemistries are further described next.

#### 4.1 Nickel-metal hydride

NiMH batteries are used for most HEVs currently sold in the United States. The primary advantage of this chemistry is its proven longevity in calendar and cycle life, and overall history of safety [12]. The primary drawbacks are limitations in energy and power density, and low prospects for future cost reductions [6]. For illustration, Fig. 16.3 presents the attributes of one NiMH PHEV battery tested at UC Davis. The NiMH cell falls far short of the power density requirements for USABC's AE-10 (333 versus 1,110 W/kg), as well as the available energy density requirements of USABC's AE-40 (72 versus 190 Wh/kg).

Although Fig. 16.3 only provides an illustrative snapshot of one NiMH battery chemistry, it does demonstrate power and energy limitations. More importantly, battery researchers generally report that there is relatively little room for further improvement [5, 6, 12]. Not only are energy and power densities unlikely to improve much further (due to limitations shown in Fig. 16.3), but NiMH costs are not expected to drop much further with increased production. Kalthammer et al. [12] estimate that at 100,000 units of production per year, NiMH battery prices may fall as low as \$530/kWh for a AE-10 and \$350/kWh for a AE-40. These forecasts are far from reaching USABC's goals of \$300/kWh and \$200/kWh, respectively.

## 4.2 Lithium-ion

In contrast to NiMH, Li-ion technology has the potential to meet the requirements of a broader variety of PHEVs. Fig. 16.3 illustrates the relative advantage of Li-ion chemistry. While still falling short of the ambitious power targets of the USABC's AE-10, and the energy targets of the AE-40, the lithium manganese spinel (LMS) battery has more than quadruple the power density and more than 30% greater energy density than the NiMH battery.

Again, more important than this illustrative snapshot is the long-term prospects for improvements to Li-ion batteries. The potential power and energy density of Li-ion batteries are much higher than other chemistries, indicating there is more room for development. Also, Li-ion battery costs are predicted to fall as low as \$395/kWh for a AE-10 and \$260/kWh for a AE-40, with 100,000 units of production [12]. Although still not sufficient to meet USABC's goals, such costs would be a substantial improvement over NiMH batteries. Note, however, that not all analysts are so optimistic about low costs; Anderman [6] expects Li-ion batteries to maintain costs around \$600/kWh even with increased production.

Although Li-ion batteries hold promise in power and energy density, and perhaps cost, Kalhammer et al. [12] describe potential drawbacks in longevity and safety. High chemical reactivity provides a greater threat to calendar life, cycle life, and safety compared to NiMH batteries. For instance, sustained high rate or voltage overcharge and shorting have potential to trigger thermal runaway, cell venting, and even burning of the electrolyte solvent and graphite. Thus, Li-ion batteries require a greater degree of control over cell voltage and temperature than do NiMH batteries [12].

Technological advances appear to be overcoming longevity problems; abuse testing of some Li-ion batteries demonstrated resistance to catastrophic failure [12]. Still, Anderman [6] states that Li-ion batteries remain far from being "proven" technologies for automotive applications. This statement was supported by Toyota's decision to halt deployment of a Li-ion battery for the third-generation Prius model (HEV) due to safety concerns; the new Prius still uses a NiMH battery pack [15]. Thus, safety and reliability remain relatively uncertain for Li-ion batteries, and further development and testing is required before mass market launch is likely.

In summary, of the battery chemistries presented in Fig. 16.3, Li-ion technologies are most capable of meeting PHEV performance requirements. In particular, Li-ion appears to be the only chemistry that is currently suited for more demanding PHEV designs, such as the AE-10 and AE-40 goals set by the USABC. NiMH batteries could play an interim role in less-demanding blended-mode designs, but it seems likely that falling Li-ion battery prices may preclude even this role. For these reasons, most current attention for PHEV battery development is on Li-ion technologies. However, the Li-ion development process is multidirectional, and the next section provides an illustrative discussion of several specific Li-ion battery chemistries that are in various stages of development.





## 5. LI-ION BATTERY PROSPECTS

Li-ion batteries can be constructed from a wide variety of materials, allowing battery developers to pursue several different paths. Specific battery chemistries are typically named according to the material used for the positive electrode, although the negative electrode material can also be a distinguishing factor. Li-ion battery designs also vary by electrolyte, packaging, structure, and shape [16]. The main Li-ion cathode material used for consumer applications (e.g., laptop computers and cell phones) is lithium cobalt oxide (LCO). However, due to safety concerns with using this chemistry for automotive applications, several alternative chemistries are being piloted, developed, or researched for PHEVs, including: lithium nickel, cobalt, and aluminum (NCA), lithium iron phosphate (LFP), lithium nickel, cobalt, and manganese (NCM), lithium manganese spinel (LMS), lithium manganese oxide (LMO), lithium titanium (LTO), and manganese titanium (MNS).

Table 16.2 presents battery performance ratings from tests of three of these chemistries: LFP, LMO, and LTO. The performance attributes among these batteries—as with batteries in general—yield trade-offs between power and energy density, as well as safety and longevity (not depicted in Fig. 16.3). The higher voltage batteries have higher energy density, and generally higher range for power density (although power is also affected by other design aspects). However, battery research is exploring newer chemistries with relatively low voltage, such as LTO, to meet battery safety and longevity goals.

A broader summary of Li-ion technologies is presented in Table 16.3. Table 16.3 is intended solely as an illustrative present snapshot of several key Li-ion technologies, and not as an exhaustive or definitive analysis of the present state of the art or prospects for future development. Instead, these brief descriptions portray the complexity and variety

**Table 16.2** Comparison of battery cell performance (testing by A. Burke at UC Davis, April 2008)

Technology type	Voltage range (V)	Cell energy density (Wh/kg)	Cell power density (W/kg)
Nickel-metal hydride (NiMH) <sup>a</sup>	1.3–1.0	72	333 <sup>b</sup>
Lithium iron phosphate (LFP)	3.6–2.5	90	1,000–1,100 <sup>c</sup>
Lithium manganese oxide (LMO)	4.0–3.0	96	1,000–2,000 <sup>c</sup>
Lithium titanium (LTO)	2.8–1.5	70	600–2,400 <sup>c</sup>

<sup>a</sup> The tested NiMH battery was designed for a HEV application, but for the purpose of this comparison, we assume the NiMH is optimized for PHEV or EV application. Thus, we assume higher energy density than HEV application and lower voltage to increase peak power (while lowering peak power efficiency as explained in the point below).

<sup>b</sup> Pulse power at 60% efficiency, at 50% SOC. At 90% efficiency, tested peak power is 90 W/kg.

<sup>c</sup> Pulse power at 90% efficiency, 50% state of charge.



**Table 16.3** Illustrative “snapshot” of PHEV battery chemistries (qualitative assessment by A. Burke at UC Davis, August 2008)

<b>Name</b>	<b>Description</b>	<b>Automotive Status</b>	<b>Power</b>	<b>Energy</b>	<b>Safety</b>	<b>Life</b>	<b>Cost</b>
NiMH	Nickel-metal hydride	Commercial production	Low	Low	High	High	Mod.
LCO	Lithium cobalt oxide	Limited production	High	High	Low	Low	High
NCA	Lithium nickel, cobalt and aluminum	Limited production	High	High	Low	Mod.	Mod.-High
LFP	Lithium iron phosphate	Pilot	Mod.-High	Mod.	Mod.-High	High	Low
NCM	Lithium nickel, cobalt and manganese	Pilot	Mod.	Mod.-High	Mod.	Low	High
LMS	Lithium manganese spinel	Development	Mod.	Low-Mod.	Mod.-High	Low-Mod.	Low-Mod.
LMO	Lithium manganese oxide	Development	High	Mod.-High	Mod.-High	Mod.-High	Mod.
LTO	Lithium titanium	Development	High	Low	High	High	Mod.
MNS	Manganese titanium	Research	High	Mod.	High	Unknown	Mod.

of Li-ion battery development, where the attributes of one particular technology may not represent Li-ion technology in general. Consistent with the USABC goals described throughout this paper, Table 16.3 presents qualitative ratings of the five main attribute categories: power, energy, safety, life and cost attributes. Note that because each battery manufacturer may follow different design strategies, it may be inappropriate to generalize our qualitative ratings for a given chemistry to all manufacturers working with that chemistry.

Table 16.3 further demonstrates the many inherent trade-offs in battery development. A single battery has yet to meet all relevant USABC PHEV goals. For instance, higher power battery chemistries have higher open circuit voltage, which also reduces life and safety. Chemistries with increased life and safety tend to limit cell voltage, which reduces power and energy capacity. The challenge is to find an appropriate balance for a particular application.

To complement Table 16.3, we summarize recent literature and assessments at UC Davis on these Li-ion chemistries as follows:

1. LCO is the most common Li-ion chemistry for non-vehicle consumer applications, but is generally not suitable for automotive applications due to concerns with safety, longevity, and cost [5, 17]. Toyota delayed the use of this chemistry in electric-drive development due to safety concerns [15].
2. Lithium NCA is currently being tested by JCS, GAIA, Matsushita, and Toyota. NCA batteries perform quite well in terms of power density, energy density, and longevity [12, 18]. However, this technology faces limitations in safety and cost [18].
3. LFP chemistries are in testing stages with A123, Valence, and GAIA. LFP technologies are thought to perform similar to NCA batteries, but with a higher degree of safety due to a more stable electrode material with less susceptibility to thermal runaway and other threats [17, 18] and potential for lower costs [5,12]. However, Kromer and Heywood [5] and Anderman [16] note there are still energy density challenges for PHEV applications.
4. Lithium NCM chemistries are being tested by Litcel, Kokam, and NEC Lamillion. Kalhammer et al. [12] indicate that NCM has lower performance than NCA and LFP batteries in terms of power, energy, safety, and life. Testing at UC Davis suggests that the high voltage of NCM holds potential for high energy density (see e.g. Table 16.3).
5. LMS is currently in development stages with GS Yuasa, Litcel, NEC, and EnerDel. Although this chemistry has limitations in power and energy density, it holds high potential for safety and low cost, although longevity is still a concern [12].
6. LMO is in development with Kokam, Enerdel, EIG and GAIA, and holds potential for higher power and energy density.
7. LTO is in development stages with Altairmano and Enerdel. LTO holds potential for high safety and longevity, but is limited in energy and affordability [18].
8. MNS chemistries are still in early research stages. These chemistries are thought to hold potential for excellent power, energy density, and safety, at moderate costs [18].



## 6. WHAT PHEV COULD BE MADE WITH NEAR-TERM BATTERY TECHNOLOGIES?

While the above review indicates that present battery technologies are not yet capable of meeting USABC or similarly ambitious PHEV-related requirements, we now turn to the question: How close are we to meeting these goals with near-term battery technologies? To explore this question, we model the performance capabilities of a PHEV version of a vehicle that is already 1) popular in the marketplace and 2) designed for high efficiency, i.e., a plug-in Toyota Prius.

The potential PHEV performance capabilities of the four battery chemistries portrayed in Table 16.2 were assessed with vehicle simulations using ADVISOR. The simulations make two assumptions that deviate from those used by USABC, MIT, and EPRI: the first produces lower demands on PHEV batteries, the second, higher demands. First, the base-simulated vehicle specifications are those of a 2004 Toyota Prius (Table 16.4); the road-load inputs (rolling resistance and drag coefficient) were selected for improved fuel efficiency relative to the midsize sedans (and one crossover SUV) analyzed to set the USABC, MIT, and EPRI battery requirements. Second, we use the US06 drive schedule to approximate realistically aggressive driving conditions and therefore to place higher power demand on batteries. For comparison, we also portray results using the UDDS drive schedule, which is more frequently applied by researchers despite being a less realistic representation of US driving behavior. To aid comparison of our simulations to the battery requirements discussed in Section 3, we held battery mass constant at the values specified by the USABC, i.e., 60 and 120 kg.

Table 16.5 summarizes the simulation results. Under the US06 drive cycle, a Prius-like PHEV with a 60-kg NiMH battery is simulated to achieve 98 miles per gallon (mpg) (not counting the 2.57 kWh of electricity used) for 15 miles in CD mode in blended

**Table 16.4** Toyota Prius modeling parameters for ADVISOR simulations

Specification	Prius
Model year	2004
Transmission	eCVT
Tire radius	41 cm
Engine power	53 kW
Curb weight	1,304 kg
Rolling resistance	0.007
Frontal area	2.16 m <sup>2</sup>
Drag Coefficient	0.26
Drag area	0.56 m <sup>2</sup>

**Table 16.5** PHEV performance with current and near-term battery technologies (ADVISOR simulations by A. Burke and E. Van Gelder at UC Davis, June 2008, Toyota Prius on US06 and UDDS drive cycles)

	Units	NiMH	LFP	LMO	LTO
<b>60 kg battery</b>					
<i>(1) Input values</i>					
Pack peak power	kW	15.0	49.5	76.5	30.6
Pack available energy <sup>a,b</sup>	kWh	2.57	3.24	3.46	2.52
<i>(2) Output performance</i>					
US06 cycle					
CD electricity use	Wh/mile	171	225	175	157
CD range	miles	15.0	14.4	19.7	16.1
CD gasoline use	mpg <sup>c</sup> (l/100 km)	98 (2.4)	3,000 (0.1)	AE (0.0)	425 (0.6)
CS gasoline use	mpg <sup>c</sup> (l/100 km)	44 (5.3)	44 (5.3)	43 (5.5)	43 (5.5)
UDDS cycle					
CD electricity use	Wh/mile	149	126	97	93
CD range	miles	17.0	25.7	35.7	27.1
CD gasoline use	mpg <sup>c</sup> (l/100 km)	800 (0.3)	AE (0.0)	AE (0.0)	AE (0.0)
CS gasoline use	mpg <sup>c</sup> (l/100 km)	67 (3.5)	73 (3.2)	69 (3.4)	71 (3.3)
<b>120 kg battery</b>					
<i>(1) Input values</i>					
Pack peak power	kW	30.0	99.0	153.0	61.2
Pack available energy <sup>a,b</sup>	kWh	5.14	6.48	6.91	5.04
<i>(2) Output performance</i>					
US06 cycle					
CD electricity use	Wh/mile	246	182	169	187
CD range	miles	20.9	35.6	40.9	27.0
CD gasoline use	mpg <sup>c</sup> (l/100 km)	329 (0.7)	AE (0.0)	AE (0.0)	AE (0.0)
CS gasoline use	mpg <sup>c</sup> (l/100 km)	43 (5.5)	44 (5.3)	45 (5.2)	42 (5.6)
UDDS cycle					
CD electricity use	Wh/mile	146	104	97	93
CD range	miles	35.2	62.3	71.2	48.5
CD gasoline use	mpg <sup>c</sup> (l/100 km)	AE (0.0)	AE (0.0)	AE (0.0)	AE (0.0)
CS gasoline use	mpg <sup>c</sup> (l/100 km)	69 (3.4)	71 (3.3)	71 (3.3)	72 (3.3)

<sup>a</sup> Packaging factor assumed to be 0.75.

<sup>b</sup> Depth of discharge assumed to be 80%.

<sup>c</sup> AE refers to all-electric operation (infinite miles per gallon or 0 liters per 100 km).

operation, and 44 mpg in CS mode.<sup>8</sup> At the other end of the power and energy spectrum of the batteries simulated, a 60-kg LMO battery in the same vehicle provides AE operation, that is, infinite gasoline fuel economy for almost 20 miles, and 43 mpg in

<sup>8</sup> In Table 16.5, we report fuel economy in miles per gallon in CD mode without accounting for the electricity from the grid that is also consumed; we report this electricity use separately.

CS mode. Doubling the battery mass to 120 kg does not allow the NiMH PHEV to operate all-electrically; however, all three Li-ion technologies can. In particular, we see that using the Prius specifications, the 120-kg LMO battery meets the USABC performance goal of 40 miles of AE range under a US06 schedule—exceeding that goal by over 30 miles using the less demanding UDDS drive cycle.

These simulations only account for the power and energy requirements, not longevity, safety, and cost. Table 16.3 suggests that for battery life and safety, the LFP or LTO chemistries may be more appropriate than the LMO—at the expense of reduced AE CD range.



## 7. DISCUSSION AND CONCLUSION

Using the USABC's goals for PHEV batteries, we have summarized the state of various battery technologies. Four main highlights can be drawn from this discussion. First, the battery “goals” or “requirements” for a PHEV are contingent on many assumptions. We compared the goals of the USABC to two alternative studies published by researchers from MIT and EPRI. The three sets of goals differ greatly based on different assumptions about CD range, CD operation (AE vs. blended), drive cycle, vehicle mass, battery mass, and other issues. The “true” requirements of PHEV technology will depend on consumers' driving and recharging behaviors as well as their valuation of different PHEV designs and capabilities. In turn, producer and consumer behavior alike can be shaped by government regulation, e.g., California's ZEV mandate. Thus, while the USABC (and others) provides a useful benchmark for the future of PHEV battery technology, there may be a role for less ambitious PHEV designs, such as lower range, blended PHEV designs (e.g., [19,20]), as well as Toyota's demonstration of a PHEV Prius using NiMH. In other words, it may not be necessary that all USABC's goals be met by a specific battery technology before the commercial production or success of PHEVs can occur. However, such advances will be required for more ambitious PHEV designs, if such designs are necessary for market success.

Second, battery development is constrained by inherent trade-offs among the five main battery attributes: power, energy, longevity, safety, and cost. No battery currently meets all of the USABC's PHEV requirements for these attributes. Increasing power density requires higher voltage that reduces longevity and safety and increases cost. Increasing energy density tends to reduce power density. Attempts to simultaneously optimize power, energy, longevity, and safety will increase battery cost. Readers must be careful to understand the complex trade-offs among these attributes and among battery technologies. Certainly we must avoid assembling the best performances from different battery technologies on different drive cycles in different vehicles as an indication of the current state of battery technology.

Third, in meeting the USABC's PHEV battery design goals, Li-ion chemistries are better suited than NiMH. We demonstrate that although a NiMH battery could achieve triple digit fuel economy for 15–20 miles in a vehicle designed for enhanced fuel economy, for example, the Toyota Prius, these performance levels do not meet the PHEV vehicle goals set by the USABC. Only Li-ion can meet the high power and energy density goals specified by USABC for vehicles with AE driving in CD mode. Although a PHEV designed to operate in blended mode will have lower power and energy density goals than the USABC goals, Li-ion technologies are still superior to NiMH in potential for lower cost. However, despite Li-ion's potential, the technology is not yet firmly established for automotive applications, and development must overcome issues of longevity and safety—and the resulting trade-offs with performance—in order to achieve commercial success.

Fourth, Li-ion technology continues to follow multiple paths of development. Table 16.3 illustrates seven such directions, each using different electrode materials in efforts to optimize power, energy, safety, life, and cost performance. In particular, we must not generalize the attributes of one battery, for example, Toyota's concerns about safety with its LCO battery, to all Li-ion batteries. Table 16.3 shows how these attributes can vary substantially among different chemistries. In addition, Table 16.3 also demonstrates the complexity and uncertainty of selecting a single technological “winner” among advanced automotive battery chemistries.

In summary, electric-drive interest groups, including researchers, policymakers, companies, advocates, and critics, should be aware of these fundamental battery issues to facilitate more grounded debates about the present and future of electric-drive vehicles, including plug-in hybrid vehicles.

## ACKNOWLEDGEMENTS

Special thanks to Eric Van Gelder for his work using ADVISOR to produce the PHEV simulation outputs used in this chapter.

## REFERENCES

1. T. Turrentine, K.S. Kurani, *Advances in Electric Vehicle Technology from 1990 to 1995: The Role of California's Zero Emission Vehicle Mandate*, TR-106274, EPRI, Palo Alto, CA, USA, 1996.
2. CARB, 2008 Proposed Amendments to the California Zero Emission Vehicle Program Regulations, California Air Resources Board, Sacramento, CA, USA, 2008.
3. CalCars, All About Plug-In Hybrids (PHEVs). <http://www.calcars.org/vehicles.html>, 2008 (accessed 17.04.2008).
4. EPRI, *The Power to Reduce CO<sub>2</sub> Emissions: The Full Portfolio*, Palo Alto, CA, USA, 2007.
5. M. Kromer, J. Heywood, *Electric Powertrains: Opportunities and Challenges in the U.S. Light-Duty Vehicle Fleet*, LFEE 2007-03 RP, Sloan Automotive Laboratory, Massachusetts Institute of Technology, Cambridge, MA, USA, 2007.
6. M. Anderman, Presentation at Society of Automotive Engineers (SAE) 2008 Hybrid Vehicle Technologies Symposium, San Diego, USA, 2008.
7. K.S. Kurani, R.R. Heffner, T. Turrentine, 23<sup>rd</sup> International Electric Vehicle Symposium and Exposition (EVS-23), Anaheim, USA, 2007.

8. J. Gonder, A. Simpson, *WEVA Journal* 1 (2007) 1.
9. CARB, Final Regulation Order: The 2003 Amendments to the California Zero Emission Vehicle Regulation, California Air Resources Board, Sacramento, CA, USA, 2003.
10. A. Pesaran, T. Markel, H. Tatara, D. Howell, 23<sup>rd</sup> International Electric Vehicle Symposium and Exposition (EVS-23), Anaheim, USA, 2007.
11. R. Graham, Comparing the Benefits and Impacts of Hybrid Electric Vehicle Options, Report #1000349, EPRI, Palo Alto, CA, USA, 2001.
12. F. Kalhammer, B. Kopf, D. Swan, V. Roan, M. Walsh, Status and Prospects for Zero Emissions Vehicle Technology: Report of the ARB Independent Expert Panel 2007, Prepared for State of California Air Resources Board, Sacramento, CA, USA, 2007.
13. J. Fahey, Remember the Pinto?, *Forbes*, October 16th, 2006.
14. D. Doughty, C. Crafts, FreedomCAR. Electrical Energy Storage System. Abuse Test Manual for Electric and Hybrid Electric Vehicle Applications. 2005-3123, Sandia National Laboratories, Albuquerque, NM, USA, 2005.
15. N. Shirouzu, Toyota puts off new type of battery for next prius, *The Wall Street Journal*, June 14th, (2007), pA14.
16. M. Anderman, 7th Advanced Automotive Batteries Conference, Long Beach, USA, 2007.
17. A. Chu, International Electric Vehicle Symposium and Exposition (EVS-23), Anaheim, USA, 2007.
18. P. Nelson, K. Amine, A. Rousseau, H. Yomoto, 23<sup>rd</sup> International Electric Vehicle Symposium and Exposition (EVS-23), Anaheim, USA, 2007.
19. C. Shiao, C. Samaras, R. Hauffe, J. Michalek, *Energy Policy* 37 (2009) 2653.
20. J. Axsen, K.S. Kurani, A. Burke, Are batteries ready for plug-in hybrid buyers?, *Transport Policy* 17 (2010) 173.



# Battery Size and Capacity Use in Hybrid and Plug-In Hybrid Electric Vehicles

Paul Albertus<sup>1</sup> and John Newman

Department of Chemical Engineering, <sup>1</sup>University of California, Berkeley, CA 94720, USA

## Contents

1. Introduction	429
2. Defining the Maximum Pulse-Power Capability	431
3. A Simple Model for Battery Size and Capacity Use	433
3.1 Defining a linear pulse-power capability	433
3.2 Applications of the simple model	436
4. A Combined Model for Battery Size and Capacity Use	441
4.1 Cell chemistries studied	442
4.2 Cell-sandwich design and performance	443
4.3 Battery model	447
4.4 Vehicle model	448
4.5 Operating configurations and driving cycle	449
4.6 Model limitations	451
4.7 Results for HEV operation	451
4.8 Results for PHEV operation	453
4.9 Pulse-power capability in a flat-potential system	457
5. Conclusions	458
Acknowledgements	459
Terminology	459
References	461



## 1. INTRODUCTION

Two of the main challenges that hinder the growth of the hybrid electric vehicle (HEV) and plug-in hybrid electric vehicle (PHEV) technologies are cost and the reduced cargo space that results from the inclusion of a large battery in a vehicle. Cost and size are linked; in general, a larger battery costs more. Thus, there is significant pressure to use a battery that, while meeting performance requirements, is as small as possible. One way to achieve a smaller battery is to find a way to increase the capacity use [1]. This could be achieved with the use of better control algorithms or with a chemistry that provides a

<sup>1</sup> Corresponding author: [albertus@berkeley.edu](mailto:albertus@berkeley.edu)



relatively flat pulse-power capability. Several battery chemistries are either in use or being considered for use in HEVs and PHEVs, including the nickel–metal hydride (Ni/MH) and lithium ion chemistries. Many types of negative- and positive-electrode materials may be used to make a lithium-ion battery, and in this chapter we relate the fundamental properties of a pair of electrode materials to the size of a battery required for a particular application and the fraction of the capacity in the battery that can be accessed during a given driving cycle.

There have been direct measurements of capacity use in the model year 2001 Toyota Prius and the model year 2000 Honda Insight. Kelly et al. connected these vehicles to a chassis dynamometer and measured the state of discharge (SOD) during a variety of driving segments [2]. They found that the Insight limited the capacity use to a maximum of 60% of the rated capacity, while the Prius limited it to 40%. While the Prius used an algorithm to return the SOD to approximately 45%, the Insight did not have a target SOD to which the control system actively returned the battery. However, while the SOD could range by up to 60% (Insight) or 40% (Prius), during normal use it varied by only a few percent. The larger SOD range occurred only when the dynamometer was used to simulate a large incline or decline. In these cases, the driving cycle influenced the capacity use.

Here, we focus on three main electrode properties: the specific capacity (in mAh/g), the magnitude of the cell equilibrium potential (in V), and the shape of the equilibrium potential (in particular, whether it is flat or sloped). Fig. 17.1 shows the equilibrium potential as a function of the specific capacity for several lithium-ion positive-electrode materials. Different materials have a different specific capacity within a potential range set by the electrolyte stability window, a different magnitude of the equilibrium potential, and a different shape of the equilibrium potential. We show a similar plot for lithium-ion

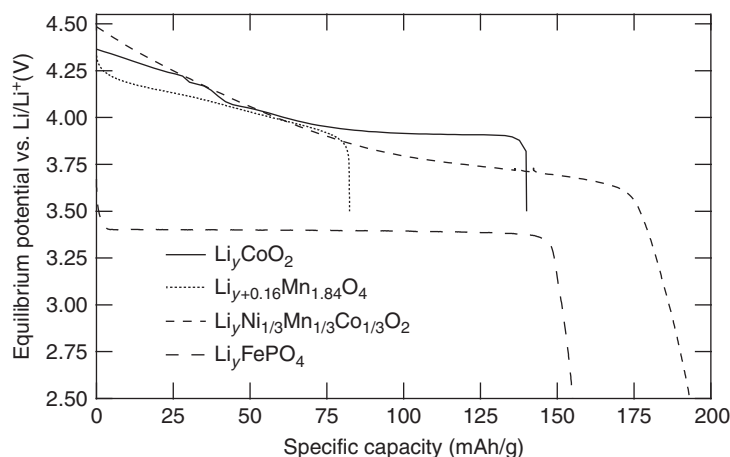


**Figure 17.1** Equilibrium potentials of several positive-electrode materials for a lithium-ion battery.

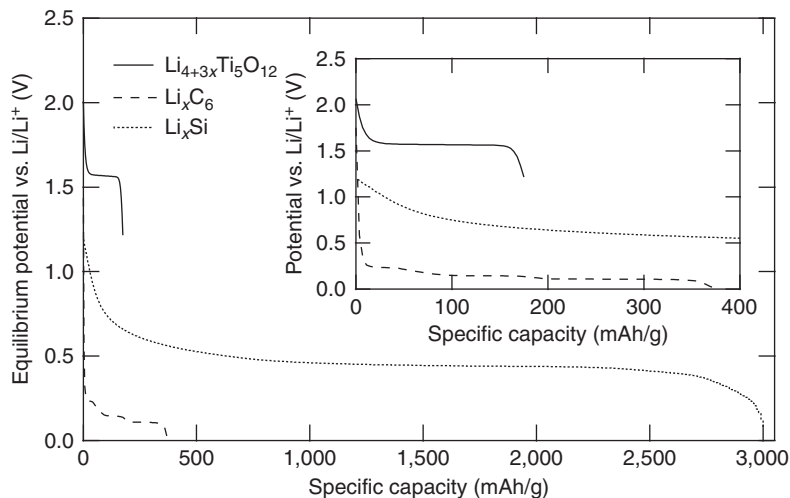


**Figure 17.2** Equilibrium potentials of several negative-electrode materials for a lithium-ion battery. The inset shows a magnification of the equilibrium potentials of the  $\text{Li}_{4+3x}\text{Ti}_5\text{O}_{12}$  and  $\text{Li}_x\text{C}_6$  materials. The  $\text{Li}_x\text{Si}$  material is still in development and typically exhibits a hysteresis between charge and discharge even at a very low rate [15].

negative-electrode materials in Fig. 17.2. The main goal of this chapter is to show how the differences evident between electrode materials in Figs. 17.1 and 17.2 affect battery size and capacity use; we also focus on the pulse-power capability.

The chapter has two main parts: one is a simple battery model (Section 3) and the other is a combined battery and vehicle model (Section 4), but both treat battery size and capacity use [3, 4]. The purpose of the simple model is to show the relationships among the major design variables, and to do this it neglects the details of actual battery operation. The model that combines a detailed battery model with a simple vehicle model includes the details and complexities. The models show that a large battery energy and maximum pulse-power capability decrease battery size and increase capacity use, but the influence of the shape of the equilibrium potential is more subtle. In particular, for a cell with a flat equilibrium potential, there is no driving force for the relaxation of concentration gradients through the depth of the electrodes. The persistence of concentration gradients can reduce performance by shifting the current distribution and resulting in more polarization for consecutive charge or discharge pulses.



## 2. DEFINING THE MAXIMUM PULSE-POWER CAPABILITY

Given the variable loads typical of a drive cycle, a battery in an electric-powered vehicle will experience a series of pulse discharges (for acceleration) and charges (for regenerative braking). Thus, in considering the performance of a battery for an

electric-powered vehicle, the pulse-power capability should be measured, and a method for this has been established by the Department of Energy (DOE) [5]. The method is called the hybrid pulse-power characterization (HPPC) protocol. Here are the major steps defined by the protocol:

1. Find the capacity of the cell (in Ah) for a 1-h discharge.
2. Fully charge the cell and allow it to relax.
3. Apply a 10 s constant-current discharge at a given C rate (e.g., 10C), recording the potential as a function of time.
4. Allow the cell to relax for 40 s.
5. Apply a 10 s constant-current charge at a C rate that is 0.75 of the discharge C rate, recording the potential as a function of time.
6. Discharge the cell at the 1C rate for a given SOD increment.
7. Allow the cell to relax for 1 h.
8. Repeat until the lower cutoff potential is reached.

From the pulse discharge and charge steps, a resistance can be defined by dividing the difference in potential between the start (before current is applied) and the end of the pulse by the applied current. With this resistance value, the maximum pulse-power capability is defined using the voltage window between the relaxed potential and either the upper (for charge) or lower (for discharge) cutoff potential. The relaxed value of the potential used in the resistance calculation is that after the 1 h relaxation for discharge and after the 40 s relaxation for charge. That is:

$$\frac{P_{\text{discharge}}}{A} = V_{\text{min}} i = V_{\text{min}} \left( \frac{U - V_{\text{min}}}{R} \right) \quad [17.1]$$

$$\frac{P_{\text{charge}}}{A} = V_{\text{max}} i = V_{\text{max}} \left( \frac{U - V_{\text{max}}}{R} \right) \quad [17.2]$$

Here,  $P$  is the pulse-power capability,  $A$  is the separator area of the cell,  $i$  is the current density,  $V_{\text{min}}$  is the lower cutoff potential,  $V_{\text{max}}$  is the upper cutoff potential,  $U$  is the equilibrium potential, and  $R$  is the appropriate resistance determined from the HPPC protocol (and in general may have a different value for charge and discharge). The resistance and pulse-power capability typically vary with the SOD, and the pulse-power capability includes contributions from the many physical processes occurring in the cell, including ohmic, kinetic, and diffusion resistances.

The theoretical maximum power of a battery with a linear current-potential relationship is  $U^2/4R$ , but the constraint of a lower cutoff potential means this maximum power is typically not feasible. Because the lower and upper cutoff potentials are often set at a given fraction of the equilibrium potential (and the lower cutoff potential is often set

at 0.55 of the upper cutoff potential for vehicle applications), the pulse-power capabilities may be written as:

$$\frac{P_{\text{discharge}}}{A} = c_1 \frac{U^2}{R} \quad [17.3]$$

$$\frac{P_{\text{charge}}}{A} = c_2 \frac{U^2}{R} \quad [17.4]$$

where  $c_1$  and  $c_2$  depend on the location of  $V_{\text{min}}$  and  $V_{\text{max}}$  relative to  $U$ .



### 3. A SIMPLE MODEL FOR BATTERY SIZE AND CAPACITY USE

#### 3.1 Defining a linear pulse-power capability

In order to facilitate an understanding of the relationships among the key design variables that influence battery size and capacity use, we develop a simple model that uses a linear pulse-power capability. As mentioned above, the pulse-power capability typically depends on the SOD, and because there are many physical processes and properties affecting the pulse-power capability (including transport, kinetic, and thermodynamic properties), it is typically nonlinear. Defining a linear pulse-power capability simplifies the mathematics and clarifies the relationships. We stress that a linear pulse-power capability is not meant to describe that of an actual cell.

First, define a linear pulse-power capability of a battery as

$$\frac{(P_{\text{req}}/A)}{(P/A)^0} = 1 - B\Delta\text{SOD} \quad [17.5]$$

$P_{\text{req}}$  is the maximum power required for a particular vehicle configuration, and numbers have been set by the DOE [6, 7].  $A$  is the total separator area of the battery.  $(P/A)^0$  is an area-specific maximum pulse-power capability and is a property of the unit cell, depending on the chemistry and cell design (e.g., increasing the electrode thicknesses increases  $(P/A)^0$ ).  $(P/A)^0$  is a maximum pulse-power capability for the cell, rather than for charge or discharge individually, and is therefore the point where the charge and discharge pulse-power curves cross, which is typically near a SOD of 0.5.  $B$  is a parameter that defines the slope of the linear pulse-power capability; higher values of  $B$  correspond to more steeply sloped pulse-power capabilities.  $\Delta\text{SOD}$  is the SOD range over which a given power requirement can be met and is equivalent to capacity use. We have plotted Eq. [17.5] in Fig. 17.3 for three arbitrarily selected values of  $B$  ( $B = 0.75, 1.0, \text{ and } 1.25$ ). Three lines start from the middle at  $(P_{\text{req}}/A) = (P/A)^0$  and descend on either side with a slope of  $B$  or  $-B$ . These lines can be interpreted as giving the power

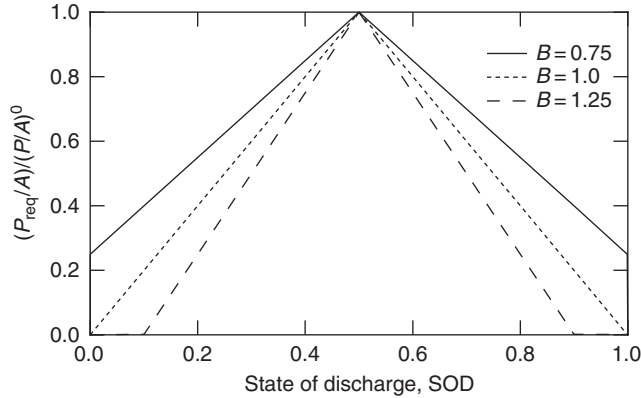


**Figure 17.3** Pulse-power capability of a hypothetical cell. The maximum value of  $(P_{\text{req}}/A)/(P/A)^0$  is equal to 1.0 at state of discharge (SOD) = 0.5, and at that point  $\Delta\text{SOD} = 0$ . The pulse-power capability for  $\text{SOD} < 0.5$  can be considered to be limited by charge, while for  $\text{SOD} > 0.5$  it is limited by discharge.

capability of three hypothetical chemistries with different linear pulse-power capabilities (resulting, for example, from differently shaped equilibrium potentials and resistance curves). Fig. 17.3 shows that as the total separator area,  $A$ , is increased, the SOD range over which the power requirement can be met,  $\Delta\text{SOD}$ , increases.

Second, specify the equivalent-electric range,  $L$ . If  $E'$  is the battery energy required to go a unit distance (J/m), then the energy required from the battery is  $E = E'L$ . This can be approximated by

$$E = E'L = AQ\langle V \rangle \Delta\text{SOD} \quad [17.6]$$

where  $Q$  is the area-specific capacity (in Ah/m<sup>2</sup>) corresponding to  $\Delta\text{SOD} = 1$  and  $\langle V \rangle$  is the average cell potential during the sequence of charge and discharge pulses of a drive cycle and is constrained between  $V_{\text{max}}$  and  $V_{\text{min}}$ . It can be approximated by  $U$ , assuming that the battery receives both charge and discharge pulses. One can solve these equations for  $A$  and  $\Delta\text{SOD}$  in terms of  $L$ . Substitute

$$A = \frac{P_{\text{req}}/(P/A)^0}{1 - B\Delta\text{SOD}} \quad [17.7]$$

into Eq. [17.6] and solve for  $\Delta\text{SOD}$  to obtain

$$\Delta\text{SOD} = \frac{E'L}{E'LB + Q\langle V \rangle P_{\text{req}}/(P/A)^0} \quad [17.8]$$

or

$$B\Delta\text{SOD} = \frac{x}{1+x} \quad [17.9]$$

where

$$x = \frac{E'LB(P/A)^0}{P_{\text{req}}Q\langle V \rangle} \quad [17.10]$$

Eq. [17.9] looks like a Langmuir isotherm.  $x$  can be considered a dimensionless energy-to-power ratio or, for a given value of  $P_{\text{req}}Q\langle V \rangle$  (i.e., for a given power requirement and area-specific battery energy), can be considered as a dimensionless equivalent-electric driving range. Fig. 17.4 shows a plot of Eq. [17.9]. The curve rises from 0 to 1 as  $x$  goes from 0 to infinity. However, for any curve with  $B < 1$ , say  $B = 0.75$ , draw a horizontal line representing the limit of  $\Delta\text{SOD} = 1.0$ , so that  $B\Delta\text{SOD} = 0.75$ .

Next, consider how the area (expressed in a dimensionless form) depends on  $x$ . By eliminating  $\Delta\text{SOD}$  and solving for  $A$  we arrive at

$$\frac{A}{P_{\text{req}}/(P/A)^0} = 1+x \quad [17.11]$$

However, for  $B < 1$ , a different line prevails for large  $L$ ,

$$\frac{A}{P_{\text{req}}/(P/A)^0} = \frac{x}{B} \quad [17.12]$$

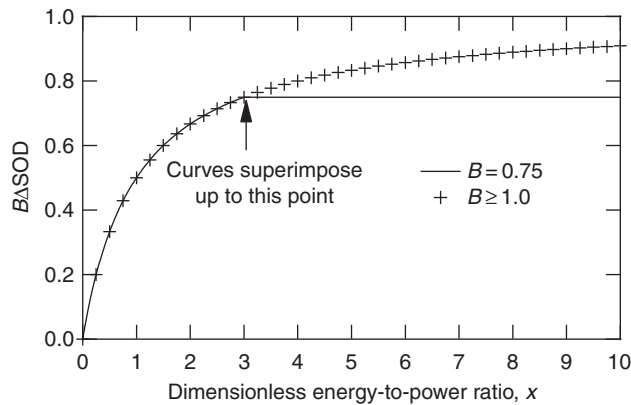


**Figure 17.4** Capacity use as a function of the dimensionless energy-to-power ratio. For  $B \geq 1.0$ , there is a single curve with an asymptote at  $B\Delta\text{SOD} = 1.0$ , while for  $B < 1.0$ , the asymptote for  $B\Delta\text{SOD}$  lies below 1.0. The case of  $B = 0.75$  is shown.

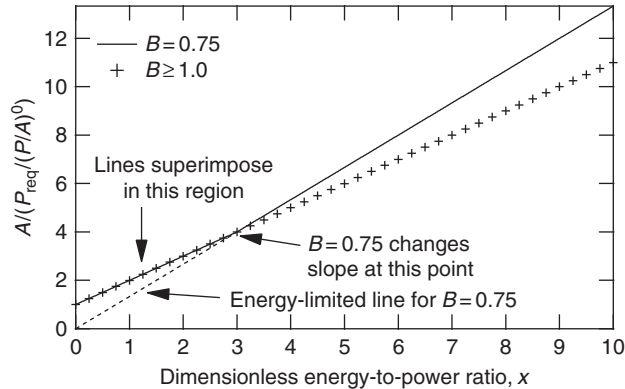


**Figure 17.5** Dimensionless area as a function of the dimensionless energy-to-power ratio. There is a single line for  $B \geq 1.0$ , while for  $B < 1.0$  there is a change of slope at the point  $x = B/(1 - B)$ .

The reason for the difference is that  $\Delta\text{SOD}$  cannot exceed 1.0 and, as shown in Fig. 17.3, this results in a change of slope when  $B < 1$  and  $P_{\text{req}}/A$  goes to zero. Eq. [17.11] for the dimensionless area can be regarded as limited by power and energy simultaneously. However, Eq. [17.12], which passes through the origin, represents a purely energy-limited battery. Fig. 17.5 shows the expected dependence of the quantity  $A/(P_{\text{req}}/(P/A)^0)$  on  $x$ . Two straight lines are shown and the intersection point is at  $x = B/(1 - B)$ . For  $B \geq 1.0$ , there is a single line with an intercept of 1 and a slope of 1. For  $B < 1.0$ , the curve will go through a bend, having a slope of 1 up to the point  $x = B/(1 - B)$ , and thereafter a slope of  $1/B$ .

A brief reiteration of the variables and parameters we are using may be helpful. The total separator area,  $A$ , is the most important variable for the design of a given battery system for a given vehicle application. Other quantities, such as the parameter  $B$  which describes the shape of the pulse-power capability curve, the average cell potential  $\langle V \rangle$ , the maximum pulse-power capability  $(P/A)^0$ , and the area-specific capacity  $Q$  are all parameters that either depend on the cell chemistry or can be changed only by altering the cell design (e.g., electrode thicknesses, volume fractions, particle sizes, etc.).  $\Delta\text{SOD}$  and the driving distance,  $L$ , can be calculated from these quantities using the equations presented above.

### 3.2 Applications of the simple model

In this section, we show how to apply the simple model to common performance representations and practical problems encountered by battery designers. First, consider battery size and capacity use in an HEV. According to United States Council of Automotive Research (USCAR), a minimum power-assist HEV should have a pulse-power capability of 25 kW ( $P_{\text{req}}$ ) and an available energy of 300 Wh ( $E$ ) [6]. To determine the required separator area for an HEV with these specifications, insert the appropriate values

**Table 17.1** HEV capacity use and separator area for three different values of  $B$ , a parameter that characterizes the shape of the pulse-power capability curve, with  $(P/A)^0 = 1625 \text{ W/m}^2$  and  $Q\langle V \rangle = 46.2 \text{ Wh/m}^2$

	$B$		
	0.75	1	1.25
$\Delta\text{SOD}$	0.384	0.351	0.322
$A, \text{ m}^2$	21.6	23.7	25.8

into Eq. [17.11], and to find the value of  $\Delta\text{SOD}$  use Eq. [17.8]. We use a value of  $1625 \text{ W/m}^2$  for  $(P/A)^0$  and a value of  $46.2 \text{ Wh/m}^2$  for  $Q\langle V \rangle$ . These values are based on the following values characteristic of a lithium-ion cell for an HEV application:  $R = 20 \Omega \text{ cm}^2$ ,  $U = \langle V \rangle = 3.8 \text{ V}$ ,  $V_{\min} = 2.5 \text{ V}$ , and  $Q = 12.2 \text{ Ah/m}^2$  (based on an electrode thickness of  $45 \mu\text{m}$ , a volume fraction of active material of 0.45, an available specific capacity of  $150 \text{ mAh/g}$ , and an active material density of  $4.0 \text{ g/cm}^3$ ). Table 17.1 summarizes the results for the separator area and  $\Delta\text{SOD}$ , and Fig. 17.6 shows the  $\Delta\text{SOD}$  values superposed on the pulse-power capability curves. From Table 17.1, we see that a value of  $B$  corresponding to a relatively flat pulse-power capability ( $B = 0.75$ ) results in a smaller required separator area and a larger capacity use. We stress that even for an HEV, both power and energy goals must be met simultaneously, and a change in either requirement results in a different battery size. In this sense, design of a battery for an HEV is qualitatively similar to the design of a battery for a PHEV, with the difference that an HEV battery requires a

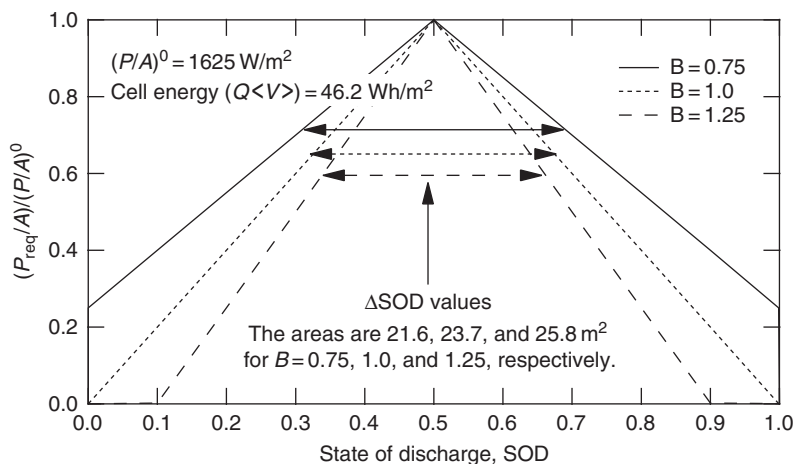


**Figure 17.6**  $\Delta\text{SOD}$  values superposed on the pulse-power capability curves for the HEV goals given by USCAR (an energy of  $300 \text{ Wh}$  and a power of  $25 \text{ kW}$  over the SOD range that the energy requirement is satisfied).



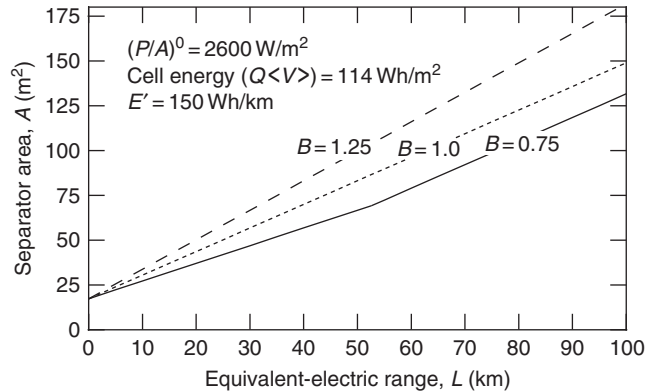


**Figure 17.7** Separator area as a function of the equivalent-electric range for a PHEV. The power requirement is 45 kW, and the energy requirement depends on the equivalent-electric range.

higher power-to-energy ratio. For a PHEV application, the lines on Fig. 17.6 would be drawn at a lower value of  $(P_{\text{req}}/A)/(P/A)^0$ , and the SOD range would be larger.

Second, consider battery size and capacity use in a PHEV. Fig. 17.7 shows a dimensional presentation of Fig. 17.5 for a power requirement of 45 kW, a value of 150 Wh/km for  $E'$ , 2600 W/m<sup>2</sup> for  $(P/A)^0$ , and 114 Wh/m<sup>2</sup> for  $Q\langle V \rangle$ . The latter two values are based on the following values characteristic of a lithium-ion cell for a PHEV application:  $R = 12.5 \Omega \text{ cm}^2$ ,  $U = \langle V \rangle = 3.8 \text{ V}$ ,  $V_{\text{min}} = 2.5 \text{ V}$ , and  $Q = 30.0 \text{ Ah/m}^2$  (based on an electrode thickness of 100  $\mu\text{m}$ , a volume fraction of active material of 0.5, an available specific capacity of 150 mAh/g, and an active material density of 4.0 g/cm<sup>3</sup>). All of the curves have the same intersection with the ordinate, although they each have a different initial slope. The curve for  $B = 0.75$  has a change in slope at a range of approximately 53 km, and after this point the slope of the line for  $B = 0.75$  and that for  $B = 1.0$  are identical. The shift is from the relationship given in Eq. [17.11] to that given in Eq. [17.12]. In Fig. 17.8, we can see the reason for the change in the slope of the  $B = 0.75$  line in Fig. 17.7; at an equivalent-electric range of approximately 53 km, the value of  $\Delta\text{SOD}$  reaches 1.0, which will cause the area to change at a different rate with respect to the equivalent-electric range. The results shown in Figs. 17.7 and 17.8 have implications for battery design; they show that a relatively flat pulse-power capability (small values of  $B$ ) should result in a smaller battery for a given equivalent-electric driving range.

Finally, consider how the magnitude of the cell equilibrium potential and cell resistance influence the capacity use and battery size. These are important considerations as developers consider whether it is better to use high-potential systems that typically form resistive films on the electrode surfaces (the anode in particular) or to shift to lower potential systems without film formation on the electrode surfaces. The value of  $(P/A)^0$ , which is chemistry- and design-specific, can be approximated by Eq. [17.3] or [17.4] for

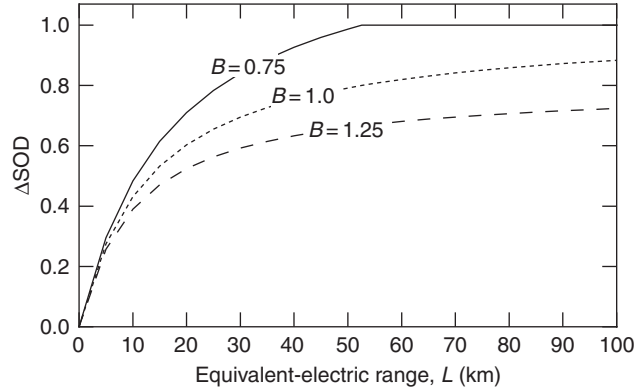


**Figure 17.8** Capacity use as a function of the equivalent-electric range for a PHEV. The power requirement is 45 kW, and the energy requirement depends on the equivalent-electric range.

a value of  $U$  and  $R$  at  $SOD = 0.5$ . Rewriting Eq. [17.10] for  $x$ , and assuming that  $\langle V \rangle = U$ , we find

$$x = \frac{E'LBc_1U}{P_{\text{req}}QR} \quad [17.13]$$

Thus, the dimensionless energy-to-power ratio is proportional to the cell potential,  $U$ , and inversely proportional to the cell resistance,  $R$ . Considering Fig. 17.4, increasing  $U$  while holding  $R$  constant would shift the value of  $B\Delta SOD$  higher, all else equal. Note that doubling the value of  $x$  at low values of  $x$  leads to a larger increase in  $B\Delta SOD$  than a doubling of  $x$  at high values of  $x$ . We can rewrite Eq. [17.8] as

$$\Delta SOD = \frac{E'L}{E'LB + (RQP_{\text{req}}/c_1U)} \quad [17.14]$$

This provides a way to determine the change in the capacity use for a change in  $U$  or  $R$ , all else equal.

Next, how does the area depend on the value of  $U$  and  $R$ ? Substitute Eq. [17.14] into Eq. [17.11],

$$A = \frac{P_{\text{req}}}{(c_1U^2/R)} + \frac{E'LB}{QU} \quad [17.15]$$

Here, we see that both the intercept and the slope depend on the value of  $U$ . Finally, we can solve for the dependence of the capacity use on the area, which results in

$$BASOD = 1 - \frac{P_{\text{req}} R}{c_1 U^2 A} \quad [17.16]$$

Eq. [17.16] can be compared with Eq. [17.5], noting that  $(P/A)^0$  has been rewritten according to Eq. [17.3]. As an example, in Fig. 17.9, we plot a battery with a PHEV design with  $B = 0.75$  (an arbitrary value),  $P_{\text{req}} = 45 \text{ kW}$ ,  $c_1 = 0.225$ , and two sets of values of  $R$  and  $U$ . One set uses  $R = 12.5 \Omega \text{ cm}^2$  and  $U = 3.8 \text{ V}$  so that  $c_1 U^2/R = 2600 \text{ W/m}^2$  (corresponding to a lithium-ion system with a graphite negative electrode), and the other set uses  $R = 7 \Omega \text{ cm}^2$  and  $U = 2.5 \text{ V}$  so that  $c_1 U^2/R = 2010 \text{ W/m}^2$  (corresponding to a lithium-ion system with a  $\text{Li}_{4+3x}\text{Ti}_5\text{O}_{12}$ , negative electrode). In Fig. 17.9A, we see that the cell with the higher value of  $U$  and  $R$  has a smaller initial size and a smaller size at long distances, and Fig. 17.9B shows that it has a larger capacity use for a given separator area. Note that the separator area for  $\Delta\text{SOD} = 0$  corresponds to the minimum separator area.

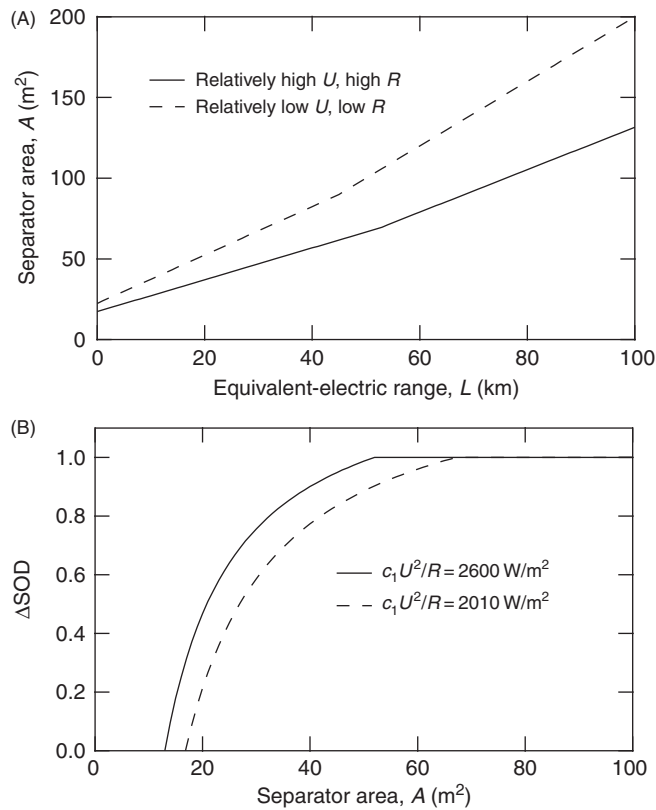


**Figure 17.9** Simple-model design plot for a cell with a PHEV cell design and two values of  $U$  and  $R$  described in the text. (A) shows the relationship between battery size and equivalent-electric range, and (B) shows the relationship between battery size and capacity use.

area required to meet the power requirement for an energy requirement of zero, and in both cases shown here the value of  $\Delta\text{SOD}$  reaches a maximum value of 1 and then levels off. After the value of  $\Delta\text{SOD}$  reaches 1.0, the battery is energy limited in the sense that it has more than enough power to meet the power requirements. Fig. 17.9 clarifies the importance of the parameters  $Q\langle V\rangle$  and  $c_1U^2/R$  for battery design.



#### 4. A COMBINED MODEL FOR BATTERY SIZE AND CAPACITY USE

Now that we have an understanding of the key system variables, we turn to a more detailed model. There has been previous work on operating modes and detailed modeling, and we briefly discuss these here to clarify our methods and assumptions [8–14]. In two important papers on system design, Markel and Simpson discuss the possible operating concepts for PHEVs [9, 10]. These authors argue that if an initial all-electric range is included, the battery must be sized to meet the peak power requirement of the drive cycle, while if the internal combustion engine (ICE) is turned on during high-power-requirement segments, the maximum required power can be reduced by the amount of power supplied by the ICE. Rather than an all-electric mode followed by an HEV mode, the authors advocate the use of a “blended strategy” in which the ICE and battery work together to meet the power demands of the drive cycle at all times. Figs. 17.10 and 17.11 of Kelly et al. clearly depict the difference between the two strategies [2]. The blended strategy, rather than an all-electric range followed by an HEV range, should be considered as a likely development pathway for PHEVs and is the one we use in our model [1].

Fellner and Newman completed a study of battery size and capacity use for HEVs. A key finding of their work was that for an HEV application less than 5% of the capacity of

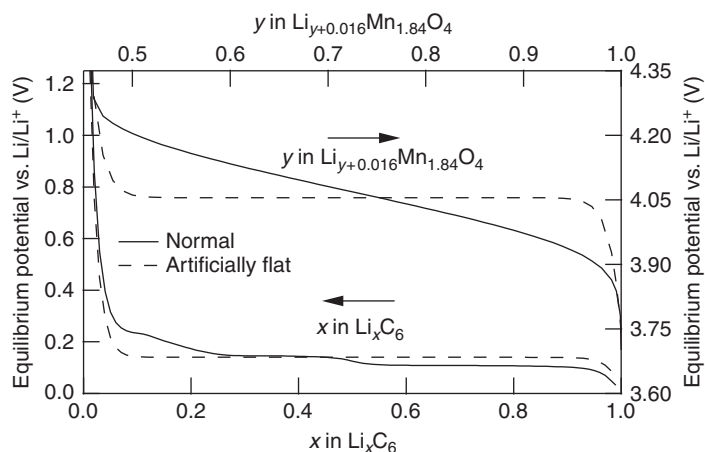


**Figure 17.10** Normal and artificially flat equilibrium potentials for the  $\text{Li}_x\text{C}_6/\text{Li}_{y+0.16}\text{Mn}_{1.84}\text{O}_4$  system.

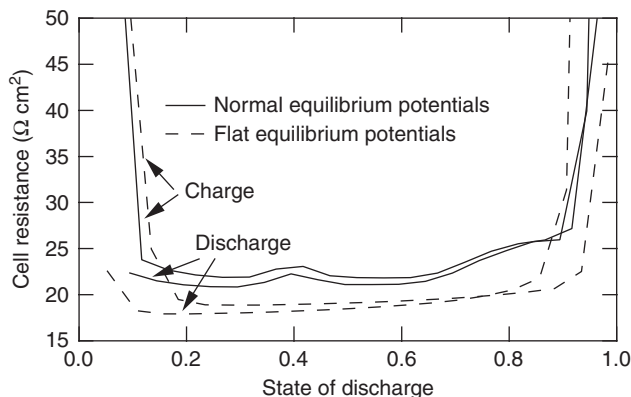


**Figure 17.11** Ten-second pulse resistance of the  $\text{Li}_x\text{C}_6/\text{Li}_{y+0.16}\text{Mn}_{1.84}\text{O}_4$  system, with normal and artificially flat equilibrium-potential curves and the HEV cell parameters. The resistance was calculated using the HPPC method.

the battery is used during a standard driving cycle [8]. These authors used a combined vehicle and battery model, performed separate optimizations for maximum mileage and minimum battery size, and found the resulting separator areas to be very similar. In their study, the battery weight ranged from 62.0 to 112.8 kg, and the thickness of the cell sandwich was around  $425\ \mu\text{m}$ , not including current collectors. The chemistry studied in their work was  $\text{Li}_x\text{C}_6$  (amorphous carbon) versus  $\text{Li}_y\text{Mn}_2\text{O}_4$ . The authors did not consider the effect of cell chemistry on their results, nor did they extend their study to PHEVs, which have received attention only in the past few years. These authors assumed that the ICE would operate at a constant load and the battery would provide all the load leveling. This accounts for the very large batteries they found (for comparison, the weight of the modules in the model year 2005 Prius is around 29 kg). Our approach in this work is different in two ways. First, we optimize our electrode thicknesses for a given power-to-energy ratio (resulting in cell sandwiches between  $150$  and  $265\ \mu\text{m}$ , depending on chemistry and vehicle configuration), while Fellner and Newman chose the thickness of their cell sandwich so it had a low resistance. Second, our power management routine limits the power at the battery leads and assumes that both the battery and the ICE assist with load leveling. As our results show, these two differences lead to an order-of-magnitude reduction in battery size and weight, which is much more realistic for the systems being designed today.

#### 4.1 Cell chemistries studied

In this section, we describe the features of the cell chemistries we chose for the present study: a  $\text{Li}_x\text{C}_6/\text{Li}_{y+0.16}\text{Mn}_{1.84}\text{O}_4$  cell with both normal and artificially flat equilibrium potentials and a  $\text{Li}_{4+3x}\text{Ti}_5\text{O}_{12}/\text{Li}_y\text{FePO}_4$  cell. The  $\text{Li}_x\text{C}_6/\text{Li}_{y+0.16}\text{Mn}_{1.84}\text{O}_4$  cell represents a relatively high-potential/high-resistance cell, while the  $\text{Li}_{4+3x}\text{Ti}_5\text{O}_{12}/\text{Li}_y\text{FePO}_4$

cell represents a relatively low-potential/low-resistance cell. The positive-electrode equilibrium potentials are shown in Fig. 17.1 (the equilibrium potential of  $\text{Li}_y\text{Mn}_2\text{O}_4$  and  $\text{Li}_{\gamma+0.16}\text{Mn}_{1.84}\text{O}_2$  are very similar), and the negative-electrode equilibrium potentials are shown in Fig. 17.2 [16, 17]. For the  $\text{Li}_{\gamma+0.16}\text{Mn}_{1.84}\text{O}_4$  and  $\text{Li}_x\text{C}_6$  materials, we also constructed artificially flat potentials at the midpoint potential, to allow direct comparison between electrode pairs with the same capacity and magnitude of the equilibrium potential, but sloped- versus flat-shaped equilibrium-potential curves. To clarify the shape of the artificially flat potentials, we show them, along with the normal potentials, in Fig. 17.10.

The cell properties and parameters are summarized in Table 17.2, which includes an indication of the source where appropriate. We set the capacity ratio of the  $\text{Li}_x\text{C}_6/\text{Li}_{\gamma+0.16}\text{Mn}_{1.84}\text{O}_4$  cells to 1.1:1 (based on a range of  $x$  values in  $\text{Li}_x\text{C}_6$  of 0–1, and a range of  $\gamma$  values in  $\text{Li}_{\gamma+0.16}\text{Mn}_{1.84}\text{O}_4$  of 0.46–1) and assume a first-cycle capacity loss of 10%, which should be applicable for synthetic graphite. We use an anode film resistance of  $0.005 \Omega \text{ m}^2$  for the  $\text{Li}_x\text{C}_6$  electrode, which results in a cell impedance of approximately  $20 \Omega \text{ cm}^2$  for the HEV cell design, a reasonable value for current state-of-the-art graphite-based cells. Because the potential of the  $\text{Li}_{4+3x}\text{Ti}_5\text{O}_{12}$  electrode is above the potential at which solid-electrolyte interphase (SEI) formation occurs, we use a capacity ratio of 1:1 (based on a range of  $x$  values in  $\text{Li}_{4+3x}\text{Ti}_5\text{O}_{12}$  of 0–0.95, and a range of  $\gamma$  values in  $\text{Li}_\gamma\text{FePO}_4$  of 0.06–1) and assume that there is no first-cycle capacity loss. The volume fraction of inert in each electrode is kept constant relative to the volume fraction of active material. We use a ratio of 1.68:1 (active-to-inert) for  $\text{Li}_x\text{C}_6$  and  $\text{Li}_{4+3x}\text{Ti}_5\text{O}_{12}$  and 2.22:1 (active-to-inert) for  $\text{Li}_{\gamma+0.16}\text{Mn}_{1.84}\text{O}_4$  and  $\text{Li}_\gamma\text{FePO}_4$ . The remaining cell properties come from previous modeling and experimental work on these materials or are set to values deemed appropriate for current state-of-the-art cells [16, 17].

## 4.2 Cell-sandwich design and performance

The electrode thicknesses and liquid-phase volume fractions result from optimizing the cells for a given power-to-energy ratio set in the goals given by USCAR [6, 7]. We use the HPPC method to determine the usable energy as a function of discharge power and vary the electrode thicknesses and porosities to maximize the energy and power, while holding the capacity ratio and power-to-energy ratio constant. This method is described in the USCAR manual and by Stewart et al. [5, 18]. We optimize HEV cells for a power-to-energy ratio of 83.3:1 and PHEV cells for a power-to-energy ratio of 13:1. The power-to-energy ratio for a PHEV will depend on its intended all-electric range; the value of 13:1 used here is for a PHEV with an intended range of 16 km. For simplicity, we do not repeat the optimization for electrode thicknesses and porosities for each range. We simulated the HPPC tests at a 10 C rate for discharge and 7.5 C for charge, with the capacity based on that available at the 1 C rate.

**Table 17.2** Cell properties and parameters used in the combined model

Design-adjustable parameters	$\text{Li}_x\text{C}_6$	$\text{Li}_{y+0.16}\text{Mn}_{1.84}\text{O}_4$	$\text{Li}_{4+3x}\text{Ti}_5\text{O}_{12}$	$\text{Li}_y\text{FePO}_4$
<b>HEV</b>				
Electrode thickness, $\mu\text{m}^a$	44.6	80	66.1	70
Volume fraction electrolyte <sup>a</sup>	0.33	0.3	0.27	0.34
Volume fraction inert filler <sup>b</sup>	0.250	0.217	0.272	0.205
<b>PHEV</b>				
Electrode thickness, $\mu\text{m}^a$	97.1	175	118	125
Volume fraction electrolyte <sup>a</sup>	0.303	0.275	0.25	0.32
Volume fraction inert filler <sup>b</sup>	0.260	0.225	0.280	0.211
<b>Electrode parameters</b>				
Diffusion coefficient in solid, $\text{m}^2/\text{s}$	$9.0 \times 10^{-14}$	$2.5 \times 10^{-15}$	$6.8 \times 10^{-15}$	$3.8 \times 10^{-19}$
Film resistance, $\Omega \text{m}^2$	0.005	0	$1 \times 10^{-5}$	$1 \times 10^{-5}$
Reaction rate constant, $\text{mol}/\text{m}^2\text{-s}$	$1 \times 10^{-3}$	$5 \times 10^{-12}$	$3 \times 10^{-3}$	$5 \times 10^{-14}$
Average particle radius, $\mu\text{m}$	5	1.75	0.1	0.02
Current collector thickness, $\mu\text{m}$	7.5 (Cu)	12.5 (Al)	7.5 (Al)	12.5 (Al)
Specific capacity, $\text{mAh}/\text{g}$	372	154	175	170
Densities, $\text{g}/\text{cm}^3$	2.27	4.40	3.50	3.60
Matrix conductivity, $\text{S}/\text{m}^c$	100	100	100	100
Cell-sandwich parameters	$\text{Li}_x\text{C}_6 / \text{Li}_{y+0.16}\text{Mn}_{1.84}\text{O}_4$ cell	$\text{Li}_{4+3x}\text{Ti}_5\text{O}_{12}/\text{Li}_y\text{FePO}_4$ cell		
Separator thickness, $\mu\text{m}$	25	25		
Cell-sandwich mass, $\text{kg}/\text{m}^2$				
HEV	0.4395	0.411		
PHEV	0.822	0.727		
Cell-sandwich capacity, $\text{Ah}/\text{m}^2$				
HEV	12.7	18.5		
PHEV	28.7	34.1		

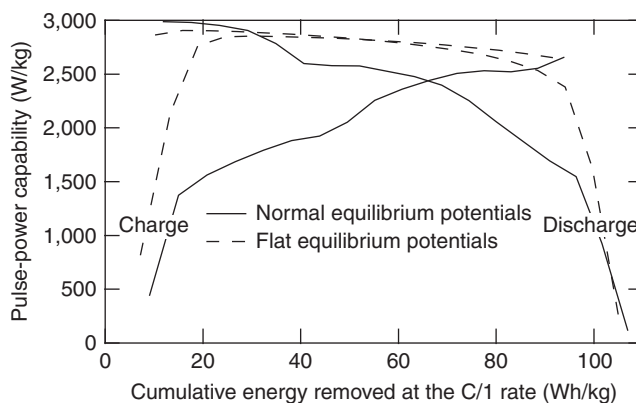
<sup>a</sup> Optimized.<sup>b</sup> Set value (see text).<sup>c</sup> Set arbitrarily high.

We present a sample of our optimization results in Fig. 17.11, which shows the 10 s pulse resistance for the  $\text{Li}_x\text{C}_6/\text{Li}_{y+0.16}\text{Mn}_{1.84}\text{O}_4$  system with both normal and artificially flat equilibrium potentials. There are two lines for each system because a separate calculation is made for the charge and discharge resistance. The resistance for the flat potential is slightly lower than that for the normal potential because a sloped equilibrium potential increases the pulse voltage change used to calculate the resistance. The resistance is relatively flat in the SOD range from 0.2 to 0.8, but increases quickly outside that range due to a more rapidly changing equilibrium potential and increased kinetic resistance. The resistance reflects the shape of the equilibrium potentials in other

ways as well; for example, the slight rise in the resistance at an SOD of approximately 0.4 is due to the change in slope of the equilibrium potential of the  $\text{Li}_x\text{C}_6$  electrode in that range. The 10s pulse resistance for the  $\text{Li}_{4+3x}\text{Ti}_5\text{O}_{12}/\text{Li}_y\text{FePO}_4$  system has a similar appearance to the flat-potential lines in Fig. 17.11. However, it has a lower magnitude at an SOD of 0.5 ( $\sim 13 \Omega \text{ cm}^2$ ) because the potential of the  $\text{Li}_{4+3x}\text{Ti}_5\text{O}_{12}$  electrode is above the potential at which SEI formation occurs, which leads to a lower film resistance and the ability to use smaller active material particles.

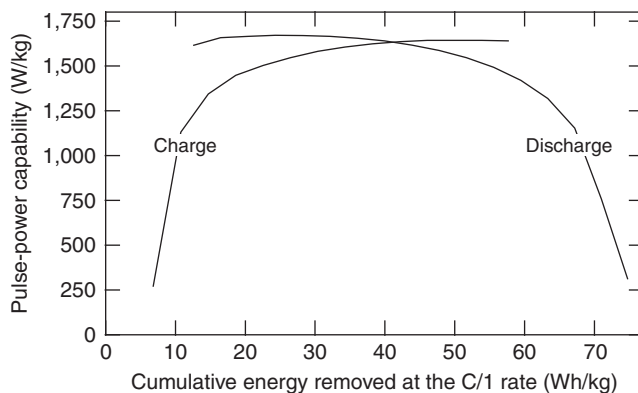
The HPPC method requires upper and lower cutoff potentials. In the case of the  $\text{Li}_x\text{C}_6/\text{Li}_{y+0.16}\text{Mn}_{1.84}\text{O}_4$  system, the upper cutoff is limited by the stability of the electrolyte; we use a value of 4.35 V. The lower cutoff is typically set to 55% of the upper cutoff, which we do for the  $\text{Li}_{4+3x}\text{Ti}_5\text{O}_{12}/\text{Li}_y\text{FePO}_4$  system, but for the  $\text{Li}_x\text{C}_6/\text{Li}_{y+0.16}\text{Mn}_{1.84}\text{O}_4$  system we set the lower cutoff potential to 3.2 V because of stability limits of the  $\text{Li}_{y+0.16}\text{Mn}_{1.84}\text{O}_4$  electrode. For the  $\text{Li}_{4+3x}\text{Ti}_5\text{O}_{12}/\text{Li}_y\text{FePO}_4$  system, the upper cutoff potential is not constrained by material stability; we use a value of 2.215 V, which we adjusted until the discharge and regeneration curves crossed at an SOD of approximately 0.5.

Fig. 17.12 shows the discharge and charge pulse-power capability as a function of cumulative energy for the  $\text{Li}_x\text{C}_6/\text{Li}_{y+0.16}\text{Mn}_{1.84}\text{O}_4$  system with both a flat and sloped equilibrium potential for the HEV cell parameters. The pulse power at which the charge and discharge curves cross (the value  $(P/A)^0$  described in the simple model) is the maximum power at which the cell could be operated, assuming that both the discharge and regeneration power goals must be satisfied. The power curves are much flatter in the case of the flat equilibrium potential. Fig. 17.13 shows a similar plot for the  $\text{Li}_{4+3x}\text{Ti}_5\text{O}_{12}/\text{Li}_y\text{FePO}_4$  system; again, the power curves are relatively flat.



**Figure 17.12** Discharge and charge power for the  $\text{Li}_x\text{C}_6/\text{Li}_{y+0.16}\text{Mn}_{1.84}\text{O}_4$  system with the HEV cell parameters as a function of the cumulative energy removed at the C/1 rate. The charge power displayed here has been divided by 0.8 according to the USCAR manual.





**Figure 17.13** Discharge and charge power for the  $\text{Li}_{4+3x}\text{Ti}_5\text{O}_{12}/\text{Li}_y\text{FePO}_4$  system with the HEV cell parameters as a function of the cumulative energy removed at the C/1 rate. The charge power displayed here has been divided by 0.8.

The usable energy is defined as the amount of energy available between the discharge and charge power curves for a given pulse-power capability. For example, at a power of 1,500 W/kg and for the normal equilibrium-potential curves shown in Fig. 17.12, the usable energy is around 75 Wh/kg. Fig. 17.14 shows the usable energy as a function of discharge power for the flat and normal equilibrium potentials for the  $\text{Li}_x\text{C}_6/\text{Li}_{y+0.16}\text{Mn}_{1.84}\text{O}_4$  system. We have also plotted the HEV power-to-energy ratio of 83.3:1 on Fig. 17.14. To optimize the electrode thicknesses and liquid-phase volume fractions for the HEV application, while holding the capacity ratio constant, we iterated to find the maximum usable energy along the power-to-energy

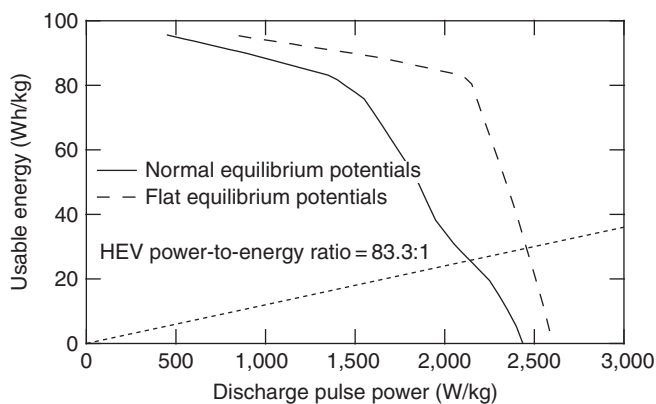


**Figure 17.14** Usable energy as a function of the discharge power for the  $\text{Li}_x\text{C}_6/\text{Li}_{y+0.16}\text{Mn}_{1.84}\text{O}_4$  system with the HEV cell parameters, for normal and artificially flat equilibrium-potential curves.

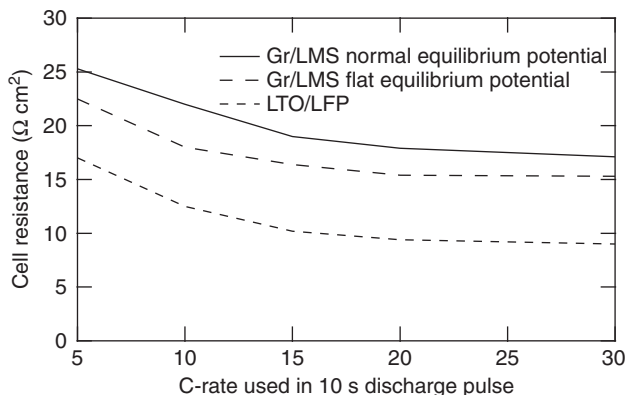


**Figure 17.15** Ten-second pulse resistance at 50% SOD as a function of C-rate for the listed chemistries with HEV cell parameters. Gr,  $\text{Li}_x\text{C}_6$ ; LMS,  $\text{Li}_{y+0.16}\text{Mn}_{1.84}\text{O}_4$ ; LTO,  $\text{Li}_{4+3x}\text{Ti}_5\text{O}_{12}$ ; LFP,  $\text{Li}_y\text{FePO}_4$ .

ratio (83.3:1) line. For the PHEV application, we used a ratio of 13:1. Optimization results are given in Table 17.2.

While exploring methods to calculate the pulse resistance and pulse-power capability, we experimented with different pulse C-rates and pulse times. Because a battery in a vehicle application will experience a wide range of applied currents and pulse durations, and the HPPC protocol defines a particular set of pulse conditions, we thought it important to examine the sensitivity of the results. In Fig. 17.15, we show the 10 s pulse resistance at an SOD of 0.5 (see Fig. 17.11) over a range of pulse currents. Clearly, the magnitude of the applied pulse current can significantly impact the resulting cell resistance. This can be explained, at least in part, by the fact that the kinetic resistance has a logarithmic relationship to the applied current at high currents (in the Tafel region). The duration of the pulse also matters. In particular, we found that for a 2 s pulse, the resistance was approximately  $10 \Omega \text{ cm}^2$  for the  $\text{Li}_x\text{C}_6/\text{Li}_{y+0.16}\text{Mn}_{1.84}\text{O}_4$  system and approximately  $6 \Omega \text{ cm}^2$  for the  $\text{Li}_{4+3x}\text{Ti}_5\text{O}_{12}/\text{Li}_y\text{FePO}_4$  system at the 30C rate. The resistance depends on the duration of the pulse because the voltage drops associated with diffusion and changes in the equilibrium potential become larger with increasing pulse duration. While it may be necessary, for the sake of benchmarking, to have a protocol for the determination of the pulse power and resistance, results may be sensitive to the applied current and pulse duration.

### 4.3 Battery model

Our simulations use a combined battery and vehicle model. The battery model is Dualfoil, and the vehicle model is based on the one developed by Fellner and Newman [8, 19–21]. The Dualfoil program employs porous electrode theory, a macrohomogenous

**Table 17.3** Equations used in the Dualfoil model

Equation description	Equation
Electrolyte material balance	$\epsilon_2 \frac{\partial c}{\partial t} = \nabla \cdot (\epsilon_2 D \nabla c) - \nabla \cdot \left[ \frac{i_2(1-t_+^0)}{F} \right]$
Intercalant material balance	$\frac{\partial c_s}{\partial t} = \frac{1}{r^2} \frac{\partial}{\partial r} (D_s r^2 \frac{\partial c_s}{\partial r})$
Liquid-phase Ohm's law	$i_2 = -\kappa \nabla \Phi_2 + \frac{2\kappa RT}{F} (1-t_+^0) \nabla \ln(f_{\pm} c)$
Solid-phase Ohm's law	$i_1 = -\sigma \nabla \Phi_1$
Butler–Volmer insertion kinetics	$j_{\text{inserter}} = \frac{i_0}{F} \left[ \exp\left(\frac{\alpha_a F}{RT} \eta_s\right) - \exp\left(-\frac{\alpha_r F}{RT} \eta_s\right) \right]$
Exchange current density	$i_0 = i'_0 (c_s)^{\alpha_c} (c_e)^{\alpha_a} (c_t - c_s)^{\alpha_a}$
Charge conservation	$\nabla \cdot i_2 = aF j_{\text{inserter}}$

approach to treating the phenomena occurring in the porous electrodes of batteries. The version used in this work has six coupled differential equations that are solved numerically and simultaneously at each time step. A summary of the equations is presented in Table 17.3. We modified the Dualfoil program to integrate it with the vehicle model; the major change was to make the time increment of the drive cycle and the time increment of Dualfoil the same. At the first time step (when the drive cycle begins), the battery is initialized, and at subsequent time steps the battery is left in its state rather than reinitialized. We discretized the driving cycle into increments of 0.25 s, and therefore the Dualfoil program is called every 0.25 s. The frequency can be increased to improve accuracy. The battery is operated in the constant-power mode.

#### 4.4 Vehicle model

The vehicle model calculates the power required at the wheels at each time step and takes into account wind resistance, rolling resistance, and acceleration. Table 17.4 lists the vehicle specifications. Eq. [17.17] provides the power at the wheels at each point in the drive cycle as

$$P_{\text{wheels}} = 0.5 \rho_{\text{air}} A_{\text{surf}} \gamma_{\text{air}} v^3 + \gamma_{\text{roll}} m_{\text{vehicle}} g v + m_{\text{vehicle}} v a \quad [17.17]$$

The mass of the vehicle is given by

$$m_{\text{vehicle}} = m_{\text{base}} + m_{\text{passengers}} + 1.5 A_{\text{sep}} m_{\text{batt}} \quad [17.18]$$

The factor of 1.5 in Eq. [17.18] accounts for the balance of system above the cell level. From Eqs. [17.17] and [17.18], it should be apparent that the battery size affects the power required at the wheels. Once the power at the wheels is determined, we use a simple algorithm to divide the power supply between the ICE and the battery. For the

**Table 17.4** Vehicle specifications

Specification	Units	Value	Description
Vehicle base mass	kg	1200	Similar to a Toyota Prius
Passenger mass	kg	135	Approximate weight of two people
$A_{\text{surf}}$	$\text{m}^2$	1.75	
$r_{\text{roll}}$		0.015	Typical value for automobiles
$r_{\text{air}}$		0.26	Value for the 2007 Toyota Prius
Powertrain efficiency		0.8	Based on Ref. [8]
Generator efficiency		0.9	Based on Ref. [8]
Electric motor efficiency		0.9	Based on Ref. [8]
Maximum regenerative braking		0.5	Amount of power available for battery charging relative to the total available power

HEV configuration, we assume that the ICE runs at a constant value (that denoted by “Base Engine Size” in Table 17.6) unless the power demanded at the wheels exceeds the power available from the battery, in which case the ICE meets the difference. Thus, the ICE is always on except when the vehicle is braking, in which case it is turned off. In this scheme, the battery serves as the load-leveling device up to its power limit, after which the ICE assists with load leveling. For the PHEV configuration, the ICE remains off unless the battery cannot supply the power demanded by the vehicle. The power from the ICE can go either to the battery through the generator or to the wheels through the powertrain (for the PHEV configuration no power from the ICE is routed to the battery during the charge-depleting mode). When power is required from the battery, it goes through the electric motor and the powertrain. Power to the battery can come either from the engine, in which case it runs through the generator, or from the wheels, in which case it runs through the powertrain and the generator. In practice, the power management system of a vehicle is much more sophisticated than this simple approach; we believe that this rough approximation is sufficient for the present purposes. Because we allow the power supplied by the ICE to vary, and the efficiency of an ICE depends on its load profile, the calculation of the fuel economy becomes difficult, and we therefore do not report fuel economy values in this work.

#### 4.5 Operating configurations and driving cycle

The HEV drive cycle must be charge neutral, which means that the final SOD must be the same as the initial SOD. In addition, the cell voltage must remain within the specified cutoff potentials. If the cell voltage goes outside the voltage bounds, the separator area is increased (a resolution of  $0.1 \text{ m}^2$  is used), and the simulation is restarted. If the final SOD does not match the initial SOD, the size of the engine is adjusted, and the simulation is restarted. In practice, this can be considered an optimization that results

**Table 17.5** Relevant USCAR specifications for the HEV and PHEV vehicle configurations

Specification	Units	HEV	PHEV
$P_{\text{req,discharge}}$	kW	25	45
$P_{\text{req,charge}}$	kW	20	30
C/1 energy over range in which power goals are met	Wh	300	Depends on desired PHEV range

in a minimum separator area. For the HEV configuration, the battery starts and ends at around 50% SOD. The power requirements for the HEV and PHEV configurations are given in Table 17.5.

In the PHEV configuration, the vehicle is charge depleting rather than charge neutral. As such, the SOD increases during the driving cycle. In this configuration, a separator area is chosen, and the vehicle runs through the driving cycle until the lower cutoff potential is reached. The initial SOD is set as low as possible without the upper cutoff potential being reached during a charging segment. Because the ICE supplements the battery during times of high power demand, it is necessary to define equivalent-electric kilometers rather than all-electric kilometers. To calculate the equivalent-electric kilometers, we calculate the distance traveled by the vehicle during its drive cycle and the net energy that it requires. The net energy calculation includes regenerative braking, which we assume captures 50% of the energy available during braking. From these numbers, we calculate an energy requirement per kilometer. Next, we calculate the net energy removed from the battery during the driving cycle. Note that this calculation includes the energy returned to the battery during the braking stages; this is necessary to calculate an energy-limited asymptote based on the total energy available in a battery. We found that if no regenerative braking is used in the calculation of the amount of energy required per kilometer traveled, the equivalent-electric range drops by approximately 25%. This choice of how to define the equivalent-electric kilometers has the disadvantage that the reported range is dependent on the fraction of regenerative braking, but has the advantage that it will give a more realistic estimate of the distance a PHEV can travel. Also note that this method accounts for the battery efficiency as well as the effect of the battery weight on vehicle weight and hence vehicle efficiency because it treats the energy flow at the battery leads. For reference, the energy requirement of our vehicles is in the range of 118–132 Wh/km. As shown in Table 17.5, we set the maximum discharge power from the battery (at the leads) to 45 kW and the maximum charge power (at the leads) to 30 kW.

We use a single driving cycle in this work, based on the urban driving cycle used by Fellner and Newman [8]. The driving cycle we use is shown in Fig. 17.16 and uses a constant acceleration rate. One of the conclusions from Fellner's work is that the precise characteristics of the driving cycle are relatively unimportant provided that it contains

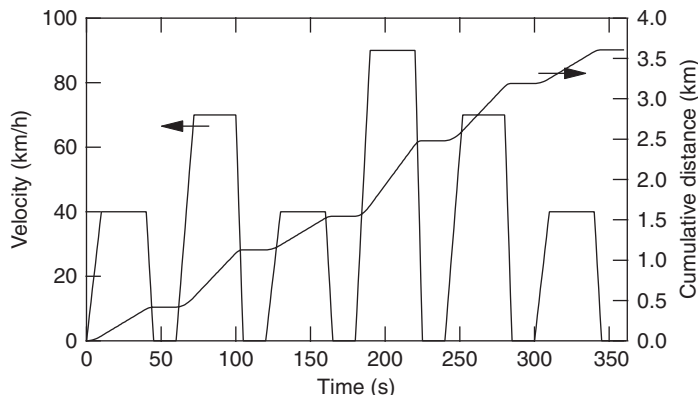


**Figure 17.16** Drive cycle used in the HEV and PHEV simulations. The drive cycle is composed of six 1 min cycles and has three 10 s accelerations, two 12 s accelerations, and one 15 s acceleration. The braking segments are 5 s, and the rests are 15 s.

essential features such as realistic braking and acceleration segments. In practice, it is the high-power peaks that determine battery sizing (at least for HEVs). We explored different driving cycles and found that the presence of high-power spikes, as well as long charge or discharge segments, can have a significant influence on battery size and capacity use. For example, a charge-neutral HEV driving cycle that involves going up and down a large hill may use a larger fraction of the battery capacity than an aggressive urban cycle primarily composed of high-power spikes. Thus, our results should be taken in the context of the drive cycle we use.

#### 4.6 Model limitations

There are several model limitations, including those related to the battery model and those related to the vehicle model. A main assumption of the battery model relevant to the present purpose is isothermal operation; in practice we expect the battery temperature in an HEV or PHEV to depend on the cycling history and ambient temperature. A good cooling system limits the error introduced by this assumption [22]. The category of vehicle-level limitations includes the fact that driving time is cut into segments of 0.25 s and a simplified power-allocation routine is used. There is also the assumption of constant-thickness electrodes for the PHEV application; in practice we would expect there to be an optimum based on the power-to-energy ratio of the particular PHEV battery under consideration.

#### 4.7 Results for HEV operation

Fig. 17.17 shows the results of the HEV simulations for the  $\text{Li}_x\text{C}_6/\text{Li}_{y+0.16}\text{Mn}_{1.84}\text{O}_4$  system with normal equilibrium potentials. The figure shows that the HEV cycle is charge neutral, and the convergence routine ensures that the cell potential comes very close to

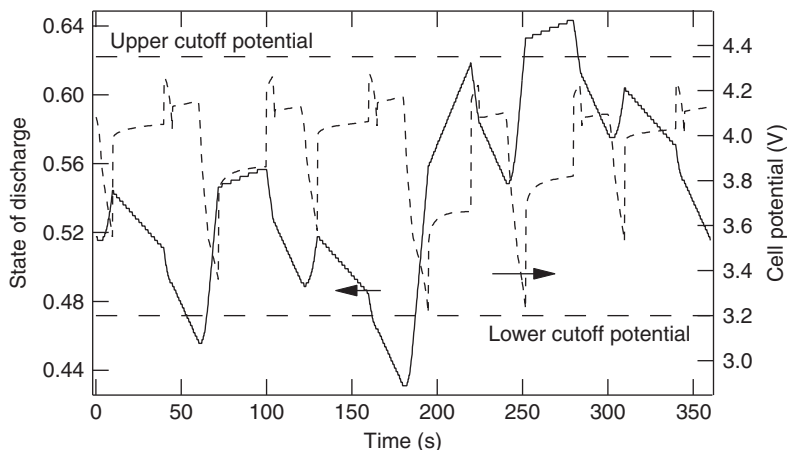


**Figure 17.17** Performance of the  $\text{Li}_x\text{C}_6/\text{Li}_{y+0.16}\text{Mn}_{1.84}\text{O}_4$  system with a normal equilibrium potential for an HEV driving cycle. For this chemistry, the separator area is  $14.1\text{ m}^2$ , and the battery mass is  $6.2\text{ kg}$ .

touching the lower cutoff potential. The performance of the  $\text{Li}_x\text{C}_6/\text{Li}_{y+0.16}\text{Mn}_{1.84}\text{O}_4$  system with artificially flat equilibrium potentials and that of the  $\text{Li}_{4+3x}\text{Ti}_5\text{O}_{12}/\text{Li}_y\text{FePO}_4$  system are qualitatively similar to the results in Fig. 17.17 and are therefore omitted. Table 17.6 presents the results for all three of the chemistries. For the  $\text{Li}_x\text{C}_6/\text{Li}_{y+0.16}\text{Mn}_{1.84}\text{O}_4$  system, the separator area is similar for the regular and artificially flat equilibrium potentials. The SOD range used by the  $\text{Li}_x\text{C}_6/\text{Li}_{y+0.16}\text{Mn}_{1.84}\text{O}_4$  system (20–25%) is much larger than that found by Fellner and Newman; as explained before, this is a result of the much smaller battery size, which is related to the much thinner, optimized cell sandwich, and the “blended” operating strategy. The separator area for the  $\text{Li}_{4+3x}\text{Ti}_5\text{O}_{12}/\text{Li}_y\text{FePO}_4$  system is substantially larger than that for the  $\text{Li}_x\text{C}_6/\text{Li}_{y+0.16}\text{Mn}_{1.84}\text{O}_4$  system. In order to

**Table 17.6** Performance results for the HEV driving cycle

Electrode system	Combined model results				
	Base engine size (kW)	SOD range (%)	Separator area ( $\text{m}^2$ )	Battery mass (cell level) (kg)	Battery efficiency (%)
$\text{Li}_x\text{C}_6/\text{Li}_{y+0.16}\text{Mn}_{1.84}\text{O}_4$ (regular equilibrium curves)	16.08	21.24	14.1	6.20	92.50
$\text{Li}_x\text{C}_6/\text{Li}_{y+0.16}\text{Mn}_{1.84}\text{O}_4$ (flat equilibrium curves)	15.90	22.27	13.5	5.93	93.22
$\text{Li}_{4+3x}\text{Ti}_5\text{O}_{12}/\text{Li}_y\text{FePO}_4$	17.32	17.44	27.4	11.27	86.7

understand this difference, it is important to consider the value of  $(U - V_{\min})V_{\min}/R$ , where  $U$  is the equilibrium potential,  $V_{\min}$  is the lower cutoff potential, and  $R$  is the area-specific cell resistance. This is what is plotted in Figs. 17.12 and 17.13, which show that the pulse-power capability of the  $\text{Li}_x\text{C}_6/\text{Li}_{y+0.16}\text{Mn}_{1.84}\text{O}_4$  system is substantially higher than the  $\text{Li}_{4+3x}\text{Ti}_5\text{O}_{12}/\text{Li}_y\text{FePO}_4$  system.

The batteries here are smaller than what would be expected for a commercial application; these results should be interpreted as a minimum separator area size to meet only the performance requirements. In practice, larger batteries are required because the performance goals are for end-of-life and battery performance declines with cycling and time. Thus, a battery that initially exceeds the requirements needs to be installed. Also, the USCAR HEV goals have an energy requirement in addition to a power requirement. The energy requirement is for 300 Wh over the SOD range over which the power goals are satisfied. A larger energy requirement allows the battery to deliver energy during a long uphill or capture energy during a long downhill; in practice this 300 Wh goal represents a tradeoff between vehicle efficiency and battery size.

Fig. 17.12 shows that, when operated at a low rate, at the cell level approximately 110 Wh/kg is available from the  $\text{Li}_x\text{C}_6/\text{Li}_{y+0.16}\text{Mn}_{1.84}\text{O}_4$  system with normal equilibrium potentials. For a battery that weighs 6.20 kg at the cell level, around 680 Wh would be available assuming the entire capacity could be used. The drive cycle shown here uses 21.24% of the SOD range, which corresponds to around 144.4 Wh. Noting that the USCAR goal is 300 Wh (over the range where the power goals are met), we can see that the battery would need to be increased in size in order to meet this energy goal.

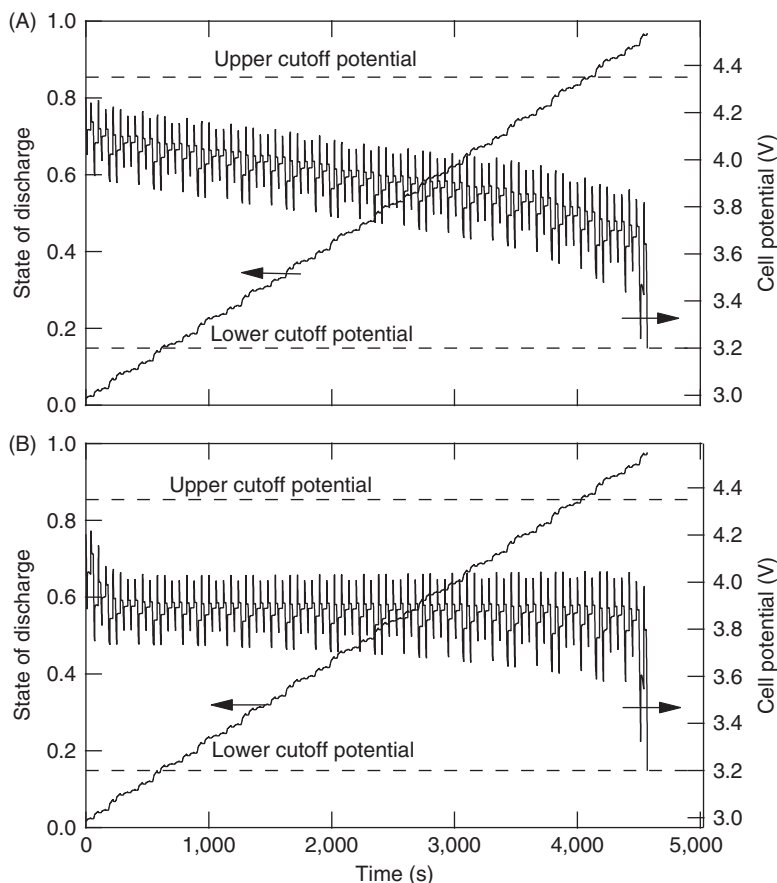
Fig. 17.12 shows that with artificially flat equilibrium potentials much more energy is available at a high power than with normal equilibrium potentials, which implies that a substantially smaller battery could be used. However, as shown in Table 17.6, the flat-potential  $\text{Li}_x\text{C}_6/\text{Li}_{y+0.16}\text{Mn}_{1.84}\text{O}_4$  system has only a slightly smaller size and larger capacity use. We discuss the reasons for this in Sections 4.8 and 4.9.

We have also listed the battery efficiencies in Table 17.6. The USCAR goals have a requirement of 90% round-trip energy efficiency for a 25 Wh cycle. The  $\text{Li}_x\text{C}_6/\text{Li}_{y+0.16}\text{Mn}_{1.84}\text{O}_4$  systems have an overall battery efficiency above 90%, while the  $\text{Li}_{4+3x}\text{Ti}_5\text{O}_{12}/\text{Li}_y\text{FePO}_4$  system has an overall efficiency below 90%. This difference may be at least partly attributable to the fact that the lower cutoff potential for the  $\text{Li}_x\text{C}_6/\text{Li}_{y+0.16}\text{Mn}_{1.84}\text{O}_4$  systems needs to be kept relatively high (at 3.2 V) because of stability considerations. In any case, all of these systems would have an efficiency above 90% for the drive cycle used here if they were sized for end-of-life requirements and were required to meet a higher energy requirement.

## 4.8 Results for PHEV operation

Fig. 17.18 shows the cell potential as a function of time for the  $\text{Li}_x\text{C}_6/\text{Li}_{y+0.16}\text{Mn}_{1.84}\text{O}_4$  system with a separator area of  $75\text{ m}^2$  and both the flat and normal equilibrium-potential

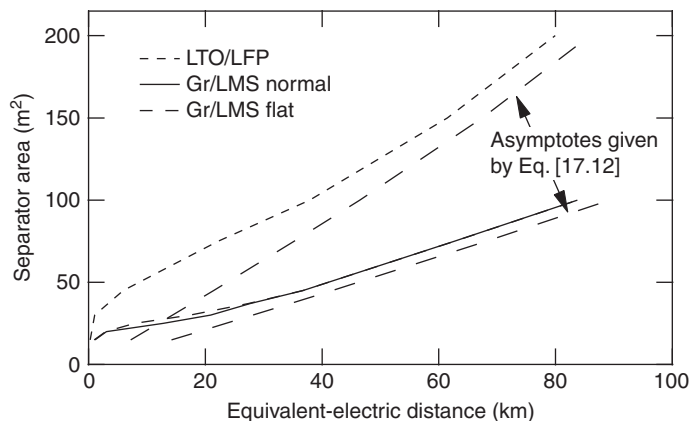




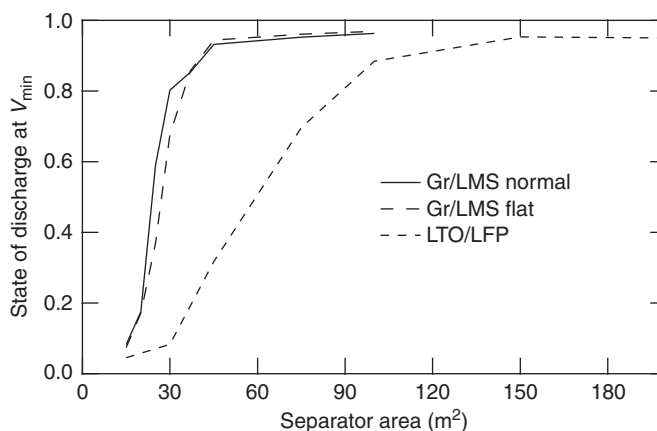
**Figure 17.18** Performance of the  $\text{Li}_x\text{C}_6/\text{Li}_{y+0.16}\text{Mn}_{1.84}\text{O}_4$  system with a normal (A) and flat (B) equilibrium potential profile for the PHEV cell parameters and configuration and a separator area of  $75\text{ m}^2$ .

curves. This figure shows clearly the magnitude of the potential spikes, as well as the shapes of the equilibrium potentials. The time at which the lower cutoff potential is reached is very similar for the flat and normal equilibrium potentials; when the potential spikes are small because of a large separator area, very similar performance should be expected from a sloped and artificially flat set of equilibrium potentials, assuming that the cells have the same capacity and average voltage. For the  $\text{Li}_{4+3x}\text{Ti}_5\text{O}_{12}/\text{Li}_y\text{FePO}_4$  system with a separator area of  $75\text{ m}^2$  the voltage spikes are much larger than in Fig. 17.18, and the time at which the lower cutoff is reached is much earlier. Although a lower resistance permits higher currents for a given voltage drop, the potential of this system is also lower, and the interplay of these effects is roughly captured by Eq. [17.1].

By running the PHEV model with a variety of separator areas, we can correlate equivalent-electric distance, separator area, and capacity use. We show results in



**Figure 17.19** Equivalent-electric distance of the  $\text{Li}_x\text{C}_6/\text{Li}_{y+0.16}\text{Mn}_{1.84}\text{O}_4$  system and the  $\text{Li}_{4+3x}\text{Ti}_5\text{O}_{12}/\text{Li}_y\text{FePO}_4$  system for a variety of separator areas.



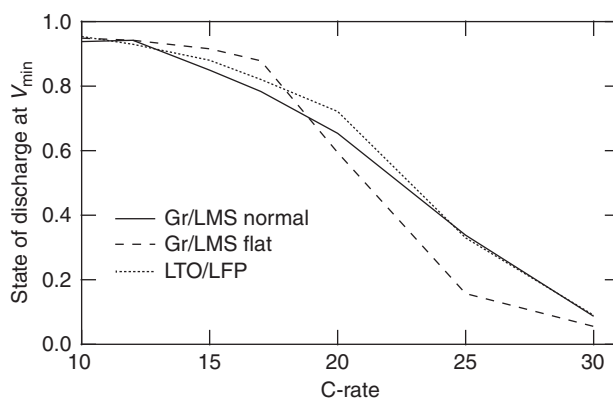
**Figure 17.20** State of discharge at the lower cutoff potential,  $V_{\min}$ , for the  $\text{Li}_x\text{C}_6/\text{Li}_{y+0.16}\text{Mn}_{1.84}\text{O}_4$  and  $\text{Li}_{4+3x}\text{Ti}_5\text{O}_{12}/\text{Li}_y\text{FePO}_4$  systems for a variety of separator areas.

Fig. 17.19 (battery size) and Fig. 17.20 (capacity use). Here we see that, for a small separator area, the equivalent-electric distance and the capacity use of the batteries are small. As the equivalent-electric distance increases, the size of the battery increases at a slope initially lower and then approaching the asymptotic value. The change in slope is also present in Figs. 17.7 and 17.9(A). As explained there, the bend is due to a change in the slope of the pulse-power capability curve, as seen in Figs. 17.12 and 17.13. We have also plotted, in Fig. 17.19, the asymptotes for an energy-limited system given by Eq. [17.12]. The slopes of the asymptotes and simulation results compare well for the  $\text{Li}_x\text{C}_6/\text{Li}_{y+0.16}\text{Mn}_{1.84}\text{O}_4$  system at distances above approximately 35 km, and for the  $\text{Li}_{4+3x}\text{Ti}_5\text{O}_{12}/\text{Li}_y\text{FePO}_4$  system at distances above approximately 60 km. As expected,

we see that a larger separator area is required for the  $\text{Li}_{4+3x}\text{Ti}_5\text{O}_{12}/\text{Li}_y\text{FePO}_4$  system than for the  $\text{Li}_x\text{C}_6/\text{Li}_{y+0.16}\text{Mn}_{1.84}\text{O}_4$  system as a result of the higher value of  $Q\langle V \rangle$  of the latter chemistry.

The simple model also helps us to understand better the results presented in Fig. 17.20. Fig. 17.9(B) shows the relationship between capacity use and separator area for the simple model, and a comparison shows that the shapes are very similar. The relevant parameter is the magnitude of the maximum pulse-power capability,  $(P/A)^0$ , and we have already shown that the  $\text{Li}_x\text{C}_6/\text{Li}_{y+0.16}\text{Mn}_{1.84}\text{O}_4$  system has a higher value than the  $\text{Li}_{4+3x}\text{Ti}_5\text{O}_{12}/\text{Li}_y\text{FePO}_4$  system.

An important question that arises from a study of Figs. 17.19 and 17.20 is why the results for the  $\text{Li}_x\text{C}_6/\text{Li}_{y+0.16}\text{Mn}_{1.84}\text{O}_4$  system with the normal and artificially flat equilibrium-potential curves are so similar. To help understand, on a common basis, the pulse rate capability of the systems, we construct a new kind of plot that can be described as a hybrid between a Peukert and HPPC plot. This hybrid plot is shown in Fig. 17.21. It is constructed by using an HPPC-like protocol in which discharge and charge pulses of a given magnitude (the abscissa in Fig. 17.21) are applied for 10 s each, separated by a 40 s rest. The SOD is increased in increments of 0.02 with a constant current at the 1C rate, and the cell is allowed to relax for an hour prior to the application of the next set of discharge and charge pulses. At some point during one of the discharge pulses, the lower cutoff potential is reached, at which point the SOD is recorded and plotted on the ordinate. We can see from Fig. 17.21 that, at C-rates in the range from approximately 18 to 30 (in the SOD range below  $\sim 0.7$ ), the rate capability of the normal-potential system is greater than the flat-potential system. We attribute this to two independent effects. First, the cell potential for the normal-potential system is greater



**Figure 17.21** Hybrid Peukert-HPPC plot showing the SOD at which the lower cutoff is reached as a function of the C-rate of the applied pulse for cells with the PHEV parameters. This method starts the cell at an SOD of 0, moves in SOD increments of 0.02 separated by a 1 h rest, and applies a 10 s charge and discharge pulse of equal magnitude separated by a 40 s rest.

than the flat-potential system below an SOD of approximately 0.5 (because the flat-potential system runs through the midpoint of potential). Second, as we discuss more in the next section, for a flat-potential system that receives consecutive discharge or charge pulses, there will be a buildup and persistence of a solid-phase concentration gradient through the electrode depth. In the SOD range from 0 to 0.5, we would expect superior performance from the normal-potential system due to its higher potential. We attribute its better performance between an SOD of 0.5 and an SOD of approximately 0.7 in Fig. 17.21 to the second effect.

#### 4.9 Pulse-power capability in a flat-potential system

Besides the differences in equilibrium potential between the normal and artificially sloped  $\text{Li}_x\text{C}_6/\text{Li}_{\gamma+0.16}\text{Mn}_{1.84}\text{O}_4$  systems, there is another effect present in flat-potential systems that affects the pulse-power capability. First, note that Fig. 17.12 has results for the HEV cell design (relatively thin electrodes), while Figs. 17.19 and 17.20 are based on the PHEV cell design. The results for the 10 s pulse-power capability of the  $\text{Li}_x\text{C}_6/\text{Li}_{\gamma+0.16}\text{Mn}_{1.84}\text{O}_4$  system with the PHEV cell parameters are shown in Fig. 17.22. The naturally flat-potential  $\text{Li}_{4+3x}\text{Ti}_5\text{O}_{12}/\text{Li}_y\text{FePO}_4$  system with the PHEV cell design has a similarly asymmetric result.

The results in this figure have an important qualitative difference from the results in Fig. 17.12; the power capability on discharge is essentially identical for the normal and flat equilibrium potentials, which helps provide a reason that the results in Figs. 17.19 and 17.20 are so similar for the  $\text{Li}_x\text{C}_6/\text{Li}_{\gamma+0.16}\text{Mn}_{1.84}\text{O}_4$  system with the two different potential profiles. Why do we see a very flat pulse-power capability in Fig. 17.12 and a sloped pulse-power discharge capability in Fig. 17.22? The PHEV cell design uses thicker electrodes and during a high-rate pulse will have a more nonuniform current distribution than an

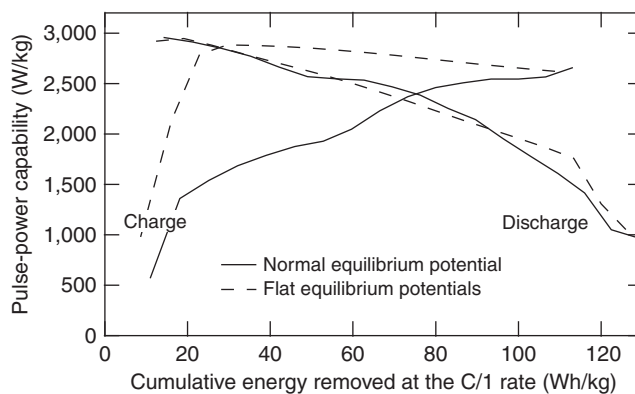


**Figure 17.22** Discharge and charge pulse-power capability of the  $\text{Li}_x\text{C}_6/\text{Li}_{\gamma+0.16}\text{Mn}_{1.84}\text{O}_4$  system with the PHEV cell parameters as a function of the cumulative energy removed at the C/1 rate. The charge power displayed here has been divided by 0.8 according to the USCAR manual.

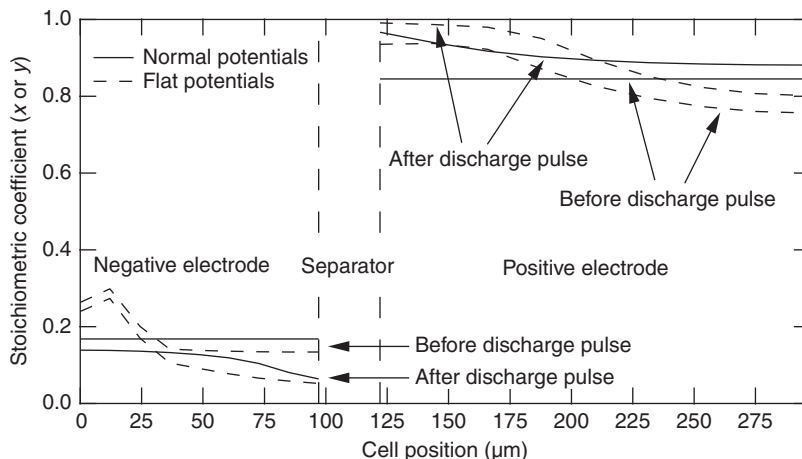


**Figure 17.23** Internal cell profiles of the stoichiometric coefficient  $x$  in  $\text{Li}_x\text{C}_6$  or  $y$  in  $\text{Li}_{y+0.16}\text{Mn}_{1.84}\text{O}_4$  immediately before and at the end of a 10C discharge pulse at an SOD of approximately 0.8. The results are for the  $\text{Li}_x\text{C}_6/\text{Li}_{y+0.16}\text{Mn}_{1.84}\text{O}_4$  system with the PHEV cell parameters.

HEV cell. This means that the region of the electrode near the separator will experience a higher C-rate than the same region for an HEV cell design. In order to explain what is occurring, we plot the detailed profiles within the cell in Fig. 17.23.

This figure shows an important characteristic of completely flat-equilibrium-potential cells; without any slope in the potential, there is no driving force for the regions of an electrode to equilibrate to a single composition. Thus, we see that at the end of a 1 h relaxation step following a 1C discharge, the flat-potential system still has a higher value of  $\gamma$  (and a lower value of  $x$ ) near the separator/positive electrode interface (and the separator/negative electrode interface). This solid-phase concentration gradient through the depth of the electrode forces current pulses to access the back of the electrode, resulting in higher polarization. This is a potential drawback of any flat-potential system. Note that the charge pulse-power curve in Fig. 17.22 is still flat; this is because the step before a pulse charge in an HPPC protocol is a pulse discharge so that concentration gradients that lead to a shift in the current distribution have not been established. Thus, pulse-power performance declines occur when a discharge pulse follows a discharge step, or a charge pulse follows a charge step. These effects have also been demonstrated in experimental cells [23].



## 5. CONCLUSIONS

For a linear set of pulse-power capability curves with a shape governed by the parameter  $B$ , a simple model can be used to show a Langmuir-like dependence of capacity use on a dimensionless energy-to-power ratio and a linear dependence of a

dimensionless area on a dimensionless energy-to-power ratio. The former means that capacity use increases rapidly at low values of the dimensionless energy-to-power ratio, while it increases slowly at high values of the dimensionless energy-to-power ratio. In dimensional terms, the parameters  $B$ ,  $Q\langle V \rangle$ , and  $(U - V_{\min})V_{\min}/R$  are each important values for determining capacity use and battery size. An ideal cell chemistry would have a small value of  $B$  (indicating a relatively flat pulse-power capability), a large value of  $Q\langle V \rangle$ , and a large value of  $(U - V_{\min})V_{\min}/R$ , resulting in a relatively high capacity use and small battery size.

A combined battery and vehicle model is required to capture the details of the complex relationships between battery chemistry and performance. For example, while it is clear that a set of relatively flat pulse-power capability curves can improve capacity use and decrease battery size, there are several scenarios in which switching to a set of flat equilibrium potentials may result in reductions in performance. One scenario is that at some values of the SOD the potential of a sloped-potential system may be higher than a flat-potential system, resulting in a lower pulse-power capability for the flat-potential system. In addition, during a sequence of consecutive pulse discharges or consecutive pulse charges, the pulse-power capability of a flat-potential system may be worse because there is no driving force for the relaxation of solid-phase concentration gradients through the electrode depth. This is especially true for relatively thick electrodes, which typically have a more nonuniform current distribution. In practice, the various aspects of cell chemistry are related, and the results from this work should be able to provide cell developers with an improved perspective on how they fit together to influence overall performance.

## ACKNOWLEDGEMENTS

Jeremy Coutts and Venkat Srinivasan made important contributions to this work.

## TERMINOLOGY

### Abbreviations

DOE	Department of Energy
Gr	$\text{Li}_x\text{C}_6$ graphite electrode
HEV	Hybrid electric vehicle
HPPC	Hybrid pulse-power characterization
ICE	Internal combustion engine
LFP	$\text{Li}_y\text{FePO}_4$ electrode
LMS	$\text{Li}_{y+0.16}\text{Mn}_{1.84}\text{O}_4$ electrode
LTO	$\text{Li}_{4+3x}\text{Ti}_5\text{O}_{12}$ electrode
PHEV	Plug-in hybrid electric vehicle
SEI	Solid-electrolyte interphase
SOD	State of discharge
USCAR	United States Council for Automotive Research

## Roman

$a$	Vehicle acceleration, $\text{m}^2/\text{s}$
$a$	Specific area, $\text{m}^2/\text{m}^3$
$A$	Total separator area of a battery, $\text{m}^2$
$A_{\text{surf}}$	Front cross-sectional area of the vehicle, $\text{m}^2$
$B$	Slope of the pulse-power capability curve
$c_1$	Constant calculated from the position of $V_{\text{min}}$
$c_2$	Constant calculated from the position of $V_{\text{max}}$
$c$	Concentration, $\text{mol}/\text{m}^3$
$D$	Diffusion coefficient, $\text{m}^2/\text{s}$
$E$	Energy required at the wheels during a driving cycle, J
$E'$	Battery energy for a vehicle to travel a given distance, J/m
$F$	Faraday's constant, 96487 C/mol
$g$	Gravitational acceleration, $\text{m}^2/\text{s}$
$i$	Current density, $\text{A}/\text{m}^2$
$j_{\text{insep}}$	Pore wall flux for insertion reaction, $\text{mol}/\text{m}^2$ interfacial
$L$	Equivalent-electric driving distance, m
$m_{\text{batt}}$	Mass of battery (cell basis), kg
$m_{\text{passengers}}$	Mass of passengers, kg
$m_{\text{vehicle}}$	Total vehicle mass, kg
$(P/A)^0$	Maximum pulse-power capability, $\text{W}/\text{m}^2$
$P_{\text{req}}$	Required power for a given vehicle configuration, W
$Q$	Specific coulombic capacity, $\text{Ah}/\text{m}^2$
$r$	Radius, m
$R$	Resistance, $\Omega$
$r_{\text{air}}$	Air drag coefficient
$r_{\text{roll}}$	Rolling resistance
$t_+$	Transference number of $\text{Li}^+$
$U$	Equilibrium potential, V
$v$	Vehicle velocity, m/s
$V$	Instantaneous cell potential, V
$\langle V \rangle$	Average cell potential, V
$V_{\text{min}}$	Lower cutoff potential, V
$V_{\text{max}}$	Upper cutoff potential, V

## Greek

$\alpha$	Transfer coefficient
$\varepsilon$	Volume fraction
$\sigma$	Conductivity, S/m
$\eta_s$	Surface overpotential, $\phi_1 - \phi_2 - U$
$\phi$	Electric potential, V
$\rho_{\text{air}}$	Density of air, $\text{kg}/\text{m}^3$

## Superscripts and subscripts

1	Solid phase
2	Liquid phase

## REFERENCES

1. T. Duong, 7th Advanced Automotive Batteries Conference, Long Beach, USA, 2007.
2. K.J. Kelly, M. Mihalic, M. Zolot, 17th Annual Battery Conference on Applications and Advances, Long Beach, USA, 2002.
3. P. Albertus, J. Newman, *J. Power Sources* 183 (2008) 376.
4. P. Albertus, J. Coutts, V. Srinivasan, J. Newman, *J. Power Sources* 183 (2008) 771.
5. FreedomCAR, Battery Test Manual for Power-Assist Hybrid Electric Vehicles, United States Council for Automotive Research, DOE/ID-11069, 2003. [http://avt.inel.gov/battery/pdf/freedomcar\\_manual\\_04\\_15\\_03.pdf](http://avt.inel.gov/battery/pdf/freedomcar_manual_04_15_03.pdf).
6. FreedomCAR, Power Assist HEV Battery Goals, United States Council for Automotive Research, 2002. [www.uscar.org/commands/files\\_download.php?files\\_id=83](http://www.uscar.org/commands/files_download.php?files_id=83)
7. United States Advanced Battery Consortium, Development of Advanced High-Performance Batteries for Plug-in Electric Vehicle Applications, 2007. [www.uscar.org/commands/files\\_download.php?files\\_id=118](http://www.uscar.org/commands/files_download.php?files_id=118).
8. C. Fellner, J. Newman, *J. Power Sources* 85 (2000) 229.
9. T. Markel, A. Simpson, 6th Advanced Automotive Battery Conference, Baltimore, Maryland, 2006.
10. T. Markel, A. Simpson, SAE Future Transportation Technology and IEEE Vehicle Power and Propulsion Joint Conferences, Chicago, USA, 2005.
11. M. Anderman, *J. Power Sources* 127 (2004) 2.
12. O. Bitshe, G. Gutmann, *J. Power Sources* 127 (2004) 8.
13. E. Karden, S. Ploumen, B. Fricke, T. Miller, K. Snyder, *J. Power Sources* 168 (2007) 2.
14. R.F. Nelson, *J. Power Sources* 91 (2000) 2.
15. V. Srinivasan, V. Sethuraman, J. Newman, Meet. Abstr. – Electrochem. Soc. 802 (607) (2008).
16. J. Christensen, V. Srinivasan, J. Newman, *J. Electrochem. Soc.* 153 (2006) A560.
17. V. Srinivasan, J. Newman, *J. Electrochem. Soc.* 151 (2004) A1530.
18. S.G. Stewart, V. Srinivasan, J. Newman, *J. Electrochem. Soc.* 155 (2008) A664.
19. M. Doyle, T.F. Fuller, J. Newman, *J. Electrochem. Soc.* 140 (1993) 1525.
20. T.F. Fuller, M. Doyle, J. Newman, *J. Electrochem. Soc.* 141 (1994) 1.
21. T.F. Fuller, M. Doyle, J. Newman, *J. Electrochem. Soc.* 141 (1994) 982.
22. A. Pesaran, Advanced Automotive Battery Conference, Las Vegas, USA, 2001.
23. P. Albertus, Ph.D. Thesis, Department of Chemical Engineering, University of California, Berkeley, 2009.





# Safety of Lithium-Ion Batteries for Hybrid Electric Vehicles

Ashish Arora<sup>1\*</sup>, Noshirwan K. Medora<sup>\*</sup>, Thomas Livernois<sup>\*\*</sup> and Jan Swart<sup>\*</sup>

<sup>\*</sup>Exponent Failure Analysis Associates, 23445 North 19<sup>th</sup> Avenue, Phoenix, AZ 85027, USA

<sup>\*\*</sup>Exponent Failure Analysis Associates, 39100 Country Club Drive, Farmington Hills, MI 48331, USA

## Contents

1. Introduction	464
2. Li-ion Flavors	465
3. Li-ion Cell Failures	465
4. Why Do Li-ion Cells Go Into Thermal Runaway?	470
4.1 External short circuit	470
4.2 Internal short circuit	471
4.2.1 Metallic contaminants	472
4.2.2 Cell defects	473
4.2.3 Cell charging algorithm	473
4.3 Cell overcharge	474
4.4 Overdischarging Li-ion cells	475
4.5 Low-temperature charging	475
4.6 High-temperature storage and charging	476
5. Typical Safety Circuits	476
6. HEV Battery Safety Standards	479
7. System Specific Safety Evaluation	482
7.1 Cell manufacturing defects	483
7.2 Design defects	485
7.3 Number of cells	486
7.4 Operating temperature	486
7.5 Operating life	487
7.6 System-based abuse testing	487
8. Voltage Introduced Safety Considerations	488
8.1 Electrical shock hazard	488
8.2 Arcing	488
9. Summary	489
Acknowledgments	490
References	490

<sup>1</sup> Corresponding author: AArora@exponent.com



## 1. INTRODUCTION

Lithium-ion (Li-ion) technology as an energy storage chemistry for hybrid and electric vehicles is developing rapidly. Wider adaptation of the technology has been limited due to factors such as cost, reliability, battery life, and safety concerns associated with the chemistry. Multiple Li-ion battery recalls have further brought safety concerns to the forefront. In the consumer electronics industry (Table 18.1), more than 2 million products containing Li-ion batteries have been recalled since October 1, 2006. These products, ranging from electronic toys to wireless headsets to bicycle lights have all been involved in recalls related to battery problems over the past few years. Other industries have experienced similar product defects and subsequent recalls. 17,000 lithium–metal–polymer batteries used in telecommunications equipment were recalled in early 2008 due to a defect which caused the cells to go into thermal runaway [1].

Although substantial interest has been expressed in the use of Li-ion batteries to power automobiles, as this chapter is written the chemistry of choice in commercially available hybrid vehicles is still nickel metal hydride (NiMH). Fig. 18.1 provides one metric that compares the Li-ion chemistry with other battery chemistries. Although Li-ion batteries have not yet been proven as a technology for electric vehicles, the chemistry

**Table 18.1** Selected Li-ion battery recalls since October 1, 2006 (from Ref. [3])

Manufacturer	Product type	Cell/battery manufacturer	Recall number	Date
Innovage LLC	Remote-controlled helicopter	N/A	685,000	7/24/2008
GN Netcom	Wireless headsets	ATL	525,000	10/14/2008
Sony	Laptop battery	Sony	340,000	10/23/2006
Jakks Pacific Inc	Toy battery	N/A	245,000	2/13/2007
Lenovo	Laptop battery	Sanyo	100,000	3/1/2007
HP	Laptop battery	N/A	70,000	5/14/2009
Estes-Cox Corp	Radiocontrolled planes	N/A	66,000	3/27/2007
Materforce	Cordless screwdriver	Great Star Industry	42,000	9/2/2008
HP/Toshiba/Dell	Laptop battery	Sony	35,000	10/30/2008
Acer	Laptop battery	Sony	27,000	4/25/2007
Gateway	Laptop battery	N/A	14,000	6/19/2007
Coby Electronics	DVD/CD/MP3	N/A	13,000	10/8/2008
Polycom, Inc.	Wireless conference phone battery	Gold Peak Industries	5,800	6/5/2008
Clarion	GPS	Kiryung Electronics	4,000	8/16/2007
Hobby-Lobby Intl.	Helicopters	N/A	3,200	4/14/2008
EV Global Motors	Electric bike	N/A	2,000	4/25/2008
DiNotte Lighting	Bicycle light	AA Portable Power Corp	1,700	11/18/2008
Toshiba	Laptop battery	Sony	1,400	8/9/2007

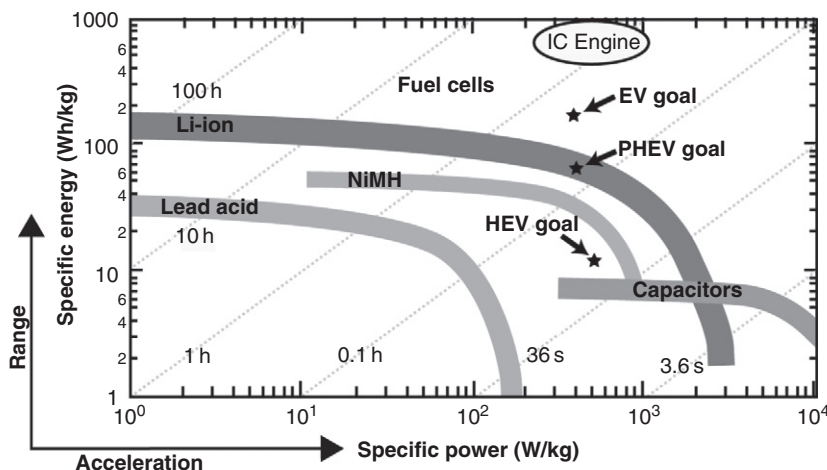


**Figure 18.1** Relative performance of various electrochemical energy storage devices (from Ref. [4]).

appears to satisfy current specific energy and power requirements for hybrid electric vehicle (HEV), plug-in hybrid vehicle (PHEV)-40, and PHEV-10 goals [2].

Similar to consumer electronic products, where NiMH batteries have been replaced by Li-ion batteries over the past few years, the automotive industry appears to be next in line. In early 2009, the Mercedes Benz S400 BlueHybrid was the first production HEV fitted with a Li-ion battery. The BlueHybrid uses the car's air conditioning system to keep the Li-ion battery cool. General Motors has indicated that the Chevrolet Volt is scheduled to be available to the general public in 2010 and will be the first major car manufacturer that will use Li-ion cells in a plug-in hybrid. The battery cells made using a manganese spinel-positive electrode are manufactured by the Korean company LG Chem [5]. The 400-pound battery system is the Volt's single most crucial component and is expected to be the most expensive element of the vehicle.



## 2. Li-ION FLAVORS

A variety of materials may be used for the construction of Li-ion cells. The selection of these materials amongst other things determines the voltage, capacity, life, and the safety of the cell. Table 18.2 provides a brief summary of selected materials that are used for the construction of high-energy Li-ion cells.



## 3. Li-ION CELL FAILURES

The consequences of a failure event in a Li-ion battery tend to be more severe compared to other rechargeable battery chemistries for two reasons. First, Li-ion batteries have a higher energy density than other battery chemistries; therefore, more heat

**Table 18.2** Selected Li-ion chemistries for high-energy designs (from Ref. [7])

Negative electrode	Separator	Electrolyte	Positive Electrode	Stoichiometry	Potential	Key attributes	Applications	Wh/kg	Wh/l
Graphite	Polyolefin	Carbonates and lithium salt	Lithiated cobalt oxide	$\text{LiCoO}_2$ (LCO)	3.6 V	High-volume production	Consumer cells for laptops, cell phones, PDAs, hand-held games	195	560
Graphite	Polyolefin	Carbonates and lithium salt	Lithiated nickel–cobalt–aluminum oxide	$\text{LiNi}_{0.8}\text{Co}_{0.15}\text{Al}_{0.05}\text{O}_2$ (NCA)	3.6 V	Most mature design for automotive	HEV, PHEV, EV, aerospace	220	600
Graphite	Polyolefin	Carbonates and lithium salt	Lithiated nickel–manganese–cobalt oxide	$\text{LiNi}_x\text{Co}_z\text{Mn}_y\text{O}_2$ (NCM)	3.7 V	Potential high-volume production for consumer cells	HEV, PHEV, aerospace, portable devices	205	580
Amorphous carbon	Ceramic-coated polyolefin	Carbonates, lithium salt and polymer	Lithiated manganese oxide	$\text{LiMn}_2\text{O}_4$ (Spinel)	3.7 V	Design developed exclusively for high power	HEV, PHEV, EV	150	420
Graphite	Polyolefin	Carbonates and lithium salt	Lithiated iron phosphate	$\text{LiFePO}_4$ (olivine)	3.2 V	Positive electrode material with increased oxygen stability	HEV, PHEV	90–130	333

can be generated by the chemical reaction between the positive and negative electrodes. Second, Li-ion batteries use a flammable organic solvent as the electrolyte that can ignite and release additional heat if exposed to the air. It is this combination of high-energy density and a flammable electrolyte that makes safety a much larger issue for Li-ion battery systems than it has been for other battery chemistries.

Generally, Li-ion cell failures can give rise to both reliability and safety concerns. Most often, a Li-ion cell will fail in a manner which makes it inoperable such that it is unable to be charged and/or discharged. However, in some instances, a Li-ion cell may fail exothermically. An exothermic failure of the cell is referred to as the cell going into “thermal runaway.” This mode of failure though is rare for the chemistry. Although infrequent, occurrences of cell thermal runaway can be highly destructive and pose a fire hazard. Accordingly, it is important to address safety concerns when designing and specifying systems using Li-ion cells.

Fig 18.2 shows the remnants of a multicell Li-ion battery after thermal runaway of the cells. In this incident, the heat generated by the exothermic failure of one of the cells caused a failure and thermal runaway of the other cells in the battery.

Thermal runaway of a Li-ion cell occurs when the heat generated within the cell exceeds the heat dissipation by the cell. The various reasons for this event are discussed in subsequent sections of this chapter. In general, whenever a charged Li-ion cell is exposed to temperatures above 60°C, there is a risk of initiating exothermic reactions within the cell. The heat generated by these reactions may result in a rise in the cell temperature, which in turn activates additional exothermic reactions.

For example, for a Li-ion cell with a lithiated cobalt oxide positive electrode, the following is one possible scenario as the cell is heated until it goes into thermal runaway (the temperatures represent approximate values) [6]:

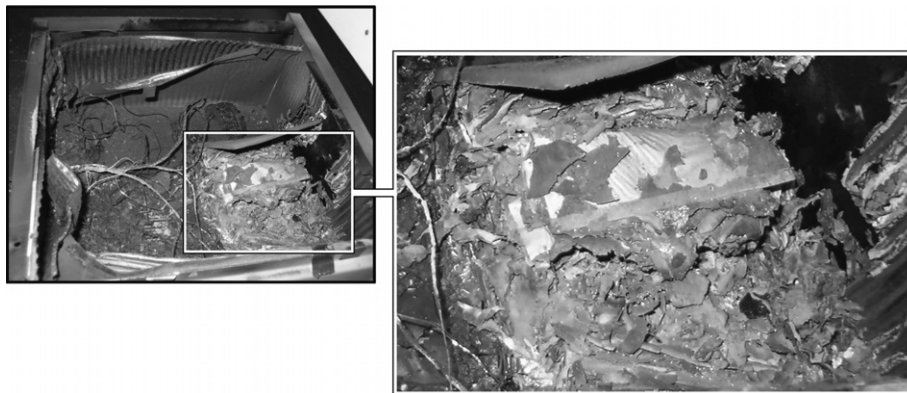


**Figure 18.2** Remnants of a multicell battery where the cells went into thermal runaway (Courtesy of Exponent, Inc.).

- Partially reduced, lithiated compounds in the passive solid electrolyte interface (SEI) layer of the negative electrode start to react with lithium in the negative electrode when the cell internal temperature reaches 60–80°C. This reaction is exothermic and can cause a further increase in the cell temperature.
- Lithium in the negative electrode starts to react thermally with the solvent once the cell's internal temperature rises to approximately 110°C. This exothermic reaction causes a further increase in the cell's temperature.
- Once the cell's internal temperature reaches approximately 125–135°C, the polyethylene component of the separator melts, closing the nanopores and resulting in a several orders of magnitude increase in the internal resistance of the cell.
- The polypropylene component of the separator starts to melt when the cell's internal temperature approaches 175–185°C, significantly reducing the mechanical strength of the separator. Above this temperature range the separator may fail mechanically, resulting in the activation of an internal short circuit.
- Once the cell's internal temperature rises to a point at which the separator starts to melt, the positive electrode reacts thermally with the solvent generating heat and in some cases causing the cell to go into irreversible thermal runaway.

Other Li-ion chemistries follow a similar sequence of events as they are heated until they enter thermal runaway. In some cases, the rapid increase in temperature can cause the cell to vent or in worst-case conditions eject its internal contents.

Fig. 18.3 shows the surface temperature of a Li-ion cell during a test based on a heating test from the Underwriters Laboratories (UL) UL1642 standard (UL1642-2003

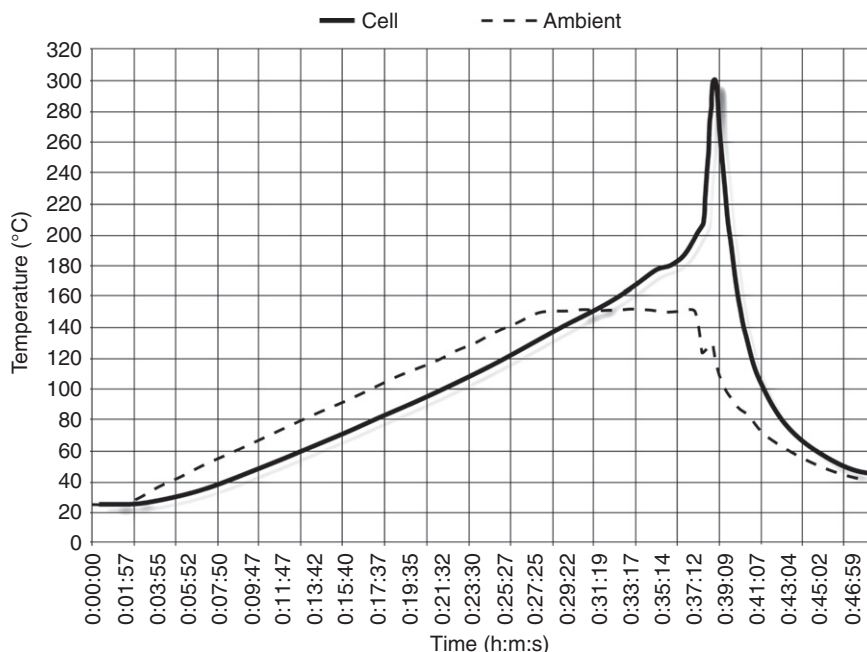


**Figure 18.3** Cell surface temperature during heating test based on the UL1642 heating test.

lowered the soak temperature to 130°C from 150°C). This test was performed with a soak temperature of 150°C. During the test performed, exothermic reactions within the cell caused its temperature to increase above the ambient temperature eventually resulting in the cell going into thermal runaway, venting and ejecting its internal contents.

The amount of heat released by the reactions between the negative electrode and the electrolyte at temperatures below 150°C are generally not sufficient to sustain a thermal runaway event. For example, if a charged Li-ion cell is heated briefly to 150°C, followed by exposure to room-temperature conditions, the cell will likely cool and return to room temperature. However, if the same Li-ion cell is held at 150°C, then the exothermic reactions at the negative electrode will eventually cause the temperature of the cell to rise as shown in Fig. 18.3 and may cause it to go into thermal runaway.

The “point of no return” is usually reached when the polypropylene component of the separator melts, around 175–185°C. Above this temperature there is a significant risk of separator failure and the initiation of an internal short circuit, which will result in a rapid increase in temperature as the stored energy within the cell is released as heat. The exact temperatures and the amount of heat released by the exothermic reactions are dependent upon the specific design attributes of the cell, such as choice of positive and negative electrode materials, surface area of these materials, and electrolyte composition.

The runaway temperature of a cell will depend on many factors including the cell’s chemistry, its construction etc. As an example, Fig. 18.4 demonstrates the results obtained by accelerated rate calorimetry (ARC) for different delithiated positive electrode materials [7].

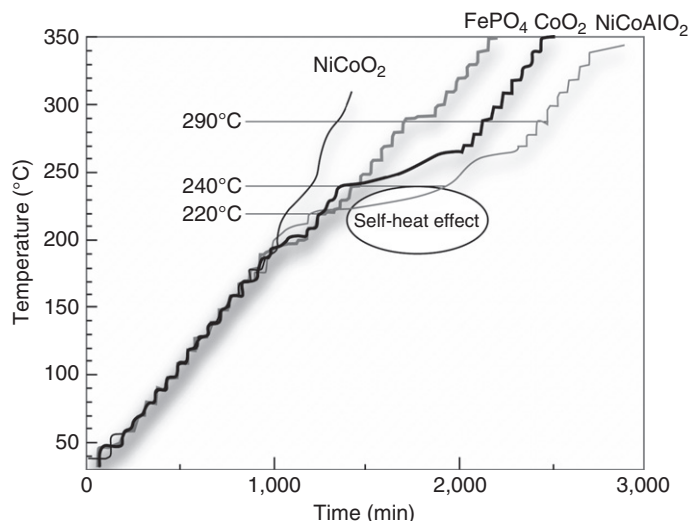


**Figure 18.4** Results obtained by ARC for different delithiated positive electrode materials using liquid electrolyte at the charge state (from Ref. [8]).

## 4. WHY DO LI-ION CELLS GO INTO THERMAL RUNAWAY?

Although most Li-ion cell failures are benign in nature and result in a nonfunctional cell (i.e., a cell which will not accept a charge or be capable of supplying output current), in rare cases a cell failure may result in a thermal runaway condition with the cell venting and releasing its contents. Thermal runaway of a Li-ion cell can occur due to a variety of reasons (Fig. 18.5). Generally, most cell failures followed by thermal runaway are a result of a cell internal fault, which is one of the most severe failure conditions for the chemistry.

The Li-ion cell has a well-defined range of operating conditions for voltage, current, and temperature. Failures generally occur when a cell is operated outside its rating and exposed to mechanical, electrical, or thermal abuse conditions. Excessive charge/discharge currents, over/undercharge conditions, over/under temperature conditions, improper manufacturing techniques, etc. are all factors that can lead to cell failure.

### 4.1 External short circuit

An external short circuit condition can occur when a conductor bridges the output terminals of a Li-ion cell. Typically, test protocols define a short circuit as a low-resistance fault condition. Throughout this chapter, reference to a short circuit would include a fault condition where the resistance is less than 50 m $\Omega$ .

A short circuit condition in a fully charged multicell Li-ion battery can generate high peak currents (typically, a 2 Ah cylindrical cell may generate peak short circuit currents in excess of 50 A). Under worst-case conditions, this can lead to cell venting with the release of flammable electrolyte, generation of toxic gases, or even a rupture of the cell can.

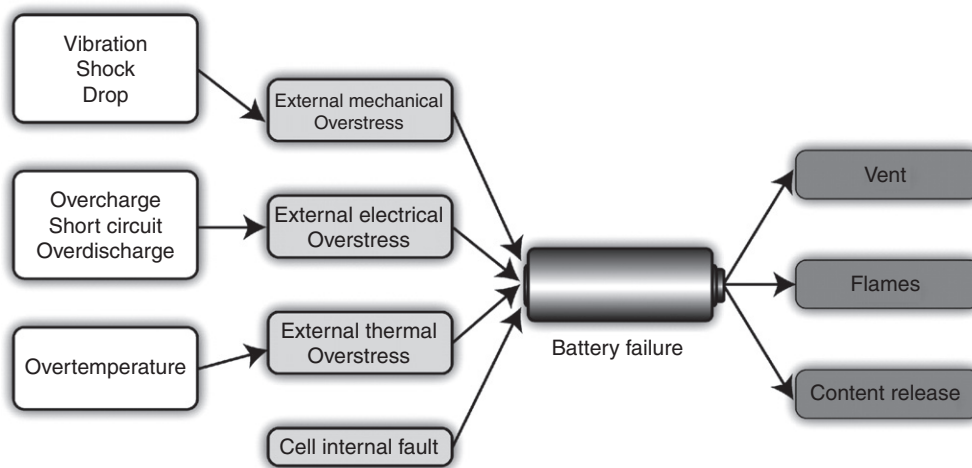


**Figure 18.5** Conditions which may cause a cell failure.



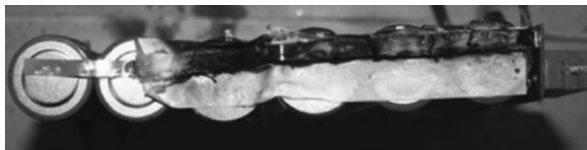


**Figure 18.6** A short circuit failure in a multicell Li-ion battery.

In a multicell application such as the HEV battery, this can start a chain reaction causing neighboring cells to fail due to the heat generated by the short circuit.

Fig. 18.6 shows a multicell Li-ion battery after a short circuit on the battery's protection circuit board caused the flow of excessive current. The large current damaged the current carrying bus bars and the positive terminals of the cell cans. Although no thermal runaway was observed in this case, an inadequate battery system design can lead to a thermal runaway during a similar fault condition.

In the example depicted in Fig. 18.6, the bus bars were probably not rated to handle the peak short circuit currents and sustained damage before the positive temperature coefficient (PTC) overcurrent protector within the cylindrical cells operated to limit the short circuit current.

## 4.2 Internal short circuit

The main components in a Li-ion cell that may be involved in an internal short circuit fault condition include the copper current collector, the positive electrode, the negative electrode, and the aluminum current collector (Fig. 18.7). The following four possible scenarios can lead to an internal short circuit fault within a Li-ion cell [9]:

- Short circuit between the two current collectors.
- Short circuit between the Cu current collector and the positive electrode active material.
- Short circuit between the Al current collector and the negative electrode active material.
- Short circuit between the active materials on both the electrodes.

The rise in local cell temperature under the four possible internal short circuit scenarios has been researched and presented by multiple authors. One such study that depicts the rise in local cell temperature as a function of time was performed by Santhanagopalan et al. [9]. The results of this study indicate that the highest temperatures result when the short occurs between the Al current collector and the negative electrode active material (Fig. 18.8). An internal short circuit within a Li-ion cell can occur due to a variety of reasons such as the following:

- Metallic contaminants
- Dendrite growth
- Lithium plating
- Charging outside rated temperature
- Separator failure
- Mechanical abuse
- Improper charging protocols

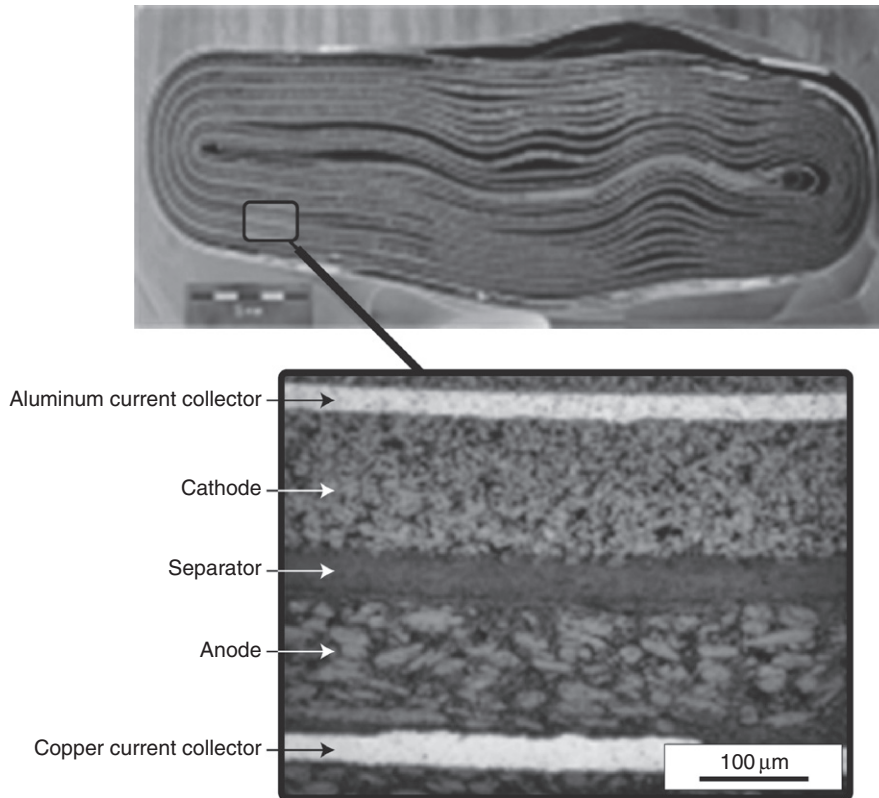


**Figure 18.7** Cell cross section showing the cell's main components (Courtesy of Exponent, Inc.).

#### 4.2.1 Metallic contaminants

Metallic contaminants introduced within the cell during the cell manufacturing process or as a result of poor incoming material quality control can result in an internal short circuit. A metallic contaminant can compromise the separator providing a path for the electric current from the positive to the negative electrode. More often than not, the metallic contaminant fuses open due to the large current flow through it. However, in some cases the contaminant may carry the current for a time period long enough to initiate exothermic reactions within the cell and eventually cause the cell to go into thermal runaway.

Additionally, metallic contaminants within the cell that do not physically bridge the gap between the negative and positive electrodes can cause a short circuit through an electrochemical dissolution and replating mechanism. For example, an iron contaminant trapped in the thickness of the active material coating will be converted to soluble iron ions when the potential of the region of the cell exceeds the oxidation potential of iron. The soluble iron ions then partition into the electrolyte, diffusing to the opposite

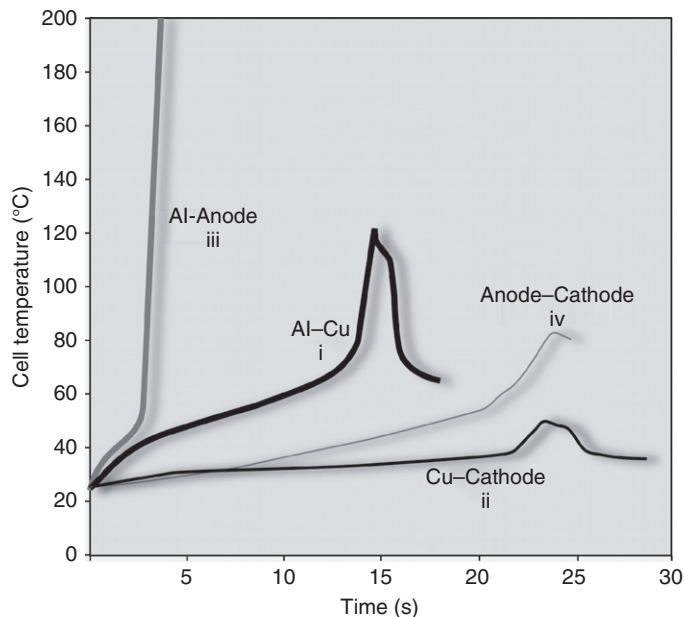


**Figure 18.8** Cell temperature under various internal short circuit scenarios. Anode: negative electrode active material; cathode: positive electrode active material (from Ref. [9]).

electrode where they are reduced back to iron. A repetition of this cycle can eventually lead to a conductive path between the positive and negative electrodes, i.e. a cell internal short circuit condition.

#### 4.2.2 Cell defects

The cell assembly process requires precision, control, and repeatability. Defects may be introduced within the cell during the assembly process which can eventually lead to an internal short circuit. Cell defects introduced during the manufacturing/assembly process are most often related to the relative positioning of critical cell components. Some examples include the following:

- Improper cell tab positioning (e.g., folding and routing of tabs, tab overhang, etc.).
- Improper cell tab insulation.
- Winding misalignments resulting in: positive/negative electrode registry problems  
crushing of the cell's electrodes.

#### 4.2.3 Cell charging algorithm

Charging a Li-ion cell is a precise operation requiring features which control when and how the cell is charged. Li-ion cells are usually charged using the constant current–constant voltage charge profile which involves the cell charged at a constant current until its voltage reaches the predetermined limit (typically 4.1 or 4.2 V)

followed by a constant voltage charge state until the current decreases to a predetermined low value [10]. No trickle charging (continuous low-current charging) is performed on these cells. Once fully charged, trickle charging Li-ion cells can result in the oxidization of the electrolytic solvents due to the high potential, physical and chemical degradation of the positive electrode material and plating of metallic lithium at the negative electrode which can eventually lead to a cell internal short circuit condition [11, 12].

### 4.3 Cell overcharge

The fully charged voltage of the most typical, commercially available Li-ion cell is specified as  $4.20 \pm 0.05$  V (some Li-ion cell chemistries may be charged to voltages as high as 4.40 V). An overcharge process initiates reactions within the cell which can cause the cell to go into thermal runaway.

Fig. 18.9 shows the temperature profile for a Li-ion cell with a  $\text{LiCoO}_2$  positive electrode, a graphitic negative electrode, and ethylene carbonate/ethyl methyl carbonate electrolyte. The following reactions occur within the cell at the various temperatures [13, 14]:

- I. As the cell overcharges, lithium ions are irreversibly removed from the positive electrode and deposited as lithium metal on the negative electrode. This delithiation of the positive electrode continues as the cell voltage increases during overcharge until eventually the lithium ions are completely depleted from the positive electrode.
- II. During the overcharge process, the cell impedance starts to rise due to an increase in the positive electrode material resistance. At the same time, the electrolyte within the cell begins to decompose, coating the active materials and further contributing to the increase in cell impedance. The increasing cell impedance results in an increase in the heat generated as charging current passes through the cell.

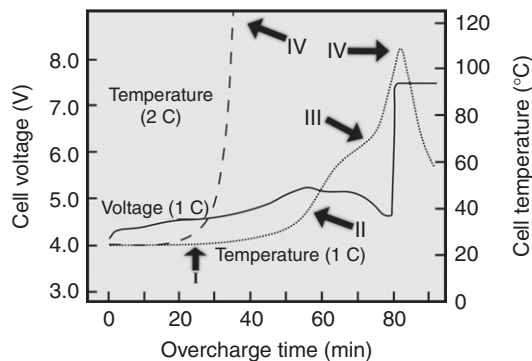


**Figure 18.9** Overcharge reaction and thermal runaway mechanism of a Li-ion cell (from Ref. [13]).

- III. The cell temperature starts to rise rapidly as an exothermic reaction between the delithiated positive electrode material and the electrolyte occurs. Once the cell temperature rises above approximately 60°C, the rate of this reaction accelerates generating a large amount of carbon dioxide.
- IV. The cell temperature continues to rise until the internal temperature reaches approximately 130–135°C. In this temperature range, the cell separator undergoes a phase transition that closes the porosity of the membrane and impedes the transport of ions between the electrodes. This engineered safety feature “shuts down” the separator terminating the charge current and ending the overcharge process. In some instances, a “shutdown” of the separator is unable to stop the self-heating of the cell which eventually leads to additional exothermic degradation processes. These “additional” processes are not well understood but if sufficiently activated can continue to generate heat within the cell and can eventually lead to a thermal runaway.

#### 4.4 Overdischarging Li-ion cells

Li-ion cells cannot generally be discharged to 0 V and rely on a cutoff scheme to terminate the discharge current before the cell voltage drops to 0 V. The cutoff voltage depends on the nuances of the cell chemistry. For a cobalt dioxide-based Li-ion cell, the cutoff voltage is generally specified in the range of 2.0–3.0 V.

Overdischarging a Li-ion cell can result in the oxidation of the Cu current collector on the negative electrode which leads to Cu dissolution into the electrolyte. As the overdischarged cell is recharged, dissolved Cu redeposits in regions of the cell capable of reducing it back to copper metal. This can reduce cell performance by, for example, blocking access to active electrode material or clogging the pores of the separator membrane. If the Li-ion cell is overdischarged frequently, dendrite growth may start to occur between the negative and positive terminal which can eventually lead to an internal short [15].

#### 4.5 Low-temperature charging

One of the steps in the manufacturing of a Li-ion cell is the “formation” step. The cell is assembled in a discharged state and the first charge results in the formation of an electrolyte decomposition layer on the surface of the negative electrode (SEI). This layer acts as a safety feature by maintaining a protective barrier between the reactive negative electrode and the electrolyte. At the same time the SEI layer is porous enough to allow the passage of  $\text{Li}^+$  for low-to-moderate rate charge and discharge currents. However, the layer limits the discharge rates and restricts the temperature range over which the battery may be charged.

The rate of  $\text{Li}^+$  transport through the SEI layer is hindered at low temperature. Hence, charging the cell in this state can result in lithium plating at the SEI/electrolyte

interface if the rate at which Li ions arrive at the surface of the negative electrode material exceeds the rate at which they can diffuse from the surface into the bulk of the particles. Lithium plating at the surface of the negative electrode material can result in dendrite growth and hence in an internal short circuit [16, 17].

#### 4.6 High-temperature storage and charging

Charging or storage of a Li-ion cell at high temperatures can lead to a failure of the cell in some cases. Failures at high temperatures may occur due to one of the following reasons:

- *SEI layer breakdown.* The SEI layer may break down and dissolve into the electrolyte if the cell temperature rises above approximately 120°C, initiating an energetic chemical reaction between the negative electrode and the electrolyte which can, under worst-case conditions, cause the cell to go into thermal runaway.
- *Electrolyte vaporization.* Li-ion cell electrolytes are based on volatile organic solvents. Under high-temperature conditions, the electrolyte may vaporize, which can result in an increase in the cell's internal pressure. This can lead to activation of the cell's current interrupt device (CID) (if so equipped). In extreme cases, the increased pressure can operate the cell's vent mechanism, resulting in the expulsion of the vaporized electrolyte from the cell.
- *State of charge.* The higher the state of charge of the cell, the more likely that the cell may fail when thermally stressed. When a charged cell is exposed to high temperatures, the positive electrode can chemically oxidize the electrolyte. This oxidation process is exothermic and may result in an increase in the cell's temperature, which may lead to a further reaction between the electrolyte and the positive electrode. If this process is allowed to continue, the temperature of the cell can become sufficiently high and cause the degradation of the separator, resulting in a cell internal short.



### 5. TYPICAL SAFETY CIRCUITS

To ensure that the Li-ion cells operate within their rated specifications, protection circuitry is relied upon. Batteries with Li-ion cells used in consumer electronics such as laptop computers, cell phones, and DVD players employ a variety of features to provide adequate protection to the cells. These include the following:

- PTC devices, thermal cut-offs, bimetal switches, and thermal fuses.
- Monitoring electronics to prevent the cells from being overcharged/overdischarged.
- Separators which prevent ionic transportation at elevated ambient temperatures.
- Additives to prevent exothermic reactions at elevated ambient temperatures.
- Safety vents to release the cell's internal pressure in a controlled manner.

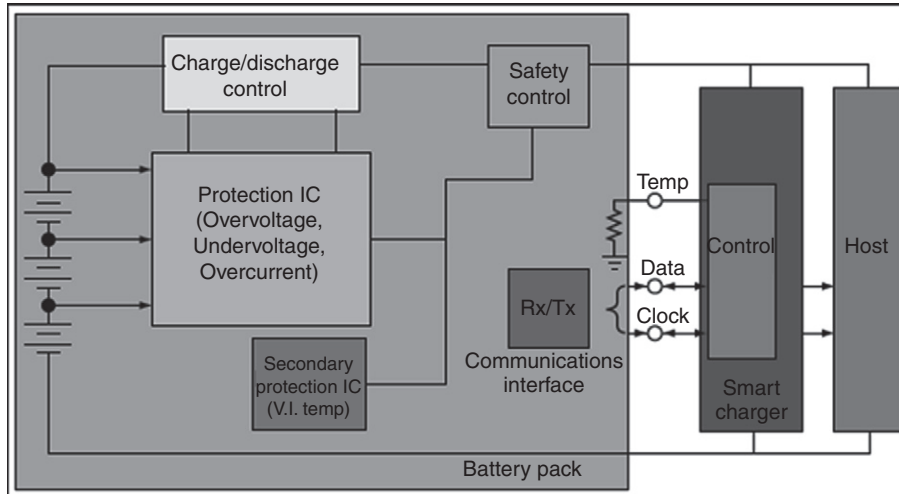


**Figure 18.10** Protection/control circuitry used in consumer electronic applications.

- Electrical disconnects such as CIDs to provide electrical disconnection at elevated cell pressures.
  - Excessive active material at the negative electrode to prevent lithium deposition.
- Fig. 18.10 shows a block diagram of the typical architecture of a Li-ion battery system for a multicell application such as a notebook computer.

Even though the Li-ion battery system in a hybrid vehicle is more demanding when compared to a consumer electronics system, the requirement of ensuring that the cells operate within their rated specifications remains the same. Additional complexity is added due to a variety of reasons such as the larger number of cells in the battery, the larger capacity of each cell, the increased energy stored by the battery, the more complex requirements for power management for the HEV application, etc. HEV requirements necessitate the introduction of safety features which are not always necessary in a consumer electronic device, such as the following:

- Cell designs that assist in the distribution of heat in the event of an internal short circuit condition.
- Ceramic separators to improve thermal stability.
- Positive electrode materials with greater thermal stability.
- Battery/cell case designs that provide better heat transfer (e.g., through the use of fins).
- Forced convection mechanisms for heat transfer.
- Electronic controls.
- The use of soft packages for the cell to provide larger aspect ratios to aid in better heat transfer.

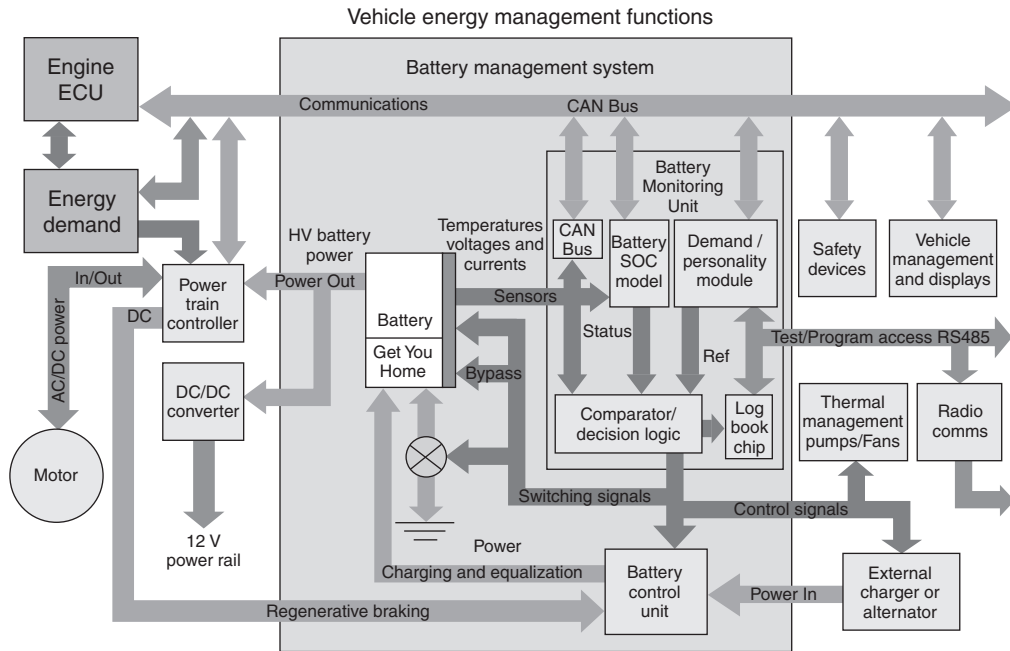


**Figure 18.11** Protection control circuit used for a HEV battery (from Ref. [18]).

Fig. 18.11 shows an example of architecture of a Li-ion battery control circuit used in a HEV [18]. The battery control unit manages the charging and equalization of the cells in the battery. This unit relies on the battery monitoring unit to provide information on when the battery should be charged and discharged. The battery monitoring unit monitors the voltages, currents, and temperatures of the cells in the battery and uses this information to determine the state of charge and state of health of the battery.

The system design goal is to ensure that the cells operate only within their specified ratings to provide safety and reliability. A typical HEV battery management system provides the following functionality [18]:

- Cell state monitoring.
- Charge and discharge current measurement and limiting.
- Cooling system management.
- Communications between the battery and the vehicle.
- High-voltage relay control.
- State of health and state of charge monitoring and estimation.

A typical HEV battery consists of multiple cell modules which may have their own control circuits. These modules are usually interconnected and controlled by a master electronic control system [19]. Fig. 18.12 shows an example of an arrangement of the controlling architecture in a HEV battery.



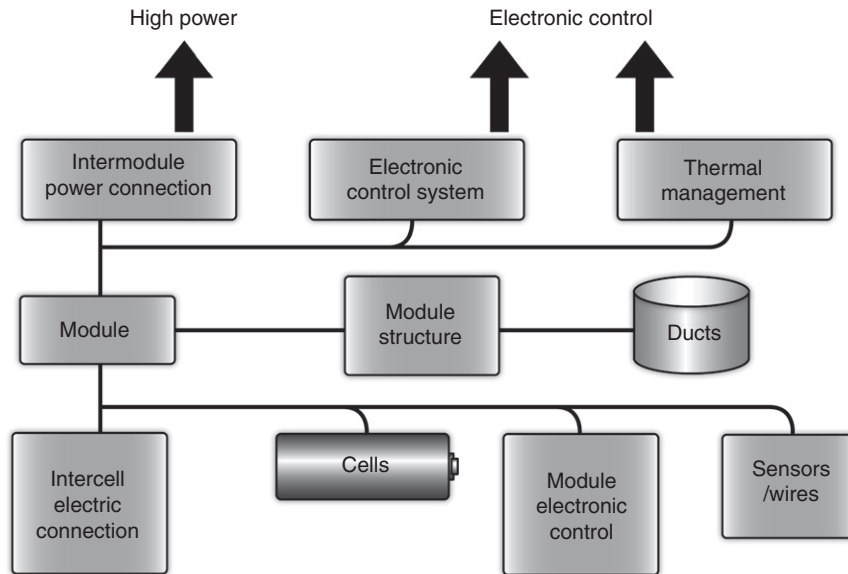


**Figure 18.12** Typical HEV battery design.



## 6. HEV BATTERY SAFETY STANDARDS

Consumer electronic product Li-ion energy storage technology has matured over the past several years and resulted in battery systems with standardized designs, similar architectures and few distinguishing features. This has allowed generic safety standards to provide a consistent and repeatable baseline for abuse and safety performance testing. However, the current state of the HEV industry with emerging and evolving vehicle designs complicates the generation and acceptance of new abuse and safety performance tests. Limited field experience and architectures which are still works in progress make it challenging to define an all encompassing standard that can provide an effective, one-size-fits-all baseline for abuse and safety characterization testing of these battery systems.

Although research continues to determine how the Li-ion HEV battery systems will react to various potential abuse conditions in the field, numerous standards exist to aid in the evaluation of the safety performance of these battery systems. These abuse tests consist of stress conditions that the batteries may be exposed to in an automotive environment. Various HEV developers and industry organizations such as the Society of Automotive Engineers (SAE) and the US Advanced Battery Consortium (USABC) have used the industry's collective knowledge base to develop a series of abuse test protocols simulating mechanical, environmental, and electrical abuse scenarios. These protocols are intended to provide a general baseline to aid in the development of safe battery systems and to provide a general reference frame for comparison between the

**Table 18.3** Potential hazard modes (from Ref. [21])

Electrical	Thermal	Mechanical	System
Short-circuit	Fire	Crush	Contactors fails closed
Overcharge	Elevated temperature	Nail intrusion	Loss of high voltage continuity
Soft short/Overload		Drop	Chassis fault

various battery systems. Table 18.3 provides a summary of the various potential abuse scenarios that a HEV battery system may be exposed to in the field.

The USABC abuse test procedures manual (FreedomCAR Electrical Energy Storage System Abuse Test for Electric and Hybrid Electric Vehicle Applications) defines a series of tests “intended to simulate use and abuse conditions that may be beyond the normal safe operating limits experienced by electrical energy storage systems used in electric and hybrid electric vehicles” [20].

The SAE J2464 (Electric Vehicle Battery Abuse Testing) standard is similar in scope and content to the USABC test procedures manual. The approach taken by the standards is to define a set of hazard modes that cells in a HEV battery system may be exposed to under various conditions. The hazard modes are divided into four subsets (Table 18.3) depending upon the type of abuse condition.

Table 18.4 provides a definition of the severity levels that are used to calibrate the battery system performance to the various abuse conditions. Table 18.5 summarizes the abuse tests defined by the various standards [21, 22].

Useful information on battery behavior and response to vehicle level misuse conditions can be gathered through the abuse tests described in Table 18.5. However, a perspective is required to calibrate the test results to determine the most effective way of reducing the risk. There are different ways in which a quantification of the risk may be performed. One such technique called the ‘Battery Hazard Modes and Risk Mitigation’ is described by Ashtiani [23]. This approach involves an identification of hazards and a calculation of the associated risks. Various hazard levels are defined to aid the quantification process. Table 18.6 provides one such definition widely used. The hazard levels are

**Table 18.4** A definition of severity for the abuse tests

Severity level	Description
1	Energy storage system expected to remain intact and functional after the test (minor repairs may be needed to make the module functional)
2	Energy storage system may become inoperable but should not expose humans to known health risks
3	Most destructive test where the energy storage system is expected to be inoperable after the test.

**Table 18.5** Abuse tests as defined by the FreedomCAR standard (from Ref. [21])

Abuse type	Test	Severity	Description
<b>Mechanical</b>	Controlled crush	3	50% displacement of the battery module's height or a force of 1,000 times the battery module's mass
	Penetration	3	Complete penetration at both the cell and battery system level
	Drop	3	Drop onto a cylindrical steel object from a height of 10 m
	Immersion	3	Salt water immersion for at least 2 h
	Roll over	1	90° increments with 1 h hold
	Vibration	1	Swept sine wave vibration testing
<b>Thermal</b>	Mechanical shock	2	20–30 g acceleration profile
	Thermal stability	3	Heat until cell self-heating occurs
	Simulated fuel fire (radiant heat test)	3	890°C exposure for 10 min
	Elevated temperature storage	2	Storage at 80°C for up to 2 months
	Rapid charge/discharge	2	Twenty continuous charge/discharge cycles at manufacturer recommended charge current and 3 kW constant power rate discharge
	Thermal shock	2	Five storage cycles between –40°C and 80°C for various time intervals
	Compromise of thermal insulation	2	Compromise insulation system integrity and determine battery response
	Extreme cold temperature test	2	Charge and discharge cycles at various temperatures down to –40°C
<b>Electrical</b>	Overheat/thermal runaway	2	Charge/discharge cycles with thermal control active and with thermal controls bypassed
	Overcharge/overvoltage	2	Charge until 200% SOC for 4 h
	Short circuit	3	Hard short (<5 mΩ) for 10 min
	Overdischarge reversal	2	50% voltage reversal of subassemblies
<b>System</b>	Partial short circuit	3	Short circuit applied to adjacent units/modules for 2 h
	Compromise of thermal insulation		Compromise thermal insulation of vehicle system and monitor temperatures until thermal equilibrium reached
	AC exposure test	2	Subject battery system to 50/60 Hz (AC) with a current limit of 60 A from a 240 V/60 A standard outlet for a period of 1 h.

**Table 18.6** Hazard levels

Hazard level	Description	Criteria and effects
0	No effect	No effect or loss of functionality
1	Reversible loss of function	No defect, leakage, venting, fire, or flame. Resetting of protective devices restores functionality.
2	Irreversible defect/damage	No defect, leakage, venting, fire or flame. Repairs needed to restore functionality.
3	Leakage (change of mass < 50%)	No defect, leakage, venting, fire, or flame. Weight loss < 50% of electrolyte weight. Light smoke.
4	Venting (change of mass > 50%)	No defect, leakage, venting, fire or flame. Weight loss $\geq$ 50% of electrolyte weight. Heavy smoke.
5	Fire or flame	No flying parts.
6	Rupture	No explosion but battery disintegrates without flying parts.
7	Explosion	Exposure to toxic substances in excess of Occupational Safety and Health Administration (OSHA) (USA) limits

combined with a number for the likelihood level. The result generates a value for the hazard risk number, which can be used to aid in the determination of whether the associated hazard of a particular occurrence is in the “high-risk zone” or in the “low-risk zone.” This information is then used to identify detection and control mechanisms required to mitigate the associated risks [24].



## 7. SYSTEM SPECIFIC SAFETY EVALUATION

The test standards discussed previously do not define pass/fail criteria. The aim of the tests defined in the standards is to provide information about the performance of the batteries under the tested abuse conditions and allow the manufacturer to decide whether the response of the battery system to these abuse conditions is acceptable. In addition to the standardized abuse tests, it is necessary to develop a set of safety tests specifically tailored to the battery and cell design and its integration into the system. For example, safety tests should be devised to investigate the following:

- The effect of the system architecture on the battery system and the interactions between the various subsystems. Ideally, the battery system should be designed to withstand all the defined abuse scenarios without going into thermal runaway or causing high cell temperatures.
- The effect of potential design and manufacturing defects and the failure modes associated with these defects.
- Any lessons learned from field failures should be utilized and incorporated into test protocols so that their effects can be understood and mitigated in the future.

## 7.1 Cell manufacturing defects

Determining the response of the cell to some of the failure modes associated with the Li-ion chemistry is challenging. This leads to the requirement of robust quality processes during cell manufacturing. For example, issues such as contamination, component latent defects, and failure modes introduced due to unique manufacturing processes are hard to test for requiring test procedures that simulate these challenging failure mechanisms. An example of such a failure mode is the introduction of contaminants within a cell which can lead to an internal short circuit. As previously discussed, this can lead to a “dead cell” condition or in some rare instances cause the cell to go into thermal runaway. Fig. 18.13 shows an example of a contaminant in a cell.

A variety of tests have been devised to simulate a cell internal short condition and its effect on the cell. Although not all encompassing, these tests allow a general understanding of the potential consequences of a cell internal short condition. Many factors can influence the test results and an understanding of the influencing factors should be gained. Variations such as ambient temperature at the time of the fault, cell age and state of charge, cell orientation, and heat dissipation in the battery will affect the response of the cell to an internal short circuit condition. Some tests commonly used to simulate a cell internal short include the following:

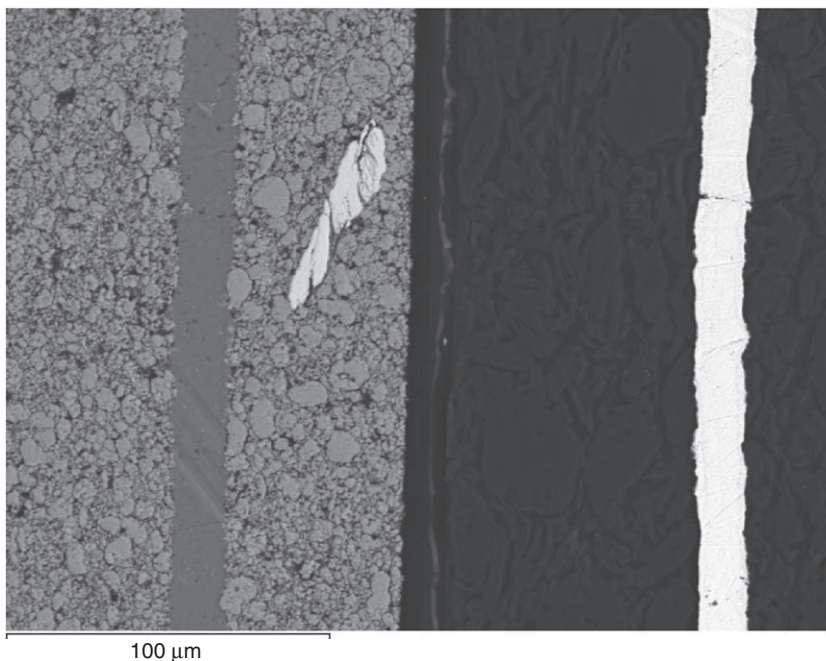


**Figure 18.13** Metal contaminant in a cell (Courtesy of Exponent, Inc.).

- Nail Test.* This test attempts to simulate a cell internal short circuit condition by using a nail to achieve a short between the cell's positive and negative electrodes. However, the test has some limitations. Test data gathered and analyzed has indicated a variation in the cell's response due to the test fixture, the diameter of the nail, the speed of nail penetration, etc. In addition, this test shorts all the windings together which may not necessarily be the fault condition that may occur in the field. Fig. 18.13 shows an example of a contaminant which may result in a short circuit between a pair of windings rather than all the windings in the cell.
- Crush Test.* This is a standard test commonly used by manufacturers and described in various industry abuse standards for Li-ion cells. In this test, a force is applied to the cell's enclosure until a cell internal short is achieved. Similar to the nail test, no control is maintained over the number of windings that are involved in the internal short condition. In addition, the crushing force required to achieve an internal short generally depends on the cell's enclosure material. For example, cells utilizing a steel can are generally disfigured during the test before an internal short is achieved.
- Forced Internal Short Circuit.* The goal of this test is to try and recreate the effect of a contaminant within a cell. The test is performed by dismantling the cell and inserting a small sliver of metallic nickel between the cell's positive and negative electrodes. The cell is then reassembled and a "pressing" force is applied until a cell internal short is achieved. Industry standards specify a particular insertion location for the metallic nickel (Fig. 18.14) [25]. Although this test provides a fair representation of an internal short circuit due to a contaminant, it is difficult to control the location of the internal short during the test. In addition, predicting the size of the contaminant that may be present in a manufactured cell is difficult.

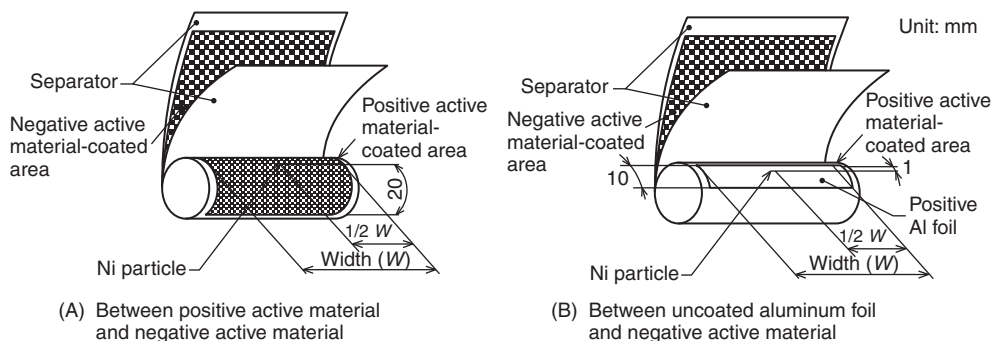


**Figure 18.14** Position of the insertion of metallic nickel in a cylindrical cell (From Ref. [25]).

## 7.2 Design defects

The determination of design defects, if any, require a thorough safety evaluation of the cell and battery system before it is released for mass production. An evaluation of all aspects of the design and safeguards present in the design is necessary to mitigate, or prevent altogether, potential unsafe failure modes. Although HEV system architectures can greatly vary, the battery and its associated architecture will generally be dependent upon the type of hybrid vehicle, that is, whether the application is a series or a parallel hybrid configuration. Figs. 18.15 and 18.16 illustrate a block diagram of the two common hybrid configurations. The charge and discharge paths in a series hybrid configuration are generally separate while in a parallel hybrid system, the battery interfaces with the rest of the vehicle through a power electronics converter which provides a path to both charge and discharge the cells in the battery. The different configurations also lead to differences in designs for the battery and its infrastructure.

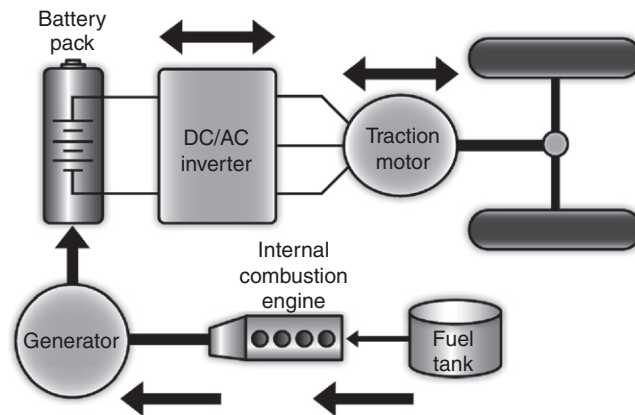


**Figure 18.15** Series hybrid configuration (from Ref. [25]).

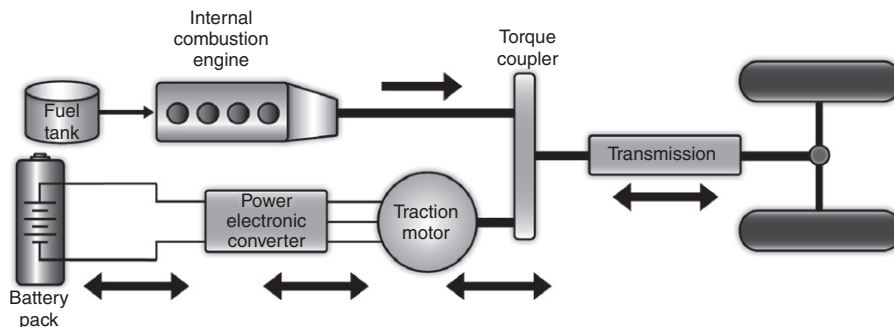


**Figure 18.16** Parallel hybrid configuration (from Ref. [25]).

Design defect testing and evaluation may be performed to ensure that the various components will perform safely under abuse conditions. For example:

- The cell passive protection devices (PTCs, fusible links, fuses, etc) should be able to handle the short circuit currents that may be generated during a fault condition. In addition, when the protection device operates, the entire circuit voltage can appear across it. As such, the device should be rated to handle the open circuit voltages generated under worst-case conditions.
- The various levels of protection circuit components should be chosen such that they have different failure modes. This ensures events causing one set of components to fail do not propagate to form a cascading event and fail the remaining components.
- The operating parameters of the various protection levels should be such that they do not overlap. For example, the operating pressure of a cell's venting mechanism should be less than the pressure at which the cell can's weld fails.

A systematic approach which includes the use of failure modes and effects analysis, fault tree analysis, and other methods can be used to evaluate the safety performance of the Li-ion battery system. Extreme operating conditions, ageing mechanisms and abuse conditions need to be considered to ensure that the system design is robust and can handle all possible conditions.

### 7.3 Number of cells

The large number of cells typically used in a HEV gives rise to other issues that need to be investigated. Tests should be performed to determine the following:

- The number of cells that must go into thermal runaway to cause the entire battery system to go into thermal runaway.
- The requirements of cell balancing and the effects of differential cell ageing on the safety and performance of the battery system.
- The probability and effect of propagating circuit board failures.
- The orientation and placement of the cells in the battery to minimize the propagation of a cell failure.

### 7.4 Operating temperature

The cells in a HEV battery system should be able to operate under all conditions. The battery systems are expected to operate and provide power in ambient temperatures as low as  $-40^{\circ}\text{C}$  and as high as  $50^{\circ}\text{C}$  (long-term goal of  $80^{\circ}\text{C}$ ) without any effect on performance, safety, or life, etc. Furthermore, storage temperatures in a HEV environment are higher than what the cells typically encounter in other applications [26]. The ambient temperature exposure of the HEV batteries will depend upon the location of the cells within the vehicle. Fig. 18.17 shows an example of temperatures within a vehicle under summer conditions. As such, the battery system design should be robust



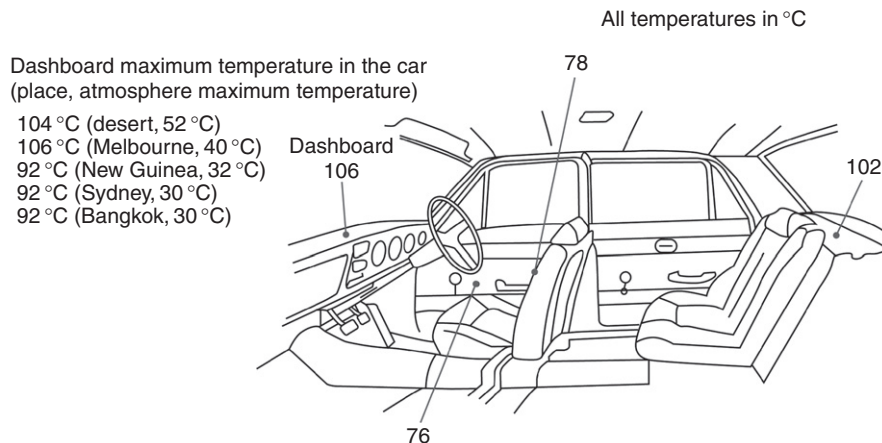


**Figure 18.17** Maximum temperature at each position in the car in Melbourne, Australia. Condition: maximum temperature on the day was 40°C (from Ref. [27]).

to handle these temperatures or have cooling systems to ensure adequate safety at the elevated ambient/operating temperatures.

## 7.5 Operating life

The operating life requirement of HEV battery systems is dictated by the requirements of the HEV itself. HEVs are generally expected to last for 10–15 years. The battery system must perform safely over the HEV's expected lifetime. The lifetime requirements in consumer electronics are relatively shorter with a typical battery expected to last for approximately 300 charge/discharge cycles. Testing should focus on determining the consequences of the prolonged cell life and also whether the performance of the cells to abuse conditions changes as the cells age.

## 7.6 System-based abuse testing

Various industries (consumer, telecommunications, aerospace, etc.) have expended significant time and effort to the development of various abuse tests in safety standards for Li-ion cells. The existing standards typically focus on evaluating the performance of the cells to electrical, mechanical, thermal, and environmental abuse conditions expected over the operating life of the cells. The consumer electronics product industry has been very proactive in developing and updating the safety standards for Li-ion cells. These standards provide a good starting point in evaluating the cells used in HEVs. Some of the known safety standards used in the consumer electronics industry are as follows:

- *UL Standard—UL1642*. This standard specifically devised for Li-ion cells provides a set of electrical and mechanical tests for cells and batteries [28].

- *ANSI Standard—ANSI C18.2*. This standard was devised for the safety evaluation of rechargeable batteries and includes various chemistries. Similar to UL1642, it provides a set of tests that give an idea of the baseline safety of Li-ion cells and batteries [29].
- UN Transportation requirements (Section 38.3) define a set of environmental, mechanical and electrical abuse tests for Li-ion cells and batteries [30].
- *IEEE Standards*. Two of the most comprehensive Li-ion battery system safety standards in the consumer electronics industry are the IEEE Std. 1625-2008 for portable computing battery systems and IEEE Std. 1725-2006 for cell phone battery systems. Both standards employ a similar approach and provide detailed requirements on cell design and quality, battery protection circuitry, host/charger and AC conversion circuit design requirements, etc. The two IEEE standards have been developed by the industry in a collective effort and have used preexisting standards as guides. As the HEV industry develops, the system-based methodology of the two IEEE standards in conjunction with the component and subsystem-based safety performance testing can provide a guide for future development of abuse test cases for electrical vehicle battery systems [27, 31].

On September 17, 2009, UL announced its intent to release a new set of requirements for large batteries in electric vehicles under UL Subject 2580. The scope of this standard according to UL will be to “mitigate the potential risk of fire and electrical hazards and enhance the overall safety of batteries for electric vehicles” [32].



## 8. VOLTAGE INTRODUCED SAFETY CONSIDERATIONS

Although not specific to the Li-ion chemistry, the use of batteries in HEVs gives rise to additional safety concerns which need to be addressed and protected against. Electrocutation, arcing resulting in ignition, and arc-flash are three of the major safety hazards for humans.

### 8.1 Electrical shock hazard

Unlike a conventional automobile with a nominal 12 Vdc lead acid battery, a HEV's Li-ion battery and its associated AC or DC propulsion system has substantially higher operating voltages. Battery output voltages are typically 160 V or higher. This voltage gives rise to a risk of electrical shock if not protected against adequately (UL defines a voltage in excess of 42.4 Vac or 60 Vdc as hazardous [33]).

### 8.2 Arcing

The hybrid vehicle may operate in harsh ambient conditions and may be subjected to a high level of environmental, mechanical, and physical abuse. The vehicle's electrical system may be exposed to large fluctuations in temperature, a high level of vibration and

may also be exposed to a variety of conductive contaminants. Electrically conductive fluids may be generated within the engine compartment during abnormal operation or from environmental conditions such as rain, snow, and salt spray. Exposed high-voltage terminals may create arcing and arc-flash hazards for humans. These electrically hazardous conditions may be exacerbated by a collision resulting in damage to the hybrid vehicle's body.

An electrically "hot" metal surface exposed to a conductive contaminant may result in an arcing fault. A "hot" connector terminal may permit a leakage current to flow along the surface of an insulating member to a grounded or low potential surface. This leakage current may eventually result in a water-tree growth with consequent degradation of the insulation. Depending on the source voltage, and the arcing path, this degradation of the insulation may result in an arcing fault.

In addition, human involvement by vehicle owners in the underhood environment such as attempting a repair may also result in hazards due to electrocution and arcing. These hazards may include accidental dropping of metal tools on exposed high-voltage terminals or improper use of measuring instruments, such as low-cost multimeters, can be a potential cause of arcing faults and arc-flash burns. Additional safeguards and protection systems may be required to minimize the risk of electrical shock and electrocution especially during handling and vehicle repairs.

The relatively confined space of an engine compartment or trunk area means that an arcing fault can also lead to arc-flash hazards. An arcing fault can result in extremely high temperatures on the order of 2,500–20,000°C. These high temperatures generate hot gases and molten metal which can result in serious burns and cause clothing to ignite.



## 9. SUMMARY

With billions of Li-ion cells being manufactured every year, the technology today is ubiquitous. Although there may be some safety concerns with the existing technology, the research performed and the safety architectures developed have helped reduce the incidents and also mitigate the effects of the incidents when they do occur.

The management of the safety aspects associated with Li-ion cells has entered a new domain with the automotive industry. Learning from the experience base developed in the toy, Uninterrupted power supply (UPS), power tools, cellular, computer, and telecom industries will be helpful to the vehicle industry in enhancing the safety performance of Li-ion cells. The adaptation of the Li-ion technology by the automotive industry will give rise to problems and issues unique to this industry which have not been faced by the consumer electronics industry. The use of adequate safeguards in the form of redundant protection circuits, well designed thermal management systems, robust manufacturing processes coupled with battery designs which can minimize the risk of safety-related failures modes is desirable.

## ACKNOWLEDGMENTS

The authors wish to thank Ms. Xiaoyun Hu, Dr. Snehal Dalal, Dr. Bala Pinnangudi, Mr. Peter Morris, Dr. Kevin White, Dr. Quinn Horn, Ms. Celina Mikolajczak, Dr. Paul Taylor, Mr. Stig Nilsson, and Mr. James Edmonds for their technical review and comments of the contents of this chapter. We would also like to thank Mr. Christopher Espinosa for his assistance with the images in this chapter.

## REFERENCES

1. The Wall Street Journal, Batteries Hamper AT&T TV Effort, <http://online.wsj.com/article/SB120045143379793329.html>, 2009 (accessed 3107.09).
2. US Department of Energy, <http://www.energy.gov/>, 2009 (accessed 2407.09).
3. US Consumer Product Safety Commission, [www.cpsc.gov](http://www.cpsc.gov), 2009 (accessed 2407.09).
4. V. Srinivasan, AIP Conf. Proc. 1044 (2008) 283.
5. SAE International Video Learning Lab, GM To Use “Stack and Fold” Manganese–Spinel Chemistry for Volt’s Batteries, <http://video.anerian.com/topics/1>, 2009 (accessed 1807.09).
6. S. Tobishima, J. Yamaki, J. Power Sources 81–82 (1999) 882.
7. R. Spotnitz, 9th International Advanced Automotive Battery & EC Capacitor Conference and Symposia, Long Beach, USA, 2009.
8. K. Zaghbi, P. Charest, A. Guerfi, J. Shim, M. Perrier, K. Striebel, J. Power Sources 134 (2004) 124.
9. S. Santhanagopalan, P. Ramadass, J. Zhang, J. Power Sources 194 (2009) 550.
10. G.M. Ehrlich, In: Handbook of Batteries, D. Linden, and T.B. Reddy (Eds.), Lithium-Ion Batteries, Chapter 35, McGraw-Hill, New York, 35–68, 2002.
11. S.S. Zhang, J. Power Sources 161 (2006) 1385.
12. I. Buchmann, Batteries in a Portable World: A Handbook on Rechargeable Batteries for Non-Engineers, second ed., Cadex Electronics, Inc., British Columbia, Canada, 2001.
13. O. Takahisa, T. Kishi, T. Kuboki, N. Takami, N. Shimura, Y. Sato, et al., J. Power Sources 146 (2005) 97.
14. L.A. Randolph, M.J. Palazzo, E.S. Takeuchi, K.J. Takeuchi, J. Power Sources 97–98 (2001) 681.
15. A. Arora, J. Swart, S. Nilsson, Y. Xu Proceedings of the 5th Advanced Automotive Battery Conference, Honolulu, USA, 2005.
16. A.N. Jansen, D.W. Dees, D.P. Abraham, K. Amine, G.L. Henriksen, J. Power Sources 174 (2007) 373.
17. H. Lin, D. Chua, M. Salomon, H.-C. Shiao, M. Hendrickson, E. Plichta, et al., Electrochem. Solid-State Lett. 4 (2001) A71.
18. G.L. Plett, M.J. Klein, SAE 2006-21-0060.
19. G. Chagnon et al., Proceedings of the 1st Advanced Automotive Battery Conference, Las Vegas, USA, 2001.
20. D.H. Doughty, C.C. Crafts, FreedomCAR. Electrical Energy Storage System. Abuse Test Manual for Electric and Hybrid Electric Vehicle Applications, Sandia National Labs, Albuquerque, NM, USA, 2005.
21. SAE J2464, Electrical Vehicle Battery Abuse Testing, SAE International, Warrendale, PA, USA, 1999.
22. C.N. Ashtiani, ECS Trans. 11(19) (2008) 1.
23. C.N. Ashtiani, US Advanced Battery Consortium, USABC August 2007, Version 0.0.
24. JIS C 8714, Safety Tests for Portable Lithium Ion Secondary Cells and Batteries for Use in Portable Electronic Applications, Battery Association of Japan, Japan, 2007.
25. A. Emadi, K. Rajashekhara, S.S. Williamson, S.M. Lukic, IEEE Trans. Veh. Technol. 54 (2005) 763.
26. US Advanced Battery Consortium, USABC Goals for Advanced Batteries for EVs, [www.usabc.org](http://www.usabc.org), 2009 (accessed 2707.10).
27. IEEE Std. 1625, IEEE Standard for Rechargeable Batteries for Multi-Cell Mobile Computing Devices, IEEE, New York, USA, 2008.
28. UL 1642, UL Standard for Safety for Lithium Batteries, Underwriters Laboratories Inc. (UL), Northbrook, IL, USA (2004).
29. ANSI C18.2, American National Standard for Portable Rechargeable Cells and Batteries – Safety Standard, American National Standards Institute, Inc., New York, USA, 2007.

30. United Nations, Recommendations on the Transport of Dangerous Goods, Manual of Tests and Criteria, United Nations, New York, USA, 2003.
31. IEEE Std. 1725, IEEE Standard for Rechargeable Batteries for Cellular Telephones, IEEE, New York, USA, 2006.
32. Underwriters Laboratories Newsroom, UL to Release Requirements for Electric Vehicle Batteries, [http://www.ul.com/global/eng/pages/corporate/newsroom/newsitem.jsp?n=ul-to-release-requirements-for-electric-vehicle-batteries\\_20090917094800](http://www.ul.com/global/eng/pages/corporate/newsroom/newsitem.jsp?n=ul-to-release-requirements-for-electric-vehicle-batteries_20090917094800), IEEE, New York, USA
33. UL 60950, Safety of Information Technology Equipment, Underwriters Laboratories Inc. (UL) Northbrook, IL, USA, 2000.



# Management of Batteries for Electric Traction Vehicles

**Daniel D. Friel**

Battery Management Solutions, Texas Instruments, Inc., 607 Herndon Parkway, Suite 100, Herndon, VA 20170, USA

## Contents

1. Introduction	494
2. Application Introduction	494
2.1 Light electric vehicles	495
2.1.1 <i>Electric bicycles</i>	495
2.1.2 <i>Electric motorcycles</i>	495
2.2 Industrial forklifts	496
2.3 Battery electric vehicle	496
2.4 Fuel-cell electric vehicle	496
2.5 Hybrid electric vehicle	497
2.5.1 <i>Microhybrid or start–stop hybrid</i>	497
2.5.2 <i>Mild hybrid</i>	498
2.5.3 <i>Full hybrid</i>	498
2.6 Plug-in hybrid electric vehicle	498
3. Battery Management Systems	499
3.1 Battery management system functions	500
3.1.1 <i>Monitoring</i>	500
3.1.2 <i>Measuring</i>	501
3.1.3 <i>Calculating</i>	502
3.1.4 <i>Communicating</i>	503
3.1.5 <i>Control</i>	503
3.1.6 <i>Balancing</i>	504
3.2 Architectures	505
3.2.1 <i>Centralized architecture</i>	505
3.2.2 <i>Distributed architecture</i>	506
3.3 Other requirements and system considerations	506
3.3.1 <i>Leakage detection or isolation breakdown detection</i>	506
3.3.2 <i>Connection sequence</i>	507
3.3.3 <i>Self-diagnostics</i>	507
3.3.4 <i>Current interruption fail-safe switches</i>	507
3.3.5 <i>System voltage and current maximums</i>	508

4. Battery Management System Examples	509
4.1 LEV or industrial	509
4.2 Microhybrid (start–stop)	509
4.3 BEV, mild or full hybrid, or PHEV	511
5. Conclusion	513
Acknowledgments	514
Glossary	514
References	514



## 1. INTRODUCTION

Electric traction vehicles can range from small pedal-assist electric e-bikes, to industrial forklifts, to full size electric vehicles (EVs) and trucks. All such EVs can also be “hybrid” in nature – sharing the battery with an internal combustion engine (ICE), fuel cell, or other source of motive force or additional electrical energy.

The field for batteries in EVs is widening as new cell chemistries are introduced along with new hybrid methods for utilizing the battery’s power and energy capabilities for motive propulsion. Traditional lead-acid (Pb-acid) batteries were replaced by nickel-metal-hydride (NiMH) cells in commercial hybrid electric vehicles (HEVs), while lithium-ion (Li-ion) cell formulations have found favor in pure battery electric vehicles (BEVs) and the next generation of plug-in hybrid vehicles (PHEVs).

In these cases, managing the high-voltage and high-current array of electrochemical cells configured into a battery pack for electric traction vehicles requires careful consideration. These larger battery packs for today’s electric traction applications are significantly different from the 12V Pb-acid batteries found in traditional motor vehicles.

This chapter will first give an overview of the types of electric traction vehicles and the characteristics of their batteries. The second part discusses battery management in general, and the third gives specific details for today’s traction vehicles.



## 2. APPLICATION INTRODUCTION

Electric traction vehicles, or simply EVs, cover a wide range of products from simple devices to assist mobility to large vehicles capable of moving thousands of pounds. The batteries to operate such devices are similarly diverse and the requirements of such batteries even more diverse depending on the economic and motive restrictions.

To simplify the following discussion, some generalizations about each EV application have been summarized. When researching a battery management system (BMS), finding a similar application will likely assist in the selection of the battery and management system.

## 2.1 Light electric vehicles

Electric scooters, bicycles (e-bikes), and motorcycles are the smallest and lightest of EVs and are categorized as “light” electric vehicles (LEVs) due to both the vehicle and the battery size, although exceptions exist. The LEV shares many of the characteristics of a full EV but with often smaller and simpler components. The battery requires charging from an external power source.

LEVs are also the most numerous, with estimates of more than 20 million produced annually in China alone – the remainder of the world adding another few million [2].

### 2.1.1 Electric bicycles

Electric bikes (e-bikes) operate with a 12, 24, 36, or perhaps 48 V motor powered by a similar voltage battery. These voltages correspond to multiples of 12 V Pb-acid battery voltages since this is the most popular battery cell chemistry used. Motor sizes range from 250 to 750 W. Smaller and lower cost e-bikes will operate at the lower voltages due to the low cost of both motor and battery. Simple Pb-acid battery powered e-bikes may utilize only basic voltage monitoring for battery management.

Typical pedal-assist e-bikes will have energy batteries ranging from 100 to 400 Wh in size while larger e-bikes may have batteries reaching 1 kWh. Government regulations often limit the size of the motor and total weight of an e-bike that does not require registration, licensing or operator training. Larger electric bikes may therefore be classified as electric motorcycles.

Higher performance e-bikes will use 36 or 48 V motors and batteries but the majority of products operate at less than 36 V. As higher voltages are used, the weight of the battery becomes a larger factor, particularly with smaller e-bikes, so some 36 and 48 V e-bikes will employ nickel-cadmium (NiCd), NiMH, or Li-ion battery packs instead of Pb-acid. These chemistries offer a higher energy density, typically faster charge times, and less weight. However, they each also require a different type of BMS.

A commercial pedal-assist example is BionX of Canada which produces retrofit motors and battery systems for traditional bicycles [2, 3].

### 2.1.2 Electric motorcycles

Full size electric motorcycles are more similar to full size EVs than to e-bikes, but are mentioned here for clarity. Electric motorcycles are often built with NiMH or Li-ion batteries due to the higher energy density provided versus Pb-acid and the higher payload capability and range requirements of full size electric motorcycles.

Typical electric motorcycles will have energy batteries with 2–5 kWh of capacity due to the performance requirements needed.

Higher voltage and higher performance motors are utilized to achieve the greater efficiencies required from electric motorcycles – often reaching 96 V or higher. Therefore, BMSs often appear more similar to full electric or HEVs than smaller e-bike electric



bicycles. This includes the use of automotive-grade components and adherence to automotive standards and specifications.

Commercial examples include the Vectrix VX1 series with a range of 30–50 miles using a 125 V, 3.75 kWh NiMH battery and a 21 kW electric motor [4].

## 2.2 Industrial forklifts

This category of electric traction vehicle is a specialty vehicle used by the material handling industry for warehouse operations. Electric forklifts, industrial movers, and similar equipment are often similar in size and power requirements to mid and full size EVs.

These vehicles are specialized in their design for lifting and moving freight and often utilize large, heavy Pb-acid batteries for motive force and counterbalancing.

Such vehicles may range in size from walk-behind pallet movers to sit-down forklifts. The electric motors operate at voltages of 12, 24, 36, and 48 V, with Pb-acid batteries of 10–75 kWh in capacity [5].

## 2.3 Battery electric vehicle

A BEV is an automobile or truck that derives all motive force from the battery itself, without the assistance of another engine – such as a fuel cell or internal combustion engine (ICE). Charging of the battery requires an external power source connection.

Modern BEVs have progressed since the “EV1” – an early commercial vehicle from General Motors (GM). Most battery EVs are special delivery vans, trucks, or high-performance sports cars such as that available commercially from Tesla Motors.

Due to range requirements of 100 miles or more, a BEV will have a 15–75 kWh battery optimized for energy. The battery is typically built using NiMH or Li-ion cells due to the high-energy density of these chemistries and will operate at voltages from 300 to 500 V. The battery is teamed with an electric motor capable of 100–200 kW continuous power.

A commercial example is the Tesla Roadster with a 244 mile range and a 60 kWh battery and the proposed Nissan Leaf with a 24 kWh battery and 100 mile range [6, 7].

## 2.4 Fuel-cell electric vehicle

Differentiated from a BEV is a fuel-cell electric vehicle (FCV) which derives electrical energy from a fuel-cell system using a form of hydrogen or methanol. The fuel-cell system makes electricity which then charges a battery which acts as the energy storage mechanism to provide the motive power. (Fuel-cell systems often cannot accommodate large or fast variations in load as well as a battery can.)

Batteries used in fuel-cell vehicles share characteristics with mild or full HEVs and are often built with NiMH or Li-ion batteries optimized for power. The typical battery size is 1–5 kWh depending on the size of the vehicle and may operate between 100 and 400 V.

## 2.5 Hybrid electric vehicle [8]

A HEV combines a traditional combustion engine with a battery to provide enhanced operating characteristics, such as lower emission, longer range, or indoor zero-emissions operation.

The major difference between hybrids and BEVs is that no external charging of the battery is required – recharge occurs from a co-located source, typically an ICE. Other “pure” EVs discussed previously must be recharged from an external source – except for a fuel-cell system in which the fuel cell acts as the onboard battery charging source.

The other critical difference is that the hybrid vehicle battery is optimized for power – the ability to deliver and receive high currents for relatively short durations. Previous systems discussed use the battery for longer periods of time with relatively constant charge and discharge rates. In a high-power battery system, the particular battery chemistry, design, and management will be different from other “pure” EVs.

Within this category, there are subclasses that may utilize different battery chemistries, sizes, and voltages due to the unique requirements of each vehicle type. In most all cases, a power battery is needed. Voltages as well as the sizes for batteries and motors are listed for typical vehicles – larger trucks and busses would have appropriately larger components.

### 2.5.1 Microhybrid or start–stop hybrid

A microhybrid or start–stop hybrid uses a simple method to achieve the hybrid operation: turn off the ICE whenever the vehicle is stopped and would otherwise be idling. By keeping the combustion engine from idling, fuel is saved and the engine economy improved, typically in the range of 5–10%.

The micro/start–stop hybrid also does not require an additional electric motor – the traditional starter motor is often sufficient. But it is important to note that the battery does not provide any motive force while waiting for the combustion engine to restart, unlike a mild or full hybrid. The vehicle’s restart mechanism is therefore different from that of mild or full hybrids.

Micro or start–stop hybrids do not require unique batteries – the traditional starting, lighting, and ignition (SLI) Pb-acid batteries common in vehicles today are suitable. However, these batteries are often made more robust, larger, and better managed since they are now starting the combustion engine more than a hundred times per day. Previously, these batteries were only starting the combustion engine a few times per day.

Due to this new requirement of the battery, the management system is even more critical: since the vehicle may turn off while in the middle of an intersection, the vehicle controller must be absolutely sure that the battery can quickly restart the vehicle before deciding to turn off the combustion engine.

A standard 12 V starting battery with a capacity of 500 Wh is often sufficient for a microhybrid or start–stop vehicle, but battery management of this battery is critical so that the vehicle is always capable of restarting the combustion engine.

Commercially available start–stop hybrids from Toyota in Japan and BMW in Germany have been available in limited markets.

### **2.5.2 Mild hybrid**

In a mild hybrid vehicle, the start–stop approach is augmented by a larger electric motor system added to the vehicle. This additional motive power can be used for an acceleration boost and to recover braking energy. A 10–20% power assist often classifies as a mild hybrid but the ability to move the vehicle solely on battery power may not be available.

The additional electric motor of approximately 15 kW is not as large or powerful as a full hybrid and therefore the battery voltage and capacity would be smaller as well, ranging from 42 to 200 V and up to 1 kWh [9].

### **2.5.3 Full hybrid**

The full hybrid builds further by increasing the capability of the electric motor drive in the vehicle – providing both motive power while the ICE is being restarted, and capturing regenerative energy when the vehicle is braking. In more recent full hybrids, motive power solely from the battery can be significant, up to a few miles at highway speeds [10].

In a full hybrid, the battery acts primarily as a large capacitor – providing limited motive force for the vehicle and recapturing energy while coasting or braking. The battery typically only provides motive force for an initial “launch” for a few meters while the ICE is started. The battery may also provide motive force for low speed or short duration high-speed movement, but typically no range of battery operation is specified.

The battery is therefore relatively small compared to a full EV, only 1–3 kWh, since it is primarily a power assist device. The HEV battery is optimized for power delivery and absorption – an energy battery is not required since operation using only the battery is minimal. Battery voltages will be between 300 and 500 V and both NiMH and Li-Ion cells have found use in full hybrids.

Full hybrids are available in multiple sizes ranging from sedans to sport utility vehicles (SUVs) from a variety of commercial manufacturers such as Toyota, Honda, Ford, GM, and others [11].

## **2.6 Plug-in hybrid electric vehicle**

Expanding on the full hybrid model, a PHEV simply has a larger battery that may be used to provide motive force for an extended period of time.

**Table 19.1** Summary of electric traction vehicle battery characteristics

Vehicle category	Battery voltage (V)	Battery energy content (kWh)	Chemistry and optimization
LEV	12, 24, 36, 48	1–2	Pb, Ni – Energy
Industrial	12, 24, 36, 48	5–50	Pb – Energy
BEV	200–500	25–75	Ni, Li – Energy
FCV	300–400	1–5	Ni – Power
HEV – Micro	12	0.50	Pb – Power
HEV – Mild	42–200	1	Ni, Li – Power
HEV – Full	300–500	2–5	Ni, Li – Power
PHEV	300–500	5–20	Li, Ni – Energy

A PHEV therefore, may have a battery of 5–25 kWh to provide an all-electric range of up to 50 miles or more. The PHEV thus shares more commonality with a BEV than a traditional HEV.

The GM Chevy Volt plans to have a 16 kWh battery and is said to achieve 40 miles of battery operation while the Fisker Automotive Karma claims 50 miles and a 22 kWh battery. In both cases, the battery size is greater than needed for the desired range in order to compensate for battery aging and to allow the vehicle to operate in hybrid mode [12, 13].

A summary of the battery characteristics of the above-mentioned vehicles is reported in Table 19.1.



### 3. BATTERY MANAGEMENT SYSTEMS

A BMS is put in place in order to ensure that the battery is operated within safe limits and achieves optimum performance over its life. In some cases, the operating limits are further constrained in order to prolong the battery's calendar life.

The complexity of a BMS can vary widely, but it must match the requirements of the chemistry of the battery cells as well as the requirements of the vehicle and the vehicle's operating conditions.

Some electrochemical battery cells have strict safe operating limits for temperature, voltage, and current, while others can be abused without much concern for safety. In all cases, the performance of the battery is maintained when the operating limits are observed.

Finally, the BMS provides information on the battery's current state and performance so that the energy and power in the battery can be fully utilized.

In any BMS, there may be one or more functions for monitoring, measuring, calculating, communicating, controlling, and balancing the electrochemical cells used in a battery pack. The goal of these functions is first to protect the battery and then to produce optimal performance over a wide range of operating and environmental conditions.

Due to the requirements of the vehicle and the battery chemistry used, not all functions will be needed. The battery chemistry may also dictate that some functions are more critical than others. For example, depending on the cell chemistry and the requirements of operation, perhaps not all physical characteristics of the battery will be observed.

A BMS may be as simple or as complex as the vehicle and cell chemistry requires. A management system could simply be a temperature monitor in the form of a fuse used to prevent thermal runaway. Alternatively, a BMS could enlist multiple electronic components and subsystems to carefully perform all of the previously mentioned functions with redundancy.

The architecture chosen to implement the BMS is also dependent on the vehicle, type of battery, and operational requirements. For some LEVs, all management functions can be easily integrated and centralized while a large hybrid vehicle may require a widely distributed management system with many redundant subcomponents and connected systems.

Finally, the BMS may not have complete control over the use of the battery itself – a higher level controller, such as a vehicle controller, may make the final decision based on information from the BMS. This is often the case with larger EVs that must consider multiple variables beyond the battery when deciding how to operate the vehicle.

### **3.1 Battery management system functions**

Battery management includes the basic functions of monitoring, measuring, calculating, communicating, controlling, and balancing – each of which are defined below. Electric traction vehicle BMSs will require some, but not necessarily all, such functions.

#### **3.1.1 Monitoring**

Monitoring refers to a function which checks a level of some characteristic of the battery cell, pack, or the management and control system.

Monitoring differs from measurement in that monitoring only indicates that a level has been exceeded. No indication is given regarding how much the level might have been exceeded.

Monitoring may have additional time delays before detecting that a level has been exceeded, in order to prevent false alarms or nuisance alerts.

Monitoring can refer to observable battery cell characteristics, such as temperature, voltage, and pressure; or battery pack characteristics such as current, coolant temperature, or leakage current.

Monitoring is typically continuous but can also be enabled only when conditions may warrant in order to reduce complexity, power consumption, or cost. The resolution and accuracy of monitoring observable characteristics is not often critical since the exact threshold level is not significant.

Monitoring is often used for maintaining safe operating limits of the battery cells, pack or management system. Safety monitoring of critical battery cell limits are often used to prevent abusive conditions from damaging the battery.

An example that relates to almost all battery systems is temperature. Monitoring can be used since exact temperature readings are not always significant, only if thresholds are exceeded. For example, a critical temperature for a battery system may be 55°C. Knowing the exact temperature to one degree is not required, only knowing that the 55°C threshold has been exceeded (perhaps with a tolerance of  $\pm 3^\circ\text{C}$ ) is crucial in order to take action to prevent further temperature abuse.

Thermal monitoring is often utilized in traction vehicle batteries for both the cells and the cooling system which must maintain the cells within specified operating temperature limits. The vehicle itself may also present a thermal load beyond that of the battery cells themselves – even when the vehicle and perhaps the BMS are not operating [14, 15].

An example of a monitoring product is the bq29410 from Texas Instruments. This product monitors the cell voltage of Li-ion cells for overvoltage using a comparator circuit on each cell which can detect a trip voltage within  $\pm 50$  mV of a preset threshold. When the preset voltage threshold is exceeded for a defined amount of time, a signal line is activated. This signal may be used to directly interrupt current flow or other similar control action [16].

A more complete example is the bq77PL900, also from Texas Instruments. This product can monitor up to 10 Li-ion cells for overvoltage, undervoltage, overcurrent, and overtemperature. All these monitoring functions are programmable as is the resulting control actions whenever the thresholds are exceeded [17].

### **3.1.2 Measuring**

Measuring refers to the direct ability to quantify a particular observable characteristic of the battery cells, pack, or management system.

Measurements convey size or magnitude information beyond what is available only from monitoring. (Although measurements may be used to compare against a threshold value, this often requires additional calculation whereas a pure monitoring approach can be much simpler.)

Measurements can vary in resolution or granularity as well as accuracy (ability to match to a known value), depending on the required use of the resulting measurement data. For example, measurements used to provide a rate-of-change of temperature require virtually no absolute accuracy and minimal resolution.

Typical measurements in a BMS often include voltage, temperature, and current – although cell pressure may also be measured in some applications. Measurements for voltage and temperature may be done at the individual battery cell level or at the pack level, or both. Current is typically measured only at the pack level but could be measured in both the positive and negative sides of the battery.

Some measurements may need to be synchronized so they can provide additional useful information, such as cell impedance, when utilizing a calculation function.

Measurement resolution and accuracy also depend on the requirements of the battery chemistry and the application. For example, in a hybrid vehicle, the battery is never fully charged or fully discharged – it is typically operated between 30 and 80% state of charge (SOC). This operating range is maintained for a variety of reasons, including the health of the battery, the ability to always accept regenerative braking energy, etc.

When operating in this region, some Li-ion battery chemistries, such as iron-phosphate, have very flat voltage profiles as shown in Fig. 19.1. These chemistries thus require a very accurate cell voltage measurement on the order of a few millivolts in order to determine the battery SOC correctly. Alternatively, in an EV or PHEV which utilizes the battery from nearly full to empty, the voltage measurement accuracy can often be reduced.

### 3.1.3 Calculating

Calculating is the act of processing measurement data of particular characteristics of the battery cells, pack, or management system in order to determine additional useful data related to these components.

Calculations may operate on one or more measurable quantities or use other nondirect measurements such as time or battery cell performance tables.

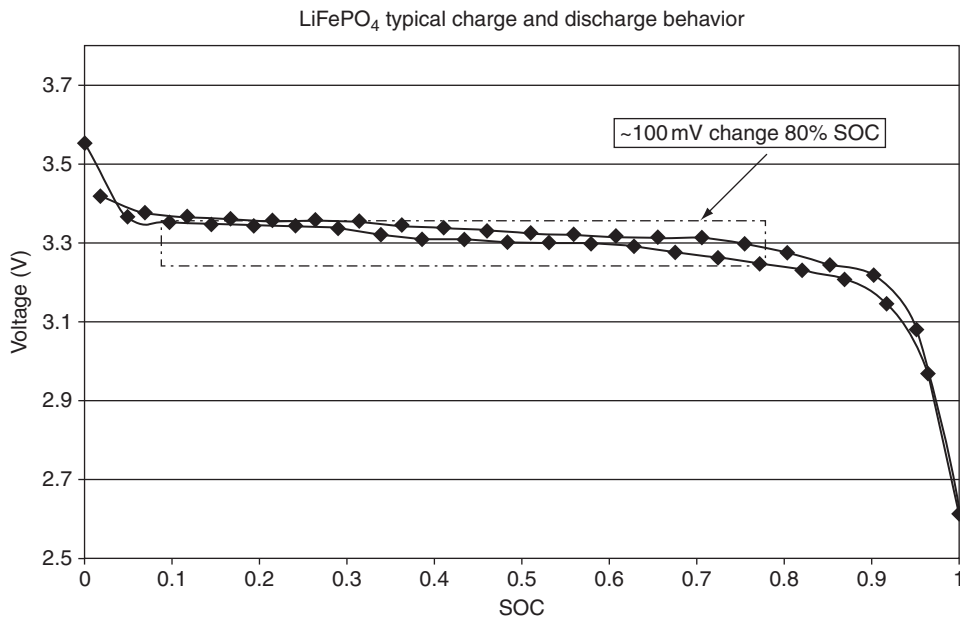


**Figure 19.1** Voltage versus SOC for Li-ion phosphate (LiFePO<sub>4</sub>) cell chemistry [18].

Calculations may occur in real time on the observed characteristics or be performed later. Calculations may be co-located with the measurement components or be handled elsewhere in a more distributed system.

Depending on the calculations required for a particular BMS, the resolution and accuracy of the measurements may be adjusted. If very coarse calculations are required, such as SOC to only  $\pm 20\%$ , then measurement requirements may be reduced in order to save complexity, power, or cost. More complex calculations may require improved measurements, such as synchronized voltage and current measurements to allow an appropriate calculation to determine cell impedance.

Examples of calculations include determining the rate of change of temperature using measurements of battery cell, pack, or system coolant temperatures. The rate of rise of the battery cell temperature is often used to determine a full charge state in NiMH rechargeable battery systems.

More advanced calculations include SOC, state of power (SOP) which is the ability of the battery to deliver a minimum amount of power, and state of health (SOH) of the battery. These calculations require measurements of the present characteristics of the battery cells as well as access to historical measurement data or other performance information for the battery.

### **3.1.4 Communicating**

Communicating refers to the ability to provide information from monitoring, measuring, and calculating functions to another subsystem or device in a useful manner.

Communicating may be as simple as a flashing indicator lamp or light-emitting diode (LED) to signal that a monitoring threshold has been exceeded.

Communicating may also be more complex and involve a defined protocol, bus structure, and data set. Common examples include the serial peripheral interface (SPI) bus and the inter integrated circuit (I<sup>2</sup>C) bus. There are also standardized vehicle interfaces such as the common automotive controller area network (CAN) bus, also known as SAE-J1939 or ISO 11898 and the slower local interconnect network (LIN) bus [19].

The information communicated may result from a monitoring function (threshold exceeded); a measurement function (voltage of the battery pack); a calculating function (SOC); or a combination of these functions. Often the information passes along multiple bus structures as it moves through the BMS.

### **3.1.5 Control**

Control implies that the BMS has direct control of critical aspects of the battery pack, such as the ability to interrupt current during charge or discharge or the ability to alter the thermal management system. This function is often separated from the battery system in order to allow other factors not directly related to the battery pack to be involved in the decision process.



In many vehicle applications, the BMS does not have direct control and therefore relies on another subsystem to take action. For example, to stop discharge if a short circuit is detected.

System control decisions in larger electric traction vehicles often must factor in external variables not known by the BMS. An example is regenerative braking which may be used to charge the battery cells. In some vehicles, the electric motor's reverse electromotive force is part of the braking equation, in addition to traditional braking mechanisms. If the battery were to reach a high charge or high-temperature state during a braking event and request the charge current to be stopped, some portion of braking force may be lost if the disconnect occurs. Although the battery system may prefer to disconnect charging current, the vehicle controller (and occupants) may not prefer to reduce braking action. In this case, the vehicle controller may risk damage to the battery system in favor of protecting the vehicle and occupants.

Smaller systems, such as LEVs, may include direct control functions since the BMS may be the only significant subsystem in the vehicle.

Control can also be split between functions – a monitoring function may have an independent control from a measurement and calculation function. This is typical in vehicles that require battery redundancy. A battery cell voltage monitoring function is employed for checking the safety limits of the cells while a separate measurement function with calculation capability also performs the same test using the numerical measurements. The control actions of these two may also differ – one may initiate a graceful decline or degradation of battery performance while the other may control a fail-safe on/off control.

### **3.1.6 Balancing**

The balancing function relates to the ability of the BMS to rebalance or equalize the battery cells in the EV's battery pack. As with the other functions, this may not be required for all battery cell chemistries or all types of electric traction vehicles. However, due to the normally larger sizes of batteries in electric traction vehicles, balancing often becomes a requirement.

Electrochemical cells can become out of balance due to slight differences in self-discharge, rates of change of internal impedance, or many other factors. In larger battery arrays typical of EVs, variations in cell temperature and cycling rates (include self-heating caused by high rate charge or discharge) are the typical causes of imbalance.

The ability to rebalance the cells during operation, such as at the end of charge, can be useful in EV applications. Some battery cell chemistries, such as Li-ion, have limitations on how rebalancing can occur while some EVs, such as full hybrids (HEVs), also restrict when and how rebalancing can be performed. For example, NiMH cells can be easily rebalanced with a low-rate overcharge. But in a HEV, the battery never reaches full charge, so an overcharge equalization method may never be possible.

Consideration for detecting imbalance and allowing for rebalancing, even if a unique operation by the vehicle controller, is an important system design decision.

Additionally, the type of balancing approach may depend on the vehicle. A hybrid vehicle that is constantly being charged and discharged can tolerate the inefficient balancing technique of “bleed” or “bypass” balancing. During charge, this approach simply connects a low value resistor across the battery cell that is at a higher voltage or SOC, thus bypassing some of the charge current around that battery cell. Multiple cells can be balanced simultaneously, but the heat produced by the bypass resistors must be managed.

Alternatively, in an EV or PHEV a charge transfer or “active” balancing approach is more suitable – energy from the higher voltage or SOC cells is transferred to the lower cells with minimal losses. This allows balancing to occur anytime, not just when charging the battery. Balancing in this manner, particularly during low rate discharge or while idle, can provide more utilization of the battery which is a critical requirement of an EV or PHEV vehicle.

## 3.2 Architectures

In addition to monitoring, measuring, calculating, communicating, control, and balancing, the BMS may also be constructed using two basic architectures – centralized and distributed.

Both architectures have unique advantages and disadvantages depending on the battery cell chemistry, the end application, physical space available, and other factors.

In general terms, a centralized approach offers less flexibility but may provide a lower total cost while a distribute architecture is more adaptable to changing design needs at a somewhat higher cost.

### 3.2.1 Centralized architecture

In a centralized architecture, most of the battery management functions are incorporated into a single subsystem, perhaps co-located within the battery pack.

This approach can be used when the physical size of the battery is not too large, such as in LEV, industrial, and microhybrid (start–stop) vehicles. In these BMSs, all functions needed for the particular battery cell chemistry may be included on a single electronic circuit module.

Larger HEV, FCV, and BEV systems may also utilize a centralized architecture when optimizing for size, volume, and cost since centralized approaches typically have fewer connectors, subcircuits, and packaging components.

A centralized architecture does not inherently assume that all functions must be in one location or circuit, but that most functions are located together and none are repeated elsewhere as would be found in a distributed architecture.

Techniques for monitoring, measurement, and communication can often be simplified in a centralized architecture where the battery cell voltages, temperatures, and currents are relatively closely located.

The centralized approach is often best for fixed sized systems which are well constrained in size and shape and are not likely to be altered, modified, or retrofitted.

An example of a small centralized electronic BMS is the previously mentioned bq77PL900 from Texas Instruments. This component can be used with up to ten series Li-ion cells and provides monitoring, communication, control, and balancing functions automatically. When paired with a small microcontroller, measurement and calculation capabilities can also be added. A battery management circuit based on this device is often used in LEVs such as e-bikes [17].

### **3.2.2 Distributed architecture**

A distributed or modular architecture splits the battery pack into subsegments of equal or similar size so that a larger battery system can be easily assembled from these smaller components. This approach increases the number of interconnections between modules but allows more flexibility in the design.

Some functions may be repeated in each module since the presence of the other modules is not necessarily known.

Techniques for monitoring and measuring are usually duplicated since signals that result from these functions must be conveyed or communicated to a remotely located central processor. Thus, with a distributed architecture, the communications interface between subsegments or modules must often be faster and more robust.

Distributed approaches have advantages when multiple sizes of battery packs are to be offered for the same vehicle system, or the same size battery is to be fitted into different sized vehicles. The added cost of connectors and wiring is offset by the flexibility provided.

The Linear Technology Corporation LTC6802 stackable voltage monitor is a product that permits the use of a distributed architecture. This part is essentially a stackable voltage and temperature measurement device with a communication interface that does not require separate isolation components [20].

Using a stackable device would then require that current monitoring and/or measurement be performed by another device and the results of the two calculated by yet another device, often none of which are co-located. In larger battery systems, this is often the case due to physical separation of these components.

## **3.3 Other requirements and system considerations**

Battery arrays found in larger vehicles often have additional requirements beyond what might be found in LEV, industrial, and microhybrid (start–stop) vehicles, although some of these principals may apply.

### **3.3.1 Leakage detection or isolation breakdown detection**

When the total battery voltage exceeds a certain level, for example, above 60 V for LEV and industrial vehicles, there are requirements for isolation from the vehicle

chassis and other electrical components. Such isolation components can fail or be incorrectly configured during maintenance and therefore a detection circuit is often employed.

One type of circuit determines if there is a breakdown in the isolation barrier such that a “leakage current” can flow between the isolation devices. If this “leakage” reaches a high level, it indicates that an isolation breakdown has occurred. Other methods can be employed to detect this function which is often required in high-voltage battery assemblies.

### **3.3.2 Connection sequence**

Most electrical systems are connected to a power source by first connecting the most negative or ground connection, then the most positive. In the case of a BMS, the power source is the battery and the connection sequence cannot always be guaranteed.

Smaller battery systems such as LEV, industrial or microhybrid (start–stop) vehicles may allow the most negative electrochemical cell to be connected first, then the next most negative, on up to the most positive cell.

But in larger battery arrays such as those in EVs, mild and full hybrids, and PHEVs, the connection of the electrochemical cells to the BMS is often random. Thus it is possible for high voltages to exist for many seconds, while the connection sequence is occurring. The BMS electronics must therefore be protected against these large voltages during this crucial time.

### **3.3.3 Self-diagnostics**

Although not required in all BMSs, onboard self-diagnostic features are becoming more critical in vehicles. Such features may simply indicate that the battery cells are properly connected, that power is available at the appropriate locations, and that monitoring levels or measurements are within expected normal operating regions.

BMSs used in commercial vehicles often must abide by certain diagnostic requirements as specified by the manufacturer or a government regulatory agency. The Society of Automotive Engineers (SAE) has numerous publications on such requirements. BMSs are increasingly being added to the list of required self-diagnostic subsystems [19].

### **3.3.4 Current interruption fail-safe switches**

Another aspect of high-voltage and high-current battery systems is the requirement for fail-safe current interruption devices.

For LEV, industrial, and perhaps microhybrid (start–stop) vehicles, standard power electronics may be used to stop the flow of battery current in a fault condition. Power MOSFETs (a type of transistor switch) are often sufficient if they are rated for the highest possible current and voltage expected during fault conditions.

However, even these devices can fail and possibly fail closed, allowing current to continue to flow. In addition, these devices are not perfect switches, they do present a series resistance, albeit in the milliohm range, but at high currents, even a small value of “on resistance” can generate a significant amount of heat which must then be dissipated.

For high current applications, such as full hybrids, EVs, and PHEVs, a powered relay, or “contactor” is employed. These are common in motor control applications since they require power in order to maintain connectivity, so in a fault state they become open and interrupt the current flow. They are often designed to reduce arcing during switching, have minimal contact resistance, and may have multiple current paths to reduce heating. For further safety and redundancy, a contactor may be placed in both the positive and negative supply paths of a high-voltage or high-current battery system.

### **3.3.5 System voltage and current maximums**

While voltages of 60 V and less are common for microhybrids, LEVs, and industrial vehicles, traction motors typically require 300 V or higher to provide sufficient motive force as required in full hybrids, EVs, and PHEVs. In buses and larger vehicles, voltages may approach 1,200 V.

In addition, when dealing with high-voltage battery arrays found in hybrids, EVs, and PHEVs, consideration must be given for the size of current carriers and their potential impact on the vehicle.

Modern battery technologies can now provide and accept very high currents for short durations, such as during vehicle start-up and launch or while capturing regenerative braking energy. These high currents require sufficiently large wiring and connectors in order to minimize heat and maintain reliability.

In some cases, the size of the power cables needed to transfer the battery current to the electric motor(s) may add substantial weight to the vehicle. A traction vehicle may choose to increase the operating voltage of the battery to reduce the peak currents, thus reducing the size and weight of the current carrying cables throughout the vehicle. Doubling the voltage will cut the current in half and reduce the effective size and weight of the wiring required.

The components used in the BMS must therefore be properly rated for the voltage and current transients and peaks expected during operation, particularly due to the electric motors. For example, a traction power inverter should have a voltage rating of 150% of the bus voltage. Practical limits of electronic components will restrict systems to operate below 1,200 V.

In [Table 19.2](#), management functions and architectures are reported for different vehicles.

**Table 19.2** Example comparison of management functions and architecture by vehicle category

Vehicle category	Typical functions	Architecture
LEV	Monitor, control	Centralized
Industrial	Monitor, measure, communicate	Centralized
BEV	Monitor, measure, calculate, communicate, balance	Distributed
FCV	Monitor, measure, calculate, communicate, balance	Centralized or Distributed
HEV – Micro	Monitor, measure, calculate, communicate	Centralized
HEV – Mild	Monitor, measure, calculate, communicate, balance	Centralized or Distributed
HEV – Full	Monitor, measure, calculate, communicate, balance	Centralized or Distributed
PHEV	Monitor, measure, calculate, communicate, balance	Distributed



## 4. BATTERY MANAGEMENT SYSTEM EXAMPLES

This section illustrates practical BMS circuits for a variety of previously discussed electric traction vehicle batteries.

### 4.1 LEV or industrial

A typical 36 V electric bike example with Li-ion cells is shown using the bq77PL900 from Texas Instruments in Fig. 19.2. This centralized all-in-one battery management device performs all the monitoring functions for voltage, temperature, and current while also providing control actions to interrupt charge or discharge current. Balancing is also activated automatically based on voltage measurements.

The bq77PL900 can be augmented by a small microcontroller to take advantage of the added functions of measurement (cell voltage and pack current) and communications available in the part. The microcontroller can also add a calculation function.

### 4.2 Microhybrid (start–stop)

A 12 V starting battery example for a microhybrid (start–stop) circuit is shown using the Analog Devices ADuC7034 product in Figs. 19.3 and 19.4. This is a complete measurement, calculation, and communication device which measures the battery voltage, current and temperature, calculates battery state, and communicates the resulting information over a LIN bus to a vehicle controller.

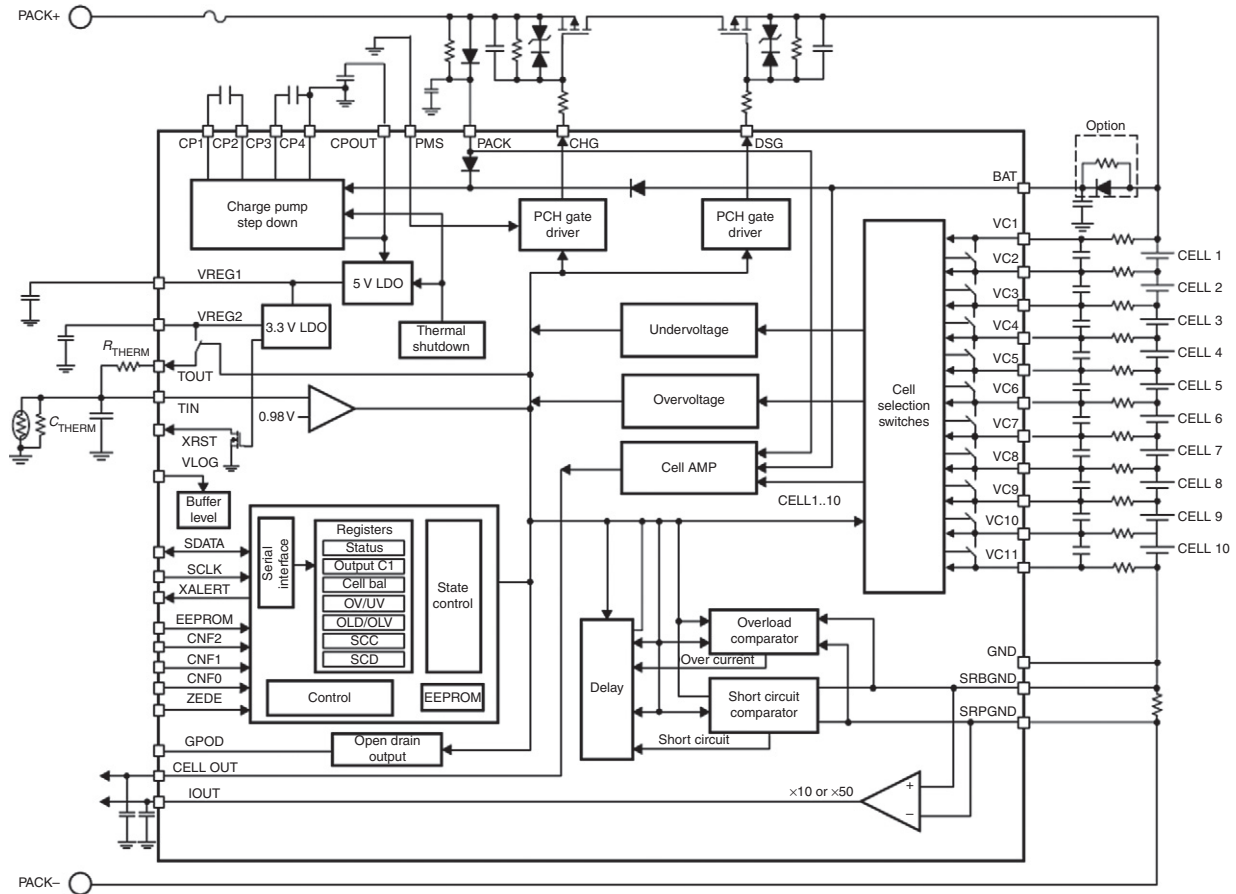
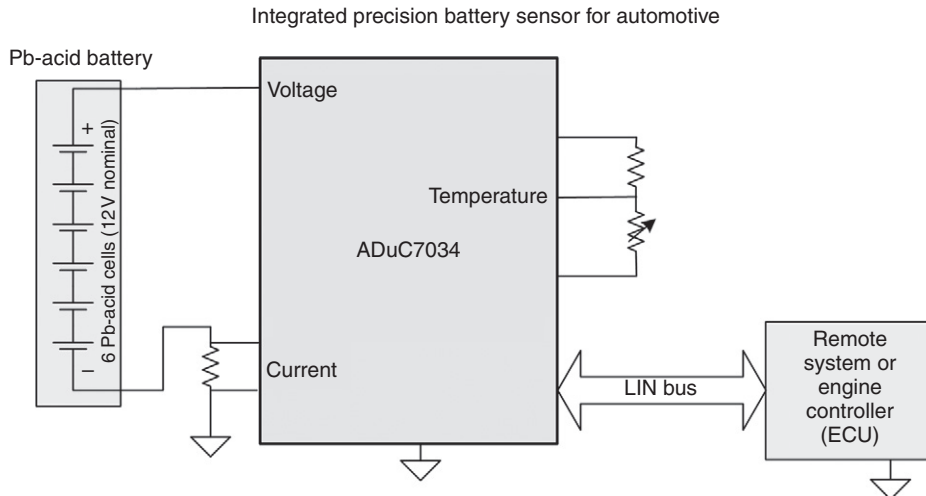
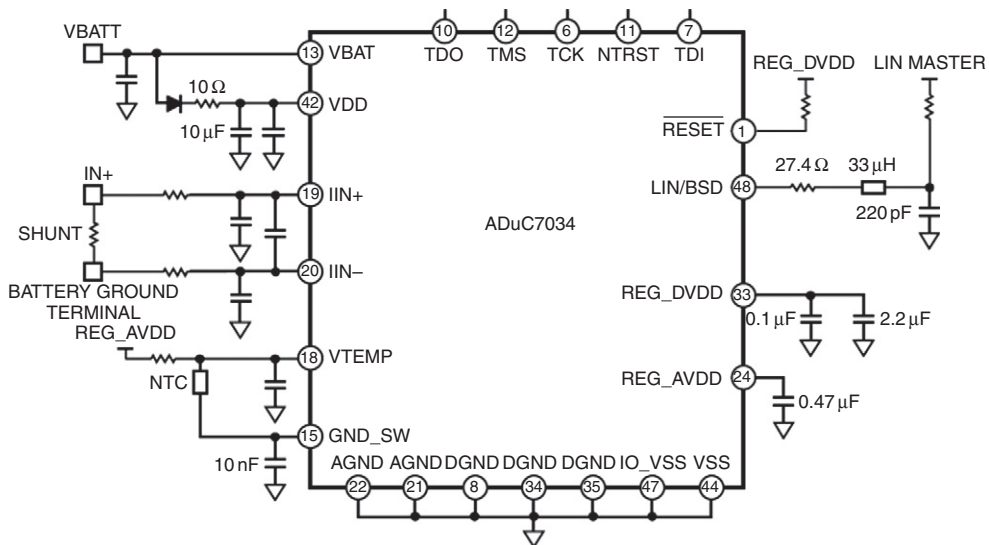


Figure 19.2 System block diagram for centralized BMS (all-in-one) using bq77pl900 from Texas Instruments, Inc [17].



**Figure 19.3** Simplified system block diagram of Pb-acid starting battery microhybrid (start-stop).



**Figure 19.4** Simplified schematic for the integrated precision battery sensor component ADuC7034 from Analog Devices, Inc [22].

### 4.3 BEV, mild or full hybrid, or PHEV

A larger battery array for a BEV, hybrid, or PHEV is shown in block diagram form in Fig. 19.5. The functions of monitoring and measuring cell voltage and temperature are combined with a circuit to enable balancing and provide



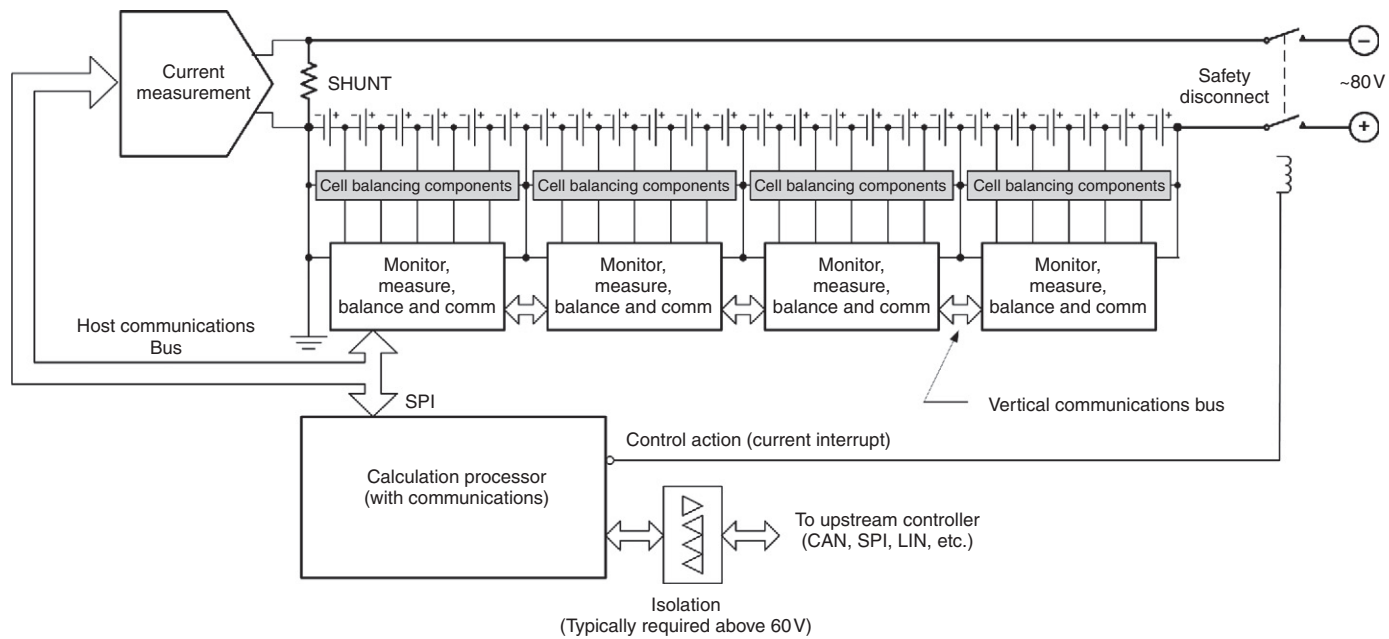


**Figure 19.5** Example BEV/HEV/PHEV high-voltage BMS block diagram [23].

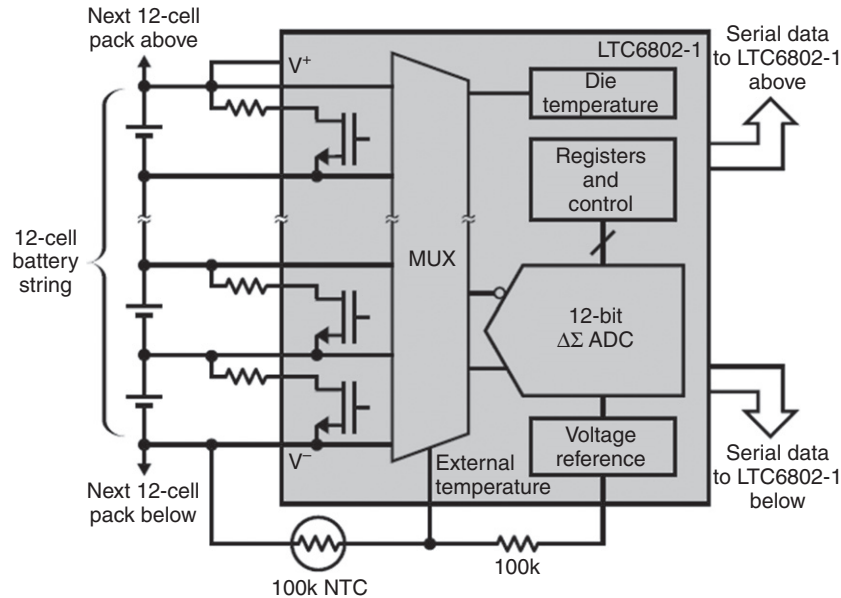


**Figure 19.6** Simplified schematic for the multicell battery stack monitor component LTC6802 from Linear Technology Corporation [20].

communications. Separate circuits measure current and a processing component provides calculation and additional communication features. Isolation and control actions are shown as well.

Such a system could utilize the integrated component in Fig. 19.6 from Linear Technology Corporation. The LTC6802 is effectively a stackable voltage and temperature monitor and measuring device with a cell balancing function and communication ability. The current measurement, calculation, control action, and isolation functions would require additional components.



## 5. CONCLUSION

BMSs for electric traction vehicles are significantly different from traditional management systems employed in consumer and industrial products such as laptops, cellular phones, two-way radios, power tools, and portable power products [24].

Although the basic functions for monitoring, measurement, calculation, communication, control and balancing exist, the implementation is more critical due to the physical size, power, energy, and end usage of such batteries in vehicles.

By selecting the appropriate functions required by the vehicle type and the battery cell chemistry, a proper BMS can ensure a robust, safe, reliable, high-performance battery system.

## ACKNOWLEDGMENTS

The author thanks the many colleagues and friends who he has worked with over the years while employed by Duracell, PowerSmart, Microchip Technologies, PowerPrecise Solutions, Honeywell Batteries, Coulomb Consulting, and Texas Instruments.

## GLOSSARY

BEV	battery electric vehicle
EV	electric vehicle
HEV	hybrid electric vehicle
ICE	internal combustion engine
IC	integrated circuit
LEV	light electric vehicle – electric bike, motorcycle, or similar size
Li-ion	lithium-ion rechargeable battery cell
NiCd	nickel–cadmium rechargeable battery cell
NiMH	nickel–metal–hydride rechargeable battery cell
Pack	a series-parallel configuration of cells, also referenced as a battery pack
Pb-Acid	lead-acid rechargeable battery cell
PHEV	plug-in hybrid electric vehicle
SOC	state of charge – percent charge remaining, typically at C/5 rate
SOH	state of health – remaining operating usefulness of battery
SOP	state of power – power delivery capacity remaining, at defined rate (SOF state-of-function – typically a metric combining SOC, SOH, and SOP)

## REFERENCES

1. M. Broussely, In *Industrial Applications of Batteries. From Cars to Aerospace and Energy Storage*, Chapter 4, M. Broussely, and G. Pistoia (Eds.), Elsevier, Amsterdam, 2007.
2. F. Jamerson with E. Benjamin, Sections 2 and 9 in *Electric Bikes Worldwide Report 2009 (EBWR09)*, Ninth Edition, Electric Battery Bicycle Company, Naples, Florida/Petoskey, Michigan, April 2009, [www.ebwr.com](http://www.ebwr.com) (accessed 19.11.09).
3. BionX, [www.bionx.ca/products/technology.php](http://www.bionx.ca/products/technology.php) (accessed 22.11.09).
4. Vectrix VX-1 specification, [www.vectrix.com](http://www.vectrix.com) (accessed 10.01.10).
5. Crown Equipment Corporation, [www.crown.com](http://www.crown.com) (accessed 10.01.10).
6. Tesla Motors, [www.teslamotors.com](http://www.teslamotors.com) (accessed 07.12.09).
7. Nissan Motors, “Leaf” website: [www.nissan-zeroemission.com/EN/LEAF/specs.html](http://www.nissan-zeroemission.com/EN/LEAF/specs.html) (accessed 22.11.09).
8. P. Onnerud, 5th Annual Lithium Mobile Power Conference, Boston, USA, November 2009.
9. C. Pillot, 26th International Battery Seminar and Exhibit, Ft. Lauderdale, USA, March 2009.
10. BMW ActiveHybrid X6, at corporate website: [www.bmw.com](http://www.bmw.com) (accessed 22.02.10).
11. Toyota Motors, hybrid vehicles website: [www.toyota.com/hybrid](http://www.toyota.com/hybrid) (accessed 02.03.10).
12. General Motors, Chevrolet Division, Chevy Volt, [www.Chevrolet.com/Volt](http://www.Chevrolet.com/Volt) (accessed 11.12.09).
13. Fisker Automotive, [www.karma.fiskerautomotive.com](http://www.karma.fiskerautomotive.com) (accessed 04.02.10).
14. K. Brandt, 26th International Battery Seminar and Exhibit, Ft. Lauderdale, USA, March 2009.
15. K. Smith, T. Markel, A. Pesaran, 26th International Battery Seminar and Exhibit, Ft. Lauderdale, USA, March 2009.
16. Texas Instruments Incorporated, bq29410 datasheet: <http://focus.ti.com/docs/prod/folders/print/bq29410.html> (accessed 07.01.10).
17. Texas Instruments Incorporated, bq77PL900 datasheet: <http://focus.ti.com/docs/prod/folders/print/bq77pl900.html> (accessed 01.10.09).

18. M. Gunderson, 26th International Battery Seminar and Exhibit, Ft. Lauderdale, USA, March 2009.
19. International Society of Automotive Engineers, [www.sae.org](http://www.sae.org) (accessed 18.03.10).
20. Linear Technology Corporation, LTC6802, [www.linear.com](http://www.linear.com) (accessed 10.11.09).
21. P. Krein, Hybrid Vehicle Workshop: The Technologies and their Potential, Cambridge, USA, November 2008.
22. Analog Devices, Incorporated, ADuC7034 datasheet: [www.analog.com/en/analog-microcontrollers/analog-microcontrollers/aduc7034/products/product.html](http://www.analog.com/en/analog-microcontrollers/analog-microcontrollers/aduc7034/products/product.html) (accessed 03.10.09).
23. R. Shoemaker, 26th International Battery Seminar and Exhibit, Ft. Lauderdale, USA, March 2009.
24. B.Y. Liaw and D.D. Friel, In Industrial Applications of Batteries. From Cars to Aerospace and Energy Storage, Chapter 13, M. Broussely, and G. Pistoia (Eds.), Elsevier, Amsterdam, 2007.



# Electric Vehicle Charging Infrastructure

**Peter Van den Bossche<sup>1</sup>**

Erasmus Hogeschool Brussel, Nijverheidskaai, Anderlecht, Belgium

## Contents

1. Introduction	518
1.1 Generalities	518
1.2 Historical background	518
1.3 Battery charging	518
2. Charging Power Levels	519
2.1 Energy usage	519
2.1.1 Background	519
2.1.2 Estimated consumption and practical example	520
2.1.3 Charging time and “charging speed”	520
2.2 Defining power levels	521
2.2.1 “Normal” charging	521
2.2.2 “Semi-fast” charging	521
2.3 Overview of power levels	523
3. Charging Modes for Conductive Charging	524
3.1 Mode 1 charging	524
3.2 Mode 2 charging	525
3.3 Mode 3 charging	526
3.3.1 Definition	526
3.3.2 Control pilot conductor	526
3.3.3 Control pilot alternatives	527
3.4 Mode 4 charging	528
4. Communication Issues	528
4.1 Control pilot communication	528
4.2 Advanced communication	529
4.2.1 Off-board chargers (Mode 4)	529
4.2.2 Communication for grid management	530
4.2.3 Billing	533
5. Accessories for charging	533
5.1 Connection cases	533
5.2 Standard accessories	535
5.3 Dedicated accessories	536
5.3.1 Early proprietary developments	536
5.3.2 Adaptation of standard accessories	536
5.3.3 New standardization proposals	536
5.4 Battery connectors	538

<sup>1</sup> Corresponding author: peter.van.den.bossche@ehb.be

6. "Fast" charging	538
7. Inductive charging	539
7.1 Introduction	539
7.2 Paddle type	540
7.3 Automatic connection	540
8. Conclusions	541
References	542



## 1. INTRODUCTION

### 1.1 Generalities

In urban traffic, due to their beneficial effect on environment, electrically propelled vehicles are an important factor for improvement of traffic and more particularly for a healthier living environment. The operation of the electrically propelled vehicle is dependent on the availability of efficient electric energy storage devices: the traction batteries. To allow the use of cheap and clean electric energy from the grid, recharging infrastructure shall be available to transfer electric energy from the distribution grid to the battery. This transfer can be done either by *conduction* or by *induction*, the first system being the most widely used.

This chapter will present the current evolution in the field of charging infrastructure, the problems involved, and the ongoing standardization efforts.

### 1.2 Historical background

The need for the availability of suitable charging infrastructure already arose in the first golden age of the electric vehicle in the early 20th century. The first ever standard to be developed for electric vehicles concerned in fact the charging plug, a standard sheet for which was presented in 1913 [1,2], which would be adopted on an international level as British Standard 74 [3]. Infrastructure needs also had their implications on the design of the vehicles. As d.c. distribution networks were still in widespread use in that period, particularly in the United States, standard battery voltages have been chosen allowing direct charging from a 110 V<sub>d.c.</sub> supply. This corresponds to the final charging voltage for a 40-cell lead-acid battery having a nominal voltage of 80 V [1]; this standard voltage was used up to the present time for battery-electric industrial vehicles [4].

The development of compact and efficient power electronic converters allowed electric vehicles to be fitted with on-board chargers, to be connected directly to the a.c. distribution network, thus greatly enhancing the flexibility of use for the vehicle.

### 1.3 Battery charging

Let us first consider the process of battery charging, which typically involves two phases:

- the main charging phase, where the bulk of energy is recharged into the battery
- the final charge phase, where the battery is conditioned and balanced

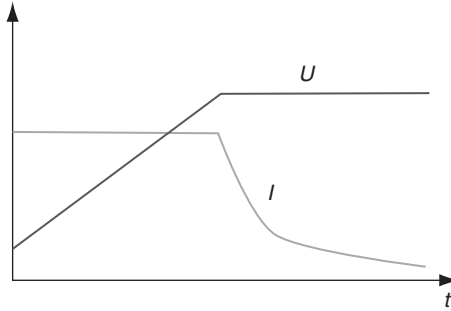


**Figure 20.1** IU charging characteristic.

Most chargers in use today use the so-called *IU* characteristic, where a constant current *I* is used for the main charge and a constant voltage *U* for the final charge (Fig. 20.1).

The duration of the main charge phase is dependent on the available current and the rating of the charger, whereas the final charge, which only needs a small current, typically takes several hours. Opportunity charging, the partial charging used in public stations, mostly involves the main charge phase only. However, for a good upkeep of most types of battery, a periodical full charge is advisable.



## 2. CHARGING POWER LEVELS

### 2.1 Energy usage

#### 2.1.1 Background

The power rating of the charging connection will depend on the energy consumed by the vehicle and the time needed for a charge.

The energy consumption of an electric vehicle, measured at the grid, can be obtained by integrating the immediate power at the wheels needed to propel the vehicle over time, taking into account the immediate efficiencies of all elements of the drive train:

$$E = \int_0^t \frac{P_w}{\eta_t \cdot \eta_m \cdot \eta_p \cdot \eta_b \cdot \eta_c} \cdot dt \quad [20.1]$$

with the efficiencies:

- $\eta_t$  of the mechanical transmission
- $\eta_m$  of the electric motor
- $\eta_p$  of the power electronics
- $\eta_b$  of the battery
- $\eta_c$  of the charger

This power  $P_w$  must be available to deliver the tractive force equal to the forces acting on the moving vehicle [5]:

$$F = F_a + F_d + F_f + F_s \quad [20.2]$$

where:

- $F_a = m' \cdot a$  is the acceleration force
- $F_d = 1/2 \cdot \rho \cdot S \cdot c_x \cdot v^2$  is the drag force
- $F_f = m \cdot g \cdot f_r \cdot \cos \alpha$  is the rolling friction force
- $F_s = m \cdot g \cdot \sin \alpha$  is the force to overcome the slope

The power, and thus the energy consumption, will depend on the vehicle characteristics (mass  $m$ , including rotating masses  $m'$ , front surface  $S$ , and drag coefficient  $c_x$ ), the road characteristics (friction coefficient  $f_r$  and slope  $\alpha$ ), the speed  $v$ , and the acceleration  $a$ . The influence of the acceleration force will be reflected through the followed drive cycle and the driving style.

Urban traffic, with its frequent accelerations, will yield much higher consumption values than constant speed driving. In extreme cases, such as postal distribution services, the energy consumption [6] may double the value measured in standardized tests based on “urban” driving schedules, as defined in international standards such as ISO 8714 [7].

### 2.1.2 Estimated consumption and practical example

A good approximation of the grid consumption of a battery-electric vehicle with current technology in mixed city traffic can be given by the empirical formula [8]:

$$E_s = 80 + 80/m \quad [20.3]$$

where:

- $E_s$  is the specific energy consumption in Wh/T km
- $m$  is the mass of the vehicle in tons

For example, a typical medium-sized vehicle weighing 1500 kg would have an energy consumption of

$$E = 1.5 \times (80 + 80/1.5) = 200 \text{ Wh/km} \quad [20.4]$$

To drive this vehicle over a distance of 50 km, a typical urban range for battery-electrics or plug-in hybrids, the following amount of energy would be needed from the grid:

$$E = 50 \text{ km} \times 200 \text{ Wh/km} = 10 \text{ kWh} \quad [20.5]$$

### 2.1.3 Charging time and “charging speed”

The time needed for charging the 10 kWh from the example above will depend on the power available and on the rating of the charger: with 2 kW available, 5 h would be needed, whereas a 10 kW outlet would deliver this power in just 1 h.



To illustrate the time needed for charging, one could define the notion of *charging speed*, corresponding to the distance covered by the amount of electrical energy charged during 1 h.

For the example, the charging speed would be 10 km/h for the 2 kW charger and 50 km/h for the 10 kW charger.

## 2.2 Defining power levels

Several power levels can be defined according to the power taken from the grid and the associated charging speed possible. However, one should be aware that the use of terms like “semi-fast” or “fast” in this context refers to the charging of typical vehicles like cars or small delivery vans as in the example of equation [20.5]. For smaller vehicles such as motorcycles, the power of a standard 16 A outlet may already allow a “fast” charge, whereas for a full-size bus a 22 kW connection will just be a “normal” charge.

### 2.2.1 “Normal” charging

*Normal* charging can be understood as using a power level corresponding to the standard power outlets typically available in residential installations. This concept corresponds to the *Level 1* charging defined in the United States [9].

The rating of standard power outlets varies in different areas of the world. In most European countries, the standard outlet is often rated 230 V, 16 A, yielding up to 3.7 kW which allows the 10 kWh from the example above to be recharged in less than 3 h. In some countries, however, the standard outlets have lower ratings (e.g., the United Kingdom 13 A, Switzerland 10 A).

With a corresponding “charge speed” of 18.5 km/h, the “normal” charging at 230 V, 16 A is thus offering a somewhat acceptable opportunity charging alternative, with adequate power for overnight charging which is typical practice for both private and commercial electric vehicles.

In North America, on the other hand, the supply of 120 V is still in general use. The standard power outlets are rated 120 V, 15 A, which corresponds to a maximum power of up to 1.8 kW. This voltage only allows a poor charging performance: with only 1.8 kW available, charging the vehicle from the example of equation [20.5] would take nearly 6 h. With a range of 50 km, one could define a “charge speed” of ~9 km/h.

### 2.2.2 “Semi-fast” charging

*Semi-fast* charging is to be understood as making use of current levels exceeding those of a standard domestic outlet, but which could be readily made available in a typical residential or commercial setting. This corresponds to *Level 2* charging in the United States.

In Europe, three-phase distribution is in general use. The most common system is a four-wire distribution as shown in Fig. 20.2, with a phase voltage of 230 V and a line

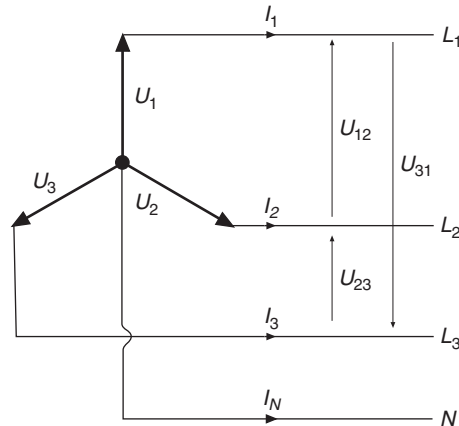


**Figure 20.2** Four-wire three-phase distribution.

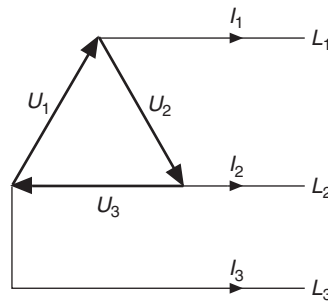


**Figure 20.3** Three-wire three-phase distribution.

voltage of 400 V. In some countries such as Belgium, three-wire  $3 \times 230$  V networks (Fig. 20.3) with a phase voltage of 230 V can be found, particularly in older installations. The neutral is not used here, its use being phased out with the demise of the former 127/220 V system. For a given current, available power levels with this system are a factor lower than with a  $3 \times 400$  V system.

The way the three-phase power is distributed to individual customers is however strongly dependent on historical developments and on the cultural tradition of every single country and its electricity distributors.

Some countries tend to allow residential connections to single phase only, even for higher power. France, for example, provides single-phase connections up to 80 A (18.4 kW). In such areas, a 230 V, 32 A connection can be readily made available, allowing 7.4 kW charge power.

On the other hand, in other areas three-phase power distribution is the norm. Switzerland mandates three-phase connections for all currents  $>16$  A, whereas a standard residential connection in Germany is  $3 \times 400$  V, 63 A.

This three-phase connection allows considerably higher power for a modest current: with just 16 A per phase, one can get:

$$P = \sqrt{3} \times 400 \times 16 \times \cos \phi = 11.1 \text{ kW} \quad (\cos \phi = 1) \quad [20.6]$$

This allows charging the example vehicle in just under 1 h for a range of 50 km, or a “charge speed” of 55 km/h.

With a current of 32 A, even up to 22.2 kW becomes available. This is already pretty fast charging for small- and medium-sized vehicles, using current levels which can be implemented more easily than the high single-phase current of nearly 100 A, which would be required to deliver this power. The use of three phases has the further advantage to be more beneficial for the load spreading of the electric network. The on-board battery charger of the vehicle shall of course be configured to accept a three-phase connection.

In North America, the three-wire split phase system illustrated in Fig. 20.4 allows a 240 V supply, effectively doubling the available power for a given current; this 240 V is indeed used for high-power devices such as cooking ranges. A 240 V, 30 A connection would give a power up to 7.2 kW, allowing charging the example vehicle of Ref. [5] in one hour and a half, or a “charge speed” of 36 km/h. Three-phase distribution is found only where asynchronous electric motors are used.

### 2.3 Overview of power levels

An overview of the available power for normal and semi-fast charging is given in Table 20.1. The last two columns give the section of copper needed for the cable (based on the standard ratings of 16 A for 2.5 mm<sup>2</sup> wire and 32 A for 6 mm<sup>2</sup> wire, and not including neutral or earth conductors) and the relationship between power and copper section. It can clearly be seen that the use of higher voltages, particularly in three phases, allows a much better utilization of the conductors, and hence the use of lighter cables and accessories.

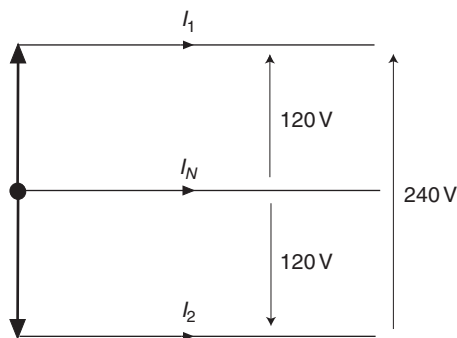


**Figure 20.4** Three-wire split-phase distribution.

**Table 20.1** Power levels for charging ( $\cos \varphi = 1$ )

	Voltage (V)	Phases	Current (A)	Power (kW)	Copper (mm <sup>2</sup> )	kW/mm <sup>2</sup>
EU Standard	230	1	16	3.7	5	0.74
EU Semi-fast	230	1	32	7.4	12	0.62
EU Semi-fast	400	3	16	11.1	7.5	1.48
EU Semi-fast	400	3	32	22.2	18	1.23
N.A. Level 1	120	1	15	1.8	5	0.36
N.A. Level 2	240	1	30	7.2	12	0.60

N.A., North America



### 3. CHARGING MODES FOR CONDUCTIVE CHARGING

The preceding section has dealt with the power levels for charging, but one should also consider the actual infrastructure used for connecting the vehicle. This leads to the definition of the so-called *charging modes*, introduced in the international standard IEC 61851-1 [10].

#### 3.1 Mode 1 charging

*Mode 1* charging refers to the connection of the electric vehicle to the a.c. supply network (mains) utilizing standardized socket outlets (i.e., meeting the requirements of any national or international standard), with currents up to 16 A. This corresponds to nondedicated infrastructure, such as domestic socket outlets, to which electric vehicles are connected for charging. These socket outlets can easily and cheaply deliver the desired power, and due to their availability, Mode 1 charging is the most common option for electric vehicles, particularly when existing infrastructure is to be used.

However, a number of safety concerns must be taken into account. The safe operation of a Mode 1 charging point depends on the presence of suitable protections on the supply side: a fuse or circuit breaker to protect against overcurrent, a proper earthing connection, and a residual current device switching off the supply if a leakage current greater than a certain value (e.g., 30 mA) is detected. Without proper earthing, a hazardous situation for indirect contact could occur with a single earth fault within the vehicle (Fig. 20.5)

In most countries, residual current devices (RCDs) are now prescribed for all new electric installations. However, still a lot of older installations are without RCD, and it is often difficult for the electric vehicle's user to know, when plugging in the vehicle, whether or not an RCD is present. Whereas some countries leave this responsibility to the user, Mode 1 has therefore been outlawed in a number of countries such as the United States.

Furthermore, some countries like Italy do not allow Mode 1 charging for charging places accessible to the public and limit its use to private premises, out of concern that live standard socket outlets in public places may be exposed to the elements, vandalism or unauthorized access.

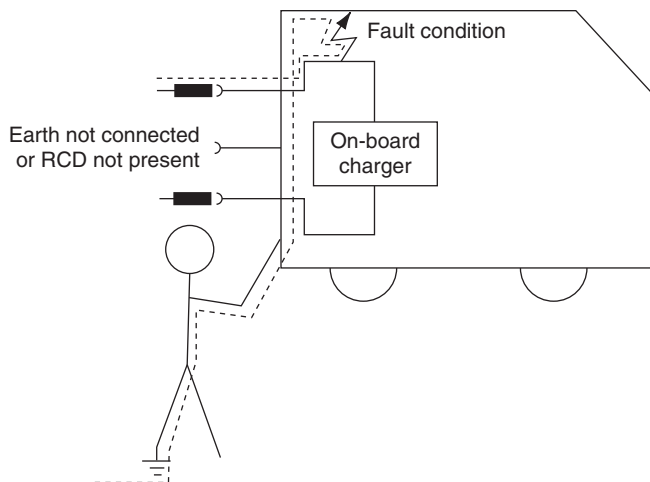


**Figure 20.5** Hazardous situation without RCD.

In countries where the use of Mode 1 charging is allowed, it will remain the most widespread charging mode for private premises (including residential garages as well as corporate parking lots) due to its simplicity and low investment cost. With a proper electrical installation including RCD, Mode 1 allows charging in full safety.

However, the uncertainty faced by the user about the presence of an RCD when plugging in the electric vehicle in an arbitrary standard outlet results in a potential hazard. For this reason, vehicle manufacturers tend to steer away from Mode 1 charging in the long term.

### 3.2 Mode 2 charging

*Mode 2* charging connection of the electric vehicle to the a.c. supply network (mains) also makes use of standardized socket outlets. It provides however additional protection by adding an in-cable control box with a control pilot conductor (see Section 3.3.2) between the electric vehicle and the plug or control box.

The introduction of Mode 2 charging, mainly aimed at the United States, reflected the American infrastructure process which developed electrical standards and code language that were adopted by the National Electrical Code [11], to ensure that personnel protection and other safety considerations were implemented in all charging systems utilized. Mode 2 was initially considered a transitional solution particularly for the United States, although it has received some new interest for replacing Mode 1 for charging at nondedicated outlets.

The main disadvantage of Mode 2 is that the control box protects the downstream cable and the vehicle, but not the plug itself, whereas the plug is one of the components more liable to be damaged in use.

### 3.3 Mode 3 charging

#### 3.3.1 Definition

*Mode 3* charging involves the direct connection of the electric vehicle to the a.c. supply network utilizing dedicated electric vehicle supply equipment. This refers to private or public charging stations. The standard IEC 61851-1 [10] mandates control pilot protection between equipment permanently connected to the a.c. supply network and the electric vehicle.

#### 3.3.2 Control pilot conductor

For Mode 3 charging, the IEC 61851-1 standard foresees additional protection measures to be provided by the so-called *control pilot*, a device which has the following functions mandated by the standard:

- verification that the vehicle is properly connected
- continuous verification of the protective earth conductor integrity
- energization and deenergization of the system
- selection of the charging rate

In the first edition of the standard [10], the control pilot is defined as an extra conductor in the charging cable assembly, in addition to the phase(s), neutral, and earth conductor. However, IEC 61851 does not specify normative requirements for the operation of the control pilot circuitry.

An example of control pilot circuit is given in Fig. 20.6, showing the operation of the system. A small current is sent through the control pilot conductor, which is connected to the vehicle body by a resistor. The current returns to the charging post through the earth conductor. When the pilot current flows correctly, the contactor in the charging post is closed and the system is energized.

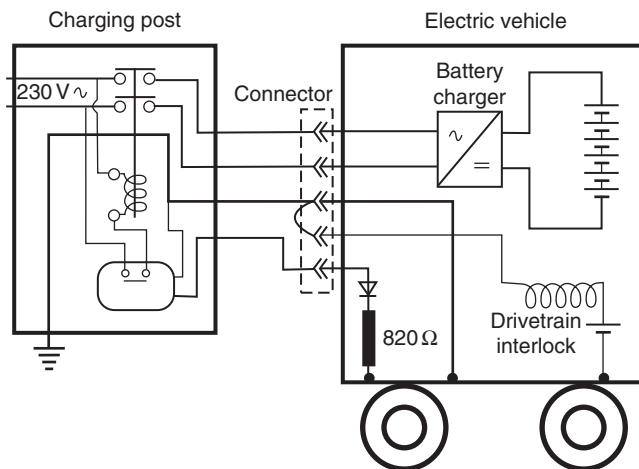


**Figure 20.6** Control pilot conductor.

When no vehicle is connected to the socket outlet, the socket is dead. This provides a key safety advantage particularly for publicly accessible charging points. Power is delivered only when the plug is correctly inserted and the earth circuit is proved to be sound.

The connection process shall be such that the earth connection is made first and the pilot connection is made last. During disconnection, the pilot connection shall be broken first and the earth connection shall be broken last. This sequence also ensures that the current is interrupted at the contactor and not at the power contact pins of the plug, thus eliminating arcing and prolonging the service life of the accessories.

The use of a control pilot conductor in charging equipment was first proposed around 1990 for charging stations for electric boats deployed in the Norfolk Broads in England [12].

The use of a control pilot function with fourth wire is also included in the Society of Automotive engineers (SAE) standard J1772 (which is now under revision) [13].

### 3.3.3 Control pilot alternatives

The use of a dedicated conductor for the control pilot necessitates an extra conductor and thus the use of special cables and accessories.

The new version of the standard 61851-1 [14] has introduced the concept of *control pilot function*, mandatory for Mode 3 charging, which has to perform the same functions as the control pilot conductor described in the previous section, but which can be realized by other means than the extra pilot conductor. The use of a physical control pilot conductor remains an option of course.

Alternative means to implement control pilot functionality include various wireless data transfer systems as well as power-line communication. An interesting implementation of the latter has been developed by Electricité de France [15]. The principle is illustrated in Fig. 20.7.

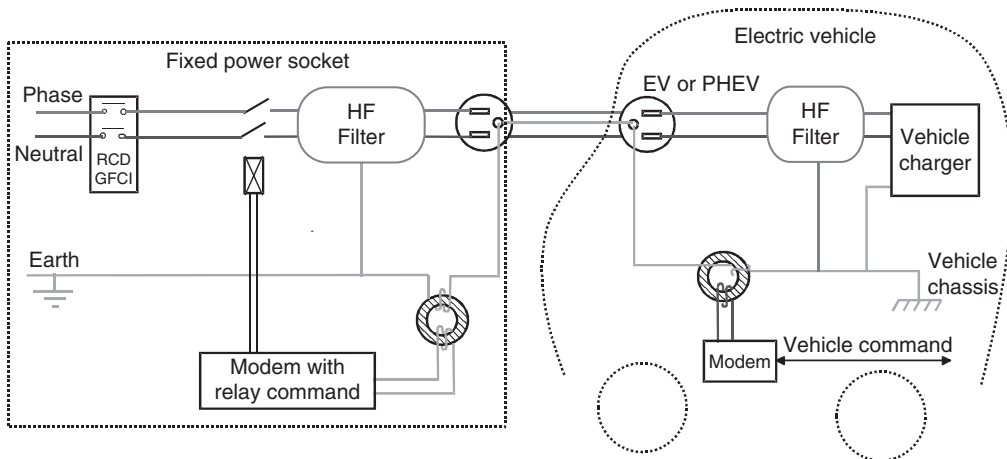


**Figure 20.7** Control pilot function with power-line communication.

The control pilot signal is a common-mode signal between the phase wires and the earth conductor, using a 110 kHz carrier frequency. This signal is generated by the vehicle electronics and transmitted to the earth wire through a transformer (ferrite torus). Filter circuits are present to avoid the unwanted transmission of data signals from the charging system to the mains, and to be compliant with relevant standards concerning electrical equipment to be connected to the grid, which proscribe any earth-line communication upstream of the electric vehicle supply equipment [16]. The associated components are small and low cost.

The system is able to perform all control pilot functionalities over a three-wire connection. This basic protection can be implemented using a cheap and minimal set of electrical components and thus would also be suited for light vehicles like electric motorcycles, where the extra cost of special accessories should be avoided.

The proposed system presents however several other interesting opportunities, since it is able not only to carry the control pilot signal but also to perform data exchange functions to be used in smart charging and billing (see also Section 4).

### 3.4 Mode 4 charging

*Mode 4* charging is defined as the indirect connection of the electric vehicle to the a.c. supply network (mains) utilizing an off-board charger where the control pilot conductor extends to equipment permanently connected to the a.c. supply.

This pertains to d.c. charging stations, which are mostly used for fast charging. As the charger is located off-board, a communication link is necessary to allow the charger to be informed about the type and state of charge of the battery, so as to provide it with the right voltage and current.



## 4. COMMUNICATION ISSUES

The communication between the vehicle and the charging post can be developed in several ways, with increasing sophistication.

In Mode 1 or Mode 2 charging, where standard, nondedicated socket outlets are used, there is no communication at all.

### 4.1 Control pilot communication

Mode 3 introduces communication through the control pilot function. In its most basic way of operation, the control pilot only fulfills its essential safety function. The signal can be just a current sent through the control pilot loop to ensure the vehicle is properly connected and the earth connection is sound.

More functionality can be added by using a pulse-width modulation (PWM) signal in the control pilot circuit. The PWM signal can convey information through the variation of its duty cycle  $D_c$  (Fig. 20.8):



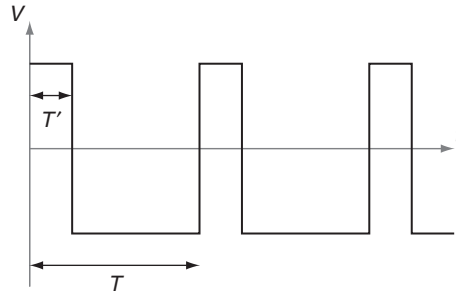


**Figure 20.8** PWM signal.

$$D_c = \frac{T'}{T} \times 100 \quad [20.7]$$

The duty cycle can be used to define the ampacity of the charger. This feature presents several operational benefits:

- The charger can adjust itself to the maximum allowable current that can be delivered by various charging points, for example, a standard value of 16 A and a higher value of 32 A for semi-fast charging points. The standard value of 16 A will usually be the default value.
- The charging point can control the amount of current absorbed by the charger, in the framework of a smart grid load management, or to optimize the billing of the electric energy.

The solution that will be proposed in the new IEC 61851-1 uses a PWM signal at a level of  $\pm 12$  V at a frequency of 1 kHz and defines the current level by a constant of  $0.6 \times D_c$  A for values of the duty cycle between 10 and 85%, and  $2.5 \times (D_c - 64)$  A for values between 85 and 96%, which will thus yield a current between 6 and 80 A, encompassing the whole range of normal and semi-fast charging.

A duty cycle  $< 5\%$  conveys the message that charging current is controlled through advanced serial communication; for duty cycles  $> 97\%$ , charging is impeded.

## 4.2 Advanced communication

### 4.2.1 Off-board chargers (Mode 4)

Off-board chargers, which supply a d.c. to the vehicle battery, must communicate with the vehicle in order to supply the battery with the correct voltage and current. This is particularly the case with nondedicated chargers as used in public charging stations, which should be able to supply vehicles with varying battery voltages and chemistries.

The communication protocol for this data link was intended to be the part 24 of IEC 61851. The document was never published by IEC however, and the European pre-standard ENV 50275-2-4 [17], which the IEC standard would supersede, was transferred in 2006 to Technical Specification 50457-2 [18].

The proposed protocol is largely based on the ISO road vehicle diagnostic standards as defined in ISO 14229 and ISO 14230 [19–22]. These concern requirements for diagnostic systems implemented on a serial data link layer, which allows a tester to control diagnostic functions in and on vehicle electronic control unit.

The protocols were specifically adapted for the selected application: after the initialization phase by the off-board charger, the vehicle's charge control unit controls the charging process of the off-board charger. Contrary to the standard communication according to ISO 14230 where the server and the client are fixed during all the session, their roles are definitively reversed after the initialization phase.

This document however is to be superseded by the new standards now under development and discussed next.

#### **4.2.2 Communication for grid management**

The development of new concepts such as “smart grid” or “vehicle to grid” has created the need for an appropriate communication protocol for electric vehicle charging beyond the mere safety functions of the control pilot, in order to provide functionalities such as:

- vehicle identification and billing, allowing payment for charging at public charging stations, but also individual billing of used energy to the user's account when the vehicle is charged at any outlets connected to a smart meter
- charge cost optimization by choosing the most appropriate time window where electricity rates are the lowest
- grid load optimization by controlling charger ampacity in function of grid demand
- peak-shaving functionality by using electric vehicles connected to the grid as a spinning reserve (vehicle-to-grid)
- appropriate billing and user compensation functions for vehicle-to-grid operation

The development of such a communication protocol involves several actors, including both vehicle manufacturers and utilities. To this effect, the standardization of this issue is being addressed by a joint working group uniting ISO TC22 SC3 (electric equipment on road vehicles, including on-board communication systems), ISO TC22 SC21 (electric road vehicles), and IEC TC69 (electric road vehicles).

The standard to be developed by this joint working group will describe the communication, in terms of data format and message content, between the electric vehicle and the electric vehicle supply equipment (charging post), as well as message content and data structure to enable billing communication and grid management. Provisions for additional communication aspects (like vehicle charge status information and configuration) will also be considered to allow for interoperability of all vehicles with all charging stations.

The communication protocols are based on the well-known seven-layer Open System Interconnection (OSI) reference model [23] (Fig. 20.9).

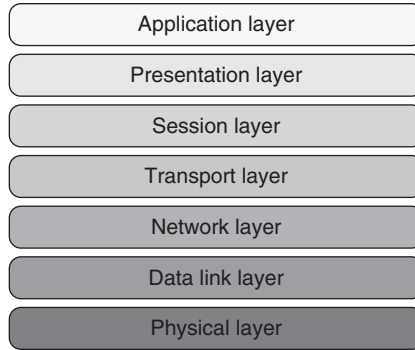


**Figure 20.9** Open System Interconnection layers.

In order to define the implementation of the communication in the lower layers, it is first necessary to analyze the real communication needs and the information to be transferred by the different “actors” involved in the charging process. These actors include physical devices such as the charging post or the vehicle controller, entities such as electricity suppliers or grid operators, and last but not least the vehicle user. An overview of actors potentially involved and the communication links between them is shown in Fig. 20.10. The local or remote communication system may have the function of a “clearing house” for the authentication, collecting and consolidation of grid and billing parameters from the actors as well as transmitting charging process information to the respective actors. Not all such functions are necessarily required for the basic charging functions, and some may be performed locally or remotely. The system can thus become rather complex, and several issues are still to be resolved.

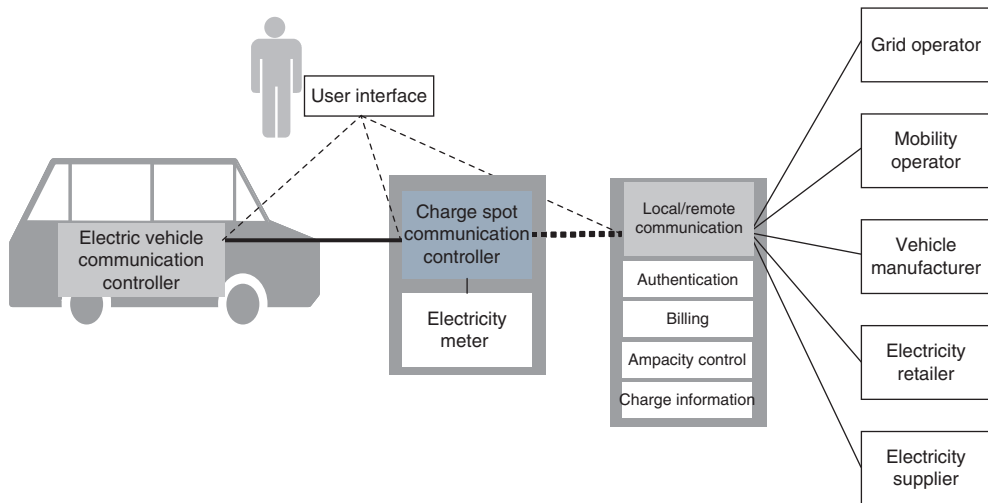


**Figure 20.10** Actors involved in the charging process.

All envisageable charging processes have to be contextualized in so-called “use cases,” where three main categories can be discerned:

- charging with no communication: this is the classical Mode 1 or 2 charging, also Mode 3 charging with only the basic control pilot safety functions
- charging with minimal communication: Mode 3 charging with ampacity control to adapt to local physical limits or to perform dynamic grid optimization
- charging with maximum communication, including automatic billing and grid control and process information

Functionalities to be implemented are illustrated in Fig. 20.11; the increase of user convenience necessitates an extension of data structures to be exchanged.

For each use case, different scenarios are to be defined, relating to the desired control of charging by the grid operator, to the used billing scheme, and to the communication system for the user. Several systems are now under consideration and/or used in experimental fleets:

- use of a radio frequency identification (RFID) tag
- communication over the control pilot conductor
- communication (at low or high data rate) through power-line communication
- communication with the vehicle’s CAN-Bus system
- wireless communication through Bluetooth or ZigBee devices
- communication via mobile phone

One typical example scenario (“plug and charge”) could be described as follows:

- The user plugs his vehicle into the charge spot without having to perform other manipulations.
- The vehicle sends its identification ID to the charge spot to get authenticated by the clearing house through GSM.

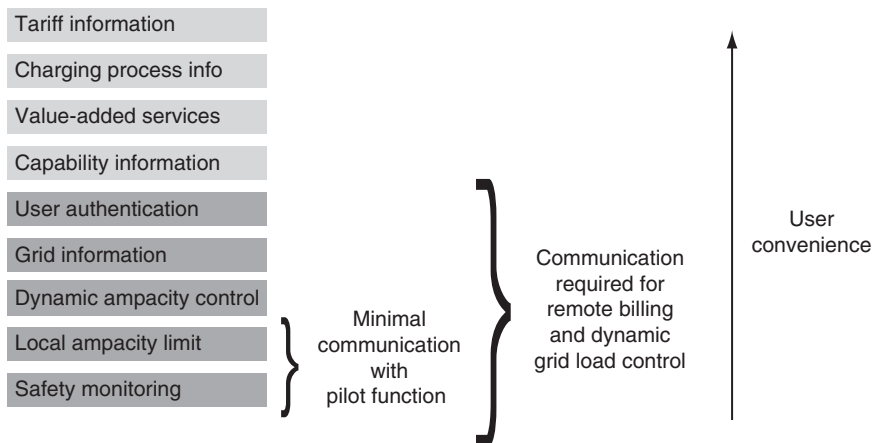


**Figure 20.11** Communication and use cases.

- Authentication is successfully processed.
- Grid and tariff parameters are negotiated.
- Charging process starts automatically.

In order to define the communication messages, every such scenario shall be translated into a sequence diagram in unified modeling language [24]. It is clear that considerable standardization work remains to be performed in this field, and that a generally applicable standard shall be drafted which does not encompass proprietary protocols so it can be used by all concerned parties, enabling a true global solution.

### 4.2.3 Billing

The practice of charging electric vehicles at public charging stations raises the problem of billing the user for the energy consumed. Payment systems can make use of coins (vulnerable to vandalism), credit cards (creating the necessity of communication systems and involving transaction costs) or dedicated access devices (cards or RFID).

As the value of the electricity typically charged in one opportunity charging session is quite low compared to the parking cost in city center environment, one can consider to charge the user according to time rather than energy used, which dispenses the need for (more expensive) electricity counters. Some legal issues have also to be considered here, as in some countries the sale of electricity as such is heavily regulated.

The new developments in communication will allow a more sophisticated approach of this issue, with user identification and communication using wireless devices or mobile phones, differential billing according to time of the day and grid load, as well as compensation for energy returned to the grid. Furthermore, vehicles being charged at varying locations in a “smart grid” environment will charge the user in a transparent “roaming” way: wherever the user charges his vehicle, it will be charged on his own bill.



## 5. ACCESSORIES FOR CHARGING

### 5.1 Connection cases

The connection of the cable between the vehicle and the charging outlet can be carried out in three ways as defined in IEC 61851-1 [10]:

- Case “A” – where the cable and plug are permanently attached to the vehicle. This case is generally found only in very light vehicles (Fig. 20.12).
- Case “B” – where the cable assembly is detachable and connected to the vehicle with a connector. This is the most common case for normal and semi-fast charging (Fig. 20.13).

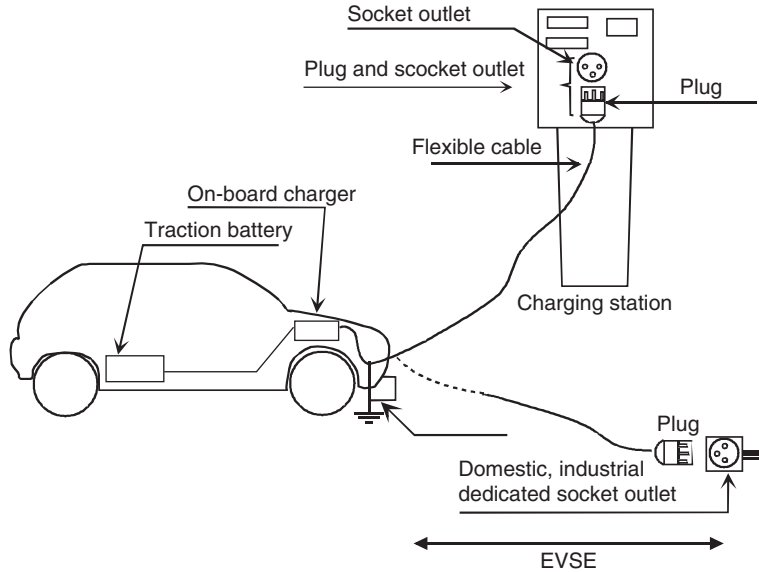


**Figure 20.12** Case “A” connection.

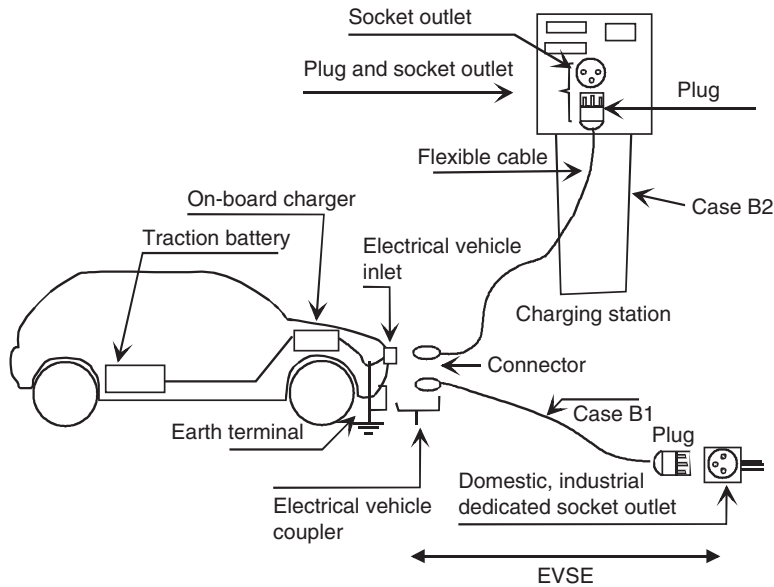


**Figure 20.13** Case “B” connection.

- Case “C” – where the cable and vehicle connector are permanently attached to the supply equipment. This arrangement is typically used for fast charging (Mode 4), so that drivers do not have to carry heavy cables around. Public charging stations using this case are however at a higher risk of copper theft (Fig. 20.14).

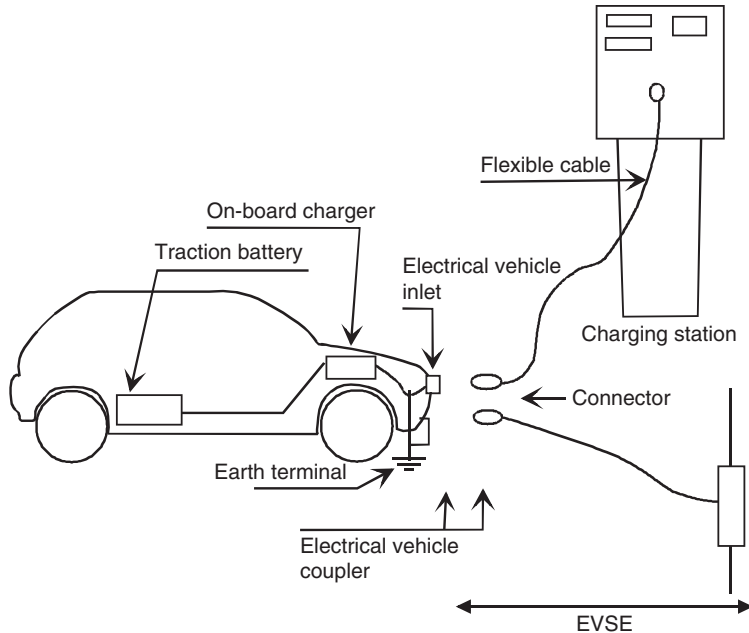


**Figure 20.14** Case “C” connection.

## 5.2 Standard accessories

For Mode 1 charging, and also for Mode 3 charging with power-line communication, standard plugs and sockets can be used encompassing only phase, neutral, and earth contacts. In most areas, this will usually be the standard domestic plugs as described in various national standards, and typically rated 10–16 A [25].

One has to recognize however that these domestic plugs, particularly not the low-cost versions mostly used on consumer grade equipment, are not really suited for the heavy-duty operation of electric vehicle charging, characterized by

- long-time operation at near rated current
- frequent operation, including disconnection under rated load
- exposure to outdoor conditions.

This leads to a shorter lifetime of the accessories and to contact problems which may cause hazardous situations.

A better alternative is to use industrial plugs and sockets as defined by the international standard IEC 60309-2 [26]. These plugs (in standard blue color for 230 V, red for 400 V) are widely used, particularly in Europe, for industrial equipment but also for outdoor uses like camping sites, marinas, etc., where they function in an operation mode comparable to an electric vehicle charging station. Both plugs/sockets and connector/inlets are available in the IEC 60309-2 family. These accessories are easily found on the

market and are inexpensive, making them the preferred choice for Mode 1 charging; they can also be used for Mode 3 charging where power-line communication is used.

### **5.3 Dedicated accessories**

The use of a physical control pilot conductor necessitates the introduction of specific accessories for electric vehicle use. Such plugs and sockets are described in the international standard IEC 62196 “Plugs, socket-outlets, vehicle couplers and vehicle inlets – Conductive charging of electric vehicles.”

Part 1 of this standard [27] gives general functional requirements; it is based on the general standard IEC 60309-1 [28], adapted with the requirements of IEC 61851-1 [10]. As the latter standard is currently being revised, a new version of IEC 61982-1 will also be drafted.

This part of the standard however states no physical dimensions of the accessories. These will be treated in part 2, which is currently under preparation.

#### **5.3.1 Early proprietary developments**

Vehicle couplers for early battery-electric vehicles used either standard accessories or proprietary connectors. One popular example of such coupler, produced by the Maréchal company, was widely used on European battery-electric vehicles, in the 1990s.

This coupler was foreseen for both Mode 1 or Mode 3 charging at 230 V<sub>a.c.</sub>, 16 A and Mode 4 d.c. charging at 200 A. One common vehicle inlet could accommodate connectors in both a lightweight version for a.c. connection and a heavier version for high-current d.c. charging. However, despite its relatively wide use, it was never adopted as an international standard sheet.

A similarly built vehicle coupler, albeit with a different arrangement of contacts, was proposed by Avcon in the United States.

#### **5.3.2 Adaptation of standard accessories**

A connector accommodating both Mode 1 and Mode 3 charging has been proposed by the German company Mennekes. It makes use of modified IEC 60309-2 accessories, with sliding side contacts added for the pilot connection, while maintaining intermateability with standard IEC 60309-2 socket-outlets. A vehicle can thus be charging in Mode 1 on a non-dedicated outlet (e.g., private garage) and in Mode 3 on a public charging station. This system has seen use in Germany and Switzerland.

#### **5.3.3 New standardization proposals**

With the new interest for battery-electric and plug-in hybrid vehicles since 2006, standardization work has started toward a global coupler design to be used for all vehicles in all countries. Parallel developments and differing needs in several regions have led



however to the proposal of three distinct designs for the vehicle coupler which will feature in IEC 61982-2, with some other proposals having been abandoned.

- *Single-phase connector.* A first proposal represents the solution which is based on the proposals made for the new forthcoming version of SAE J1772 and on a proposal made by the Japanese company Yazaki. This plug is rated for 250 V and 32 A (30 A in the United States and Japan). It is fitted with two extra contacts: one for the control pilot (CP) and one for an auxiliary coupler contact (CS) which can be used to indicate the presence of the connector to the vehicle and to signal the correct insertion of the vehicle connector into the vehicle inlet. With a diameter of 44 mm, this connector is made in a compact way.
- *Three-phase connector.* The connector proposed in the former paragraph is single phase only. The advantages of three-phase connections and the availability of three phase supply in most European countries led to a second proposal based on a prototype developed by the German company Mennekes. The connector is rated for currents up to 63 A and has two auxiliary contacts. One interesting feature of this proposal is that the same device is designed to be used both as plug and vehicle connector (Fig. 20.15) - if national regulations permit such use - with a supplementary insulation of contact pin tips to prevent direct contact with live conductors.
- *Italian national standard plug.* Based on the first edition of IEC 62196-1 [27], a national standard was drafted in Italy [29] for a single-phase plug with pilot contact. These

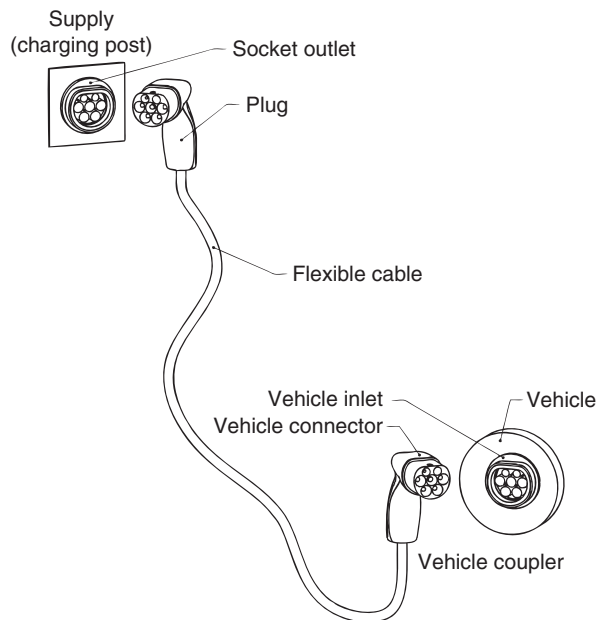


**Figure 20.15** Proposed three-phase connector with nomenclature of accessories.

accessories are in widespread use in Italy, particularly for light electric vehicles such as motorcycles. Based on this standard, a third proposal has been drafted, with either one or two auxiliary (pilot) contacts. This accessory comes with a rating of either 16 A or 32 A; the dimensions of the plug housing and the contacts are actually identical for both, but a different keyway is provided to disallow introduction of a 32 A plug in a 16 A socket outlet. A three-phase version of this concept is also being proposed.

## 5.4 Battery connectors

Battery connectors are widely standardized for use in industrial electric vehicles. Functional requirements are given in the European standard EN 1175-1 [30]. Several families of connectors in use conform to this standard, such as the so-called Euroconnectors [31,32] and the “Anderson” connectors. These connectors are available with or without auxiliary contacts, for d.c. currents up to 350 A.

Although such connectors are sometimes found in electric road vehicles for internal connections, their use for (Mode 4) charging of road vehicles is not advisable, particularly by the general public, as they are designed neither for the higher battery voltage levels now in use nor for connecting to cable assemblies. Furthermore, they lack earth conductors and are not designed to break a load.



## 6. “FAST” CHARGING

For “fast” charging (called *Level 3* charging in the United States), higher power levels are used which create the need for specific infrastructure beyond standard domestic or industrial socket outlets. The charging can be performed with either a d.c. or an a.c. connection between the vehicle and the charging post.

In the d.c. case, a fixed battery charger (rectifier) is connected to the battery, and more heavy and expensive fixed infrastructure is thus needed, whereas for a.c. fast charging the rectifying is done on-board the vehicle, most commonly using the traction inverter which is able to recharge the battery at a high current (for regenerative braking) and can also be fed by the grid (Fig. 20.16).

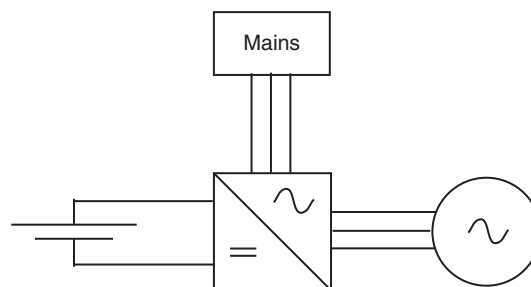


**Figure 20.16** Charging with inverter.

Fast charging infrastructure is being proposed for power levels up to 250 kW [33], claiming to be able to charge an electric vehicle in less than 10 min, comparable with the refueling time of a gasoline-powered legacy vehicle.

The enhancing of the user flexibility associated with this fast charging comes however with a number of drawbacks:

- the high cost of the fixed infrastructure involved compared with semi-fast charging
- the need for heavy cables, which for practical purposes are usually fixed to the charging station (Case “C”), exposing them to copper thieves
- the high burden on the distribution network if point loads of this level are introduced, and the high cost of the electric energy particularly at peak times. This can be alleviated by providing an energy buffer such as a stationary battery at the charging station (which would be charged overnight at low rates), but such solution increases the investment cost even more while introducing additional losses due to battery and charger efficiencies
- the fast charging cycle provides only opportunity charging and does not allow final charge which takes a certain time at a low current; periodical (overnight) charging will thus remain necessary

It thus seems likely that the mainstay of the infrastructure will make use of normal or semi-fast charging points located both at private locations (residential garages or corporate parking places) and at publicly accessible charging points.

The presence and availability of fast charging stations however provides a psychological advantage to electric vehicle drivers, allowing them to fully exploit the range envelope of their vehicle and to overcome “range anxiety.” A few well-located fast charging stations in an urban area can fulfill this need. They will be accessed mostly for “emergency” uses or in case of an unexpected change in mission, with the bulk of the electric energy delivered to the vehicles by cheap overnight charging.

The psychological advantage of the fast charging stations is comparable in fact to the plug-in hybrid vehicle, where the presence of an auxiliary power unit gives users the confidence to use the full range of their battery, overcoming the range anxiety typical for many battery-electric drivers who do not have specialist knowledge of the behavior of their battery.

The high power connection of the “fast” charging station makes it furthermore particularly interesting for “vehicle-to-grid” applications.



## 7. INDUCTIVE CHARGING

### 7.1 Introduction

Inductive charging is defined as the transfer of energy from the supply network to the vehicle in an electromagnetic way, using a two-part transformer with the primary connected to the network and the secondary installed on the vehicle. Charging can be performed after juxtaposition of the two parts.

The introduction of inductive charging systems has been proposed to allow a considerable improvement of charging safety. The nonconductive energy transfer virtually eliminates all risk of electric shock for the user. Furthermore, the opportunity for automatic connection dispenses with the use of electric cables, thus removing both electrical (handling of power connectors) and mechanical (trailing cables) hazards which are usually associated with the use of electric vehicle charging equipment.

## 7.2 Paddle type

One type of inductive charging has been introduced and extensively promoted by General Motors in the 1990s. The secondary coils were arranged around a slot in the vehicle, the primary coil being a paddle to be inserted in the slot (Fig. 20.17). The system was able to accommodate all three levels of charging. The use of high frequencies for the inductor circuit allowed for lightweight construction [34].

The 1990s saw a heavy competition between inductive and conductive charging technologies. Due to the higher cost of the inductive solution on one hand, particularly for the off-board part, and the sufficiently high level of safety that can be reached with conductive solutions on the other hand, conductive charging has taken the lead and the inductive paddle solution has fallen into oblivion. Efforts for international standardization, which had to lead to the publication of a document with general requirements for inductive charging, as well as a document defining the geometry of the paddles, did not proceed further than CD stage, work being halted in 2000 [35,36].

## 7.3 Automatic connection

The paddle system presented an inherently safe “plug” but still necessitated the use of cables.

Cable-free charging can be made possible by appropriate design and location of the inductors so it is sufficient to park the vehicle adjacent to the primary inductor, which can be done in one of the following ways [34] (Fig. 20.18):

1. special charging post design
2. fixed devices, flush with road surface

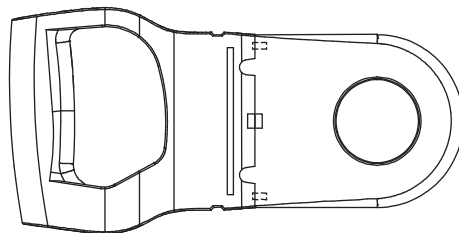


**Figure 20.17** Inductive charging paddle.

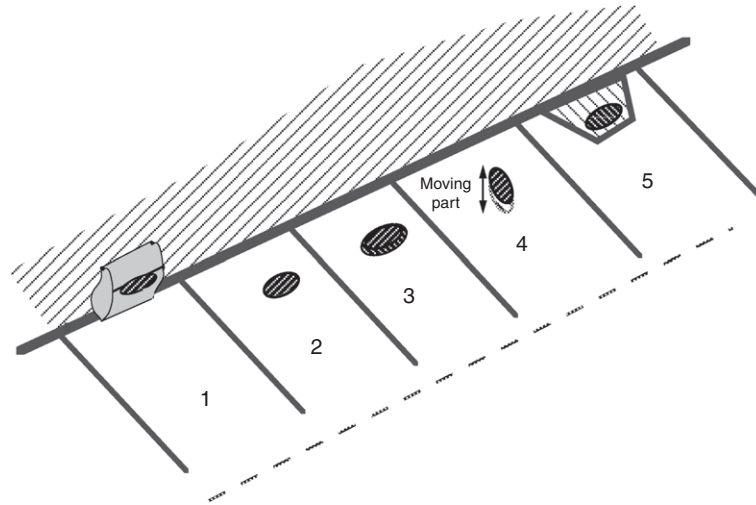


**Figure 20.18** Automatic charger connections.

3. fixed devices, not flush with road surface
4. devices on road surface which include moving parts
5. special kerb designs

As such systems require a specific approach to both the vehicle and the charging point architecture, their use will be mostly limited to niche applications such as captive fleets for special use and automatic rent-a-car systems, for which inductive charging systems have recently known a renewed interest. This should also be seen in the framework of the inductive energy transfer systems now being implemented for powering trams and electric buses without overhead cables.

## ➤ 8. CONCLUSIONS

Battery-electric and plug-in hybrid vehicles can be charged on several levels.

“Normal” charging, making use of standard domestic socket outlets, can be used potentially anywhere but is limited in power. It remains suitable for overnight home charging or improvised opportunity charging. On private premises, Mode 1 charging can be done in perfect safety with a properly fitted electrical installation, making use of standard accessories, preferably of the IEC 60309-2 type.

“Semi-fast” charging allows a higher charging power, up to 22 kW, which is very suitable for most vehicles. It makes use of power levels which are easily delivered by existing distribution networks and will be the mainstay for dedicated electric vehicle charging points in both private and public settings. The use of three-phase supply allows a considerable increase in the charging power available. Dedicated accessories are being

standardized to allow a flexible operation of the system including power management and vehicle to grid.

“Fast” charging needs a more expensive infrastructure, particularly where a d.c. connection with off-board charger is used and may thus be less interesting for routine charging, but the availability of selected fast charging stations provides opportunities for enhancing the operational flexibility of the vehicles, as well as high-power bidirectional energy transfer.

Inductive charging may offer interesting opportunities by eliminating plugs and cables, but its infrastructure requirements limit it to specific applications.

Battery-electric and plug-in hybrid vehicles should be considered equally for their infrastructure needs, both depending on the electric grid for their energy supply; it is in fact to be expected that most plug-in hybrids will mainly be operated in electric mode, allowing the use of cheaper (and cleaner!) electric energy.

Intensive work is now being performed by international standardization committees in order to realize unified solutions which will be a key factor in allowing the deployment of electrically propelled vehicles on a global level.

## REFERENCES

1. P. Van den Bossche, *The Electric Vehicle: Raising the Standards*. Ph.D. Thesis, Vrije Universiteit Brussel, 2003.
2. Electric Vehicle Association of America, Standard Charging Plugs and Receptacles, *The Central Station* 13 (1914) 304.
3. BS74, British Standard Specification for Charging Plug and Socket for Vehicles Propelled by Electric Secondary Batteries. BSI, 1917.
4. ISO 1044, Industrial Trucks – Lead-Acid Traction Batteries – Preferred Voltages. ISO, 1993.
5. J. Van Mierlo, *Simulation Software for Comparison and Design of Electric, Hybrid Electric and Internal Combustion Vehicles with Respect to Energy, Emissions and Performances*. Ph.D. Thesis, Vrije Universiteit, Brussel, 2000.
6. EVD-Post, *Electric Vehicle Delivery Post – Final Report*. European Project TR140/97, CITELEC, 2001.
7. ISO 8714, *Electric Road Vehicles – Reference Energy Consumption and Range – Test Procedures for Passenger Cars and Light Commercial Vehicles*. ISO, 2002.
8. P. Van den Bossche, *Proceedings of EVS-11*, Firenze, Italy, 1992.
9. C. Toepfer, *EV Charging Systems, Report of the Connector and Connecting Station Committee*. TR-104623-V2, Project 2882.EPRI, 1994.
10. IEC 61851-1, *Electric Vehicle Conductive Charging System – Part 1: General Requirements*. IEC, 1st ed., 2001.
11. NEC 625, *Electric Vehicle Charging System*. National Fire Protection Association, 1999.
12. Benning Ltd, *Safe Power for Electric Boats*. Brochure, 1990.
13. SAE J1772, *Electric Vehicle Conductive Charge Coupler*. SAE, 2001.
14. IEC 61851-1/CDV, *Electric Vehicle Conductive Charging System – Part 1: General Requirements*. 69/160/CDV. IEC TC69 WG4, 2009.
15. C. Bleijs, *Proceedings of EVS-24*, Stavanger, Norway, 2009.
16. EN 50065-1, *Signalling on Low-Voltage Electrical Installations in the Frequency Range 3 KHz to 148.5 KHz – Part 1: General Requirements, Frequency Bands and Electromagnetic Disturbances*. CENELEC, 2002.
17. ENV 50275-2-4, *Conductive Charging for Electric Vehicles – Part 2: Communication Protocol Between Off-Board Charger and Electric Vehicle*. CENELEC, 1998.

18. TS 50457-2, Conductive Charging for Electric Vehicles – Part 2: Communication Protocol Between Off-Board Charger and Electric Vehicle. CENELEC, 2006.
19. ISO 14229-1, Road Vehicles – Unified Diagnostic Services (UDS) – Part 1: Specification and Requirements. ISO, 2006.
20. ISO 14230-1, Road Vehicles – Diagnostic Systems – Keyword Protocol 2000 – Part 1: Physical Layer. ISO, 1999.
21. ISO 14230-2, Road Vehicles – Diagnostic Systems – Keyword Protocol 2000 – Part 2: Data Link Layer. ISO, 1999.
22. ISO 14230-3, Road Vehicles – Diagnostic Systems – Keyword Protocol 2000 – Part 3: Application Layer. ISO, 1999.
23. ISO/IEC 7498-1, Information Technology – Open Systems Interconnection – Basic Reference Model: The Basic Model. ISO/IEC, 1994.
24. ISO/IEC 19501, Information Technology – Open Distributed Processing – Unified Modeling Language (UML) Version 1.4.2. ISO/IEC 2005.
25. IEC/TR 60083, Plugs and Socket-Outlets for Domestic and Similar General Use Standardized in Member Countries of IEC. IEC, 6th ed., 2009.
26. IEC 60309-2, Plugs, Socket-Outlets and Plugs for Industrial Purposes – Part 2: Dimensional Interchangeability Requirements for Pin and Contact-Tube Accessories. IEC, 4.1 ed., 2005.
27. IEC 62196-1, Plugs, Socket-Outlet and Vehicle Couplers – Conductive Charging of Electric Vehicles – Part 1: Charging of Electric Vehicles up to 250 A a.c. and 400 A d.c. IEC, 2003.
28. IEC 60309-1, Plugs, Socket-Outlets and Plugs for Industrial Purposes – Part 1: General Requirements. IEC, 2005.
29. CEI-69-6, Foglio di Unificazione di Prese a Spina per la Connessione alla Rete Elettrica di Veicoli Elettrici Stradali. CEI – Italian Electrotechnical Committee, 2001.
30. EN 1175-1, Safety of Industrial Trucks. Electrical Requirements. General Requirements for Battery Powered Trucks. CEN, 1998.
31. DIN 43589-1, Geräte-Steckvorrichtungen 80, 160, 320 A, 150 V für Elektro-Flurförderzeuge – Teil 1: Anschlußmaße, Werkstoff, Kennzeichnung. DIN, 1994.
32. FEM 4.007b, Industrial Trucks – Connectors for Traction Batteries up to and Including 96V – Dimensions. Fédération Européenne de la Manutention, 1993.
33. A. Szczepanek and C. Botsford, Proceedings of EVS-24, Stavanger, Norway, 2009.
34. G. Maggetto, P. Van den Bossche and W. Li, Proceedings of EVS-17, Montreal, Canada, 2000.
35. IEC 61980-1/CD, Electric Vehicle Inductive Charging Systems – Part 1: General Requirements. 69/125/CD. IEC TC69 WG4, 2000.
36. IEC 61980-2/CD, Electric Vehicle Inductive Charging Systems – Part 2: Manual Connection System Using a Paddle. 69/126/CD. IEC TC69 WG4, 2000.



# Market Prospects of Electric Passenger Vehicles

Peter Mock, Stephan A. Schmid<sup>1</sup>, and Horst E. Friedrich

Institute of Vehicle Concepts, German Aerospace Center (DLR), Stuttgart, Germany

## Contents

1. Introduction	546
2. Technical Aspects	548
2.1 Batteries and fuel cells	548
2.2 Definition of vehicles	549
2.2.1 General definitions	549
2.2.2 Vehicle energy consumption	551
2.2.3 Vehicle production costs	554
3. Relevant Stakeholders and Outline of Calculation Model	554
3.1 Customers	555
3.2 Vehicle manufacturers	558
3.3 Politics	559
3.4 Prices for fuel and electricity	560
3.5 Verification of model results	560
4. Scenario Calculations	561
4.1 Scenario 1 – “baseline”	562
4.1.1 Assumptions of input parameters	562
4.1.2 Results: new vehicle fleet	563
4.1.3 Results: vehicle stock	566
4.2 Scenario 2 – “climate protection”	566
4.2.1 Results: new vehicle fleet	567
4.2.2 Results: vehicle stock	570
4.3 Sensitivities	570
4.3.1 Scenarios 1a and 2a – “soaring crude oil price”	571
4.3.2 Scenario 1b – “reduced efforts for climate protection and lower costs for emission after-treatment of diesel vehicles”	571
4.3.3 Scenario 2b: “optimistic development of battery technology”	573
4.4 Comparison of results	573
5. Conclusions and Future Opportunities	575
Nomenclature	576
References	577

<sup>1</sup> Corresponding author: stephan.schmid@dlr.de





## 1. INTRODUCTION

According to the United Nations Intergovernmental Panel on Climate Change (UN IPCC), “warming of the climate system is unequivocal” and “most of the observed increase in globally averaged temperatures since the mid-20th century is very likely due to the observed increase in anthropogenic greenhouse gas (GHG) concentrations” [1]. In order to limit the expected future increase of temperature to a maximum of 2°C above the preindustrial level and avoid irreversible effects, it is necessary to dramatically decrease GHG emissions from industrialized countries and furthermore to slowdown emissions from developing nations.

Transport constitutes a significant portion of carbon dioxide (CO<sub>2</sub>) and therefore GHG emissions (Fig. 21.1). For example, in the western part of the European Union (EU-15) approximately 24% of an overall 3.15 billion tons (Gt) of CO<sub>2</sub> emissions are assigned to transport activities. More than 90% of these emissions are from road transport, with cars and vans making up the largest proportion [2]. Emissions from pollutants are decoupling from a continuously increasing mileage for the most part due to the ongoing introduction of emission after treatment systems for vehicles (Fig. 21.2). In contrast, for CO<sub>2</sub> emissions there is no clear reversal of trend observable to date, making it necessary to find solutions for lowering emissions in the future.

Electric vehicles are one important pillar of strategies to reduce GHG emissions from transport in the long run. At the local level, they do not emit any pollutants and in combination with electricity from renewable energy sources they allow reaching an emission level close to zero even on a well-to-wheel (WTW) basis. Furthermore, they could provide a way to end dependence on liquid fuels based on crude oil and ensure a drastic reduction of noise emission level especially for inner cities.

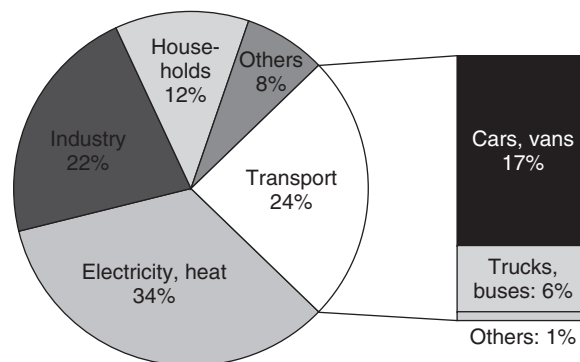


**Figure 21.1** CO<sub>2</sub> emissions in EU-15 in 2004 – total: 3.15 billion tons (Refs. [1,2]). Emissions from aviation are calculated according to the official Kyoto protocol calculation method, including only territorial emissions. Overall, civil aviation accounts for approximately 12% of CO<sub>2</sub> emissions from transport.

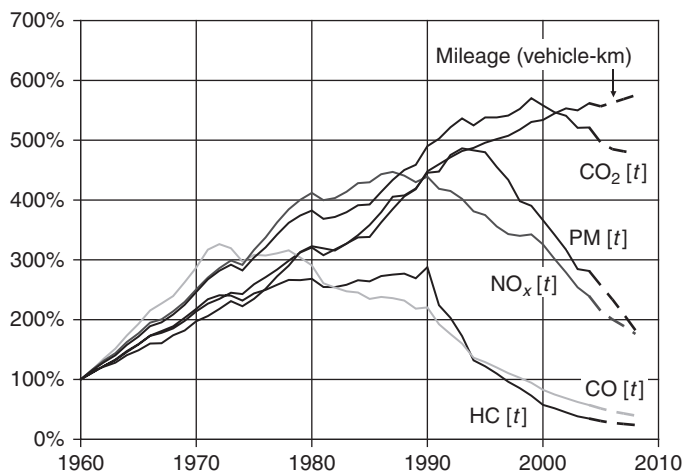


**Figure 21.2** Mileage and emissions from road transport in Germany 1960–2008 (Ref. [3]).

In view of these numerous advantages one could expect large quantities of electric vehicles driving on our roads today. And indeed, in 1900 approximately 40% of all new road vehicles sold in the United States were powered electrically. Another 40% relied on steam propulsion and only 20% were based on gasoline fuel [4]. However, by 1905 gasoline-powered vehicles already achieved a market share of 85% and today internal combustion engines (ICEs) entirely dominate the vehicle markets worldwide, as either gasoline or diesel vehicles.

As it can be seen from a historical analysis there have been periods of times with a larger number of electric vehicles brought to the roads and times with fewer numbers, but always at a very low level compared to the total number of vehicle registrations. Currently, the impression often transported to the public is that electric vehicles are advancing fast and that their further development is self-evident. But as we have seen from looking at past evolutions a reverse of this trend is not impossible and it is not certain that the current increased level of activity will again decrease in the future – a definite prognosis of future trends is not possible.

On the other hand, the assessment of well-based scenarios of market prospects for electric vehicles is urgently needed. Society and political decision makers need to know what contribution for a lasting reduction of GHG emissions may be expected from the introduction of electric vehicles into the market and what framework conditions are to be set in order to ensure a successful diffusion into the mass market. Manufacturers depend on planning reliability in order to justify investments in capital-intensive research activities and machinery investments for a new generation of vehicles.

Market prospects of electric vehicles are influenced by a variety of parameters and a solely intuitive assessment of future developments is not feasible. Computer models

incorporating at least some of the most important influencing parameters can help to develop coherent scenarios on future progress.

This chapter includes a brief analysis of technical aspects relevant for a future success of electric vehicles. Based on a description of relevant stakeholders and influencing factors in reality, the development of a new computer model called *VECTOR21* is outlined. The model is then applied for a detailed assessment of future scenario pathways not only for market shares of new vehicles and vehicle population but also with regard to CO<sub>2</sub> emissions and costs. Focus of the current examination is on the example of the vehicle market in Germany but the results are transferable to other vehicle markets in Europe and eventually worldwide.



## 2. TECHNICAL ASPECTS

### 2.1 Batteries and fuel cells

Key factor for the success of electric vehicles is the technical development of electric components and in particular batteries and fuel cells. The current status of research activities and technical parameters of battery and fuel cell systems for traction applications can be found in other chapters of this book. Here, we limit ourselves to stress the dependence of costs on the diffusion of alternative vehicles.

Production costs for high-energy lithium-ion batteries for vehicles are currently estimated at about \$1,000/kWh. Recent assessments of future costs, taking into account materials needed and their chemicals as well as physical properties, conclude that approximately \$200–300/kWh could be a realistic value for mass production volumes [5, 6]. Potential for cost reduction mainly comes from application of improved materials for electrodes and conducting salts, optimization of production processes, and higher quantities of raw materials and preproducts being ordered (economies of scale).

Summarizing publicly available recent cost estimates for lithium-ion batteries leads to the conclusion that future cost reduction would follow a learning curve with a rate of approximately 90% (Fig. 21.3). This means that manufacturing costs would be reduced by  $100 - 90 = 10\%$  for each doubling of the cumulative number of units produced.

For fuel cells, while decreasing platinum loading and increasing power density already have contributed to production cost reductions, for achieving a cost level acceptable for introducing fuel cell vehicles into the market further efforts are required. This also includes improvements of production processes and upscaling of production volumes. A bottom-up assessment of possibly achievable production costs for proton exchange membrane (PEM) fuel cell stacks at mass production levels has resulted in an estimated value of \$12–40/kWh for a cumulative number of 1 million fuel cell vehicles produced, compared to approximately \$1,000/kWh today (Fig. 21.4) [7].

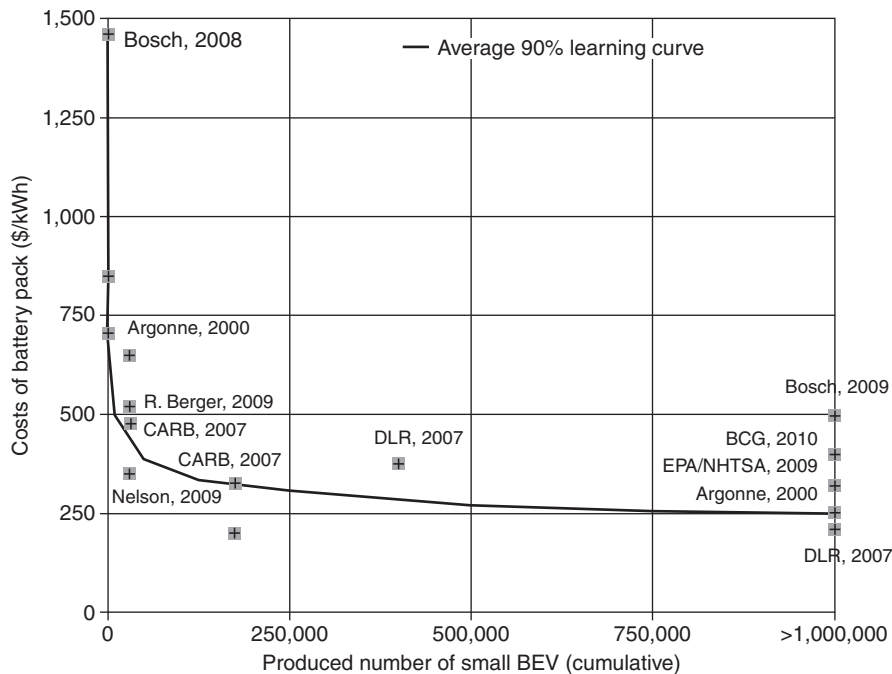


**Figure 21.3** Comparison of estimates of production costs for lithium-ion batteries with increasing production volumes. Source: reports published by manufacturers and research institutions.

## 2.2 Definition of vehicles

It is important to realize that electric vehicles compete with conventional vehicles dominating the market today. For the upcoming years, advancements of conventional ICE engines and vehicle technologies are to be expected and future market prospects of electric vehicles always have to be looked at in view of this general evolution of competing technologies. For example, hybrid vehicles with a small battery and electric motor may be seen as a step toward fully electrified vehicles but at the same time may also be considered as a potential competitor for them.

Furthermore, even within the broad category of electric vehicles, there are numerous concepts available in principle and most of them are competing with each other: depending on the daily needs of customers, a plug-in hybrid vehicle (PHEV) or extended range electric vehicle (EREV) may be sufficient whereas for others a full battery electric vehicle (BEV) or fuel cell hybrid electric vehicle (FCHEV) might be a better choice.

### 2.2.1 General definitions

In order to limit calculation times necessary in the *VECTOR21* model, it is essential to select only a restricted number of exemplary vehicle technologies for the assessment. The

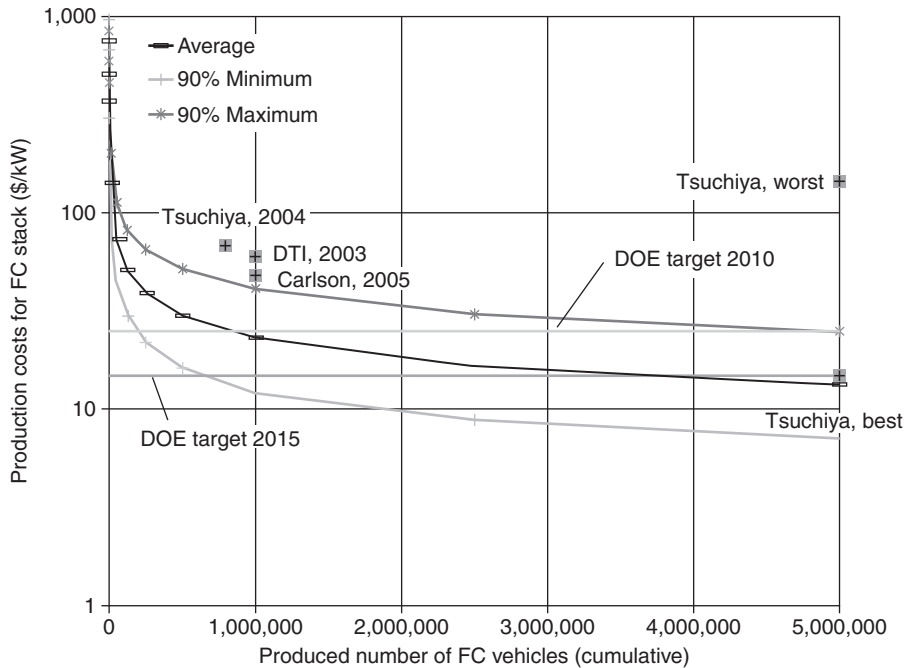


**Figure 21.4** Production cost estimate for fuel cell stacks. Cost estimate is for a platinum market price of \$20,000/kg (Ref. [7]).

following combinations of types of vehicle propulsion and energy storage are currently covered by the underlying database:

- gasoline and gasoline hybrid electric vehicles (HEVs)
- diesel and diesel HEVs
- compressed natural gas (CNG) and CNG HEVs
- EREVs
- BEVs
- FCHEVs

In particular for HEV and EREV, there exist actually a number of different variants, each with an individual range of electric driving depending on the battery capacity of the vehicle. Due to the need of simplification for the following assessment, only one variant as described further below had to be chosen.

Table 21.1 gives details on technical properties of the vehicles assessed in the model. Currently there are three vehicle size categories included in the database: small, medium, and large passenger cars. More detailed differentiations of types of passenger vehicles as well as extensions to include other types of vehicles will be part of a future work.

For the assessment it is assumed that BEVs are suitable for small and medium size passenger vehicles only, with respect to their limited range of driving, high battery weight, and costs. For EREVs, it is assumed that they will be offered for the medium and

**Table 21.1** Technical properties of the vehicles evaluated

	G	D	CNG	G-HEV	D-HEV	CNG-HEV	EREV	BEV	FCHEV
<b>Small size passenger car</b>									
Power: ICE (kW)	51	51	51	51	51	51	n.a.	n.a.	n.a.
Power: electric motor (kW)	n.a.	n.a.	n.a.	30	30	30	n.a.	55	55
Capacity: battery (kWh)	n.a.	n.a.	n.a.	1	1	1	n.a.	16	1
Driving range (CADC): fuel (km)	>700	>700	>300	>700	>700	>300	n.a.	n.a.	400
Driving range (CADC): battery (km)	n.a.	n.a.	n.a.	<5	<5	<5	n.a.	80	<5
<b>Medium size passenger car</b>									
Power: ICE (kW)	77	77	77	77	77	77	40	n.a.	n.a.
Power: electric motor (kW)	n.a.	n.a.	n.a.	40	40	40	80	80	80
Capacity: battery (kWh)	n.a.	n.a.	n.a.	2	2	2	13	36	2
Driving range (CADC): fuel (km)	>700	>700	>300	>700	>700	>300	>500	n.a.	400
Driving range (CADC): battery (km)	n.a.	n.a.	n.a.	<5	<5	<5	50	120	<5
<b>Large size passenger car</b>									
Power: ICE (kW)	140	140	140	140	140	140	55	n.a.	n.a.
Power: electric motor (kW)	n.a.	n.a.	n.a.	80	80	80	125	n.a.	125
Capacity: battery (kWh)	n.a.	n.a.	n.a.	3	3	3	18	n.a.	3
Driving range (CADC): fuel (km)	>700	>700	>300	>700	>700	>300	>500	n.a.	400
Driving range (CADC): battery (km)	n.a.	n.a.	n.a.	<5	<5	<5	50	n.a.	<5

BEV, battery electric vehicle; CADC, Common Artemis driving cycle; CNG, compressed natural gas; D, diesel; EREV, extended range electric vehicle; FCHEV, fuel cell hybrid electric vehicle; G, gasoline; HEV, hybrid electric vehicle; ICE, internal combustion engine.

large size categories only. Furthermore, it is expected that EREVs would be driven on average 60% powered by electricity and 40% powered by gasoline fuel.

### 2.2.2 Vehicle energy consumption

For each type of vehicle and size category, specific energy consumption of a baseline variant is estimated, using data from in-house simulations and from literature [8, 9]. As real-world driving conditions are reflected by simulations based on the Common Artemis driving cycle (CADC), consumption generally tends to be higher than in the New European driving cycle (NEDC).

In addition to the baseline energy consumption, a number of potential technical measures for reducing specific energy consumption are identified. These include, for example, direct injection for gasoline vehicles, downsizing and turbo charging, variable valve control, and reduction of vehicle curb weight. For each individual measure the effect on specific energy consumption of the baseline vehicle is estimated using detailed data from various literature sources (e.g., [10, 11]).

Individual potentials for reduction of specific energy consumption may not be added up because of overlapping effects [11]. Hence, for each type of vehicle and size category, several fuel economy packages are defined. These packages combine a set of suitable individual technical measures and indicate an overall influence on specific energy consumption of the baseline vehicle.

Table 21.2 shows details on the effectiveness and costs of analyzed fuel economy packages for medium size passenger cars. For a baseline configuration of a gasoline car,

**Table 21.2** Effectiveness and production costs of assumed fuel technology packages compared to the baseline vehicle (e.g., medium size passenger cars)

	Baseline	FE#01	FE#02	FE#03	FE#04	FE#05
G	0.74 kWh/km, €9,400	-8.0%, +€300	-17.0%, +€870	-24.0%, +€1,490	-34.0%, +€2,645	-40.0%, +€3,615
D	0.57 kWh/km, €11,000	-9.0%, +€300	-11.0%, +€620	-17.0%, +€1,220	-23.0%, +€1,870	-27.0%, +€2,415
CNG	0.74 kWh/km, €11,350	-11.0%, +€400	-24.0%, +€1,320	-30.0%, +€2,270	-37.0%, +€3,015	n.a.
G-HEV	0.60 kWh/km, €14,500	-4.0%, +€100	-14.0%, +€570	-20.0%, +€1,190	-28.0%, +€1,945	-35.0%, +€2,915
D-HEV	0.48 kWh/km, €16,100	-5.0%, +€100	-8.0%, +€420	-16.0%, +€1,170	-20.0%, +€1,715	n.a.
CNG-HEV	0.60 kWh/km, €16,450	-5.0%, +€220	-16.0%, +€870	-21.0%, +€1,320	-32.0%, +€2,315	n.a.
EREV	0.32 kWh/km, €22,600	-4.0%, +€220	-11.0%, +€970	-21.0%, +€1,765	n.a.	n.a.
BEV	0.18 kWh/km, €32,425	-5.0%, +€405	-8.0%, +€825	n.a.	n.a.	n.a.
FCHEV	0.43 kWh/km, €108,940	-5.0%, +€405	-8.0%, +€825	n.a.	n.a.	n.a.

All costs are initial costs for 2009, excluding costs for Euro 6 compliance and learning curve effects. Assumption for EREV energy consumption: 60% electric driving, 40% ICE driving. BEV, battery electric vehicle; CNG, compressed natural gas; D, diesel; EREV, extended range electric vehicle; FCHEV, fuel cell hybrid electric vehicle; FE, fuel economy package number; G, gasoline; HEV, hybrid electric vehicle; n.a, not applicable.

a reduction of specific energy consumption by 40% appears feasible applying technical measures known today. For diesel vehicles, the reduction potential is assessed to be less, given the fact that some technical measures (e.g., direct injection) are assumed already to be applied in the baseline configuration today. In the future, a convergence of specific energy consumption for gasoline and diesel cars is expected.

Energy consumption of CNG vehicles is similar to that of gasoline vehicles but with a higher potential for reduction if optimization of the combustion process with regard to the specific fuel properties of CNG is carried out. For FCHEVs and especially for BEVs, specific energy consumption is significantly lower than for ICE vehicles, given their higher degree of efficiency of energy conversion.

In *VECTOR21* all fuel economy packages are treated as optional add-ons for a baseline vehicle. Consequently, the model automatically generates a range of vehicle variants in addition to the baseline configurations previously defined, each equipped with a different fuel economy package, representing the supply side of a virtual new vehicle market. Fig. 21.5 visualizes the specific energy consumption of the resulting vehicle variants, with energy consumption of the baseline vehicle on the right side of the resulting bands and minimum specific consumption of the technically most advanced vehicle variant on the left side. For example, for gasoline vehicles a range of vehicle variants with specific energy consumption between 0.74 and 0.44 kWh/km is

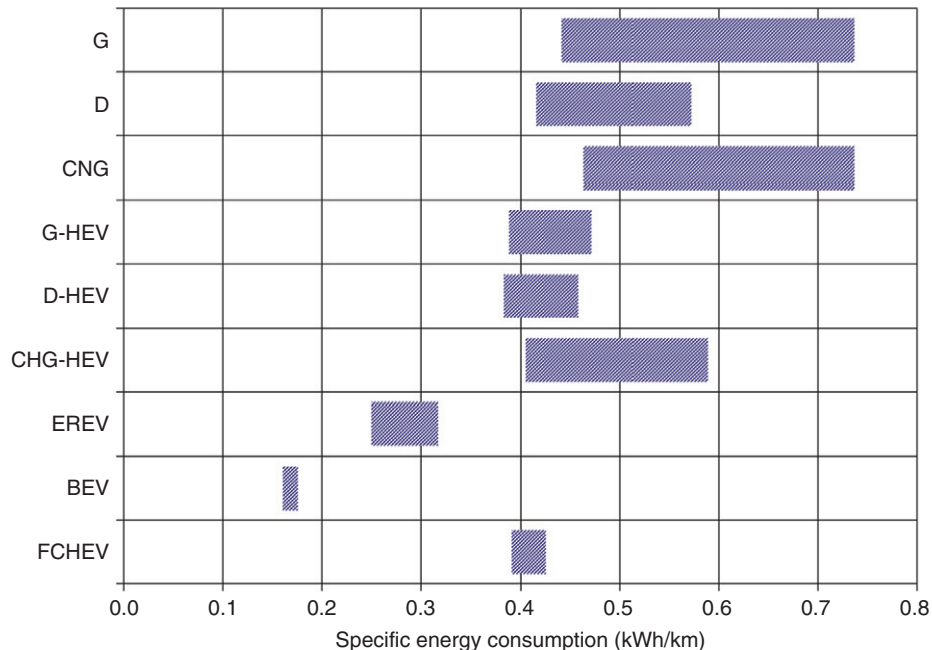


**Figure 21.5** Visualization of the range of specific energy consumption for types of vehicles assessed (for a medium size passenger car).



available whereas for diesel vehicles the range is narrower, ranging from 0.57 to 0.42 kWh/km due to a lower potential for reductions of the level of specific energy consumption.

### 2.2.3 Vehicle production costs

Manufacturing costs for baseline gasoline, diesel, and CNG vehicles are estimated based on sales prices of currently available passenger car variants. In order to derive overall production costs for other types of vehicles, individual costs for nonnecessary technical parts are deducted and costs for supplementary necessary parts, according to literature data (e.g., [8, 10]), are added. For example, for HEV vehicles, costs for a standard ICE alternator and starter are credited, while costs for a battery, an electric motor and several other system components are added.

Furthermore, for each technical measure to reduce energy consumption previously identified, production costs are assessed based on various literature and manufacturer data. Individual measures are combined and costs are summarized to reflect the composition of fuel economy packages previously defined.

From Table 21.2, it becomes obvious that ambitious fuel economy packages come at high investment costs, for example, more than €3,600 for package #05 for a gasoline vehicle with a potential of reducing specific energy consumption by 40%. For diesel vehicles, costs tend to be lower but at the same time initial costs of a baseline diesel vehicle are higher than for a baseline gasoline vehicle and energy reduction potentials associated are lower. Therefore, a convergence of gasoline and diesel vehicles, not only with regard to their specific energy consumption but also with regard to their costs, is expected for the future.

Costs given in Table 21.2 all are initial production costs for the vehicles assessed, without any learning curve effects. For example, costs given for HEVs include initial costs for a lithium-ion battery, electric motor, and electric components, all with significant potential for cost reduction as production volume increases over time. Similarly, costs for FCHEVs are initially prohibitively high but will decrease as the technology diffuses into the vehicle market at high volumes. Fig. 21.6 illustrates initial production costs for all types of vehicles considered, including different variants with fuel economy packages applied.



## 3. RELEVANT STAKEHOLDERS AND OUTLINE OF CALCULATION MODEL

Following the consideration of technical aspects, key stakeholders involved (customers, vehicle manufacturers, and politics) as well as their possible behavior have to be evaluated in the next step. Based on the results, an appropriate structure and algorithm for the *VECTOR21* calculation model is outlined – anticipating reality as much as

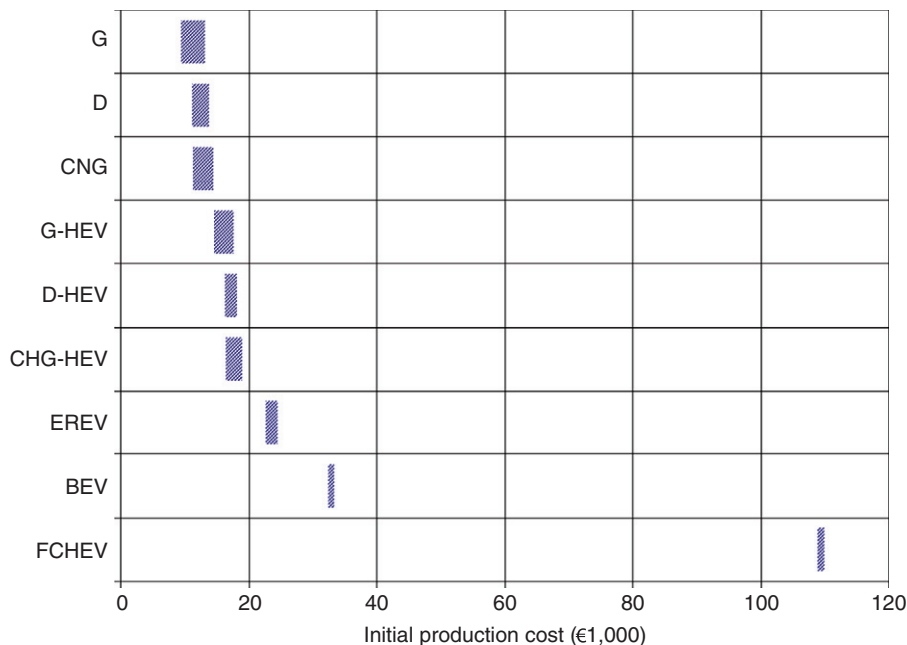


**Figure 21.6** Range of initial production costs, reflecting different variants of vehicle types assessed in the *VECTOR21* model (medium size passenger car).

possible but at the same time simplifying where necessary in order to ensure reasonable calculation times. Finally, practicability and plausibility of the model developed are tested by application to a historic case study.

### 3.1 Customers

Research indicates that vehicle purchase decision involves a high cognitive effort. Vehicle size, safety, and price are ranking at top priority of the most important criteria for customers. Environmental issues are often also considered important, however, at almost no willingness-to-pay an additional price. For electric vehicles, many customers today state that they would be willing to buy them, especially with respect to their image of clean, quite, and innovative vehicles.

However, in particular for BEVs these statements have to be taken with a grain of salt. Today's general expectation of most customers is to have an all-purpose car to be used for short-distance trips as well as longer trips, for example for annual vacation. But BEVs are not suitable for meeting these expectations as this would require enormous amounts of battery capacity to be built into vehicles at very high costs.

On the other hand, analysis shows that daily driving range of a majority of customers is as low as ~40 km in Europe and 60 km in the United States. Therefore, vehicles with a

maximum driving range of 100 km would be sufficient for most customers for daily commuting, even when considering challenging climate conditions with application of heating or air conditioning systems requiring additional energy. This is especially true when taking into account that many households own more than one car, therefore being able to choose a different car for longer trips on weekends or for vacations. This would allow limiting the daily amount of energy capacity needed by a vehicle and therefore the size and costs of the necessary battery for BEVs. Yet, it would imply a dramatic change in customer's expectations and the way we use our vehicles.

Less demanding with regard to a change in customer behavior are ideas that are based on a network of switch stations for batteries for backup purposes when regular charging is not an option. Another bridging function could be fulfilled by vehicle concepts combining a battery as a primary source of energy to the electric motor with an ICE or fuel cell as a range extender to provide additional energy and to charge the battery when going for longer trips.

For modeling customer purchase decision, a three-step approach is implemented in *VECTOR21*:

- Step 1: Reduce the number of available vehicle variants by choosing a size category and filtering for general compulsory requirements.
- Step 2: Within the remaining variants, choose the ones with lowest relevant cost of ownership (RCO).
- Step 3: Finally, choose the vehicle variant with lowest WTW CO<sub>2</sub> emissions.

Step 1 is based on the assumption that customers generally select an appropriate vehicle size category based on their everyday needs, as well as a vehicle variant which satisfies basic requirements, for example, regarding a certain minimum driving range as discussed above. Nevertheless, it is evident that this decision is often made on a nonrational basis, for example, when buying a vehicle excessively large due to prestige reasons or when demanding for an all-purpose vehicle with high maximum driving range. Therefore, for step 1, market shares of vehicle size categories, as well as general compulsory requirements to be satisfied by the vehicles considered, have to be pre-defined by the user and are not modeled implicitly.

Following the preselection step 1, customers are supposed to react rationally on the basis of RCO when choosing a vehicle variant within a certain size category. RCO in this analysis includes all relevant costs, such as vehicle purchase price, vehicle purchase tax or subsidy, annual ownership tax, and costs for fuel. It is therefore different from total cost of ownership (TCO) in a way that it neglects cost aspects that are considered being less relevant for purchase decision (e.g., insurance costs). RCO is calculated for a time period of 4 years to reflect the average time horizon for expected return of investment of customers purchasing new passenger cars. Depreciation of vehicles is not considered in the model as it is assumed that the rate of depreciation is identical for all types of vehicles. Eventually, new vehicle technologies are only to be offered if they are technically

mature enough compared to conventional vehicles. Hence, lifetime is assumed to be identical for all vehicles and therefore not a limitation in the model.

Depending on the type of customer examined, an additional willingness-to-pay for technically more advanced vehicles is found. In order to reflect this behavior adequately, five different types of adopters are defined in the *VECTOR21* model: a small group of *innovators*, a somewhat larger group of *early adopters*, two major groups *early majority* and *late majority*, as well as a group of *laggards* [12]. Willingness-to-pay, and more generally the degree of innovativeness, is highest for the group of *innovators* and gradually decreases toward the group of *laggards*. Each adopter group furthermore is differentiated into subgroups, with different annual mileages to reflect varying driving behaviors. Fig. 21.7 illustrates the distribution of annual mileages of passenger cars in Germany based on an analysis of data collected by vehicle dealers' workshops. It is obvious that average annual mileage of larger vehicles is higher than that of smaller vehicles and the distribution curve is more flat in shape. In total, currently there exist 900 different types of customers in the model.

In step 3, among the remaining vehicle variants with lowest RCO, the one with lowest WTW CO<sub>2</sub> emissions is selected in order to reflect customer's general awareness for environmental performance, but only within their individual price range. WTW examination includes all emissions for producing, distributing, and using the respective fuel. This implies that customers are to be informed about the WTW emissions of potential vehicle variants they might purchase. Today's focus, for example, of vehicle test reports in automobile magazines is on tank-to-wheel (TTW) emissions. Nevertheless, it

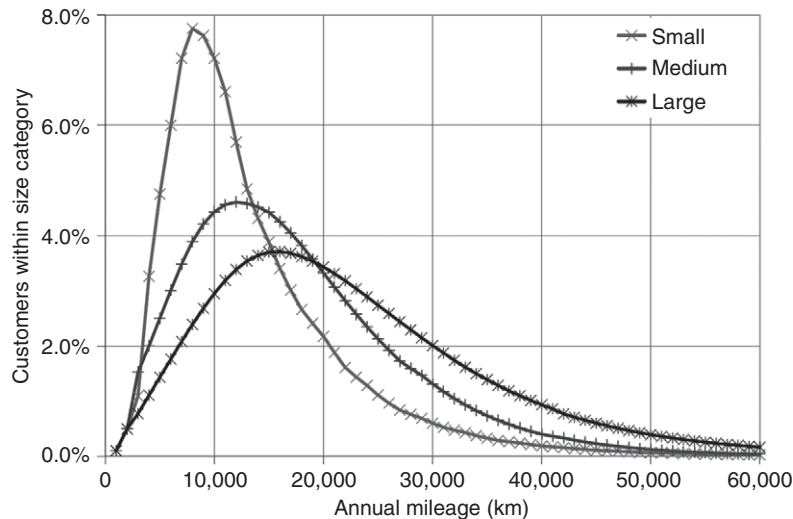


**Figure 21.7** Distribution of annual mileage of passenger cars in Germany.

is assumed that this is likely to change, as environmental awareness of the public will continue to grow in the future.

### 3.2 Vehicle manufacturers

Vehicle manufacturers ensure that there is a selection of different variants of vehicles available for customers to choose from. An important objective of their business strategy is maximization of profits. Changing the structure of vehicle supply and introducing new vehicle technologies may implicate risks for manufacturers. Investment in research and development (R&D) as well as new production facilities have to be made and a shift of revenues, for example, from mechanical engineering toward chemical engineering for batteries and fuel cells, may occur. Nevertheless, introduction of new technologies might get inevitable for political reasons or changes in customer demand. In order to minimize risks, vehicle manufacturers are likely to prefer an evolutionary shift of vehicle technologies rather than a revolutionary.

Introducing innovative technologies sometimes requires accepting lower or even negative profit margins for manufacturers for a limited period of time. High initial investments in R&D as well as production facilities cannot be passed on to customers in full as otherwise the price of the new technology would be too high for a significant number of customers deciding to purchase it. After some time has passed, increasing production volumes and associated learning curve effects result in lower production costs. This situation finally allows increasing profit margins while maintaining reasonable prices for customers. An example for such an approach is the *Toyota Prius* hybrid car, which supposedly did not contribute to the company's earnings until the launch of the third generation of the vehicle.

In *VECTOR21* a broad range of vehicle variants with individual energy consumption and retail price is offered to customers in each year of the analysis, by combining baseline vehicles with the previously identified fuel economy packages. For innovative vehicle technologies with a learning curve rate used to describe future development of production costs, the cumulative number of units sold in previous years is used by the model to derive manufacturing costs for the current year.

For the conversion of manufacturing costs (including manufacturer overhead) into retail prices (excluding tax), an average factor of 1.35 is applied, as discussed in literature [10]. This markup includes profit of the vehicle manufacturer as well as costs and profit of dealership. Note that – in reality – it is likely that the conversion factor will vary for different technologies, depending on their technical complexity and the timeframe considered [11]. Furthermore, value-added tax (VAT) is added on top, resulting in an overall conversion factor of 1.6 for the German market.

In the beginning of production of a new technology, it is necessary for the manufacturer to subsidize these vehicle variants by partly forgoing markups, whereas, with increasing units produced, manufacturer subsidies are automatically reduced by the

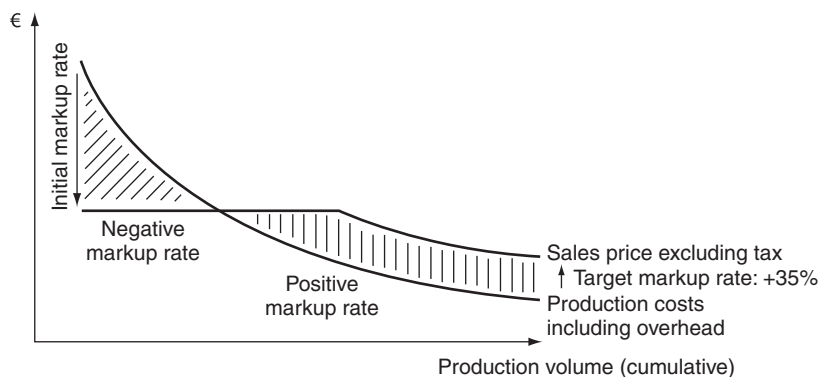


**Figure 21.8** Schematic illustration of pricing for new technologies in *VECTOR21*.

model. This means that markup rates increase toward the previously defined value of 1.35 (Fig. 21.8).

### 3.3 Politics

National as well as local regulations may significantly influence market prospects of vehicle technologies and fuels. Financial subsidies for specific technologies as well as penalties for others directly intervene with market development. Also changes of the taxation structure, for example, by introducing a CO<sub>2</sub> component into annual circulation tax for cars, might have a significant impact on customer purchase decisions. Manufacturer's actions can be affected by imposing legislative regulations, for example, by introducing emission levels for new vehicles, or by introducing financial instruments, for example, when funding private research initiatives.

Politics therefore has a significant impact on both the supply and the demand side in *VECTOR21*. There exist several options in the model to intervene with market action. For example, it is possible to pay one-time subsidies for the purchase of certain vehicle variants, raise annual ownership taxes, raise fuel taxes, raise VAT, dictate the use of certain technological measures (e.g., technologies for complying with Euro 6 standard), and raise penalties for exceeding a CO<sub>2</sub> target value.

Imposing incentives and regulations may also help to ensure the development of a new infrastructure, for example, for battery charging devices or hydrogen fueling stations, and therefore overcoming the chicken or the egg dilemma when not having enough vehicles to justify a new infrastructure and vice versa.

For vehicle technologies which require installation of a novel infrastructure for refueling and maintenance services, the investment and time necessary in *VECTOR21* is reflected by restricting the technology to more innovative and therefore less demanding customer types at first and slowly opening it to other groups of customers in later years of a simulation run.

### 3.4 Prices for fuel and electricity

Prices for conventional fuels, electricity, and hydrogen have a significant influence on RCO and therefore customer purchase behavior. For modeling the supply side for fuel and electricity, sales prices are either predefined by the user or calculated internally according to crude oil price development and applying historical correlation factors.

A linear relationship between crude oil price and price for gasoline fuel (excluding taxes) has been found valid for the past (Fig. 21.9). It is assumed that a similar correlation will continue to be valid in the future. Therefore, it is possible to calculate fuel prices based on crude oil price development. Sales prices for electricity and hydrogen have to be predefined by the user.

For all energy parameters, it is possible to differentiate numerous pathways for fuels and electricity, each having a different prechain well-to-tank (WTT) CO<sub>2</sub> emission and price.

### 3.5 Verification of model results

The functionality and plausibility of the *VECTOR21* model is verified using a historical case study, that is, the increasing proportion of diesel passenger cars in Germany between 1995 and 2008. All relevant input data, for example, fuel prices, vehicle prices, and taxation, are aligned to historical data and model calculation is carried out. Fig. 21.10

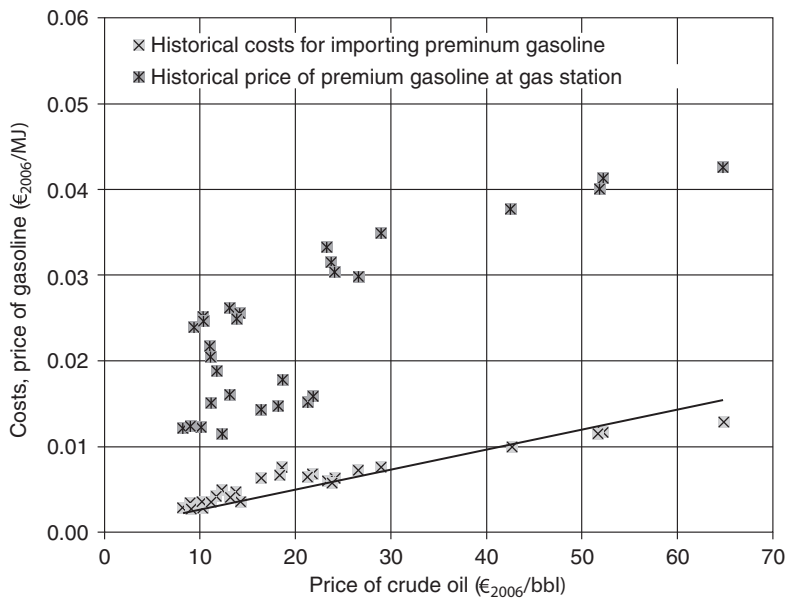


**Figure 21.9** Historic correlation of crude oil price and fuel net costs (straight line) as well as fuel prices in Germany for the years 1980–2008. Source: MWV, BP.

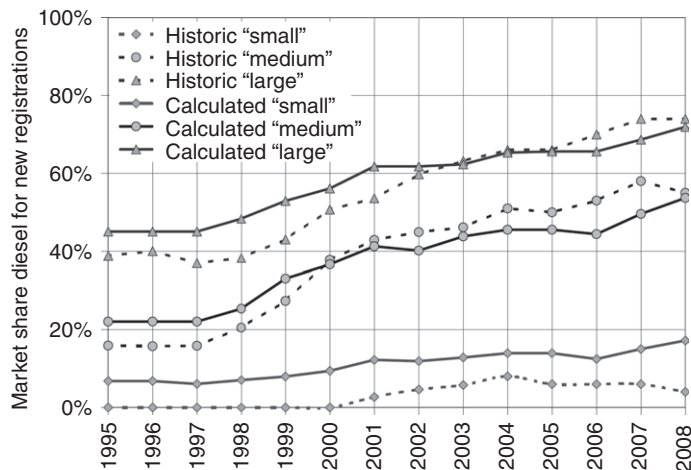


**Figure 21.10** Historical development of diesel market share for new passenger car registrations in Germany: reality vs. model results. Source: VECTOR21 [3].

demonstrates the results: the development of the proportion of diesel passenger cars for three individual vehicle size categories.

For medium and large passenger vehicles, the calculated development is close to real historical developments. For small size vehicles, the calculated market share of diesel is higher than historical values. This is due to the unavailability of a broad selection of small diesel passenger vehicles during the 1990s. Furthermore, there are investment budget restrictions for many small vehicle size customers preventing them from buying diesel vehicles, with initially higher investment costs than for gasoline cars. Overall, the calculated evolution for average diesel passenger cars share corresponds very well to historical values.



#### 4. SCENARIO CALCULATIONS

In the following section, the *VECTOR21* model is applied to analyze future market prospects of electric vehicles. Calculations are carried out for two major scenarios and four additional sensitivity checks, each with a different set of framework conditions defined.

It is important to realize that none of the scenarios presented may be seen as a forecast of future market developments. Rather, the purpose of the calculations is to evaluate the influence of determining factors and the effects of possible outcome.

The focus of the current analysis lies on the passenger car market in Germany up to 2030. Nevertheless, framework conditions and results are seen as exemplary for a number of European vehicle markets, and an extension of the analysis to additional regions worldwide is planned.



## 4.1 Scenario 1 – “baseline”

Considered a baseline for the following simulations, [scenario 1](#) is calculated assuming conservative input parameters reflecting relatively minor changes of political and social framework conditions.

### 4.1.1 Assumptions of input parameters

The price of crude oil is assumed to decrease from €54/bbl<sup>1</sup> in 2009 to €50/bbl in 2020 and then increase to €65/bbl in 2030, based on a prognosis on behalf of the German government [13]. Compared to peaks of prices during 2007 and 2008, this development appears to be conservative. Prices for gasoline increase from €1.27/l in 2009 to €1.39/l by 2030; for diesel fuel the increase is from €1.16/l to €1.25/l (all based on historical correlation factors for crude oil price). For biofuels a stepwise increase of the market share from approximately 3/9/0% for gasoline/diesel/CNG in 2009 to 15% for all fuel types in 2030 is assumed. It is important to note that CNG fuel is currently subsidized in Germany, as fuel tax is lower for CNG than it is for other fuels. By 2017, this partly tax exemption will phase-out, a development which is reflected in the scenario assumptions.

Electricity for transportation in [scenario 1](#) is assumed to be taken from the German electricity grid. Electricity mix in Germany is currently dominated (~50%) by coal as a primary energy source. The CO<sub>2</sub> intensity was 600 g/kWh in 2009 and is expected to decrease to 550 g/kWh by 2030. The price for electricity today is approximately 18 c/kWh and is not expected to rise significantly in the context of the scenario assumptions. However, as an increasing share of electric vehicles would result in a decreasing amount of fuel tax revenue, it is assumed that starting in 2018 a fuel tax on electricity for transport will be applied in order to maintain tax revenues at a constant level. Price for electricity therefore increases to 35 c/kWh by 2030. For hydrogen, it is assumed that it will initially be produced from natural gas and later on from electricity. CO<sub>2</sub> emissions therefore increase from 400 g/kWh to 650 g/kWh by 2030 (for electrolysis of hydrogen, an efficiency loss of 20% is assumed).

For maximum CO<sub>2</sub> emissions of the new vehicle fleet in Germany, a value of 140 g/km is assumed for 2015. This corresponds to the target of the European Union (setting a limit of 130 g/km) as the vehicle fleet in Germany historically has approximately 8% higher CO<sub>2</sub> emissions than the European average. For [scenario 1](#), it is assumed that the long-term target of the European Union (105 g/km = ~113 g/km for the German market) will be hit with a 5-year delay by 2025. For exceeding the target values, a uniform penalty of €95/(g/km) is defined.

For BEVs and FCHEVs initial public subsidies of €3,000 per vehicle are assumed, while for EREVs the subsidy is €2,000. These subsidies are expected to decrease annually and to be phased out after 5 years.

<sup>1</sup> All prices in €<sub>2009</sub>.

**Table 21.3** Summary of relevant input parameters for **scenario 1** (“baseline”)

	2010	2015	2020	2025	2030
Crude oil price (€/bbl)	54	52	50	58	65
Share of biofuels (%)	0–8	4–11	8–13	11–14	15
<b>Electricity: source</b>		<b>National mix Germany</b>			
Electricity: CO <sub>2</sub> intensity (g/kWh)	600	610	620	590	550
Electricity: price (€/kWh)	0.18	0.18	0.35	0.35	0.35
<b>Hydrogen: source</b>		<b>Natural gas</b>		<b>Electricity</b>	
Hydrogen: CO <sub>2</sub> intensity (g/kWh)	350	350	740	700	650
Hydrogen: price (€/kWh)	0.16	0.16	0.35	0.35	0.35
CO <sub>2</sub> : target value new vehicle fleet (g/km)	n.a.	140	125	113	113
CO <sub>2</sub> : penalty for exceeding target value (€/g/km)	n.a.	95	95	95	95
Customers: willingness-to-pay (%)	0–10	0–10	0–10	0–10	0–10
Market share size categories (S/M/L) (%)	22/55/20	26/52/21	28/50/23	29/47/24	30/45/25

n.a., not applicable.

For customer behavior, a willingness-to-pay of 0–10% (0–5% for small size cars) is assumed. For example, customers of the type “innovators” are expected to be willing to pay up to 10% more in terms of RCO for a vehicle variant with lower WTW CO<sub>2</sub> emissions than other variants. “Laggards” are assumed to be unwilling to pay any premium price; values for other types of customers are interpolated. Furthermore, it is assumed that the market share of medium size passenger cars will generally decrease in favor of small and large size vehicles over time. [Table 21.3](#) summarizes the assumptions for relevant input parameters for [scenario 1](#).

#### 4.1.2 Results: new vehicle fleet

[Fig. 21.11](#) shows calculation results for [scenario 1](#) differentiated by vehicle size categories (small, medium, large) and in total.

The majority of today’s small cars in Germany are gasoline vehicles. In [scenario 1](#), their proportion remains nearly constant over time but with substitution of conventional gasoline cars (G) by G-HEVs, especially as CO<sub>2</sub> emission targets are introduced beginning in 2015. The market share of diesel vehicles (D) decreases with introduction of costly technical measures to comply with Euro 6. In the long run, small diesel passenger cars, even as hybrids, remain below a market share of 5%. CNG vehicles are successful during the years 2015–2017. This is due to introduction of CO<sub>2</sub> emission targets that add penalties to conventional gasoline and diesel vehicles but favor CNG vehicles because of their lower CO<sub>2</sub> emissions. However, as soon as the partly tax exemption

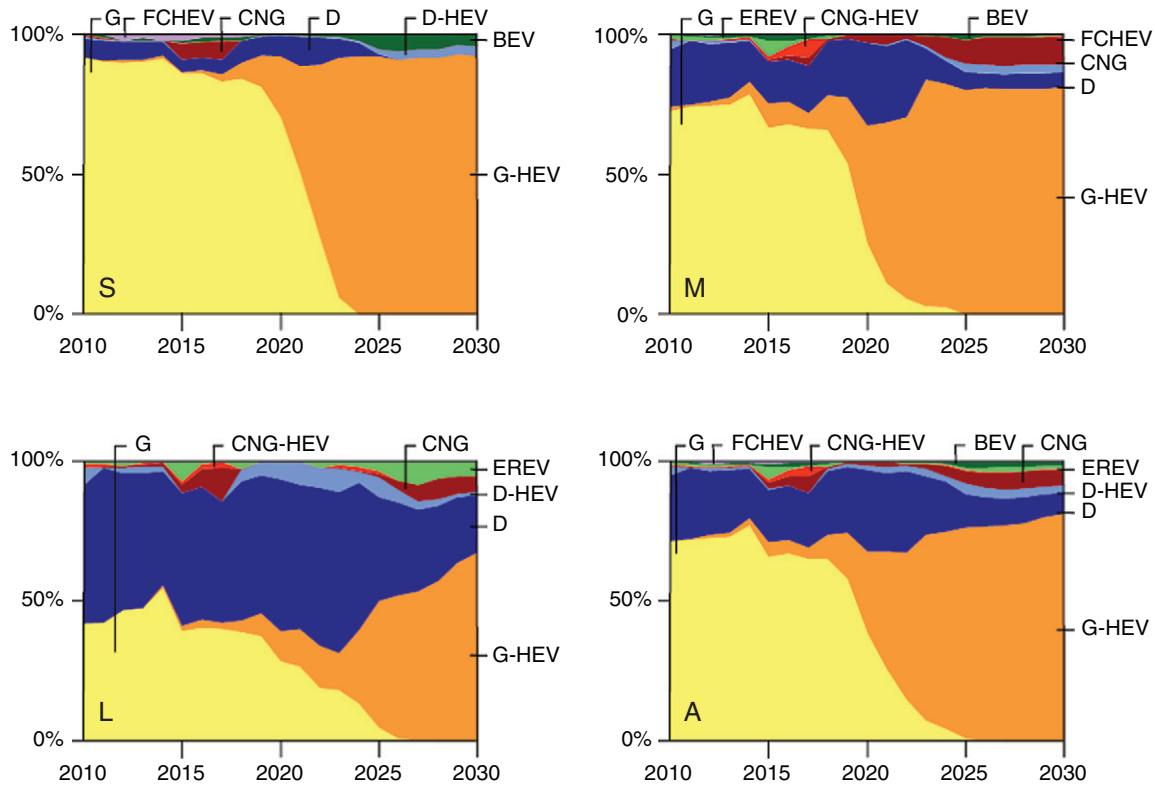


**Figure 21.11** Market shares of new passenger cars in **scenario 1** differentiated by vehicle size categories (S, small; M, medium; L, large) and in total (A, all) (see color plate 5).

for CNG fuel fades out in 2018, CNG vehicles become too expensive to retain a significant market share. FCHEVs for small passenger cars in [scenario 1](#) are to be seen for a short period only, as long as there are public subsidies being paid. From 2019 on, after the phasing out of public funding, FCHEVs are not able to remain in the market. BEVs are first introduced into the market for small cars in significant numbers in 2016. After the introduction of a tax on electricity for transport, they become more expensive compared to other vehicle variants and disappear from the market. By 2021 they diffuse into the market again in small numbers (5% market share) as WTT emissions of electricity decrease and learning curve effects help to decrease production costs and retail prices of BEVs.

The development for medium size passenger cars is similar to the one for small cars. Differences can be seen in the generally higher proportion of diesel vehicles and in a higher market share of CNG vehicles. This is due to higher annual mileages of customers in this segment facilitating shorter amortization periods for additional investments for vehicle variants with higher fuel economy. Electric vehicles are not able to claim significant market shares in [scenario 1](#). Reasons are as follows: relatively high TTW emissions of electricity and hydrogen as well as low costs for vehicles with low fuel economy, as there are only limited penalties to be paid with regard to less challenging emission target values.

For large passenger vehicles historically the market share of diesel vehicles is considerably higher than that for the other segments. Therefore, the reduction of diesel market share is more evident than that for small and medium vehicles. Main reasons are as follows: additional costs for diesel engines to comply with Euro 6 standards as well as a convergence of gasoline and diesel vehicles in terms of CO<sub>2</sub> emissions and costs for fuel economy measures. Large EREVs are able to sustain a market share of 5% by 2030. As CO<sub>2</sub> emissions of electricity production decrease and learning curve effects result in lower costs for batteries and electronic components, these vehicles become attractive for a relevant number of customers.

In total, the market shares in [scenario 1](#) in 2030 are 80% for G and G-HEVs, 10% for D and D-HEVs, and 7% for CNG vehicles. Electric vehicles are of almost no relevance for the results.

TTW CO<sub>2</sub> emissions of new vehicles in [scenario 1](#) decrease from 170 g/km to 114 g/km (−33%) and WTW CO<sub>2</sub> emissions decrease to 126 g/km (−35%).

Average total costs for customers in terms of RCO increase from €24,600 in 2010 to €27,100 in 2030 (+10%). Higher vehicle prices are due to a more widespread application of complex and costly vehicle technologies. At the same time, learning curve effects as well as decreasing costs for fuel due to improving fuel economy slow down the increase of RCO.

Public funding of EREVs, BEVs, and FCHEVs totals €550 million in [scenario 1](#). In comparison with a recent subsidy program of the German government for the purchase of new vehicles (€5 billion), the amount appears to be realistic.

Earnings of manufacturers (in terms of the markup factor applied to direct technology costs) initially decrease by 14% in [scenario 1](#) as new vehicles (EREVs, BEVs, FCHEVs) are

subsidized by the manufacturers themselves. It is not before 2017 that the increase of earnings again follows the increase of total revenue. In the long run, revenue and earnings increase by 25%. This is due to sales of more technologically advanced and more expensive vehicle variants as well as the assumption of a constant markup rate even at high sales volumes. In reality, it appears to be more realistic that manufacturers would transfer a portion of their additional earnings to limit the increase of sales prices for customers.

#### 4.1.3 Results: vehicle stock

The development of market shares for the entire vehicle stock follows the development for the new vehicle fleet with some delay (Fig. 21.12). In *scenario 1*, the proportion of gasoline cars increases from 70% to 80% by 2030, the proportion of diesel vehicles decreases from 30% to 15%, and CNG vehicles achieve a market share of 5%. The number of electric vehicles (BEVs, FCHEVs, and EREVs) rises to 850,000 in 2030, which is significantly lower than the target value of the German government (5 million vehicles by 2030).

TTW CO<sub>2</sub> emissions of the vehicle stock decrease from 100 million tons to 75 million tons and WTT emissions from 17 million tons to 6 million tons under the assumption that the total mileage driven remains constant at 600 billion km per year.

Implications for the amount of fuel needed for passenger cars in Germany (Fig. 21.13) include a significant reduction of diesel fuel from 520 PJ in 2009 to 240 PJ by 2030 (the total amount of diesel fuel consumed in Germany today is approximately 1,000 PJ per year). For CNG the amount of fuel needed in 2030 sums up to 45 PJ (2% of the total amount of natural gas consumed in Germany per year today). Electricity needed in *scenario 1* amounts to 8 PJ (one-third of the power of an average single nuclear reactor).

## 4.2 Scenario 2 – “climate protection”

Intention of *scenario 2* is to assess potential effects of increased activities in climate protection for the transportation sector. Particularly, use of electricity and hydrogen from renewable energy sources, increased application of biofuels, tightened CO<sub>2</sub> emission

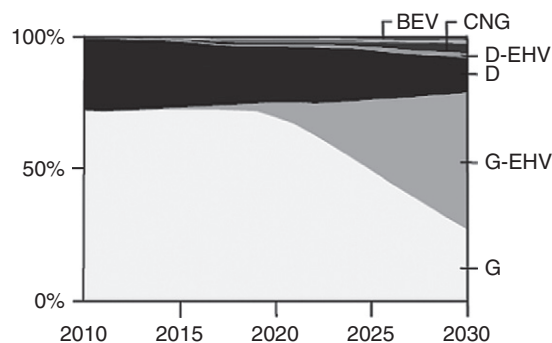


**Figure 21.12** Development of market shares of vehicle stock in *scenario 1*.

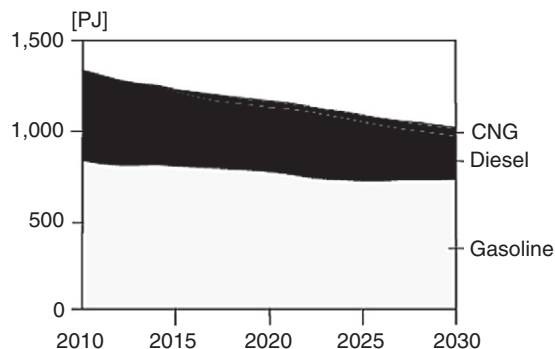


**Figure 21.13** Energy consumption of passenger cars in [scenario 1](#) differentiated by fuel.

**Table 21.4** Summary of input parameters for [scenario 2](#) (“climate protection”)

	2010	2015	2020	2025	2030
Crude oil price (€/bbl)	54	52	50	58	65
Share of biofuels (%)	0–8	<b>6–14</b>	<b>13–18</b>	<b>19–21</b>	<b>25</b>
<b>Electricity: source</b>					
Electricity: CO <sub>2</sub> intensity (g/kWh)	<b>20</b>	<b>20</b>	<b>20</b>	<b>20</b>	<b>20</b>
Electricity: price (€/kWh)	<b>0.21</b>	<b>0.21</b>	<b>0.37</b>	<b>0.37</b>	<b>0.37</b>
<b>Hydrogen: source</b>					
Hydrogen: CO <sub>2</sub> intensity (g/kWh)	<b>25</b>	<b>25</b>	<b>25</b>	<b>25</b>	<b>25</b>
hydrogen: price (€/kWh)	<b>0.21</b>	<b>0.21</b>	<b>0.38</b>	<b>0.38</b>	<b>0.38</b>
CO <sub>2</sub> : target value new vehicle fleet (g/km)	n.a.	140	<b>113</b>	<b>95</b>	<b>76</b>
CO <sub>2</sub> : penalty for exceeding target value (€/g/km)	n.a.	95	<b>105</b>	<b>113</b>	<b>120</b>
Customers: willingness-to-pay (%)	<b>0–20</b>	<b>0–20</b>	<b>0–20</b>	<b>0–20</b>	<b>0–20</b>
Market share size categories (S/M/L) (%)	22/55/20	26/52/21	28/50/23	29/47/24	30/45/25

Changes compared to [scenario 1](#) are printed in bold letters. n.a., not applicable.

standards for new passenger cars, and increasing awareness of customers for environmental issues are taken into account. At the same time, assumptions for future crude oil price developments are in line with [scenario 1](#) for focusing solely on the effects of political efforts. [Table 21.4](#) summarizes main input parameters for calculation of [scenario 2](#).

#### 4.2.1 Results: new vehicle fleet

[Fig. 21.14](#) shows the results of model runs for [scenario 2](#).

The most obvious difference between the results of [scenario 1](#) and [scenario 2](#) is a significantly higher proportion of electric vehicles in [scenario 2](#). For small passenger cars,

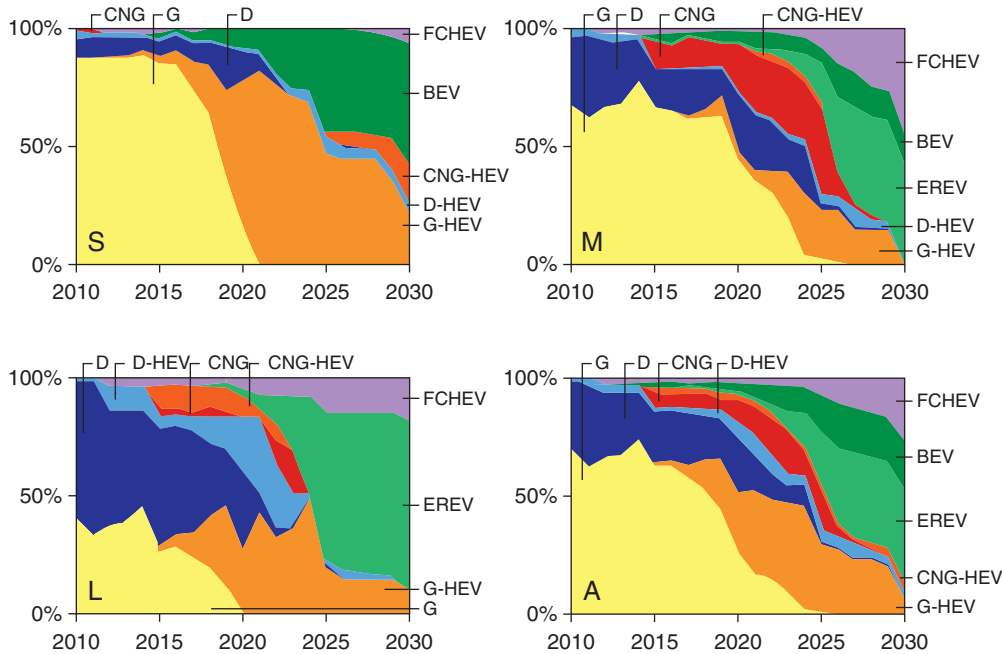


**Figure 21.14** Market shares of new passenger cars in [scenario 2](#) differentiated by vehicle size categories (S, small; M, medium, L, large) and in total (A, all) (see color plate 6).

BEVs achieve a market share of 50% by 2030. Additionally, FCHEVs are able to diffuse into the market to some extent even after phasing out of public funding. For medium size passenger cars, EREVs and FCHEVs dominate the market in 2030; BEVs are less important due to the higher average mileage of medium size passenger cars which make BEVs seem less suitable for them due to limited maximum driving range. For large size passenger cars, EREVs (80%) and FCHEVs (18%) are most important vehicle types in 2030.

The dramatic success of electric vehicles in [scenario 2](#) compared to [scenario 1](#) has several reasons:

1. Especially after 2020 stringent CO<sub>2</sub> emission standards and high penalties for exceeding the restrictions result in higher costs for the purchase of conventional types of vehicles with high CO<sub>2</sub> emissions. Therefore, electric vehicles, even if initial investment costs are high, are able to compete at least within some customer segments.
2. Electricity is solely based on renewable energy in [scenario 2](#). WTW CO<sub>2</sub> emissions of electric vehicles are close to zero and therefore significantly lower than in [scenario 1](#) and than for any conventional propulsion concept even if ambitious fuel economy packages are applied. As WTW CO<sub>2</sub> emissions are one aspect of the underlying customer purchase decision process, this results in a more likely choice of electric vehicles in [scenario 2](#) as long as they are competitive in terms of RCO.

3. It is assumed for [scenario 2](#) that customer's willingness-to-pay for vehicles with lower CO<sub>2</sub> emissions is higher than in [scenario 1](#). This assumption favors electric vehicles due to their low WTW CO<sub>2</sub> emissions in [scenario 2](#) and supports their market introduction especially in the beginning as purchase prices are still high.
4. As electric vehicles are being purchased and the cumulative sales volume increases, learning curve effects result in decreasing production costs and eventually decreasing purchase prices.

Especially during the time period 2015–2025, when CO<sub>2</sub> emission levels are introduced for the first time and tightened in the following years and when electric vehicles are still too expensive to be competitive, CNG vehicles diffuse into the market in significant numbers. For medium size passenger cars, the market share of CNG vehicles temporarily hits 20%. However, as electric vehicles become more attractive in terms of costs, CNG vehicles are pushed out of the market as their CO<sub>2</sub> emissions are still significantly higher than those of electric vehicles.

Investment costs for infrastructure are not implicit part of the model. Money and time necessary to build up a charging or fueling network are currently controlled by restricting these vehicle types to a small group of customers at first and then slowly expanding the number of customers allowed to purchase. In reality, sustaining a significant market share of BEVs and FCHEVs would cause substantial monetary burdens, therefore possibly slowing down introduction of those vehicles even more.

Due to the high market share of electric vehicles powered by electricity from renewable energy sources, CO<sub>2</sub> emissions of the new vehicle fleet decrease considerably in [scenario 2](#). TTW emissions fall from 165 g/km in 2009 to 30 g/km by 2030. WTT emissions decrease to close to zero, so that overall WTW emissions in 2030 are 30 g/km compared to 188 g/km in 2009.

Average retail price of cars (including any penalties for exceeding CO<sub>2</sub> target values) increases from €19,000 in 2009 to €25,000 by 2025 due to the more widespread application of fuel economy measures. It is not before 2025 that learning curve effects help to compensate additional costs imposed by tightening CO<sub>2</sub> emission standards so that the average retail price decreases again to €24,000. Average expenditures for fuel remain almost constant in [scenario 2](#) even as fuel prices increase, due to a constantly improving fuel economy of vehicles. In total, RCO increases from €25,000 in 2009 to €30,000 in 2030.

Public funding in [scenario 2](#) amounts to €1.5 billion in total, compared to €0.5 billion in [scenario 1](#). Main reason for the higher sum of subsidies paid is a lasting success of FCHEV in [scenario 2](#), even before phasing out of the assumed subsidy program. Although the order of magnitude of public funding in [scenario 2](#) is still comparable to recent national subsidy programs for the automotive industry, it appears to be realistic to assume that in reality subsidy programs for FCHEV would be ended sooner if it becomes obvious that the vehicles are able to remain on the market without any further support



by public funds. Therefore, the volume of €1.5 billion in *scenario 2* is likely higher than it would be in reality.

Manufacturer's earnings initially decrease by 35% in *scenario 2* as manufacturers accept low or even negative markup rates for getting new vehicle technologies into the market. In the long run, total revenue and also earnings increase by 50% due to sales of technically more advanced and more expensive vehicles. However, as it was true for *scenario 1*, it is likely that part of this increase in earnings would be passed on to customers in reality.

#### 4.2.2 Results: vehicle stock

The total number of BEVs in the vehicle stock in *scenario 2* (Fig. 21.15) amounts to 5 million vehicles by 2030, for FCHEVs it is 3 million vehicles, and for EREVs it is 6 million vehicles. This is considerably more than the target value of the German government of having 5 million electric vehicles in the market by 2030.

TTW CO<sub>2</sub> emissions are reduced from 100 million tons in 2010 to 50 million tons by 2030. Due to use of electricity from renewable energy sources, WTW emissions decrease from 117 million tons to 53 million tons.

Total energy consumption of passenger vehicles in Germany (Fig. 21.16) decreases from 1,300 PJ in 2010 to 800 PJ by 2030. The decrease of the amount of diesel fuel needed is from 530 PJ to 140 PJ. The amount of CNG needed is 100 PJ in 2030 (3% of all natural gas used in Germany today). The total amount of electricity needed for passenger vehicles is 80 PJ compared to production of 190 PJ electricity from renewable energy sources in Germany today. Hydrogen needed in *scenario 2* is 55 PJ (220 PJ of total production in Germany today).

### 4.3 Sensitivities

In order to test sensitivity of the previous calculations, additional scenarios are calculated applying the model.

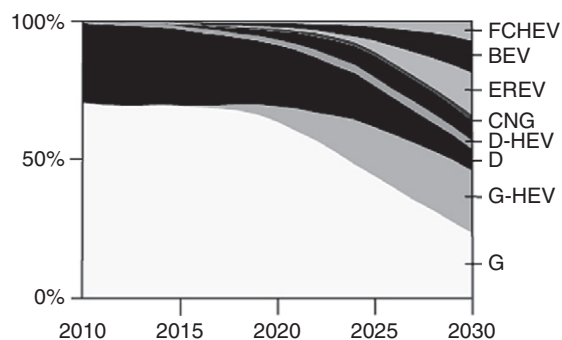


**Figure 21.15** Development of market shares of vehicle stock in *scenario 2*.

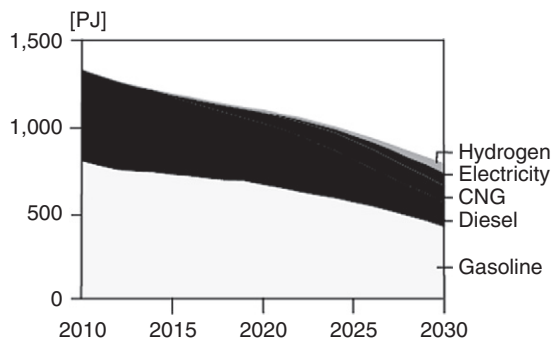


**Figure 21.16** Energy consumption of passenger cars in [scenario 2](#) differentiated by fuel.

#### 4.3.1 Scenarios 1a and 2a – “soaring crude oil price”

To assess the influence of an increasing crude oil price, the assumptions for [scenarios 1 and 2](#) are changed so that crude oil price increases from initially €54/bbl to €100/bbl in 2030 compared to previously €65/bbl. The level of €100/bbl corresponds to the market price assumed in the 2008 reference scenario of the International Energy Agency [14]. Price for gasoline and diesel fuel increases to €1.65/l and €1.56/l, respectively. Price for electricity has not been modified.

As shown in [Fig. 21.17](#), changing crude oil prices to a higher level does not influence the results of both scenarios significantly. Market shares of electric vehicles increase only slightly. Although CNG fuel prices correlate to crude oil prices to a lesser extent than prices for gasoline and diesel, the number of CNG vehicles decreases at the same rate as the number of electric vehicles increases due to an intensified competition of these concepts in [scenarios 1a and 2a](#).

The reason for the observed low influence of crude oil price is the relatively small proportion of expenditures for fuel (~20%) with regard to overall RCO. In comparison, costs for new vehicle technologies or penalties to be paid for exceeding CO<sub>2</sub> target values are significantly higher and therefore have a considerable influence on model results [15].

#### 4.3.2 Scenario 1b – “reduced efforts for climate protection and lower costs for emission after-treatment of diesel vehicles”

For [scenario 1b](#), it is assumed that following the introduction of a CO<sub>2</sub> target value of 130 g/km for the European average passenger car fleet in 2015 there would occur no further tightening of this standard. This assumption is deliberately inconsistent with the long-term target value already specified by the European Union in order to demonstrate the effects of reduced efforts for climate protection.

Additionally, for diesel vehicles it is assumed that costs for technical measures necessary for complying with Euro 5 and Euro 6 emission standards are lower than

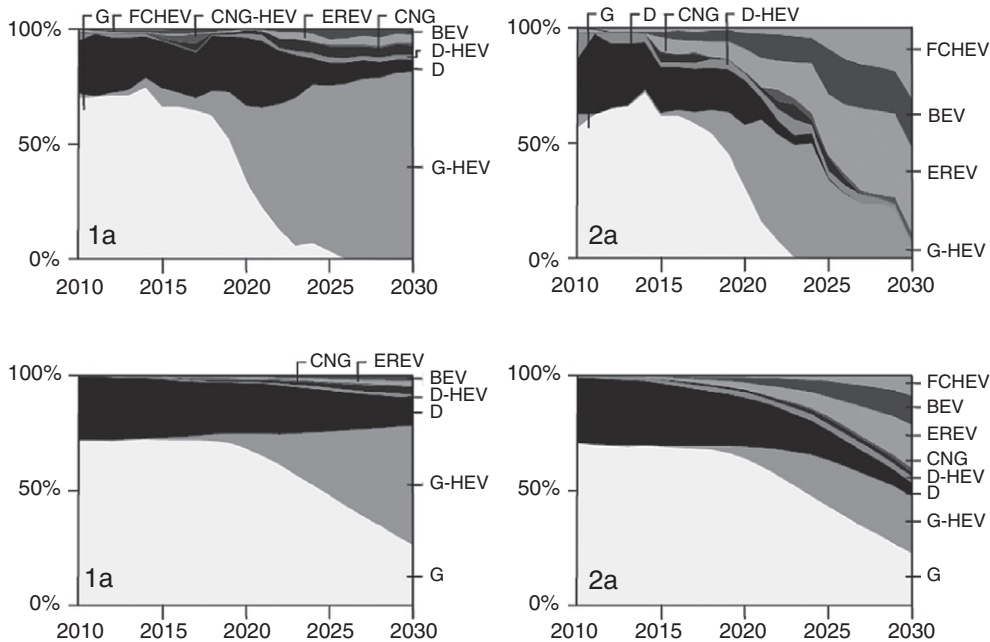


**Figure 21.17** Development of market shares for new passenger cars (top) and vehicle stock (bottom) for *scenarios 1a and 2a*.

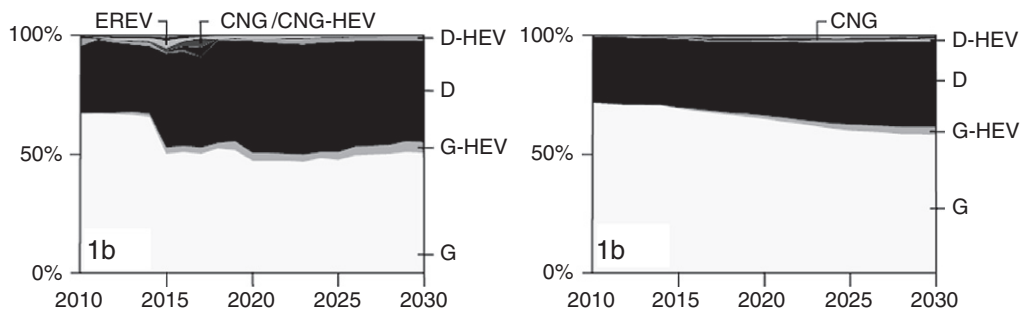


**Figure 21.18** Development of market shares for new passenger cars (left) and vehicle stock (right) for *scenario 1b*.

previously assumed in *scenario 1*. Production costs are set at €50 for Euro 5 and additionally €50 for complying with Euro 6, in contrast to €200 and €250 in *scenario 1*.

As shown in *Fig. 21.18*, the market development for *scenario 1b* is by far more conservative than for all previously assessed scenarios. Prices of diesel vehicles are lower and given the convergence of efficiency and costs of gasoline and diesel vehicles, even a relatively small change in purchase prices can lead to a competitive advantage for diesel vehicles as it is demonstrated in *scenario 1b*. When CO<sub>2</sub> emission standards are

introduced in 2015 for the first time, there is a change of 10% of customers switching from gasoline to diesel vehicles – customers who previously would have changed to technically more advanced gasoline vehicles. In general, the market distribution remains relatively constant at today's levels. Innovative propulsion concepts like HEVs and electric vehicles do not gain any significant market shares. This is due to missing incentives for purchasing low-CO<sub>2</sub> emission vehicles as CO<sub>2</sub> target values and penalties for exceeding are too low to change customer behavior.

#### 4.3.3 Scenario 2b: "optimistic development of battery technology"

For [scenario 2b](#), a more optimistic development of battery technology is assumed, resulting in a maximum utilizable capacity of 90% for Li-ion batteries compared to 75% assumed in the scenarios previously assessed. This implies that less excess capacity is needed to ensure availability of electric energy from the battery over the entire lifetime period of the vehicle. Therefore, average costs of batteries are lower in [scenario 2b](#) than in [scenario 2](#). Furthermore, a more optimistic development regarding the availability of charging stations and of the maximum driving range of BEVs is assumed, resulting in 75% of customers potentially being interested in BEVs by 2030 compared to 50% in previous scenarios.

As shown in [Fig. 21.19](#), optimistic assumptions for battery technology and infrastructure cause an increased diffusion of HEVs and BEVs. Introduction of HEVs occurs 1 year earlier than in [scenario 2](#). The market share of BEVs increases to 55% by 2030 compared to 20% in [scenario 2](#), as BEVs benefit the most from improved battery properties. On the other hand, market shares of CNG vehicles, EREVs, and FCHEVs are lower in [scenario 2b](#), given the fact that BEVs are now more attractive for many customers due to lower costs and improved comfort aspects.

## 4.4 Comparison of results

[Fig. 21.20](#) summarizes the results of all scenarios with regard to CO<sub>2</sub> emissions, RCO, public funding, and manufacturer earnings. It is obvious that [scenarios 2, 2a, and 2b](#)

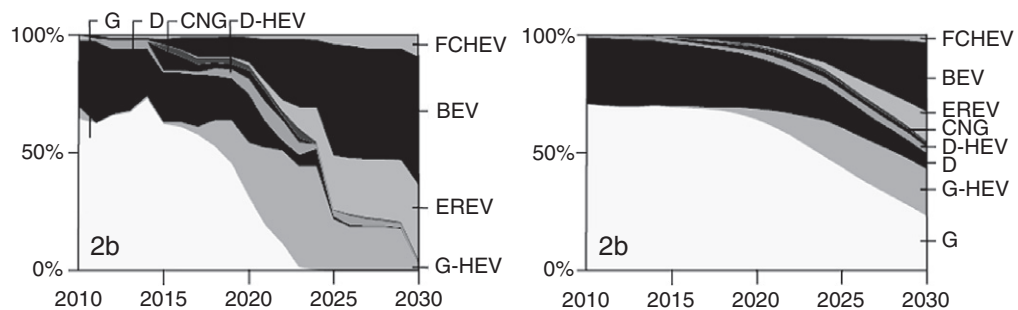


**Figure 21.19** Development of market shares for new passenger cars (left) and vehicle stock (right) for [scenario 2b](#).

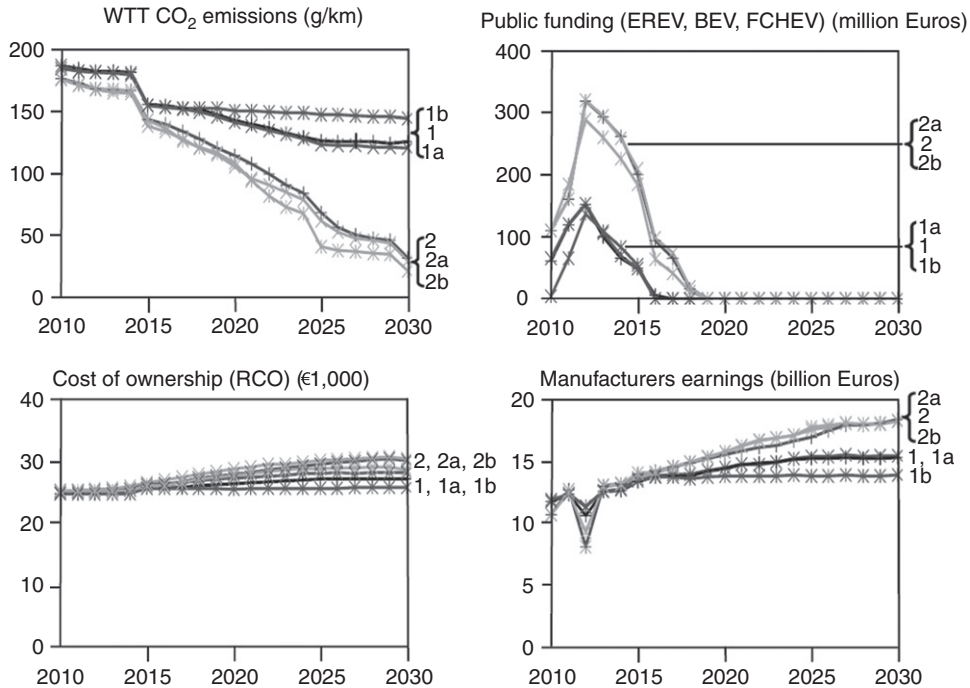


**Figure 21.20** Comparison of results for new passenger cars for all scenarios.

**Table 21.5** Additional costs to stakeholders and reductions of CO<sub>2</sub> emissions in comparison to scenario 1

	1a	1b	2	2a	2b
Additional costs to customers (billion Euros)	47	-40	101	137	75
Additional costs to government (billion Euros)	<0.1	-0.1	1.0	1.0	0.8
Additional costs to manufacturers (billion Euros)	-2	13	-23	-26	-28
WTW CO <sub>2</sub> emission reduction (million tons)	17	-42	230	276	285
Average costs for reduction of CO <sub>2</sub> (€/ton)	2,647	-643	343	406	168

result in significantly lower CO<sub>2</sub> emissions but at higher costs to customers and government while at the same time manufacturers have higher earnings.

Table 21.5 shows costs and benefits for all relevant stakeholders for all scenarios in comparison to baseline scenario. Efficiencies of the scenarios are assessed in terms of additional costs per reduced ton of CO<sub>2</sub>. Scenario 1a appears to be a non-cost-effective scenario at €2,647/ton: increasing fuel prices impose a burden for customers while at the same time only few vehicles with advanced technological measures are sold. Therefore, benefits in terms of CO<sub>2</sub> emissions reduced as well as manufacturer revenues are

counterbalanced. **Scenario 1b** has a negative efficiency rate, given the fact that more CO<sub>2</sub> is emitted than in baseline **scenario 1**. **Scenarios 2, 2a, and 2b** are between €168/ton and €406/ton, with **scenario 2b** being the most cost-effective due to cheaper battery technology and **scenario 2a** being the most expensive due to a higher crude oil price.



## 5. CONCLUSIONS AND FUTURE OPPORTUNITIES

The newly developed model *VECTOR21* allows taking into account a number of influencing parameters and to better quantify possible outcomes of future developments in the vehicle market. However, it is important to understand that the results shown are not predictions of the future. They have to be interpreted as scenarios examining different pathways and demonstrating the relevance of specific variables.

With respect to future market prospects of electric vehicles, the scenarios shown made clear that there exist several pathways with significantly different results. When taking into consideration competitive technologies, especially advanced ICE and hybrid vehicles, a fast diffusion of electric vehicles into the mass market is not to be taken for granted. In the baseline scenario – based on a set of plausible assumptions for framework conditions – only a slight proportion of EREVs and BEVs will be found on the market for new vehicles and also in the vehicle stock by 2030. Nevertheless – in another scenario with more challenging but not unrealistic conditions – electric vehicles will dominate the market in the long run.

Battery cost development as well as CO<sub>2</sub> target values and penalties have been identified as key influencing factors for the German market. An increasing price of crude oil was found to be less significant. This is in line with an earlier analysis of the effect of target values versus oil price [15] and likely to be similar for other European vehicle markets.

Given the range of possible outcomes and the relevance of specific influencing parameters, it is obvious that there is a need to set favorable framework conditions well in advance to ensuring sustainable transport for the future while allowing for security in planning processes. This requires primarily action from politics shaping responsible targets and incentives but also addresses manufacturers and their strategy for R&D investments and marketing as well as pricing of new vehicle technologies. Finally, a change of consumer's expectations regarding the performance of their vehicles could assist in accelerating the pace toward sustainable mobility.

Focusing on technical parameters for both batteries and fuel cells, remarkable breakthroughs have been achieved in the past. However, a number of issues are still to be solved in order to ensure performance and safety in the long run while significantly decreasing costs. Especially smaller hybrid vehicles that today make use of the NiMH technology could benefit from lithium-ion batteries with high power and energy density allowing to apply smaller and therefore cheaper battery packs [16].

Additional electricity demand from the transport sector is relatively low even for [scenario 2](#) with a high market share of electric vehicles (~4% of total electricity demand in Germany in 2030). However, in order to decrease CO<sub>2</sub> emissions on a WTW basis, it is necessary to ensure use of electricity from renewable energy sources as shown in [scenarios 2, 2a, and 2b](#).

A temporary increase of costs from a customer's perspective is anticipated for all scenarios. Eventually learning curve effects and a balancing of costs and benefits between customers and manufacturers could limit the increase of RCO, depending on the development of the price for crude oil and electricity.

When interpreting the results, it is important to keep in mind existing limitations of the model. Customer behavior with respect to the choice of vehicles based on individual driving cycles and possibly irrational expectations of the maximum driving range of vehicles may not be modeled in an entirely realistic way. Also, aspects of the creation of a new infrastructure, for example, for charging stations, as well as lead time for manufacturers to invest in new production facilities could only partially be considered. Finally, a life cycle analysis (LCA), including the production of battery packs and fuel cell stacks as well as an assessment of possible negative effects resulting from a dependence on raw materials like lithium, neodymium, and platinum would be desirable.

Hence, further research and a refinement of the *VECTOR21* model are intended. This will also include extending the number of vehicle technologies covered, allowing for additional hybrid vehicle concepts and commercial vehicles, as well as adapting it to other regional or geographic areas.

## NOMENCLATURE

BEV	Battery electric vehicle
CADC	Common Artemis driving cycle
CNG	Compressed natural gas
EREV	Extended range electric vehicle
FCHEV	Fuel cell hybrid electric vehicle
FE	Fuel economy package number
GHG	Greenhouse gas
Gt	Billion tons
HEV	Hybrid electric vehicle
ICE	Internal combustion engine
NEDC	New European driving cycle
PEM	Proton exchange membrane
PJ	10 <sup>15</sup> joule
PHEV	Plug-in hybrid electric vehicle
RCO	Relevant cost of ownership
R&D	Research and development
TCO	Total cost of ownership
TTW	Tank-to-wheel
WTT	Well-to-tank
WTW	Well-to-wheel

## REFERENCES

1. IPCC, Climate Change 2007: Synthesis Report. Summary for Policymakers. (Summary approved at IPCC Plenary XXVII, Valencia, Spain, November 2007.)
2. TREMOVE. Transport emission model TREMOVE version 2.7. Brussels, European Commission DG ENV, 2008.
3. TREMOD. Transport emission model TREMOD version 4.17. Dessau/Heidelberg, Umweltbundesamt (UBA)/Institut für Energie- und Umweltforschung (IFEU), 2006.
4. F.W. Geels, *Technol. Anal. Strateg. Manag.* 17 (2005) 445.
5. P. Mock, S.A. Schmid, *Techno-Economic Assessment of Fuel Cells and Batteries*, Encyclopedia of Electrochemical Power Sources, J. Garche (Ed.), Elsevier B.V., Amsterdam, The Netherlands, 2009.
6. P.A. Nelson, D.J. Santini, J. Barnes, EVS-24, Stavanger, Norway, May 2009.
7. P. Mock, S.A. Schmid, *J. Power Sources* 190 (2009) 133.
8. R. Edwards, J.-F. Larivé, V. Mahieu, P. Rouveïrolles, *Well-to-Wheels Analysis of Future Automotive Fuels and Powertrains in the European Context*, Tank-to-Wheels Report, Version 2c, CONCAWE/EUCAR/JRC, 2007.
9. A. Bandivadekar, K. Bodek, L. Cheah, C. Evans, T. Groode, J. Heywood, et al., *On the Road in 2035 – Reducing Transportation’s Petroleum Consumption and GHG Emissions*, Laboratory for Energy and the Environment, Massachusetts Institute of Technology, Cambridge, MA, 2008.
10. R. Smokers, R. Vermeulen, I. Skinner, M. Fergusson, G. Fontaras, Z. Samaras, *Review and Analysis of the Reduction Potential and Costs of Technological and Other Measures to Reduce CO<sub>2</sub> Emissions from Passenger Cars*, Final Report, C. n. SI2.408212, Delft, The Netherlands, 2006.
11. EPA/NHTSA, *Draft Joint Technical Support Document. Proposed Rulemaking to Establish Light-Duty Vehicle Greenhouse Gas Emission Standards and Corporate Average Fuel Economy Standards*, Washington, D.C., 2009.
12. E.M. Rogers, *Diffusion of Innovations*, fourth ed., Free Press, New York, 1995.
13. D. Lindenberger, M. Bartels, A. Seelinger, R. Wissen, P. Hofer, M. Schlesinger, *Auswirkungen höherer Ölpreise auf Energieangebot und -nachfrage – Ölpreisvariante der Energiewirtschaftlichen Referenzprognose 2030*. Köln, Basel, Energiewirtschaftliches Institut an der Universität zu Köln (ew)/Prognos AG, 2006.
14. International Energy Agency (IEA), *World Energy Outlook*, Paris, France, 2008.
15. S. Clerides, T. Zachariadis, *Are Standards Effective in Improving Automobile Fuel Economy? Discussion Paper 2006-06 – Department of Economics, University of Cyprus*, 2006.
16. *Lithium Ion Batteries Will Help Hybrids More Than Electric Cars*. Interview with John German, HybridCars, December 14, 2009.





# Automakers' Powertrain Options for Hybrid and Electric Vehicles

Fabio Orecchini and Adriano Santiangeli<sup>1</sup>

GRA (Automotive Research Group) and CIRPS (Interuniversity Research Centre for Sustainable Development), "La Sapienza" University of Rome, Piazza S. Pietro in Vincoli 10, 00184 Rome, Italy

## Contents

1. Introduction	580
1.1 Electrified powertrains	581
2. Hybrid Electric Vehicles	581
2.1 Micro hybrids	582
2.1.1 <i>BMW efficient dynamics</i>	583
2.1.2 <i>Volkswagen blue motion technologies</i>	583
2.1.3 <i>FIAT PUR-O2</i>	583
2.1.4 <i>Volvo DRIVE</i>	583
2.1.5 <i>SEAT ecomotive</i>	584
2.1.6 <i>Smart MHD</i>	584
2.1.7 <i>Toyota optimal drive</i>	584
2.2 Mild hybrids (Mild HEVs)	584
2.2.1 <i>Honda integrated motor assist</i>	584
2.2.2 <i>Mercedes S-Class (Mild hybrid)</i>	587
2.2.3 <i>BMW active hybrid (Mild hybrid)</i>	588
2.3 Full hybrids (Full HEVs)	590
2.3.1 <i>Toyota hybrid synergy drive and Lexus hybrid synergy drive</i>	590
2.3.2 <i>BMW active hybrid (Full hybrid)</i>	594
2.3.3 <i>Mercedes M-Class Hybrid</i>	596
2.3.4 <i>Audi Q7 Hybrid</i>	597
2.3.5 <i>Porsche Cayenne Hybrid</i>	597
2.3.6 <i>Volkswagen full hybrid</i>	598
2.3.7 <i>PSA Peugeot Citroën Hybrid</i>	599
2.4 Plug-in hybrids (PHEVs)	600
2.4.1 <i>Toyota Prius Plug-in</i>	601
2.4.2 <i>General motors E-Flex system</i>	602
2.4.3 <i>MP3 Hybrid</i>	605
3. Battery Electric Vehicles	606
3.1 Renault–Nissan alliance	607
3.1.1 <i>Renault Z.E.</i>	607
3.1.2 <i>Twizy Z.E. concept</i>	608

<sup>1</sup> Corresponding author: [Adriano.santiangeli@uniroma1.it](mailto:Adriano.santiangeli@uniroma1.it)

3.1.3	<i>Zoe Z.E. Concept</i>	609
3.1.4	<i>Kangoo Z.E. Concept</i>	609
3.1.5	<i>Fluence Z.E. Concept</i>	609
3.1.6	<i>Nissan Leaf</i>	610
3.2	Smart Fortwo Electric Drive	611
3.3	Mitsubishi i-MiEV	612
3.4	PSA Peugeot Citroën–Mitsubishi partnership	613
3.4.1	<i>Citroën C-Zero</i>	613
3.4.2	<i>Peugeot iOn</i>	613
3.5	PSA Peugeot Citroën–Venturi Automobiles agreement	613
3.6	Audi E-tron	616
3.7	Fiat 500 BEV	617
3.8	BMW Concept ActiveE – 1-Series Electric	617
3.9	MINI E	619
3.10	Ford Focus EV	620
3.11	Volvo C30 BEV	620
3.12	Ape Calessino 2009 Electric Lithium	621
3.13	Nissan – Land Glider	622
3.14	Rinspeed	622
4.	Fuel Cell Hydrogen Electric Vehicles	624
4.1	Honda FCX Clarity	624
4.2	Toyota FCHV-adv	626
4.3	Mercedes-Benz B-Class F-Cell	626
4.4	Nissan X-Trail	628
5.	Multi-Purpose Electrified Traction Platforms and Architectures, and Auto Innovation Design	629
5.1	Host	629
5.2	General motors' Voltec technology	633
6.	Conclusions	635



## 1. INTRODUCTION

The dark surrounding the world's automotive industry is about to be lit up by dazzling blinks, aiming at providing completely different cars for the next decade. The epoch-making change has been in the air for a long time, but it is the financial downturn started in 2008 that will bring in the inexorable and final verdict, and the next few years will tell us whether vehicles can really make it. The environmental issue alone did not turn out to be sufficient to lead car manufacturers and drivers beyond the era of polluting substances, nor was the oil issue – with its geopolitical and economic unbalances – able to give a shove off to a product that remained unchanged for over one century.

The global crisis brought the great fear, but also the great occasion: cars can finally speed up their development processes. Electrified powertrain is really starting to take shape; the pathway leading to the future has a clear route that increasingly sees fuel freed from its burdensome relationship with petroleum and with the other fossil hydrocarbons,

a significant increase in on-board efficiency, and the increasing capacity of providing zero emission mobility.

Through the proposals of the major car manufacturers and the new brands that are about to reach the market of electric vehicles, this chapter intends to describe the evolution of vehicle electrification: from hybrid electric vehicles (micro, mild-medium, full) and from plug-in hybrid electric vehicles to battery electric vehicles (BEVs), from fuel cell hydrogen electric vehicle to multi-purpose electrified traction platforms and architectures.

## 1.1 Electrified powertrains

The development of increasingly electric vehicles, able not only to better use fuel but also to travel for longer and longer distances in a zero emissions vehicle (ZEV) mode, that is, at zero emissions, is the main focus of the industrial policies of the largest world countries.

The electrification of vehicles in the most important motor shows of the last few years has been increasing: from hybrid to all-electric vehicles, batteries and engines were shown in any exhibition area of large carmakers. It is noteworthy that the NAIAS 2010 (North American International Auto Show) of Detroit devoted an area of nearly 3,500 m<sup>2</sup> – the ‘Electric Avenue’ – to electric mobility in its different configurations.

A car electrification ‘pathway’ can be identified in the following sequence: non-hybrid vehicles – namely internal combustion engine (ICE) drive, hybrid electric vehicle (HEV; micro hybrid, mild hybrid, full hybrid, plug-in hybrid), extended range EV (EREV), BEV, fuel cell electric vehicle (FCEV). Table 22.1 shows an overview of the functions and features (described in the next paragraphs) existing or possible in a vehicle according to the different types.



---

## 2. HYBRID ELECTRIC VEHICLES

The hybrid solution allows to obtain a marked reduction of consumption and emissions. In the case of hybrid-electric systems, the presence of the electric motor allows using the heat engine more efficiently, and the presence of electric power accumulators and electric motors allows energy recovery during braking and its subsequent use for traction purposes.

A traditional classification of hybrid is proposed on the basis of the system architecture: (a) series hybrid (only the electric motor supplies power to the wheels), (b) parallel hybrid (both the heat engine and the electric motor supply, in parallel, power to the wheels), and (c) series-parallel hybrid (the heat engine can both drive the wheels directly [as in the parallel hybrid] and be disconnected from the wheels, so that only the electric motor powers the wheels [as in the series hybrid]).

**Table 1** Different types of vehicles and their main functions/characteristics

	Function				
	Stop&start	Electric traction	Regenerative braking	Electric driving only	External battery charge
<b>System</b>					
Conventional vehicle	Possible	No	No	No	No
Micro HEV	Yes	No	Minimum	No	No
Mild HEV/ Medium HEV	Yes	Limited	Yes	Minimum	No
Full HEV	Yes	Yes	Yes	Yes	No
Plug-in HEV (PHEV)	Yes	Yes	Yes	Yes	Yes
Extended range EV (EREV)	Yes	Yes	Yes	Yes	Yes
Battery electric vehicle (BEV)	Yes	Yes	Yes	Yes	Yes
Fuel cell electric vehicle (FCEV)	Yes	Yes	Yes	Yes	Yes (electric and/or hydrogen refuelling)

However, the classification that is at present adopted by all car manufacturers and by the experts of this sector refers to the degree of hybridisation of the car, that is, the ratio between the power of the heat engine/generator and the power of the electric motor. Therefore, on the basis of this criterion, the hybrid traction solutions classified according to the possibility of performing given functions by the electric system are the following:

- Micro hybrid
- Mild (or medium) hybrid
- Full hybrid.

## 2.1 Micro hybrids

The functions performed by the electric component in a micro hybrid vehicle are mainly the following:

- Power supply to electrically driven accessories, including air-conditioning
- Stop&start (putting the ICE in standby as soon as the vehicle stops, and automatically switching it on at restarting)
- Brake energy regeneration (possibility of recovering part of the braking energy).

Many carmakers adopt micro hybrid solutions on their models to actively intervene on emission and consumption reduction. Examples of these models are given in the following.

### **2.1.1 BMW efficient dynamics**

At BMW the micro hybrid is part of the EfficientDynamics technological solutions for the reduction of emissions and consumption. Both stop&start and brake energy regeneration functions are available. With the stop&start function, when the vehicle stops, the engine is automatically switched off as the clutch is disengaged, and it is restarted when the clutch is engaged again. Brake energy regeneration allows, during deceleration or braking, to recover and store in the battery the energy produced by the movement of the vehicle. In this way, the battery is recharged by converting the kinetic energy of the vehicle, without using the ICE. This system allows saving up to 3% fuel. In fact, the generator normally works continuously when the engine (that activates it through a V-belt) is in motion to produce the electric energy that is increasingly necessary for the comfort and safety functions of the car. With the brake energy regeneration, on the contrary, the generator is only activated during deceleration or braking, this providing a further advantage: in case of maximum acceleration, the engine also avails itself of the driving force that the generator would need in case of conventional charging. In extreme cases, when the battery state of charge reaches its lower limit, the system is activated to charge it during the acceleration phase as well, hence avoiding its excessive discharge.

### **2.1.2 Volkswagen blue motion technologies**

Volkswagen gathers its ecological innovations under the brand name Blue Motion Technologies. Different models include innovations as the stop&start system and the brake energy regeneration.

### **2.1.3 FIAT PUR-O2**

FIAT has introduced the PUR-O2 line in a range of models (city-car, sedan and station-wagon) availing themselves of different systems for the reduction of polluting emissions and of the level of CO<sub>2</sub>, including the stop&start function developed by Bosch. For instance, Fiat 500 PUR-O2 reaches CO<sub>2</sub> emissions of 115 g/km, the lowest ones among petrol cars.

### **2.1.4 Volvo DRIVE**

The name DRIVE indicates the most environmentally friendly cars of the entire Volvo's fleet. Besides a series of specific measures aimed at improving car efficiency (tyres with a low rolling resistance, optimised aerodynamics) these vehicles also adopt the stop&start system (which alone contributes to 5–8% fuel saving) and the regenerative brake system, which – during braking – allows to store energy in a supplementary battery, for the use of entertainment systems when the engine is switched off (stop&start is activated).

### **2.1.5 SEAT ecomotive**

SEAT gathers its vehicles that allow fuel saving and emission reduction under the brand name Ecomotive. In this case as well, the solutions adopted include the stop&start system and regenerative braking.

### **2.1.6 Smart MHD**

In the Smart micro hybrid drive (MHD), the heart of the system is represented by a special stop&start alternator that efficiently exploits the 'phases of rest' of the engine. According to the manufacturer, fuel saving amounts to nearly 8% on the basis of the global consumption in the European combined cycle. Indeed, consumption is reduced by about 0.41 per 100 km (from 4.7–4.3 l).

### **2.1.7 Toyota optimal drive**

Toyota labels its low-emission and low-consumption vehicles as optimal drive. These vehicles have the stop&start system in addition to the weight reduction of engine and transmission, the decrease of friction and the increase of the combustion efficiency.

## **2.2 Mild hybrids (Mild HEVs)**

Mild (or medium) hybrids indicate a range of vehicles in which the electric systems perform functions additional to those of the micro hybrid. A summary of all functions include:

- Power supply to electrically driven accessories, including air conditioning (as in micro hybrids).
- Stop&start (as in micro hybrids)
- Inactive timing system (when torque is not requested by the ICE, valves go to a sleep mode and do not absorb any energy, the ICE stops without really switching off)
- Power supply for traction purposes; in particular the electric motor provides power to the wheels when torque peaks must be reached (for instance at the start).<sup>1</sup>
- Brake energy regeneration.

The main difference between this solution and the micro hybrid consists in the fact that in this case the electric system significantly contributes to the powertrain. On the basis of the ratio between the power of the electric motor and the power of the ICE, reference is made to mild or medium hybrid. In any case, traction with the electric motor alone is not possible except for very particular conditions.

### **2.2.1 Honda integrated motor assist**

The hybrid technology of Honda is characterised by the integrated motor assist (IMA) system with a petrol-electric hybrid engine, stop&start and brake energy regeneration. It

<sup>1</sup>In this way the torque provided by the ICE 'flattens' with remarkable reductions in consumption and emissions.

was the first carmaker to commercialise a hybrid vehicle outside Japan in 1999 with the coupé Insight (first generation of the IMA system), and is now present in the European market with two models, Civic Hybrid and the new Insight.

Nickel-metal hydride (NiMH) batteries are adopted, and are recharged both through the petrol engine and the recovery of kinetic energy during deceleration. The electric motor supports the heat engine and provides the additional power during acceleration that allows the ICE to work at a more efficient rpm.

The hybrid system of Honda Civic Hybrid includes a four-cylinder i-VTEC petrol engine (1.3l) of 70 kW at 6,000 rpm with the support of an electric motor of 15 kW at 2,000 rpm that allows a 30% torque increase as well as a power increase. With an overall power of 85 kW, the consumption is 4.6l per 100 km, with CO<sub>2</sub> emissions amounting to 109 g/km in the European homologation combined cycle.

The new Insight has adopted the fifth generation of IMA with an extremely thin electric motor [always included between the heat engine – 65 kW at 5800 rpm – and continuously variable transmission (CVT)] (10 kW power at 1,500 rpm) (Fig. 22.1). The engine-generator, placed in the front bonnet of the vehicle is connected to the 100.8-V Ni-MH battery pack, which is conversely located, with the intelligent power unit (IPU), in the rear underbody of the vehicle (Fig. 22.2). It is endowed with a stop&start system as well as with the brake energy regeneration systems; its consumption under the European combined cycle amounts to 4.4l per 100 km, with CO<sub>2</sub> emissions of 101 g/km.

In the Insight the electric motor provides the necessary power when higher performances are requested, and acts as a generator during deceleration and braking, allowing all-electric operation in particular motion conditions. In fact, the variable cylinder

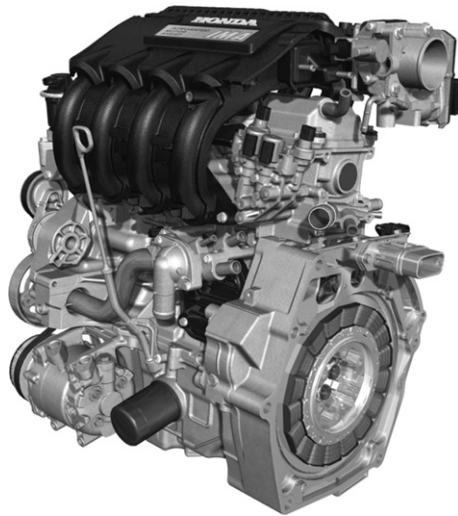


**Figure 22.1** IMA System (Integrated Motor Assist).



**Figure 22.2** 2010 Honda Insight: hybrid system layout.

management (VCM) technology is also used to block the valve mechanism in the four cylinders when proceeding at low constant speed. In this way, Insight automatically shifts to the ‘electric only’ all-electric mode, reducing the pumping losses of all the cylinders, up to an official range of nearly 2 km.

Obviously, also the transmission system plays a major role in hybrid powertrain in consideration of the global efficiency of the system. The Insight adopts an evolution of the high torque CVT of civic hybrid, with a lower gear ratio (4,200 vs. 3,937), which improves standing starts.

A further system installed on the Insight, which aims at contributing to reducing consumption and CO<sub>2</sub> emissions, is the Ecological Drive Assist System (Eco Assist), which shows drivers whether their driving style is low-consumption, and provides assistance to ‘educate’ drivers to an ‘Eco Drive’.

A step forward, again linked to the IMA system, is the CR-Z hybrid (sport hybrid) presented at the 2010 NAIAS in Detroit (Fig. 22.3). The subsequent step is represented by the adoption of the IMA system on compact Honda Jazz as well as the development of another hybrid system for medium–large vehicles. It is not a ‘light’ IMA hybrid system, but probably a new full-hybrid system, supporting the driving of large-size SUV and sedans also in all-electric mode.

On the CR-Z the IMA system includes a traditional four-cylinder 1.5 i-VTEC and a 10-kW electric motor. The result is a power of 91 kW and a robust torque of 174 Nm,





**Figure 22.3** Honda CR-Z.

already available at only 1,500 rpm. These are nearly the same values as Honda Civic 1.8, but with CO<sub>2</sub> emissions of 117 g/km and a range of 20 km/l.

### **2.2.2 Mercedes S-Class (Mild hybrid)**

Mercedes S-Class, although put on the market over 10 years later than the world première of a hybrid model and 4 years after the launch of hybrid cars in the sector of premium brands – occurred with Lexus RX 400h in June 2005 – is the first European car with a powertrain system including electric motor and batteries together with the traditional ICE, and the first hybrid car in the world that adopted lithium-ion (Li-ion) batteries on a production vehicle.

The hybrid technology onboard of an S-Class of the mild hybrid type has a 15-kW electric motor with stop&start function, and a V6 petrol engine (3,500 cm<sup>3</sup>, 205 kW),

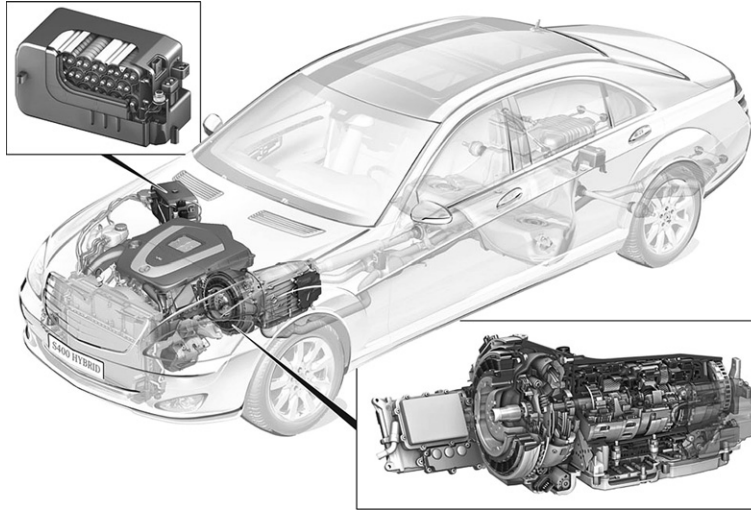


**Figure 22.4** Mercedes S400 Class Hybrid: system layout.

this leading to a combined power of 220 kW with a maximum torque of 385 Nm. The lithium battery pack is compact (directly installed inside the engine compartment) and light, but also with a rather limited energy capacity. The Li-ion battery (produced by Continental with cells by the French Saft) guarantees an energy supply only sufficient to put the electric powertrain in action for a few seconds. However, the difference versus the analogous car without electric motor is clear and driving the hybrid is extremely pleasant. Furthermore, the lithium-ion battery, easily accessed in an upper corner of the engine compartment, can directly support the air-conditioning system of the car (Fig. 22.4).

Compared to the other hybrid cars on the market, Mercedes S-Class uses the electric support for much shorter times; however, in the homologation data, these small repeated interventions lead to achieve excellent results, which can be summed up in the consumption of 7.91 of petrol every 100 km, amounting to the emission of 186 g/km of CO<sub>2</sub>. For a flagship vehicle with a mass of over 2 tons and a 3.5-l V6 petrol engine, these values represent a real record.

### 2.2.3 BMW active hybrid (Mild hybrid)

The 7-series ActiveHybrid model is the first mild hybrid BMW entering the market. The rationale at the basis of this premium luxury vehicle is not represented by a consumption reduction, but rather the achievement of performances comparable to the higher category (V12) with a lower weight and higher range. For this reason, it has a 330-kW twin-turbo V8 engine, backed by an 8-speed automatic transmission, in addition to an electric motor of 15 kW and 210 Nm. In this way, the total power of

ActiveHybrid 7 reaches 342 kW (slightly less than the arithmetic sum given the different output of the electric motor), with a maximum overall torque of 700 Nm and an acceleration from 0 to 100 km/h in 4.9 s. The average consumption in the testing cycle amounts to 9.4 l/100 km, 10.6 km/l, with CO<sub>2</sub> emissions of 219 g/km.

The engine/generator block is coupled on the shaft before the torque converter and connected through a 120-V inverter to an 800-Wh lithium battery that ensures the vehicle 4 min of boost between 0 and 3,500 revolutions (with higher number of revolutions, the torque fall of the electric motor penalises its efficient use).

The battery charge during normal driving occurs both through brake energy regeneration and (whenever the battery management system deems it suitable according to the charge conditions) directly through the engine. The active hybrid system obviously endows the vehicle with a stop&start solution to avoid engine idling when the car is stopped. The electric motor also performs the starting function and replaces the 12-V generator, through a DC–DC converter.

The BMW Active Hybrid system uses the hybrid technology to optimise services already adopted, for example, the circuit of the two liquid intercoolers is also used to cool the DC–DC converter and all the power electronics. The 7-series ActiveHybrid does not allow all electric drive.

Fig. 22.5 shows the ActiveHybrid (mild hybrid) system adopted, which includes BMW V8 petrol engine with High Precision Injection and Twin Turbo (1); the electric motor, integrated in the gearbox with its 210 Nm and 15 kW (2), replacing the engine starter and the generator, supporting at the same time the petrol engine; the 8-speed automatic transmission (3), on which high performance electronics is directly installed (4); a 120-V Li-ion battery (5).

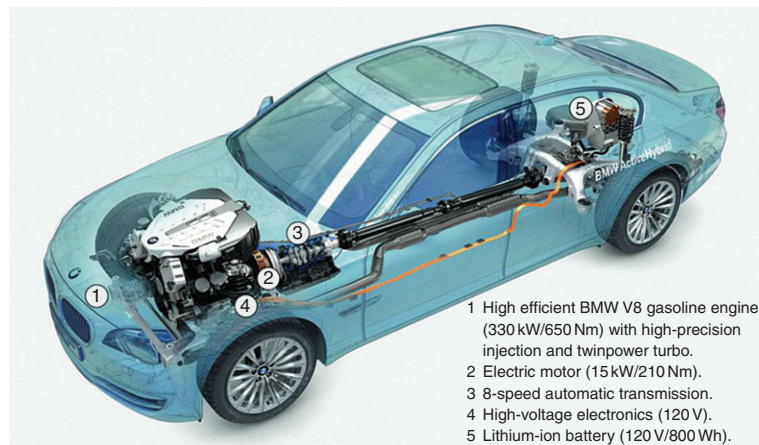


**Figure 22.5** BMW 7 Series ActiveHybrid: system layout (see color plate 7).

## 2.3 Full hybrids (Full HEVs)

In addition to the functions envisaged for micro and mild hybrids, a full hybrid vehicle allows starting and driving with the electric motor alone. Obviously, due to the limited size of electric motor and batteries, the all-electric range is limited.

Therefore, summing up all the functions of a full-hybrid system, the following characteristics are present:

- Power supply to electrically driven accessories, including air-conditioning (as in micro, mild and medium hybrids)
- Stop&start (as in micro, mild and medium hybrids)
- Inactive timing system (when the ICE is not requested to supply torque, valves go to a sleep mode and do not draw any energy, and the ICE stops without really switching off) (as in mild and medium hybrids)
- Power supply for traction purposes; in particular the electric motor provides power when torque peaks must be reached, e.g. at the start (as in mild and medium hybrids)
- Brake energy regeneration<sup>2</sup> (as in mild and medium hybrids)
- Possibility of starting and running in electric mode only with the ZEV function.

### 2.3.1 Toyota hybrid synergy drive and Lexus hybrid synergy drive

As a result of 30 years of research and development in the field of hybrid vehicles, Toyota has brought to the market the first hybrid car.

Toyota Prius and Lexus are endowed with series-parallel hybrid systems, called hybrid synergy drive. The heat engine and the electric motor operate in complete synergy and both have the possibility of providing traction. The hybrid cars by Toyota and Lexus can therefore guarantee efficiency, noiselessness and 'zero emissions' of the full-hybrid solution, which allows standing start and all-electric drive in many conditions. Thanks to its capacity to operate in electric mode alone, the hybrid synergy drive system guarantees the advantages of the series hybrid system in terms of energy saving, and of the parallel hybrid system in terms of performance. Consequently, it offers a uniform and homogeneous acceleration, reduced consumption, and the lowest level of emissions, while a high comfort is guaranteed without any change in the usual driving style.

In the third generation Toyota Prius (Fig. 22.6) a new 1.8-l inline-4 Atkinson-cycle engine (2ZR-FXE) is rated at 73 kW @ 5,200 rpm and 142 Nm @ 4,000 rpm; the DOHC 16-valve unit includes variable valve timing with intelligence (VVT-i). Toyota's hybrid transaxle uses a dual planetary reduction gear set to integrate the two motor generators (MG1 and MG2) with the ICE. MG1 is a permanent magnet motor generator rated at 42 kW, while the bigger 60 kW MG2 produces 207 Nm of torque and spins to 13,500 rpm; the combined hybrid powertrain produces a peak power of

<sup>2</sup> As a matter of fact, it is possible to really recover only a part of the energy wasted during braking.



**Figure 22.6** Third-generation 2010 Toyota Prius: hybrid system layout.

100 kW, supplied to the front wheels via an electronically controlled CVT Fig. 22.7 shows motor generators for the second and third Prius generations.

The main characteristic of the hybrid synergy drive technology is that the electric motor, the generator and the power divider are all located in a light and compact transmission housing, whose size is comparable to a conventional gearbox.

A 201.6 V NiMH battery pack powers the dual electric motor generators. The pack, shown in Fig. 22.8, is composed of 28 9.6-V modules (for a total of 168 cells) with a



**Figure 22.7** Motor-generators: the second-generation Prius transaxle (left) and the new 2010 Prius transaxle (right).



**Figure 22.8** Nickel-Metal Hydride (NiMH) battery pack.

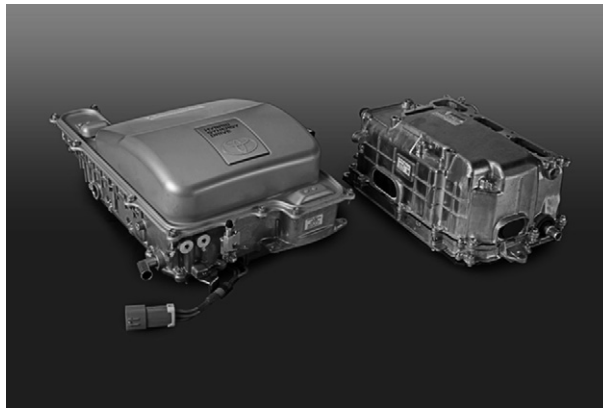








**Figure 22.9** The second-generation inverter (left) vs. the 2010 Prius inverter (right).

capacity of 6.5 Ah and a maximum power output of 27 kW. The battery pack voltage jumps to 650 V before an inverter converts it to 3-phase AC for the MG1 and MG2 motor generators. A DC/DC converter provides 12 VDC for electrical accessories and the auxiliary battery. The recyclable battery pack is warranted for 10 years/240,000 km. Inverters are shown in Fig. 22.9.

The second electric motor of Toyota's Hybrid Synergy Drive® system can independently recharge the battery at any time. Additionally, in specific driving situations such as deceleration and braking, the high-power 60-kW electric motor acts as a high-output generator by recovering kinetic energy (normally wasted as heat) and supplying it as electrical energy to the high-performance battery.

The operation phases of the hybrid system can be divided into Starting, Driving, Overtaking, Braking, Electric mode, Stopping. A description of the main features is contained in Fig. 22.10.



Starting	Driving	Overtaking
 <p data-bbox="247 336 451 478"><i>From start-up the new Prius can drive under electric motor power alone up to 45 km/h until the petrol engine kicks in.</i></p>	 <p data-bbox="482 336 872 455"><i>Above medium speed new Prius uses its petrol engine and its two electric motors in synergy. Depending on driving conditions the battery can also be recharged by the electric motor which then acts as a generator.</i></p>	 <p data-bbox="915 336 1208 525"><i>When overtaking or during sudden acceleration, seamless power comes from both energy sources. The 1.8l petrol engine is supported by the 60 kW electric motor providing additional boosting power while offering an impressive, seamless acceleration.</i></p>
 <p data-bbox="247 707 451 843"><i>When braking and during deceleration the electric motor acts as a high-output generator and recharges the high-power battery.</i></p>	 <p data-bbox="482 707 886 795"><i>The driver can activate electric vehicle mode (EV) to drive in pure electric mode for speeds up to 45 km/h. In this mode, no fuel is consumed and the car provides zero emissions.</i></p>	 <p data-bbox="915 707 1208 843"><i>When stopping the petrol engine is switched off by the stop&amp;start system to lower fuel consumption even further. All other systems, including the electric air conditioning, continue to function.</i></p>

**Figure 22.10** Prius hybrid energy flow.

The official consumption and emissions of Prius III in a combined cycle indicate 3.9 l/100 km with CO<sub>2</sub> emissions of 89 g/km.

Lexus RX 450h (4 × 4) with 'full hybrid' technology (Fig. 22.11) has CO<sub>2</sub> emissions of 148 g/km with consumption of 6.3 l/100 km in a combined cycle. Its characteristics can be summarised as follows: heat engine: 3,456 cm<sup>3</sup> Dual VVT-i, max power of 183 kW @ 6,000 rpm, max torque of 317 Nm @ 4,800 rpm; two permanent magnet synchronous electric motors: front motor with 132 kW of max power with max torque of 335 Nm and rear motor with 50 kW of max power with max torque of 139 Nm; E-Four four-wheel drive and CVT.

Lexus GS 450h (rear-drive) is, on the contrary, a V6 providing a performance comparable to a V8, with lower consumption and emissions. CO<sub>2</sub> emissions amount to 180 g/km with combined cycle consumption of 7.6 l/100 km. The engines of this hybrid drive sedan have maximum power of 218 kW at 6,400 rpm with 638 Nm at 4,800 rpm in the case of heat engine, and 147 kW with max torque of 275 Nm in the case of electric motor.

Lexus LS 600h as well (four-wheel drive) (Fig. 22.12), the flagship vehicle of the Japanese carmaker, is endowed with the Lexus hybrid drive with CO<sub>2</sub> emissions of 219 g/Km. In the combined cycle, consumption amounts to nearly 9.3 l/100 km. The

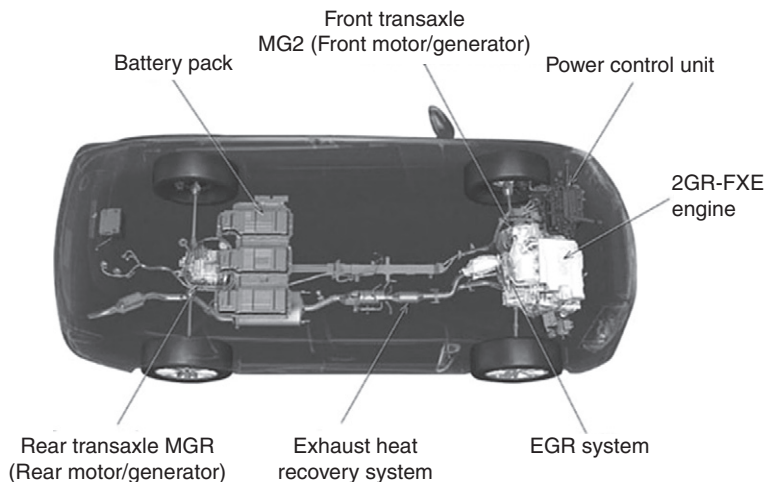


**Figure 22.11** Lexus RX 450h: hybrid system layout.

overall maximum power of 327 kW is supplied by 290 kW at 6,400 rpm of maximum power (with a max torque of 520 Nm at 4,000 rpm) of the heat engine and 165 kW of the permanent magnet synchronous motor, with a torque of 300 Nm.

### **2.3.2 BMW active hybrid (Full hybrid)**

BMW X6 ActiveHybrid is the first Sports Activity Coupé of the German carmaker equipped with a full-hybrid motor. In BMW X6 ActiveHybrid, the combination of a V8 petrol engine and an electric motor produces a powerful vehicle, while affording approximately 20% reduction of fuel consumption and emissions. This vehicle is an



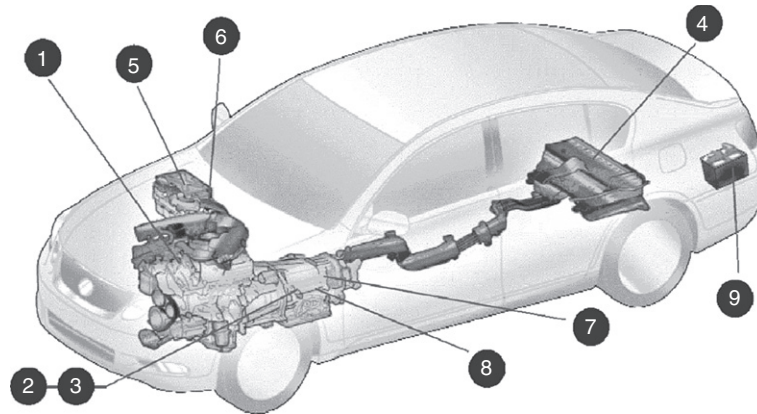


**Figure 22.12** Lexus LS 600h: hybrid system layout. (1) ICE: V-6 VVT-i, 3,456 cm<sup>3</sup>, 218 kW; (2) electric start-up – generator; (3) electric motor (147 kW, 650 V) – generator; (4) 288-V NiMH traction batteries; (5) inverter; (6) electronic control system; (7) brake energy regeneration system; (8) electronic-control speed changer; (9) 12-V batteries.

integral part of the BMW EfficientDynamics development strategy, in the framework of the progressive reduction of consumption and emissions.

As shown in Fig. 22.13, the innovative, full-hybrid, two-mode active transmission (1) is the main hybrid component of the BMW X6 ActiveHybrid. The two-mode active transmission comprises power electronics (2) with an integrated inverter module and a high-performance battery (3). This combines the driving dynamics and efficiency of the combustion engine (4) and the electric drive system in an innovative, intelligent manner.

The two-mode active transmission is developed at the Global Hybrid Cooperation in Troy (USA) together with General Motors (GM), Chrysler and Daimler. This

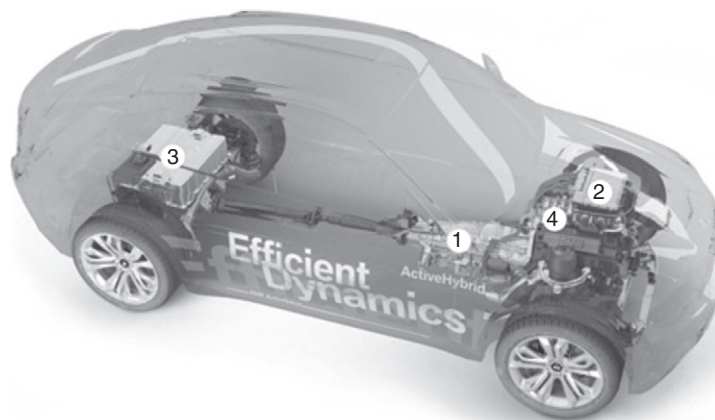


**Figure 22.13** BMW X6 ActiveHybrid: system layout.

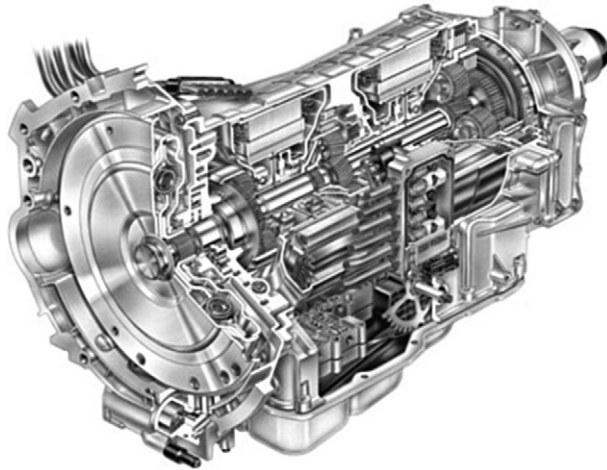


**Figure 22.14** GM Two-Mode Hybrid cutaway view.

innovative technology enables the interplay between the electric motors and the engine to be varied according to the situation. It features two different transmission modes: one that ensures maximum torque when pulling away and in low-speed driving, and another that is optimised for higher speeds and bursts of acceleration – e.g. when overtaking. The active transmission allows the BMW X6 ActiveHybrid to get maximum performance and efficiency from its powertrain at all speeds.

The sectional view of [Fig. 22.14](#) shows the complex arrangement of electric motors & planet gears that comprise the two-mode transmission.

The traction of BMW X6 ActiveHybrid can occur thanks both to the electric motors alone and the ICE, and to a combination of the two propulsion systems. According to the driving characteristics, electric motors can be used both for acceleration and to perform regenerative braking. In this case, the braking torque generated by the two electric motors during the release or deceleration phases produces current for high-voltage energy storage. In the acceleration phases, the boost effect of electric motors determines a highly quick response with an important reduction of consumption and emissions.

In power divider propulsion systems, one of the two electric motors takes on the function of generator, transforming part of the motor power into electric current that is supplied to the battery and the second electric motor, which converts this current into mechanic power. The Two-Mode active transmission (see figure) manages the ratio between electric and mechanic motor, hence allowing an optimised efficiency.

### **2.3.3 Mercedes M-Class Hybrid**

Mercedes launched in the US market its M-Class luxury SUV with a full hybrid system. In its first commercialisation phase, M-Class Hybrid is not envisaged for the European

market, where the manufacturer intends to protect as long as possible the spreading of Diesel engines in its models.

Mercedes ML450 Hybrid, the first 'full hybrid' model of the German manufacturer, contrasts Lexus RX 450h in the North-American market. ML450 shares with S400 Hybrid the 205 kW Atkinson cycle 3.5l V6 engine, but the hybrid system is more complex and the electric part outweighs the one of the flagship vehicle. The system adopted is the bimodal one fine-tuned jointly with BMW, GM and Chrysler as already described above, that is to say endowed with two electric motors (both of 63 kW, although one with 260 Nm and the other with 235 Nm) and three planetary gears, whose composition generates four fixed ratios and two variable ratios. The 288-V battery adopted by Mercedes ML450 Hybrid (produced by the American Cobasys and located under the luggage compartment), is liquid cooled NiMH and therefore does not belong to the present Daimler agreements for lithium batteries. The propulsion can rely upon a total power of 250 kW and 517 Nm.

ML450 Hybrid, as a full-hybrid, is able to move at low speed and in an electric mode alone for short ranges, all depending on the charge level of the battery, which can be monitored from the instrumentation onboard. The start is therefore usually silent, but when pressing the throttle pedal to accelerate the heat engine V6 is started.

### **2.3.4 Audi Q7 Hybrid**

After presenting functional prototypes of Q7 Hybrid, Audi's present commitment with hybrid vehicles is addressed to the development of a hybrid version of the medium SUV Q5, which should be equipped with lithium batteries, and a 3.2-l V6 engine matched with an electric motor.

### **2.3.5 Porsche Cayenne Hybrid**

The choice made by Porsche as regards hybrid models is the parallel full-hybrid. The difference between the full-hybrid series-parallel and the full-hybrid parallel being developed by Porsche resides in the dynamo that in the latter case is integrated in the drive chain. The hybrid module is positioned between gear and combustion engine, where it is joined to a clutch. Porsche Cayenne Hybrid (Fig. 22.15) is announced with consumption below 9 l/100 km, this meaning a reduction of over 25% compared to the non-hybrid version. The optimal management of the powertrain is entrusted to the Hybrid-Manager that activates or excludes the combustion engine or the electric motor according to the driving conditions. The battery (240 cells, 288 V, 38 kW of power) is located in the spare wheel housing and its temperature is guaranteed below 40°C through a dedicated cooling system.



**Figure 22.15** Porsche Cayenne Hybrid: system layout.

### 2.3.6 Volkswagen full hybrid

Volkswagen has launched a hybrid version of Touareg (Fig. 22.16). The heat engine of the system is the 3.0-l V6 TSI (petrol direct injection equipped with a variable geometry turbo compressor) with a power of 245 kW @ 5,500 rpm and 440 Nm of maximum torque starting from 3,000 rpm. The electric motor (E-motor) located between the V6 and the gear is able to supply 38 kW of power and a torque up to 300 Nm. The batteries, deriving from a specific agreement with Sanyo, are NiMH.

Electric traction is possible up to 50 km/h, beyond which the petrol engine starts up. In the driving situations in which particular power is requested, the heat engine receives the support of the electric motor. The total power of Touareg TSI Hybrid is 275 kW and

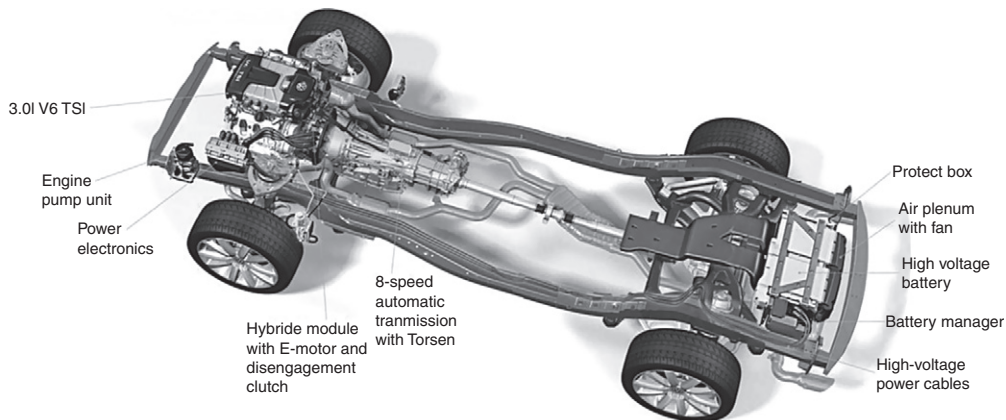


**Figure 22.16** Volkswagen Touareg Hybrid: system layout.

with a peak of driving force at 550 Nm. As with Porsche Cayenne Hybrid, the manufacturer declares for the final model of Volkswagen Touareg V6 TSI Hybrid an average consumption of 9 l/100 km, with average CO<sub>2</sub> emissions of 210 g/km (25% less than a similar non-hybrid vehicle in urban driving and 17% in trunk roads and motorways).

Volkswagen has also presented at the 2010 Detroit Auto Show the prototype of the New Compact Coupé (NCC); it is a full hybrid that can be placed between sports car Scirocco and Passat CC.

The German manufacturer stated that the NCC is equipped with a petrol TSI engine (1.4 l and 110 kW) and a 20-kW electric unit powered by Li-ion batteries. The system is managed by a 7-speed automatic DSG. The official consumption, in combined driving, amounts to 4.2 l/100 km and CO<sub>2</sub> emissions amount to 98 g/km, with a maximum speed of 227 km/h and an acceleration from 0 to 100 km/h in 8.6 s. The vehicle is also endowed with the stop&start system to reduce fuel consumption, and with a system for the recovery of kinetic energy during braking.

### **2.3.7 PSA Peugeot Citroën Hybrid**

PSA Peugeot Citroën relies upon the diesel hybrid technology to increasingly exploit the characteristic of diesel engines to be less consuming than petrol engines. The two prototypes proposed were Citroën C4 Hdi Hybride and Peugeot 307 Hdi Hybride (Fig. 22.17) with official consumption of 3.4 l/100 km on the European mixed cycle and a 30% reduction compared to the present series version. CO<sub>2</sub> emissions, therefore, reach the record level of 90 g/km, while the vehicles have better dynamic performances both in acceleration and pick-up.

The French manufacturer has the merit of raising the issue and showing the real feasibility of the technological solution that in its opinion is particularly interesting for European customers, that is to say hybrid vehicles with diesel engine and electric motor (Fig. 22.18). It is to be noted that this idea is applied to the major sector in Europe, that is to say compact cars as C4 and 307.

Furthermore, the availability of a ZEV button allowing the car to operate in electric mode for 5 km with a speed up to 50 km/h, entirely noiseless and without any exhaust emission, is an important characteristic of these vehicles.

At the 2010 Detroit Auto Show, Peugeot presented SR1, a hybrid concept-car with HYbrid4 technology, which will be adopted as a standard equipment on Peugeot 3008 as from 2011, and subsequently will be included in other models. The petrol engine is 1.6-l THP (160 kW), located in the front side, whereas the 70-kW electric propeller is in the rear part. SR1, therefore, can run either with the heat engine alone, or in an exclusively electric mode for nearly 12 km, or can combine the action of the two types of powertrains to become a 4-wheel drive sports car with a power of 230 kW. The official consumption is 4.9 l/100 km, with CO<sub>2</sub> emissions of 119 g/km. SR1 is also

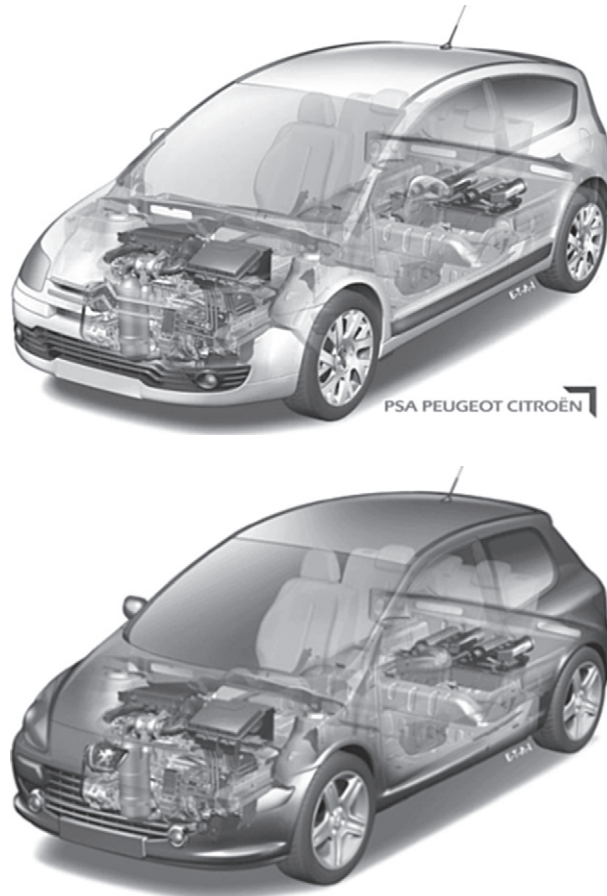


**Figure 22.17** PSA Peugeot Citroën HDi Hybrid system layout (up, Peugeot; down, Citroën).

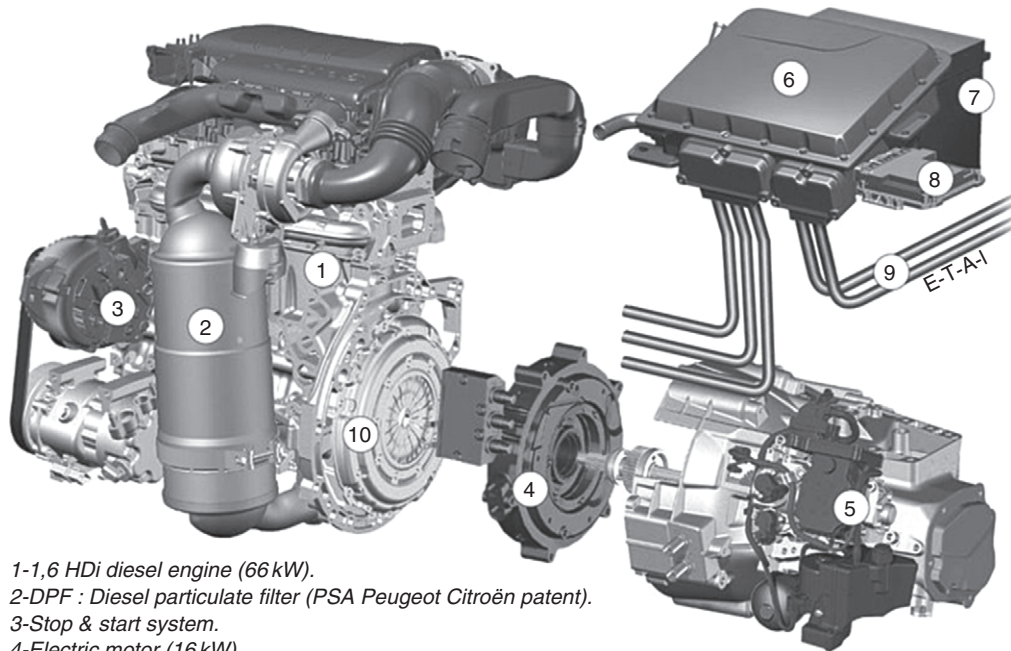
endowed with integral steering, with the rear wheels that can rotate by following the ‘indications’ of the electronic control unit.

As concerns Citroën, the full hybrid DS5, with 2.0 l HDi heat engine (125 kW of power) and 27 kW electric motor, will be commercialised in 2011 together with Peugeot 3008.

## 2.4 Plug-in hybrids (PHEVs)

Plug-in hybrid vehicles offer – as main differences compared to present hybrid cars – the possibility of recharging the batteries onboard from an electrical socket and the capacity to guarantee all-electric driving for a distance that is sufficient at least for daily average urban driving, i.e. from approximately 15 to above 100 km. Just as HEVs, PHEVs can be an intermediate step, if successful, towards purely electric vehicles.





- 1-1,6 HDi diesel engine (66 kW).  
 2-DPF : Diesel particulate filter (PSA Peugeot Citroën patent).  
 3-Stop & start system.  
 4-Electric motor (16 kW).  
 5-Automatized manual transmission (AMT - 6 gears).  
 6-Power electronics (inverter and converter).  
     Inverter : drives the electric motor.  
     Converter : converts high-voltage to 12 V onboard network.  
 7-Low-voltage battery (12 V).  
 8-PTMU : Powertrain mangement unit.  
 9- High-voltage cables.  
 10-Dry clutch.

CITR  
Direct

**Figure 22.18** PSA Peugeot Citroën Hdi Hybride powertrain.

### 2.4.1 Toyota Prius Plug-in

The production of the first fleet for a large international project of road tests for over 600 Plug-in Prius (Fig. 22.19) started at the end of October 2009 and the delivery of the first 350 units at the end of the same year, whereas the remaining cars are delivered as follows in 2010: 230 units in Japan, 150 in the United States, 200 in Europe and 20 between Oceania (Australia and New Zealand) and Canada. France was the first European country in which this vehicle was circulating, thanks to a special project envisaging the development of a version with Li-ion batteries rechargeable from the house electric socket.

According to the Japanese homologation regulations, Plug-in Prius can run for 57 km with 1 l of petrol (and with the battery fully recharged). These data indicate an 86% improvement compared to 30.6 km/l of the non-plug-in version. Emissions amount to 41 g/km of CO<sub>2</sub> versus 89 g/km for the normal version in the same



**Figure 22.19** Toyota Prius Plug-in.

conditions. This is due to the adoption of 5.2 kWh Li-ion batteries that, according to the Japanese cycle, afford a driving range of 23.4 km in all-electric mode, during which the plug-in vehicle can also reach a speed of 100 km/h. Toyota has also tested the Li-ion batteries with temperatures from  $-30^{\circ}\text{C}$  to  $+40^{\circ}\text{C}$  in three different continents for a total of 10.5 million km. As concerns the recharge from the home socket, the official time is 100 min with a voltage of 220 V.

An additional functionality compared to the normal version is the EV driving ratio, which allows evaluating at best the difference between the all-electric use of Prius and the mixed one. Another 'educational' aspect is represented by the possibility of visualising the quantity of  $\text{CO}_2$  not released into the environment. Toyota considers putting Plug-in Prius on the market in 2012 with an initial volume of several tens of thousands of units.

#### **2.4.2 General motors E-Flex system**

1. Chevrolet Volt. The propulsion and supply system proposed with Chevrolet Volt (Fig. 22.20) will determine, according to GM, the definition of a new class of vehicles called extended-range electric vehicle (EREV). The system is a series hybrid, therefore the wheels of Volt are always activated by the electric motor. The energy stored in a 16-kWh Li-ion battery guarantees a range of nearly 60 km (64 km is the official value of the test, in the MVEG urban cycle), but when the battery is almost exhausted, the petrol/ethanol engine is activated. Indeed, there is a 'traditional' petrol tank fuelling an electricity generator that recharges the battery or supplies the electric motor when the battery is discharged. Therefore, the Volt can still cover several



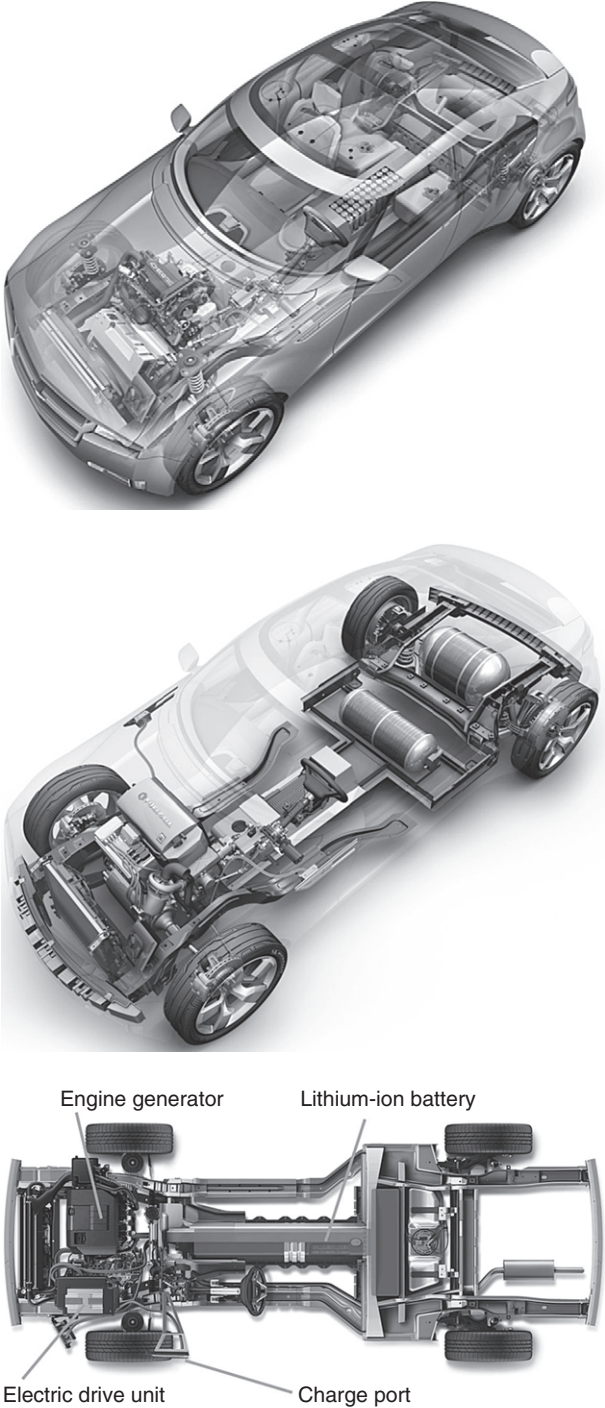


**Figure 22.20** Chevrolet Volt E-Flex system layout.

hundreds of kilometres with the battery exhausted. The total range (with a full tank and full electricity) of the Chevrolet Volt should be four times that of an electric vehicle, i.e. about 480 km.

Chevrolet Volt is conceived as a plug-in, with the possibility of recharging the battery through a normal 220-V socket; a complete recharge takes less than 3 h. The battery can provide a power of approximately 110 kW, with an instantaneous torque of 370 Nm and a maximum speed of over 160 km/h. Chevrolet has also prepared a 1.5-min video in which the vehicle is shown while plunging at high speed in a water course that almost entirely covers its bonnet. This kind of tests, passed by Volt, aims at reassuring drivers about the waterproof characteristics of the battery. This car is produced at the GM factory of Hamtramck (Detroit) and its commercialisation is scheduled in the USA at the end of 2010, and in Europe at the end of 2011.

2. Opel Ampera. Opel Ampera will be in Europe what Chevrolet Volt is in America (Fig. 22.21). In fact, this is the electric vehicle that the German manufacturer will put on the market in Europe at the end of 2011; in the UK, it will be branded as Vauxhall.
3. Mercedes Vision S500 Plug-in Hybrid. The hybrid system of Mercedes Vision S500 Plug-in Hybrid (based on the S-Class) combines a 3.5-l petrol heat engine and a 44-kW electric motor able to guarantee an all-electric range of 30 km. Batteries include a 10-kWh Li-ion pack, also rechargeable through a normal home socket in only 4.5 h. If connection to a 20-kW socket is possible, a full recharge of the battery is completed in 1 h.

In this case as well, the logical management of the two engines allows shifting from a purely electric powertrain, with limited support of the heat engine, to traditional



**Figure 22.21** Opel Ampera.

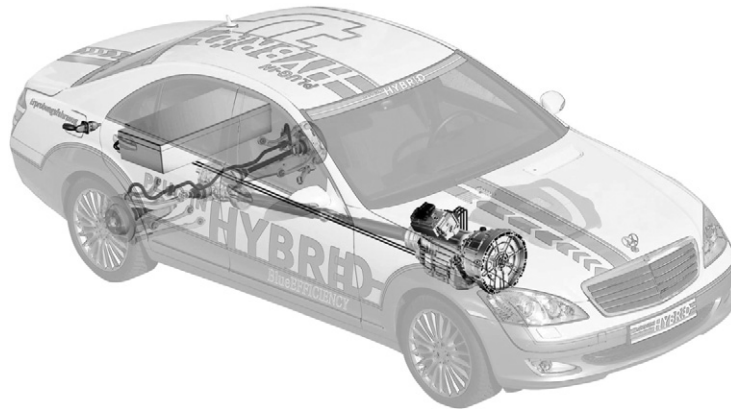


**Figure 22.22** Mercedes Vision S500 Plug-in HYBRID: system layout.

petrol propulsion with electric ‘boosting’ during fast acceleration. This luxury sedan (Fig. 22.22) can reach a top speed of 250 km/h, with an acceleration from 0 to 100 km/h in 5.5 s. Its consumption is 3.2 l/100 km, with CO<sub>2</sub> emissions of 74 g/km.

### 2.4.3 MP3 Hybrid

In May 2009, the Piaggio Group presented a three-wheel hybrid scooter, MP3 Hybrid (Fig. 22.23). The technology of MP3 Hybrid allows reduction of both petrol consumption and CO<sub>2</sub> emissions by over 50% compared to the average of petrol scooters.



**Figure 22.23** Piaggio MP3 HYBRID: system layout.

First in the two-wheeler world, Piaggio has developed for MP3 Hybrid a 'parallel' hybrid propulsion in which both the electric motor and the combustion engine are mechanically and electronically integrated, and are able to simultaneously supply power to the wheels. Endowed with automatic transmission, electric starting and an innovative ride-by-wire system, during normal running the heat engine also allows battery recharging. Furthermore, whenever a fast acceleration is needed, as it happens in standing starts, the electric motor intervenes and backs the heat engine, thus providing improved performances up to 85%. Furthermore, in deceleration and braking conditions, the control system recovers and stores energy in the battery.

MP3 Hybrid can cover up to 60 km/l compared to an average range of 26 km/l of medium-power petrol scooters. CO<sub>2</sub> emissions drop to 40 g/km compared to an average of 90 g/km of traditional heat scooters (the values for MP3 Hybrid are calculated by considering a 65% utilisation in hybrid mode and 35% in electric mode).

MP3 Hybrid can also work with the electric motor only. By rotating the selector placed on the handlebar, the heat engine is disconnected and MP3 Hybrid is transformed into a ZEV scooter, thus allowing its use in restricted traffic areas. By acting on the same selector, the heat engine may become once again the main engine of the vehicle, thus recharging the battery while running in areas open to normal traffic.

The battery charge level is marked by an indicator installed in the dashboard. Battery recharge (MP3 Hybrid is a hybrid plug-in) can also take place through the electric network, with the battery charger integrated in the on-board electronics. A full recharge is carried out in about 3 h.



### **3. BATTERY ELECTRIC VEHICLES**

Three main elements underlie the revival of purely electric vehicles. The first element is the increasing willingness of society, political world and, therefore, the market, to have vehicles not only less polluting and consuming, but not consuming fossil fuels at all and not releasing any harmful substances from exhaust pipes. The second element is represented by the increasing technological success of hybrid vehicles, even though their commercial success was limited thus far. In fact, these systems described by sceptics as complex, expensive and delicate, are practically proving to be even more reliable than conventional vehicles, to be able to guarantee profits to those who decided to put them on the market, and to allow, if properly used, remarkable fuel savings and reductions in CO<sub>2</sub> emissions.

The third factor is linked to the large spreading and technological success of the ubiquitous Li-ion batteries. The extensive market created by portable applications allowed huge capitals to be allocated to R&D of these batteries to such an extent that they entered other markets as the one of hybrid and electric vehicles.

### 3.1 Renault–Nissan alliance

At the end of 2009, the Renault–Nissan alliance<sup>3</sup> announced in Los Angeles that Nissan and Energy Reliant of Huston, Texas (one of the most important US electric power suppliers), signed an agreement to promote the development of zero emission mobility in the United States. This announcement facilitates the introduction in 2010 of Nissan Leaf, the first all-electric zero emissions vehicle (ZEV) designed for the mass market. ‘The Renault–Nissan Alliance aims at becoming a global leader in zero emissions’, stated Carlos Ghosn, Chairman and Chief Executive Officer of Nissan, as well as CEO of Renault. ‘Nissan and Reliant Energy share the idea that electric vehicles represent the best solution to reduce CO<sub>2</sub> emissions’.

The first results of this alliance available for the market are represented by a range of four ZEVs by Renault (ready for the market in 2011) and Leaf by Nissan (2010).

#### 3.1.1 Renault Z.E.

Since 2011 Renault will put on the market a complete range of electric vehicles (marked by the acronym Z.E. –Zero Emissions), endowed with a cutting-edge Li-ion battery technology and destined to mass spreading. The range, presented at the 2009 Frankfurt Motor Show, includes four models: the city car Twizy Z.E., the compact sedan Zoe Z.E., the estate car Fluence Z.E. and the minivan Kangoo Z.E. (Fig. 22.24)

The Renault Z.E. range will be supported by an innovative economic proposal, so that the cost of an electric vehicle will be comparable to that of a heat-engine vehicle, thus representing a convenient and accessible purchasing solution.



**Figure 22.24** Renault’s Zero Emissions (ZE) range.

<sup>3</sup>The Renault–Nissan Alliance was set up in 1999 with the objective of being among the three main world car manufacturers in terms of quality, technology and profitability.

### 3.1.2 Twizy Z.E. concept

The latest concept cars presented by Renault at the Frankfurt Motor Show can be included among the electric plug-in vehicles with an all-electric powertrain.

Twizy Z.E. is the smallest car in the range of Renault's Z.E. vehicles. It is a micro car with four faired wheels and a seat format that puts the driver and the passenger behind one another (as in a tandem), and is powered by a 70-Nm, 15-kW electric motor (Fig. 22.25). The maximum speed is limited to 75 km/h, whereas a 100-km range is guaranteed by the lithium batteries located under the seats. A complete recharge from a home socket lasts nearly 3.5 h. Thanks to its reduced weight (420 kg) and its extremely small size ( $2.30 \times 1.13$  m), this concept vehicle should be as practical and quick in urban traffic as a two-wheeler, also thanks to a turning radius of only 3 m.



**Figure 22.25** Renault Twizy ZE concept.



Renault will produce the electric vehicle derived from the Twizy Z.E. Concept in Valladolid, Spain.

### 3.1.3 Zoe Z.E. Concept

The Zoe Z.E. Concept ( $4.1 \times 1.8 \times 1.5$  m, with a wheelbase of 2.6 m, similar to Clio) has a 226-Nm and 70-kW electric motor that allows the modern 1,400-kg coupé to reach 140 km/h and to run up to 160 km with a full charge. The Li-ion battery recharge can be carried out in three different ways, just as for the other concepts presented by Renault in Frankfurt: standard (4–8 h), fast (20 min) in dedicated facilities, and with the 'Quickdrop' (3 min) in special stations where the entire battery is replaced.

Renault has chosen to produce its future zero emission electric compact sedan in the industrial area of Flins, in the region of Paris. The Zoe Z.E. Concept, see Fig. 22.26, prefigures this new vehicle.

### 3.1.4 Kangoo Z.E. Concept

Kangoo Z.E. Concept (Fig. 22.27) is powered by an electric motor (70 kW, 225 Nm of maximum torque) allowing to reach a maximum speed of 130 km/h. The motor is powered by a Li-ion battery located under the car floor, with a maximum range of 160 km and allowing two recharge options: standard, in 8 h, or fast, in 20 min.

Renault will produce the electric version of Kangoo in its factory of Maubeuge, in the north of France, since the first half of 2011.

### 3.1.5 Fluence Z.E. Concept

Renault Fluence Z.E. Concept (Fig. 22.28), an electric version of the worldcar Fluence produced in Turkey, has a 70-kW electric motor and allows a range of 160 km. As in the



**Figure 22.26** Renault Zoe ZE concept.



**Figure 22.27** Renault Kangoo ZE concept.



**Figure 22.28** Renault Fluence ZE concept.

case of Zoe, there are three battery recharge options: standard, fast and instant ('Quickdrop').

Renault will produce at the factory OYAK-Renault of Bursa, in Turkey, the electric version of Fluence, unveiled with the Fluence Z.E. Concept. The production of this model will begin in the first half of 2011.

### **3.1.6 Nissan Leaf**

Leaf is produced in the Japanese factory of Oppama (50,000 units/year) and in the American factory in Tennessee (200,000 units/year). The building of facilities in Portugal and the United Kingdom is also envisaged, which should serve Renault first and, subsequently, also a European factory of the Japanese brand.





**Figure 22.29** Nissan Leaf.

Leaf (Fig. 22.29) is a hatchback, 4.44-m long car with five doors, five seats, an 80-kW and 280-Nm torque electric motor (comparable to a 1.6-l diesel engine). The 24-kWh, 90-kW Li-ion batteries are 80% rechargeable in 30 min from a fast recharge unit, or in 8 h from a normal socket. The commercial formula selected envisages to sell the vehicle to customers and to lease the battery pack in order to reduce the price impact.

### 3.2 Smart Fortwo Electric Drive

The first Smart Electric Drive produced are assigned to customers involved in different projects carried out by Daimler in the main European and US cities, including e-mobility Italy, joint project for electric mobility launched in December 2009 by Smart and Enel, the largest Italian electric utility, and second utility in terms of installed capacity in Europe. Since 2012, Smart Fortwo Electric Drive (Fig. 22.30) will become an integral part of the Smart range, and it will be commercialised through the network of Smart centres. Endowed with an innovative 17-kWh high-efficiency Li-ion battery, the 30-kW electric motor provides this Smart with very good acceleration and high agility

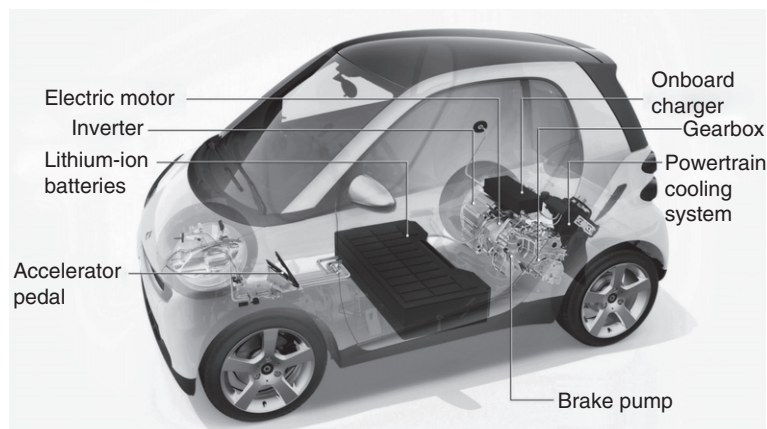


**Figure 22.30** Smart Fortwo Electric Drive: system layout.

thanks to an immediately available 120-Nm torque. A full battery recharge affords—according to manufacturer’s data—a range of 135 km, which is considered more than sufficient for the urban mobility needs.

### 3.3 Mitsubishi i-MiEV

Mitsubishi Innovative Electric Vehicle (i-MiEV) is the result of 40 years devoted by Mitsubishi to the development of electric vehicles; i-MiEV is the first ZEV really available in the Japanese and European markets (Fig. 22.31). It is endowed with an efficient 47-kW permanent magnet synchronous electric motor powered by high energy density Li-ion batteries, and with a lightweight speed reduction gear transmission, which



**Figure 22.31** Mitsubishi i-MiEV.

allows to exploit a typical characteristic of electric motors—high torque at low rpm. Mitsubishi i-MiEV has an official range of 130 km with a single charge. The charge can be made in three different ways: with regenerative braking, by connecting the vehicle to a normal 100–200 V domestic socket, or in a fast charge mode in special high-voltage stations. The system configuration is shown in Fig. 22.32.

In view of the fiftieth anniversary of the foundation of Mitsubishi Motors Corporation, the Japanese Group announced the ‘roadmap’ of Mitsubishi Motors Group Environmental Vision 2020, containing a description of their general principles of an environmental policy destined to maximise the benefits offered by electric vehicles.

### 3.4 PSA Peugeot Citroën–Mitsubishi partnership

Thanks to a partnership agreement in the development of electric vehicles signed by PSA Peugeot Citroën and Mitsubishi, two new electric city cars were developed by the French carmaker: Peugeot iOn and Citroën C-Zero, which will be put on the European market at the end of 2010. Both are based on Mitsubishi i-MiEV's technology.

#### 3.4.1 Citroën C-Zero

The all-electric vehicle developed by Citroën (Fig. 22.33) will be characterised by zero petrol consumed, zero CO<sub>2</sub> emitted, zero noise. It has a permanent magnet synchronous motor that develops 47 kW from 3,000 to 6,000 rpm. The maximum torque reaches 180 Nm, from 0 to 2,000 rpm, and the power is supplied to the rear wheels via a single-speed reduction gear.

The motor is powered by a last-generation Li-ion battery, placed at the centre of the vehicle: 88 50-Ah cells (for a total energy of 16 kWh) provide power at 330 V. The battery can be fully recharged in 6 h with a 220-V socket, whereas an 80% charge is possible in only 30 min using a dedicated station with a single-phase current of 125 A, 400 V, for a maximum power of 50 kW.

The performance of this vehicle (top speed of 130 km/h, from 0 to 100 km/h in nearly 15 s and 60–90 km/h in 6 s) and an asserted range of 130 km in a standard combined cycle allows driving in extra-urban roads as well.

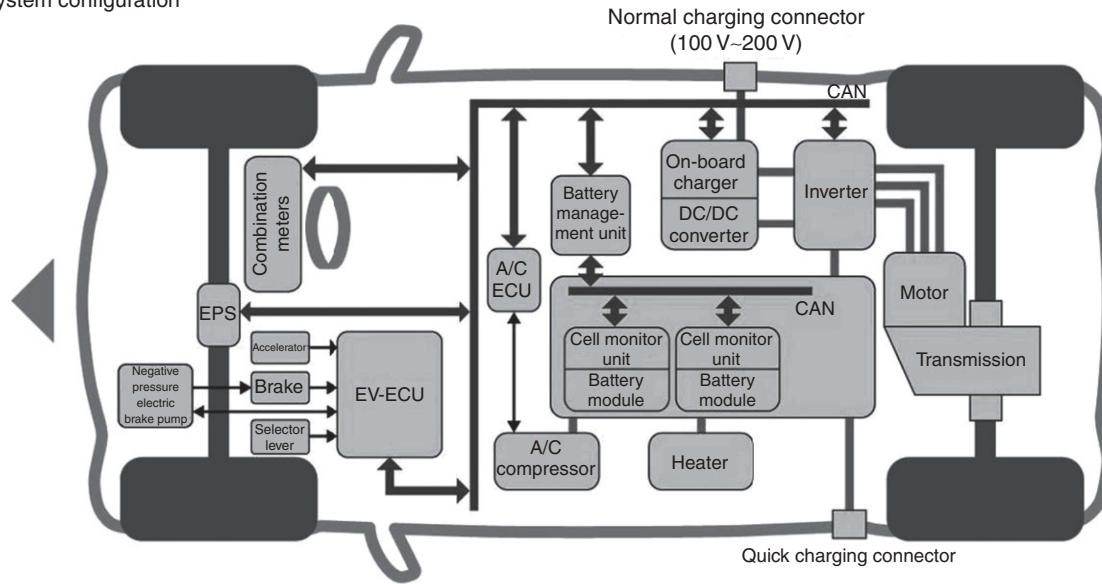
#### 3.4.2 Peugeot iOn

Peugeot iOn (Fig. 22.34), presented at the 2009 Frankfurt Motor Show, represents Peugeot's city-car developed on the basis of Mitsubishi i-MiEV (as Citroën C-Zero) and comes from an agreement between the two carmakers for commercialising the electric vehicle under the brand of Peugeot by the end of 2010.

### 3.5 PSA Peugeot Citroën–Venturi Automobiles agreement

PSA Peugeot Citroën signed an agreement with Venturi Automobiles to produce the electric version of Citroën Berlingo First (Fig. 22.35).

■ EV system configuration



Charging-to-driving process

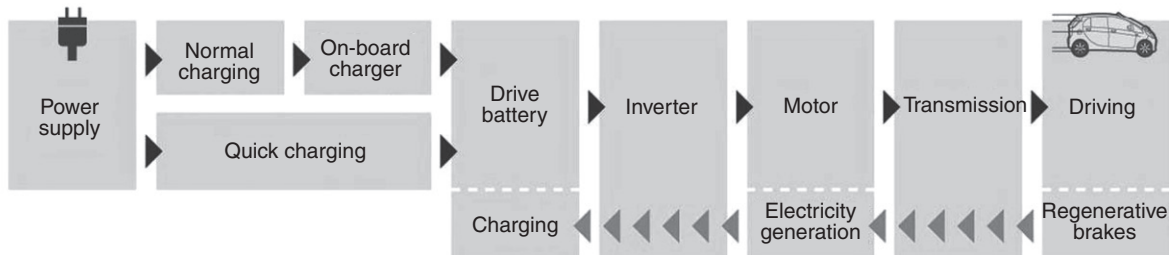


Figure 22.32 Mitsubishi i-MiEV: EV system configuration.



**Figure 22.33** Citroën C-Zero.



**Figure 22.34** Peugeot iOn.

Thanks to the development of a compact powertrain, Berlingo First Electric houses all its electric components (battery, motor + reducer, inverter, charger, DC–DC converter, vacuum pump, electric power steering) in the front bonnet, so replacing the ICE system.

Its commercialisation is scheduled for March 2010 and in the first instance it will meet the demands of fleets of electric vehicles by large companies for carrying out some of their services.

Berlingo First is equipped with 'Zebra for Venturi' (Nickel-sodium chloride) 23.5-kWh batteries allowing a driving range of 100 Km. These high-temperature batteries (270–350 °C) feature a high specific energy (120 Wh/Kg), no maintenance,

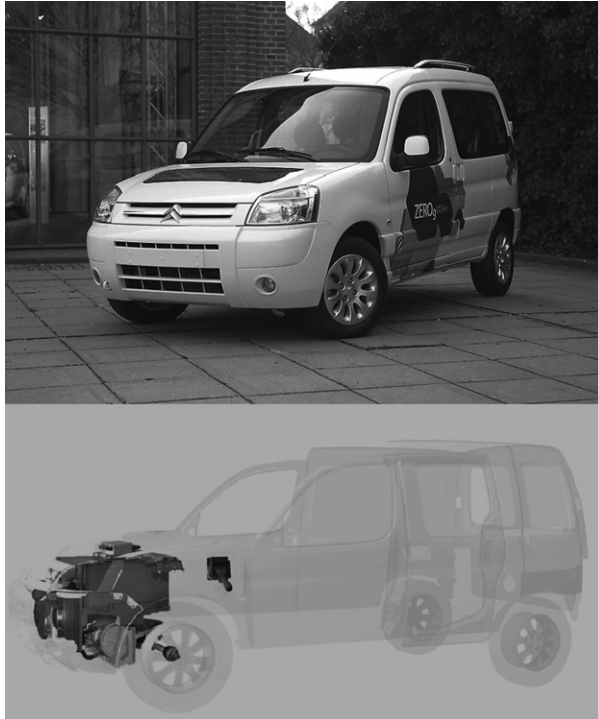


**Figure 22.35** Berlingo First Electric.

no memory effects and an expected life equal to the vehicle's expected life (10 years, 1,000 cycles). The powertrain relies upon a 42-kW asynchronous three-phase motor with a max torque of 180 Nm and a maximum speed of 110 Km/h.

### 3.6 Audi E-tron

Audi E-tron, presented at the 2010 Detroit Auto Show (Fig. 22.36), is a prototype representing an evolution of the electric powertrain sports concept seen at the 2009 Frankfurt Motor show. Compared with the R8 model of September 2009, E-tron is even more compact and lightweight. It is endowed with two asynchronous electric motors supplying over 147 kW in total, with an acceleration time from 0 to 100 km/h <6 s, and a maximum speed limited to 200 km/h in order not to negatively impact on the battery's state of charge.

The range in a mixed driving (according to the NEDC – New European Driving Cycle) is nearly 250 km. Endowed with an energy brake regeneration thanks to the electromechanical brake system, it is powered by a 45-kWh Li-ion battery able to guarantee a driving range up to 250 km in normal conditions. The charging time of a



**Figure 22.36** Audi E-tron.

fully discharged battery is around 11 h (domestic current at 230 V, 16 A), while a high-voltage recharge (400 V, 32 A) lasts nearly two hours.

### 3.7 Fiat 500 BEV

At the 2010 Detroit Auto Show, Fiat presented 500 BEV (Fig. 22.37), the electric version of 500 (ready to enter the US market in its traditional version). Still in its prototype phase, 500 BEV is endowed with the technology that Chrysler developed in the last 3 years within the ENVI project. Technical data on performance and range is not available.

### 3.8 BMW Concept ActiveE – 1-Series Electric

BMW Concept ActiveE is a prototype presented at the 2010 Detroit Auto Show—a zero-emission 1-Series powered by an electric motor (Fig. 22.38).





**Figure 22.37** Fiat 500 BEV.

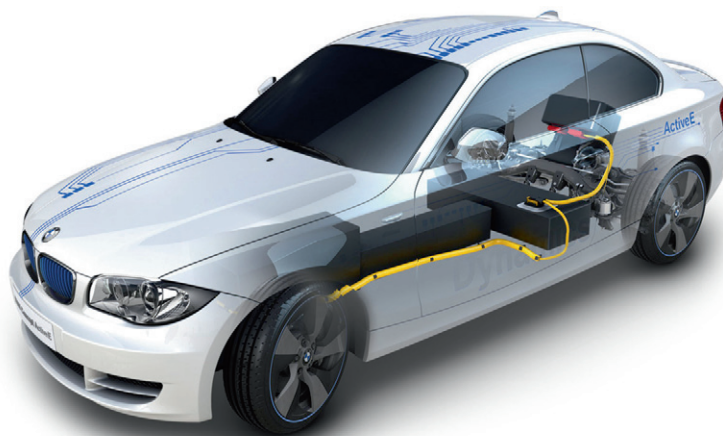


**Figure 22.38** BMW Concept ActiveE: system layout (see color plate 8).



Based on the same principles as MINI E, Concept ActiveE is a front-drive vehicle with a 125-kW electric motor mounted on the rear axle. This vehicle exploits two different Li-ion battery packs, the first in the traditional area of the fuel tank, and the second replacing the engine.

The official acceleration is 0–100 km/h in <9 s, whereas maximum speed is limited to 145 km/h to protect the level of battery charge. The range is 160 km and the batteries are recharged through a normal socket. Fast charge allows having a 'full battery' in 3 h.

### 3.9 MINI E

BMW performed a number of tests on powertrains powered by lithium batteries using a fleet of 500 MINI. The vehicles were directly delivered to customers since March 2009: 250 in South California and 200 in the metropolitan area of New York. The formula adopted provides for an annual leasing agreement that also includes maintenance (both ordinary and extraordinary) and the installation of a recharge station directly in the garage: \$850 per month (nearly €640).

MINI E (Fig. 22.39) is equipped with a 150-kW electric motor having a torque of 220 Nm (8.5 s from 0 to 100 km) powered by a 35-kWh last-generation Li-ion battery able to guarantee a range of nearly 200 km. A full recharge can be done in 2.5 h by connecting the vehicle to a socket provided by BMW – the so-called Wall Box – which can be mounted where the car is usually parked. BMW declares great economic advantages deriving from this vehicle, also considering that the consumption for a full recharge amounts to 28 kWh of current. The maximum speed is electronically limited to 152 km/h.



**Figure 22.39** MINI E: system layout.

A cost estimate comparing a MINI E and a petrol engine MINI underlined that with an average monthly range for both vehicles of slightly less than 2,000 km, the cost for charging MINI E would be lower than 40% compared to the cost of petrol-engine MINI.

Ian Robertson, member of the BoD of the BMW Group, at the 2010 Detroit Auto Show explained the decision of extending the pilot project launched in the United States with a fleet of MINI E put at customers' disposal through the payment of a monthly fee, stating that '*American drivers prefer this solution*'.

This project involved 600 electric vehicles and made them available in Germany, the United States and Great Britain, and within 2010 will also reach France in order to collect data on the economic, behavioural and practical problems connected with the use of electric vehicles.

### 3.10 Ford Focus EV

At the 2009 Frankfurt Motor show, a prototype Focus EV was presented (Fig. 22.40), with which Ford intends to participate in the demonstration programme 'Ultra-Low Carbon Vehicles' in the United Kingdom. Thanks to a research carried out by a consortium including Ford, Scottish and Southern Energy and Strathclyde University, 15 electric prototypes of Ford Focus will be tested to evaluate the suitability of the EV technology for future applications in Europe of Ford cars in daily use.

The Focus electric prototype uses a 100-kW, 320-Nm permanent magnet motor developed by Magna. Focus EV reaches a maximum speed of 136 km/h and is powered by a 23-kWh Li-ion battery pack. Full charge can be achieved with a normal 230-V domestic socket in 6–8 h, thus providing a range of 120 km.

### 3.11 Volvo C30 BEV

Volvo C30 BEV, shown in Fig. 22.41, has an 82-kW electric front motor, which allows the vehicle to reach 130 km/h with 0–100 km/h acceleration in <11 s. The range of 150 km is ensured by the 24-kWh Li-ion battery (data similar to Ford Focus).



**Figure 22.40** Ford Focus EV.



**Figure 22.41** Volvo C30 BEV: system layout.

In this case as well, Volvo's testing aims at collecting indications on the pros and cons of fully electric vehicles, with zero emissions at the exhaust pipe, designed for urban and extra-urban use, besides assessing technical data and how to improve the level of weight, volume and battery charge capacity.

### 3.12 Ape Calessino 2009 Electric Lithium

Ape Calessino is an Italian three-wheel vehicle that has been successfully produced for over 60 years (two million vehicles sold worldwide). Ape Calessino 2009 'Electric Lithium' (Fig. 22.42) is a 'zero environmental impact' electrified powertrain version, made in only 100 units by the Piaggio Group. The heart of the 'green



**Figure 22.42** Ape Calessino 2009 Electric Lithium.

revolution' of Ape Calessino is the electric motor supported by the innovative power system Aenerbox with the last generation of Li-ion batteries. The adoption of this new technology allowed outperforming the previous systems with lead-gel and sodium-nickel batteries in terms of range (75 km), weight, volume and recharging time.

The Aenerbox storage system, in fact, is extremely performing, with a specific power exceeding 500 W/kg (more than doubled compared to the previous systems), which translates into excellent performances through a remarkable weight and volume reduction. Indeed, for the same power, the weight of the new Li-ion batteries is less than one-third that of lead-gel batteries. The recharge times are more than halved; Ape Calessino Electric Lithium can be completely recharged in less than 4 h using a normal 220-V electric network.

The Aenerbox system has a further advantage: when the vehicle is not running, even for a long time, the battery tends to maintain its state of charge; this is a rather important characteristic contributing to battery's longevity. The lifecycle of this battery, in fact, is 15 years (or over 800 recharge cycles amounting to nearly 60,000 km) versus 7–10 years of traditional systems.

### 3.13 Nissan – Land Glider

Nissan has proposed a new model of urban mobility that falls within the concept of zero emissions: Land Glider (Fig. 22.43). This vehicle is developed to be a new city car; the linear acceleration and the narrow bodywork, which are possible only in an ultra-light and ultra-compact EV, allow to relief traffic congestions and to promote an effective use of car parks. A characteristic of this vehicle is the possibility of moving its barycentre through inclination, as it happens when going round a bend with a motorbike, which offers 'different' driving emotions compared to a 4-wheel vehicle, besides a feeling of precision and power.

### 3.14 Rinspeed

Rinspeed, a company specialised in the development of projects in the framework of sustainable mobility, presented during the 80<sup>th</sup> Geneva Motor Show (March 2010), the 'UC' Urban Commuter, an electric concept car (Fig. 22.44). It is a two-seat, 2.5-m vehicle able to reach maximum speeds of 110 km/h with a range of 120 km.

A characteristic of this vehicle is the possibility of being transported (in case of long distances) onboard of a railway carriage, where it can recharge its batteries (through a simple booking on the internet).

'UC' sounds just like 'you see', thus meaning that the zero emission solution exists and anyone can see it.

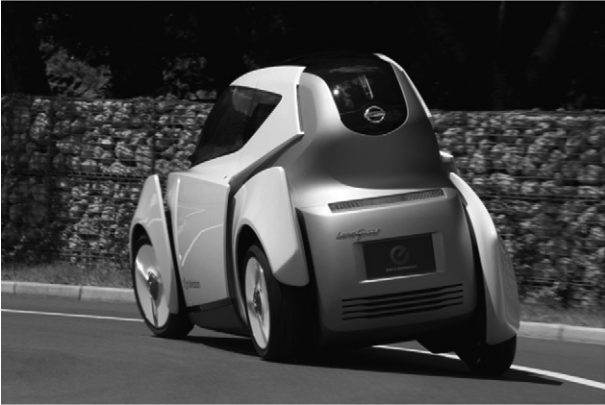


Figure 22.43 Nissan – Land Glider.



Figure 22.44 Rinspeed.



## 4. FUEL CELL HYDROGEN ELECTRIC VEHICLES

On September 2008, the European Parliament adopted a regulation that sets the European rules relating to the homologation of hydrogen vehicles.

The great interest on battery-powered electric vehicles decreased the interest of the large public vis-à-vis hydrogen vehicles. On the one side, this entails some risks, as for instance the possible reduction in terms of efforts and investments by carmakers, by the energy companies potentially interested in producing hydrogen, by the civil society and by the political world. All these stakeholders should concur to the creation of economic and market conditions favouring diffusion of this new fuel. On the other side, the new situation, in which the possible future powered by hydrogen does not receive enough attention, also leads to positive effects: the complex system devoted to the fine-tuning of rules, which presently do not absolutely exist for the production, storage, use and trading of hydrogen, has the opportunity of being shaped. In addition, the development of efficient and reliable solutions for motor vehicles can proceed along an easier situation compared to a few years ago. Expectations appear less pressing, having considered that some even believe the hydrogen technology has already been put aside. In the meantime, the workgroups produce results, the prototypes show more and more interesting performances and economic stakeholders are preparing themselves to become profitably part of the new business.

It is important to note that rules have been issued, at the European level, for the homologation of hydrogen vehicles. In fact, whilst everybody talked about hydrogen, these vehicles did not even exist in regulations, and homologation of a fuel cell car was therefore impossible. The new regulation has bridged this gap.

### 4.1 Honda FCX Clarity

An overview of dates and events linked to the FCX Clarity explains how the project was developed and is going on:

- September 2006: Honda presents the new-generation FCX Concept endowed with the new V-Flow FC Stack, notable for its compact design and high power
- June 2007: First driving tests for Honda FCX Concept in the isle of Gotland (Sweden) by European mass-media
- 14 November 2007: Honda FCX Clarity—characterised by advanced driving performance, high-level comfort and environmental performances, and endowed with an elegant and futuristic design—makes première at the Los Angeles International Auto Show
- 16 June 2008: Ceremony for the launch of the production of the first fuel cell vehicle in the world: FCX Clarity
- November 2008: Honda launches the commercialisation through leasing of FCX Clarity in Japan
- September 2009: The first two FCX Clarity prototypes are available in Europe.

Honda FCX Clarity is a front-drive vehicle, with a 100-kW permanent magnet electric motor (maximum torque, 256 Nm), a 100-kW polymer electrolyte fuel cell stack and 288-V Li-ion batteries (Figs. 22.45–22.47). It has a range of 460 km guaranteed by a full tank of hydrogen (171 l) stored at 350 bar. Its maximum speed is 160 km/h.

Honda FCX Clarity is a vehicle produced in a very small series, with the objective of reaching a total of 200 units put on the road within 2012. The costs of fuel cells, converting onboard hydrogen into electricity, and of the tank are still very high and

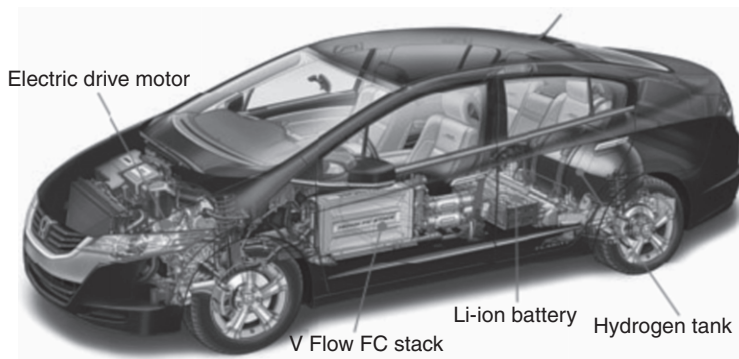


**Figure 22.45** Honda FCX Clarity: system layout.

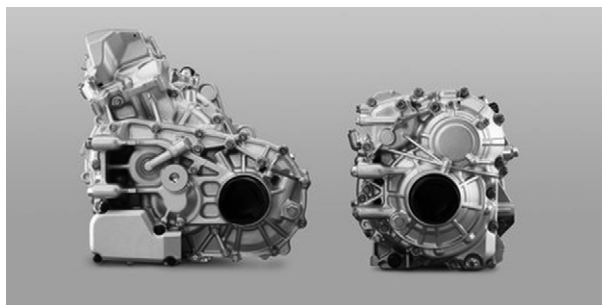


**Figure 22.46** The new Honda FCX Concept transmission (right) and previous generation (left).

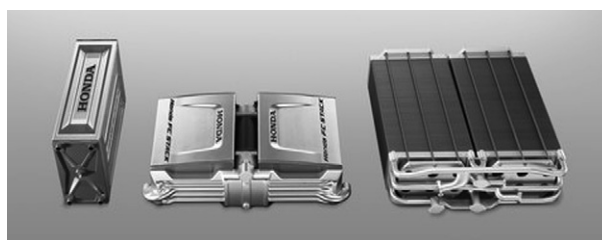


**Figure 22.47** Three generations of the Honda FC stack.



**Table 2** Innovations of hydrogen-powered Honda FCX Clarity

Honda FCX Clarity	Present technology	Possible developments	Short-term market spin-offs
Fuel cells	The 'Vertical flow' technology is exclusive of Honda and allows a great compactness	The present version dates back to 2006. The next generation will be ready within 2012	'V-flow' fuel cells will be put on the market within 2012 as electric generators for remote sites
Electrified powertrain	Small-size coaxial electric motor	The system for motor control and power flows will be integrated	Developed control systems and motors for the next hybrid models
Lithium batteries	The lithium batteries of Clarity outperform supercapacitors	Development of similar batteries also in terms of higher energy capacity and power	High-efficiency and high-capacity lithium batteries for urban electric cars
Hydrogen storage	Pressurised tank at 350 bar	Pressure increase at 700 bar, or tank hybridisation with sponge materials inside	New nanostructured materials for lithium batteries and for onboard materials and components

cannot certainly be lowered unless a potential market of hundreds of thousands of units looms on the horizon. Clarity's technological characteristics are summarised in [Table 22.2](#), along with their effect on the marketable vehicle.

## 4.2 Toyota FCHV-adv

Toyota FCHV-adv is a crossover equipped with a fuel cell system ([Fig. 22.48](#)), presented to the press – with a test-drive – during the G8 meeting in Hokkaido, Japan, in July 2008.

The FCHV-adv is built on the Toyota Highlander platform, which is the previous version. Homologated by the Japanese Ministry of Transports, it is able to start at  $-30^{\circ}\text{C}$  and can rely upon a full tank of hydrogen able to ensure a range of 830 km, more than doubled compared to the previous version: Toyota Highlander, in fact, has a range of 431 km with a full tank of hydrogen. Furthermore, being endowed with a regenerative brake system, it increased its energy efficiency by 25%. It can reach a maximum speed of 155 km/h.

## 4.3 Mercedes-Benz B-Class F-Cell

Mercedes-Benz B-Class F-Cell, shown in [Fig. 22.49](#), has a range of nearly 400 km and, when powered with compressed hydrogen, allows a consumption of about 6.8–7.2 l/100 km in the combined cycle.





**Figure 22.48** Toyota FCHV-adv: system layout.



**Figure 22.49** Mercedes-Benz B-Class F-Cell: system layout.

In a couple of minutes it is possible to store – by anybody, as in a normal self-service station – 4 kg of gaseous hydrogen at 700 bar in the tanks, made with a strong composite material, placed under the car floor. This is made possible by the sandwich-shaped structure of the double-bottom bodywork, which can also allocate the lithium batteries. Compared to the A-Class F-Cell, the range of 177 km at 350 bar is more than doubled.

The 100-kW electric motor is directly connected to the wheels (without interposition of the gear or clutch). The need of being endowed with batteries is linked to their 'buffer' function, since fuel cells, although improved, still need 0.9 s to switch from the rest position to the maximum energy. This time span is not compatible with the driving needs—just think of overtaking—and the battery must intervene. Mercedes' engineers confirm that, besides working on the response time, they also improved the longevity of the polymer membrane. The official time declared amounts to about 2,000 h, corresponding to nearly 70,000 km. Some prototypes also reached 2,800 h without any significant drops, and researches are being developed to make regeneration of the pack possible, in order to keep performances always close to their top. B-Class F-Cell has distance tests for over 100,000 km, but Daimler also has the largest hydrogen fleet in the world that has covered more than 4.5 million km.

In 2010, US and European customers will receive 200 units of F-Cell vehicles in the framework of a special leasing programme.

#### 4.4 Nissan X-Trail

In November 2009 Nissan North America, Inc. (NNA) signed in Sacramento, California, a leasing contract with Sacramento Coca-Cola Bottling Co., Inc., for the long-term renting of an X-TRAIL FCV. Nissan, which has been studying fuel cell technologies since 1996, has already used its FCVs in the framework of demonstration fleets in Japan and California through the California Fuel Cell Partnership (CaFCP), but this is the first commercial leasing of a fuel cell vehicle in North America.

Nissan X-TRAIL FCV (Fig. 22.50) is based on the X-TRAIL SUV commercialised in Mexico, Japan and Europe. It is endowed with a compact fuel cell stack, tuned up by Nissan, a compact Li-ion battery, and a high-pressure cylinder for hydrogen storage. Its

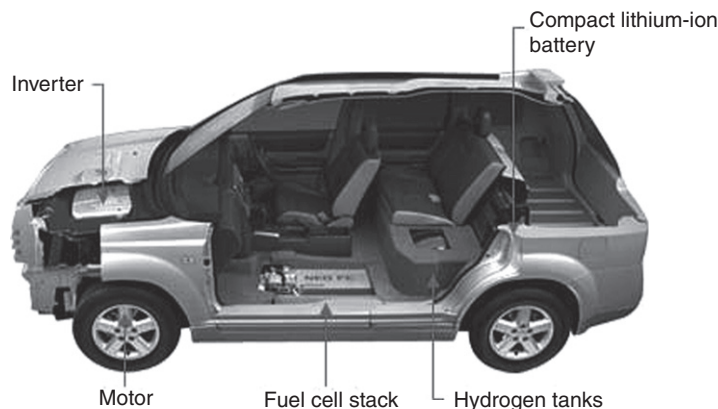


**Figure 22.50** Nissan X-Trail FCV.

performance is similar to that of an ICE of the same size. X-TRAIL FCV exceeds 150 km/h and has a range of over 480 km.



## **5. MULTI-PURPOSE ELECTRIFIED TRACTION PLATFORMS AND ARCHITECTURES, AND AUTO INNOVATION DESIGN**

The correct implementation, and therefore the success, of innovation design depends on a new relationship between style and technology. With the car innovation design, new forms and new concepts of vehicles come to light, based on new technological solutions for power supply, powertrain, drive and connection with the outside world. This is not a design seeking charming forms to dress known technologies, but rather a design that invents new forms and new functionalities, adequate to present and future needs of mobility, comfort and aesthetic appearance. At the same time, technological innovation shall not just follow the development of new solutions to be adjusted in already known forms and proportions; conversely, it must suggest new styles to designers, and even new possible uses of the vehicle led by the technological potential available.

The vehicle that nowadays comes out of an innovation design process moves towards all directions, changes its appearance, function and purpose even during the same day; it can travel alone or lined-up with its 'fellows' in a sort of train that integrates it to public transports. And, most of all, it does not pollute, not even during manufacturing or dismantling, since many components can already be made with entirely recyclable materials.

Two vehicle prototypes, already presented to the large public, are close to this concept: human-oriented sustainable transport (HOST), manufactured by a consortium of nine European companies and Universities led by 'La Sapienza' University of Rome, presented (statically) in a world première during the 2007 edition of H2 Roma, and (dynamically) to the Bologna Motor Show; and Nissan Pivo 2, presented during the 2007 Tokyo Motor Show. Both prototypes, shown in Fig. 22.51, allow to change their direction without making any manoeuvring (HOST rotates on itself, Nissan Pivo 2 makes its cabin rotate), and both have a totally electrified powertrain. HOST is powered by a diesel-electric and lithium-battery system; Pivo 2 is powered by batteries alone and recharged from the electric network.

This section will also provide more details on the Voltec Technology proposed by GM. A vehicle based on this technology is a plug-in, extended range vehicle with an autonomous range of about 500 km, that is, four times that of an electric vehicle.

### **5.1 Host**

HOST is the result of a €3.2-million project (co-financed by the European Commission). The pool working to this project, in the timeframe 2005–2009, comprised nine

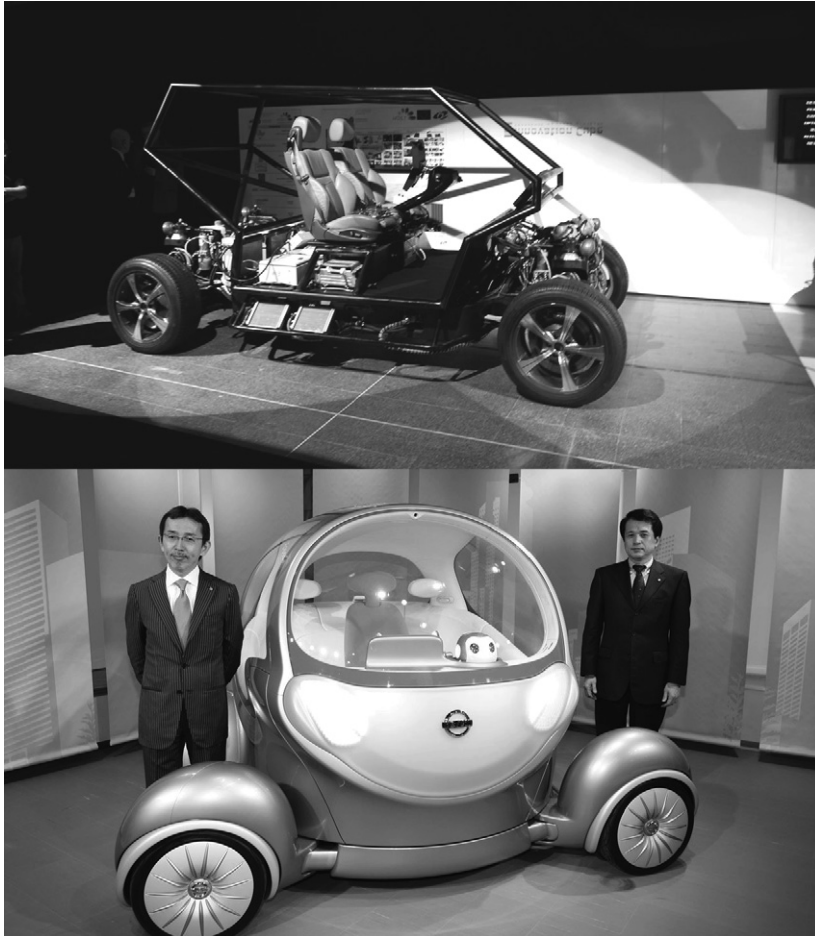


**Figure 22.51** Two innovative vehicles: HOST (up) and Nissan Pivo (down).

European partners of seven EU nations and was coordinated by CIRPS-‘La Sapienza’, University of Rome.

HOST (Fig. 22.52) is an innovative vehicle concept suitable for the urban transport of both persons and goods. To lower the impact of mobility on urban environment, cleaner vehicles must be better than conventional ones under all respects, including costs. To lower such costs, thus really starting up the low polluting vehicles (LPVs) market, the versatility of LPVs has to be enhanced.

HOST aims at developing a fully versatile low-cost LPV concept, where versatility is achieved by making the vehicle modular, and cost reduction is obtained by using the same vehicle for different purposes, simply fitting different cabins to the same chassis.

The main tasks HOST is conceived for are (Fig. 22.53):

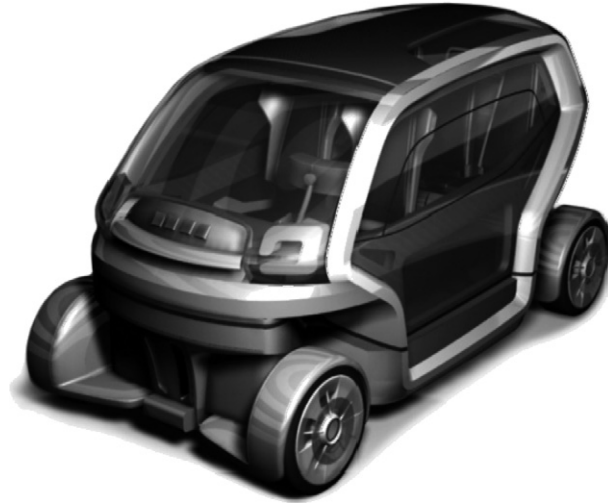


**Figure 22.52** HOST (human-oriented sustainable transport) vehicle.



**Figure 22.53** HOST: four services for one chassis (see color plate 9).

- Nighttime collective taxi
- Daytime car-sharing services
- Daytime freight collection and distribution
- Nighttime garbage collection.

The four services above are not the only ones HOST may be used for, but are those for which it is specifically studied. Such choice is based on the fact that these tasks belong to the same family of 'municipal services'.

Using the same chassis to operate all the different services is feasible and can create the critical mass of final users that allow price reduction. The four services chosen, two addressing passenger mobility and two addressing freight mobility, all aim at reducing

urban mobility impact. Car sharing and nighttime collective taxi systems, if integrated with public transport, can increase HOST's attractiveness, thus pushing more people to use it.

Freight pick-up and delivery and garbage collection may be re-organised and become more sustainable if a low-pollution alternative, such as the one proposed by HOST, is made available.

The powertrain layout and the possibility of easily varying the platform's main dimensions enable HOST to be equipped with very different bodyworks, thus allowing the car manufacturer to provide both private and public bodies, such as municipalities or urban mobility authorities. In more detail, the energy system is all included in the HOST platform and is conceived in shaped boxes, so that its modules become interchangeable.

HOST has a series hybrid configuration (Fig. 22.54) and its ICE is coupled with an energy recovery system (batteries + supercapacitors). It is already designed for utilising hydrogen fuel cells by just changing the energy module (and the tank), this being the final purpose of the concept design. Thanks to these two solutions, HOST is able to run as a ZEV for a limited period of time (with ICE) or for the whole driving cycle (with fuel cells).

A full drive-by-wire solution is adopted and the only mechanical connection between the cabin and the platform will be a specifically designed mechanical anchorage, this solution allowing the easy installation/removal of any cabin.

The vehicle has 4-wheel drive capability (4WD), thus featuring a good grip even on slippery roads. The four electric motors (one per wheel) allow an easy traction control, ensuring stability and safety. The chassis has a 4-wheel total steering (4WS) configuration that enables the vehicle to rotate around its vertical axis as well as to shift laterally (Fig. 22.55). These characteristics give HOST decisive advantages in the missions it has been conceived for.

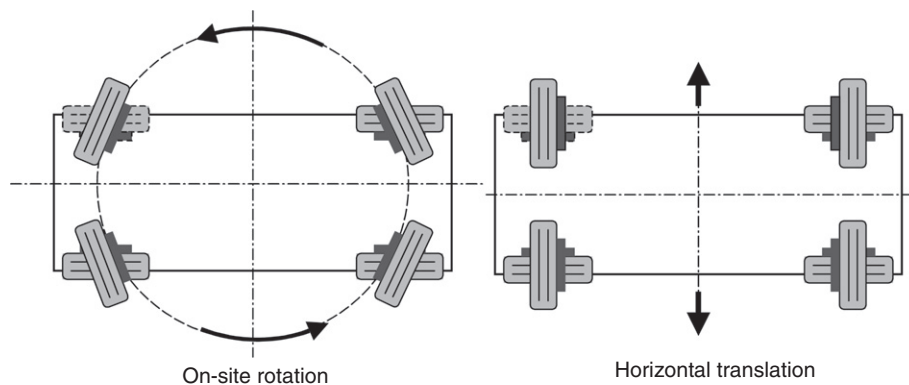


**Figure 22.54** HOST: four-wheel drive capability.



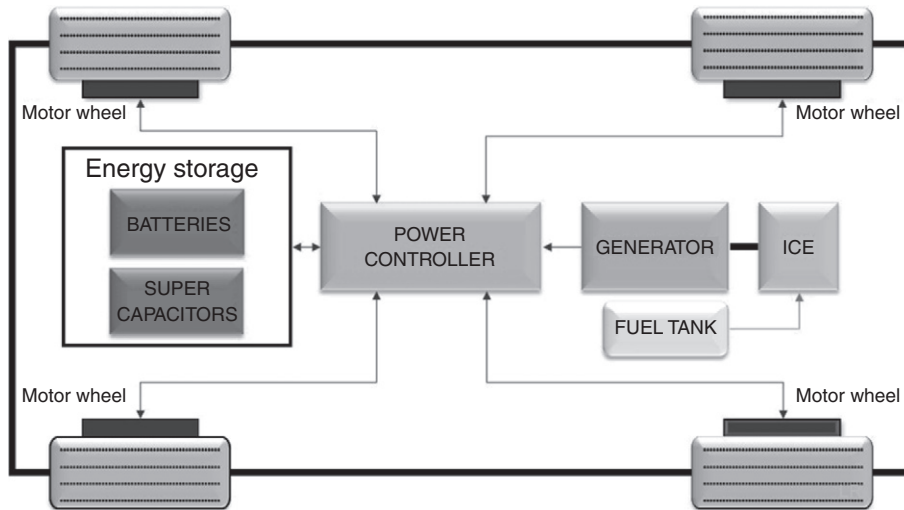


**Figure 22.55** HOST: system layout.

The 4WS capability endows the vehicle with easy manoeuvring in narrow streets in the cities centres, and it is useful for an accurate positioning of trucks during freight loading/unloading operations and while they run as garbage collectors.

HOST's powertrain features can be summarised as

- Batteries plus ultracapacitors
- ZEV range
- MIMOPEC (multi input multi output power energy control)
- Series-hybrid
- Plug-in
- Drive-by-wire.

Chassis features are

- 4-Wheel drive
- 4-Wheel steering (docking)
- Transhipment predisposition
- From city car to trucks.

HOST was also on exhibition, in 2009, at the Future Science Museum – The Miraikan of Tokyo (Fig. 22.56).

## 5.2 General motors' Voltec technology

All 'historic' car manufacturers are faced with a choice: targeting on the maximum enhancement of today's models and technologies, trying to highlight their environmental strengths and advances compared to past models, or working to speed up the

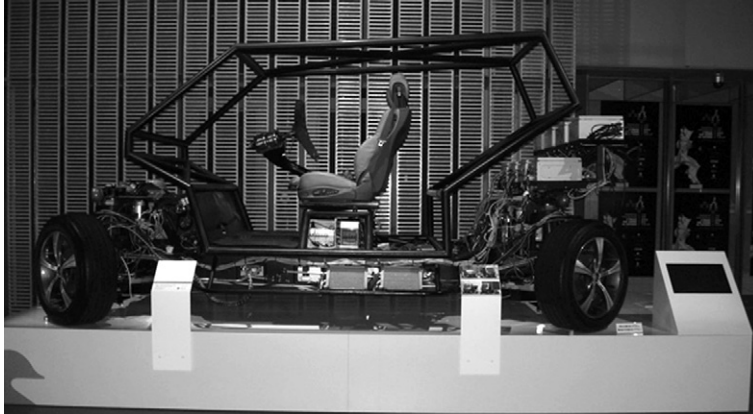


**Figure 22.56** HOST at the Future Science Museum – the Miraikan of Tokyo.

availability on the market of new technologies, able to achieve higher driving efficiency and even the long-awaited zero emissions.

The GM group, dealing with a difficult economic and organisational restructuring at a global level, has a key project for its future, strongly and continuously advertised since 2008, i.e. the Voltec Technology. This project was formerly known as E-Flex system or, more simply, Volt – the first prototype that was equipped with it (see Section 2.4).

The Voltec technology was first unveiled in Russelsheim, at the Opel research and development centre. The definition of E-REV was used by GM to indicate its future extended range electric vehicle, based on a hybrid-series system. As is well known, in hybrid-series, batteries provide a certain range, and a combustion engine acting as a current generator allows extending this range far beyond the capacity of accumulators alone. Indeed, the range in all-electric mode is rather penalised (~60 km max for Volt), although the total efficiency is excellent and emission of polluting substances is limited.

After approximately 60 km, a small (1.4l) petrol engine creates electricity on-board using a 53-kW generator to extend the Volt's range to about 500 km. The electrical power from the generator is sent primarily to the electric motor, while the excess goes to the batteries, this depending on their state of charge and the power demanded at the wheels. The energy supplied by the petrol engine is entirely converted into electricity and the car's powertrain continues to be all electric. Regenerative braking will also contribute to create electricity.

This choice for the Voltec system is therefore entirely new for a car destined to series production, and is aimed at maximising the electric range that batteries are able to guarantee with a domestic recharge usually made overnight. A range of approximately 500 km with a full tank of petrol (or ethanol E85) is reassuring. This allows the driver to overcome the 'range anxiety' that a driving depending on the battery charge would generate, and corresponds to the GM experience gained with the very short



period of commercialisation of the first electric vehicle, EV1, during the 1990s in California.

The future Chevrolet Volt and Opel Ampera (described in Section 2.4) will be commercialised, as scheduled, in 2010 in the United States and from 2011 in Europe.



## 6. CONCLUSIONS

The ways out of the oil dependence are manifold. Vehicles can use other fuels (LPG, methane, biofuels) and energy vectors (electricity, hydrogen) not necessarily produced from petroleum.

Very soon there will be a number of proposals to supply vehicles with LPG (gas mixture also obtainable from non-oil sources, although at present mainly derived from petroleum refining process) and methane (now made by almost all manufacturers). As far as biofuels are concerned, on the contrary, bioethanol and biodiesel, able to play an important role for the reduction of petroleum dependency, need clear and long-term strategies to favour their diffusion. The economic cost is high, and the use of lands for the cultivation of plants necessary for their production is challenging.

The new entry in the world of vehicles 'that really matter' is electricity—just look at (a) the pilot projects by the main automakers all over the world; (b) new brands; (c) vehicles ready for the market in all motor shows. And hydrogen fuel cell-powered vehicles, which in the public opinion had a slight drop from their forefront position in favour of battery powered vehicles, are still the subject of continued applied research and testing. The expectation of a large diffusion of electric vehicles could in fact lead to reconsider hydrogen fuel cells as one of the solutions for these vehicles in the next decades.

Chances for hydrogen fuel cells will not be substantial before around 2015. The hydrogen architecture will probably hybridise the battery-powered electric system with a stack of fuel cells and a tank, thus allowing an extension of the range compared to battery-powered electric vehicles. The electricity produced by fuel cells will be supplied to the batteries or the electric motor (according to the different configurations and needs), while releasing in the process water vapour only.

There are now many solutions, ready to enter the market, for consumption reductions. All brands have, or will have, some clearly identified low-consumption product lines. The main systems so far adopted to cut consumption include the stop&start system, the brake energy regeneration and the hybrid architecture with heat engine—batteries—electric motor. In the next decade many car manufacturers will put on the market all-electric vehicles endowed with lithium batteries, and other completely new manufacturers will start to operate on the market.

ZEVs are feasible and in the year 2010 they will also be on the road, besides being the subject of massive testing. An all-electric traction can be obtained in different ways, with

different architectures that range from full-hybrid configurations, allowing driving in electric mode for short ranges, to solutions with electric batteries and motor, up to the adoption of electric systems with the double possibility of supplying onboard electricity from both hydrogen-powered fuel cells and batteries.

ZEVs will be increasingly available, although with a slow initial pace. This green revolution is bound to continue, especially at the high levels of car hierarchy, involving models at the top of the range.

# Appendix



## 1. SELECTED REFERENCES FOR TOPICS NOT SPECIFICALLY TREATED IN THIS BOOK (TO JANUARY 2010)

### Incentives for Hybrid and Electric Vehicles

US DOE, Alternative Fuels & Advanced Vehicles Data Center, “Hybrid Electric Vehicle Incentives and Laws”; “Plug-In Hybrid Electric Vehicle Incentives and Laws”; “Hydrogen and Fuel Cell Vehicle Incentives and Laws”; “Electric Vehicle Incentives and Laws”.

Wikipedia, Electric Vehicle (Incentives and Promotion), (accessed December 2009).

Labour's £5,000 Sweetener to Launch Electric Car Revolution, Guardian.Co.UK, 16 April 2009.

G. Passier, H. Driever, Early Market for Electric Mobility: Possible Win-Win for 4 Major Stakeholders, 24th Electric Vehicle Symposium, EVS-24, Stavanger, Norway, May 2009.

D. Taylor, Plugging in to an Electric Transportation Future: Existing Federal Incentives, Plug-in 2008, San José, CA, USA, July 2008.

D. Taylor, Up-Front Cost versus Life-Cycle Cost Dilemma, California Electric Fuel Implementation Strategies (CEFIS) Workshop, Berkeley, CA, USA, November 2008.

M. Thornton, Vehicle Modeling and Simulation, DOE Vehicle Technologies Program Overview of DOE Vehicle Modeling and Simulation R&D, Bethesda, Maryland, USA, February 2008.

N. Lutsey, D. Sperling, America's bottom-up climate change mitigation policy, Energy Policy 36 (2008) 673.

B.D. Yacobucci, Alternative Fuels and Advanced Technology Vehicles: Issues in Congress, CRS Report for Congress, July 2006.

F. Joseck, U.S. Government's Role Towards Sustainable Transportation, 24th Electric Vehicle Symposium, EVS-24, Stavanger, Norway, May 2009.

D. Pedelmas, Electric Vehicles. Challenges and Status, 4th International Conference Enertech '09, October 2009, Athens, Greece.

## Buses and Trucks

- R. Barnitt, Case Study: Ebus Hybrid Electric Buses and Trolleys, Technical Report NREL/TP-540-38749, July 2006.
- R. Barnitt, In-Use Performance Comparison of Hybrid Electric, CNG, and Diesel Buses at New York City Transit, 2008 SAE International Powertrains, Fuels & Lubricants Conference, Shanghai, China, June 2008.
- R. Barnitt, BAE/Orion Hybrid Electric Buses at New York City Transit. A Generational Comparison, Technical Report NREL/TP-540-42217, Revised March 2008.
- J.S. Campbell, D.B. Kittelson, Superbus Phase I: Accessory Loads Onboard a Parallel Hybrid-Electric City Bus, Center for Transportation Studies, University of Minnesota, Final Report 01/08, August 2009.
- L. Callaghan, S. Lynch, Analysis of Electric Drive Technologies for Transit Applications: Battery-Electric, Hybrid-Electric, and Fuel Cells, U.S. Department of Transportation, Federal Transit Administration, Final Report, August 2005.
- U.S. Department of Transportation, Federal Transit Administration, Transit Research Update January-February 2009.
- M.J. Kellaway, Hybrid Buses – What their batteries really need to do, *J. Power Sources* 168 (2007) 95.
- K. Chandler, K. Walkowicz, L. Eudy, NYCT Diesel Hybrid-Electric Buses: Final Results, DOE/NREL Transit Bus, Evaluation Project, July 2002.
- S.B. Han, et al., Fuel economy comparison of conventional drive trains with series and parallel hybrid electric step vans, *Int. J. Automotive Technol.* 10 (2009) 235.
- International Energy Agency (IEA), Status Overview of Hybrid and Electric Vehicle Technology (2007), Final Report Phase III, Annex VII, IAHEV, IEA, December 2007.
- Current (Electric Transportation, Southern California Edison), Vol. 8, Issue 3, Winter 2003.
- N. Omar, Effectiveness Evaluation of a Super Capacitor-Battery Parallel Combination for Hybrid Heavy Lift Trucks, 24th Electric Vehicle Symposium, EVS-24, Stavanger, Norway, May 2009.
- Y. Chang, Hybrid Drives Design for Minibus by Simulation, 24th Electric Vehicle Symposium, EVS-24, Stavanger, Norway, May 2009.
- E. Tazelaar, Driving Cycle Characterization and Generation for Design and Control of Fuel Cell Buses, 24th Electric Vehicle Symposium, EVS-24, Stavanger, Norway, May 2009.
- M. Hairr, Data Acquisition System for Electric- and Hybrid-Electric Buses, 24th Electric Vehicle Symposium, EVS-24, Stavanger, Norway, May 2009.
- L. Cheng, Study on Intelligent Control System of Pure Electric Bus Based on the Fuzzy Decision Theory, 24th Electric Vehicle Symposium, EVS-24, Stavanger, Norway, May 2009.

- W.Z. Po, Study on Operation System of Pure Electric Bus, 24th Electric Vehicle Symposium, EVS-24, Stavanger, Norway, May 2009.
- Q. Bin, A Study on Energy Efficiency of Fuel Cell Bus Under Transit Cycle, 24th Electric Vehicle Symposium, EVS-24, Stavanger, Norway, May 2009.
- R. Barrero, Hybrid Buses: Defining the Power Flow Management Strategy and Energy Storage System Needs, Electric Vehicle Symposium, 24th EVS-24, Stavanger, Norway, May 2009.
- J. Halme, Power Bus Control for Series Hybrid Heavy-Duty Vehicles, 24th Electric Vehicle Symposium, EVS-24, Stavanger, Norway, May 2009.
- G.-H. Tzenga, C.-W. Lina, S. Opricovic, Multi-criteria analysis of alternative-fuel buses for public transportation, *Energy Policy* 33 (2005) 1373.
- C.-C. Lin, S. Jeon, H. Peng, J. M. Lee, Driving Pattern Recognition for Control of Hybrid Electric Trucks. [www.personal.umich.edu/~hpeng/VSD\\_from\\_AVEC\\_DPR.pdf](http://www.personal.umich.edu/~hpeng/VSD_from_AVEC_DPR.pdf)
- T.A.C. van Keulen, A.G. de Jager, A.F.A. Serrarens, M. Steinbuch, Optimal energy management in hybrid electric trucks using route information, *Oil Gas Sci. Technol.* 65 (2010) 103.
- L. Callaghan Jerram, 2008 Bus Survey, Fuel Cell Today, December 2008. [www.fuelcelltoday.com/.../survey?...2008-12%2F2008-Bus](http://www.fuelcelltoday.com/.../survey?...2008-12%2F2008-Bus)

### **Individual Mobility (Scooters and Bikes)**

- F. Jamerson, Electric Bikes Worldwide Reports 2009 (EBWR09), Electric Bicycle Battery Company, Naples, Florida/Petoskey, Michigan, April 2009.
- U.N. Schwegler, Electric Scooters: Technologies and Markets, 24th Electric Vehicle Symposium, EVS-24, Stavanger, Norway, May 2009.
- R. Widmer, Developing a Simple Test Method to Compare the Mileage of E-Scooters, 24th Electric Vehicle Symposium, EVS-24, Stavanger, Norway, May 2009.
- J.-M. Timmermans, A Comparative Study of 12 Electrically Assisted Bicycles, 24th Electric Vehicle Symposium, EVS-24, Stavanger, Norway, May 2009.
- U. Schwegler, Political Support for E-Scooters, 23rd Electric Vehicle Symposium, EVS-23, Anaheim, CA, USA, December 2007.
- K.-B. Sheu, Simulation for the analysis of a hybrid electric scooter powertrain, *Appl. Energy* 85 (2008) 589.
- Karl T. Ulrich, Estimating the technology frontier for personal electric vehicles, *Transport. Res. Part C* 13 (2005) 448.
- J. X. Weinert, A. F. Burke, X. Wei, Lead-acid and lithium-ion batteries for the chinese electric bike market and implications on future technology advancement, *J. Power Sources* 172 (2007) 938.
- J. Weinert, J. Ogden, D. Sperling, A. Burke, The future of electric two-wheelers and electric vehicles in china, *Energy Policy* 36 (2008) 2544.

Y. Chou, C. Sun, M. Lee, P. Tseng, B. Lin, A Uniformly Full-charging Scheme for Multi-cells Li-ion Battery Packs of Electric Bikes, 22nd Electric Vehicle Symposium, EVS-22, Yokohama, Japan, 2006.

### City Cars (Neighborhood Electric Vehicles)

International Energy Agency (IEA), Clean Vehicle-Award: Ceremony at the EVS-24; the Personal Awards: S.V. Jensen, Stavanger, Norway, May 2009.

THINK Electric Car – The All Electric and Highway Safe Think City. [www.think.no/2009 THINK City – Electric Car](http://www.think.no/2009%20THINK%20City%20-%20Electric%20Car). <http://alternativefuels.about.com/.../electricvehicles/...electric-cars-/2009-th-nk-city-electric-car.htm>

Green Car Congress: Battery/Ultracapacitor System for Small Electric Vehicles. [www.greencarcongress.com/.../batteryultracapacitor-system-for-small-electric-vehicles.html](http://www.greencarcongress.com/.../batteryultracapacitor-system-for-small-electric-vehicles.html)

Agreement Between PSA and Mitsubishi on Electric Cars. [www.h2roma.org/.../agreement\\_between\\_psa\\_and\\_mitsubishi\\_on\\_electric\\_cars](http://www.h2roma.org/.../agreement_between_psa_and_mitsubishi_on_electric_cars)

J. Francfort, M. Carroll, US DOE's Field Operations Program. Neighborhood Electric Vehicle Fleet Use, INEEL Report, July 2001.

NEVs. [www.evfinder.com/NEVs.htm](http://www.evfinder.com/NEVs.htm)

Inhabitat. Robot-Equipped Electric Eco Car: Nissan Pivo 2. [www.inhabitat.com/.../transportation-tuesday-robotic-eco-nissan-pivo-2/](http://www.inhabitat.com/.../transportation-tuesday-robotic-eco-nissan-pivo-2/)

J. Francfort, L. Slezak, US DOE's Field Operations Program. Electric and Hybrid Vehicle Testing, INEEL Report, 2002.

D. Karner, J. Francfort, Hybrid and plug-in hybrid electric vehicle performance testing by the US department of energy advanced vehicle testing activity, J. Power Sources 174 (2007) 69.

Wikipedia, Neighborhood Electric Vehicle (accessed December 2009).

Department Of Transportation (DOT), National Highway Traffic Safety Administration, 49 CFR Part 571, Federal Motor Vehicle Safety Standards, June 1998.

Chrysler's Huggable 2009 GEM Peapod Debuts. [www.insideline.com/.../gem/chryslers-huggable-2009-gem-peapod-debuts.html](http://www.insideline.com/.../gem/chryslers-huggable-2009-gem-peapod-debuts.html)

ExxonMobil/Electrovaya's Electric Car, the Maya 300. [www.green.autoblog.com/.../exxonmobil-electrovayas-electric-car-the-maya-300-gets-detail/](http://www.green.autoblog.com/.../exxonmobil-electrovayas-electric-car-the-maya-300-gets-detail/)



## 2. FURTHER READING ON RECHARGING NETWORKS AND MARKET ISSUES (TO JANUARY 2010)

### Recharging Networks

R. Winkel, M. Notenboom, Cost Effective Introduction of Electric Vehicles, 24th Electric Vehicle Symposium, EVS-24, Stavanger, Norway, May 2009.

- J. A. Peças Lopes, F. J. Soares, P. M. Almeida, M. Moreira da Silva, Smart Charging Strategies for Electric Vehicles: Enhancing Grid Performance and Maximizing the Use of Variable Renewable Energy Resources, 24th Electric Vehicle Symposium, EVS-24, Stavanger, Norway, May 2009.
- Report on Electric Vehicle Charging 2009-06-22. <http://vancouver.ca/ctyclerk/documents/penv3.pdf>
- E. Kjaer, What is SCE Going to Prepare and What Needs to Be Done Now?... By Utilities, Grid Operators and Government, 24th Electric Vehicle Symposium, EVS-24, Stavanger, Norway, May 2009.
- E. Kjaer, Integrating Transportation into a Changing Utility System. [www.pjm.com/.../kjaer-electrifying-presentation-role-of-the-electricity-sector.ashx](http://www.pjm.com/.../kjaer-electrifying-presentation-role-of-the-electricity-sector.ashx)
- C. Bleijs, Charging Infrastructure for Electric Vehicles and PHEVs, IEC TC69, Standards for EV, London, October 2008.
- C. Bleijs, Utility Perspective: Understanding the Key Issues Faced by Utilities for Plug-In Hybrids and Electric Vehicles, Enabling Electric+Hybrid Vehicle Market 2008, Detroit, MI, USA, May 2008.
- K. Nansai, S. Tohno, M. Kono, M. Kasahara, Y. Moriguchi, Life-cycle analysis of charging infrastructure for electric vehicles, Appl. Energy 70 (2001) 251.
- G. Cullen, International Perspectives on Market Issues and Supportive Policies: Current State of U.S. Initiatives, PHEV '09, Montreal, Canada, September 2009.
- T. Anegawa, Desirable Characteristics of Public Quick Charger, PHEV '09, Montreal, Canada, September 2009.
- D. Pedelmas, Electric Vehicles. Challenges and Status, 4th International Conference Enertech '09, October 2009, Athens, Greece.
- H. Gerbracht, Implications of E-Mobility for the Energy System, Smart Grids Conference Salzburg 09, Salzburg, Austria, May 2009.
- C. Wittwer, Bi-Directional Grid-Integration of E-Vehicles with New Smart Metering Systems, Fleet Test of VW-Eon, Smart Grids Conference Salzburg 09, Salzburg, Austria, May 2009.
- C. Leitinger, Power Requirement and Charge Strategies of E-Mobility for Future Energy Systems, Smart Grids Conference Salzburg 09, Salzburg, Austria, May 2009.
- F. Heider, M. Büttner, J. Link, C. Wittwer, Vehicle to Grid: Realization of Power Management for the Optimal Integration of Plug-In Electric Vehicles into the Grid, 24th Electric Vehicle Symposium, EVS-24, Stavanger, Norway, May 2009.
- R. Horbaty, Plug-In Vehicles and Smart Grids: From Simple Charging at Home to Grid Regulating Ancillary Services, IAMF-2009, Geneva, Switzerland, 2009.
- Coulomb Technologies Announces New Smart Charging Infrastructure for Plug-In Vehicles, Campbell, CA, USA, July 2008.

- P. H. Andersen, J. A. Mathews, M. Rask, Integrating private transport into renewable energy policy: the strategy of creating intelligent recharging grids for electric vehicles, *Energy Policy* 37 (2009) 2481.
- Efrain Ornelas, PHEV Infrastructure: Smart Charging, Vehicle to Home and Future Vehicle to Grid, AFVi PHEV Workshop, Las Vegas, Nevada, USA, May 2008.
- E. Kjaer, Future of Transportation...It's Electrifying, July 2006. [www.scag.ca.gov/rcp/ewg/presentations/EdKjaerPresentation.pdf](http://www.scag.ca.gov/rcp/ewg/presentations/EdKjaerPresentation.pdf)
- D. Tuttle, N. Johns, P. Sivaraman, K. Houlihan, J. Serface, The grid-connected vehicle primer, CleanTX Forum on Grid-Connected Vehicles, Austin, TX, USA, September 2007.
- P. Clasquin, M. Kierk, 365 Energy Group Fueling Electric Transportation, Düsseldorf, February 2009. [www.energieregion.nrw.de/\\_database/\\_data/.../090224-12\\_365\\_Energy.pdf](http://www.energieregion.nrw.de/_database/_data/.../090224-12_365_Energy.pdf)
- P. Clasquin, Changing the Way People Move, Frost & Sullivan's Workshop on Electric Vehicles, London, UK, June 2009.
- B. Daniel, Electric Vehicle Infrastructure and Emergence of Key Business Models, Frost & Sullivan's Workshop on Electric Vehicles, London, UK, June 2009.
- K. Clement, Analysis of the Impact of Plug-In Hybrid Electric Vehicles on the Residential Distribution Grids by Using Quadratic and Dynamic Programming, 24th Electric Vehicle Symposium, EVS-24, Stavanger, Norway, May 2009.
- P. Clasquin, The Need for a Smart Charging Infrastructure, 24th Electric Vehicle Symposium, EVS-24, Stavanger, Norway, May 2009.
- K. J. Dyke, Analysis of Electric Vehicles on Utility Networks, 24th Electric Vehicle Symposium, EVS-24, Stavanger, Norway, May 2009.
- Electric Vehicle Plug-In Charging Stations – Coulomb Technologies. [www.coulombtech.com/products.php](http://www.coulombtech.com/products.php)
- Renault-Nissan, EDF in Electric Car Partnership. [cleantech.com/.../renault-nissan-edf-electric-car-partnership](http://cleantech.com/.../renault-nissan-edf-electric-car-partnership)
- Wiring Wars: The Race to Charge the World's EVs Industry. [bnet.com/.../wiring-wars-the-race-to-charge-the-worlds-evs/](http://bnet.com/.../wiring-wars-the-race-to-charge-the-worlds-evs/)
- Toyota Large-Scale Demonstration of Plug-in Hybrid Vehicles in France. [www.gizmag.com/toyota-large-scale.../11288/](http://www.gizmag.com/toyota-large-scale.../11288/)
- EDF Energy Working Together with Elektromotive Ltd. [www.edfenergy.com/elektromotive/](http://www.edfenergy.com/elektromotive/)
- E.On Utility – Autoblog Green. [Green.autoblog.com/tag/e.on+utility/](http://Green.autoblog.com/tag/e.on+utility/)
- Better Place | The Global Provider of Electric Vehicle Services. [www.betterplace.com/company/](http://www.betterplace.com/company/)
- Daimler, RWE to Roll out Electric Cars in Berlin. [www.dw-world.de/dw/article/0,,3621836,00.html](http://www.dw-world.de/dw/article/0,,3621836,00.html)
- ENEL and Daimler e-Mobility Italy. [theirearth.com/index.../enel-and-daimler-e-mobility-italy](http://theirearth.com/index.../enel-and-daimler-e-mobility-italy)



## HEV/EV Market

- C. Pillot (Avicenne), Electric, PHEV & Hybrid Vehicle Trends & Impact on the Battery Market, 24th Electric Vehicle Symposium, EVS-24, Stavanger, Norway, May 2009.
- HIEDGE Institute, Hybrid Vehicle Market Report. [hiedge.co.jp/dm/HEV2009W](http://hiedge.co.jp/dm/HEV2009W)
- HIEDGE Institute, Electric Vehicle Market 2009. [hiedge.co.jp/EV2009](http://hiedge.co.jp/EV2009)
- Yole Developpement, SiC'08 Silicon Carbide Market: from Material to Systems, December 2007.
- Darnell Group, Vehicle Electrification: Worldwide Forecasts, February 2009.
- Freedonia Group, World Light Hybrid-Electric Vehicles, October 2006.
- Paumanok Publications, Hybrid Electric Vehicle Production Forecasts: 2006–2015, July 2006.
- Research and Markets, 2009 Report on Global and China's Electric-Vehicle (EV) Markets.
- H. Takeshita, Worldwide Market Update on NiMH, Li Ion and Polymer Batteries for Portable Applications and HEVs, 26th International Battery Seminar & Exhibit, Fort Lauderdale FL, USA, March 2009.
- Frost & Sullivan, World HEV/PHEV Battery Market, 2008. [www.reportbuyer.com/samples/027641e0f1b4ebedd4ce869cddc7843b.pdf](http://www.reportbuyer.com/samples/027641e0f1b4ebedd4ce869cddc7843b.pdf)
- Frost & Sullivan, EV Study List, October 2009. (This list contains 14 reports by Frost and Sullivan, from December 2007 to September 2009, on HEVs, EVs, and related infrastructure).

# INDEX

## A

### Alternative vehicles

- comparison with conventional vehicles, 4*t*, 6*t*, 10*t*, 12*t*
  - specific vehicles on the market, 2–3
- electric, 2–3
- environmental impact criteria, 5
  - GHG and AP emissions, 5
- hybrid, 2–3, 7, 11
- hydrogen in ammonia-fueled vehicle, 2–3
- hydrogen fuel cell, 2–3
- hydrogen internal combustion, 2
- normalization and the general indicator, 10
- technical and economical criteria, 3
- see also specific vehicles*

## B

### Batteries

- aging, **214–224**, **310–324**, **376–396**
  - accelerated, 383
  - calendar life, 312–313
  - capacity fade, 217–218, 220–222
    - with different charging scenarios, 220
  - electrode reactions, 312
  - life-cycle, 385, 386*f*, 393
  - models, 217, 313
  - resistance growth, 217, 220–224, 391, 396
    - with temperature, 313, 396
- electric vehicles, 329
- for HEVs, 319
  - Li-ion battery safety, **463–492**
- impact of different technologies on the environment, 357
- LCA (life cycle assessment), 348
- life modeling, 214
- management for electric traction vehicles, **493–513**
  - management systems, 500
    - architectures, 505
    - balancing, 504
    - calculating, 502
    - communicating, 503
    - connection sequence, 507
    - control, 503
    - current interruption fail-safe switches, 507

- examples, 509
- isolation breakdown detection, 506
- leakage detection, 506
- measuring, 501
- monitoring, 500
- self-diagnostics, 507
  - system voltage and current maximums, 508
- performance in electric and hybrid vehicle
  - operation, **375–404**
    - battery pack modeling, 398
    - field test data collection and analysis, 378
    - laboratory battery tests, 382
    - single cell modeling, 395
    - vehicle drivetrain platform modeling, 399
- for PHEVs
  - battery technologies, 417
    - Li-ion, 419
    - NiMH, 418, 424*t*
  - design architectures, 408
  - goals, 410, 411*t*
    - costs, 416
    - energy capacity, 413
    - life, 413
    - power, 412
    - safety, 415
  - size and capacity use in HEVs and PHEVs
    - combined model, 441
      - battery model, 447
      - cell chemistries, 442, 444*t*
      - cell sandwich design, 443
      - operating configurations and driving cycle, 449
      - pulse-power capability in a flat-potential system, 457
    - results for HEV operation, 451
    - results for PHEV operation, 453
      - vehicle model, 448, 449*t*
    - maximum pulse power capability, 431
    - simple model, 433
      - applications, 436
- Battery environmental analysis
  - boundary conditions, 364
  - electric vehicles traction batteries, 358
  - functional unit, 359

- Battery environmental analysis (*Continued*)
  - impact of the different battery technologies, 357
    - assembly and recycling of the battery, 357
  - impact of the different stages, 362
  - importance of recycling, 369
  - LCA (life cycle assessment), 348
    - eco-indicator points, 352
    - LCIA (life cycle impact assessment) method, 349
  - model, 352
    - assembly, 355
    - composition, 353
      - lead-acid, 353*t*
      - lithium-ion, 354*t*
      - nickel-cadmium, 354*t*
      - nickel-metal hydride, 353*t*
      - sodium-nickel chloride, 354*t*
    - electricity production, 356
    - recycling, 355
    - use of the battery in the vehicle, 355
  - qualitative analysis, less widespread battery technologies, 371
  - sensitivity analysis, 365
- Battery performance in electric and hybrid vehicle operation
  - battery pack modeling, 398
  - cell-to-cell variations, 393
  - field test data collection and analysis, 378
    - representative usage schedule, 380
    - vehicle usage pattern analysis, 378
  - laboratory battery tests, 382
    - assessing battery performance, 384
    - battery degradation mechanisms, 385
      - incremental capacity analysis, 389
      - mechanisms that contribute to battery capacity fading, 391
    - polarization resistance, 389
    - SOC determination by relaxed cell voltage, 387
  - roadmap to allow better understanding of, 377*f*
  - single cell modeling, 395
  - vehicle drivetrain platform modeling, 399
- Battery requirements for HEVs, PHEVs, EVs
  - fuel cell hybrid vehicles, 340
  - general requirements, 306
    - cost, 307, 308*t*
    - energy/power, 306, 307*t*, 331*t*, 331
    - life, 310
      - calendar life, 312
      - cycle life, 311
    - recycling and environmental issues, 315
    - safety, 314
    - temperature control, 313
  - specific requirements, 316
    - EVs, 329
      - Li-ion, 334
      - lithium metal polymer (LMP), 337, 338*t*
      - sodium/nickel chloride (ZEBRA), 338, 339*t*
    - USABC's goals, 332*t*
  - full hybrids, 319
    - Li-ion, 322, 323*t*
    - NiMH, 320, 336*t*
  - micro hybrids, 316
  - PHEVs, 326
    - Li-ion, 328
      - Li-ion battery pack, 329*t*
      - USABC's goals, 328*t*
  - soft hybrids, 317
  - summary of Li-ion chemistries, 340
- Battery vehicles, types or prototypes
  - Audi, 616
  - BMW, 617, 619
  - Chevrolet Volt, 336–341, 602–604, 635
    - Voltec technology, 633
  - Fiat, 617
  - Ford Focus, 620
  - GM EV1, 228–229
  - HOST, 629
  - MINI, 619
  - Opel Ampera, 229, 231, 240–241, 604
  - Pivo, 629, 630*f*
  - PSA Peugeot Citroën – Mitsubishi, 613
  - PSA Peugeot Citroën – Venturi Automobiles, 613
  - Renault–Nissan, 607
  - simulation, **247–274**
  - Volvo, 620
- BEVs (battery electric vehicles)
  - comparison of GHG emissions estimates with FCVs, 126
  - cost of, 22
  - Fiat 500, 617
  - GREET – emission results, 134
  - LEM – emission results, 126
  - management of batteries, **493–513**
  - Volvo C30, 620
  - See also* Electric vehicles (EVs)

**C**

- Carbon constrained world
    - atmospheric CO<sub>2</sub> levels, 91–93
      - carbon capture and storage (CCS), 92, 104
      - concentrating solar power (CSP), 104
  - Charging infrastructure
    - accessories for charging, 533
      - battery connectors, 538
      - dedicated accessories, 536
        - adaptation of standard accessories, 536
        - new standardization proposals, 536
      - standard accessories, 535
    - battery charging, 518
    - charging modes for conductive charging, 524
      - mode 1 charging, 524
      - mode 2 charging, 525
      - mode 3 charging, 526
      - mode 4 charging, 528
    - charging power levels, 519
      - defining power levels, 521
        - normal charging, 521
        - semi-fast charging, 521
      - energy usage, 519
        - charging time, 520
        - estimated consumption, 520
    - communication issues, 528
      - advanced communication, 529
        - billing, 533
        - grid management, 530
        - off board chargers, 529
      - control pilot communication, 528
    - fast charging, 538
    - historical background, 518
    - inductive charging, 539
  - Cost of battery, fuel-cell, and plug-in hybrid electric vehicles
    - battery electric vehicles (BEVs), 22
      - accessory systems for BEVs, 26
      - batteries for BEVs, 24
    - BEV drivetrain costs, 24
      - electric motors and motor controllers for BEVs, 26
      - energy-use costs for BEVs, 27
      - external costs of BEVs, 28
        - nonenergy operating and maintenance costs, 27, 37, 50
    - fuel-cell electric vehicles (FCEVs), 45
      - component costs, 32, 45
      - fuel-cell system, 46
        - hydrogen storage system, 49
  - energy-use costs, 53
    - cost of fuel, 54
      - HyPro, 54
      - SSCHISM, 54
    - energy use of FCEVs, 53
      - ADVISOR, 54
      - AVCEM, 53–54
  - external costs of FCEVs, 55
  - nonenergy operating and maintenance costs, 37
    - maintenance and repair costs, 37
    - other nonenergy operating costs, 39
  - plug-in hybrid electric vehicles (PHEVs), 31
    - component costs, 32
      - accessory power, 37
      - batteries, 32
        - ADVISOR, 34
      - electric motor and motor controller, 35
      - engine, exhaust system, and transmission, 35
    - energy-use costs, 39
      - energy use of PHEVs, 39
        - GPS-based cycle, 40–42
        - UDDS/HWFET cycle, 40–42
        - US06 cycle, 40–42
      - the price of electricity and the total annual electricity cost, 42
    - external costs of PHEVs, 42
      - nonenergy operating and maintenance costs, 37
        - maintenance and repair costs, 37
        - other nonenergy operating costs, 39
- Cost(s)
  - of batteries, 307, 416
  - in battery-fuel cell hybrids, 247–249, 267, 270
  - of battery, fuel-cell, and plug-in hybrid electric vehicles, 22, 31, 45
  - cost-effective vehicles and fuel technology choices, 104
    - four scenarios, 104
    - impact of CCS and CSP, 104
    - impact of vehicle technology cost, 107
  - in PHEVs, 206
  - of vehicle production, 554

**D**

- DOE's fuel cell vehicle project – NREL's data analysis results
  - composite data products (CDPs), 288–291

- DOE's fuel cell vehicle project – NREL's data analysis results (*Continued*)
- Fleet Analysis Toolkit (FAT), 290–291
  - fuel cell
    - durability, 293
    - factors affecting, 297
    - efficiency, 292,
      - at ¼ power, 292
      - at full power, 292
    - stack degradation, 295, 297
    - system power, 293
    - vehicle freeze capability, 301
  - geographic regions, 289
  - hydrogen production technologies, 290
    - electrolyzing water, 290
      - efficiency, 290
    - reforming natural gas, 290
      - efficiency, 290
  - hydrogen refueling stations, 290, 298
  - Hydrogen Secure Data Center (HSDC), 288–289, 289*f*
  - industry teams, 288
    - Chevron/Hyundai-Kia, 288
    - Daimler/BP, 288
    - Ford/BP, 288
    - GM/Shell, 288
  - infrastructure maintenance, 298
  - total number of vehicles deployed, 289
  - vehicle driving range, 291
  - vehicle fuel economy, 291
    - generation 1 vehicles, 291
    - generation 2 vehicles, 291
  - vehicle greenhouse gas emissions, 300
  - vehicle maintenance, 298
    - maintenance events, 298
  - vehicle refueling rates, 298
    - fills for 350 and 700 bar pressure, 298
- Drive cycles
- Australian urban, 63, 64*f*, 69*t*, 74*f*, 74–75, 80–81
  - FUDES, 383
  - GPS-based, 40–42
  - HWFET, 196, 196*t*, 197
  - JCO8, 196*t*, 200
  - NEDC, 63, 63*f*, 69*t*, 79*f*, 85*f*, 86*f*, 87*f*, 196*t*, 200
  - UDDS, 193–194, 196
  - UDDS/HWFET, 40–42
  - US06, 40–42
  - US-FTP, 63, 64*f*, 69*t*, 84
- E**
- Electric vehicles (EVs)
- battery management, 499
  - fuel cell, 232
  - light (LEV), 495
  - traction batteries, 358
  - see also specific vehicles*
- Emissions
- of GHG, 5–7, 6*t*, 7*t*, 7–9, 9*t*, 10*t*, 11–13, 118, 123–124, 134–135, 145, 147, 275, 277–281, 281*t*, 281–282, 282*f*, 282*t*, 283*f*, 300
  - in PHEVs, 195, 200, 203
    - CO<sub>2</sub>, 119–120, 123, 201*t*
    - FTP, 198, 200
- Energy
- consumed in fuel cycle of fuel cell vehicles, 278–281, 281*f*, 281*t*, 281–282, 282*t*, 282–283, 283*f*, 284*f*
  - consumption
    - in fuel cell vehicle cycle, 278–281, 281*f*, 281*t*, 281–282, 282*t*, 282–283, 283*f*, 284*f*
    - in vehicles, 551
  - goals for PHEV batteries, 413
  - management strategies in PHEVs, 174
  - and power requirements for HEVs, PHEVs, EVs, 306
  - storage systems in PHEVs, 168
  - systems modeling, 94
    - Global Energy Transition (GET) model, 92
      - constraints, 95
      - cost data, 95
      - energy demand, 94
      - model structure, 93
      - personal transportation, 95
    - usage in charging infrastructure, 519
- Environmental
- battery analysis, **347–374**
    - and recycling issues, 315
  - comparison of conventional and alternative vehicles, **1–18**
    - impact criteria, 5
- EVs (electric vehicles)
- battery requirements for, 329
  - fuel cycles, 118, 123–124, 149
  - Li-ion, 334
  - lithium metal polymer (LMP), 334, 338*t*
  - scaling up, 147
  - sodium/nickel chloride (ZEBRA), 338, 339*t*
  - USABC's goals, 332*t*
  - See also* BEVs (battery electric vehicles)

**F**

## Fuel cell

- durability, 293
- factors affecting, 297
- efficiency, 292
  - at ¼ power, 292
  - at full power, 292
- stack degradation, 295, 297
- system power, 293
- vehicle freeze capability, 301

Fuel-cell electric vehicles (FCEVs),  
**227–246**

- cost of, 45
- DOE's project, 291
- driving range, 291
- filling station infrastructure, 242
- freeze capability, 301
- fuel economy, 291
- GM HydroGen, 233, 233*f*, 234*f*, 235*t*
  - vs.* Chevrolet Equinox, 235*t*, 236*f*
- greenhouse gas emissions, 300
- Honda FCX Clarity, 624
- hybrids, battery-fuel cell, 267
- hydrogen, **275–287**
- maintenance, 298
- management of batteries, 496
- Mercedes, 626
- Nissan, 628
- PEM, 7*t*, 8*t*, 8, 232–233, 546, 280
- refueling rates, 257
- Toyota, 626
- VW Lupo simulation, 257–258, 259*f*

## Fuel economy

- in fuel cell vehicles, 291
- hybrid vehicles, 80
- intelligent-hybrid vehicles/intelligent vehicles,  
**61–90**
- in PHEV, 206
  - CAFE, 200, 201*t*
- in PHEV-20, 212–213, 215, 215*t*, 219–221
- in PHEV-40, 212–213, 215–216, 215*t*, 218–220,  
221*f*, 222–224

## Full hybrids, 67, 319, 590

**G**

- GHG. See Greenhouse gas emission reductions
- Global Energy Transition (GET) model, 92
- Greenhouse gas emission reductions
  - background and previous research, 115

- comparison of GHG emissions reductions from  
EV types, 145
- comparison of major modeling  
efforts, 135
  - comparison of GHG emissions estimates for  
BEVs and FCVs, 135
- comparison of GHG emissions reductions from  
PHEVs, 144
  - overview of GHG emissions estimates for  
PHEVs, 137
  - review of estimates of GHG emissions from  
PHEVs, 140
- emissions of CO<sub>2</sub> and other GHGs from the  
vehicle life cycle, 123
- estimates of GHG emissions from EV fuel cycles,  
124
  - GREET model – overview, 133
    - GREET – GHG emission results for BEVs  
and FCVs, 134
  - LEM – overview, 124
    - LEM – emission results for BEVs and FCVs,  
126
- formation of GHG emissions from EV fuel cycles,  
118
  - combustion or “in-use” emissions, 119
    - combustion emissions of carbon dioxide –  
overview, 120
    - emissions of methane from combustion  
engines, 120
    - emissions of nitrous oxide from power  
plants, 122
    - emissions of other greenhouse gases, 123
    - formation and emissions of nitrous oxide  
from combustion engines, 122
  - upstream emissions, 119
- key uncertainties and areas for further research,  
148
- magnitude of possible GHG reductions – scaling  
up the EV industry, 147

**H**

## HEVs (hybrid electric vehicles)

- battery requirements, 319
  - size and capacity use, 451
  - combined model, 441, 444*t*, 452*t*
- battery safety standards, 479
- power assist, 319

## Hybrid

- electric vehicles (HEVs), 581

Hybrid (*Continued*)

- full hybrids, 590
    - Toyota Prius, 590–593
  - management of batteries for, 497
  - micro hybrids, 582
  - micro/soft/full, batteries for, 316–317, 319
  - mild hybrids, 584
    - Honda Insight, 585–586, 586*f*
  - plug-in hybrids, 600,
    - See also* PHEVs (plug-in hybrid electric vehicles)
  - powertrain vehicle model, 65–67
  - vehicles with telematics, 80
- Hybrids, battery-fuel cell
- configuration optimization, 268
    - estimate of the cost, 270–271, 272*f*
  - simulation, 267
- Hydrogen
- in ammonia-fueled vehicle, 2, 4, 4*t*, 6
  - filling infrastructure, 242
  - fuel cell, 2–3
  - fuel cell vehicles, **275–287**
  - fuel cycle, natural gas reforming, 279
  - internal combustion, 2
  - production technologies, 290
  - refueling stations, 290
  - Secure Data Center (HSDC), 288–289, 289*f*

**I**

- Internal combustion vehicle, VW Lupo, 249
  - emissions, 249–250, 252, 254
  - performance simulation, 249

**L**

- Life cycle assessment (LCA), **275–287**
  - of gasoline vehicles, **275–287**
  - of hydrogen fuel cell vehicles, **275–287**
  - of vehicle technology, 275–276, 278–279, 284*f*
- Light electric vehicles (LEVs)
  - electric bicycles, 495
  - electric motorcycles, 495
- Li-ion cell safety
  - failures, 465
  - system specific safety evaluation, 482
  - thermal runaway, 470
  - typical safety circuits, 476
  - voltage introduced safety considerations, 488
- Lithium metal polymer (LMP), 337

**M**

- Management of batteries for electric traction vehicles
  - battery electric vehicle (BEV), 496
  - battery management systems, 499
    - architectures, 505
      - centralized, 505
      - distributed, 506
    - balancing, 504
    - calculating, 502
    - communicating, 503
    - connection sequence, 507
    - control, 503
    - current interruption fail-safe switches, 507
    - examples, 509
      - BEV, mild or full hybrid, or PHEV, 511
      - LEV or industrial, 509
      - micro hybrid, 509
    - isolation breakdown detection, 506
    - leakage detection, 506
    - measuring, 501
    - monitoring, 500
    - self-diagnostics, 507
      - system voltage and current maximums, 508
  - fuel cell electric vehicle (FCV), 496
  - hybrid electric vehicle (HEV), 497
  - industrial forklifts, 496
  - light electric vehicle (LEV), 495
    - electric bicycles, 495
    - electric motorcycles, 495
  - plug-in hybrid electric vehicle (PHEV), 498
- Market prospects of electric passenger vehicles
  - relevant stakeholders, 554
    - customers, 555
    - politics, 559
    - vehicle manufacturers, 558
- Vector21* model, 548
  - scenario 1: baseline, 562
    - results: new vehicle fleet, 563
    - results: vehicle stock, 566
  - scenario 2: climate protection, 566
    - results: new vehicle fleet, 567
    - results: vehicle stock, 570
  - verification of model results, 560
- Micro hybrids, 316, 582
- Mild hybrids, 66, 498, 584
- Models, for simulation
  - ADVISOR, 40–42, 54, 65, 142, 144, 199–200, 208, 212–213, 215, 399, 423, 423*t*, 424*t*

- AVCEM, 50–56
  - GREET, 55, 95–99, 117–118, 123–124, 133–134, 204, 277–278
  - HyPro, 54
  - LEM, 124, 125*t*, 126, 126*t*, 134
  - PSAT, 65, 399
  - SSCHISM, 54
  - VECTOR21*, 548–550, 553–561
  - VPSET, 399
- P**
- PHEVs (plug-in hybrid electric vehicles)
    - batteries for, **405–426**
    - case studies, 168
      - Chevrolet Volt, 186
      - Daimler Chrysler Sprinter, 185
      - Escape, 185
      - Hymotion Prius, 183*t*, 185
    - design, 161
      - literature review, 162
      - methods for studying, 163
      - process, 161, 163
    - Li-ion, 328
    - Li-ion battery pack, 329*t*
    - requirements
      - general, 306
      - specific, 316
    - size and capacity
      - combined model, 441
      - simple model, 433
    - subsystem and tradeoff analysis
      - accessory systems, 177
      - drivetrain architecture, 164
      - energy management strategies, 173
      - energy storage systems (ESS), 168
      - ESS charging system, 179
      - secondary power sources, 167*t*, 170
      - USABC's goals, 328*t*
  - PHEVs, evaluation of energy consumption/
    - emissions/cost
      - all electric range, 193–194, 202
      - charge depleting (CD), 193–195, 197–202, 204
      - charge sustaining (CS), 200, 203
    - costs, 31, 206
    - driving profile database, 216
    - driving profile impacts, 219
    - emissions, 195
      - CO<sub>2</sub>, 203
      - FTP, 201*t*
    - fuel consumption, 195, 200
      - CAFE, 201*t*
    - impact on the electric grid, 205
    - management of batteries, 498
    - NREL research and development, 212
    - parallel, 199*t*
    - petroleum displacement potential, **211–224**
      - enhanced charging scenario, 220
      - NREL research and development, 212
      - PHEV-20, 212–213, 215–216, 218–224
        - opportunity charging, 215, 219–220
      - PHEV-40, 212–213, 215–216, 215*t*, 219–220, 222–224
        - single evening charge, 215, 219–220
    - SAEJ1711 applied to, 196
    - series, 199*t*
  - Powertrain
    - conventional, vehicle model, 65
    - hybrid, vehicle model, 65
  - Powertrain options for hybrid and electric vehicles
    - battery electric vehicles, 606
      - Audi E-Tron, 616
      - BMW Concept ActiveE – 1-Series Electric, 617
      - Fiat 500 Bev, 617
      - Ford Focus EV, 620
      - MINI E, 619
      - Mitsubishi i-MiEV, 612
      - PSA Peugeot Citroën – Mitsubishi Partnership, 613
      - PSA Peugeot Citroën – Venturi Automobiles Agreement, 613
      - Renault–Nissan Alliance, 607
      - Smart Fortwo Electric Drive, 611
      - Volvo C30 BEV, 620
    - fuel cell hydrogen electric vehicles, 624
      - Honda FCX Clarity, 624
      - Mercedes-Benz B-Class F-Cell, 626
      - Nissan X-Trail, 628
      - Toyota FCHV-adv, 626
    - hybrid electric vehicles, 581
      - full hybrids, 590
        - Toyota Prius, 590–591
      - micro hybrids, 582
      - mild hybrids, 584
        - Honda Insight, 581
    - multi-purpose electrified traction platforms and architectures, and auto innovation design, 629
      - General Motors' Voltec technology, 633
      - HOST, 629
    - plug-in hybrids, 600



**S**

- Safety of lithium-ion batteries for HEVs
  - HEV battery safety standards, 479
  - Li-ion cell failures, 465
  - Li-ion cell thermal runaway, 470
    - cell overcharge, 474
    - external short circuit, 470
    - high temperature storage and charging, 476
  - internal short circuit, 471
    - cell charging algorithm, 473
    - cell defects, 473
    - metallic contaminants, 472
    - low temperature charging, 475
    - overdischarging Li-ion cells, 475
- system specific safety evaluation, 482
  - cell manufacturing defects, 483
  - design defects, 485
  - number of cells, 486
  - operating life, 487
  - operating temperature, 486
  - system-based abuse testing, 487
- typical safety circuits, 476
- voltage introduced safety considerations, 488
  - arcing, 488
  - electrical shock hazard, 488